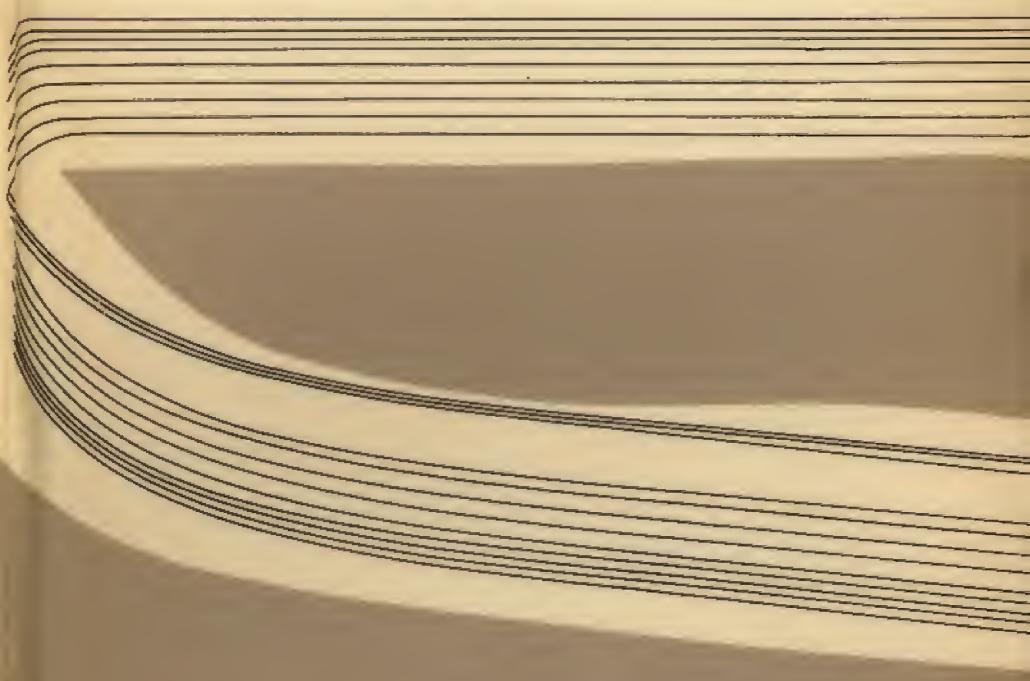
KING

Transmission-line Theory

BY RONOLD W. P. KING



Transmission-line Theory

Dover

S1285

£1.96 net
In UK only

DOVER BOOKS ON ENGINEERING AND ENGINEERING PHYSICS

Theory of Wing Sections, Ira H. Abbott and Albert E. von Doenhoff. $3.25

De Re Metallica, Georgius Agricola. Clothbound $10.00

Charles Babbage and His Calculating Engines, edited by Philip Morrison and Emily Morrison. $2.00

Treatise on Hydrodynamics, A. B. Basset. Two volume set $3.50

Traveling Waves on Transmission Systems, L. V. Bewley. $3.00

Two-Dimensional Fields in Electrical Engineering, L. V. Bewley. $1.50

Flux Linkages and Electromagnetic Induction, L. V. Bewley. $1.25

The Measurement of Power Spectra from the Point of View of Communications Engineering, Ralph B. Blackman and John W. Tukey. $1.85

Theory of Ship Motions, S. N. Blagoveshchensky. Two volume set $4.00

The Thermodynamics of Electrical Phenomena in Metals, and A Condensed Collection of Thermodynamic Formulas, Percy W. Bridgman. $1.75

Analytical Mechanics of Gears, Earle Buckingham. $2.75

Piezoelectricity, Walter G. Cady. Two volume set $5.00

Mathematical Tables and Formulas, Robert D. Carmichael and Edwin R. Smith. $1.00

Operational Methods in Applied Mathematics, H. S. Carslaw and John C. Jaeger. $2.25

Gaseous Conductors: Theory and Engineering Applications, James D. Cobine. $2.95

Applied Optics and Optical Design, A. E. Conrady. Two volume set $5.90

Electrical Theory on the Giorgi System, P. Cornelius. Clothbound $6.00

Mechanics of the Gyroscope: Dynamics of Rotation, Richard F. Deimel. $1.65

Mechanics, J. P. Den Hartog. $2.00

Strength of Materials, J. P. Den Hartog. $2.00

Teach Yourself Heat Engines, E. De Ville. Clothbound $2.00

A Diderot Pictorial Encyclopedia of Trades and Industry: Manufacturing and the Technical Arts in Plates Selected from L'Encyclopédie ou Dictionnaire Raisonné des Sciences, des Arts, et des Métiers, edited by Charles Gillispie. Clothbound. Two volume set $18.50

Hydrodynamics, Hugh L. Dryden, Francis D. Murnaghan, and Harry Bateman. $2.75

A Guide to Operational Research, Eric Duckworth. Clothbound $3.50

Aerodynamic Theory, William F. Durand, editor-in-chief. Clothbound. Three volume set $17.50

(continued on back flap)

Transmission-line Theory

RONOLD W. P. KING, Ph.D.

Gordon McKay Professor of Applied Physics
Harvard University

DOVER PUBLICATIONS, INC.
NEW YORK

Copyright © 1965 by Dover Publications, Inc.
Copyright © 1955 by Ronold W. P. King.

All rights reserved under Pan American and International Copyright Conventions.

Published in the United Kingdom by Constable and Company Limited, 10 Orange Street, London W. C. 2.

This Dover edition, first published in 1965, is an unabridged and corrected republication of the work first published by the McGraw-Hill Book Company, Inc., in 1955, to which has been added a new Index of Symbols.

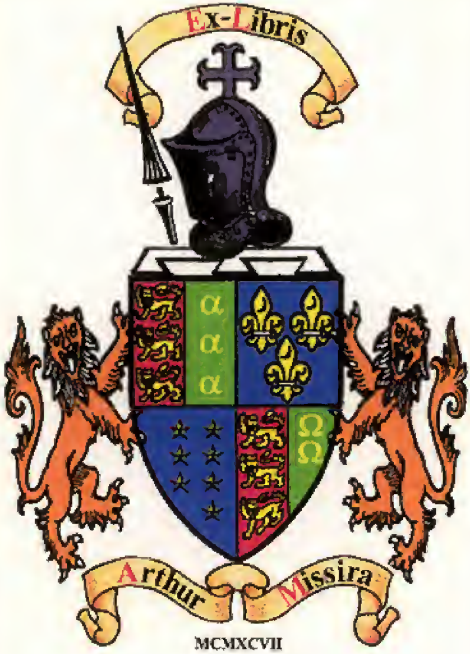
Library of Congress Catalog Card Number: 64-8269

Manufactured in the United States of America

Dover Publications, Inc.
180 Varick Street
New York 14, N. Y.

Theory as such is of no use except in so far as it makes us believe in the coherence of phenomena.

GOETHE, *Maxims and Reflections*


Ex-Libris
α α α
Ω Ω
Arthur Missira
MCMXCVII

PREFACE TO THE DOVER EDITION

Although a decade has passed since *Transmission-line Theory* was first published, the material it contains is still modern and complete. This characterization is likely to apply for many years to come. Indeed, as technology continues to require ever greater precision, the scientifically accurate treatment provided in *Transmission-line Theory* may find increasing appreciation and use by engineers.

In this second edition a number of misprints and minor errors have been corrected. In addition, an index of symbols has been provided.

RONOLD W. P. KING

Gordon McKay Laboratory of Applied Science
Harvard University
Cambridge, Mass., August, 1964

PREFACE

As a consequence of the ever-increasing preoccupation of physicists with problems in nuclear and solid-state physics, the scientific and technical advance of electrical science is rapidly becoming the concern and responsibility of the engineer. As the research scientist knows only too well, an understanding of recent progress in applied electricity, especially in the generation, transmission, and radiation of electromagnetic energy at ever higher frequencies, requires a deeper appreciation of physical and mathematical fundamentals than can be provided by even a most thorough knowledge of electric-network theory as applied to lumped elements. This deeper and more fundamental approach involves a knowledge of general electromagnetic theory.

Perhaps the most interesting bridge between the specialized point of view of lumped-constant electric circuits and the general and fundamental approach of electromagnetic theory is the conventional transmission line. Since its transverse dimensions satisfy the conditions of lumped-constant circuits, whereas its length is unrestricted, the electromagnetic aspect involving the concept of propagation is one-dimensional. Moreover, by demanding that equal and opposite currents and charges be sufficiently close together, the smooth line may be approximated by a recurrent network of lumped elements for most purposes. This is found to be a consequence of the application of general electromagnetic theory and its specialization, subject to appropriate restrictions, to the boundaries of conventional transmission lines. Significantly it is possible to introduce some of the most fundamental concepts of electromagnetic theory without becoming involved in all the complications of vector field theory.

In Chap. I the well-known transmission-line equations for an infinite line are deduced in the conventional manner *and* from electromagnetic fundamentals for various important cross sections. In Chap. II the derivation of the equations is specialized to lines of finite length, and the basic method of treating terminated lines is formulated. Chapter III is concerned with the impedance of sections of transmission line and their use as shunt and series elements in insulators, transformers, matching networks, unbalanced loads, baluns, shielded loops, and hybrid junctions. An important feature of the treatment of terminal impedance and input impedance is the use of complex terminal functions. These are very closely related to experimentally measured quantities, and they are

more convenient in analyzing many types of problems than are the reflection coefficients. Chapter IV is devoted to the study of distributions of current and voltage, the transfer of power, and an analysis of distribution and resonance curves and their application in transmission-line measurements. Chapter V involves the analysis of discontinuities and nonuniformities along smooth lines. Included are discussions of the Weissfloch tangent relation and Deschamps's method for determining the properties of junctions. Also treated are dielectric slabs as discontinuities, the measurement of dielectric constants and permeabilities, changes in cross section, terminations, bends, T junctions, and end corrections, including those for transmission lines used to drive antennas. Chapter VI is concerned with transmission-line oscillators, coupled-circuit phenomena on lines, and radiation.

Most of this book has developed from lecture notes for a one-semester graduate course on transmission-line theory which has been given at Harvard University for the last 10 years. It is concerned primarily with the high-frequency aspects of transmission lines and with their steady-state operation. It is designed to serve as a necessary and fundamental introduction preceding serious work in wave guides and cavities as well as antennas. Although the treatment is predominantly analytical, little more than a sound knowledge of differential and integral calculus and elementary differential equations is presupposed, together with a thorough background in alternating currents. Although the foundation of transmission-line theory on electromagnetic principles is a special feature of this book, it is possible to pursue a more conventional course simply by omitting Chap. I, Secs. 3 to 12, and Chap. II, Secs. 1 to 4. It is to be expected that Chaps. V and VI would not be covered in such a plan.

The author is indebted to several of his students for contributions and assistance. These include, in particular, J. Eisenstein, D. D. King, J. Porter, L. S. Sheingold, J. E. Storer, C. T. Tai, and K. Tomiyasu. D. B. Brick and J. E. Storer assisted with the proofs. The entire manuscript was typed by Phyllis Kennedy. The figures were prepared by E. Rising and his assistants.

Ronold W. P. King

CONTENTS

Preface vii

Note on the Numbering of Equations and Figures and on the Notation . . . xiii

CHAPTER I: THE INFINITELY LONG LINE. 1

1. Methods of Analyzing the Transmission Line 1
2. The Conventional Derivation of the Differential Equations of the Transmission Line 3
3. Potential Functions and Electromagnetic Preliminaries 7
4. Electromagnetic Derivation of the Equations and Parameters for Balanced Infinitely Long Two-wire Lines 13
5. The Balanced Four-wire Line 19
6. The Coaxial Line 20
7. The Closely Spaced Two-wire Line with Unequal Conductors. . . . 23
8. The Shielded Line with Eccentric Inner Conductor. 31
9. The Shielded-pair Line 34
10. Three-wire Polyphase Line; Three-phase Cable 39
11. The Coaxial Cage Transmission Line 43
12. Strip Lines 45
13. General Solution of the Differential Equations for an Infinite Line . . 48
14. Interpretation of the Solution for the Voltage along an Infinite Line. Phase and Group Velocities 50

Problems 56

CHAPTER II: THE TERMINATED LINE. 58

1. Potential Functions for a Terminated Line 58
2. Generalized Differential Equations 64
3. Terminal Zones; Coupling and End Effects 68
4. Equivalent Uniform Line with Terminal-zone Network 71
5. Evaluation of Constants in Terms of Boundary Conditions; Exponential Solution for a Terminated Line 73
6. Infinite-series Form of the Exponential Solution 77
7. Incident- and Reflected-wave Form of the Exponential Solution . . . 79
8. Hyperbolic Forms of the Solution 83
9. Instantaneous Values of the Hyperbolic Solutions 86
10. The Propagation Constant 91
11. The Characteristic Impedance 93
12. The Phase and Group Velocities of the Infinite Line 94
13. Special Forms of the General Parameters of the Line 95
14. Relation between Reflection Coefficient and Terminal Functions . . 101
15. The Phase and Attenuation Functions of the Terminations 102
16. Graphical Representation of the Terminal Functions in the Normalized Impedance or Admittance Plane; Circle Diagram 104
17. Graphical Representation of the Normalized Impedance or Admittance in the Reflection-coefficient Plane; Smith Chart 108

18. Special Forms of the Terminal Functions and of the Reflection Coefficient —Resistive Termination 112
19. Special Forms of the Terminal Functions—the Predominantly Reactive Termination 117
20. The Conducting Wire Bridge as a Termination; Resistive Wire . . . 120
21. Conducting Pistons and Disks as Terminations 127
22. Terminations with Negative Attenuation Function or Reflection Coefficient Greater than Unity 128
Problems 130

Chapter III: Impedance and Admittance. 133

1. Normalized Input Impedance and Admittance of a Terminated Section of Line 133
2. Input Impedance and Admittance 147
3. Extreme Values of the Input Resistance and Conductance 153
4. Extreme Values of the Input Reactance and Susceptance 157
5. Summary of Critical Values of Input Impedance and Admittance for a Section of Low-loss Line 160
6. Section of Transmission Line as an Insulator 164
7. Impedance Transformation Using a Network of Transmission-line Sections—General Formulation 172
8. The Series Transformer 174
9. Matching Section with a Single Movable Stub 177
10. Matching Section Consisting of a Double-stub Tuner 184
11. Matching with a Shunt Section 190
12. Representation of a Section of Transmission Line by Lumped Equivalents; Impedance, Admittance, and Scattering Matrices 194
13. Unbalanced Load Terminating a Symmetrically Driven Shielded-pair Line 203
14. Series Stubs and Unbalanced Sections of Line; Folded Dipole; Balun; Shielded Loop 209
15. The Hybrid Junction for Transmission Lines 225
Problems 241

Chapter IV: General Amplitude Relations for Current and Voltage . 243

1. The Distribution of Current and Voltage and the Transfer of Power along a Nonresonant Line 243
2. General Expressions for Current and Voltage for an Arbitrarily Terminated Line When Driven by a Single Pair of Equal and Opposite Point Generators (or Their Equivalent) Anywhere along the Line 244
3. General Expressions for Current and Voltage for an Arbitrarily Terminated Line When Driven by Two Pairs of Equal and Opposite Point Generators (or Their Equivalent) Anywhere along the Line 246
4. General Expressions for Current and Voltage for an Arbitrarily Terminated Line When Driven by Three Pairs of Generators (or Their Equivalent) Anywhere along the Line 248
5. Polar Form of the General Expressions for Current and Voltage . . . 249
6. The Transfer of Power along a Transmission Line 251
7. Resonance Curves and the Condition for Resonance 254
8. Distribution Curves 257
9. Resonance-curve and Distribution-curve Ratios; the Standing-wave Ratio 259

10. Distributions of Current and Voltage in a Resonant Line; Components of Current and Voltage 262
11. The Widths of Resonance and Distribution Curves. 266
12. The "Q" of a Transmission Line 269
13. Theory of Transmission-line Measurements 272
Problems 286

CHAPTER V: DISCONTINUITIES AND NONUNIFORMITIES IN TRANSMISSION LINES. 288

1. Two-terminal-pair Networks in Transmission Lines 288
2. Equivalent Transformer for Two-terminal-pair Network That Includes Sections of Transmission Line. Weissfloch Tangent Relation . . . 294
3. Experimental Determination of an Equivalent Ideal Transformer for a Reactive Network 298
4. Deschamps's Graphical Method for Determining the Scattering Matrix and Equivalent Circuit of a Junction 304
5. Measurement of Impedance and Reflection Coefficient through a Junction. 314
6. Theory of a Dielectric and Magnetic Slab or Bead in a Transmission Line 317
7. The Maximum-Minimum-shift Method for Determining Dielectric Constants and Permeabilities of Solids and Liquids and Equivalent Sections of Transmission Line for Symmetrical Two-terminal-pair Networks . . 329
8. Determination of Losses in Dielectric and Magnetic Materials Using the Maximum-shift Method 341
9. The Double Bead and the Spacing of Beads for No Change in Impedance . 346
10. The Double-slug Transformer 351
11. Lossy Terminations for Nonresonant Shielded Lines 358
12. Closed and Open Ends as Reactive Terminations in Two-wire and Coaxial Lines 364
13. Junction of Two Open-wire Lines with Conductors of Different Radii . 368
14. Change of Radius in a Coaxial Line 377
15. Bend in a Two-wire Line 382
16. T Junction in a Two-wire Line. 389
17. Junction Networks for Series Branches in Two-wire Lines; Terminal-zone Networks for Stub-supported and Center-driven Antennas and Folded Dipoles 397
18. Change in Spacing of a Two-wire Line 411
19. Right-angle Bend in the Plane of a Two-wire Line 418
20. Bends and T Junctions in Balanced Shielded-pair Lines 426
21. Bend in a Coaxial Line; T Junction 426
22. End Correction for a Coaxial Line When Driving an Antenna over a Ground Screen 430
Problems 437

CHAPTER VI: TRANSMISSION-LINE OSCILLATORS AND COUPLED SECTIONS OF TRANSMISSION LINE 439

1. Frequency Characteristics of Simple Triode Oscillators with Transmission Lines as Tank Circuits 439
2. Frequency Characteristics of a Transmission-line Oscillator with Coupled Secondary 447
3. Electric Field of a Conductor with Sinusoidally Distributed Current. . 454
4. The Electric Field of a Driven Section of Two-wire Line 457

5. Current and Voltage in a Line Driven by a Coupled Section of Transmission Line; Directional Coupler 463
6. Coupled Transmission Lines 468
7. Admittance of Bridge-coupled Sections of Low-loss Transmission Line; Coupled-circuit Effects Involving Minima and Double Peaks . . . 470
8. Transmission-line Measurements with a Multiple-frequency Source; Filter Sections 482
9. Radiation from Open-wire Lines 487
Problems 492

Bibliography 494

Indexes 501

NOTE ON THE NUMBERING OF EQUATIONS AND FIGURES AND ON THE NOTATION

Chapters are numbered with roman numerals; sections are numbered with arabic numerals beginning with 1 in each chapter; equations are numbered consecutively (1), (2), . . . , in each section with no reference to section number. At the top of each left-hand page is the chapter number; at the top of each right-hand page is the section number. When reference is made to an equation in the same section, only the equation number is given, e.g., (5). When reference is made to an equation in another section in the same chapter, the section and equation numbers are given in the form Sec. 6, Eq. (12). When reference is made to an equation in another chapter, the chapter number, section number, and equation number are given, e.g., Chap. II, Sec. 4, Eq. (36). Figures are numbered with both section and figure numbers; thus Fig. 6.2 is the second figure in Sec. 6. Reference to a figure in another chapter includes the chapter number, e.g., Chap. II, Fig. 7.5. By referring to chapter and section numbers at the tops of the pages, any equation or figure is quickly found.

Superior numbers refer to the Bibliography at the end of the book. The following symbolism is used: Space vectors, whether real or complex, are in boldface roman type, $\mathbf{A}$, $\mathbf{x}$. Complex scalars (phasors) are in boldface italic, $\boldsymbol{Z}$, or boldface Greek, $\boldsymbol{\gamma}$. Real scalars are in lightface italic or lightface Greek, X, α. Matrices are represented by boldface roman, $\mathbf{Y}$.

CHAPTER I

THE INFINITELY LONG LINE

1. Methods of Analyzing the Transmission Line. The distributions of current and potential difference and the transfer of power along open and shielded transmission lines may be determined by several methods. The choice of method may appear to be of no practical concern, since it is assumed, quite naturally, that all methods must give the same correct answer. Actually the mathematical analysis of many physical phenomena is not easily reduced to right and wrong. A so-called solution is in almost every instance an approximation or idealization, and in consequence its correctness is a matter of degree. This is true, in a peculiar way, of the current in a transmission line. But this fact does not in itself dictate a choice between the several different approaches to a problem if they lead to the same final result. Obviously, in this event, all methods are correct to the same degree, and it would seem that one must be as good as another. Insofar as the ultimate formula is concerned, this is true. On the other hand, it is never sufficient to be provided merely with a formula that is to be used to compute actual results in an engineering problem without a complete statement of the circumstances to which it applies and of the conditions under which it will yield accurate results. Such a statement is an essential part of every mathematical formula, notwithstanding the fact that it is often not provided and that correct answers are often obtained without it. It is the function of a mathematical derivation of a formula from fundamental principles to supply information regarding all restrictions, approximations, and limitations that are imposed, as well as to produce the formula itself. But even this is not enough. It is necessary also to examine the generality and the applicability of the fundamental principles that are accepted at the outset.

The methods that may be pursued in analyzing the transmission line fall into two groups, those which are based on electric-circuit theory and those which proceed from electromagnetic theory. In the first group are two well-known methods. The one divides the transmission line into small elements each of which is represented by an "equivalent" circuit of suitably arranged elements of inductance, resistance, and capacitance to which Kirchhoff's laws may be applied. By allowing the length of the element to vanish, the difference equations so obtained become the

familiar first-order differential equations of the transmission line. The second method in the first group is related closely to the one described. It treats the transmission line as a limiting form of an artificial line constructed of recurrent sections of unrestricted impedances and analyzed in general terms by network theory.

In the second group, which depends on electromagnetic theory, the attempt may be made to analyze the transmission line as a boundary-value problem, or it may be merely a question of deriving the transmission-line equations. In either case it is possible to proceed from the Maxwell equations defining the electromagnetic field or from the defining relations for the scalar and vector potentials.

A detailed, critical evaluation of these several methods cannot be made at this point. The following comments, however, are offered as an introduction to further work. Throughout the first group it is assumed without proof that the methods of electric-circuit theory, in particular, the application of Kirchhoff's laws and the description of circuits entirely in terms of resistance, inductance, and capacitance, are sufficiently general to serve as first principles. Actually this is true for the transmission line subject to definite conditions, which, moreover, cannot be determined in any derivation that ignores them in its initial postulates. None of the methods in this group can provide formulas for the circuit parameters, which must therefore always be derived separately. On the other hand, the entire first group, and particularly the first of the two methods mentioned, is characterized by the analytical simplicity of network theory. This is no mean advantage. The second method also brings into clear perspective the important relationships that exist between transmission lines and artificial lines.

The methods of the second group have the advantage over all others that they directly depend upon the first and most fundamental principles of macroscopic electrodynamics. They have the almost equally great disadvantage of sharing in the complexity of electromagnetic theory. This latter is especially true of methods that attempt to analyze the transmission line as a boundary-value problem, but also, though to a smaller degree, of methods that specialize the Maxwell equations or the equations for the potential functions in order to obtain the transmission-line equations. In carrying out such a specialization all necessary restrictions and approximations may be made available, and formulas for all parameters of the line are derived in the process. As a consequence, it may be shorter as well as more rigorous and complete than the simplest method based on circuit theory, if the separate determinations of the several parameters are added to this. Finally the more general analysis using electromagnetic principles permits a study of transmission-line end effects and coupling effects in a region near the junction of the transmission line with its terminations or with another line of different charac-

teristics. These play a significant role in determining the apparent impedance of a termination as an actual load, as distinct from its ideal or theoretical impedance as an isolated entity independent of the line to which it is connected. However, to a degree satisfactory for most practical purposes, such junction effects can be represented by an appropriate circuit of lumped reactances. It follows that, subject to suitable restrictions that define the limits of conventional transmission-line analysis, the entire problem can be solved in a form that makes use of the symbolism of network theory. That is, the variables are currents, voltages, and charges; the parameters are resistances and reactances. Just as in network theory, the specific values of resistance and reactance associated with a particular configuration of conductors must either be determined theoretically from electromagnetic principles or measured. It may be concluded that electromagnetic investigations are required in order to (1) specify the nature of the circuit, (2) evaluate the parameters involved, and (3) provide the restrictions on the generality of the circuit and the formulas for the parameters. However, electromagnetic theory is not needed to determine the properties of a given network of resistances and reactances.

In order to simplify the analysis of a problem that in its fundamental sense is highly complicated, it seems desirable to begin with a study of the transmission line as a limiting case of a recurrent network of lumped resistances, inductances, and capacitances. The soundness of this method is then verified by reanalyzing the infinite line using the scalar and vector potential functions of general electromagnetic theory. In this way the formulas for the line constants are obtained with the differential equations. At a later point this same method is appropriately generalized to the finite line so that account may be taken of junction and end effects.

2. The Conventional Derivation of the Differential Equations of the Transmission Line. Short sections of two- and four-wire lines and of coaxial and shielded-pair lines are shown schematically in Fig. 2.1. For the open-wire lines the conductors are identical. Each is circular in cross section; its radius is a, and the separation between centers is b. In the case of the coaxial line the smaller conductor has an outer radius a_1, and the larger conductor has an inner radius a_2 and an outer radius a_3. In carrying out the analysis it is *assumed* that each section of length Δz may be treated as if equivalent to the circuit shown in Fig. 2.2, with fixed values of r, l, c, and g in the limit as Δz is made to approach zero. For the open-wire lines r_1 and l_1 are assumed to be equal, respectively, to r_2 and l_2, r_3 and l_3, r_4 and l_4. In the case of the coaxial line r_1 and l_1 are not equal to r_2 and l_2. Clearly, to replace each length Δz of a transmission line by the circuit of Fig. 2.2 implies that all such lengths are exactly alike, *a condition true only for a line that is infinitely long.* Inductance

and capacitance and, to a smaller degree, resistance and leakage conductance per unit length differ near the ends of a line of finite length, however terminated, from their values far from the ends. Moreover the load may be coupled to the conductors of the line in a short region near their common junctions. If the assumption is made, nevertheless, that inductance and capacitance as well as resistance and leakage conductance

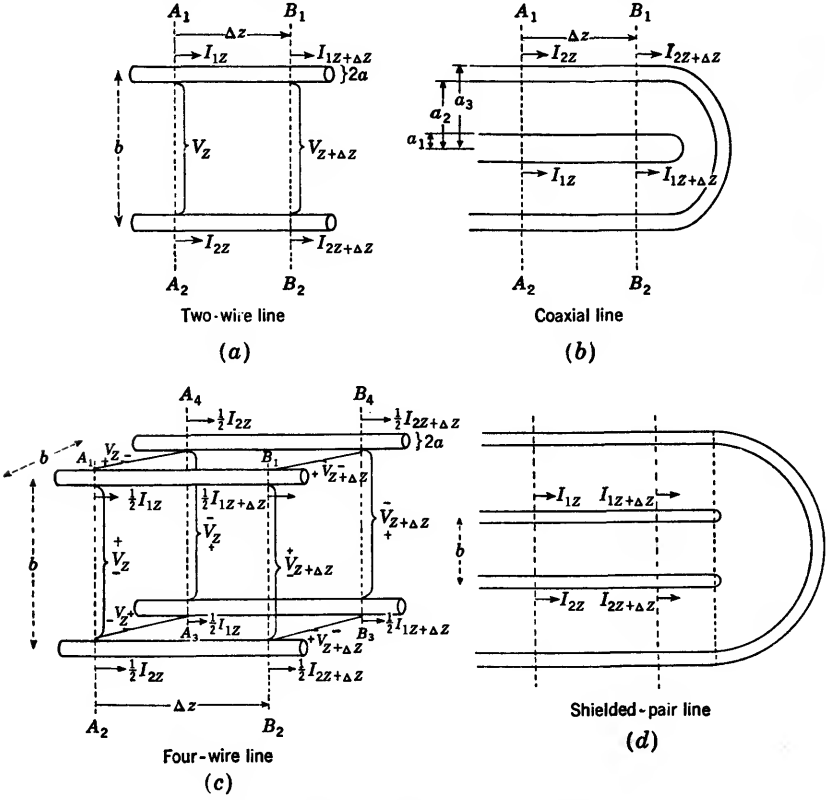


FIG. 2.1. Sections of infinite transmission lines.

per unit length are *constants independent of the location* of the element Δz along the line, and coupling between line and load is ignored, the over-all error so introduced can be made negligible only by making the separation of the conductors of the line sufficiently small compared with both the length of the line and the wavelength. In practice, the error involved in this assumption either is disregarded and consequently included with the terminal impedance or is designated as an end effect. Note that the assumed equivalence between the circuits in Figs. 2.1 and 2.2 is in no way qualified by restrictions limiting its generality, thus suggesting that there are no restrictions. This is a consequence of the fact that the

restrictions that actually obtain are limitations on network theory as a whole and not on this particular application alone. Nor is the argument that the calculated results are verified experimentally entirely satisfactory except in a limited way, since for any given line the agreement ceases to be a good one when the frequency is raised to a sufficiently high value. It is shown at a later point that network theory is a good approximation in transmission lines only if the conditions

$$b \ll \lambda \qquad a_2 \ll \lambda$$

are satisfied, where b is the spacing of a two-wire line and a_2 is the inner radius of the outer conductor of a coaxial line.

The circuit of Fig. 2.2 may be analyzed as follows: First, since Δz is small, the currents and the potential difference at the point $z + \Delta z$ may be

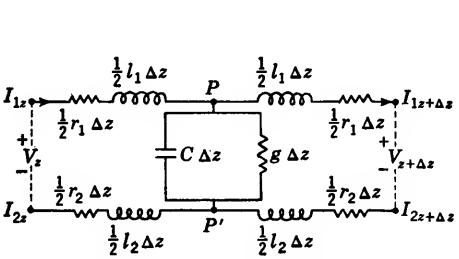


FIG. 2.2. Equivalent circuit of a section of an infinite transmission line.

expressed in terms of the currents and the potential difference at the point z by means of Maclaurin's expansion:

$$I_{z+\Delta z} = I_z + \left(\frac{dI}{dz}\right)_z \Delta z + \left(\frac{d^2I}{dz^2}\right)_z \frac{(\Delta z)^2}{2} + \cdots \tag{1}$$

$$V_{z+\Delta z} = V_z + \left(\frac{dV}{dz}\right)_z \Delta z + \left(\frac{d^2V}{dz^2}\right)_z \frac{(\Delta z)^2}{2} + \cdots \tag{2}$$

Next, upon applying Kirchhoff's emf law around the rectangle formed by the input and output terminals of the section, the following result is obtained:

$$\tfrac{1}{2}(I_{1z} + I_{1z+\Delta z})(r_1 + j\omega l_1)\,\Delta z + V_{z+\Delta z} - \tfrac{1}{2}(I_{2z} + I_{2z+\Delta z})(r_2 + j\omega l_2)\,\Delta z - V_z = 0 \tag{3}$$

With (1) and (2) this gives

$$\tfrac{1}{2}\left[2I_{1z} + \left(\frac{dI_1}{dz}\right)_z \Delta z + \cdots\right](r_1 + j\omega l_1)\,\Delta z - \tfrac{1}{2}\left[2I_{2z} + \left(\frac{dI_2}{dz}\right)_z \Delta z + \cdots\right](r_2 + j\omega l_2)\,\Delta z + \left(\frac{dV}{dz}\right)_z \Delta z + \cdots = 0 \tag{4a}$$

Collecting terms, dividing by Δz, and then allowing Δz to approach zero give

$$I_{1z}(r_1 + j\omega l_1) - I_{2z}(r_2 + j\omega l_2) + \left(\frac{dV}{dz}\right)_z = 0 \tag{4b}$$

The current in an open-wire line can be resolved into two components, to be distinguished in the following by subscripts C (for codirectional) and O (for opposite). These components are defined to satisfy the following relations:

$$I_{1z} = I_{C1z} + I_{O1z} \qquad I_{2z} = I_{C2z} + I_{O2z} \tag{5a}$$

$$I_{C2z} = I_{C1z} \qquad I_{O2z} = -I_{O1z} \tag{5b}$$

It is possible and, for purposes of transmission, desirable to drive and arrange open-wire lines symmetrically in such a manner that

$$I_{Cz} = 0 \qquad I_{O2z} = -I_{O1z} = -I_z \tag{6}$$

Open-wire lines that satisfy (6) are *balanced;* if (6) is not true, the line is unbalanced.

The components of current I_{Cz}, if they exist on an open-wire line, are codirectional antenna currents that do not depend upon the constants r, l, c, and g; hence they cannot be determined by transmission-line theory or ordinary electric-circuit theory. Whether codirectional currents exist or not, transmission-line theory is meaningful only for the component I_{Oz}. If I_{Cz} is not zero, the total current is given by (5*a*), with I_{Cz} obtained from antenna theory and I_{Oz} from line theory. In the following only I_{Oz} is determined, and for simplicity it is assumed that (6) is satisfied, so that the subscript O may be omitted.

For practical purposes (6) is always satisfied for the currents on the inner conductor and on the inner surface of the outer conductor of a coaxial line. Antenna currents, if they exist on a coaxial line, as they often do, are on the outer surface of the outer conductor. In a shielded-pair line unbalanced currents treat the line like a coaxial line, with the two inner conductors in parallel as one line and the inner surface of the sheath as the other. Antenna currents on the outside of the shield are also possible.

Let the following shorthand be introduced and applied to a balanced open-wire line or a coaxial line:

$$r \equiv r_1 + r_2 \qquad l = l_1 + l_2 \qquad z \equiv r + j\omega l \tag{7}$$

The quantities r, l, and z are the total resistance, inductance, and impedance *per loop unit length.* In two- and four-wire lines and shielded-pair lines with identical conductors,

$$r_1 = r_2 \qquad l_1 = l_2$$

Assuming (6) to be true and using (7), (4*b*) becomes

$$zI_z = -\left(\frac{dV}{dz}\right)_z \tag{8}$$

Before Kirchhoff's current law is applied at the point P, it is to be noted that the voltage across PP' is $\frac{1}{2}(V_z + V_{z+\Delta z})$. Then

$$I_{1z} = I_{1z+\Delta z} + \tfrac{1}{2}(V_z + V_{z+\Delta z})(g + j\omega c)\,\Delta z \tag{9}$$

If use is made of (1) and (2) and the expression so obtained is divided by Δz before allowing this to approach zero, the following equation is the result:

$$yV_z = -\left(\frac{dI}{dz}\right)_z \tag{10}$$

In (10) the symbol y stands for the total shunt admittance per loop unit length:

$$y \equiv g + j\omega c \tag{11}$$

The first-order differential equations (8) and (10) are the well-known transmission-line, or long-line, equations. The variables are readily separated, and the equations replaced by two of the second order, as follows:

$$-z\left(\frac{dI}{dz}\right)_z = \left(\frac{d^2V}{dz^2}\right)_z = yzV_z \tag{12}$$

$$-y\left(\frac{dV}{dz}\right)_z = \left(\frac{d^2I}{dz^2}\right)_z = yzI_z \tag{13}$$

It is convenient to define a quantity γ, known as the *complex propagation constant*, as follows:

$$\gamma^2 \equiv yz = (g + j\omega c)(r + j\omega l) \tag{14}$$

The real and imaginary parts of γ are α and β. Thus $\gamma = \alpha + j\beta$. The law of conservation of electric charge is expressed by the equation of continuity. In complex form it is

$$\frac{dI_z}{dz} + j\omega q_z = 0 \tag{15}$$

where q_z is the charge per unit length on one conductor. With (10), $q_z = -(jy/\omega)V_z$.

3. Potential Functions and Electromagnetic Preliminaries. From the point of view of general electromagnetism the determination of distributions of current and charge in a configuration of metallic conductors (such as a transmission line) embedded in a poorly conducting or nonconducting dielectric medium is a boundary-value problem involving the field equations of Maxwell† subject to appropriate boundary conditions.

† Maxwell's equations are formulated in standard books on electromagnetic theory. See, for example, Refs. 9, 21, 27, 28.

Maxwell's equations may be regarded essentially as definitions of the fundamental electromagnetic-field vectors **E** and **B** in terms of current and charge. For many purposes it is convenient to introduce the scalar potential ϕ and the vector potential **A** in terms of **E** and **B**. In a homogeneous isotropic medium characterized by the permittivity (dielectric constant) ϵ, the permeability μ, and the conductivity σ, these are defined as follows:

$$-\operatorname{grad}\phi = \mathbf{E} + \frac{\partial \mathbf{A}}{\partial t} \tag{1}$$

$$\operatorname{curl}\mathbf{A} = \mathbf{B} \tag{2a}$$

$$\operatorname{div}\mathbf{A} = -\sigma\mu\phi - \epsilon\mu\frac{\partial\phi}{\partial t} \tag{2b}$$

The three vector operators in (1) to (2*b*) have the following forms in cartesian coordinates (unit vectors in the directions of the coordinate axes are $\hat{\mathbf{x}}$, $\hat{\mathbf{y}}$, $\hat{\mathbf{z}}$):

$$\operatorname{grad}\phi = \hat{\mathbf{x}}\frac{\partial\phi}{\partial x} + \hat{\mathbf{y}}\frac{\partial\phi}{\partial y} + \hat{\mathbf{z}}\frac{\partial\phi}{\partial z} \tag{3}$$

$$\operatorname{div}\mathbf{A} = \frac{\partial A_x}{\partial x} + \frac{\partial A_y}{\partial y} + \frac{\partial A_z}{\partial z} \tag{4}$$

$$\operatorname{curl}\mathbf{A} = \begin{vmatrix} \hat{\mathbf{x}} & \hat{\mathbf{y}} & \hat{\mathbf{z}} \\ \dfrac{\partial}{\partial x} & \dfrac{\partial}{\partial y} & \dfrac{\partial}{\partial z} \\ A_x & A_y & A_z \end{vmatrix} \tag{5}$$

With a periodic time dependence

$$\phi_{inst} = \phi e^{j\omega t} \qquad \mathbf{A}_{inst} = \mathbf{A}e^{j\omega t} \tag{6}$$

the formulas (1) and (2*a*,*b*) become complex and independent of the time. They are

$$-\operatorname{grad}\phi = \mathbf{E} + j\omega\mathbf{A} \tag{7}$$

$$\operatorname{curl}\mathbf{A} = \mathbf{B} \tag{8a}$$

$$\operatorname{div}\mathbf{A} = -j\omega\mu\xi\phi = -j\frac{\beta^2}{\omega}\phi \tag{8b}$$

where the complex dielectric factor ξ is defined by

$$\xi \equiv \epsilon - \frac{j\sigma}{\omega} = \epsilon(1 - jh_e) \tag{9a}$$

and the loss tangent is

$$h_e \equiv \frac{\sigma}{\omega\epsilon}\dagger \tag{9b}$$

† If the dielectric constant and the conductivity are functions of the time in the sense that time lags occur and ϵ and σ become complex in the form $\epsilon = \epsilon' - j\epsilon''$ and

and where $$\beta^2 \equiv \omega^2 \mu \xi \tag{10}$$

The relative dielectric constant or permittivity ϵ_r and permeability μ_r satisfy the relations

$$\epsilon_r = \frac{\epsilon}{\epsilon_0} \qquad \mu_r = \frac{\mu}{\mu_0} \tag{11a}$$

where $\epsilon_0 = 8.85 \times 10^{-12}$ farad/m $\qquad \mu_0 = 4\pi \times 10^{-7}$ henry/m (11b)

In order to emphasize symmetry between analogous electric and magnetic quantities, the reluctivity ν (or reciprocal permeability) is useful:

$$\nu = \frac{1}{\mu} \qquad \nu_r = \frac{1}{\mu_r} \qquad \nu_0 = \frac{1}{\mu_0} = 7.95 \times 10^5 \text{ m/henry} \tag{11c}$$

In most applications the relative permeability is real. However, when time lags in magnetization are involved, it is complex. Thus

$$\frac{1}{\nu} \equiv \mu \equiv \mu' - j\mu'' = \mu'(1 - jh_m) \doteq \mu(1 - jh_m) \tag{12a}$$

where $$h_m \equiv \frac{\mu''}{\mu'} \qquad \mu = \mu' \sqrt{1 + h_m^2} \doteq \mu' \tag{12b}$$

The last step in (12*a*) and (12*b*) assumes

$$h_m^2 \ll 1 \tag{12c}$$

Subject to (12*c*) and

$$h_e^2 \ll 1 \qquad h_e h_m \ll 1 \tag{13a}$$

the following approximate expressions are useful:

$$\mu\xi \doteq \mu\epsilon[1 - j(h_e + h_m)] = \mu\epsilon(1 - jh_v) \tag{13b}$$

$$\frac{\mu}{\xi} \doteq \frac{\mu}{\epsilon}[1 + j(h_e - h_m)] = \frac{\mu}{\epsilon}(1 + jh_r) \tag{13c}$$

$$\frac{\xi}{\mu} \doteq \frac{\epsilon}{\mu}[1 - j(h_e - h_m)] = \frac{\epsilon}{\mu}(1 - jh_r) \tag{13d}$$

where $$h_v = h_e + h_m \qquad h_r = h_e - h_m \tag{13e}$$

Note that, when $h_m = 0$, $h_v = h_r = h_e$. Convenient combinations of these

---

$\sigma = \sigma' - j\sigma''$, the real effective quantities

$$\epsilon_e = \epsilon' - \frac{\sigma''}{\omega} \qquad \sigma_e = \sigma' + \omega\epsilon'' \tag{9c}$$

must be introduced and substituted for ϵ and σ in (9*a*) and (9*b*). In order to avoid the distinguishing subscripts, ϵ and σ are retained with the understanding that where required they must be replaced by ϵ_e and σ_e as defined in (9*c*).

factors include the characteristic velocities:

$$v_0 \equiv \frac{1}{\sqrt{\mu_0\epsilon_0}} \doteq 3 \times 10^8 \text{ m/sec} \tag{14a}$$

$$v \equiv \frac{1}{\sqrt{\mu\epsilon}} = \frac{v_0}{\sqrt{\mu_r\epsilon_r}} \tag{14b}$$

$$\boldsymbol{v} \equiv \frac{1}{\sqrt{\boldsymbol{\mu}\boldsymbol{\xi}}} \doteq \frac{v}{\sqrt{1 - jh_v}} \tag{14c}$$

the phase constants:

$$\beta_0 \equiv \frac{\omega}{v_0} = \omega\sqrt{\mu_0\epsilon_0} \tag{15a}$$

$$\beta \equiv \frac{\omega}{v} = \omega\sqrt{\mu\epsilon} \tag{15b}$$

$$\boldsymbol{\beta} \equiv \frac{\omega}{\boldsymbol{v}} = \omega\sqrt{\boldsymbol{\mu}\boldsymbol{\xi}} \doteq \beta\sqrt{1 - jh_v} \tag{15c}$$

and the characteristic impedances:

$$\zeta_0 \equiv \sqrt{\frac{\mu_0}{\epsilon_0}} \doteq 376.7 \text{ ohms} \tag{16a}$$

$$\zeta \equiv \sqrt{\frac{\mu}{\epsilon}} = \zeta_0\sqrt{\frac{\mu_r}{\epsilon_r}} \tag{16b}$$

$$\boldsymbol{\zeta} \equiv \sqrt{\frac{\boldsymbol{\mu}}{\boldsymbol{\xi}}} \doteq \frac{\zeta}{\sqrt{1 - jh_r}} \tag{16c}$$

The elimination of the electric and magnetic vectors from (1) and (2*a*,*b*) using the field equations leads to the equations

$$\nabla^2\boldsymbol{\phi} + \boldsymbol{\beta}^2\boldsymbol{\phi} = 0 \tag{17}$$

$$\nabla^2\mathbf{A} + \boldsymbol{\beta}^2\mathbf{A} = 0 \tag{18}$$

where the laplacian operator ∇^2 (nabla squared), when applied to a scalar, is defined by

$$\nabla^2\boldsymbol{\phi} \equiv \text{div grad } \boldsymbol{\phi} \tag{19}$$

When applied to a vector it is

$$\nabla^2\mathbf{A} \equiv \text{grad div } \mathbf{A} - \text{curl curl } \mathbf{A} \tag{20}$$

In cartesian coordinates

$$\nabla^2\mathbf{A} = \hat{\mathbf{x}}\,\nabla^2 A_x + \hat{\mathbf{y}}\nabla^2 A_y + \hat{\mathbf{z}}\nabla^2 A_z \tag{21}$$

and

$$\nabla^2\psi = \left(\frac{\partial^2}{\partial x^2} + \frac{\partial^2}{\partial y^2} + \frac{\partial^2}{\partial z^2}\right)\psi \tag{22}$$

where ψ stands for any scalar such as $\boldsymbol{\phi}$, A_x, A_y, and A_z.

Solutions of (17) and (18) which give the scalar and vector potentials at all points in a homogeneous isotropic medium due to distributions of

current and charge in arbitrary configurations of conductors are

$$\phi = \frac{1}{4\pi\xi} \iint \mathfrak{n}' \frac{e^{-j\beta R}}{R} dS' \tag{23}$$

$$\mathbf{A} = \frac{1}{4\pi\nu} \iiint \mathfrak{i}' \frac{e^{-j\beta R}}{R} dV' \tag{24}$$

where $\mathfrak{n}'$ is the charge density on the surface element dS' of the conductor at a point $Q'(x',y',z')$ and $\mathfrak{i}'$ is the volume density of current in the interior element dV' at $Q'(x',y',z')$. The potentials are *calculated* at a point $Q(x,y,z)$ outside the conductors in the medium in which they are embedded. The distance between the point $Q'(x',y',z')$ locating the element of charge or current on or in the conductor and the point $Q(x,y,z)$ where the potential is calculated is

$$R = \sqrt{(x - x')^2 + (y - y')^2 + (z - z')^2} \tag{25}$$

The integration in (23) is over all charged surfaces; that in (24) is over the interior of all current-carrying conductors. Note that the solutions (23) and (24) take account of the boundary conditions automatically. If the current density is expressed in cartesian coordinates,

$$\mathfrak{i} = \hat{\mathbf{x}}\mathfrak{i}_x + \hat{\mathbf{y}}\mathfrak{i}_y + \hat{\mathbf{z}}\mathfrak{i}_z \tag{26}$$

the three cartesian components of (24) are

$$\mathbf{A} = \hat{\mathbf{x}}A_x + \hat{\mathbf{y}}A_y + \hat{\mathbf{z}}A_z \tag{27}$$

$$A_x = \frac{1}{4\pi\nu} \iiint \mathfrak{i}_x' \frac{e^{-j\beta R}}{R} dV' \tag{28a}$$

$$A_y = \frac{1}{4\pi\nu} \iiint \mathfrak{i}_y' \frac{e^{-j\beta R}}{R} dV' \tag{28b}$$

$$A_z = \frac{1}{4\pi\nu} \iiint \mathfrak{i}_z' \frac{e^{-j\beta R}}{R} dV' \tag{28c}$$

If all conductors are of sufficiently small cross section, for example, a circle of radius a which satisfies the condition

$$|\beta|a \ll 1 \tag{29}$$

it is proper to define the total axial current and the total charge per unit length in each conductor. Specifically the potentials calculated from currents and charges in a cylindrical conductor of small cross section along a direction $\hat{\mathbf{z}}$ are given by†

$$\phi = \frac{1}{4\pi\xi} \int_z q' \frac{e^{-j\beta R}}{R} dz' \qquad q' = \int_0^{2\pi} \mathfrak{n}' a \, d\theta' \tag{30a}$$

$$\mathbf{A} \doteq \hat{\mathbf{z}}A_z \qquad A_z = \frac{1}{4\pi\nu} \int_z I_z' \frac{e^{-j\beta R}}{R} dz' \qquad I_z' = \int_0^a \int_0^{2\pi} \mathfrak{i}_z' r' \, dr' \, d\theta' \tag{30b}$$

† These formulas are good approximations if the axial integration extends over distances at least as great as $5a$ (Refs. 9, 10, 61). Near the ends of a cylindrical

Since no currents are excited around the axis of the conductor, $i_\theta = 0$, and therefore $A_\theta = 0$. As a consequence of the fact that the radial current density i_r must be small compared with i_z if (29) is satisfied, and that the contributions of oppositely directed elements in $i_r' \cos\theta'$ virtually cancel in computing

$$A_r = \frac{1}{4\pi\nu}\int_z\int_0^{2\pi}\int_0^a i_r'\frac{e^{-j\beta R}}{R}\,r\,dr'\cos\theta'\,d\theta'\,dz' \tag{30c}$$

it follows that A_r is so small compared with $\mathbf{A}_z$ that it may be neglected. That is, $A_r \doteq 0$.

Note that (30*a*) and (30*b*) must satisfy (8*b*), which, with $\mathbf{A} = \hat{\mathbf{z}}A_z$, reduces to

$$\frac{dA_z}{dz} + j\frac{\beta^2}{\omega}\phi = 0 \tag{31}$$

If the configuration of conductors consists of several conductors in different directions, contributions to the vector potential by currents in each are like (30*b*), with $\hat{\mathbf{z}}$ replaced by a unit vector in the appropriate direction. The resultant vector potential is the *vector* sum of all these contributions. The resultant scalar potential may be obtained by integrating (30*a*) over all surfaces. Alternatively, as a consequence of (31) and the equation of continuity:

$$\frac{dI_z}{dz} + j\omega q = 0 \tag{32}$$

in terms of the total current I_z and charge per unit length q, it is possible to associate specific parts of ϕ and $\mathbf{A}$ with one another *and* with specific parts of the distributions of charge and current. For example, if a transmission line with its terminations includes conductors lying parallel to the x axis, others parallel to the y axis, and yet others parallel to the z axis, the vector potential is given by (27) with

$$A_x = \frac{1}{4\pi\nu}\int I_x'\frac{e^{-j\beta R}}{R}\,dx' \tag{33a}$$

$$A_y = \frac{1}{4\pi\nu}\int I_y'\frac{e^{-j\beta R}}{R}\,dy' \tag{33b}$$

$$A_z = \frac{1}{4\pi\nu}\int I_z'\frac{e^{-j\beta R}}{R}\,dz' \tag{33c}$$

where A_x is determined entirely by currents in the conductors parallel to the x axis, A_y by the currents in the conductors parallel to the y axis,

---

conductor or at bends, small errors corresponding to a change in the length of the z integration by at most $\pm a$ are involved. Note that the formulas are, in effect, the accurate potentials for a charge q or a current I concentrated along the axis of the conductor.

etc. The *associated* parts of the scalar potential are

$$\phi_{(x)} = \frac{1}{4\pi\xi} \int q'_{(x)} \frac{e^{-j\beta R}}{R} dx' \tag{34a}$$

$$\phi_{(y)} = \frac{1}{4\pi\xi} \int q'_{(y)} \frac{e^{-j\beta R}}{R} dy' \tag{34b}$$

$$\phi_{(z)} = \frac{1}{4\pi\xi} \int q'_{(z)} \frac{e^{-j\beta R}}{R} dz' \tag{34c}$$

The following continuity relations must be satisfied:

$$\frac{\partial A_x}{\partial x} + j\frac{\beta^2}{\omega}\phi_{(x)} = 0 \qquad \frac{\partial I_x}{\partial x} + j\omega q_{(x)} = 0 \tag{35a}$$

$$\frac{\partial A_y}{\partial y} + j\frac{\beta^2}{\omega}\phi_{(y)} = 0 \qquad \frac{\partial I_y}{\partial y} + j\omega q_{(y)} = 0 \tag{35b}$$

$$\frac{\partial A_z}{\partial z} + j\frac{\beta^2}{\omega}\phi_{(z)} = 0 \qquad \frac{\partial I_z}{\partial z} + j\omega q_{(z)} = 0 \tag{35c}$$

Note that $q_{(x)}$ is the charge associated with the current I_x and that $\phi_{(x)}$, which is derived from $q_{(x)}$, is the scalar potential associated with the vector potential A_x, which in turn is derived from the current I_x.

4. Electromagnetic Derivation of the Equations and Parameters for Balanced Infinitely Long Two-wire Lines.[9,10,47–49]† Since the transmission-line equations derived by network theory apply strictly only to an unending line in which every section is like every other, it is appropriate as a first application of electromagnetic methods to rederive these

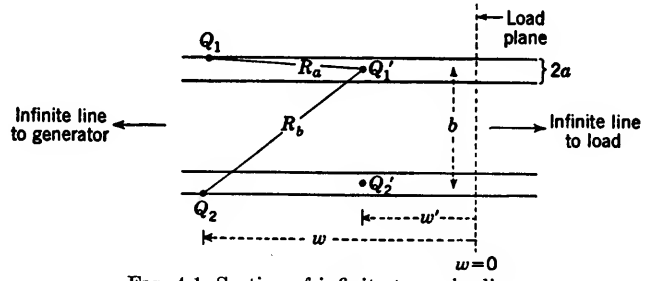


FIG. 4.1. Section of infinite two-wire line.

equations for the infinitely long line. The equations so obtained apply approximately to all parts of a uniform line of finite length except near terminations or other discontinuities. The specific conditions are derived in Chap. II.

Consider a uniform two-wire line (Fig. 4.1) extending along the z axis of a rectangular system of coordinates. The two wires lie in the yz plane with the center of wire 1 at $y = b/2$ and the center of wire 2 at $y = -b/2$.

† Superior numbers refer to the Bibliography at the end of this book.

The radius of each wire is a. It satisfies the inequality

$$|\beta|a \ll 1 \tag{1}$$

Let it be assumed for the present that the inequality

$$b^2 \gg a^2 \tag{2}$$

is satisfied, so that distributions of current and charge in each conductor may be assumed rotationally symmetrical. Let the section of line to the right of a plane $z = s$ or $w = s - z = 0$ be designated the load. The distance along the axis of each conductor to the left of this plane to axial elements dw' at points Q_1' and Q_2' is w'. The total axial current at the point Q_1' in conductor 1 is $I_{1z}(w')$; the charge per unit length near this point is $q_1(w')$. The current at point Q_2' in conductor 2 is $I_{2z}(w')$; the charge per unit length near point Q_2' is $q_2(w')$. The conditions for a balanced line are assumed to be satisfied. They are

$$I_{2z}(w) = -I_{1z}(w) = -I_z(w) \qquad q_2(w) = -q_1(w) = -q(w) \tag{3}$$

$$A_{2z}(w) = -A_{1z}(w) \qquad \phi_2(w) = -\phi_1(w) \tag{4}$$

The vector and scalar potentials in (4) are defined at the equipotential surface of the cross section at w of the conductor indicated by the subscript.

The current and charge per unit length satisfy the one-dimensional equation of continuity:

$$\frac{dI_z(w)}{dw} - j\omega q(w) = 0 \tag{5a}$$

The corresponding relation for the potentials that are defined in terms of $I_z(w)$ and $q(w)$ is Sec. 3, Eq. (31), with $\partial/\partial w = -\partial/\partial z$, namely,

$$\frac{\partial A_z(w)}{\partial w} - j\frac{\beta^2}{\omega}\phi(w) = 0 \tag{5b}$$

Note that, with the z component of Sec. 3, Eq. (7), viz.,

$$\frac{\partial \phi}{\partial w} = -\frac{\partial \phi}{\partial z} = E_z + j\omega A_z \tag{6a}$$

and (5b), the following equations are obtained by differentiation and substitution:

$$\frac{\partial^2 \phi}{\partial w^2} + \beta^2 \phi = \frac{\partial E_z}{\partial w} \tag{6b}$$

$$\frac{\partial^2 A_z}{\partial w^2} + \beta^2 A_z = j\frac{\beta^2}{\omega} E_z \tag{6c}$$

so that for points on the surface of a perfect conductor, where $E_z = 0$, ϕ and A_z satisfy the equations

$$\frac{\partial^2 \phi}{\partial w^2} + \beta^2 \phi = 0 \qquad \frac{\partial^2 A_z}{\partial w^2} + \beta^2 A_z = 0 \tag{6d}$$

The potential differences between equipotential rings around the surfaces of conductors 1 and 2 at opposite points Q_1 and Q_2 at equal distances w from the plane of the load at $w = 0$ are defined as follows:

$$V(w) \equiv \phi_1(w) - \phi_2(w) = 2\phi_1(w) \tag{7}$$
$$W_z(w) \equiv A_{1z}(w) - A_{2z}(w) = 2A_z(w) \tag{8}$$

The last step in each equation follows from (4). The differential equations satisfied by $V(w)$ and $W_z(w)$ are obtained readily by combining (6*b*,*c*) with (7) and (8). The results are

$$\frac{\partial^2 V(w)}{\partial w^2} + \beta^2 V(w) = \frac{\partial}{\partial w}(E_{1z} - E_{2z}) \tag{9a}$$
$$\frac{\partial^2 W_z(w)}{\partial w^2} + \beta^2 W_z(w) = j\frac{\beta^2}{\omega}(E_{1z} - E_{2z}) \tag{9b}$$

where E_{1z} and E_{2z} are defined on the surfaces of the conductors.

The evaluation of the potential differences in terms of the current is accomplished as follows: Using Sec. 3, Eqs. (30*a*,*b*), the general definitions are

$$V(w) = \frac{1}{2\pi\xi}\int_{-\infty}^{\infty} q(w')P_L(w,w')\,dw' \tag{10a}$$
$$W_z(w) = \frac{1}{2\pi\nu}\int_{-\infty}^{\infty} I_z(w')P_L(w,w')\,dw' \tag{10b}$$

where
$$P_L(w,w') = \frac{e^{-j\beta R_a}}{R_a} - \frac{e^{-j\beta R_b}}{R_b} \tag{11}$$

and
$$R_a = \sqrt{(w - w')^2 + a^2} \qquad R_b = \sqrt{(w - w')^2 + b^2} \tag{12}$$

In order to evaluate (9) and (10) the charge per unit length and the current at the point Q' may be expanded in Taylor series in terms of the charge per unit length and the current at the point Q. Thus the leading and first correction terms are

$$q(w') = q(w) + (w' - w)\frac{\partial q(w)}{\partial w} + \cdots \tag{13a}$$
$$I_z(w') = I_z(w) + (w' - w)\frac{\partial I_z(w)}{\partial w} + \cdots \tag{13b}$$

Using (5*a*), Eqs. (13*a*,*b*) may be expressed as follows:

$$q(w') \doteq q(w) + \frac{1}{j\omega}\frac{\partial^2 I_z(w)}{\partial w^2}(w' - w) \tag{14a}$$
$$I_z(w') \doteq I_z(w) + j\omega q(w)(w' - w) \tag{14b}$$

Finally the substitution of (14*a*) and (14*b*) in (10*a*) and (10*b*) gives the following general expressions for the potential differences along an infinite

uniform line:

$$V(w) = \frac{1}{2\pi\xi}\left[q(w)k_0(w) + \frac{1}{j\omega}\frac{\partial^2 I_z(w)}{\partial w^2}\frac{k_1(w)}{\beta}\right] \tag{15a}$$

$$W_z(w) = \frac{1}{2\pi\nu}\left[I_z(w)k_0(w) + j\omega q(w)\frac{k_1(w)}{\beta}\right] \tag{15b}$$

where

$$k_0(w) \equiv \int_{-\infty}^{\infty} P_L(w,w')\,dw' = \int_{-\infty}^{\infty}\left(\frac{1}{R_a} - \frac{1}{R_b}\right)dw' + \int_{-\infty}^{\infty}[F(a) - F(b)]\,dw' \tag{16}$$

$$\frac{k_1(w)}{\beta} = \int_{-\infty}^{\infty}(w' - w)P_L(w,w')\,dw' = \int_{-\infty}^{\infty}(w' - w)\left(\frac{1}{R_a} - \frac{1}{R_b}\right)dw' + \int_{-\infty}^{\infty}(w' - w)[F(a) - F(b)]\,dw' \tag{17}$$

and where $$F(a) \equiv \frac{e^{-j\beta R_a} - 1}{R_a} \qquad F(b) \equiv \frac{e^{-j\beta R_b} - 1}{R_b} \tag{18}$$

The first integrals, in the expanded forms (16) and (17), may be evaluated directly. They yield

$$\int_{-\infty}^{\infty}\left(\frac{1}{R_a} - \frac{1}{R_b}\right)dw' = 2\ln\frac{b}{a} \tag{19}$$

and

$$\int_{-\infty}^{\infty}(w - w')\left(\frac{1}{R_a} - \frac{1}{R_b}\right)dw' = 0 \tag{20}$$

It will now be shown that, subject to the condition

$$|\beta b|^2 \ll 1 \tag{21}$$

the second integrals in (16) and (17) may be neglected. Evidently, over that part of the integration for which $(w' - w)^2$ is large compared with b^2 and a^2, R_a and R_b differ negligibly from $|w' - w|$ and from each other. It follows that $F(a) \doteq F(b)$, so that there are no contributions to the integrals. The principal contributions to the integrals occur when $|w' - w|$ is small, so that R_a and R_b are of order of magnitude b. But when this is true, it follows with (21) that

$$|\beta^2 R^2| \ll 1 \qquad e^{-j\beta R} \doteq 1 - j\beta R - \beta^2 R^2 + j\beta^3 R^3 \tag{22}$$

where R stands for R_a or R_b. Hence the integrand of the second integral on the right in (16) is of the order of magnitude

$$|F(a) - F(b)| = |\beta^2(R_b - R_a) - j\beta^3(R_b^2 - R_a^2)| \tag{23}$$

whereas the integrand of the first integral is

$$\frac{1}{R_a} - \frac{1}{R_b} = \frac{R_b - R_a}{R_b R_a} \tag{24}$$

The ratio of the integrand in the first to that in the second integral in

both (16) and (17) is

$$1 : |\beta^2 R_a R_b - j\beta^3 R_a R_b (R_b + R_a)| \tag{25}$$

over a range where (22) is valid, so that with (22) the second integral is negligible. It follows that, for the infinitely long line subject to (21),

$$\boldsymbol{k}_0(w) \doteq k_0 = 2 \ln \frac{b}{a} \tag{26}$$

$$\boldsymbol{k}_1(w) \doteq 0 \tag{27}$$

It is interesting to note that the imaginary part of (25) determines the radiation, which (21) makes negligible.

With (26) and (27) the potential differences at a point Q along the line are

$$\boldsymbol{V}(w) \doteq \boldsymbol{q}(w) \frac{j\omega}{\boldsymbol{y}} = \frac{d\boldsymbol{I}_z(w)}{dw} \frac{1}{\boldsymbol{y}} \tag{28}$$

$$\boldsymbol{W}_z(w) = \boldsymbol{I}_z(w) \boldsymbol{l}^e \tag{29}$$

The following symbolism is introduced in (28) and (29):

$$\boldsymbol{y} \equiv g + j\omega c \equiv j\omega \frac{2\pi\xi}{k_0} = \frac{j\omega\pi\xi}{\ln (b/a)} \tag{30a}$$

$$g \equiv \frac{\pi\sigma}{\ln (b/a)} \qquad c \equiv \frac{\pi\epsilon}{\ln (b/a)} \qquad \boldsymbol{l}^e = \frac{\boldsymbol{\mu}}{\pi} \ln \frac{b}{a} \tag{30b}$$

These are the leakage conductance, the capacitance, and the external inductance per unit length of the *infinite* two-wire line. If $\boldsymbol{\mu}$ is complex, $\boldsymbol{l}^e$ also is complex. In the last step in (28) use is made of (5a). Note that

$$\beta^2 = \omega^2 \boldsymbol{\mu} \xi = -\boldsymbol{z}^e \boldsymbol{y} \tag{31}$$

where $\boldsymbol{z}^e = j\omega \boldsymbol{l}^e$ is the external impedance per unit length of the parallel line.

It is noteworthy that the correction terms in (13a,b) and (14a,b) make no significant contribution to the potential differences when the line is infinitely long and (21) is satisfied. *The assumption of uniform current and charge per unit length is adequate in evaluating the potential differences and the constants for an infinite line.*

One of the differential equations for the two-wire line is contained in (28). The other is obtained from (6a) using (7) and (8). Thus

$$\frac{d\boldsymbol{V}(w)}{dw} - j\omega \boldsymbol{W}_z(w) = \boldsymbol{E}_{1z}(w) - \boldsymbol{E}_{2z}(w) \tag{32}$$

where $\boldsymbol{E}_{1z}(w)$ and $\boldsymbol{E}_{2z}(w)$ are the axial tangential components of the electric field at the surfaces of the two conductors. This electric field is proportional to the total current, so that

$$\boldsymbol{E}_{1z}(w) = \boldsymbol{I}_{1z}(w) \boldsymbol{z}_1^i = \frac{\boldsymbol{I}_z(w) \boldsymbol{z}^i}{2} \tag{33a}$$

$$\boldsymbol{E}_{2z}(w) = \boldsymbol{I}_{2z}(w) \boldsymbol{z}_2^i = -\frac{\boldsymbol{I}_z(w) \boldsymbol{z}^i}{2} \tag{33b}$$

Note that $I_{2z}(w) = -I_{1z}(w)$ for a balanced line and $z_2^i = z_1^i$ for identical conductors. Hence

$$z^i = z_1^i + z_2^i \tag{33c}$$

The complex quantity $z^i = r^i + jx^i$ is the *internal impedance per unit length of the two-wire line.* Its real part r^i is the internal or ohmic resistance of a unit length of the *two* conductors. The evaluation of z^i from the ratio $E_z(w)/I_z(w)$ along a cylindrical conductor is in the literature (Ref. 9, Chap. V). The formula for high frequencies subject to (2) is

$$z_1^i = r_1^i + jx_1^i = \frac{1+j}{2\pi a}\sqrt{\frac{\mu_c\omega}{2\sigma_c}} \qquad a\sqrt{\omega\mu_c\sigma_c} \geqq 10 \tag{34}$$

where μ_c and σ_c apply to the conductor. Note that $z^i = 2z_1^i$ for a two-wire line. Using (33) and (29), (32) becomes

$$\frac{\partial V(w)}{\partial w} = (z^i + j\omega l^e)I(w) \tag{35a}$$

With (30*a*) in (28), this becomes

$$\frac{\partial I(w)}{\partial w} = (g + j\omega c)V(w) \tag{35b}$$

These are the familiar one-dimensional transmission-line equations. If desired, $-\partial/\partial z$ may be substituted for $\partial/\partial w$, so that, with

$$z = z^i + j\omega l^e = r^i + j\omega(l^i + l^e) = r + j\omega l \tag{36}$$

the final equations are

$$-\frac{\partial V(z)}{\partial z} = zI(z) \tag{37a}$$

$$-\frac{\partial I(z)}{\partial z} = yV(z) \tag{37b}$$

These are the equations derived in Sec. 2 by assuming that the line is equivalent to a recurrent network of resistive and reactive networks. This assumption has now been justified. Note that the constants of the line have been derived except for z^i, which presents a special problem.

In the rest of this chapter transmission-line theory is formulated under the assumption that the permeability of all media is real. If, as outlined in Sec. 3 and implied in (30*b*), (35*a*), and (36), μ is complex and given by Sec. 3, Eq. (12*a*), i.e.,

$$\mu = \mu' - j\mu'' = \mu(1 - jh_m) \tag{38a}$$

the complex external inductance

$$l^e = l^e(1 - jh_m) \tag{38b}$$

must be used instead of the real value l^e. Then

$$z^e = j\omega l^e = j\omega l^e(1 - jh_m) \tag{39a}$$

and in (36) it follows that

$$z = z^i + j\omega l^e = r^i + \omega l^e h_m + j\omega(l^i + l^e) = r + j\omega l \tag{39b}$$

Clearly the generalized value of r is

$$r = r^i + \omega l^e h_m \tag{40}$$

where h_m is the ratio of the imaginary to the real part of the complex permeability μ. It follows that, whenever a magnetic medium with a time lag in magnetization response is involved, r as given in (40) must be used.

For an infinitely long two-wire line (or approximately for the section of a long finite line that is sufficiently far from terminations or discontinuities) (37a,b) are the correct equations for current and voltage. The following conditions have been assumed or imposed:

$$\left.\begin{array}{l}(1)\ \text{The two conductors are parallel and identical}\\ (2)\ |\beta a| \ll 1\\ (3)\ |\beta b|^2 \ll 1\\ (4)\ b^2 \gg a^2\\ (5)\ \text{The line is infinitely long}\end{array}\right\} \tag{41}$$

It is shown later that, by a modification in the formulas for the line constants, condition (4) can be removed and that, by introducing an appropriate lumped-constant network at each termination or discontinuity, condition (5) may be eliminated. Condition (1) is modified to include conductors of unequal size in Sec. 7.

5. The Balanced Four-wire Line.[9] The method of analysis used in Sec. 4 is readily applied to the balanced four-wire line constructed of identical and parallel conductors (each of radius a) which are so driven that conductors 1 and 3 on one diagonal of a square of side b are in parallel, as are conductors 2 and 4 on the other diagonal. The two parallel pairs form the transmission line (Fig. 5.1). The following conditions are assumed:

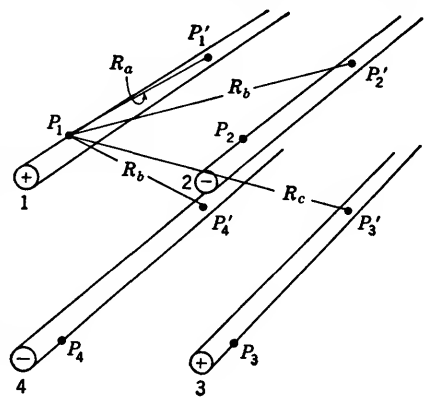


FIG. 5.1. Four-wire line.

$$|\beta a| \ll 1 \qquad b^2 \gg a^2 \tag{1}$$

$$I_4(w) = I_2(w) = -I_1(w) = -I_3(w) = -\tfrac{1}{2}I(w) \tag{2}$$

$$q_4(w) = q_2(w) = -q_1(w) = -q_3(w) = -\tfrac{1}{2}q(w) \tag{3}$$

where $I(w)$ is the total current in the line and $q(w)$ is the total charge per unit length.

$$\phi_4(w) = \phi_2(w) = -\phi_1(w) = -\phi_3(w) \tag{4}$$

$$A_{4z}(w) = A_{2z}(w) = -A_{1z}(w) = -A_{3z}(w) \tag{5}$$

The potential differences are

$$V(w) = \phi_1(w) - \phi_2(w) = \phi_3(w) - \phi_4(w) = 2\phi_1(w) \tag{6}$$

$$W_z(w) = A_{1z}(w) - A_{2z}(w) = A_{3z}(w) - A_{4z}(w) = 2A_{1z}(w) \tag{7}$$

$$V(w) = \frac{1}{4\pi\xi}\int_{-\infty}^{\infty} q(w)P_L(w,w')\,dw' \tag{8}$$

$$W_z(w) = \frac{1}{4\pi\nu}\int_{-\infty}^{\infty} I_z(w')P_L(w,w')\,dw' \tag{9}$$

where

$$P_L(w,w') = \frac{e^{-j\beta R_a}}{R_a} - 2\frac{e^{-j\beta R_b}}{R_b} + \frac{e^{-j\beta R_c}}{R_c} \tag{10}$$

and

$$R_a = \sqrt{(w'-w)^2 + a^2} \qquad R_b = \sqrt{(w'-w)^2 + b^2}$$
$$R_c = \sqrt{(w'-w)^2 + 2b^2} \tag{11}$$

It is readily verified that, subject to the condition

$$|\beta b|^4 \ll 1 \tag{12}$$

it follows that

$$k_0(w) = \int_{-\infty}^{\infty} P_L(w,w')\,dw' \doteq 2\ln\frac{b}{a\sqrt{2}} = 2\left(\ln\frac{b}{a} - 0.3464\right) \tag{13}$$

Hence

$$g = \frac{2\pi\sigma_e}{\ln(b/a\sqrt{2})} \qquad c = \frac{2\pi\epsilon_e}{\ln(b/a\sqrt{2})} \qquad l^e = \frac{\mu}{2\pi}\ln\frac{b}{a\sqrt{2}} \tag{14}$$

Also

$$z^i = z_1^i + z_2^i + z_3^i + z_4^i = 4z_1^i \tag{15}$$

where, subject to

$$b^2 \gg a^2 \tag{16}$$

z_1^i is given by Sec. 4, Eq. (34), at high frequencies. The same differential equations as for the two-wire line apply to the four-wire line, but with these new values of the parameters.

6. The Coaxial Line. The analysis of the infinite coaxial line (consisting of a conductor 1 of radius a_1 in a conducting sheath 2 of inner radius a_2 and outer radius a_3) may be carried out in the manner used for the two-wire line. If the conditions of balance for current and charge in Sec. 4, Eq. (3), are postulated, the potentials at an arbitrary point $Q(r,\theta,z)$ in the dielectric medium ($a_1 \leqq r \leqq a_2$) are given by

$$\phi(w) = \frac{1}{4\pi\xi}\int_0^{2\pi}\int_{-\infty}^{\infty} q(w')P_r(w,w',\theta')\,dw'\frac{d\theta'}{2\pi} \tag{1}$$

$$A_z(w) = \frac{1}{4\pi\nu}\int_0^{2\pi}\int_{-\infty}^{\infty} I_z(w')P_r(w,w',\theta')\,dw'\frac{d\theta'}{2\pi} \tag{2}$$

where

$$P_r(w,w',\theta') \equiv \left[\frac{e^{-j\beta R_{s1}}}{R_{s1}} - \frac{e^{-j\beta R_{s2}}}{R_{s2}}\right] \tag{3}$$

and (Fig. 6.1)

$$R_{s1} = \sqrt{(w - w')^2 + s_1^2} \qquad s_1^2 = r^2 + a_1^2 - 2a_1 r \cos\theta' \tag{4}$$

$$R_{s2} = \sqrt{(w - w')^2 + s_2^2} \qquad s_2^2 = r^2 + a_2^2 - 2a_2 r \cos\theta' \tag{5}$$

The charge per unit length and the total current in each conductor are defined as follows in terms of the surface density of charge $\mathbf{n}$ and the axial component of the volume density of current i_z:

$$\begin{aligned} q_1(w) &= 2\pi a_1 \mathbf{n}_1(w) \\ q_2(w) &= 2\pi a_2 \mathbf{n}_2(w) = -q_1(w) \end{aligned} \tag{6}$$

$$\begin{aligned} I_{1z}(w) &= 2\pi \int_0^{a_1} i_{1z}(w,r) r\, dr \\ I_{2z}(w) &= 2\pi \int_{a_2}^{a_2} i_{2z}(w,r) r\, dr \\ &= -I_{1z}(w) \end{aligned} \tag{7}$$

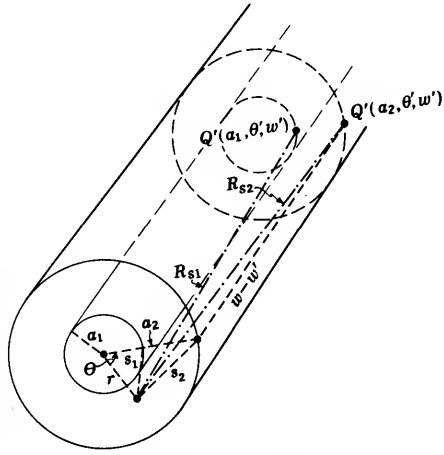


FIG. 6.1. Coaxial line.

In defining s in (5) it is assumed for simplicity that the entire current $I_{2z}(w)$ is concentrated in a thin layer on the inner surface of the sheath as for a perfect conductor. For a good but imperfect conductor, the field in the sheath is included in the evaluation of the internal impedance. Note that only R_s in $P_r(w,w',\theta')$ involves θ'.

In evaluating (1) and (2) for the infinite line, $q(w')$ may be replaced by $q(w)$, and $I_z(w')$ by $I_z(w)$, as shown for the two-wire line. This leaves only $P_r(w,w',\theta')$ under the sign of integration. The integration with respect to z may be carried out just as for the two-wire line. After the condition

$$|\beta a_2|^2 \ll 1 \tag{8}$$

is imposed to eliminate higher modes, the steps in the analysis parallel those in Sec. 4, Eqs. (16), (18), and (19). The result is

$$\int_{-\infty}^{\infty} P_r(w,w'\,\theta')\, dw' \doteq \int_{-\infty}^{\infty} \left(\frac{1}{R_{s1}} - \frac{1}{R_{s2}}\right) dw' = 2 \ln \frac{s_2}{s_1} \tag{9}$$

The integration with respect to θ' (which does not occur with the two-wire line) may be carried out using Pierce formula 523. Thus

$$\begin{aligned} \Phi(w) &= \frac{q(w)}{2\pi\xi} \left\{ \int_0^{\pi} [\ln (r^2 + a_2^2 - 2a_2 r \cos\theta')] \frac{d\theta'}{2\pi} \right. \\ &\qquad \left. - \int_0^{\pi} [\ln (r^2 + a_1^2 - 2a_1 r \cos\theta')] \frac{d\theta'}{2\pi} \right\} \\ &= \frac{q(w)}{2\pi\xi} \ln \frac{a_2}{r} \end{aligned} \tag{10}$$

Similarly
$$A_z(w) = \frac{I_z(w)}{2\pi\nu} \ln \frac{a_2}{r} \tag{11}$$

The potential differences between points $Q_1(a_1,\theta,w)$ and $Q_2(a_2,\theta,w)$ on the surfaces of the two conductors are

$$V(w) = \phi_1(w) - \phi_2(w) = \frac{q(w)}{2\pi\xi} \ln \frac{a_2}{a_1} \tag{12}$$

$$W_z(w) = A_{1z}(w) - A_{2z}(w) = \frac{I_z(w)}{2\pi\nu} \ln \frac{a_2}{a_1} \tag{13}$$

Note that these results may be obtained even if the term $1/R_s$ is omitted in (9) and $V(w)$ is evaluated directly. This shows that the potential differences may be determined *entirely* from the charges and currents in the *inner* conductor. The potential differences in (12) and (13) may be expressed in the form of Sec. 4, Eqs. (28) and (29), viz.,

$$V(w) = \frac{dI_z(w)}{dw} \frac{1}{y} \tag{14}$$

$$W_z(w) = I_z(w) l^e \tag{15}$$

with
$$y = g + j\omega c \qquad g = \frac{2\pi\sigma}{\ln (a_2/a_1)} \qquad c = \frac{2\pi\epsilon}{\ln (a_2/a_1)}$$
$$l^e = \frac{\mu}{2\pi} \ln \frac{a_2}{a_1} \tag{16}$$

As for the two-wire line, the internal impedance per unit length is

$$z^i = z_1^i + z_2^i \tag{17}$$

where z_1^i and z_2^i are the internal impedances per unit length of the inner and outer conductors. At high frequencies ($a_1 \sqrt{\omega\sigma_c\mu_c} \geqq 10$)

$$z_1^i = \frac{1+j}{2\pi a_1} \sqrt{\frac{\mu_c\omega}{2\sigma_c}} \qquad z_2^i = \frac{1+j}{2\pi a_2} \sqrt{\frac{\mu_c\omega}{2\sigma_c}} \tag{18}$$

The remaining steps follow those for the two-wire line and lead to the same differential equations, but with the line parameters (16) and (17) instead of Sec. 4, Eqs. (30) and (33*c*). The general conditions on the equations are like those in Sec. 4, Eq. (41), for the two-wire line except that conditions (1) and (4) in Sec. 4, Eq. (41), are not imposed.

The electric and magnetic fields in the dielectric medium in the coaxial line are obtained from the potential functions. Since rotational symmetry obtains and A_z is the only component of the vector potential, the vector relation [Sec. 3, Eq. (2*a*)] reduces to

$$B_r = 0 \qquad B_\theta = -\frac{\partial A_z}{\partial r} \qquad B_z = 0 \tag{19}$$

in cylindrical coordinates. Hence, with (11),

$$\mathbf{B} = \hat{\theta} B_\theta \qquad B_\theta = \frac{I_z}{2\pi\nu r} \tag{20}$$

The electric field is given by Sec. 3, Eq. (1). With $\mathbf{A} = \hat{z}A_z$ and rotational symmetry the only transverse component of the electric field is

$$E_r = -\frac{\partial \phi}{\partial r} = \frac{q}{2\pi\xi r} \tag{21}$$

The last step follows from (10).

If the space between the two conductors of a coaxial line is not filled by a single homogeneous isotropic dielectric, complications arise which cannot be solved without the introduction of more advanced mathematical methods. Two cases are of interest: (*a*) If the inner conductor is coated with a good dielectric of uniform thickness and the rest of the space between the two conductors is air, a so-called *guided field* exists in the dielectric which propagates in a manner related to that of the single-wire dielectric-coated line.[45] It cannot be analyzed by ordinary transmission-line theory. (*b*) If the space between the conductors is filled with two different dielectrics each extending from the inner to the outer conductor, but the one only over an angle θ and the other over the remaining angle $2\pi - \theta$, the line behaves essentially in the transverse electromagnetic (TEM) manner characteristic of the coaxial line with a single dielectric, provided a_2 is sufficiently small. The capacitance per unit length of the two-dielectric line is a parallel combination of the capacitances per unit length of the two sectors with different dielectrics.[34]

7. The Closely Spaced Two-wire Line with Unequal Conductors.[1,9,40] In the general study of the two-wire line in Sec. 4 the conductors are assumed to be of equal radius, and the condition $b^2 \gg a^2$ is imposed from the outset in order to keep the transverse part of the analysis simple while the complications resulting from the occurrence of both transverse and axial variables are unresolved. An important result of this analysis is the demonstration that, subject to the conditions imposed, the *transverse and axial problems are independent* to a high degree of approximation. Indeed the final differential equations are the same for all the lines investigated. They involve only the axial variable z, whereas the solutions of the several transverse problems appropriate to the cross-sectional boundaries are contained in the formulas for the parameters of the particular line. Since the conditions ensuring this effective independence of axial and transverse problems are primarily those requiring the cross-sectional dimensions to be small, these are better satisfied for more closely spaced two-wire lines. So long as the conditions $|\beta a_1| \ll 1$ and $|\beta a_2| \ll 1$ are satisfied, there is nothing in the analysis which requires the two radii to be equal. It follows that the formulation of the problem of a balanced two-wire line consisting of two parallel conductors of radii a_1 and a_2 separated a distance b between centers which satisfies the conditions

$$b > a_1 + a_2 \qquad |\beta b| \ll 1 \tag{1}$$

where the first inequality merely means that the two conductors may not actually make contact, is readily achieved.

The separation of the axial and transverse parts of a function, such as the potential difference

$$V \equiv \phi_1 - \phi_2 \qquad \text{or} \qquad W_z \equiv A_{1z} - A_{2z}$$

which satisfies the scalar wave equation

$$\frac{\partial^2 W_z}{\partial x^2} + \frac{\partial^2 W_z}{\partial y^2} + \frac{\partial^2 W_z}{\partial z^2} + \beta^2 W_z = 0 \tag{2}$$

is accomplished by the separation of variables. By setting

$$W_z = F(x,y)f(z) \tag{3}$$

and substituting this in (2), the following result is obtained:

$$-\frac{1}{F(x,y)}\left[\frac{\partial^2 F(x,y)}{\partial x^2} + \frac{\partial^2 F(x,y)}{\partial y^2}\right] = \frac{1}{f(z)}\frac{\partial^2 f(z)}{\partial z^2} + \beta^2 \tag{4}$$

In order that the mutually independent sides of this equation may be equal for *all* values of the variables, they must both equal a constant, which, however, may be multivalued. Let this constant be k^2. Then, with (3), the following equations are obtained:

$$\frac{\partial^2 W_z}{\partial z^2} + (\beta^2 - k^2) W_z = 0 \tag{5}$$

$$\frac{\partial^2 W_z}{\partial x^2} + \frac{\partial^2 W_z}{\partial y^2} + k^2 W_z = 0 \tag{6}$$

For a two-wire line with identical conductors, the axial equation for W_z is Sec. 4, Eq. (9*b*), with Sec. 4, Eqs. (33*a*,*b*,*c*), viz.,

$$\frac{\partial^2 W_z}{\partial z^2} + \beta^2 W_z = j\frac{\beta^2}{\omega} z^i I_z \tag{7}$$

where z^i is the internal impedance per unit length of the two-wire line. It is now clear that the approximations involved in the analysis of Secs. 4 and 5 in which

$$W_z = I_z l^e \tag{8}$$

are equivalent to setting

$$k^2 = j\frac{\beta^2}{\omega l^e} z^i \tag{9}$$

in (5). Note that the equation is then valid only on the surfaces of the conductors, since the right side is obtained from the electric fields on these surfaces. With $z^i/\omega l^e$ extremely small for good conductors, k^2 is small in magnitude compared with $|\beta|^2$. Nevertheless k^2 must be retained in (5), since when the dielectric medium is perfect and β^2 is

real, the propagation constant γ in

$$\gamma^2 = k^2 - \beta^2 \tag{10}$$

is a pure imaginary unless k differs from zero. A nonzero value of k implies imperfect conductors and is necessary to maintain W_z and I_z finite. On the other hand, the contribution of a very small value of k^2 to the *transverse* problem defined by (6) is insignificant. Accordingly (6) is replaced by

$$\frac{\partial^2 W_z}{\partial x^2} + \frac{\partial^2 W_z}{\partial y^2} \doteq 0 \tag{11}$$

The solution actually obtained in Sec. 4 is for W_z as determined from (7) and (11). Thus account is taken of the large but *finite* conductivity of the conductors in determining *axial* distributions that involve an unrestricted length of conductor, but not in determining the transverse distributions that involve only the very much restricted cross sections.

The problem is to solve the two-dimensional Laplace equation (11) subject to the condition that A_z have a constant but different value on each of two circles of given radii a_1 and a_2. These are the circular cross sections of the conductors. The appropriate solution is

$$A_z = K \ln \frac{r_2}{r_1} \tag{12}$$

where $$r_2 = \sqrt{(x+d)^2 + y^2} \qquad r_1 = \sqrt{(x-d)^2 + y^2} \tag{13}$$

and d is a constant length to be determined. K in (12) is not a function of x and y, but of z alone. It is verified by substitution that (12) satisfies (11). It remains to be shown that the equipotential surfaces are circles. For this purpose let

$$2\rho \equiv \ln \frac{r_2}{r_1} = \text{const.} \tag{14a}$$

so that

$$\frac{r_2}{r_1} = e^{2\rho} \tag{14b}$$

and

$$A_z = 2K\rho \tag{15}$$

Thus contours of constant ρ define equipotential lines in the plane or infinite cylinders in space. Next let (14*b*) be squared and (13) substituted in it. The result is

$$(x+d)^2 + y^2 = e^{4\rho}[(x-d)^2 + y^2] \tag{16}$$

This can be rearranged as follows:

$$(x - d\coth 2\rho)^2 + y^2 = d^2(\coth^2 2\rho - 1) = \frac{d^2}{\sinh^2 2\rho} \tag{17}$$

This equation defines two families of circles—the one with positive and the other with negative values of ρ as parameter. Thus it has been

proved that contours of constant ρ, which coincide with contours of constant vector potentials, are circles. Since an entirely similar analysis can be made for the scalar potential ϕ, it follows that *equipotential lines for both scalar and vector potentials are circles of constant* ρ. The range of ρ is from $-\infty$ to $+\infty$. The centers of the circles are at

$$x = d \coth 2\rho \qquad y = 0 \tag{18}$$

Their radii are

$$a = \frac{d}{|\sinh 2\rho|} \tag{19}$$

The two families of circles are shown in Fig. 7.1. They are divided by

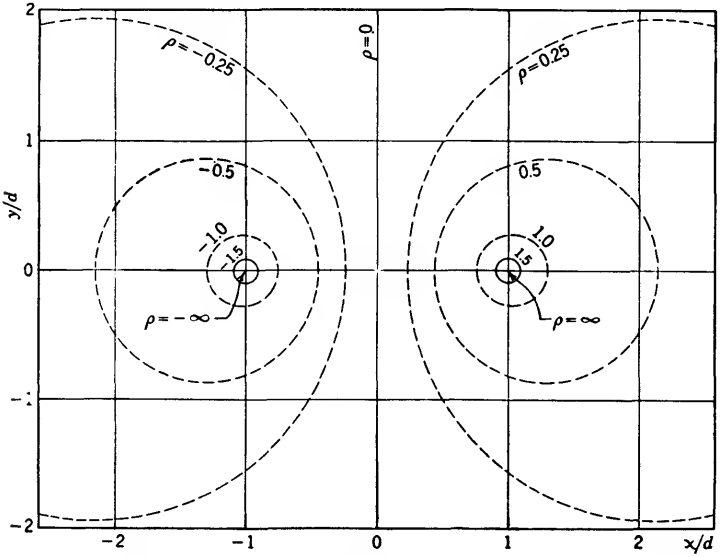


FIG. 7.1. Equipotential circles for two-wire line.

the straight line $x = 0$ or $\rho = 0$. The points $x = \pm d$, $y = 0$ are for $\rho = \pm\infty$.

Consider a particular pair of circles defined by $\rho = \rho_1 = |\rho_1|$ and $\rho = \rho_2 = -|\rho_2|$. The centers of the circles coincide with the axes of the two conductors at

$$x = x_1 = d \coth 2\rho_1 \qquad y = y_1 = 0 \tag{20a}$$

$$x = x_2 = -d \coth 2|\rho_2| \qquad y = y_2 = 0 \tag{20b}$$

The radii are the same as the radii of the two conductors, viz.,

$$a_1 = \frac{d}{\sinh 2\rho_1} \qquad a_2 = \frac{d}{\sinh 2|\rho_2|} \tag{21a}$$

Note that

$$a_2 \sinh 2|\rho_2| = a_1 \sinh 2\rho_1 \tag{21b}$$

With (21a) in (20a,b) the locations of the centers may be expressed as follows:

$$x_1 = a_1 \cosh 2\rho_1 \qquad y_1 = 0 \tag{22a}$$

$$x_2 = -a_2 \cosh 2\rho_2 \qquad y_2 = 0 \tag{22b}$$

The distance between centers, which is the spacing between centers of the two-wire line, is

$$b = x_1 - x_2 = a_1 \cosh 2\rho_1 + a_2 \cosh 2\rho_2 \tag{23}$$

In order to express ρ_1 and ρ_2 (and with them the potentials on the two circles) in terms of b and a_1 and a_2, ρ_2 (or ρ_1) may be eliminated between (21b) and (23). Thus

$$b = a_1 \cosh 2\rho_1 + \sqrt{a_2^2 + a_1^2 \sinh^2 2\rho_1} \tag{24}$$

This can be solved for ρ_1 to obtain

$$2\rho_1 = \cosh^{-1} \frac{b^2 + a_1^2 - a_2^2}{2a_1 b} \equiv \cosh^{-1} \psi_1 \tag{25a}$$

Similarly $$2\rho_2 = -\cosh^{-1} \frac{b^2 + a_2^2 - a_1^2}{2a_2 b} \equiv -\cosh^{-1} \psi_2 \tag{25b}$$

The symbols ψ_1 and ψ_2 are defined in (25a) and (25b). It follows with (15) that the components of vector potential on the surfaces of the two conductors of radii a_1 and a_2, with centers separated a distance b, are

$$A_{1z} = 2K\rho_1 = K \cosh^{-1} \psi_1 \tag{26a}$$

$$A_{2z} = 2K\rho_2 = -2K|\rho_2| = -K \cosh^{-1} \psi_2 \tag{26b}$$

The vector potential difference is

$$W_z = A_{1z} - A_{2z} = K(\cosh^{-1} \psi_1 + \cosh^{-1} \psi_2) \tag{27}$$

The constant K in (27) may be evaluated by comparing the solution of Sec. 4, Eq. (29), with (27) when this is specialized to wires of equal radius and sufficiently great separation by setting $a_1 = a_2 = a$ and utilizing the inequality $b^2 \gg a^2$. Subject to these special conditions,

$$\psi_1 = \psi_2 = \frac{b}{2a} \tag{28}$$

Using the standard relation between arc-hyperbolic and logarithmic functions, viz.,

$$\cosh^{-1} \frac{b}{2a} = \ln \left[\frac{b}{2a} + \sqrt{\left(\frac{b}{2a}\right)^2 - 1} \right] \tag{29}$$

it follows that with $b^2 \gg a^2$

$$\cosh^{-1} \psi_1 = \cosh^{-1} \psi_2 = \ln \frac{b}{a} \tag{30}$$

Hence after the substitution of (30) in (27) it follows from a comparison with Sec. 4, Eqs. (29) and (30*b*), and $\mathfrak{y} = \mu = 1/\nu$, that

$$K = \frac{I_z}{2\pi\nu} \tag{31}$$

so that the vector potential difference is

$$W_z = \frac{I_z}{2\pi\nu} (\cosh^{-1} \psi_1 + \cosh^{-1} \psi_2) \tag{32}$$

The corresponding solution for the scalar potential difference has a different constant. It is

$$V = \frac{q}{2\pi\xi} (\cosh^{-1} \psi_1 + \cosh^{-1} \psi_2) \tag{33}$$

It is now convenient to define the external inductance per unit length l^e and the admittance per unit length $y = g + j\omega c$ as factors of current and charge in the relations

$$W_z = I_z l^e \qquad V = q \frac{j\omega}{y} \tag{34}$$

as in Sec. 4, Eqs. (28) and (29). The use of (32) and (33) in (34) gives the following formulas for the parameters of the closely spaced two-wire line:

$$l^e = \frac{\mu}{2\pi} (\cosh^{-1} \psi_1 + \cosh^{-1} \psi_2) \tag{35a}$$

$$g = 2\pi\sigma(\cosh^{-1} \psi_1 + \cosh^{-1} \psi_2)^{-1} \tag{35b}$$

$$c = 2\pi\epsilon(\cosh^{-1} \psi_1 + \cosh^{-1} \psi_2)^{-1} \tag{35c}$$

The arguments are

$$\psi_1 \equiv \frac{b^2 + a_2^2 - a_1^2}{2a_1 b} \qquad \psi_2 \equiv \frac{b^2 + a_1^2 - a_2^2}{2a_2 b} \tag{36}$$

where b is the distance between centers of the two parallel conductors of radii a_1 and a_2.

For widely separated conductors for which the conditions $b^2 \gg a_1^2$ and $b^2 \gg a_2^2$ are satisfied,

$$\psi_1 \doteq \frac{b}{2a_1} \qquad \psi_2 \doteq \frac{b}{2a_2} \tag{37}$$

and

$$l^e = \frac{\mu}{\pi} \ln \frac{b}{\sqrt{a_1 a_2}} \qquad g = \frac{\pi\sigma}{\ln (b/\sqrt{a_1 a_2})} \qquad c = \frac{\pi\epsilon}{\ln (b/\sqrt{a_1 a_2})} \tag{38}$$

The most interesting and important special case is when $a_1 = a_2 = a$. In this case

$$\psi_1 = \psi_2 = \frac{b}{2a} \tag{39a}$$

so that

$$l^e = \frac{\mu}{\pi} \cosh^{-1} \frac{b}{2a} \qquad g = \frac{\sigma\pi}{\cosh^{-1} (b/2a)} \qquad c = \frac{\epsilon\pi}{\cosh^{-1} (b/2a)} \tag{39b}$$

Note that with (29) it is possible to express the general parameters for arbitrary spacing of identical conductors in the same form as for a spacing that satisfies the inequality $b^2 \gg a^2$ merely by defining an *effective* spacing b_e, which replaces b. This effective spacing is obtained from (29) to be

$$b_e = \frac{b}{2}\left[1 + \sqrt{1 - \left(\frac{2a}{b}\right)^2}\right] \tag{40a}$$

With (40*a*), (39*b*) may be expressed as follows:

$$l^e = \frac{\mu}{\pi} \ln \frac{b_e}{a} \qquad g = \frac{\sigma\pi}{\ln (b_e/a)} \qquad c = \frac{\epsilon\pi}{\ln (b_e/a)} \tag{40b}$$

Clearly, when b^2 is sufficiently great compared with a^2, these formulas reduce to those in Sec. 4, since $b_e \doteq b$ when the condition $b^2 \gg a^2$ is satisfied.

A second special case is when conductor 2 has an infinite radius, so that its surface becomes the xz plane, given by $\rho = \rho_2 = 0$. In this case it follows from (22*a*) that

$$\rho_1 = \cosh^{-1} \frac{x_1}{a} \qquad \rho_2 = 0 \tag{41}$$

where x_1 is the distance from the center of conductor 1 to the plane. Since with (26*b*) $A_{2z} = 0$, it follows with (27) and (31) that

$$W_z = A_{1z} = \frac{I_z}{2\pi\nu} \cosh^{-1} \frac{x_1}{a} \tag{42}$$

Let the distance x_1 be expressed in terms of the full line spacing b between the conductor and its image in the conducting plane. That is, let

$$x_1 = \frac{b}{2} \tag{43}$$

Then, with (32) and (35),

$$l^e = \frac{\mu}{2\pi} \cosh^{-1} \frac{b}{2a} \qquad g = \frac{2\pi\sigma}{\cosh^{-1} (b/2a)} \qquad c = \frac{2\pi\epsilon}{\cosh^{-1} (b/2a)} \tag{44}$$

Note that l^e is one-half and g and c double the corresponding value for a two-wire line of identical conductors spaced a distance b between centers. This follows from the fact that W_z and V measured between the conductor and conducting plane, a distance $b/2$, are one-half the values measured between two identical conductors separated a distance b and carrying equal and opposite currents and charges. The same results can be derived directly from the theory of images.

The internal impedance per unit length is modified when two parallel conductors are close together by the so-called proximity effect. The density of axial current is increased in adjacent parts of parallel conductors with oppositely directed currents and is decreased at more remote parts. This increases the effective internal impedance, since more current is confined to a smaller volume. Accurate formulas for z_1^i for one cylindrical conductor in the presence of another with different radius are not available. If the two conductors are identical, an approximate high-frequency formula involves an effective radius

$$a_e = a\sqrt{1 - (2a/b)^2} \tag{45}$$

in place of a in the formula for z_1^i for a cylindrical rotationally symmetrical conductor.† Thus for each conductor[40]

$$z_1^i \doteq \frac{1+j}{2\pi a}\sqrt{\frac{\mu_c\omega}{2\sigma_c[1 - (2a/b)^2]}} \tag{46}$$

The internal impedance per unit length of a two-wire line is $z^i = 2z_1^i$. For the single wire over the conducting plane, $z^i = z_1^i$ if losses in the plane are neglected.

The transverse electric and magnetic fields in the medium surrounding the two conductors are readily obtained. Since by definition $\mathbf{B} = \text{curl}\,\mathbf{A}$, it follows from Sec. 3, Eq. (5), that, when $\mathbf{A} = \hat{\mathbf{z}}A_z$,

$$B_x = \frac{\partial A_z}{\partial y} \qquad B_y = -\frac{\partial A_z}{\partial x} \tag{47}$$

The slope of a magnetic line is

$$\frac{dy}{dx} = \frac{B_y}{B_x} \tag{48}$$

so that its contour must satisfy the equation

$$B_x\,dy - B_y\,dx = \frac{\partial A_z}{\partial y}\,dy + \frac{\partial A_z}{\partial x}\,dx = dA_z = 0 \tag{49}$$

Integration yields

$$A_z = \text{const.} \tag{50}$$

Thus the magnetic field is directed along contours of constant vector potential, that is, along the circles $\rho = \text{constant}$. The direction is speci-

† More accurate formulas for use at lower frequencies and with tubular conductors of outer radius a and inner radius ka are[57]

$$r_1^i \doteq r_0(1 - k^2)\left[\frac{BA}{2\sqrt{2}} + \frac{B(2 - B^2)}{4} + \frac{B(9 - 10B^2 + 4B^4)}{16\sqrt{2}\,A} + \cdots\right] \tag{45a}$$

$$l_1^i \doteq \frac{\mu_c}{\pi}\left[\frac{1}{2}\ln\frac{B+1}{B-1} + \frac{B}{2\sqrt{2}} - \frac{B(9 - 10B^2 + 4B^4)}{9\sqrt{2}\,A^3} + \cdots\right] \tag{45b}$$

where $A \equiv a\sqrt{\mu_c\sigma_c\omega}$, $B \equiv a/a_e \equiv [1 - (2a/b)^2]^{-\frac{1}{2}}$, and $r_0 = 1/\pi\sigma a^2$. These formulas are good approximations provided that $r/r_0 \geqq 2$. Still more accurate but also much more complicated formulas are given in the literature.[35]

fied by the right-hand screw relation with respect to **A**. Since **A** reverses with ρ, the direction of **B** around the circles ρ = constant, with $\rho > 0$, is opposite to that around the circles ρ = constant, with $\rho < 0$.

The electric field satisfies the relation

$$\mathbf{E} = -\operatorname{grad} \phi - j\omega\mathbf{A} \tag{51}$$

Hence, with $\mathbf{A} = \hat{z}A_z$, the transverse components are

$$E_x = -\frac{\partial \phi}{\partial x} \qquad E_y = -\frac{\partial \phi}{\partial y} \tag{52}$$

Since the gradient of a scalar function is a vector in the direction of the greatest rate of increase of the function, it must be perpendicular to the equipotential lines given by ρ = constant. Thus the electric lines must be circles perpendicular to the circles of constant ρ. As such they pass through the points $x = \pm d$, $y = 0$. Since the volume density of current in the dielectric medium if this is imperfect is given by

$$\mathbf{i} = \sigma\mathbf{E} \tag{53}$$

where **E** is the field in the dielectric and σ is its conductivity, it follows that the **E** lines are also the lines of flow of electric charges from one conductor to the other through the medium.

8. The Shielded Line with Eccentric Inner Conductor.[1,33] If the inner conductor (radius a_1) of a coaxial line is displaced so that its axis is at a distance D from the central axis of the enclosing sheath (inner radius a_2), as shown in Fig. 8.1, the solution of the transverse problem may be obtained from the results of Sec. 7. It is shown in Sec. 7 that the circles ρ = constant are equipotential lines in each transverse plane of a two-wire line. The solution of the transverse problem of the two-wire line was achieved by identifying the circular metallic surfaces of the two conductors which have radii a_1 and a_2 and centers at $x = x_1 = |x_1|$, $y = 0$ and $x = x_2 = -|x_2|$, $y = 0$ with the circles $\rho = \rho_1 = |\rho_1|$ and $\rho = \rho_2 = -|\rho_2|$ according to the relations

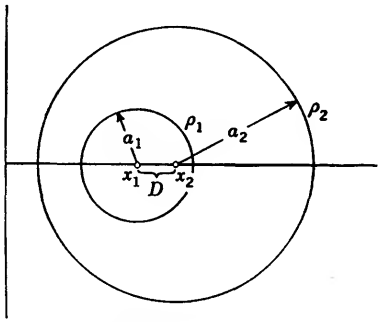


FIG. 8.1. Shielded line with eccentric inner conductor.

$$x_1 = a_1 \cosh 2\rho_1 \qquad x_2 = -a_2 \cosh 2|\rho_2| \tag{1}$$

The same identification with equipotential circles may be carried out for a shielded line (with circular metal surfaces of radii a_1 and a_2 with centers at $x = x_1 = |x_1|$, $y = 0$ and $x = x_2 = |x_2|$, $y = 0$, shown in Fig. 8.1)

by setting

$$x_1 = a_1 \cosh 2\rho_1 \qquad x_2 = a_2 \cosh 2\rho_2 \tag{2}$$

Note that for the two-wire line ρ_1 is positive and ρ_2 is negative, whereas for the shielded line ρ_1 and ρ_2 are both positive. The axial separation of the two conductors of the shielded line is

$$D = x_2 - x_1 = a_2 \cosh 2\rho_2 - a_1 \cosh 2\rho_1 \tag{3}$$

Since, as shown in Sec. 7, the following relation is satisfied:

$$a_1 \sinh 2\rho_1 = a_2 \sinh 2\rho_2 \tag{4}$$

it is possible to eliminate first ρ_1, then ρ_2, from (3). The results are

$$2\rho_1 = \cosh^{-1} \frac{a_2^2 - a_1^2 - D^2}{2a_1 D} \equiv \cosh^{-1} \psi_{1c} \tag{5a}$$

$$2\rho_2 = \cosh^{-1} \frac{a_2^2 - a_1^2 + D^2}{2a_2 D} \equiv \cosh^{-1} \psi_{2c} \tag{5b}$$

where ψ_{1c} and ψ_{2c} are defined by (5*a*) and (5*b*). Thus it has been shown that a shielded line with inner conductor of radius a_1 and outer conductor of inner radius $a_2 > a_1$, with axes separated a distance D, may be identified with two circles of constant ρ defined by (5*a*,*b*). The vector and scalar potentials are obtained from the values of ρ by multiplying by the appropriate constant. Thus

$$\boldsymbol{A}_{1z} = \frac{\boldsymbol{I}_z}{2\pi\nu} \cdot 2\rho_1 + \boldsymbol{C}_A \qquad \boldsymbol{A}_{2z} = \frac{\boldsymbol{I}_z}{2\pi\nu} \cdot 2\rho_2 + \boldsymbol{C}_A \tag{6a}$$

$$\phi_1 = \frac{\boldsymbol{q}}{2\pi\xi} \cdot 2\rho_1 + \boldsymbol{C}_\phi \qquad \phi_2 = \frac{\boldsymbol{q}}{2\pi\xi} \cdot 2\rho_2 + \boldsymbol{C}_\phi \tag{6b}$$

It is evidently possible to add the arbitrary constant potentials $\boldsymbol{C}_A$ and $\boldsymbol{C}_\phi$ and still satisfy the two-dimensional Laplace equation. This is done so that the potentials may be referred to zero at the shield by setting

$$\boldsymbol{C}_A = -\frac{\boldsymbol{I}_z}{2\pi\nu} \cdot 2\rho_2 \qquad \boldsymbol{C}_\phi = -\frac{\boldsymbol{q}}{2\pi\xi} \cdot 2\rho_2 \tag{7}$$

so that $\boldsymbol{A}_{2z} = 0$ and $\phi_2 = 0$. The potentials of the inner conductor are then equal to the potential differences as follows:

$$\boldsymbol{W}_z = \boldsymbol{A}_{1z} - \boldsymbol{A}_{2z} = \boldsymbol{A}_{1z} = \frac{\boldsymbol{I}_z}{2\pi\nu} (\cosh^{-1} \psi_{1c} - \cosh^{-1} \psi_{2c}) \tag{8a}$$

$$\boldsymbol{V} = \phi_1 - \phi_2 = \phi_1 = \frac{\boldsymbol{q}}{2\pi\xi} (\cosh^{-1} \psi_{1c} - \cosh^{-1} \psi_{2c}) \tag{8b}$$

With the general formula

$$\cosh^{-1} x - \cosh^{-1} y = \cosh^{-1} [xy - \sqrt{(x^2 - 1)(y^2 - 1)}] \tag{9a}$$

it follows that

$$\cosh^{-1} \psi_{1c} - \cosh^{-1} \psi_{2c} = \cosh^{-1} \frac{a_2^2 + a_1^2 - D^2}{2a_1 a_2} \tag{9b}$$

Hence
$$W_z = \frac{I_z}{2\pi\nu} \cosh^{-1} \frac{a_2^2 + a_1^2 - D^2}{2a_1a_2} \tag{10a}$$
$$V = \frac{q}{2\pi\xi} \cosh^{-1} \frac{a_2^2 + a_1^2 - D^2}{2a_1a_2} \tag{10b}$$

so that the external inductance per unit length of an infinite line is

$$l^e = \frac{W_z}{I_z} = \frac{\mu}{2\pi} \cosh^{-1} \frac{a_2^2 + a_1^2 - D^2}{2a_1a_2} \tag{11a}$$

Similarly
$$\frac{j\omega}{y} = \frac{V}{q} = \frac{1}{2\pi\xi} \cosh^{-1} \frac{a_2^2 + a_1^2 - D^2}{2a_1a_2} \tag{11b}$$

where $y = g + j\omega c$ is the admittance per unit length. It follows that

$$g = \frac{2\pi\sigma}{\cosh^{-1} [(a_2^2 + a_1^2 - D^2)/2a_1a_2]} \tag{12}$$
$$c = \frac{2\pi\epsilon}{\cosh^{-1} [(a_2^2 + a_1^2 - D^2)/2a_1a_2]} \tag{13}$$

Note that, when the distance D between axes is sufficiently small so that the following inequality is satisfied:

$$D^2 \ll a_1^2 + a_2^2 \tag{14}$$

it is correct to set

$$\cosh^{-1} \frac{a_2^2 + a_1^2 - D^2}{2a_1a_2} \doteq \cosh^{-1} \frac{a_2^2 + a_1^2}{2a_1a_2} \doteq \ln \frac{a_2}{a_1} \tag{15}$$

so that the line parameters reduce to the simple form of the coaxial line, viz.,

$$l^e = \frac{\mu}{2\pi} \ln \frac{a_2}{a_1} \qquad g = \frac{2\pi\sigma}{\ln (a_2/a_1)} \qquad c = \frac{2\pi\epsilon}{\ln (a_2/a_1)} \tag{16}$$

It is significant that the functions in (8a,b) may be interpreted as *either* of the following: (1) The potential difference between the surface

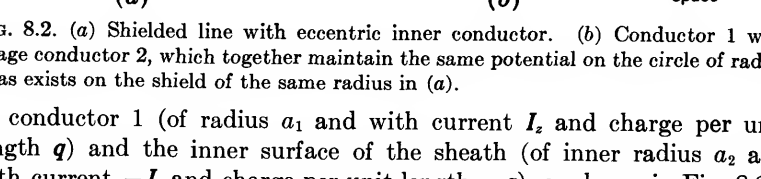


FIG. 8.2. (a) Shielded line with eccentric inner conductor. (b) Conductor 1 with image conductor 2, which together maintain the same potential on the circle of radius a_2 as exists on the shield of the same radius in (a).

of conductor 1 (of radius a_1 and with current I_z and charge per unit length q) and the inner surface of the sheath (of inner radius a_2 and with current $-I_z$ and charge per unit length $-q$), as shown in Fig. 8.2a. (2) The potential difference between the surface of conductor 1 (of radius a_1 and with current I_z and charge per unit length q) and a circle of radius

a_2 *in space* when in the presence of a second conductor 2 (of radius a_1 and with current $-I_z$ and charge per unit length $-q$). This second conductor (image) has its center at a distance

$$b_i = 2a_1 \cosh 2\rho_1 = \frac{a_2^2 - a_1^2 - D^2}{D} \tag{17}$$

from the center of conductor 1, as shown in Fig. 8.2*b*. This distance b_i in (17) is obtained from (5*a*) and Sec. 7, Eq. (23), with appropriate specialization and changes in notation simply by requiring the potentials on conductor 1 to be the same in the two cases, so that (5*a*) may be substituted in Sec. 7, Eq. (23), with $a_2 = a_1$. If the radius a_1 is sufficiently small so that

$$a_2^2 - D^2 \gg a_1^2 \tag{18}$$

(17) reduces to

$$b_i + D = \frac{a_2^2}{D} \tag{19}$$

This is the fundamental relation between the distance D of a line source from the axis of a metal cylinder of radius a_2 and the distance $b_i + D$ from the same axis to the image of the line source.

9. The Shielded-pair Line. Consider four infinitely long parallel conductors each of radius a arranged side by side, as shown in Fig. 9.1.

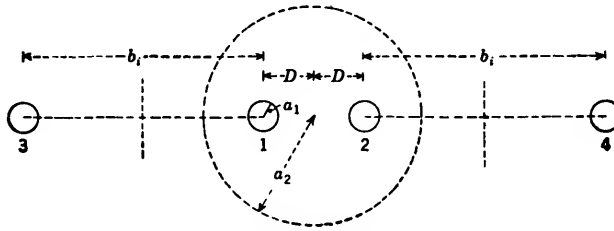


FIG. 9.1. Four-conductor line that maintains a constant potential on the circle of radius a_2.

From left to right the conductors are numbered 3, 1, 2, 4. The currents and charges in the four conductors are related as follows:

$$I_{2z} = I_{3z} = -I_{1z} = -I_{4z} \tag{1a}$$
$$q_2 = q_3 = -q_1 = -q_4 \tag{1b}$$

The distance between conductors 1 and 2 is $b = 2D$; that between 1 and 3 and that between 2 and 4 are b_i, where, from Sec. 8, Eq. (17),

$$b_i = \frac{a_2^2 - a_1^2 - D^2}{D} = 2a_1 \cosh 2\rho_1 \tag{2}$$

With this choice of distances it follows from Sec. 8 that the currents and

charges in conductors 1 and 3 make the circle of radius a_2 an equipotential surface with $\rho = \rho_2 =$ constant, as given by Sec. 8, Eq. (5*b*). By symmetry the currents and charges in conductors 2 and 4 (which are oppositely directed from those in 1 and 3, respectively) also make this same circle an equipotential surface with $\rho = -|\rho_2| =$ constant. It follows by superposition that the currents and charges in *all four* conductors make $\rho = \rho_2 - \rho_2 = 0$ on the circle of radius a_2, provided the two pairs of conductors do not interact sufficiently to alter significantly the distribution of current in the conductors. This is true approximately if the condition

$$b^2 = 4D^2 \gg a_1^2 \tag{3a}$$

is satisfied. Subject to this condition, the circle of radius a_2 in space may be replaced by a conducting sheath of radius a_2 enclosing conductors 1 and 2, and the image conductors 3 and 4 removed without changing anything electrically within this circle. Conductors 1 and 2 in the sheath thus form a balanced shielded-pair line, as shown in Fig. 9.2.

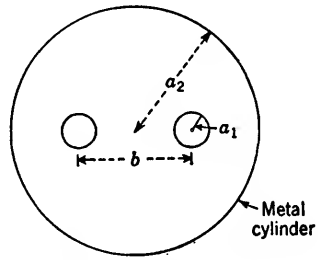


FIG. 9.2. Shielded-pair line.

The potential differences between conductors 1 and 2 in Figs. 9.1 and 9.2 are the same. Whereas they cannot be readily obtained when the radius a_1 of the conductors is unrestricted, they are evaluated easily when a_1 is sufficiently small so that the conditions (3*a*) and

$$a_2^2 - D^2 \gg a_1^2 \tag{3b}$$

are satisfied. Since the two-wire line consisting of conductors 1 and 2 is balanced, it follows, just as for the open two-wire line in Sec. 4, that, in the notation of Sec. 4,

$$I_{2z}(w) = -I_{1z}(w) \qquad q_2(w) = -q_1(w) \tag{4a}$$
$$A_{2z}(w) = -A_{1z}(w) \qquad \phi_2(w) = -\phi_1(w) \tag{4b}$$

where the potentials are determined *on the surfaces of the conductors*. It follows that the potential differences are

$$W_z(w) = A_{1z}(w) - A_{2z}(w) = 2A_{1z}(w) \tag{5a}$$
$$V(w) = \phi_1(w) - \phi_2(w) = 2\phi_1(w) \tag{5b}$$

Hence it is merely necessary to determine the scalar and vector potentials on conductor 1 as maintained by the charges and currents in *all four* conductors in Fig. 9.1. This potential is equal to that maintained by the charges and currents in the two conductors and in the sheath in Fig. 9.2.

Using the notation of Sec. 4, the two-conductor problem is readily

extended to four. Thus for the infinite line

$$W_z(w) = \frac{I_z(w)}{2\pi\nu} k_0 \qquad V(w) = \frac{q(w)}{2\pi\xi} k_0 \tag{6}$$

where
$$k_0 = \int_{-\infty}^{\infty} \left(\frac{1}{R_{11}} - \frac{1}{R_{12}} - \frac{1}{R_{13}} + \frac{1}{R_{14}} \right) dw' \tag{7a}$$

and
$$R_{11} = \sqrt{(w - w')^2 + a_1^2} \qquad R_{12} = \sqrt{(w - w')^2 + 4D^2}$$
$$R_{14} = \sqrt{(w - w')^2 + (b_i + 2D)^2} \qquad R_{13} = \sqrt{(w - w')^2 + b_i^2} \tag{7b}$$

The integration gives

$$k_0 = 2 \ln \frac{2D}{a_1} - 2 \ln \frac{b_i + 2D}{b_i} \tag{8}$$

The distance b_i may be eliminated using (2). Thus, with (3b),

$$k_0 = 2 \ln \frac{2D(a_2^2 - D^2)}{a_1(a_2^2 + D^2)} = 2 \ln \frac{b(a_2^2 - b^2/4)}{a_1(a_2^2 + b^2/4)} \tag{9}$$

where $b = 2D$ is the distance between centers of the shielded pair, each of radius a_1, and a_2 is the radius of the shield. It follows, as in Sec. 4, that the line parameters for the balanced shielded-pair line are

$$l^e = \frac{\mu k_0}{2\pi} \qquad g = \frac{2\pi\sigma}{k_0} \qquad c = \frac{2\pi\epsilon}{k_0} \tag{10a}$$

where k_0 is as in (9).

Note that, when the shield is so large that the inequality $a_2^2 \gg b^2/4$ is satisfied, (8) reduces to the values for the open-wire line.

Since the conductors are sufficiently far apart and far enough from the shield to satisfy (3a,b), the internal impedance per unit length $z^i = r^i + jx^i$ of the shielded two-wire line is obtained from the same formula [Sec. 4, Eq. (34)] as for the open two-wire line. To this must be added the impedance per unit length of the shield, in which equal and opposite currents are induced on opposite sides. An approximate formula (Ref. 4, page 44) is

$$z_s^i = \frac{4(1 + j)}{\pi a_2} \sqrt{\frac{\mu_c \omega}{2\sigma_c}} \frac{(b/2a_2)^2}{1 - (b/2a_2)^4} \tag{10b}$$

The total internal impedance per unit length is $2z^i + z_s^i$. If the shield is made of material different from that of the inner conductors, σ_c and μ_c in (10b) differ from these quantities in Sec. 4, Eq. (34).

It is possible to drive the shielded-pair line so that the two inner conductors are in parallel, with equal and codirectional currents and equal charges of the same sign, and the sheath is the return conductor, with a total current that is equal in magnitude to the sum of the currents in the inner conductors, but opposite in direction, and a total charge per unit length which is equal in magnitude to the sum of the charges per

unit length in the two inner conductors, but of opposite sign. For this method of driving, the line has properties similar to those of a shielded line with eccentric inner conductor. If the radius a_1 of the identical inner conductors is sufficiently small to satisfy (3*a*,*b*), there is no significant proximity effect. For each conductor the sheath is an equipotential surface, as analyzed in Sec. 8. Its potential with only one of the inner conductors present is proportional to ρ_2, where, from Sec. 8, Eq. (5*b*),

$$2\rho_2 = \cosh^{-1} \frac{a_2^2 - a_1^2 + D^2}{2a_2D} \tag{11}$$

Since the second inner conductor maintains the same potential on this circle, the total potential of the sheath is proportional to $4\rho_2$. For a current $I_z(w)/2$ and a charge per unit length $q(w)/2$ in *each* inner conductor and a current $-I_z(w)$ and a charge per unit length $-q(w)$ in the sheath, the potentials of the sheath are

$$A_{2z}(w) = \frac{I_z(w)/2}{2\pi\nu} 4\rho_2 + C_A = \frac{I_z(w)}{2\pi\nu} \cosh^{-1} \frac{a_2^2 - a_1^2 + D^2}{2a_2D} + C_A \tag{12a}$$

$$\phi_2(w) = \frac{q(w)/2}{2\pi\xi} 4\rho_2 + C_\phi = \frac{q(w)}{2\pi\xi} \cosh^{-1} \frac{a_2^2 - a_1^2 + D^2}{2a_2D} + C_\phi \tag{12b}$$

The potential on each inner conductor may be obtained from

$$A_{1z}(w) = \frac{I_z(w)/2}{4\pi\nu} k_0 + C_A \tag{13a}$$

$$\phi_1(w) = \frac{q(w)/2}{4\pi\xi} k_0 + C_\phi \tag{13b}$$

where k_0 is determined for the two conductors with their images shown in Fig. 9.1, but with currents and charges that satisfy the conditions

$$I_{1z}(w) = I_{2z}(w) = -I_{3z}(w) = -I_{4z}(w) \tag{14a}$$

$$q_1(w) = q_2(w) = -q_3(w) = -q_4(w) \tag{14b}$$

Thus k_0 is like (7*a*) but with different signs. Specifically

$$k_0 = \int_{-\infty}^{\infty} \left(\frac{1}{R_{11}} + \frac{1}{R_{12}} - \frac{1}{R_{13}} - \frac{1}{R_{14}} \right) dw' \tag{15}$$

where the R's are as defined in (7*b*). The integration gives

$$k_0 = 2 \ln \frac{b_i(b_i + 2D)}{2Da_1} \tag{16}$$

It is assumed that the conductors are sufficiently far apart to satisfy the conditions

$$a_1^2 \ll 4D^2 \qquad a_1^2 \ll b_i^2 \tag{17}$$

where b_i is given by

$$b_i \doteq \frac{a_2^2 - D^2}{D} \tag{18}$$

With (17) and (18)

$$k_0 = 2 \ln \frac{a_2^4 - D^4}{2D^3 a_1} \tag{19}$$

so that

$$A_{1z}(w) = \frac{I_z(w)}{4\pi\nu} \ln \frac{a_2^4 - D^4}{2D^3 a_1} + C_A \tag{20a}$$

$$\phi_1(w) = \frac{q_1(w)}{4\pi\xi} \ln \frac{a_2^4 - D^4}{2D^3 a_1} + C_\phi \tag{20b}$$

With (12a,b) the potential differences are

$$W_z(w) = A_{1z}(w) - A_{2z}(w) = \frac{I_z(w)}{4\pi\nu} \left(\ln \frac{a_2^4 - D^4}{2D^3 a_1} - 2 \cosh^{-1} \frac{a_2^2 + D^2}{2a_2 D} \right)$$

$$= \frac{I_z(w)}{4\pi\nu} \ln \frac{a_2^4 - D^4}{2Da_1 a_2^2} \tag{21}$$

Similarly

$$V(w) = \phi_1(w) - \phi_2(w) = \frac{q(w)}{4\pi\xi} \ln \frac{a_2^4 - D^4}{2Da_1 a_2^2} \tag{22}$$

From their definitions, $l^e = W_z(w)/I_z(w)$ and $y = g + j\omega c = q(w)/V(w)$, it follows that the parameters for the shielded-pair line used with its inner conductors in parallel are

$$l^e = \frac{\mu k_0}{8\pi} \qquad c = \frac{8\pi\epsilon}{k_0} \qquad g = \frac{8\pi\sigma}{k_0} \tag{23a}$$

where

$$k_0 = 2 \ln \frac{a_2^4 - b^4/16}{ba_1 a_2^2} \tag{23b}$$

and $b = 2D$ is the distance between the inner conductors. Although these formulas are restricted by (17), so that the distance $2D$ between the inner conductors must be large compared with their radius a_1, the limiting case in which the two inner conductors coincide is readily obtained by setting $D = b/2 = 0$ in the numerator of the logarithm [since this comes from (12a,b)] and setting $b = 2D = a_1$ in the denominator [since this comes from (15), in which coincidence is specified by $R_{11} = R_{12}$]. The result is the formula for the coaxial line.

The internal impedance per unit length of line is obtained approximately by treating the outer conductor as the shield in the coaxial line and each inner conductor as if rotationally symmetrical. Thus

$$z^i = \tfrac{1}{2} z_1^i + z_2^i \tag{24a}$$

where

$$z_1^i = \frac{1 + j}{2\pi a_1} \sqrt{\frac{\mu_c \omega}{2\sigma_c}} \qquad z_2^i = \frac{1 + j}{2\pi a_2} \sqrt{\frac{\mu_c \omega}{2\sigma_c}} \tag{24b}$$

If the shield is of rectangular cross section, as shown in Fig. 9.3, the following line constants apply when the inner conductors are balanced, i.e., have equal and opposite currents and charges:[43]

$$l_0^e = \frac{\mu k_0}{2\pi} \qquad g = \frac{2\pi\sigma}{k_0} \qquad c = \frac{2\pi\epsilon}{k_0} \tag{25}$$

where

$$k_0 = 2\left[\ln \frac{2h \tanh (\pi b/2h)}{\pi a} - \sum_{m=1}^{\infty} \ln \frac{1 + \dfrac{\sinh^2 (\pi b/2h)}{\cosh^2 (m\pi w/2h)}}{1 - \dfrac{\sinh^2 (\pi b/2h)}{\sinh^2 (m\pi w/2h)}}\right] \tag{26}$$

These formulas are good approximations provided the radius a of the inner conductors is small compared with the distance b between them and small compared with the distance from the wire to any side of the surrounding surface. Usually it is not necessary to go beyond $m = 1$ in the sum in (26) to obtain an adequate approximation. As a numerical example with $a = 0.0625$ in., $h = 0.4$ in., $b = 0.5$ in., and $w = 0.9$ in., (26) converges rapidly to give $k_0 = 2.564$. The internal impedance $z^i = r^i + jx^i$ per unit length is the internal impedance of the two-wire line, as given in Sec. 4, Eq. (34), plus a small contribution z_s^i from losses in the shield. Since this carries only small equal and opposite currents on the two sides—the total axial current is zero—the value of z_s^i is small. In the absence of an accurate formula, and since the shield is assumed far from the wires as compared with their radius, a reasonable estimate is obtained if the value of z_s^i in (10b) for a circular shield is used, if its circumference $2\pi a_2$ is made equal to the perimeter $2wh$ of the rectangle. That is, (10b) is used with $a_2 = wh/\pi$.

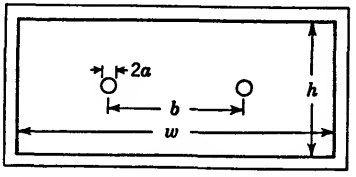


FIG. 9.3. Two-wire line in shield of rectangular cross section.

If the line with rectangular shield is driven with the two inner conductors in parallel, so that the entire return current is in the shield, the line constants defined in (25) apply with

$$k_0 = 2\left[\ln \frac{2h \coth (\pi b/2h)}{\pi a} + \sum_{m=1}^{\infty} (-1)^m \ln \frac{1 + \dfrac{\cosh^2 (\pi b/2h)}{\sinh^2 (m\pi w/2h)}}{1 - \dfrac{\cosh^2 (\pi b/2h)}{\cosh^2 (m\pi w/2h)}}\right] \tag{27}$$

For $a = 0.0625$ in., $h = 0.4$ in., $b = 0.5$ in., and $w = 0.9$ in., (27) gives $k_0 = 0.677$. At high frequencies the internal impedance per unit length is given by (24a), with z_1^i as in (24b) and

$$z_2^i = \frac{1 + j}{2hw}\sqrt{\frac{\mu_c \omega}{2\sigma_c}} \tag{28}$$

10. Three-wire Polyphase Line; Three-phase Cable.[1,59] A three-wire polyphase transmission line (Fig. 10.1) consists of three identical parallel wires each of radius a_1 located at the vertices of an equilateral

triangle of side b. It is assumed that the conditions

$$|\beta|a_1 \ll 1 \qquad |\beta b|^2 \ll 1 \qquad b^2 \gg a_1^2 \tag{1}$$

are satisfied.

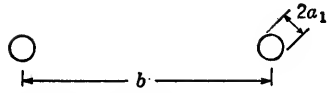


FIG. 10.1. Three-wire line with conductors at the vertices of an equilateral triangle.

The line is driven so that the currents in all three wires are equal in magnitude and have a progressive phase change of 120° from one wire to the next. Specifically

$$I_{3z} = pI_{2z} = p^2 I_{1z} \tag{2}$$

where

$$p \equiv e^{j2\pi/3} \qquad p^2 + p + 1 = 0 \tag{3}$$

The vector potential at a point $Q_1(x,y,z)$ on the surface of conductor 1 is the superposition of contributions maintained by all three currents. Thus

$$A_{1z}(w) = \frac{1}{4\pi\nu}\int_{-\infty}^{\infty}\left[I_{1z}(w')\frac{e^{-j\beta R_a}}{R_a} + I_{2z}(w')\frac{e^{-j\beta R_b}}{R_b} + I_{3z}(w')\frac{e^{-j\beta R_b}}{R_b}\right]dw' \tag{4}$$

where $$R_a = \sqrt{(w-w')^2 + a^2} \qquad R_b = \sqrt{(w-w')^2 + b^2} \tag{5}$$

With (2) and (3) the expression for the vector potential may be simplified. Thus

$$A_{1z}(w) = \frac{1}{4\pi\nu}\int_{-\infty}^{\infty} I_{1z}(w')P_L(w,w')\,dw' \tag{6}$$

Similarly $$\phi_1(w) = \frac{1}{4\pi\xi}\int_{-\infty}^{\infty} q_1(w')P_L(w,w')\,dw' \tag{7}$$

where $$P_L(w,w') = \frac{e^{-j\beta R_a}}{R_a} - \frac{e^{-j\beta R_b}}{R_b} \tag{8}$$

The corresponding expressions for the potentials on conductors 2 and 3 are

$$A_{2z}(w) = pA_{1z}(w) \qquad \phi_2(w) = p\phi_1(w) \tag{9}$$

$$A_{3z}(w) = p^2 A_{1z}(w) \qquad \phi_3(w) = p^2\phi_1(w) \tag{10}$$

The potential differences between conductors 1 and 2 are

$$W_{12z}(w) = A_{1z}(w) - A_{2z}(w) = \frac{1-p}{4\pi\nu}\int_{-\infty}^{\infty} I_{1z}(w')P_L(w,w')\,dw' \tag{11a}$$

$$V_{12}(w) = \phi_1(w) - \phi_2(w) = \frac{1-p}{4\pi\xi}\int_{-\infty}^{\infty} q_1(w')P_L(w,w')\,dw' \tag{11b}$$

The potential differences between the outer pairs of conductors differ only in substituting for $1 - p$ the factors $p(1 - p)$ or $p^2 - 1$ if referred to the current I_1 in conductor 1. They are like (11a,b) if the subscripts are cyclically permuted so that $W_{23}(w)$ is referred to I_2 and $W_{31}(w)$ to I_3.

A comparison of (11a,b) with Sec. 4, Eqs. (10a,b), shows that the

integrals are the same. It follows that their approximate evaluation must be the same, subject to the conditions imposed in (1). Thus

$$W_{12}(w) = \tfrac{1}{2}(1 - p)I_{1z}(w)l^e \tag{12}$$

$$V_{12}(w) = \tfrac{1}{2}(1 - p)q(w)\frac{j\omega}{y} = \tfrac{1}{2}(1 - p)\frac{dI_{1z}(w)}{y\,dw} \tag{13}$$

where l^e and y are as in Sec. 4, Eq. (30a,b). Subject to $b^2 \gg a_1^2$, the internal impedance per unit length z_1^i of each conductor is the same as in Sec. 4, Eq. (34). Since (12) and (13) differ from Sec. 4, Eqs. (28) and (29), only in the constant factor $\frac{1}{2}(1 - p)$, the final differential equations can differ from Sec. 4, Eqs. (37a,b), only in this factor. Thus the differential equations for the voltage and current in one pair of a three-conductor three-phase line are

$$-\frac{\partial V_{12}(z)}{\partial z} = \tfrac{1}{2}(1 - p)zI_{1z}(z) \tag{14a}$$

$$-\frac{\partial I_{1z}(z)}{\partial z} = \frac{2}{1 - p}yV_{12}(z) \tag{14b}$$

where I_{1z} is the current in conductor 1 and $V_{12}(z)$ is the potential difference between conductors 1 and 2. The equations for the other two phases are obtained from (14a,b) by cyclical permutation of the subscripts. The factor $\frac{1}{2}(1 - p)$ is unchanged. Thus the problem of the three-phase line is reduced to that of three two-wire lines with currents related according to (2) and (3).

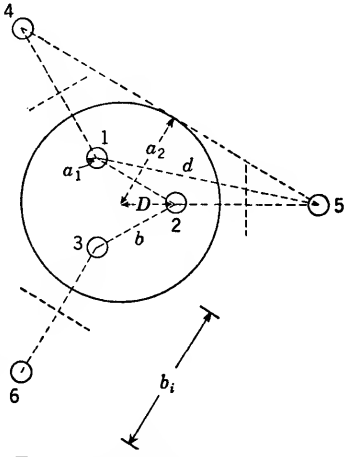


FIG. 10.2. Shielded three-wire line with image conductors equivalent to the shield.

The analysis is readily extended to the n-phase n-wire transmission line and the single-phase multiwire transmission line.[59]

The Three-phase Cable. If the three-phase line in Fig. 10.1 is placed symmetrically in a cylindrical metal shield of radius a_2, the constants for each phase may be obtained by the method used in Sec. 9. This consists in imagining the conducting shield removed and three image conductors so arranged that the resultant potential from the six conductors vanishes on a circle of radius a_2 corresponding to the circumference of the metal shield. The currents and charges in the six conductors shown in Fig. 10.2 are related as follows:

$$I_3 = pI_2 = p^2I_1 \tag{15a}$$

where

$$p \equiv e^{j2\pi/3} \qquad p^2 + p + 1 = 0 \tag{15b}$$

$$I_6 = -I_3 \qquad I_5 = -I_2 \qquad I_4 = -I_1 \tag{15c}$$

The distance between each conductor and its image is b_i. It is given

by the equivalent of Sec. 9, Eq. (2), in Fig. 10.2:

$$b_i = \frac{a_2^2 - a_1^2 - D^2}{D} \tag{16}$$

Subject to the inequalities

$$a_2^2 - D^2 \gg a_1^2 \qquad b^2 \gg a_1^2 \tag{17a}$$

which are implied in the solution as explained in Sec. 9,

$$b_i \doteq \frac{a_2^2 - D^2}{D} \tag{17b}$$

The distance d from the image of one conductor to one of the other two conductors is

$$d = \sqrt{(D + b_i)^2 + D^2 + D(D + b_i)} = \sqrt{\left(\frac{a_2}{D}\right)^2 + D^2 + a_2^2} \tag{18}$$

The last step follows with (17b).

The potential functions at w on the surface of conductor 1 within the shield are equal to the potentials calculated from the currents and charges in the three actual conductors and in the three image conductors without the shield. Thus, with (15c),

$$A_{1z}(w) = \frac{1}{4\pi\nu}\int_{-\infty}^{\infty} \left\{ I_{1z}(w')\left(\frac{e^{-j\beta R_a}}{R_a} - \frac{e^{-j\beta R_i}}{R_i}\right) + [I_{2z}(w') + I_{3z}(w')]\left(\frac{e^{-j\beta R_b}}{R_b} - \frac{e^{-j\beta R_d}}{R_d}\right)\right\} dw' \tag{19}$$

where
$$R_a = \sqrt{(w - w')^2 + a_1^2} \qquad R_b = \sqrt{(w - w')^2 + b^2}$$
$$R_i = \sqrt{(w - w')^2 + b_i^2} \qquad R_d = \sqrt{(w - w')^2 + d^2} \tag{20}$$

In (20) a_1 is the radius of each conductor; b is the axial distance between pairs of conductors; b_i is the distance between each conductor and its image, as given in (17b); and d is the distance from the image of one conductor to one of the other conductors.

With (15a,b,c) the vector potential (19) may be expressed as follows:

$$A_{1z}(w) = \frac{1}{4\pi\nu}\int_{-\infty}^{\infty} I_z(w')P_d(w,w')\,dw' \tag{21a}$$

Similarly the scalar potential at w on conductor 1 is

$$\phi_1(w) = \frac{1}{4\pi\xi}\int_{-\infty}^{\infty} q(w')P_d(w,w')\,dw' \tag{21b}$$

where
$$P_d(w,w') = \left(\frac{e^{-j\beta R_a}}{R_a} - \frac{e^{-j\beta R_b}}{R_b}\right) - \left(\frac{e^{-j\beta R_i}}{R_i} - \frac{e^{-j\beta R_d}}{R_d}\right) \tag{22}$$

The corresponding expressions for the potentials on conductors 2 and 3 are

$$A_{2z}(w) = pA_{1z}(w) \qquad \phi_2(w) = p\phi_1(w) \tag{23a}$$
$$A_{3z}(w) = p^2A_{1z}(w) \qquad \phi_3(w) = p^2\phi_1(w) \tag{23b}$$

The potential differences between conductors 1 and 2 at the coordinate w are

$$\boldsymbol{W}_{12z}(w) = \boldsymbol{A}_{1z}(w) - \boldsymbol{A}_{2z}(w) = \frac{1-p}{4\pi\nu}\int_{-\infty}^{\infty} \boldsymbol{I}_z(w')\boldsymbol{P}_d(w,w')\,dw' \quad (24a)$$

$$\boldsymbol{V}_{12}(w) = \boldsymbol{\phi}_1(w) - \boldsymbol{\phi}_2(w) = \frac{1-p}{4\pi\nu}\int_{-\infty}^{\infty} \boldsymbol{q}(w')\boldsymbol{P}_d(w,w')\,dw' \quad (24b)$$

These integrals are like those in (11a,b). They differ only in the occurrence of $\boldsymbol{P}_d(w,w')$ in place of $\boldsymbol{P}_L(w,w')$. Hence the differential equations that are satisfied by $\boldsymbol{V}_{12}(z)$ and $\boldsymbol{I}_1(z)$ must be the same as (14a,b) but with different values of the line constants. By imposing the condition

$$|\beta a_2|^2 \ll 1 \quad (25)$$

and carrying out the analysis as in Sec. 4, the following results are obtained:

$$k_0 = \int_{-\infty}^{\infty} P_d(w,w')\,dw' \doteq \int_{-\infty}^{\infty}\left[\left(\frac{1}{R_a}-\frac{1}{R_b}\right)-\left(\frac{1}{R_i}-\frac{1}{R_d}\right)\right]dw'$$
$$= 2\ln\frac{bd}{a_1 b_i} \quad (26)$$

where d and b_i are as in (17b) and (18). The line constants are

$$l^e = \frac{\mu}{\pi}\ln\frac{bd}{a_1 b_i} \qquad g = \frac{\pi\sigma}{\ln(bd/a_1 b_1)} \qquad c = \frac{\pi\epsilon}{\ln(bd/a_1 b_1)} \quad (27)$$

The internal impedance per unit length of each conductor $z_1^i = r_1^i + jx_1^i$ is the same as in Sec. 4, Eq. (34), subject to (17a).

11. The Coaxial Cage Transmission Line. A conventional coaxial line is shown in Fig. 11.1a. If its outer cylinder is replaced by $2N$† conductors each of radius a_1 symmetrically arranged in a circle of radius b

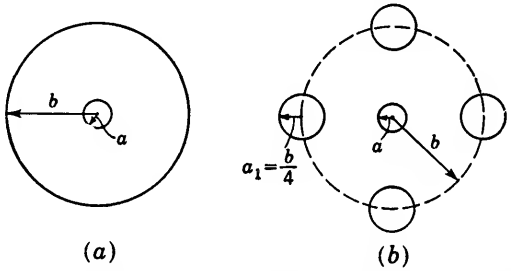


FIG. 11.1. (a) Coaxial line; $c_0 = 2\pi\epsilon/[\ln(b/a)]$ and $l_0^e = [\ln(b/a)]/2\pi\nu$. ($b$) Cage line with the same values of c_0 and l_0^e.

around the central conductor, as in Fig. 11.1b, and these $2N$ conductors are operated in parallel, the properties of the coaxial line in Fig. 11.1a may be closely approximated. In order to demonstrate this, let it be

† An odd number $2N + 1$ conductors may also be used to form the cage. For simplicity only the even numbers are considered here.

assumed as usual that the following inequalities are satisfied:

$$b^2 \gg a^2 \qquad b^2 \gg a_1^2 \tag{1}$$

The parameters of the cage transmission line may be quickly determined. Thus the scalar potential at the coordinate w on the surface of the central conductor (number 0), when this has a positive charge $q(w')$ per unit length at w', whereas each of the $2N$ outer conductors (numbered from 1 to $2N$) has a charge $-q(w')/2N$, is given by

$$\begin{aligned}\phi_0(w) &= \frac{1}{4\pi\xi}\int_{-\infty}^{\infty} q(w')\left(\frac{e^{-j\beta R_a}}{R_a} - \frac{e^{-j\beta R_b}}{R_b}\right)dw' \\ &\doteq \frac{q(w)}{4\pi\xi}\int_{-\infty}^{\infty}\left(\frac{1}{R_a} - \frac{1}{R_b}\right)dw'\end{aligned} \tag{2}$$

where $$R_a = \sqrt{(w' - w)^2 + a^2} \qquad R_b = \sqrt{(w' - w)^2 + b^2} \tag{3}$$

It is assumed that the following inequality is satisfied

$$|\beta b|^2 \ll 1 \tag{4}$$

The potential on the surface of each of the $2N$ outer conductors at the same axial coordinate w is the same as the potential $\phi_1(w)$ on conductor 1. This is

$$\phi_1(w) \doteq -\frac{q(w)}{4\pi\xi}\int_{-\infty}^{\infty}\left[\frac{1}{2N}\left(\frac{1}{R_{a1}} + \frac{1}{R_{1,N+1}} + 2\sum_{i=2}^{N}\frac{1}{R_{1i}}\right) - \frac{1}{R_b}\right]dw' \tag{5}$$

where $$R_{1i} = \sqrt{(w' - w)^2 + \left[2b\sin\frac{\pi(i-1)}{2N}\right]^2} \qquad 2 \leqq i \leqq N \tag{6a}$$

$$R_{1,N+1} \equiv \sqrt{(w' - w)^2 + 4b^2} \qquad R_{a1} = \sqrt{(w' - w)^2 + a_1^2} \tag{6b}$$

The potential difference is

$$\begin{aligned}V(w) = \phi_0(w) - \phi_1(w) \doteq \frac{q(w)}{4\pi\xi}\int_{-\infty}^{\infty}\Bigg[\frac{1}{R_a} + \frac{1}{2N}\Bigg(\frac{1}{R_{a1}} + \frac{1}{R_{1,N+1}} \\ + 2\sum_{i=2}^{N}\frac{1}{R_{1i}}\Bigg) - \frac{2}{R_b}\Bigg]dw'\end{aligned} \tag{7}$$

This expression may be integrated term by term and rearranged to give

$$V(w) \doteq \frac{q(w)k_0}{2\pi\xi} \tag{8}$$

where

$$\begin{aligned}k_0 &= \ln\frac{b}{a} + \frac{1}{2N}\left\{\ln\frac{b}{a_1} - (2N-1)\ln 2\right. \\ &\qquad \left. - 2\ln\left[\sin\frac{\pi}{2N}\sin\frac{2\pi}{2N}\sin\frac{3\pi}{2N}\cdots\sin\frac{(N-1)\pi}{2N}\right]\right\} \\ &= \ln\frac{b}{a} + \frac{1}{2N}\ln\frac{b}{2Na_1}\end{aligned} \tag{9}$$

It follows that

$$c_0 = \frac{2\pi\epsilon}{k_0} \qquad g_0 = \frac{2\pi\sigma}{k_0} \qquad l_0^e = \frac{v_p^2}{c_0} = \frac{k_0}{2\pi\nu} \tag{10}$$

Since the formulas (10) apply to the coaxial line of Fig. 11.1*a* with $k_0 = \ln (b/a)$, it follows that the cage line will have the same values of c_0, g_0, and l_0^e as the coaxial line, provided the radius of the conductors of the cage has a value such that

$$a_1 = \frac{b}{2N} \tag{11}$$

The internal impedance per unit length of the cage is approximately

$$z^i = z_0^i + \frac{z_1^i}{2N} \tag{12a}$$

where

$$z_0^i = \frac{1+j}{2\pi a}\sqrt{\frac{\mu_c\omega}{2\sigma_c}} \qquad z_1^i \doteq \frac{1+j}{2\pi a_1}\sqrt{\frac{\mu_{c1}\omega}{2\sigma_{c1}}} \tag{12b}$$

whereas that for the coaxial line is

$$z^i = z_0^i + z_b^i \tag{13a}$$

where z_0^i is as in (12*b*) and

$$z_b^i = \frac{1+j}{2\pi b}\sqrt{\frac{\mu_c\omega}{2\sigma_c}} \tag{13b}$$

Since the principal ohmic loss is in the inner conductor, which is the same in the cage line as in the coaxial line, z^i in (12*a*) usually does not differ sufficiently from z^i in (13*a*) to make it necessary to adjust σ_{c1} so that $z_1^i = z_b^i$. In the case of low-loss lines it is adequate to impose (11) in order to make the properties of the cage line equal to those of the coaxial line.

12. Strip Lines. The two conductors of the open-wire line analyzed in Sec. 7 are of circular but not necessarily equal cross section. In particular, one of the conductors may be of infinite radius, i.e., may consist of a highly conducting image plane. Although conductors of circular shape are usually most convenient in practice, there are special applications where flat strip conductors are useful. These may take several forms, the simplest of which is shown in cross section in Fig. 12.1. A parallel two-conductor line made of flat strips of small thickness is shown in Fig. 12.1*a*; the corresponding single-conductor line over an image plane is shown in Fig. 12.1*b*. The properties of strip lines of these simple types do not differ significantly from those of lines with circular cross section. The analyses in preceding sections indicate that the capacitance per unit length c_0 may be determined by electrostatic methods irrespective of the nature of the cross section, provided the width b of each strip and the

distance $2h$ between the two strips are both small compared with the wavelength (or other means are provided to ensure the existence of exclusively axial currents, which, for lossless conductors, are in the TEM mode).

The capacitance per unit length of a very thin strip (conductivity σ_c, permeability μ_c, and thickness d) in a homogeneous infinite medium

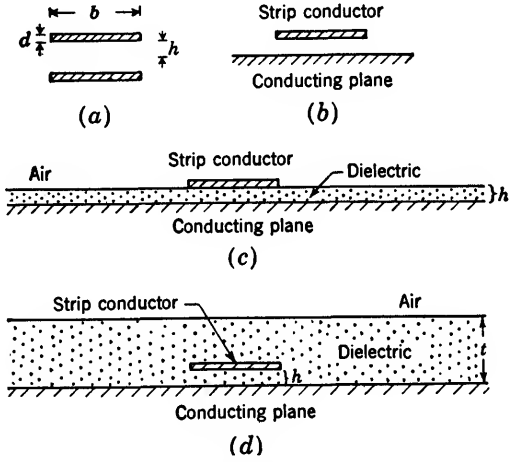


FIG. 12.1. Cross sections of strip lines: (*a*) two-conductor strip line; (*b*) strip line over conducting plane; (*c*) strip conductor on dielectric-coated conducting plane (microstrip); (*d*) strip conductor in dielectric over conducting plane (sandwich line).

(dielectric constant ϵ, permeability μ, and small conductivity σ) over a highly conducting infinite plane surface (conductivity σ_c and permeability μ_c) has been determined[36] by conformal transformation subject to the inequalities $d \ll h \ll b$. It is

$$c = \frac{\epsilon b}{h} \frac{F(x)}{x} \tag{1}$$

where

$$F(x) = 1 + x + \ln (1 + x) \qquad x = \frac{\pi b}{2h} \tag{2}$$

It follows directly that

$$g = \frac{\sigma b}{h} \frac{F(x)}{x} \tag{3}$$

and

$$l^e = \frac{\mu \epsilon}{c} = \frac{\mu h}{b} \frac{x}{F(x)} \tag{4}$$

As usual, $Z_c = \sqrt{l^e/c}$, using (1) and (4). The approximate internal impedance per unit length $z^i = z^i_{\text{strip}} + z^i_{\text{plane}}$ is obtained from

$$z^i_{\text{strip}} = \frac{1}{b} \sqrt{\frac{\omega \mu_c}{2\sigma_c}} \frac{x[1 + x + \pi - 2 \ln (\delta/2)]}{F(x)} \tag{5a}$$

$$z^i_{\text{plane}} = \frac{1}{b} \sqrt{\frac{\omega \mu_c}{2\sigma_c}} \frac{x(1 + x)}{F(x)} \tag{5b}$$

where σ_c and μ_c apply to the conductor and

$$\delta = k^2 - 1 + k\sqrt{k^2 - 1} \qquad k = 1 + \frac{d}{h} \tag{6}$$

The above formulas are good approximations for a plane of finite width, provided it extends a distance equal to the width b of the strip on each side.

An important practical application of the strip line is to provide a more compact and more readily manufactured substitute for wave guides and coaxial lines. One form of strip line known as microstrip[83] is made of thin sheets of a low-loss plastic dielectric material, with continuous films of copper laminated to both sides. Appropriate portions of the film are removed on one side to leave a design having the shape of the desired strip-line circuit. The strip line obtained in this manner differs from the simple line already described in having a layer of dielectric of thickness h covering the entire conducting plane, as shown in Fig. 12.1*c*. Thus the strip conductor is not completely immersed in a single infinite dielectric as assumed in deriving (1). Actually the presence of the two dielectrics, plastic for a thickness h above the conducting plane and air beyond this, introduces complications that result from the fact that it is no longer possible to maintain currents only in the TEM mode. An electric field between the strip line and the conducting plane may excite modes in the thin layer of dielectric which propagate outward in a manner quite different from that characteristic of the TEM mode and with magnitudes that decrease much less rapidly with distance.[37] It follows that two strip lines on the same dielectric-coated metal surface may be closely coupled even though so far apart that their interaction would be negligible if there were only a single homogeneous dielectric. Note that this interaction is due not to radiation in the TEM mode but to so-called guided modes. In an elementary sense the propagation in the thin layer of dielectric is a consequence of total internal reflection at the air-dielectric boundary. An analysis of the electromagnetic field and the constants of the line when a guided mode exists is beyond the scope of this book. However, for many purposes satisfactory approximations are obtained by assuming that only a TEM mode exists.

In order to reduce the guided modes, the thickness of the dielectric layer may be increased so that the strip conductor is completely immersed in it, as shown in Fig. 12.1*d*. Such a line is known as a sandwich line. If the thickness t of dielectric is quite large compared with the height h of the strip line above the metal plate, conditions approximating those in an infinite dielectric are approached, and the formulas given earlier in this section are good approximations. Alternatively the dielectric may itself consist of a strip not much wider than the metal strip conductor.

Since losses in the dielectric must be kept as low as possible, it is

advantageous to have air rather than a solid material between the metal strip and the conducting plane.[44] A symmetrical arrangement resembling a flattened shielded-pair line operated with the two inner conductors in parallel is shown in Fig. 12.2. In this construction the two inner conductors are separated by a dielectric that serves as the support, as shown.

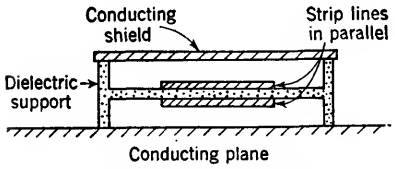


FIG. 12.2. Shielded-pair strip line.

Since the two inner conductors are at the same potential, there is no field in the dielectric, so that no guided mode is excited in it. Thus it is essentially only the TEM mode which is maintained, and there is no solid dielectric between the inner conductors and the outer ones, where the field is great. Moreover, if the conducting shield extends sufficiently far out beyond the edges of the strip lines, losses by radiation are reduced below those for the unshielded strip line shown in Fig. 12.1*c*.

13. General Solution of the Differential Equations for an Infinite Line. The first-order differential equations that are satisfied by the scalar potential difference and the current in all the several types of line analyzed in the preceding sections have the form

$$-\frac{\partial V}{\partial z} = zI_z \qquad -\frac{\partial I_z}{\partial z} = yV \tag{1}$$

where

$$y = g + j\omega c \qquad z = z^i + j\omega l^e = r^i + j\omega l \tag{2}$$

It is customary to define the total inductance per unit length by

$$l = l^e + l^i \qquad l^i = \frac{x^i}{\omega} \tag{3}$$

Since x^i is not a linear function of the frequency, it follows that l^i is not independent of frequency. The formulas for l^e, g, c, and z^i differ for different cross sections. The equations for the polyphase lines derived in Sec. 10 are the same as (1), but with the individual currents multiplied by the factor $(1 - p)/2$, where $p = e^{j2\pi/3}$. It follows that I_{1z} in conductor 1 is obtained from the solution of (1) for I by setting

$$I_z = I_{1z}\frac{1 - p}{2} \tag{4}$$

By differentiation with respect to z and appropriate substitution, the first-order equations (1) may be transformed into second-order equations. Since the equations in I_z and V are alike in form, it is sufficient to examine one of them.

The differential equation for the voltage is

$$\left(\frac{d^2V}{dz^2}\right)_z - \gamma^2 V_z = 0 \tag{5}$$

where, as defined in Sec. 2, Eq. (14), the complex propagation constant is

$$\gamma \equiv \sqrt{zy} = \alpha + j\beta \tag{6}$$

The general solution of the well-known Eq. (5) may be expressed in different ways, such as

$$V_z = B_1 e^{\gamma z} + B_2 e^{-\gamma z} = C_1 \cosh \gamma z + C_2 \sinh \gamma z = D \cosh (\gamma z + \theta) \tag{7}$$

as may be verified by direct substitution. Alternatively $w = s - z$ may be substituted for z in the several forms of (7). The B's, C's, D, and θ are complex constants of integration. The expression for the current is most easily obtained from

$$zI_z = -\left(\frac{dV}{dz}\right)_z \tag{8}$$

Thus, for the exponential form of (7),

$$zI_z = -\gamma(B_1 e^{\gamma z} - B_2 e^{-\gamma z}) \tag{9}$$

It is convenient to introduce Z_c, called the characteristic impedance, for the ratio z/γ. Thus

$$Z_c \equiv R_c + jX_c \equiv \sqrt{\frac{r + j\omega l}{g + j\omega c}} \tag{10a}$$

$$Y_c \equiv \frac{1}{Z_c} \equiv G_c + jB_c \tag{10b}$$

The current is then given by

$$I_z = Y_c(-B_1 e^{\gamma z} + B_2 e^{-\gamma z}) \tag{11}$$

Similar expressions for the other forms of (7) are readily derived using (8). The relations (7) and (11) are general solutions for the complex currents and potential differences. Although strictly correct only for an infinitely long line, they are good approximations for finite sections of line which satisfy the conditions

$$|\gamma b|^2 \ll 1 \qquad z^2 \gg b^2 \qquad (s - z)^2 \gg b^2 \tag{12}$$

as is shown later.

Alternative exponential forms of (7) and (11) which are convenient in the analysis of junctions (Chap. V) are obtained by redefining the arbitrary constants. They are

$$V_z = \sqrt{Z_c}\,(Ae^{-\gamma z} + Be^{\gamma z}) \tag{13}$$

$$I_z = \sqrt{Y_c}\,(Ae^{-\gamma z} - Be^{\gamma z}) \tag{14}$$

where $A = B_1\sqrt{Y_c}$ and $B = B_2\sqrt{Y_c}$. The coefficients B_1 and B_2 in (7) and (11) are dimensionally voltages; the squares of the coefficients in (13) and (14) are dimensionally powers.

14. Interpretation of the Solution for the Voltage along an Infinite Line. Phase and Group Velocities.[17,28] Before proceeding to evaluate $\boldsymbol{B}_1$ and $\boldsymbol{B}_2$ (Sec. 13) in terms of general terminal conditions, it is instructive to apply the solutions obtained to an infinite line. Consider a section of line beginning at $z = 0$ and ending at $z = s = \infty$. For physical reasons the voltage must vanish at infinity, so that $\boldsymbol{B}_1 = 0$. It follows directly from Sec. 13, Eq. (7), that $\boldsymbol{B}_2$ is the voltage $\boldsymbol{V}_0$ at $z = 0$. Thus

$$s = \infty \qquad \boldsymbol{V}_z = \boldsymbol{I}_z \boldsymbol{Z}_c = \boldsymbol{V}_0 e^{-(\alpha+j\beta)z} \tag{1}$$

Upon multiplying through by $e^{j\omega t}$ and selecting the real part as the solution that is consistent with an assumed time dependence of the form

$$v_0 = V_0 \cos \omega t = \text{Re}\,(V_0 e^{j\omega t}) \tag{2}$$

which refers the phase to the maximum value of the instantaneous voltage, one obtains

$$v_z = V_0 e^{-\alpha z} \cos (\omega t - \beta z) \tag{3}$$

This solution has an instructive physical interpretation. Note that the voltage v_z is a function of *two* independent variables, the time t and the distance z along the wire. At any fixed point $z = z_1$ the voltage varies periodically. The potential is positive on one wire and negative on the other for one half period. The amplitude increases from zero to a maximum of $V_0 e^{-\alpha z_1}$ and decreases to zero in a sinusoidal fashion. Then the polarity reverses, and the voltage decreases to an equal negative extreme, then again is reduced to zero. The phase lag of the voltage at z behind the voltage at $z = 0$ is βz. The cycle repeats. The same variation occurs at every other point z, but the amplitude $V_0 e^{-\alpha z}$ is different, and the phase lags that at $z = 0$ by βz. The amplitude decreases exponentially, and the phase lag increases linearly with distance from $z = 0$.

If, instead of concentrating on a fixed point along the line, the amplitude all along the line is examined at a given instant, such as $t = 0$, then

$$v_z = V_0 e^{-\alpha z} \cos \beta z \tag{4a}$$

At a quarter period later $t = T/4$, and

$$v_z = V e^{-\alpha z} \sin \beta z \tag{4b}$$

At a half period later $t = T/2$, and

$$v_z = -V_0 e^{-\alpha z} \cos \beta z \tag{4c}$$

The three distributions are shown in Fig. 14.1. It appears that, as time passes, any given curve, such as the one for $t = 0$, moves down the line with amplitude confined between the limiting curves $V_0 e^{-\alpha z}$ and $-V_0 e^{-\alpha z}$.

In order to investigate this motion, let attention be focused specifically on the phase of the voltage. This is given by the argument of the

trigonometric function in (3), that is, by $\omega t - \beta z$. Points and times in the distribution of voltage along the semi-infinite line at which the voltages are all in the same phase relative to a complete cycle are defined by $\psi = \omega t - \beta z = \text{constant}$. Because the trigonometric function is multivalued, the current at all points for which the constant differs by $2n\pi$

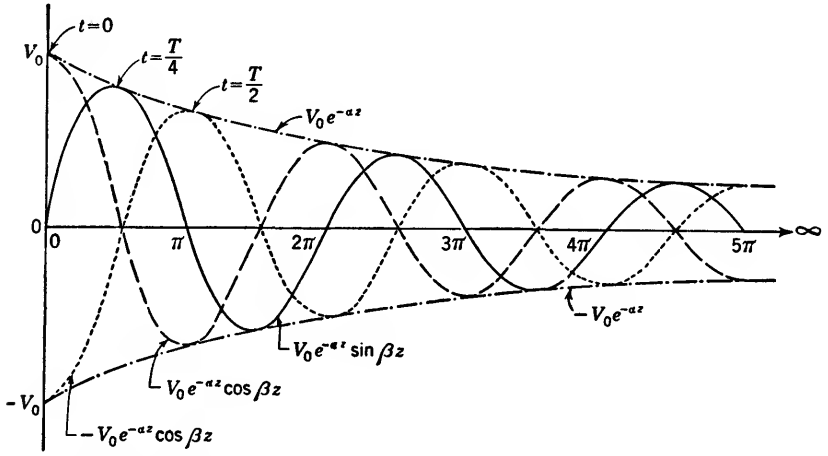


FIG. 14.1. Instantaneous distribution of voltage along a semi-infinite line at instants differing by a quarter period.

(where n is any integer) is in the same phase as at $z = 0$. The currents at different times and different points along the line which differ in phase by integral multiples of 2π are defined by

$$\omega t - \beta z = \psi_n = \psi_0 - 2n\pi \qquad n = 0, 1, 2, 3, \ldots \tag{5}$$

where ψ_0 is a constant. The significance of this relation may be disclosed, first, by determining the distances z from the input end at which the voltages differ instantaneously in phase by integral multiples of 2π and, secondly, by discovering what happens to these particular phases as time passes. If an arbitrary instant t_1 is selected, the points characterized by voltages in the phases $\psi_0 - 2n\pi$ are given by

$$z_n = \frac{1}{\beta}(\omega t_1 - \psi_0 + 2n\pi) \qquad n = 0, 1, 2, 3, \ldots \tag{6}$$

The distance between two points that are adjacent and differ in phase by 2π is

$$z_{m+1} - z_m = \frac{2\pi}{\beta} \qquad m \text{ is any integer} \tag{7}$$

This distance is the same for all choices of m. It is a fundamental constant of the distribution called the *wavelength on the line*. It is assigned

the symbol λ. Thus, by definition,

$$\lambda \equiv \frac{2\pi}{\beta} \tag{8}$$

At any given instant of time, voltages along the semi-infinite line which differ in phase by 2π are separated by *distances* λ.

With the points in the distribution which are characterized by voltages in a particular phase at a given instant determined, it remains to discover how the distance z locating any one such point varies in time. This is determined by differentiating both sides of (5) with respect to time. In this way

$$\omega - \beta \frac{dz}{dt} = 0 \tag{9}$$

or, defining v_p,

$$v_p \equiv \frac{dz}{dt} = \frac{\omega}{\beta} \tag{10}$$

In (10) v_p is the velocity with which a given phase travels along the line. In general, it has nothing to do with the propagation of energy, but only with the arrangement of phases; it applies only to periodic phenomena of infinite duration. Thus each particular phase of the voltage travels along the infinite line in the positive z direction with a constant velocity ω/β. This phenomenon, in which points of constant phase are separated by constant distances λ and all travel with a constant velocity v_p, is called *traveling* or *running waves of constant phase.* Depending on whether attention is directed to a constant phase of voltage or of current, the traveling waves are called *voltage waves* or *current waves.* Any particular phase reaching a distance z at a selected instant must have started at $z = 0$ at an earlier time given by $t - z/v_p$ or by $t - \beta z/\omega$. Consequently a voltage in this particular phase always lags the voltage at $z = 0$ at any time t by a phase angle βz. Similarly, if the distribution of voltage is viewed along the entire line at any single instant, as in Fig. 14.1, the phase lag at any distance z from 0 (with respect to the voltage at $z = 0$ at that instant) is βz. Thus β measures the phase angle characteristic of a given semi-infinite line per unit of its length. It is the *phase constant* (per unit length) of the (infinite) line. It is measured in radians per meter if z is in meters.

The amplitude of voltage in a particular phase is reduced according to $e^{-\alpha z}$. Thus α measures the natural logarithm of the ratio of amplitudes $|V_0/V_z|$ per unit length:

$$\alpha = \frac{1}{z} \log \left| \frac{V_0}{V_z} \right| \tag{11}$$

It is the *attenuation constant* (per unit length) of the (infinite) line. In the relation (11) it is measured in nepers per meter if z is in meters.

If the phase constant β is a linear function of the frequency, so that

$$\beta = \frac{\omega}{v} \tag{12}$$

where v is a constant independent of frequency, then the phase velocity v_p is the same for all frequencies and equal to the constant v introduced in (12). Under all other conditions the phase velocity is different for each frequency, so that, for any complex voltage that is a superposition of components of several frequencies, these components have different phase velocities. In this case *dispersion* is said to occur.

The significance of dispersion may be determined by investigating the propagation along a semi-infinite transmission line of a voltage that is modulated in amplitude at an angular frequency $\delta\omega$ which is small compared with ω. In this case the input voltage at $z = 0$ may be written as follows:

$$v_0 = V_0[1 + m \cos(\delta\omega t)] \cos \omega t \tag{13}$$

where m is the degree of modulation (usually multiplied by 100 and expressed in percent). Using a standard trigonometric formula, this may be rewritten in the following equivalent form:

$$v_0 = V_0\left[\cos \omega t + \frac{m}{2}\cos(\omega + \delta\omega)t + \frac{m}{2}\cos(\omega - \delta\omega)t\right] \tag{14}$$

Since the differential equation is linear, the voltage at any point z along the infinite line is the superposition of the voltages due to the three components. Thus

$$v_z = V_0\left\{e^{-\alpha z}\cos(\omega t - \beta z) + \frac{m}{2}e^{-(\alpha+\delta\alpha)z}\cos[(\omega + \delta\omega)t - (\beta + \delta\beta)z] + \frac{m}{2}e^{-(\alpha-\delta\alpha)z}\cos[(\omega - \delta\omega)t - (\beta - \delta\beta)z]\right\} \tag{15}$$

Here $\alpha \pm \delta\alpha$ and $\beta \pm \delta\beta$ are, respectively, the attenuation constants and phase constants associated with the angular frequencies $\omega \pm \delta\omega$. If $\delta\omega$ is sufficiently small, it may be assumed that the changes in α and β for an increase in ω by $\delta\omega$ are the same in magnitude as the changes when ω is decreased by $\delta\omega$. Since α is very small along a highly conducting line, as will be shown later, $\delta\alpha$ is a small quantity of higher order and of negligible importance in determining the nature of the propagation, at least over moderate distances. Specifically $e^{\pm\delta\alpha z} \doteq 1 \pm \delta\alpha z$. The last term is negligible if z is not so great that it is not possible to require $\delta\alpha z \ll 1$. If $\delta\alpha z$ is neglected, the result is

$$v_z = V_0 e^{-\alpha z}\left\{\cos(\omega t - \beta z) + \frac{m}{2}\cos[(\omega + \delta\omega)t - (\beta + \delta\beta)z] + \frac{m}{2}\cos[(\omega - \delta\omega)t - (\beta - \delta\beta)z]\right\} \tag{16}$$

This may be transformed trigonometrically, without further approximation, into the following expression:

$$v_z = V_0 e^{-\alpha z}[1 + m \cos(\delta\omega\, t - \delta\beta\, z)] \cos(\omega t - \beta z) \tag{17}$$

The transmission properties of the modulation-amplitude are contained in the function in square brackets. Thus a particular phase in the modulation amplitude is defined by

$$\delta\omega\, t - \delta\beta\, z = \text{const.} \tag{18}$$

Differentiation with respect to t yields the *velocity of propagation* (dz/dt) *of a particular phase of the modulation amplitude along the infinite line.* It is the *group velocity* and is defined by

$$v_g \equiv \frac{dz}{dt} \equiv \frac{\delta\omega}{\delta\beta} \tag{19a}$$

In the limit as $\delta\omega$ approaches zero,

$$v_g = \lim_{\delta\omega \to 0} \frac{\delta\omega}{\delta\beta} = \frac{d\omega}{d\beta} \tag{19b}$$

An alternative form is obtained using $\delta\omega = \delta(\beta v_p) = v_p \delta\beta + \beta\, \delta v_p$:

$$v_g = v_p + \beta \frac{dv_p}{d\beta} \tag{19c}$$

Since $\beta = 2\pi/\lambda$, $\beta(d/d\beta) = -\lambda(d/d\lambda)$, so that

$$v_g = v_p - \lambda \frac{dv_p}{d\lambda} \tag{19d}$$

If there is no dispersion, ω is linearly related to β by the simple relation $\beta = \omega/v$, with v a constant independent of frequency. In this case (19) together with (12) gives

$$v_g = v = v_p \tag{20}$$

When there is no dispersion, a modulation envelope travels along the transmission line at the same velocity as any particular phase of the carrier frequency. If there is dispersion, the velocity of the modulation envelope is different from that of the carrier. If the phase velocity decreases with frequency so that $dv_p/d\beta$ is negative, a particular phase travels more slowly at a higher frequency than at a lower one, the dispersion is normal, and the group velocity is less than the phase velocity. If the phase velocity increases with frequency so that $dv_p/d\beta$ is positive, a particular phase travels more rapidly at higher than at lower frequencies, the dispersion is anomalous, and the group velocity is greater than the phase velocity.

It is easily shown that the group velocity is also approximately the velocity of propagation of a pulse that can be represented in terms of a

narrow frequency band between $\omega_0 + \delta\omega$ and $\omega_0 - \delta\omega$, with $\delta\omega$ very small. If this is true,

$$\beta_0 + \delta\beta \geqq \beta_0 \geqq \beta_0 - \delta\beta \tag{21}$$

If a voltage pulse composed of a narrow band of frequencies (note that this does not mean a narrow, sharp pulse that is composed of a very wide band of frequencies) is impressed across an infinite line at $z = 0$, the instantaneous complex value of the resulting voltage pulse on the line can be represented in terms of a complex Fourier integral of the form

$$v_z = \int_{-\infty}^{\infty} V(\beta) e^{j(\omega t - \beta z)}\, d\beta \doteq \int_{\beta_0 - \delta\beta}^{\beta_0 + \delta\beta} V(\beta) e^{j(\omega t - \beta z)}\, d\beta \tag{22}$$

Here $V(\beta)$ is an amplitude function of the frequency, and hence of β, which has any shape in the interval $\beta_0 - \delta\beta$ to $\beta_0 + \delta\beta$ but is *vanishingly small outside this interval.* (A pulse of any shape can be expressed by a Fourier integral with limits extending from $-\infty$ to $+\infty$. A sharp pulse contains such a wide range of frequencies, each with a different phase velocity, that the shape of the pulse changes so rapidly that a group velocity cannot be defined.) Because it is required that $\delta\omega$ be small, the angular velocity ω in the integrand can be expanded as a function of β in a rapidly converging Taylor series about the value at β_0, and higher-power terms may be neglected:

$$\omega(\beta) = \omega_{\beta=\beta_0} + \left(\frac{d\omega}{d\beta}\right)_{\beta=\beta_0} (\beta - \beta_0) + \cdots \tag{23}$$

$$\omega t - \beta z \doteq \left[\omega_0 + \left(\frac{d\omega}{d\beta}\right)_0 (\beta - \beta_0)\right] t - (\beta_0 + \beta - \beta_0) z$$

$$= \omega_0 t - \beta_0 z + (\beta - \beta_0)\left[\left(\frac{d\omega}{d\beta}\right)_0 t - z\right] \tag{24}$$

Hence

$$v_z = \left\{\int_{\beta_0 - \delta\beta}^{\beta_0 + \delta\beta} V(\beta) e^{j(\beta - \beta_0)[(d\omega/d\beta)_0 t - z]}\, d\beta\right\} e^{j(\omega_0 t - \beta_0 z)} = V_z e^{j(\omega_0 t - \beta_0 z)} \tag{25}$$

The complex amplitude V_z varies with z only in the phase factor in the exponential. Accordingly V_z is the same at all points and times where

$$\left(\frac{d\omega}{d\beta}\right)_0 t - z = \text{const.} \tag{26}$$

Differentiating with respect to the time gives the velocity

$$\frac{dz}{dt} = v_g = \left(\frac{d\omega}{d\beta}\right)_0 \tag{27}$$

of the pulse. It is the same as the velocity of a modulation envelope (19). The concept of group velocity is precise only in the limit as $\delta\omega$ approaches zero. If $\delta\omega$ is sufficiently small, the shape of the modulation envelope

or of a pulse remains approximately the same over a long distance, so that a velocity of propagation is meaningful. This is the group velocity.

The velocity of a signal whose transmission can be described in terms of electromagnetic waves is, in general, neither the phase velocity nor the group velocity, but a third velocity called the signal velocity. This is not easy to define in general terms, but it corresponds physically to the arrival of a sufficiently large amplitude to activate a receiver. In the case of normal and small dispersion the signal velocity practically coincides with the group velocity, and both are smaller than 3×10^8 m/sec. When dispersion is normal but large, both group and signal velocities are difficult to define at all; when dispersion is anomalous, complicated conditions may obtain in which the group velocity may differ greatly from the signal velocity. In no case does the signal velocity exceed 3×10^8 m/sec; in all practical cases it is less. Theoretically an infinitely sensitive receiver should detect the extremely small amplitude of the so-called first precursor of a signal. This always has the so-called wavefront velocity, 3×10^8 m/sec for all media.

PROBLEMS

1. Derive the transmission-line equations using the general method of Sec. 2 as applied to an equivalent Π section.

2. Determine the line constants of a four-wire line in which adjacent pairs (instead of diagonal pairs) of conductors are in parallel. The four conductors are at the corners of a square.

3. Determine the line constants of a four-wire line with conductors arranged at the corners of a rectangle of sides b and c. The diagonal pairs of conductors are in parallel.

4. The inner conductor of a horizontal coaxial slotted line is supported along its entire length by a wedge of polystyrene ($\epsilon_r = 2.6$) which occupies a 9° angle. If the wavelength measured along the line is 1.2 m, what would it be if the line were completely air-filled?

5. A trough line consists of a single wire placed symmetrically parallel to the intersecting line of two highly conducting planes. The planes meet at an angle of 60°; the conductor lies on the bisector of this angle at a perpendicular distance $b/2$ from each plane. Determine the line constants, indicating what approximations are made. (HINT: Use images.)

6. A shielded cable consists of four copper conductors at the corners of a square in an iron shield of circular cross section. The dielectric is polystyrene.

(*a*) Determine the line constants l^e, c, and β for each of the possible phase-sequence voltages, assuming simple image theory to apply.

(*b*) What are the associated phase velocities? Obtain an estimate of their numerical magnitudes by assuming the copper conductors to be No. 10 wire, the square to have a side of 1 cm, and the shield to have an inner diameter of 3 cm.

7. A transmission line terminated at $z = s$ in its characteristic impedance of 300 ohms is driven at $z = 0$ by a generator with an emf of 100 volts and an impedance of $8 + j40$ ohms. The frequency is 100 Mc/sec. The attenuation constant of the line is 0.01 neper/m. Determine the instantaneous current and voltage at $z = 10$ m if the instant $t = 0$ is chosen to occur when the emf has a positive maximum in its cycle.

8. The amplitude of the current in a long line terminated in its characteristic impedance is measured at two points 100 m apart. The ratio of the two values is 1.1.

(*a*) What is the attenuation constant of the line in nepers per meter?

(*b*) What is the ratio of potential differences between the two conductors of the line at two points 20 m apart?

9. Plot curves showing $|I_z/I_0|$ along an infinite line (or a line terminated in Z_c) for which $\alpha = 10^{-3}$ neper/m over a range from $z = 0$ to $z = 2\lambda$ and over a second range from $z = 100\lambda$ to $z = 102\lambda$. Sketch the instantaneous current i_z/I_0 at $t = 0$ in both ranges with $\beta = 3.14$ radians/m ($i_0 = I_0 \cos \omega t$).

10. A flexible two-wire line consists of two copper wires joined by a thin ribbon of dielectric. The characteristic impedance of the line is specified by the manufacturer. The wire size and spacing can be determined by direct measurement. How could the wavelength along this line be determined by calculation for a specified frequency?

CHAPTER II

THE TERMINATED LINE

1. Potential Functions for a Terminated Line.[9,10,49] Since the differential equations derived in Chap. I are valid strictly only for an infinitely long line, it is not correct to assume that they may be applied to a line of finite length with arbitrary impedances as the load at $z = s$ and in series with the generator at $z = 0$. In order to investigate this problem of termination, let the infinitely long line to the right of the line-load plane

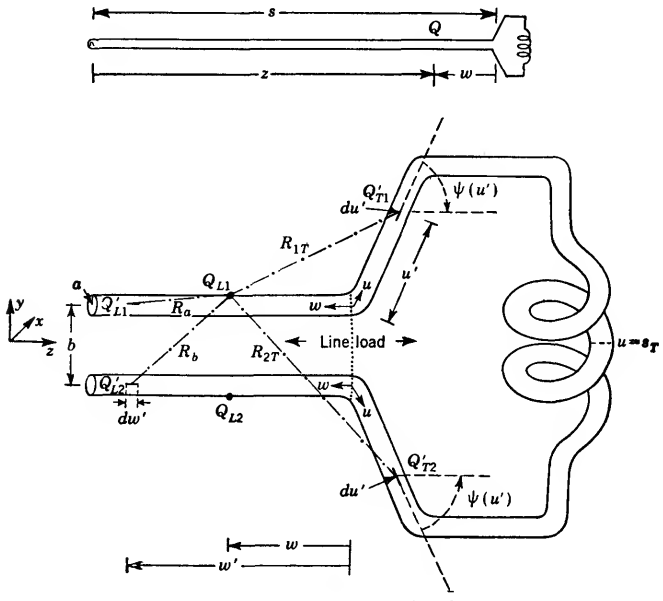


FIG. 1.1. Line with termination.

at $z = s$ be replaced by a terminal impedance of finite length. Since there is a different specific solution for each type of termination, it is not possible to derive general results valid for all terminations and types of lines. However, the general method of analysis can be formulated in terms of the configuration of conductors shown in Fig. 1.1, consisting of a symmetrical coil terminating a two-wire line with identical conductors

of radius a and spaced a distance b that satisfies the inequality

$$b^2 \gg a^2 \tag{1}$$

This restriction may be removed as in Chap. I, Sec. 7.

As a first step in the derivation of a generalized set of differential equations, let the scalar and vector potential differences be evaluated. Let $w = s - z$ be measured from the line-load plane along the transmission line to the ring $Q_L(w,x,y)$ on the surface of each conductor where the potentials are evaluated. Similarly let w' be the distance from the line-load plane to the elements dw' at $Q'_L(w',x,y)$ at opposite points on the axes of the conductors. The coordinate u is measured from the line-load plane along each side of the *symmetrical* load. The distance from this plane $w = 0$, $u = 0$ to the elements du' at Q'_T on the axes of the conductors forming the load is u'.

In order that the line may be balanced with equal and opposite currents and charges on the two conductors, that is,

$$q_{2L}(w) = -q_{1L}(w) \qquad I_{2zL}(w) = -I_{1zL}(w) \tag{2}$$

(where the subscript L stands for line), it is necessary that the line and the load be symmetrical, so that

$$\phi_2(w) = -\phi_1(w) \qquad A_{2z}(w) = -A_{1z}(w) \tag{3}$$

Since $\phi_2(w)$ and $\phi_1(w)$ must be calculated from all the charges and $A_{2z}(w)$ and $A_{1z}(w)$ from all the z components of current in both the line *and* the load, this latter must be symmetrical in its geometry and in its charges and currents. Thus it is necessary that

$$q_{2T}(u) = -q_{1T}(u) \qquad I_{2uT}(u) = -I_{1uT}(u) \tag{4}$$

where the subscript T stands for termination. If the halves of the load are geometrical images of each other in the plane $y = 0$ (Fig. 1.1), but with signs of charges and directions of currents opposite to those of mirror images, all conditions (2) to (4) are satisfied. However, there are configurations of conductors in which the halves are *not* geometrical images in the plane $y = 0$ which also satisfy these conditions.

With (2) the potential differences between opposite points on the equipotential surfaces of the two conductors are

$$V(w) = \phi_1(w) - \phi_2(w) = 2\phi_1(w) \tag{5a}$$
$$W_z(w) = A_{1z}(w) - A_{2z}(w) = 2A_{1z}(w) \tag{5b}$$

Note that these are the sums of the potential differences calculated from the charges and currents in the line (subscript L) and in the termination (subscript T):

$$V(w) = V_L(w) + V_T(w) \qquad W_z(w) = W_{zL}(w) + W_{zT}(w) \tag{6}$$

Equations (5) are true if subscripts L or T are added to each potential.

The evaluation of the potential differences at w on the line may be carried out as in Chap. I, Sec. 4, but with finite limits. Thus

$$\boldsymbol{W}_{zL}(w) = \frac{1}{2\pi\nu}\int_0^s \boldsymbol{I}_{zL}(w')\boldsymbol{P}_L(w,w')\,dw' \tag{7a}$$

$$\boldsymbol{W}_{zT}(w) = \frac{1}{2\pi\nu}\int_0^{s_T} \boldsymbol{I}_{zT}(u')\boldsymbol{P}_T(w,u')\,du' \tag{7b}$$

$$\boldsymbol{V}_L(w) = \frac{1}{2\pi\xi}\int_0^s \boldsymbol{q}_L(w')\boldsymbol{P}_L(w,w')\,dw' \tag{8a}$$

$$\boldsymbol{V}_T(w) = \frac{1}{2\pi\xi}\int_0^{s_T} \boldsymbol{q}_T(u')\boldsymbol{P}_T(w,u')\,du' \tag{8b}$$

where

$$\boldsymbol{P}_L(w,w') = \frac{e^{-j\beta R_a}}{R_a} - \frac{e^{-j\beta R_b}}{R_b} \tag{9a}$$

$$\boldsymbol{P}_T(w,u') = \frac{e^{-j\beta R_{1T}}}{R_{1T}} - \frac{e^{-j\beta R_{2T}}}{R_{2T}} \tag{9b}$$

and where

$$R_a = \sqrt{(w-w')^2 + a^2} \qquad R_b = \sqrt{(w-w')^2 + b^2} \tag{9c}$$

The distances R_{1T} and R_{2T} are measured from the symmetrically placed elements of integration du' in the termination to the point $Q_L(w,x,y)$ on one of the conductors of the line where the potentials are calculated, as shown in Fig. 1.1. The half distance around the contour of the termination is s_T. It is assumed that the length s of the line is sufficiently great so that the direct coupling between the generator and the load is negligible. It follows that it is sufficient to determine the potential differences far from the generator end of the line. By interchanging z and w the results so obtained apply to the part of the line far from the load end.

In order to evaluate the potential differences in (7) and (8), the charges and currents at w' on the line and at u' in the termination are expanded in Taylor series, as in Chap. I, Sec. 4. The distributions of current and charge are continuous at the line-load junctions, so that

$$\boldsymbol{q}_L\ (w' \to 0) = \boldsymbol{q}_T\ (u' \to 0) \tag{10a}$$

$$\boldsymbol{I}_{zL}\ (w' \to 0) = \boldsymbol{I}_{uT}\ (u' \to 0) \tag{10b}$$

With $d\boldsymbol{I}_s/ds + j\omega\boldsymbol{q} = 0$, the following expansions are obtained (as in Chap. I, Sec. 4) for $\boldsymbol{q}_L(w')$ and $\boldsymbol{I}_{zL}(w')$ (only the first two terms are retained):

$$\boldsymbol{q}_L(w') \doteq \boldsymbol{q}_L(w) + (w'-w)\frac{1}{j\omega}\frac{\partial^2 \boldsymbol{I}_{zL}(w)}{\partial w^2} \tag{11a}$$

$$\boldsymbol{I}_{zL}(w') \doteq \boldsymbol{I}_{zL}(w) + (w'-w)j\omega\boldsymbol{q}_L(w) \tag{11b}$$

$$\boldsymbol{q}_T(u') \doteq \boldsymbol{q}_L(w) - (u'+w)\frac{1}{j\omega}\frac{\partial^2 \boldsymbol{I}_{zL}(w)}{\partial w^2} \tag{11c}$$

$$\boldsymbol{I}_{uT}(u') \doteq \boldsymbol{I}_{zL}(w) - (u'+w)j\omega\boldsymbol{q}_L(w) \tag{11d}$$

Note that

$$\boldsymbol{I}_{zT}(u') = \boldsymbol{I}_{uT}(u')\cos\psi(u') \tag{12}$$

where $\boldsymbol{I}_{uT}(u')$ is the total axial current at u' in the termination and $\psi(u')$ is the angle between the direction of the current at u' and the z axis.

The substitution of (11) and (12) in (7*a*,*b*) and (8*a*,*b*) and the subsequent substitution of the integrals so obtained in (6) give

$$\boldsymbol{W}_z(w) = \frac{1}{2\pi\nu}\left\{\boldsymbol{I}_{zL}(w)[\boldsymbol{k}_0(w) + \boldsymbol{k}_{0T}(w)] + \frac{j\omega\boldsymbol{q}_L(w)[\boldsymbol{k}_1(w) + \boldsymbol{k}_{1T}(w)]}{\beta}\right\} \tag{13}$$

$$\boldsymbol{V}(w) = \frac{1}{2\pi\xi}\left\{\boldsymbol{q}_L(w)[\boldsymbol{k}_0(w) + \boldsymbol{k}'_{0T}(w)] + \frac{\frac{1}{j\omega}\frac{\partial^2\boldsymbol{I}_{zL}(w)}{\partial w^2}[\boldsymbol{k}_1(w) + \boldsymbol{k}'_{1T}(w)]}{\beta}\right\} \tag{14}$$

where, with $w = s - z$,

$$\begin{aligned}\boldsymbol{k}_0(w) &\equiv \int_0^s \boldsymbol{P}_L(w,w')\,dw' \doteq \int_0^s \left(\frac{1}{R_a} - \frac{1}{R_b}\right) dw' \\ &= \sinh^{-1}\frac{w}{a} - \sinh^{-1}\frac{w}{b} + \sinh^{-1}\frac{z}{a} - \sinh^{-1}\frac{z}{b}\end{aligned} \tag{15a}$$

For a sufficiently long line ($s^2 \gg b^2$) this reduces to

$$\begin{aligned}\boldsymbol{k}_0(w) \doteq k_0(w) &\doteq \sinh^{-1}\frac{w}{a} - \sinh^{-1}\frac{w}{b} + \ln\frac{b}{a} \\ &= 2\ln\frac{b}{a} - \ln\frac{w + \sqrt{w^2 + b^2}}{w + \sqrt{w^2 + a^2}}\end{aligned} \tag{15b}$$

$$\boldsymbol{k}_{0T}(w) \equiv \int_0^{s_T} \boldsymbol{P}_T(w,u')\cos\psi(u')\,du' \doteq \int_0^{s_T}\left(\frac{1}{R_{1T}} - \frac{1}{R_{2T}}\right)\cos\psi(u')\,du' \tag{15c}$$

$$\boldsymbol{k}'_{0T}(w) \equiv \int_0^{s_T} \boldsymbol{P}_T(w,u')\,du' \doteq \int_0^{s_T}\left(\frac{1}{R_{1T}} - \frac{1}{R_{2T}}\right)du' \tag{15d}$$

$$\begin{aligned}\boldsymbol{k}_1(w) &\equiv \beta\int_0^s (w' - w)\boldsymbol{P}_L(w,w')\,dw' \doteq \beta\int_0^s (w' - w)\left(\frac{1}{R_a} - \frac{1}{R_b}\right)dw' \\ &= \beta(\sqrt{w^2 + b^2} - \sqrt{w^2 + a^2} - \sqrt{z^2 + b^2} + \sqrt{z^2 + a^2})\end{aligned} \tag{15e}$$

$$\begin{aligned}\boldsymbol{k}_{1T}(w) &\equiv -\beta\int_0^{s_T} (u' + w)\boldsymbol{P}_T(w,u')\cos\psi(u')\,du' \\ &\doteq -\beta\int_0^{s_T}(u' + w)\left(\frac{1}{R_{1T}} - \frac{1}{R_{2T}}\right)\cos\psi(u')\,du'\end{aligned} \tag{15f}$$

$$\begin{aligned}\boldsymbol{k}'_{1T}(w) &\equiv -\beta\int_0^{s_T}(u' + w)\boldsymbol{P}_T(w,u')\,du' \\ &\doteq -\beta\int_0^{s_T}(u' + w)\left(\frac{1}{R_{1T}} - \frac{1}{R_{2T}}\right)du'\end{aligned} \tag{15g}$$

Note that the integrals (15*a*) and (15*e*) are the same as those in Chap. I, Sec. 4, Eqs. (16) and (17), except that the limits of integration are from 0 to s instead of from $-\infty$ to $+\infty$. Just as in Chap. I, Sec. 4, it is a

good approximation to replace the first integrals in (15*a*) and (15*e*) by the second integrals, provided the following restriction is imposed on the separation b of the two conductors of the line:

$$|\beta b|^2 \ll 1 \tag{16}$$

It is not clear whether this restriction is sufficient to make the second integrals in (15*c*), (15*d*), (15*f*), and (15*g*) good approximations of the first integrals. The approximation actually made is

$$\left| \int_0^{s_T} \left(\frac{1}{R_{1T}} - \frac{1}{R_{2T}} \right) du' \right| \gg \left| \int_0^{s_T} (F_{1T} - F_{2T})\, du' \right| \tag{17a}$$

where

$$F_{1T} \equiv \frac{e^{-j\beta R_{1T}} - 1}{R_{1T}} \qquad F_{2T} \equiv \frac{e^{-j\beta R_{2T}} - 1}{R_{2T}} \tag{17b}$$

In order to evaluate (17*a*) it is necessary to specify the geometry of the termination. As a convenient and rather general case, let all significant contributions to the potential differences on the line come from currents and charges in the straight parts of the termination in Fig. 1.1 which make a constant angle ψ with the line. This means that these parts are relatively longer compared with the line spacing b than in Fig. 1.1. Note that R_{1T} and R_{2T} may be expressed as follows:

$$R_{1T} = \sqrt{(w + u' \cos \psi)^2 + (u' \sin \psi)^2 + a^2} \tag{18a}$$

$$R_{2T} = \sqrt{(w + u' \cos \psi)^2 + (u' \sin \psi + b)^2} \tag{18b}$$

Significant contributions to both integrals in (17*a*) are obtained only from values of the integrand for which R_{1T} and R_{2T} are of the order of magnitude of small multiples of b and therefore sufficiently small to satisfy the inequalities

$$|\beta R_{1T}|^2 \sim |\beta b|^2 \ll 1 \qquad |\beta R_{2T}|^2 \sim |\beta b|^2 \ll 1 \tag{19}$$

For larger values of R_{1T} and R_{2T}, these distances approach each other, and the integrands in both integrals in (17*a*) become small. Over the ranges specified in (19) the exponentials in (17*b*) may be expanded as in Chap. I, Sec. 4. The result is

$$F_{1T} - F_{2T} = \beta^2(R_{2T} - R_{1T}) - j\beta^3(R_{2T}^2 - R_{1T}^2) \cdots \tag{20}$$

It follows that the ratio of the magnitude of the integrand on the left in (17*a*) to that on the right is

$$1 : |\beta^2 R_{1T} R_{2T}| \ll 1 \tag{21}$$

Since over this range (19) is satisfied, the integrand on the right in (17*a*) is small compared with the integrand on the left over the entire significant range of the integral. Therefore the representation of the first integrals in (15*c*,*d*) and (15*f*,*g*) by the second integrals may be assumed to be a good approximation, subject to (16). Let the following symbols be

defined (note that $\boldsymbol{k}$ in (15*b*,*c*) is essentially real):

$$l^e(w) \equiv l_0^e(w) + l_T^e(w) = \frac{k_0(w) + k_{0T}(w)}{2\pi\nu} \tag{22a}$$

$$j\omega\boldsymbol{y}^{-1}(w) \equiv j\omega[\boldsymbol{y}_0^{-1}(w) + \boldsymbol{y}_T^{-1}(w)] = \frac{k_0(w) + k'_{0T}(w)}{2\pi\xi} \tag{22b}$$

$$\boldsymbol{y}(w) \equiv g(w) + j\omega c(w) \tag{22c}$$

$$\boldsymbol{p}(w) \equiv \frac{\boldsymbol{k}_1(w) + \boldsymbol{k}_{1T}(w)}{k_0(w) + k_{0T}(w)} \tag{22d}$$

$$\boldsymbol{p}'(w) \equiv \frac{\boldsymbol{k}_1(w) + \boldsymbol{k}'_{1T}(w)}{k_0(w) + k'_{0T}(w)} \tag{22e}$$

$$\boldsymbol{p}_0(w) \equiv \frac{\boldsymbol{k}_1(w)}{k_0(w)} \tag{22f}$$

Note that

$$\beta^2 \equiv \frac{\omega^2\xi}{\nu} = \frac{-j\omega l_0^e(w)\boldsymbol{y}(w)[k_0(w) + k'_{0T}(w)]}{k_0(w)} \tag{22g}$$

If (22*a*) to (22*f*) are substituted in (13) and (14), the final expressions for the vector potential difference and the scalar potential difference are

$$\boldsymbol{W}_z(w) = l^e(w)\left[\boldsymbol{I}_{zL}(w) + \frac{j\omega\boldsymbol{q}_L(w)\boldsymbol{p}(w)}{\beta}\right] \tag{23a}$$

$$V(w) = \frac{j\omega}{\boldsymbol{y}(w)}\left[\boldsymbol{q}_L(w) + \frac{1}{j\omega}\frac{\partial^2\boldsymbol{I}_{zL}(w)}{\partial w^2}\frac{\boldsymbol{p}'(w)}{\beta}\right] \tag{23b}$$

For some purposes the ratio functions $\boldsymbol{a}_1(w)$ and $\boldsymbol{\Phi}_1(w)$ are useful. They are

$$\boldsymbol{a}_1(w) \equiv \frac{\boldsymbol{W}_z(w)}{\boldsymbol{W}_{zL}(w)} \doteq \frac{l^e(w)}{l_0^e(w)} \doteq a_1(w) \tag{24a}$$

$$\boldsymbol{\Phi}_1(w) \equiv \frac{\boldsymbol{V}_L(w)}{\boldsymbol{V}(w)} \doteq \frac{\boldsymbol{y}(w)}{\boldsymbol{y}_0(w)} \tag{24b}$$

Note that, when the leakage conductance is small, as is usual,

$$\boldsymbol{\Phi}_1(w) \doteq \Phi_1(w) \doteq \frac{c(w)}{c_0(w)} \tag{24c}$$

It is now readily verified from (15*a*) to (15*g*) that, subject to the inequalities

$$w^2 \gg b^2 \qquad z^2 \gg b^2 \tag{25}$$

the general expressions (23*a*) and (23*b*) for the potential differences are well approximated by the simple formulas derived in Chap. I, Sec. 4, for the infinite line. With (25) it follows that

$$k_0(w) \doteq k_0 = 2\ln\frac{b}{a} \qquad \boldsymbol{k}_1(w) \doteq 0 \tag{26a}$$

$$k_{0T}(w) \doteq 0 \qquad k'_{0T}(w) \doteq 0 \qquad \boldsymbol{k}_{1T}(w) \doteq 0 \tag{26b}$$

$$\boldsymbol{p}_0(w) \doteq 0 \qquad \boldsymbol{p}(w) \doteq 0 \qquad \boldsymbol{p}'(w) \doteq 0 \tag{26c}$$

$$\boldsymbol{\Phi}_1(w) \doteq 1 \qquad \boldsymbol{V}_L(w) \doteq \boldsymbol{V}(w) \tag{26d}$$

$$\boldsymbol{a}_1(w) \doteq 1 \qquad \boldsymbol{W}_{zL}(w) \doteq \boldsymbol{W}_z(w) \tag{26e}$$

so that $$\boldsymbol{W}_z(w) = l^e \boldsymbol{I}_{zL}(w) \qquad \boldsymbol{V}(w) = \frac{j\omega}{\boldsymbol{y}} \boldsymbol{q}_L(w) \tag{27}$$

where $$l^e = \frac{k_0}{2\pi\nu} \qquad \frac{\boldsymbol{y}}{j\omega} = \frac{2\pi\xi}{k_0} \tag{28}$$

It follows that, whereas the general equations (23*a*) and (23*b*) for the potential differences *must be used* within distances of the termination at both ends which do not satisfy (25), the simple formulas for the infinite line are good approximations at sufficient distances from the ends.

Although the discussion in this section was carried out specifically for a two-wire line, it applies with slight modification in detail to the other types of line analyzed in Chap. I. In all cases there is a region near each termination where the more general equations (23*a*,*b*) must be used, whereas the formulas for the infinite line apply at distances from the termination which are large compared with the cross-sectional dimensions of the particular type of line. For each type of line the appropriate formula for k_0 must be used in the general expressions (28) for the parameters l^e and $\boldsymbol{y} = g + j\omega c$.

For example, in the case of the coaxial line,

$$k_0(w) \doteq \frac{1}{2\pi} \int_0^{\pi} \int_0^{\infty} \left(\frac{1}{R_1} - \frac{1}{R_2} \right) dw'\, d\theta' \tag{29}$$

where, as in Chap. I, Sec. 6, with $r = a_1$,

$$R_1 = \sqrt{(w - w')^2 + a_1^2} \qquad R_2 = \sqrt{(w - w')^2 + s_{12}^2} \tag{30a}$$

$$s_{12} = \sqrt{a_2^2 + a_1^2 - 2a_1 a_2 \cos\theta'} \tag{30b}$$

The integration with respect to w' may be carried out directly to give

$$k_0(w) = 2 \ln \frac{a_2}{a_1} - \int_0^{\pi} \ln \frac{w + \sqrt{w^2 + a_2^2 + a_1^2 - 2a_2 a_1 \cos\theta'}}{w + \sqrt{w^2 + a_1^2}} \frac{d\theta'}{2\pi} \tag{31}$$

The integral in (31) has not been evaluated, but a satisfactory approximation is readily obtained. Since a_2 is always greater, and usually much greater, than a_1 and since the expression under the radical in the numerator ranges between $\sqrt{w^2 + (a_2 - a_1)^2}$ and $\sqrt{w^2 + (a_2 + a_1)^2}$, it is clear that a reasonable mean value is obtained simply by neglecting the terms in a_1 in the numerator. The result is

$$k_0(w) \doteq 2 \ln \frac{a_2}{a_1} - \ln \frac{w + \sqrt{w^2 + a_2^2}}{w + \sqrt{w^2 + a_1^2}} \tag{32}$$

This is seen to be the same in form as (15*b*) for the two-wire line, with a_2 occurring in place of b and a_1 in place of a.

2. Generalized Differential Equations.[9,10,49] The derivation of the differential equations for the scalar and vector potential differences which

are valid at all points along a terminated line parallels the derivation in Chap. I, Sec. 4, for the infinite line but proceeds from more general forms of the fundamental relations. Specifically, since the vector potential at points on the conductors of the line near its terminations may have components perpendicular to the line as well as parallel to it, the general relation [Chap. I, Sec. 3, Eq. (8*b*)] must be used. The desired general equation of continuity for the vector potential at points on the conductors of the line is

$$\frac{\partial A_x}{\partial x} + \frac{\partial A_y}{\partial y} + \frac{\partial A_z}{\partial z} + j\frac{\beta^2}{\omega}\phi = 0 \tag{1}$$

where A_x, A_y, and A_z are the components of the *total* vector potential due to the currents I_{zL} in the line and such of the components I_{xT}, I_{yT}, and I_{zT} as may exist in the terminations; ϕ is the total scalar potential due to charges q_L in the line and charges q_T in the terminations. As pointed out in Chap. I, Sec. 3, it is possible to replace the single equation (1) by several equations involving related components of the potentials such as the following:

$$A_x = A_{xT} \qquad A_y = A_{yT} \qquad A_z = A_{zL} + A_{zT} \tag{2a}$$

$$\phi = \phi_T + \phi_L \tag{2b}$$

A_{zL} and ϕ_L are computed at points on the line from currents and charges in the line, whereas A_{xT}, A_{yT}, A_{zT}, and ϕ_T are computed at the same points on the line from currents and charges in the termination. These components satisfy the following equations:

$$\frac{\partial A_{xT}}{\partial x} + \frac{\partial A_{yT}}{\partial y} + \frac{\partial A_{zT}}{\partial z} + j\frac{\beta^2}{\omega}\phi_T = 0 \tag{3a}$$

$$\frac{\partial A_{zL}}{\partial z} + j\frac{\beta^2}{\omega}\phi_L = 0 \tag{3b}$$

If the scalar and axial vector potential differences are introduced as defined in Sec. 1, Eqs. (5*a*,*b*), it follows from (3*b*) and with $\partial/\partial w = -\partial/\partial z$ that

$$\frac{\partial W_{zL}(w)}{\partial w} = j\frac{\beta^2}{\omega}V_L(w) \tag{4}$$

Similarly, proceeding from the general equation [Chap. I, Sec. 4, Eq. (6*a*)], viz.,

$$\frac{\partial \phi(w)}{\partial w} = E_z(w) + j\omega A_z(w) \tag{5}$$

and making use of the defining relation [Chap. I, Sec. 4, Eq. (33*a*)] for the internal impedance per unit length z_1^i, namely, $E_{1z}(w) = I_{1z}(w)z_1^i$, the following equation is obtained directly:

$$\frac{\partial V(w)}{\partial w} = z^i I_{zL}(w) + j\omega W_z(w) \tag{6}$$

where $V(w)$ and $W_z(w)$ are the total potential differences between points on the two conductors of the line at a distance w from the load-line junction, $I_{1z}(w) = I_{zL}(w)$ is the total current in conductor 1 at this distance, and $z^i = z_1^i + z_2^i$. The desired differential equations may now be obtained from (4) and (5) with Sec. 1, Eqs. (23a) and (23b). As a first step, let $q_L(w)$ be eliminated from Sec. 1, Eq. (23a), using Sec. 1, Eq. (23b), to give

$$W_z(w) = l^e(w)\left[I_{zL}(w) + \frac{V(w)y(w)p(w)}{\beta} - \frac{\partial^2 I_{zL}(w)}{\partial w^2}\frac{p(w)p'(w)}{\beta^2}\right] \tag{7}$$

Since the last term on the right in (7) is a small correction term, it is satisfactory to assume in evaluating its order of magnitude that the current satisfies the uncorrected equation. Moreover, since the term includes the small factor $p(w)p'(w)$, it is negligible beyond a distance $10b$ from each end of the line. In the short lengths $10b$ the small internal impedance of the conductors may be ignored, and $j\beta$ substituted for γ. Under these conditions the differential equation for the current as obtained in Chap. I, Sec. 13, is

$$\frac{\partial^2 I_{zL}(w)}{\partial w^2} + \beta^2 I_{zL}(w) = 0 \tag{8}$$

If (8) is used in (7), the first and last terms on the right become

$$I_{zL}(w)[1 + p(w)p'(w)] \tag{9}$$

However, since both $p(w)$ and $p'(w)$ are correction terms, their product is of higher order and may be neglected. Hence, subject to the condition

$$|p(w)p'(w)| \ll 1 \tag{10}$$

the z component of the vector potential difference in (7) may be expressed as follows:

$$W_z(w) \doteq l^e(w)\left[I_{zL}(w) + \frac{V(w)y(w)p(w)}{\beta}\right] \tag{11}$$

$W_z(w)$, as given in (11), may be substituted in (6) to obtain

$$I_{zL}(w) = \frac{1}{z(w)}\left[\frac{\partial V(w)}{\partial w} - \frac{j\omega l^e(w)y(w)p(w)}{\beta}V(w)\right] \tag{12}$$

where the impedance per unit length has been defined as follows:

$$z(w) \equiv z^i + j\omega l^e(w) \tag{13}$$

The correction factor on the right may be expressed in terms of the ratios $a_1(w)$ and $\Phi_1(w)$ defined in Sec. 1, Eqs. (24a,b), if use is made of Sec. 1, Eqs. (22). The result

$$I_{zL}(w) = \frac{1}{z(w)}\left[\frac{\partial V(w)}{\partial w} + \beta a_1(w)\Phi_1(w)p(w)V(w)\right] \tag{14}$$

is the generalized first-order equation for the current.

The second-order equation for the voltage is obtained by differentiating (6) with respect to w and using (4) together with

$$\boldsymbol{W}_z(w) = \boldsymbol{W}_{zL}(w) + \boldsymbol{W}_{zT}(w)$$

Thus
$$\frac{\partial^2 \boldsymbol{V}(w)}{\partial w^2} + \mathfrak{g}^2 \boldsymbol{V}_L(w) = \frac{\partial}{\partial w}\left[z^i \boldsymbol{I}_{zL}(w) + j\omega \boldsymbol{W}_{zT}(w)\right] \tag{15}$$

In this relation $\boldsymbol{W}_{zT}(w)$ is the axial component of the vector potential difference due to currents in the termination only, and the term with z^i as a factor takes account of the very small internal impedance of the line. Thus the entire term on the right in (15) is a first-order correction in which the vector potential difference and the current may be represented by their leading terms, i.e., by their uncorrected values. Thus with Sec. 1, Eq. (23*a*), the leading part of the total vector potential is

$$\boldsymbol{W}_z(w) \doteq \boldsymbol{I}_{zL}(w) l^e(w) = \boldsymbol{I}_{zL}(w)[l_0^e(w) + l_T^e(w)] \tag{16}$$

Evidently, since $\boldsymbol{W}_z(w) = \boldsymbol{W}_{zL}(w) + \boldsymbol{W}_{zT}(w)$, it follows that

$$\boldsymbol{W}_{zT}(w) \doteq \boldsymbol{I}_{zL}(w) l_T^e(w) \tag{17}$$

If (17) is substituted in the brackets in (15) and $\boldsymbol{I}_{zL}(w)$ is replaced by its leading term from (14), viz.,

$$\boldsymbol{I}_{zL}(w) \doteq \frac{1}{\boldsymbol{z}(w)} \frac{\partial \boldsymbol{V}(w)}{\partial w} \tag{18}$$

the right side of (15) becomes

$$\frac{\partial}{\partial w}\left[\frac{\boldsymbol{z}(w) - j\omega l_0^e(w)}{\boldsymbol{z}(w)} \frac{\partial \boldsymbol{V}(w)}{\partial w}\right] \tag{19}$$

Since the principal part of $\boldsymbol{z}(w)$ is $j\omega l_0^e(w)$, the leading term in (19) is

$$\frac{\boldsymbol{z}(w) - j\omega l_0^e(w)}{\boldsymbol{z}(w)} \frac{\partial^2 \boldsymbol{V}(w)}{\partial w^2} \tag{20}$$

The substitution of (20) in (15) and a subsequent rearrangement of terms give the following homogeneous equation:

$$\frac{\partial^2 \boldsymbol{V}(w)}{\partial w^2} + \frac{\boldsymbol{z}(w)}{j\omega l_0^e(w)} \mathfrak{g}^2 \boldsymbol{V}_L(w) = 0 \tag{21}$$

However, with Sec. 1, Eqs. (22) and (24*b*), it follows that

$$\frac{\mathfrak{g}^2}{j\omega l_0^e(w)} = -\frac{\boldsymbol{y}(w)}{\boldsymbol{\Phi}_1(w)} \tag{22}$$

Hence, since with Sec. 1, Eq. (24*b*), $\boldsymbol{V}_L(w)/\boldsymbol{\Phi}_1(w) = \boldsymbol{V}(w)$, the final equation for the total voltage along the line is

$$\frac{\partial^2 \boldsymbol{V}(w)}{\partial w^2} - \gamma^2(w) \boldsymbol{V}(w) = 0 \tag{23}$$

The generalized propagation constant $\gamma^2(w)$ is defined by

$$\gamma^2(w) \equiv z(w)y(w) \doteq z_0(w)y_0(w)a_1(w)\Phi_1(w) \tag{24}$$

When there is no inductive coupling between the termination and the line, $a_1(w) = 1$; when there is no capacitive coupling, $\Phi_1(w) = 1$. At distances that satisfy the condition $w^2 \gg b^2$,

$$\gamma^2(w) \doteq \gamma^2 = zy = (z^i + j\omega l^e)(g + j\omega c) \tag{25}$$

where l^e, g, and c are the parameters of the infinite line. Thus, when w^2 is large compared with b^2, the generalized Eq. (23) reduces to the equation for the infinite line given by Chap. I, Sec. 13, Eq. (5).

3. Terminal Zones; Coupling and End Effects.[10,49] It was shown in the preceding section that the scalar potential difference between the two conductors of a transmission line of finite length and terminated in arbitrary impedances is given in first approximation by the equation

$$\frac{d^2V(w)}{dw^2} - \gamma^2(w)V(w) = 0 \tag{1}$$

where
$$\gamma^2(w) = z(w)y(w) \doteq a_1(w)\Phi_1(w)z_0(w)y_0(w) \tag{2}$$

The current in one of the conductors of the balanced line, in which $I_{2z}(w) = -I_{1z}(w) = -I_z(w)$, is obtained from the scalar potential difference by differentiation:

$$I_z(w) = \frac{1}{z(w)}\left[\frac{\partial V(w)}{\partial w} + \beta p(w)a_1(w)\Phi_1(w)V(w)\right] \tag{3}$$

Since the variable w, in general, occurs in $\gamma^2(w)$ in an intricate manner, Eq. (1) cannot be solved by conventional methods that apply to equations with constant coefficients. Indeed, since $\gamma(w)$ is a different function of w for each type of termination and line, a general solution of (1) is not possible. Fortunately, precise knowledge about the distribution of current or voltage in the parts of a line near its ends at $w = 0$ and $z = s - w = 0$, which are excluded by the conditions

$$w^2 \gg b^2 \qquad z^2 = (s - w)^2 \gg b^2 \tag{4}$$

is relatively unimportant, provided the currents and voltages are known accurately everywhere else. Although at all points outside the terminal zones of length

$$d \leqq 10b \qquad d \doteq 0.1\lambda \tag{5}$$

currents and voltages satisfy the simple equations

$$\frac{d^2V(w)}{dw^2} - \gamma^2V(w) = 0 \qquad \gamma^2 = zy \tag{6}$$

$$I_z(w) = \frac{1}{z}\frac{\partial V(w)}{\partial w} \tag{7}$$

for which general solutions are given in Chap. I, Sec. 13, the currents and voltages actually cannot be determined from (6) and (7) without specifying boundary conditions; and *these necessarily involve the terminal zones* in which (1), (2), and (3) but not (6) and (7) are valid.

The differences between the general Eqs. (1) and (3) for the terminated line and the special Eqs. (6) and (7) for the infinite line and for points sufficiently far from the ends of a finite line may be summarized under

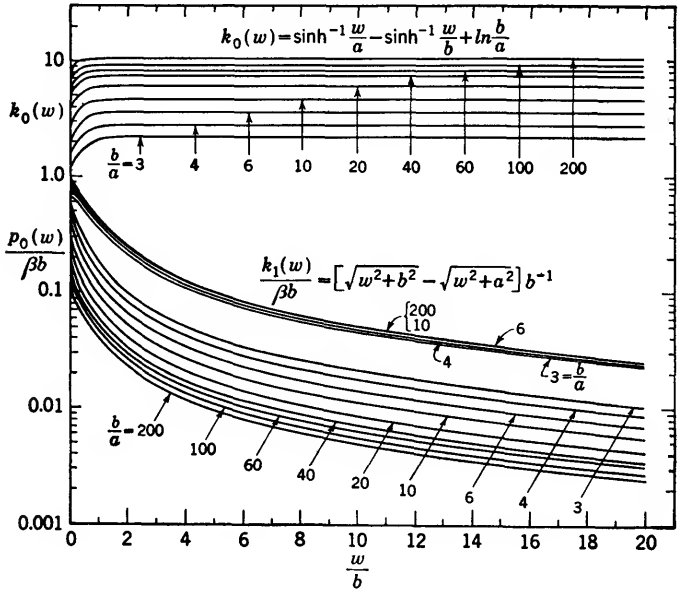


FIG. 3.1. The functions $k_0(w)$, $k_1(w)/\beta b$, and $p_0(w)/\beta b$ for a two-wire line in a perfect dielectric.

the headings of coupling between the load and the line and transmission-line end effects.

1. Coupling between the load and the line may be inductive owing to a nonvanishing z component of current in the load, so that $W_{zT}(w)$ and $l_T^e(w)$ are not zero and $a_1(w)$ differs from unity; it may be capacitive, so that $V_T(w)$ and $c_T(w)$ in $y_T(w)$ are not zero and $\Phi_1(w)$ differs from unity. The absence of inductive coupling is defined by $a_1(w) = 1$; the absence of capacitive coupling is defined by $\Phi_1(w) = 1$. It is significant to note that the infinite line is *not* characterized by an absence of either inductive or capacitive coupling between the sections of line on each side of an arbitrary line-load junction at $w = 0$. On the contrary, in the infinite line the following relations are true:

$$l_T^e(w) + l_0^e(w) = l^e \tag{8a}$$

$$y_T^{-1}(w) + y_0^{-1}(w) = y^{-1} = (g + j\omega c)^{-1} \tag{8b}$$

so that the constancy of l^e and $\boldsymbol{y}$ *presupposes inductive and capacitive coupling.* Note that, at $w = 0$,

$$l_T^e(0) = l_0^e(0) = \tfrac{1}{2}l^e \qquad \boldsymbol{y}_T(0) = \boldsymbol{y}_0(0) = 2\boldsymbol{y} \tag{9a}$$

whereas, when $w^2 \gg b^2$ or $w \to \infty$,

$$l_T^e(\infty) = 0 \qquad l_0^e(\infty) = l^e \qquad \boldsymbol{y}_T(\infty) = 0 \qquad \boldsymbol{y}_T(\infty) = \boldsymbol{y} \tag{9b}$$

It is clear that the equations for the infinite line do not apply even to a section of line with an open end, since $|2\boldsymbol{y}| \geqq |\boldsymbol{y}(w)| \geqq |\boldsymbol{y}|$.

2. Transmission-line end effects arise from the fact that, even when there is no capacitive or inductive coupling between the line and the load or when there is no load, the general Eqs. (1) and (3) do not both reduce to the simple forms (6) and (7). This is readily seen by setting

$$\boldsymbol{\Phi}_1(w) = 1 \qquad \boldsymbol{a}_1(w) = 1 \tag{10}$$

It follows that

$$\begin{aligned} \boldsymbol{z}(w) &= \boldsymbol{z}_0(w) \\ \boldsymbol{y}(w) &= \boldsymbol{y}_0(w) \end{aligned} \tag{11}$$

$$\boldsymbol{\gamma}^2(w) = \boldsymbol{z}_0(w)\boldsymbol{y}_0(w) = \boldsymbol{z}\boldsymbol{y} = \boldsymbol{\gamma}^2 \tag{12}$$

so that

$$\frac{d^2V(w)}{dw^2} - \boldsymbol{\gamma}^2 V(w) = 0 \tag{13}$$

which is the infinite-line equation. On the other hand,

$$\boldsymbol{I}_z(w) = \frac{1}{\boldsymbol{z}(w)} \left[\frac{\partial V(w)}{\partial w} + \boldsymbol{\beta}\boldsymbol{p}_0(w) V(w) \right] \tag{14}$$

where

$$\boldsymbol{p}_0(w) = \frac{\boldsymbol{k}_1(w)}{\boldsymbol{k}_0(w)} \tag{15}$$

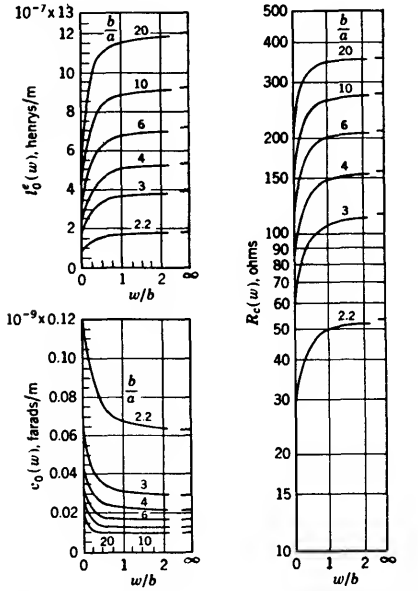


FIG. 3.2. The functions $l_0^e(w)$, $c_0(w)$, and $R_c(w)$.

Note that it is *only* the product $\boldsymbol{z}_0(w)\boldsymbol{y}_0(w)$ which is independent of w, not the functions $\boldsymbol{z}_0(w)$ and $\boldsymbol{y}_0(w)$ individually. It is due to the fact that $\boldsymbol{z}_0(w)$ is proportional to $k_0(w)$ and $\boldsymbol{y}_0(w)$ to $1/k_0(w)$ that the product $\boldsymbol{z}_0(w)\boldsymbol{y}_0(w)$ is constant. Clearly the ratio $\boldsymbol{z}_0(w)/\boldsymbol{y}_0(w)$ is not independent of w, and it is this ratio which defines the generalized characteristic impedance $\boldsymbol{Z}_c(w)$.

The functions $k_0(w)$, $k_1(w)$, and $p_0(w)$ are shown in Fig. 3.1 for an open two-wire line as a function of the normalized distance w/b from the load

at $w = 0$. The line spacing is b. The inductance and capacitance per unit length, $l_0^e(w)$ and $c_0(w)$, are shown in Fig. 3.2 together with the ratio $R_c(w) = l_0^e(w)/c_0(w) \doteq z_0(w)/y_0(w)$. A perfect dielectric is assumed.

The section of line near a termination (or other discontinuity) in which the equations of the infinite lines, (6) and (7), are not valid is called a *terminal zone*, and the conditions that are responsible for the differences between (1) and (3), on the one hand, and (6) and (7), on the other, are called *terminal-zone effects.*

4. Equivalent Uniform Line with Terminal-zone Network. Since the principal purpose of an analytical solution of the transmission-line problem is to predetermine quantities actually measured on a transmission line, it is necessary to formulate an approximate solution of the general equations [Sec. 3, Eqs. (1) and (3)] for practical use. Transmission-line measurements usually involve the distributions of current and voltage on parts of the line which are outside the terminal zones. The data so obtained are then interpreted using conventional formulas derived from the solutions of the special equations [Sec. 3, Eqs. (6) and (7)] for an infinite line. Although these equations are valid in the region of measurement, their range of application does not extend to the actual terminations. Hence this procedure is correct only if a sufficiently long section of line is included as a *part of the termination*, so that $z = s$ may not be the actual end of the smooth line. If the conventional formulas are assumed (incorrectly) to apply to the terminal zones and $z = s$ or $w = s - z = 0$ coincides with the actual junction of the line with an impedance, the impedance *apparently* terminating the line includes the effect of errors made in using incorrect parameters and formulas in the terminal zone. This *apparent terminal impedance* $\boldsymbol{Z}_{sa}$ at $z = s$ (or $\boldsymbol{Z}_{0a}$ at $z = 0$) is not, in general, the ratio of the actual scalar potential difference across, to the current entering, the terminating impedance. Since $\boldsymbol{Z}_{sa}$ involves the properties of the transmission line, the same impedance may have quite different apparent impedances when connected as a load to different transmission lines. Merely by varying the spacing of the line or by changing the relative orientation of line and termination, the apparent terminal impedance of a given load may be altered.

For reasons similar to those which make it impossible to have the uniform properties of a long transmission line continue to its junction with an arbitrary impedance, it is also impossible to define for an arbitrary circuit element an impedance that is independent of the circuit to which it is connected. The degree of coupling of such an element to the adjacent parts of the circuit, e.g., the transmission line, varies with the configuration of conductors and the separation of its terminals; it may be large or almost zero in specially designed arrangements. Only when the separation of the terminals of a circuit element is vanishingly small, as when it is driven by a fictitious extensionless generator or by an equally

fictitious transmission line with zero spacing, is it possible to define a self-impedance Z_s that is an independent characteristic of the circuit element, which then becomes a complete self-contained circuit.

It is possible to separate formally the circuit properties of, and the coupling between, two parts of a single complete circuit into two self-impedances and a mutual impedance.[9] Except when the distribution of current is greatly affected by the mutual term, the self-impedance of the load differs negligibly from its ideal self-impedance when isolated and driven by a potential difference maintained across its terminals by a fictitious source. This is true of the coupling between a transmission line and its load. Accordingly the transmission line may be analyzed as if it had a physically extensionless load, and the load may be analyzed as if it were driven by a fictitious source that maintains the required potential difference $V(s) = \phi_1(s) - \phi_2(s)$ at its terminals, as shown in Fig. 4.1, *provided* separate account is taken of the actual coupling between them. This may be done approximately by means of a suitable equivalent network that represents the coupling as if lumped at the junction instead of distributed over short distances near it. By concentrating coupling effects and transmission-line end effects in such a network of lumped elements, the actual terminal zone in which $z(w)$ and $y(w)$ are functions of position may be replaced by a fictitious section of line in which the variable parameters $z(w)$ and $y(w)$ are replaced by the constants z and y of the infinite line. That is, the length of the terminal zone is reduced from, say, $d \doteq 10b$ to zero, and its distributed circuit properties, insofar as they depart from those of a smooth line, are concentrated as a lumped network at the line-load junction. If this is done, the impedance terminating the hypothetical completely uniform line with constant parameters everywhere is the *apparent terminal impedance* Z_{sa}. This consists of the impedance of the idealized *isolated* load $Z_s = V(s)/I(s)$, as obtained from Fig. 4.1, in combination with the lumped network that takes account of all terminal-zone effects. This is shown schematically in Fig. 4.2, where the lumped elements of the terminal-zone network consist of a series impedance $Z_T = j\omega L_T$ and a shunt admittance $Y_T = j\omega C_T$.

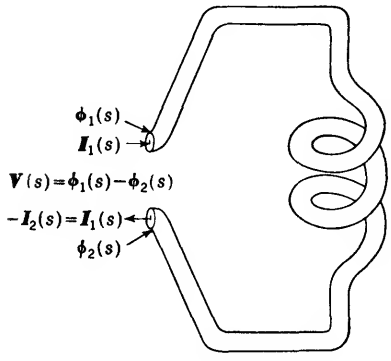


FIG. 4.1. Typical termination for two-wire line.

The lumped elements Z_T and Y_T are to compensate for the difference between the series impedance and shunt admittance of the actual terminal zone and the series impedance and shunt admittance of a section of line which is equal to the terminal zone in length but has the line constants

of an infinite line. These elements are defined as follows:

$$Z_T = \int_0^d [z(w) - z]\,dw \doteq j\omega \int_0^d [l^e(w) - l^e]\,dw = j\omega L_T \qquad (1)$$

$$Y_T = \int_0^d [y(w) - y]\,dw \doteq j\omega \int_0^d [c(w) - c]\,dw = j\omega C_T \qquad (2)$$

where $y(w)$ is as defined in Sec. 1, Eq. (22c), $z(w)$ as in Sec. 2, Eq. (13), and z and y as in Sec. 2, Eq. (25). Alternatively, with Sec. 2, Eqs. (24a,c),

$$L_T = \int_0^d [l_0^e(w)a_1(w) - l^e]\,dw \qquad (3)$$

$$C_T = \int_0^d [c_0(w)\Phi_1(w) - c]\,dw \qquad (4)$$

With Z_T in series and Y_T in parallel with the load (the order is not important), $z(w)$ and $y(w)$ in the terminal zone may be replaced by

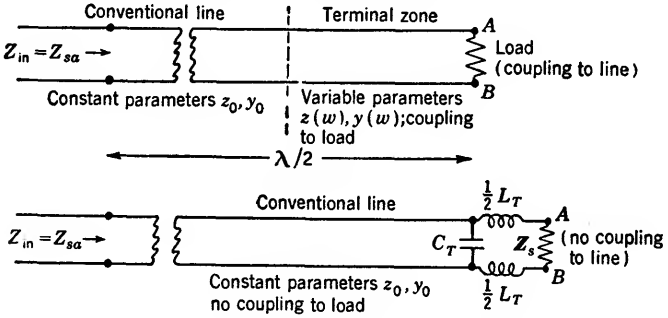


FIG. 4.2. Actual and equivalent transmission lines. The configuration of conductors between A and B is the same in both cases.

z and y, so that $\gamma(w)$ becomes γ and $p(w) = 0$. It follows that the infinite-line equations [Sec. 3, Eqs. (6) and (7)] apply to the *entire line including terminal zones*, provided an appropriate lumped network is connected between the line and each termination, as shown in Fig. 4.2, so that the apparent terminating impedances are Z_{sa} at $z = s$ and Z_{0a} at $z = 0$. The constants of this network must be evaluated separately for each impedance and each type of line. Specific application of this general theory to impedances of various types terminating different lines and to the junction of two different lines is made in later sections. For use in the next section it has been shown that the constants of integration in the general solution of the infinite-line equations [Sec. 3, Eqs. (6) and (7)] may be applied to finite lines, provided the boundary conditions are expressed in terms of apparent terminal impedances Z_{sa} which include an appropriate terminal-zone network.

5. Evaluation of Constants in Terms of Boundary Conditions; Exponential Solution for a Terminated Line.[17] If the transmission line is of finite length extending from $z = 0$ to $z = s$, as shown in Fig. 5.1a, the

ends of the conductors may be connected by terminal impedances of the most general sort, provided a section of transmission line which is long compared with the line spacing b is included as a part of each termination. The impedances are defined by

$$Z = \frac{V}{I} \tag{1}$$

where V is the complex potential difference across the terminals of the impedance and I is the complex current in each terminal. The currents

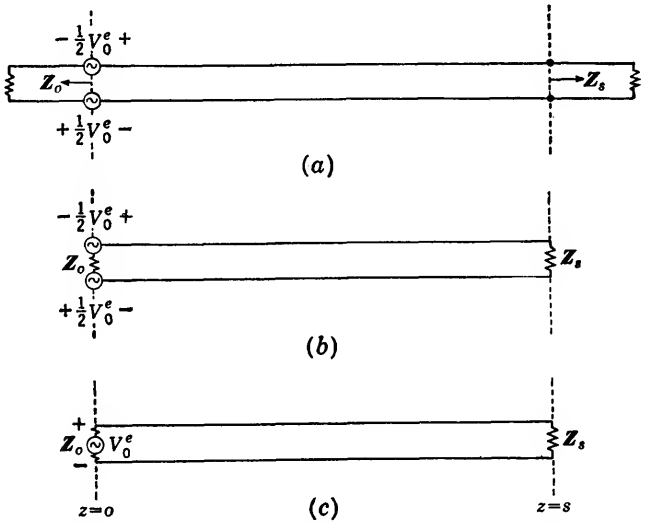


FIG. 5.1. Terminated transmission lines. (*a*) Terminations at both ends include sections of transmission line. (*b*) Lumped terminations. (*c*) Lumped terminations with single generator at center of Z_0.

in the two terminals are equal and opposite. At the input end the impedance is $Z_0 = R_0 + jX_0$; at the output end it is $Z_s = R_s + jX_s$. The generator at the input end is separated into two identical parts each maintaining an emf $\frac{1}{2}V_0^e$. The superscript e is to distinguish an externally applied potential difference or emf from a voltage drop. The subscript 0 locates the generators at $z = 0$.

For lines in which b is so small that it makes no significant difference in any length of line whether it is increased or decreased by an amount b, terminal-zone effects are negligible, and the circuit of Fig. 5.1*b* or Fig. 5.1*c* is adequate with $Z_{sa} \doteq Z_s$ and $Z_{0a} \doteq Z_0$. If the current at all points in Z_0 is the same as I_0 (the current into or out of the line), the halves of the generator may be combined into a single generator connected in series with Z_0 in any desired manner. If the current amplitude is not constant throughout Z_0, the generator must be in two parts in order to have the

currents equal and in reversed directions at opposite points along the two conductors or at the center of a symmetrical structure.

If the termination does not include a section of line and the spacing is not so small that terminal-zone effects are negligible, these may be assumed to be localized in a network of lumped elements at the junction of the line and the termination, as explained in the preceding section. By combining such a corrective network with the ideal impedance Z_0 or Z_s of the impedance when isolated, the apparent impedance Z_{0a} or Z_{sa} is obtained. This is the fictitious impedance that would have to terminate the line if uniform conditions prevailed to the ends and the same currents and voltages existed everywhere on the line as on the actual line with the actual termination except in the terminal zones. The apparent impedance *is that determined from measurements made on the line* if solutions of the conventional or uniform-line equations are used in the reduction of the data.

In the following it is assumed for simplicity in the notation that terminal-zone effects are negligible, so that Z_0 and Z_s are the terminations. The solution obtained may be applied to general terminations merely by adding the additional subscript a to Z_0 and Z_s and to other functions introduced to describe the terminations.

The boundary conditions for the circuit of Fig. 5.1 are

For $z = 0$, $\quad V_0 = V_0^s - I_0 Z_0$ (2a)

For $z = s$, $\quad V_s = I_s Z_s$ (2b)

If the appropriate currents and voltages as given by the first equation in Chap. I, Sec. 13, Eq. (7), and by Chap. I, Sec. 13, Eq. (11), namely, $V_z = B_1 e^{\gamma z} + B_2 e^{-\gamma z}$ and $I_z = \frac{1}{Z_c}(-B_1 e^{\gamma z} + B_2 e^{-\gamma z})$, are substituted in (2), two equations are obtained for evaluating the arbitrary constants B_1 and B_2 in terms of the impedances Z_0 and Z_s and the parameters of the line. These equations are

$$V_0^s = B_1 + B_2 + \frac{Z_0}{Z_c}(-B_1 + B_2) \tag{3}$$

$$\frac{Z_s}{Z_c}(-B_1 e^{\gamma s} + B_2 e^{-\gamma s}) = B_1 e^{\gamma s} + B_2 e^{-\gamma s} \tag{4}$$

Rearranging and collecting terms lead to

$$-B_1 \frac{Z_0 - Z_c}{Z_0 + Z_c} + B_2 = V_0^s \frac{Z_c}{Z_0 + Z_c} \tag{5}$$

$$-B_1 + B_2 \frac{Z_s - Z_c}{Z_s + Z_c} e^{-2\gamma s} = 0 \tag{6}$$

For convenience let the following shorthand be introduced in (5) and (6):

$$\Gamma_0 \equiv \frac{Z_0 - Z_c}{Z_0 + Z_c} = \Gamma_0 e^{i\psi_0} \qquad \Gamma_s = \frac{Z_s - Z_c}{Z_s + Z_c} = \Gamma_s e^{i\psi_s} \tag{7}$$

The complex factors Γ_0 and Γ_s are called *coefficients of reflection* of voltage. Their properties are studied in later sections. Solving (5) and (6) for B_1 and B_2, using (7), gives

$$B_1 = V_0^s \frac{Z_c}{Z_0 + Z_c} \frac{\Gamma_s e^{-2\gamma s}}{1 - \Gamma_0 \Gamma_s e^{-2\gamma s}} \tag{8}$$

$$B_2 = V_0^s \frac{Z_c}{Z_0 + Z_c} \frac{1}{1 - \Gamma_0 \Gamma_s e^{-2\gamma s}} \tag{9}$$

Upon substituting these in Chap. I, Sec. 13, Eqs. (7) and (11), the final solutions in exponential form are obtained. They are

$$V_z = \frac{V_0^s Z_c}{Z_c + Z_0} \frac{e^{-\gamma z} + \Gamma_s e^{-\gamma(2s-z)}}{1 - \Gamma_0 \Gamma_s e^{-2\gamma s}} \tag{10}$$

$$I_z = \frac{V_0^s}{Z_c + Z_0} \frac{e^{-\gamma z} - \Gamma_s e^{-\gamma(2s-z)}}{1 - \Gamma_0 \Gamma_s e^{-2\gamma s}} \tag{11}$$

The solutions for a terminated line must, of course, reduce to the solutions previously obtained in Chap. I, Sec. 14, Eq. (1), for a semi-infinite line of length s that is allowed to increase without limit. If $s \to \infty$ in (10) and (11), all exponential terms involving s vanish, provided γ has a positive real part, so that

$$V_z = I_z Z_c = \frac{V_0^s Z_c}{Z_c + Z_0} e^{-\gamma z} = V_0 e^{-\gamma z} \tag{12}$$

This is like Chap. I, Sec. 14, Eq. (1); note that

$$V_0 = \frac{V_0^s Z_c}{Z_c + Z_0} \tag{13}$$

It is significant that solutions like (12) and (13) are obtained for a line terminated so that

$$Z_s = Z_c \qquad \text{or} \qquad \Gamma_s = 0 \tag{14}$$

The input current given in (12) is like that in a simple circuit consisting of Z_c in series with Z_0. It follows that an infinitely long transmission line, or a line of any length terminated in $Z_s = Z_c$, behaves at its input terminals like an impedance Z_c. Since Z_c is defined by Chap. I, Sec. 13, Eq. (10*a*), entirely in terms of parameters characteristic of the line itself, Z_c is properly called the *characteristic impedance* of the line. Note that a transmission line behaves like an impedance Z_c *only if it is infinitely long or if it is terminated in* Z_c. Its behavior under other circumstances is quite different.

6. Infinite-series Form of the Exponential Solution.[17] The exponential solutions of Sec. 5, Eqs. (10) and (11), may be modified either in order to make them more convenient mathematically or in order to facilitate their interpretation in terms of a physical picture or model. In this section Sec. 5, Eq. (10), is rearranged into a form with a physical interpretation that helps to explain the significance of the parameters appearing in the solution. From the analytical point of view such a physical interpretation is not required. On the other hand, pictures or models that illuminate a mathematical formula in terms of a readily visualized physical mechanism often serve a valuable purpose.

A physically fundamental transformation of Sec. 5, Eq. (10), is derived below. The procedure is contrary to that usually followed by the mathematician, who prefers a closed formula to a physical interpretation, in that Sec. 5, Eq. (10), is expanded into an infinite series by dividing the numerator by the denominator. The result is

$$V_z = \frac{V_0^e Z_c}{Z_0 + Z_c}\,[e^{-\gamma z} + \Gamma_s e^{-\gamma(2s-z)} + \Gamma_0\Gamma_s e^{-\gamma(2s+z)} + \Gamma_0\Gamma_s^2 e^{-\gamma(4s-z)} + \Gamma_0^2\Gamma_s^2 e^{-\gamma(4s+z)} + \cdots] \quad (1)$$

In order to obtain the instantaneous real voltage, (1) must be multiplied by $e^{j\omega t}$ and the real part selected. This is

$$\begin{aligned} v_z = V_0^e \left|\frac{Z_c}{Z_0 + Z_c}\right| \{ & e^{-\alpha z}\cos(\omega t - \beta z + \Phi) \\ & + \Gamma_s e^{-\alpha(2s-z)}\cos[\omega t - \beta(2s - z) + \psi_s + \Phi] \\ & + \Gamma_0\Gamma_s e^{-\alpha(2s+z)}\cos[\omega t - \beta(2s + z) + \psi_0 + \psi_s + \Phi] \\ & + \Gamma_0\Gamma_s^2 e^{-\alpha(4s-z)}\cos[\omega t - \beta(4s - z) + \psi_0 + 2\psi_s + \Phi] \\ & + \Gamma_0^2\Gamma_0^2 e^{-\alpha(4s+z)}\cos[\omega t - \beta(4s + z) + 2\psi_0 + 2\psi_s + \Phi] \\ & + \cdots\} \end{aligned} \quad (2)$$

Note that

$$\frac{Z_c}{Z_0 + Z_c} = \left|\frac{Z_c}{Z_0 + Z_c}\right| e^{j\Phi} \quad (3)$$

and

$$\Gamma_0 = \Gamma_0 e^{j\psi_0} \qquad \Gamma_s = \Gamma_s e^{j\psi_s} \quad (4)$$

The velocity of a constant phase associated with each term in (2) is obtained by setting the phase equal to a constant and differentiating with respect to the time. Thus

For the first term,

$$\frac{d}{dt}(\omega t - \beta z + \Phi) = \text{const.} \qquad \frac{dz}{dt} = \frac{\omega}{\beta} = v_p$$

For the second term,

$$\frac{d}{dt}(\omega t - 2\beta s + \beta z + \psi_s + \Phi) = \text{const.} \qquad \frac{dz}{dt} = -\frac{\omega}{\beta} = -v_p$$

For the third term,

$$\frac{d}{dt}(\omega t - 2\beta s - \beta z + \psi_0 + \psi_s + \Phi) = \text{const.} \qquad \frac{dz}{dt} = \frac{\omega}{\beta} = v_p$$

For the fourth, sixth, and every even-numbered term $dz/dt = -v_p$; for the fifth, seventh, and every odd-numbered term $dz/dt = v_p$.

The series (2) may be interpreted term by term. By allowing the length s of the line to increase without limit, the first term in (2) is seen to be the complete solution for the instantaneous voltage at z on a *semi-infinite* line. It is like Chap. I, Sec. 14, Eq. (1), for a generator impedance $\boldsymbol{Z}_0$ instead of zero. The interpretation previously applied to Sec. 4, Eq. (1), may be applied to the first term in (2). That is, the contribution to the instantaneous voltage at z by the first term may be visualized as a voltage wave traveling in the positive z direction with a constant phase velocity v_p, the amplitude of the voltage diminishing exponentially with z. At the instant t when the wave reaches the point z, the wave will have traveled a total distance z from $z = 0$ to $z = z$. The voltage measured at z at the particular instant t may be regarded as having originated at the generator at an appropriate earlier time t_1 such that $t_1 = t - z/v_p$. Thus the first term may be assumed to represent a voltage wave that has traveled only the distance z from the generator to the point of observation at z with velocity v_p. It involves a phase lag βz and a decrease in amplitude by the factor $e^{-\alpha z}$ compared with the point $z = 0$ at the same instant.

The instantaneous voltage at z on the *terminated* line at time t_1 differs from that which would be observed at the same point and time if the line were *infinite* by the addition of the series of terms following the first one in (2). Viewed in the same light as the first term, the second term in (2) represents a voltage wave moving in the negative z direction which has traveled the distance $2s - z$, starting at the generator, proceeding to the end of the line at $z = s$, and returning to the point z, where it arrives simultaneously with the first wave. The entire distance was traversed with the constant phase velocity v_p. The starting time was $t_1 - (2s - z)/v_p + \psi_s/\omega$. It involves a phase lag $\beta(2s - z)$ and a decrease in amplitude by the factor $e^{-\alpha(2s-z)}$. In addition, there is an amplitude factor $\Gamma_s = |(\boldsymbol{Z}_s - \boldsymbol{Z}_c)/(\boldsymbol{Z}_s + \boldsymbol{Z}_c)|$ and a phase shift $\psi_s = \arg (\boldsymbol{Z}_s - \boldsymbol{Z}_c)/(\boldsymbol{Z}_s + \boldsymbol{Z}_c)$. Since Γ_s and ψ_s depend only on the terminal impedance $\boldsymbol{Z}_s$ at $z = s$ and on the parameter of the line $\boldsymbol{Z}_c$, it is plausible to regard $\boldsymbol{\Gamma}_s = \Gamma_s e^{j\psi_s}$ as a *coefficient of reflection* characterizing the impedance $\boldsymbol{Z}_s$ when this terminates the line of characteristic impedance $\boldsymbol{Z}_c$. The effect of the coefficient is to change the amplitude of an incident voltage wave by a factor Γ_s and the phase by ψ_s after the wave reaches $\boldsymbol{Z}_s$ and before it starts back as a reflected wave.

The third term in (2) may be interpreted in an analogous manner as a wave which originated at the generator at a time $t_1 - (2s + z) + \psi_s/\omega + \psi_0/\omega$ and which has traveled to the end at $z = s$, back to the generator at $z = 0$, and finally back to the point of observation at z, where it arrives simultaneously with the other waves. When it arrives at z, it is traveling in the positive z direction along with the first wave. In transit the wave

is attenuated by the factor $e^{-\alpha(2s+z)}$ due to the line, by a factor Γ_s due to reflection at Z_s, and by a factor Γ_0 due to reflection at Z_0. Similarly there is a phase lag $\beta(2s + z)$ due to the distance traversed on the line and phase shifts ψ_s and ψ_0 due to reflection at Z_s and Z_0. All succeeding terms in (2) may be interpreted in a manner analogous to that used to describe the first three terms. Each is a contribution to the voltage at the point z from components that started at $z = 0$ sufficiently early to travel as a constant phase back and forth along the line. In so doing the amplitude suffers a continuous exponential attenuation, and the phase suffers a linearly increasing lag with respect to the voltage at $z = 0$. In successive reflections at each of the two ends, discontinuous changes in amplitude and phase supplement the effect of the line. The number of reflections at each end is given by the powers to which the factors Γ_0 and Γ_s, which characterize a single reflection, are raised. The total distance traveled by each component is given by the factor of α in the exponents or of β in the phases. In terms of this physically attractive picture the instantaneous potential difference at any point along a terminated transmission line is the resultant of all the contributions reaching that point simultaneously from both directions after an infinity of successive reflections at the ends. The terminated line is thus seen to play the role of an infinite line folded back and forth upon itself, with discontinuities at intervals equal to the actual length and with the potential difference in these folded parts actually superimposed and combined algebraically into a single value.

This interpretation can be obtained directly from the complex series (1) if it is recalled that a complex quantity involves a real amplitude and a phase shift. That is, once the relationship between complex and real instantaneous values is understood, the essential points may be determined directly from the complex form without the real solution. A similar expansion and interpretation may be used for the current.

7. Incident- and Reflected-wave Form of the Exponential Solution.[11] An alternative physical picture of the exponential solution of the transmission-line equations is often given in a form of Sec. 5, Eqs. (10) and (11), in which the voltage V_s across, and the current $I_s = V_s/Z_s$ in, the terminal impedance Z_s are introduced explicitly. The voltage V_s is obtained by setting $z = s$ in Sec. 5, Eq. (10). It is

$$V_s = \frac{V_0^s Z_c}{Z_c + Z_0} \frac{e^{-\gamma s}(1 + \Gamma_s)}{1 - \Gamma_0 \Gamma_s e^{-2\gamma s}} \tag{1}$$

Similarly, from Sec. 5, Eq. (11),

$$I_s = \frac{V_0^s}{Z_c + Z_0} \frac{e^{-\gamma s}(1 - \Gamma_s)}{1 - \Gamma_0 \Gamma_s e^{-2\gamma s}} \tag{2}$$

If (1) and (2) are substituted in Sec. 5, Eqs. (10) and (11), and the notation

$$w \equiv s - z \tag{3}$$

is introduced, the following expressions are obtained:

$$\boldsymbol{V}_z = \frac{\boldsymbol{V}_s}{1 + \boldsymbol{\Gamma}_s}(e^{\gamma w} + \boldsymbol{\Gamma}_s e^{-\gamma w}) = \frac{\boldsymbol{I}_s \boldsymbol{Z}_c}{1 - \boldsymbol{\Gamma}_s}(e^{\gamma w} + \boldsymbol{\Gamma}_s e^{-\gamma w}) \tag{4}$$

$$\boldsymbol{I}_z = \frac{\boldsymbol{V}_s}{\boldsymbol{Z}_c(1 + \boldsymbol{\Gamma}_s)}(e^{\gamma w} - \boldsymbol{\Gamma}_s e^{-\gamma w}) = \frac{\boldsymbol{I}_s}{1 - \boldsymbol{\Gamma}_s}(e^{\gamma w} - \boldsymbol{\Gamma}_s e^{-\gamma w}) \tag{5}$$

It is clear that the *distribution* of current depends on $w = s - z$, not on z alone. The instantaneous real solutions are obtained by multiplying by $e^{j\omega t}$ and selecting the real parts. Thus, for example, the first equation in (4) leads to

$$v_z = \text{Re } \boldsymbol{V}_z e^{j\omega t} = \left|\frac{\boldsymbol{V}_s}{1 + \boldsymbol{\Gamma}_s}\right| [e^{\alpha w} \cos(\omega t + \beta w + \Phi) + \Gamma_s e^{-\alpha w} \cos(\omega t - \beta w + \psi_s + \Phi)] \tag{6}$$

where Φ is given by

$$\frac{\boldsymbol{V}_s}{1 + \boldsymbol{\Gamma}_s} = \left|\frac{\boldsymbol{V}_s}{1 + \boldsymbol{\Gamma}_s}\right| e^{j\Phi} \tag{7}$$

This instantaneous voltage consists of two terms. The phase velocity for the first term is obtained by holding the total phase constant and differentiating with respect to time. This gives

$$-\frac{dw}{dt} = \frac{dz}{dt} = \frac{\omega}{\beta} = v_p \tag{8}$$

The phase velocity of the second term is

$$-\frac{dw}{dt} = \frac{dz}{dt} = -\frac{\omega}{\beta} = -v_p \tag{9}$$

Accordingly the first term in (6) represents a voltage wave traveling in the positive z direction with phase velocity v_p, whereas the second term represents a wave traveling in the negative z direction with the same velocity. Thus the instantaneous voltage v_z at z may be considered to be made up of the sum of a composite wave of amplitude $|\boldsymbol{V}_s/(1 + \boldsymbol{\Gamma}_s)|e^{\alpha w}$ traveling toward $\boldsymbol{Z}_s$ and a composite wave of amplitude $|\boldsymbol{V}_s/(1 + \boldsymbol{\Gamma}_s)|\boldsymbol{\Gamma}_s e^{-\alpha w}$ traveling in the opposite direction. The two waves differ in phase by $\psi_s - 2\beta w$, corresponding to a greater distance of travel for the second wave from the point z to $\boldsymbol{Z}_s$ and back to z, with a phase shift ψ_s on reflection at $\boldsymbol{Z}_s$. The wave traveling toward $\boldsymbol{Z}_s$ is the *incident* wave; that traveling away from $\boldsymbol{Z}_s$ is the *reflected* wave. Note that these *composite* waves have amplitudes that are intricate functions of the parameters of the line and of both $\boldsymbol{Z}_0$ and $\boldsymbol{Z}_s$, and that the origin of the waves is not readily determined by noting the distance traveled.

The relative phases and amplitudes of the two terms in (4) and (5) are represented in the following alternative formulas:

$$V_z = \frac{V_s}{1 + \Gamma_s} e^{\gamma w}[1 + \Gamma_s e^{-2\alpha w} e^{j(\psi - 2\beta w)}] \tag{10}$$

$$I_z = \frac{V_s}{Z_c(1 + \Gamma_s)} e^{\gamma w}[1 - \Gamma_s e^{-2\alpha w} e^{j(\psi - 2\beta w)}] \tag{11}$$

A plot of the bracket in (10) is given with $\alpha = 0$ in Fig. 7.1 and with $\alpha \neq 0$ in Fig. 7.2.

It is instructive to compare the representation of the exponential solution [Sec. 5, Eq. (10)], first, by an infinite series as in Sec. 6, Eq. (1) and, secondly, by two terms as in (6). The first representation expresses the instantaneous solution as an infinite sum of individually simple terms, each of which is the solution of an infinite line folded back upon itself.

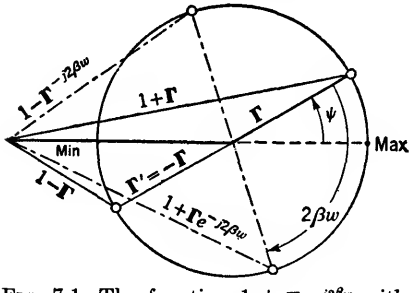


FIG. 7.1. The function $1 + \Gamma e^{-j2\beta w}$ with $\Gamma = \Gamma e^{j\psi}$; $\Gamma = 0.6$, $\psi = 30°$.

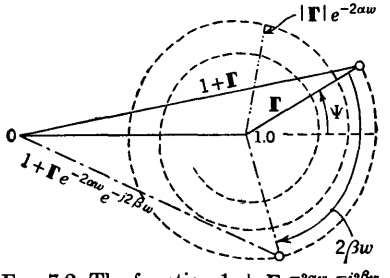


FIG. 7.2. The function $1 + \Gamma e^{-2\alpha w} e^{-j2\beta w}$ with $\Gamma = \Gamma e^{j\psi}$; $\Gamma = 0.6$, $\psi = 30°$.

The contribution by each term is made up of the fraction of the generator voltage impressed across the line, modified in amplitude and phase by the effect of the over-all distance traversed on the line and by the coefficient of reflection at each end appearing as a factor for *each* reflection. The instantaneous voltage at a given point is thus made up of the simultaneously arriving contributions of an infinite number of simple waves that have traveled back and forth, with one term for each possible distance between generator and point of determination.

The second representation, using only two composite terms, in effect separates the infinite series into two parts, as determined by the direction of motion at the point z at the instant t. Thus all terms representing waves traveling in the positive z direction are combined into a single composite wave, the *incident* wave; similarly all terms representing waves traveling in the negative z direction are combined into a composite *reflected* wave. Each of the two resulting composite waves is the superposition of an infinite number of simple waves traveling simultaneously in one direction. As such, its amplitude involves the effect of all reflections at both ends and does not represent each by an explicit factor.

The regrouping of an infinite number of simple waves into two composite ones traveling in opposite directions is analytically convenient but not physically so transparent as the superposition of an infinite number of simple waves. In particular, the physical interpretation of the coefficients of reflection Γ_0 and Γ_s as modifying amplitude and phase at *each* reflection is lost, and the expressions (4) and (5) may as well be made more symmetrical by substituting for Γ_s the equivalent $(Z_s - Z_c)/(Z_s + Z_c)$. The resulting expressions are

$$\begin{aligned} V_z &= \frac{V_s}{2Z_s}(Z_s + Z_c)e^{\gamma w} + \frac{V_s}{2Z_s}(Z_s - Z_c)e^{-\gamma w} \\ &= \tfrac{1}{2}I_s(Z_s + Z_c)e^{\gamma w} + \tfrac{1}{2}I_s(Z_s - Z_c)e^{-\gamma w} \end{aligned} \tag{12}$$

$$\begin{aligned} I_z &= \frac{V_s}{2Z_cZ_s}(Z_s + Z_c)e^{\gamma w} - \frac{V_s}{2Z_cZ_s}(Z_s - Z_c)e^{-\gamma w} \\ &= \frac{I_s}{2Z_c}(Z_s + Z_c)e^{\gamma w} - \frac{I_s}{2Z_c}(Z_s - Z_c)e^{-\gamma w} \end{aligned} \tag{13}$$

Some writers introduce the notation

$$V_z \equiv V_z^+ + V_z^- \qquad I_z = I_z^+ + I_z^- \tag{14}$$

$$V_z^+ \equiv \frac{V_s}{2Z_s}(Z_s + Z_c)e^{\gamma w} = \tfrac{1}{2}I_s(Z_s + Z_c)e^{\gamma w} \qquad I_z^+ = \frac{V_s^+}{Z_c} \tag{15}$$

$$V_z^- \equiv \frac{V_s}{2Z_s}(Z_s - Z_c)e^{-\gamma w} = \tfrac{1}{2}I_s(Z_s - Z_c)e^{-\gamma w} \qquad I_z^- = -\frac{V_z^-}{Z_c} \tag{16}$$

Then $V_z = V_s^+e^{\gamma w} + V_s^-e^{-\gamma w}$; $I_z = I_s^+e^{\gamma w} + I_s^-e^{-\gamma w}$ $\quad w \equiv s - z$ (17)

where

$$\begin{aligned} V_s^+ &= \frac{I_s}{2}(Z_s + Z_c) = \frac{V_s}{2Z_s}(Z_s + Z_c) \\ V_s^- &= \frac{I_s}{2}(Z_s - Z_c) = \frac{V_s}{2Z_s}(Z_s - Z_c) \end{aligned} \tag{18}$$

$$\begin{aligned} I_s^+ &= \frac{I_s}{2Z_c}(Z_s + Z_c) = \frac{V_s}{2Z_cZ_s}(Z_s + Z_c) \\ I_s^- &= -\frac{I_s}{2Z_c}(Z_s - Z_c) = -\frac{V_s}{2Z_cZ_s}(Z_s - Z_c) \end{aligned} \tag{19}$$

Clearly, from (10) and (11), with $j\psi = 2\gamma w = j2\beta w$, for $\gamma = j\beta$ and $\alpha = 0$,

$$\left.\begin{aligned} V_z &= V_s^+e^{\gamma w}(1 + |\Gamma_s|) = V_{z,\max} \\ I_z &= I_s^+e^{\gamma w}(1 - |\Gamma_s|) = I_{z,\min} \end{aligned}\right\} \text{ at } \psi - 2\beta w = 0,\ 2\pi,\ 4\pi,\ \ldots \tag{20}$$

Similarly, at $j\psi = 2\gamma w + j\pi$,

$$\left.\begin{aligned} V_z &= V_s^+e^{\gamma w}(1 - |\Gamma_s|) = V_{z,\min} \\ I_z &= I_s^+e^{\gamma w}(1 + |\Gamma_s|) = I_{z,\max} \end{aligned}\right\} \text{ at } \psi - 2\beta w = \pi,\ 3\pi,\ \ldots \tag{21}$$

The terms with the superscript + are for waves traveling in the positive z direction; those with the superscript − are for waves traveling in the negative z direction.

Note that

$$\Gamma_s = \frac{V_s^-}{V_s^+} = -\frac{I_s^-}{I_s^+} = -\Gamma_s' \tag{22}$$

so that the reflection coefficient Γ_s may be interpreted as measuring the ratio of the reflected composite voltage wave at Z_s divided by the composite incident wave. Similarly Γ' measures the ratio of current waves. No such interpretation for Γ_0 exists. In fact, Γ_0 does not appear in any of the formulas for two composite waves, being contained exclusively in the amplitudes V_s and I_s.

8. Hyperbolic Forms of the Solution.[7,81] The formulas [Sec. 5, Eqs. (10) and (11)] for the complex current and voltage may be expressed in terms of hyperbolic functions of complex argument by eliminating the reflection factors Γ_0 and Γ_s using Sec. 5, Eq. (7), and the definitions of the hyperbolic sine and cosine, viz.,

$$\cosh u \equiv \tfrac{1}{2}(e^u + e^{-u}) \qquad \sinh u \equiv \tfrac{1}{2}(e^u - e^{-u}) \tag{1}$$

where u stands for γs in the denominators and $\gamma(s - z)$ in the numerators of Sec. 5, Eqs. (10) and (11). With $w = s - z$ the two expressions are

$$V_z = \frac{V_0^e Z_c}{D}(Z_s \cosh \gamma w + Z_c \sinh \gamma w) \tag{2}$$

$$I_z = \frac{V_0^e}{D}(Z_s \sinh \gamma w + Z_c \cosh \gamma w) \tag{3}$$

where

$$D = (Z_c^2 + Z_0 Z_s) \sinh \gamma s + Z_c(Z_0 + Z_s) \cosh \gamma s \tag{4}$$

These expressions explicitly involve γ and Z_c and the terminal impedances Z_0 and Z_s; coefficients of reflection do not appear. These alternative forms of Sec. 5, Eqs. (10) and (11), do not lend themselves to a simple physical interpretation in terms of successive reflections.

The formulas (2) and (3) are too complicated to permit a direct visualization or simple graphical representation of the distributions of current and voltage. Very considerable simplification from this point of view may be achieved by employing the same method previously used in simplifying the exponential forms, viz., introducing the voltage and current at $z = s$ explicitly. These are

$$V_s = \frac{V_0^e Z_c Z_s}{D} = I_s Z_s \qquad I_s = \frac{V_0^e Z_c}{D} \tag{5}$$

If these values are substituted in (2) and (3) to eliminate V_0^e/D, the following formulas are easily deduced:

$$V_z = V_s \cosh \gamma w + I_s Z_c \sinh \gamma w \tag{6}$$

$$I_z = \frac{V_s}{Z_c} \sinh \gamma w + I_s \cosh \gamma w \tag{7}$$

It is clear from (6) and (7) that the voltage and current at any point along a terminated transmission line depend on the distance $w = s - z$ of the point from the *output* end. Furthermore they may be expressed entirely in terms of the voltage across, and the current into, the terminal impedance $\boldsymbol{Z}_s$. The formulas (2) and (3) are in this way divided into two somewhat simpler parts. The first permits the investigation of the current and voltage at any point along the line in terms of the current and voltage at the output end. The second, as given in (5), involves the current and the voltage at the output end.

It is evidently possible to express Eqs. (6) and (7) in the following general form:

$$\boldsymbol{V}_z = \boldsymbol{A}\boldsymbol{V}_s + \boldsymbol{B}\boldsymbol{I}_s \tag{8a}$$

$$\boldsymbol{I}_z = \boldsymbol{C}\boldsymbol{V}_s + \boldsymbol{D}\boldsymbol{I}_s \tag{8b}$$

where, in the present case of a transmission line, the four complex coefficients $\boldsymbol{A}$, $\boldsymbol{B}$, $\boldsymbol{C}$, and $\boldsymbol{D}$ have the following values:

$$\boldsymbol{A} = \boldsymbol{D} = \cosh \gamma w \tag{9a}$$

$$\boldsymbol{B} = \boldsymbol{Z}_c^2\boldsymbol{C} = \boldsymbol{Z}_c \sinh \gamma w \tag{9b}$$

Since (8*a*) and (8*b*) are, in fact, the general equations of a four-terminal network of lumped elements, it is clear that a section of line between the points z and s must be equivalent to such a four-terminal network. This is considered in Chap. III, Sec. 12.

An alternative method of simplifying (2) and (3) involves the definition of functions to replace the reflection coefficients $\boldsymbol{\Gamma}_0$ and $\boldsymbol{\Gamma}_s$. It will be recalled that $\boldsymbol{\Gamma}_0$ and $\boldsymbol{\Gamma}_s$ may be interpreted as a measure of the change in amplitude and the shift in phase produced by *each* of an infinite number of successive reflections of a wave traveling back and forth along the line. The new functions that are to replace $\boldsymbol{\Gamma}_0$ and $\boldsymbol{\Gamma}_s$ are defined to be a measure of *the complete or over-all attenuation and phase shift* by the termination, that is, to represent as a single effect the composite effect of all the reflections at a given termination.

The complex terminal function $\boldsymbol{\theta}$ and its real and imaginary parts, the terminal *attenuation function* ρ and the terminal *phase function* Φ, are defined as follows:

$$\boldsymbol{\theta} \equiv \rho + j\Phi \equiv \coth^{-1} \frac{\boldsymbol{Z}}{\boldsymbol{Z}_c} \tag{10}$$

A subscript 0 or s is used on $\boldsymbol{\theta}$, ρ, Φ, and $\boldsymbol{Z}$ to distinguish between the terminations at $z = 0$ and $z = s$. An alternative definition that is at times more convenient is

$$\boldsymbol{\theta}' \equiv \rho + j\Phi' \equiv \tanh^{-1} \frac{\boldsymbol{Z}}{\boldsymbol{Z}_c} \tag{11}$$

It is readily verified that the primed functions differ from the unprimed

by the following very simple relation:

$$\theta' = \theta \pm \frac{j\pi}{2} \qquad \Phi' = \Phi \pm \frac{\pi}{2} \tag{12}$$

The proof reduces to showing that

$$\coth (\rho + j\Phi) = \tanh \left(\rho + j\Phi \pm \frac{j\pi}{2}\right) \tag{13}$$

Using Dwight formulas 655.3 and 655.4, this is accomplished at once. It is shown later that Φ is measured from zero current into the termination and Φ' from zero voltage across the termination.

If the numerator and denominator of (2) are divided by Z_c^2 and Z_0/Z_c and Z_s/Z_c are replaced, respectively, by $\coth \theta_0$ and $\coth \theta_s$, according to (10) it follows that

$$V_z = V_0^e \frac{\coth \theta_s \cosh \gamma w + \sinh \gamma w}{(1 + \coth \theta_0 \coth \theta_s) \sinh \gamma s + (\coth \theta_0 + \coth \theta_s) \cosh \gamma s} \tag{14}$$

With suitable rearrangements this expression becomes

$$V_z = V_0^e \frac{\sinh \theta_0 \cosh (\gamma w + \theta_s)}{\sinh (\gamma s + \theta_0 + \theta_s)} \tag{15}$$

Similarly

$$I_z = \frac{V_0^e}{Z_c} \frac{\sinh \theta_0 \sinh (\gamma w + \theta_s)}{\sinh (\gamma s + \theta_0 + \theta_s)} \tag{16}$$

If the definition (11) is used instead of (10), the corresponding formulas are

$$V_z = V_0^e \frac{\cosh \theta_0' \sinh (\gamma w + \theta_s')}{\sinh (\gamma s + \theta_0' + \theta_s')} \tag{17}$$

$$I_z = \frac{V_0^e}{Z_c} \frac{\cosh \theta_0' \cosh (\gamma w + \theta_s')}{\sinh (\gamma s + \theta_0' + \theta_s')} \tag{18}$$

These relations may be referred to voltage and current at $z = s$. Thus, from (15) and (16),

$$V_s = V_0^e \frac{\sinh \theta_0 \cosh \theta_s}{\sinh (\gamma s + \theta_0 + \theta_s)} \tag{19}$$

$$I_s = \frac{V_0^e}{Z_c} \frac{\sinh \theta_0 \sinh \theta_s}{\sinh (\gamma s + \theta_0 + \theta_s)} \tag{20}$$

For convenience let the *modified terminal voltage* $\bar{V}_s$ be defined as follows:

$$\bar{V}_s \equiv V_0^e \frac{\sinh \theta_0}{\sinh (\gamma s + \theta_0 + \theta_s)} = \frac{V_s}{\cosh \theta_s} = \frac{I_s Z_c}{\sinh \theta_s} \tag{21}$$

Using (21), (15) and (16) reduce to

$$V_z = \bar{V}_s \cosh (\gamma w + \theta_s) = \bar{V}_s \cosh [(\alpha w + \rho_s) + j(\beta w + \Phi_s)] \tag{22}$$

$$I_z = \frac{\bar{V}_s}{Z_c} \sinh (\gamma w + \theta_s) = \frac{\bar{V}_s}{Z_c} \sinh [(\alpha w + \rho_s) + j(\beta w + \Phi_s)] \tag{23}$$

These formulas reduce to a particularly simple form for a lossless line with a dissipationless load, for which, as is discussed later in detail,

$$\alpha = 0 \qquad \gamma = j\beta \qquad Z_c = R_c \tag{24}$$

$$\rho_s = 0 \qquad \theta_s = j\Phi_s = j\left(\Phi_s' + \frac{\pi}{2}\right) \tag{25}$$

$$V_z = \bar{V}_s \cos(\beta w + \Phi_s) = -\bar{V}_s \sin(\beta w + \Phi_s') \tag{26}$$

$$I_z R_c = \bar{V}_s \sin(\beta w + \Phi_s) = \bar{V}_s \cos(\beta w + \Phi_s') \tag{27}$$

For a short-circuited line for which $Z_s = 0$, $\Phi_s = \pi/2$, and $\Phi_s' = 0$ (as shown in Sec. 15),

$$V_z = -\bar{V}_s \sin \beta w \tag{28}$$

$$I_z R_c = \bar{V}_s \cos \beta w \tag{29}$$

For an open-circuited line for which $Z_s = \infty$, $\Phi_s = 0$, and $\Phi_s' = -\pi/2$ (as shown in Sec. 15),

$$V_z = \bar{V}_s \cos \beta w \tag{30}$$

$$I_z R_c = \bar{V}_s \sin \beta w \tag{31}$$

The completely hyperbolic forms of the solution, as expressed in (22) and (23), represent the general case with arbitrary terminations in a form analogous to the simple form of a lossless line. The phase function Φ_s represents the over-all phase shift due to the termination at $z = s$ (as distinguished from the phase shift per reflection given by the argument of the reflection coefficient). The function Φ_0 plays a similar part for the termination at $z = 0$.

The part played by the attenuation functions ρ_0 and ρ_s is best seen in the amplitude factor $\bar{V}_s$ in (21). Thus in

$$\bar{V}_s \equiv V_0^e \frac{\sinh(\rho_0 + j\Phi_0)}{\sinh[\alpha s + \rho_0 + \rho_s + j(\beta s + \Phi_0 + \Phi_s)]} \tag{32}$$

ρ_0 and ρ_s contribute the over-all attenuation due to the terminations in the same manner as αs contributes the over-all attenuation due to the line.

9. Instantaneous Values of the Hyperbolic Solutions. The instantaneous voltage and current are obtained by multiplying the respective complex quantities by $e^{j\omega t}$ and taking the real parts. For this purpose it is necessary to express the complex quantities in polar form, which, in turn, involves the polar forms of complex hyperbolic functions. These are

$$\sinh(u + jv) = \boldsymbol{S} = Se^{j\sigma} \tag{1}$$

$$\cosh(u + jv) = \boldsymbol{C} = Ce^{j\epsilon} \tag{2}$$

where

$$S = \sqrt{\tfrac{1}{2}(\cosh 2u - \cos 2v)} = \sqrt{\sinh^2 u + \sin^2 v} \tag{3}$$

$$C = \sqrt{\tfrac{1}{2}(\cosh 2u + \cos 2v)} = \sqrt{\sinh^2 u + \cos^2 v} \tag{4}$$

$$\sigma = \tan^{-1} \frac{\tan v}{\tanh u} \tag{5}$$

$$\epsilon = \tan^{-1}(\tan v \tanh u) \tag{6}$$

With this notation Sec. 8, Eqs. (15) and (16), become

$$\boldsymbol{V}_s = V_0^e \frac{\boldsymbol{S}_0\boldsymbol{C}_w}{\boldsymbol{S}_s} = V_0^e \frac{S_0 C_w}{S_s} e^{j(\sigma_0+\epsilon_w-\sigma_s)} \tag{7}$$

$$\boldsymbol{I}_s = \frac{V_0^e}{\boldsymbol{Z}_c}\frac{\boldsymbol{S}_0\boldsymbol{S}_w}{\boldsymbol{S}_s} = \frac{V_0^e}{Z_c}\frac{S_0 S_w}{S_s} e^{j(\sigma_0+\sigma_w-\sigma_s-\phi_c)} \tag{8}$$

where

$$\boldsymbol{S}_0 = S_0 e^{j\sigma_0} = \sinh \boldsymbol{\theta}_0 = \sinh (\rho_0 + j\Phi_0) \tag{9}$$

$$\boldsymbol{S}_w = S_w e^{j\sigma_w} = \sinh (\gamma w + \boldsymbol{\theta}_s) = \sinh [\alpha w + \rho_s + j(\beta w + \Phi_s)]$$
$$\equiv \sinh (A_w + jF_w) \tag{10}$$

$$\boldsymbol{C}_w = C_w e^{j\epsilon_w} = \cosh (\gamma w + \boldsymbol{\theta}_s) = \cosh [\alpha w + \rho_s + j(\beta w + \Phi_s)]$$
$$\equiv \cosh (A_w + jF_w) \tag{11}$$

$$\boldsymbol{S}_s = S_s e^{j\sigma_s} = \sinh (\gamma s + \boldsymbol{\theta}_0 + \boldsymbol{\theta}_s) = \sinh [\alpha s + \rho_0 + \rho_s + j(\beta s + \Phi_0 + \Phi_s)]$$
$$\equiv \sinh (A_s + jF_s) \tag{12}$$

$$\boldsymbol{Z}_c = Z_c e^{j\phi} \tag{13}$$

In particular $$\boldsymbol{V}_s = V_0^e \frac{\boldsymbol{S}_0}{\boldsymbol{S}_s} = V_0^e \frac{S_0}{S_s} e^{j(\sigma_0-\sigma_s)} = V_s e^{j(\sigma_0-\sigma_s)} \tag{14}$$

$$V_s = V_0^e \frac{S_0}{S_s} = V_0^e \sqrt{\frac{\cosh 2\rho_0 - \cos 2\Phi_0}{\cosh 2A_s - \cos 2F_s}} = V_0^e \sqrt{\frac{\sinh^2 \rho_0 + \sin^2 \Phi_0}{\sinh^2 A_s + \sin^2 F_s}} \tag{15a}$$

$$\sigma_0 - \sigma_s = \tan^{-1} \frac{\tan \Phi_0}{\tanh \rho_0} - \tan^{-1} \frac{\tan F_s}{\tanh A_s} \tag{15b}$$

The instantaneous real voltage is obtained by multiplying both sides of (7) by $e^{j\omega t}$ and taking the real part to correspond to a driving voltage

$$v_0^e = V_0^e \cos \omega t \tag{16a}$$

Thus $$v_z = V_0^e \frac{S_0 C_w}{S_s} \cos (\omega t + \sigma_0 - \sigma_s + \epsilon_w) \tag{16b}$$

For fixed terminations (16*b*) may be interpreted as a *single wave of composite amplitude and phase.*

The distribution of voltage along the line at particular instants may be investigated conveniently by setting $\omega t' = \omega t + \sigma_0 - \sigma_s$, so that

$$v_z = V_0^e \frac{S_0}{S_s} \sqrt{\sinh^2 A_w + \cos^2 F_w} \cos \epsilon_w (\cos \omega t' - \tan \epsilon_w \sin \omega t') \tag{16c}$$

With (6) and (11) this may be expressed as follows:

$$v_z = V_0^e \frac{S_0}{S_s} \sqrt{\frac{\sinh^2 A_w + \cos^2 F_w}{1 + \tanh^2 A_w \tan^2 F_w}} [\cos \omega t' - (\tanh A_w \tan F_w) \sin \omega t'] \tag{16d}$$

Rearrangement gives

$$v_z = V_0^e \frac{S_0}{S_s} (\cosh A_w \cos F_w \cos \omega t' - \sinh A_w \sin F_w \sin \omega t') \tag{17a}$$

Note that, for a matched line with $\rho_s = \infty$, (17*a*) reduces to the expression previously obtained in Chap. I, Sec. 14, using the exponential form

of the solution. Specifically, when $\rho_s \to \infty$, $\sigma_s \to \beta s + \Phi_0 + \Phi_s$, and

$$\frac{\sinh A_w}{S_s} \to \frac{\cosh A_w}{S_s} \to \frac{e^{\alpha w+\rho_s}}{e^{\alpha s+\rho_0+\rho_s}} = e^{-\rho_0}e^{-\alpha z} \qquad \text{where } z = s - w \quad (17b)$$

so that $$v_z = V_0^e S_0 e^{-\rho_0} e^{-\alpha z} \cos(\omega t - \beta z + \sigma_0 - \Phi_0) \quad (17c)$$

This is the same as Chap. I, Sec. 14, Eq. (3), when $\rho_0 = 0$ and $\Phi_0 = \pi/2$.

Convenient instants for studying the distribution of voltage in the general case (17*a*) are $\omega t' = 0$ and $\omega t' = \pi/2$. At these instants the voltage distributions are

For $\omega t' = 0$: $$v_z = \frac{V_0^e S_0}{S_s} \cosh A_w \cos(\beta w + \Phi_s) \quad (18a)$$

For $\omega t' = \frac{\pi}{2}$: $$v_z = \frac{V_0^e S_0}{S_s} \sinh A_w \sin(\beta w + \Phi_s) \quad (18b)$$

Note that these distributions resemble (17*c*) in that they are sinusoidal, but that the amplitude factors behave quite differently in that they have different values at different instants of time. This means that, for a wave traveling along the line with a finite (but not necessarily constant) velocity, the amplitude varies with location. Note that, for $\alpha w \ll \rho_s$, A_w is essentially constant.

The phase velocity of the sinusoidal wave with variable amplitude may be determined in the usual manner by selecting an arbitrary phase ψ and differentiating it with respect to time. Let

$$\psi = \omega t + \sigma_0 - \sigma_s + \epsilon_w = \text{constant}$$

Then $$\frac{d\psi}{dt} = \omega + \frac{d\epsilon_w}{dt} = 0 \quad (19)$$

(Note that σ_0 and σ_s are constants that do not involve t, z, or w.) Introducing the variable $w = s - z$, (19) may be expressed as follows:

$$\omega + \frac{d\epsilon_w}{dw}\frac{dw}{dt} = \omega - \frac{d\epsilon_w}{dw}\frac{dz}{dt} = 0 \quad (20)$$

Hence the phase velocity is given by

$$v_p = \frac{dz}{dt} = -\frac{dw}{dt} = \frac{\omega}{d\epsilon_w/dw} \quad (21)$$

where $$\epsilon_w = \tan^{-1}[\tan(\beta w + \Phi_s) \tanh(\alpha w + \rho_s)] \quad (22)$$

Differentiation using the formula

$$\frac{d}{dw}(\tan^{-1} x) = \frac{1}{1 + x^2}\frac{dx}{dw} \quad (23)$$

gives $$\frac{d\epsilon_w}{dw} = \frac{d/dw[\tan(\beta w + \Phi_s) \tanh(\alpha w + \rho_s)]}{1 + \tan^2(\beta w + \Phi_s) \tanh^2(\alpha w + \rho_s)} \quad (24)$$

Using the standard relations

$$\frac{d}{dw}\tan x = \sec^2 x \frac{dx}{dw} \tag{25a}$$

$$\frac{d}{dw}\tanh x = \operatorname{sech}^2 x \frac{dx}{dw} \tag{25b}$$

in (24), the result is

$$\frac{d\epsilon_w}{dw} = \frac{\beta \tanh(\alpha w + \rho_s)\sec^2(\beta w + \Phi_s) + \alpha \tan(\beta w + \Phi_s)\operatorname{sech}^2(\alpha w + \rho_s)}{1 + \tan^2(\beta w + \Phi_s)\tanh^2(\alpha w + \rho_s)} \tag{26}$$

Accordingly, with $\beta = \omega/v$, $F_w \equiv \beta w + \Phi_s$, and $A_w \equiv \alpha w + \rho_s$,

$$v_p = \frac{\omega}{d\epsilon_w/dw} = v\frac{1 + \tan^2 F_w \tanh^2 A_w}{\tanh A_w \sec^2 F_w + (\alpha/\beta)\tan F_w \operatorname{sech}^2 A_w} \tag{27}$$

Note that v is the phase velocity previously obtained for an *infinitely long or matched line.* Equation (27) can be rearranged by multiplying numerator and denominator by $\cosh^2 A_w \cos^2 F_w$. Thus

$$v_p = v\frac{\cosh^2 A_w \cos^2 F_w + \sinh^2 A_w \sin^2 F_w}{\sinh A_w \cosh A_w + (\alpha/\beta)\sin F_w \cos F_w} \tag{28}$$

The division of (28) by $\cosh A_w \sinh A_w$ and the introduction of double arguments give

$$(v_p)_{\text{voltage}} = v\frac{\coth A_w \cos^2 F_w + \tanh A_w \sin^2 F_w}{1 - \frac{\alpha}{\beta}\frac{\sin 2F_w}{\sinh 2A_w}} \tag{29}$$

The corresponding expression for the phase velocity of the current is obtained in the same manner. It is

$$(v_p)_{\text{current}} = v\frac{\coth A_w \sin^2 F_w + \tanh A_w \cos^2 F_w}{1 - \frac{\alpha}{\beta}\frac{\sin 2F_w}{\sinh 2A_w}} \tag{30}$$

A simple special case is that of a transmission line with low attenuation per unit length (α small) but sufficiently end-loaded so that

$$\frac{\alpha}{\beta \sinh 2A_w} = \frac{\alpha}{\beta \sinh 2(\alpha w + \rho_s)} \ll 1 \tag{31}$$

In this case the phase velocities for the voltage and current in (29) and (30) are

$$(v_p)_{\text{voltage}} \doteq v(\coth A_w \cos^2 F_w + \tanh A_w \sin^2 F_w) \tag{32}$$

$$(v_p)_{\text{current}} \doteq v(\coth A_w \sin^2 F_w + \tanh A_w \cos^2 F_w) \tag{33}$$

On a low-loss line α/β may be of the order of magnitude of 10^{-3}, so that (31) is satisfied if $\sinh 2(\alpha w + \rho_s) \geqq 0.1$. This is true when $\alpha w + \rho_s \geqq$

0.05. If the line is not loaded, so that $\rho_s = 0$, it follows that

$$\frac{\alpha}{\beta \sinh 2\alpha w} \ll 1 \tag{34a}$$

or, with $\alpha/\beta \doteq 10^{-3}$, $\sinh 2\alpha w \doteq 2\alpha w \geqq 0.1$. This is equivalent to

$$\frac{1}{2\beta w} \leqq 10^{-2} \qquad \beta w \geqq 50 \qquad w \geqq 8\lambda \tag{34b}$$

That is, on a line with low attenuation and no load the phase velocity given by (32) or (33) is accurate only at eight or more wavelengths from the end $z = s$. Nearer to the end than this (29) or (30) must be used.

If the attenuation on the line is small compared with the load,

$$A_w \equiv \alpha w + \rho_s \doteq \rho_s \qquad \alpha w \ll \rho_s \tag{35}$$

The amplitude of the voltage and current distribution along the line as functions of $w = s - z$ is given by

$$V_z \sim C_w = \sqrt{\sinh^2 A_w + \cos^2 F_w} \tag{36}$$

$$I_z \sim S_w = \sqrt{\sinh^2 A_w + \sin^2 F_w} \tag{37}$$

If (35) is true, as is usual on a loaded line, $A_w \doteq \rho_s$ is independent of w, so that V_z is *greatest where* $\cos^2 F_w$ *is greatest and smallest where* $\cos^2 F_w$ *is smallest.* Similarly I_z is greatest where $\sin^2 F_w$ is greatest. Specifically

For $F_w = n\pi$,

$$(V_z)_{\max} \sim C_w = \sqrt{\sinh^2 A_w + 1} = \cosh A_w$$
$$(v_p)_{\text{voltage}} = v \coth A_w = (v_p)_{\max} \tag{38a}$$

$$(I_z)_{\min} \sim S_w = \sinh A_w \qquad (v_p)_{\text{current}} = v \tanh A_w = (v_p)_{\min} \tag{38b}$$

For $F_w = n\pi + \pi/2$,

$$(V_z)_{\min} \sim C_w = \sinh A_w \qquad (v_p)_{\text{voltage}} = v \tanh A_w = (v_p)_{\min} \tag{39a}$$

$$(I_z)_{\max} \sim S_w = \sqrt{\sinh^2 A_w + 1} = \cosh A_w$$
$$(v_p)_{\text{current}} = v \coth A_w = (v_p)_{\max} \tag{39b}$$

Note that $(v_p)_{\max}(v_p)_{\min} = v^2$. Thus the phase velocity is greatest ($v \coth A_w$) where the amplitude is greatest ($\sim \cosh A_w$); the phase velocity is smallest ($v \tanh A_w$) where the amplitude is smallest ($\sim \sinh A_w$). From the behavior of the hyperbolic tangent and cotangent, the extreme values of the phase velocity increase with decreasing A_w and decrease with increasing A_w. In particular, if $\rho_s = \infty$, so that $A_s = \infty$, $\tanh A_w = \coth A_w = 1$, so that $v_p = v =$ constant at all points along the line. This is the *matched* or *infinite line* with running or traveling waves. On the other hand, if the line is essentially lossless with a very small load, $\tanh A_w \doteq A_w$ is very small and $\coth A_w$ is very large, so that the phase velocity is very large where the amplitude is large and extremely small where the amplitude is small.

Since the shape of the voltage (or current) wave *changes as it travels*, the motion of a given phase is not readily visualized. However, two points are always located easily. These are the *zero points* and the points where the *trigonometric factor* has its maximum value of unity. Since the value 1 is multiplied by a varying amplitude, it is not always at the maximum of the traveling wave. However, it is always *at the point of contact* of the varying traveling disturbance, with the amplitude variation plotted as a fixed function of z. Thus the picture is that of a wave of varying shape moving between boundary lines defined by the amplitude, in such a manner that the wave is in contact with these lines at one point in each wavelength. This point of contact and the zero value travel with a phase velocity that increases and decreases along the line with the fixed amplitude distribution. Thus, when the zero point in the instantaneous wave passes the maximum of the amplitude, it is moving with high speed if the transmission line has only a small load. On the other hand, when it passes the minimum in the amplitude, it travels very slowly. The same is true for the point of contact.

10. The Propagation Constant. The complex propagation constant γ defined in Chap. I, Sec. 13, is

$$\gamma = \alpha + j\beta = \sqrt{(r + j\omega l)(g + j\omega c)} = \sqrt{(rg - \omega^2 lc) + j\omega(lg + cr)} \quad (1)$$

The real and imaginary parts of the radical on the right may be separated in two ways leading to equivalent but different formulas for the attenuation constant α and the phase constant β. In the first method both sides of (1) are squared, and the real and imaginary parts equated separately. By solving for α and β and selecting positive roots to make α and β real and positive, the results are

$$\alpha = \sqrt{\tfrac{1}{2}(yz - \omega^2 lc + rg)} \quad (2)$$

$$\beta = \sqrt{\tfrac{1}{2}(yz + \omega^2 lc - rg)} \quad (3)$$

where $$y = \sqrt{g^2 + \omega^2 c^2} \qquad z = \sqrt{r^2 + \omega^2 l^2} \quad (4)$$

In the second method for obtaining explicit expressions of α and β, (1) is arranged as follows:

$$\gamma = \alpha + j\beta = j\sqrt{\omega^2 lc - rg}\,\sqrt{1 - jh_\gamma} \qquad \omega^2 lc > rg \quad (5)$$

$$= \sqrt{rg - \omega^2 lc}\,\sqrt{1 + jh_\gamma} \qquad rg > \omega^2 lc \quad (6)$$

$$= \frac{1 + j}{\sqrt{2}}\sqrt{\omega(lg + rc)} \qquad rg = \omega^2 lc \quad (7)$$

where $$h_\gamma = \left| \frac{\omega(lg + rc)}{\omega^2 lc - rg} \right| \quad (8)$$

The second square root in (5) and (6) is in the form used in defining the tabulated functions $f(h)$ and $g(h)$ (Ref. 9, Appendix II). These functions

are the real and imaginary parts of the square root. Thus

$$\sqrt{1 \pm jh} = f(h) \pm jg(h) \tag{9}$$

The functions $f(h)$ and $g(h)$ are defined as follows:

$$f(h) \equiv \sqrt{\tfrac{1}{2}(\sqrt{1+h^2}+1)} = \cosh\left(\tfrac{1}{2}\sinh^{-1} h\right) \tag{10}$$

$$g(h) \equiv \sqrt{\tfrac{1}{2}(\sqrt{1+h^2}-1)} = \sinh\left(\tfrac{1}{2}\sinh^{-1} h\right) \tag{11}$$

For $h^2 \ll 1$, $\qquad f(h) \doteq 1 \qquad g(h) \doteq \dfrac{h}{2}$ (12)

For $h^2 \gg 1$, $\qquad f(h) \doteq g(h) \doteq \sqrt{\dfrac{h}{2}}$ (13)

Using the notation of (9) in (5), the result is

$$\alpha + j\beta = j\sqrt{\omega^2 lc - rg}\,[f(h_\gamma) - jg(h_\gamma)] \qquad \omega^2 lc > rg \tag{14}$$

$$\alpha + j\beta = \sqrt{rg - \omega^2 lc}\,[f(h_\gamma) + jg(h_\gamma)] \qquad \omega^2 lc < rg \tag{15}$$

For all practical transmission lines $\omega^2 lc$ is always greater than rg. However, in some attenuators rg may exceed $\omega^2 lc$. It follows that

$$\left.\begin{aligned}\alpha &= \sqrt{\omega^2 lc - rg}\, g(h_\gamma)\\ \beta &= \sqrt{\omega^2 lc - rg}\, f(h_\gamma)\end{aligned}\right\} \qquad \omega^2 lc > rg \tag{16}$$

$$\left.\begin{aligned}\alpha &= \sqrt{rg - \omega^2 lc}\, f(h_\gamma)\\ \beta &= \sqrt{rg - \omega^2 lc}\, g(h_\gamma)\end{aligned}\right\} \qquad \omega^2 lc < rg \tag{17}$$

$$\alpha = \beta = \sqrt{\tfrac{1}{2}\omega(lg + rc)} \qquad \omega^2 lc = rg \tag{18}$$

These formulas are more convenient for computing α and β than are (2) and (3) if tables of $f(h)$ and $g(h)$ functions are available. The condition $\omega^2 lc > rg$ is satisfied for all practical high-frequency transmission lines. The important ratio α/β is given by

$$\frac{\alpha}{\beta} = \frac{g(h_\gamma)}{f(h_\gamma)} = \sqrt{\frac{\sqrt{1+h_\gamma^2}-1}{\sqrt{1+h_\gamma^2}+1}} = \frac{1}{h_\gamma}(\sqrt{1+h_\gamma^2}-1) \qquad \omega^2 lc > rg \tag{19a}$$

$$\frac{\beta}{\alpha} = \frac{g(h_\gamma)}{f(h_\gamma)} = \frac{1}{h_\gamma}(\sqrt{1+h_\gamma^2}-1) \qquad rg > \omega^2 lc \tag{19b}$$

Clearly

$$\begin{aligned}&\text{For } \frac{\alpha}{\beta} < 1, && \omega^2 lc > rg\\ &\text{For } \frac{\alpha}{\beta} > 1, && \omega^2 lc < rg\\ &\text{For } \alpha = \beta, && \omega^2 lc = rg\end{aligned} \tag{20}$$

It is readily verified that for $\omega^2 lc > rg$ the following relations are true:

$$\frac{h_\gamma^4}{4} \ll 1 \qquad \frac{\alpha}{\beta} \doteq \frac{h_\gamma}{2} < 1 \tag{21}$$

or, specifically, for an error not exceeding 1 per cent,

$$h_\gamma^2 \leqq 0.2 \qquad h_\gamma \leqq 0.45 \qquad \frac{\alpha}{\beta} \leqq 0.225 \qquad \frac{\alpha^2}{\beta^2} \leqq 0.05 \tag{22}$$

Consequently a good approximation is obtained if α^2/β^2 is neglected in comparison with unity if h_γ does not exceed 0.45.

On the other hand, for $rg > \omega^2 lc$,

$$\frac{h_\gamma^2}{4} \gg 1 \qquad \frac{\beta}{\alpha} \doteq 1 - \frac{1}{h_\gamma} \qquad \frac{\alpha}{\beta} \doteq 1 + \frac{1}{h_\gamma} \tag{23}$$

11. The Characteristic Impedance. The general definition of the characteristic impedance is

$$\boldsymbol{Z}_c \equiv R_c + jX_c \equiv \sqrt{\frac{r + j\omega l}{g + j\omega c}} \tag{1}$$

This also may be separated into real and imaginary parts in two ways corresponding to those used for the propagation constant. In the first manner $\boldsymbol{Z}_c$ is obtained in polar form. Using $\tan^{-1} x = \pi/2 - \tan^{-1}(1/x)$,

$$\boldsymbol{Z}_c = \sqrt[4]{\frac{r^2 + \omega^2 l^2}{g^2 + \omega^2 c^2}}\, exp\, \{(j/2)[\tan^{-1}(g/\omega c) - \tan^{-1}(r/\omega l)]\} \tag{2}$$

In order to make use of the $f(h)$ and $g(h)$ functions, let

$$\boldsymbol{Z}_c = \sqrt{\frac{\omega^2 lc + rg}{\omega^2 c^2 + g^2}} \sqrt{1 - j\,\frac{\omega(rc - lg)}{\omega^2 lc + rg}} \tag{3}$$

and define

$$h_c = \left| \frac{\omega(rc - lg)}{\omega^2 lc + rg} \right| \tag{4}$$

so that (3) is equivalent to

$$\boldsymbol{Z}_c = \sqrt{\frac{\omega^2 lc + rg}{\omega^2 c^2 + g^2}}\, [f(h_c) \pm jg(h_c)] \tag{5}$$

The upper sign is to be used when $rc < lg$; the lower sign is to be used when $rc > lg$, as is usual in all transmission lines immersed in *good* dielectrics. Then

$$R_c = \sqrt{\frac{\omega^2 lc + rg}{\omega^2 c^2 + g^2}}\, f(h_c) \tag{6}$$

$$X_c = \pm \sqrt{\frac{\omega^2 lc + rg}{\omega^2 c^2 + g^2}}\, g(h_c) = \pm R_c \frac{g(h_c)}{f(h_c)} \tag{7}$$

Here the upper sign applies when $rc < lg$; the lower sign applies when $rc > lg$, as is usual. If $rc = lg$, $X_c = 0$ and $f(h_c) = 1$. It is convenient to introduce the quantity ϕ_c, called the distortion factor, by setting

$$\phi_c \equiv \frac{g(h_c)}{f(h_c)} \tag{8}$$

By the same reasoning as was used to establish Sec. 10, Eq. (20), it follows that ϕ_c cannot exceed 1. That is,

For $h_c < \infty$: $$\phi_c < 1 \tag{9}$$

In particular,

For $h_c \leqq 0.45$: $$\phi_c^2 \leqq 0.05 \quad \text{or} \quad \phi_c^2 \ll 1 \tag{10}$$

In terms of (3) to (5) it follows that

$$\begin{aligned} \boldsymbol{Z}_c &= R_c(1 - j\phi_c) && rc > lg \\ \boldsymbol{Z}_c &= R_c(1 + j\phi_c) && rc < lg \\ \boldsymbol{Z}_c &= R_c && rc = lg \end{aligned} \tag{11}$$

$\boldsymbol{Z}_c$ may be expressed in polar form as follows:

$$\boldsymbol{Z}_c = R_c \sqrt{1 + \phi_c^2}\, e^{-j \tan^{-1}\phi_c} \doteq R_c \epsilon^{-j\phi_c} \qquad \text{for } \phi_c^2 \ll 1 \text{ and } rc > lg \tag{12}$$

For $rc < lg$ the sign of ϕ_c is changed; for $rc = lg$, $\phi_c = 0$.

12. The Phase and Group Velocities of the Infinite Line. The velocity of a particular phase of current or voltage traveling along an infinite line or reflected back and forth along a terminated line is defined in Chap. I, Sec. 14, Eq. (10). It is

$$\begin{aligned} v_p \equiv \frac{\omega}{\beta} &= \frac{1}{\sqrt{lc - (rg/\omega^2)\, f(h_\gamma)}} \\ &= \frac{\omega}{\sqrt{\tfrac{1}{2}[\sqrt{(g^2 + \omega^2c^2)(r^2 + \omega^2l^2)} + \omega^2lc - rg]}} \end{aligned} \tag{1}$$

Numerical values may be determined using tables of $f(h)$. At sufficiently high frequencies h_γ, as defined by Sec. 10, Eq. (8), becomes small; $f(h_\gamma)$, as defined by Sec. 10, Eq. (10), approaches unity; and rg/ω^2 in (1) becomes negligible. Hence the upper limit of v_p as the frequency is increased without limit is

$$v_p \to \frac{1}{\sqrt{lc}} \text{ as } \omega \to \infty \tag{2}$$

The lower limit as ω becomes small is obtained most easily using the second form of (1). It is

$$v_p \to 2\sqrt{\frac{rg}{r^2c^2 + g^2l^2}} \text{ as } \omega \to 0 \tag{3}$$

Since v_p is not independent of the frequency, there must be dispersion. The group velocity as defined by Chap. I, Sec. 14, Eq. (19*a*), may be calculated directly from Sec. 10, Eq. (3), or from Sec. 10, Eqs. (16) to (18), using Chap. I, Sec. 14, Eq. (19*a*) or (19*b*). The expression obtained is intricate, and, in general, the group velocity is *not* equal to the phase velocity.

13. Special Forms of the General Parameters of the Line. The general formulas for the complex parameters γ and Z_c of a transmission line may be simplified by imposing restrictive conditions upon the relative magnitudes of some or all of the parameters r, l, c, and g. Although considerable simplification in the form of the general solutions for the current and voltage along the line may be achieved in this manner, it is obtained at the expense of generality. Wherever the particular restrictions imposed are consistent to a satisfactory degree of approximation with the experimental circumstances for which the final formulas are to be used, such simplification is desirable and valuable. Otherwise it must be used with great caution, if at all, and with the realization that results are not dependable in any general sense.

From the point of view of high-frequency circuits the most important special cases are those associated with low values of resistance and leakage conductance. The simplifications leading to the so-called distortionless line or the ocean cable are of minor importance in the high-frequency field.

The Line with Low Attenuation per Unit Length. The conditions that define a transmission line with low attenuation per unit length are

$$\left(\frac{r}{\omega l}\right)^2 \ll 1 \qquad \left(\frac{g}{\omega c}\right)^2 \ll 1 \qquad \frac{rg}{\omega^2 lc} \ll 1 \tag{1}$$

Subject to these conditions,

$$h_\gamma \doteq \frac{1}{\omega}\left(\frac{r}{l} + \frac{g}{c}\right) \qquad h_c \doteq \frac{1}{\omega}\left(\frac{r}{l} - \frac{g}{c}\right) \tag{2}$$

so that

$$h_\gamma^2 \ll 1 \qquad h_c^2 \ll 1 \tag{3}$$

It follows directly from Sec. 10, Eqs. (10) and (11), using (3), that, for $h^2 \ll 1$,

$$f(h) \doteq 1 \qquad g(h) \doteq \frac{h}{2} \tag{4}$$

These relations apply for both subscripts γ and c. Accordingly

$$\alpha \doteq \frac{\sqrt{lc}}{2}\left(\frac{r}{l} + \frac{g}{c}\right) \tag{5}$$

$$\beta \doteq \omega\sqrt{lc} \tag{6}$$

$$\frac{\alpha}{\beta} = \frac{1}{2\omega}\left[\frac{r}{l} + \frac{g}{c}\right] \qquad \text{so that } \frac{\alpha^2}{\beta^2} \ll 1 \tag{7}$$

$$R_c \doteq \sqrt{\frac{l}{c}} \tag{8}$$

$$\phi_c \doteq \frac{h_c}{2} = \frac{1}{2\omega}\left(\frac{r}{l} - \frac{g}{c}\right) \qquad \text{so that } \phi_c^2 \ll 1 \tag{9}$$

$$v_p \doteq \frac{1}{\sqrt{lc}} \doteq v_0 \tag{10}$$

In this special case the phase velocity is to a *first approximation*, equal to the upper limit given in Sec. 12, Eq. (2), which is independent of the frequency, so that no dispersion occurs. It is to be noted that this is only approximately true and that even a small difference in v_p for different frequencies may lead to great over-all dispersion on a line of sufficient length. As shown in the small type below, more accurate formulas are

$$\beta = \omega\sqrt{l^e c}\,(1 + \delta) \tag{11}$$

$$v_p = v_e(1 - \delta) \tag{12}$$

$$v_g = v_e\left(1 - \frac{\delta}{2}\right) \tag{13}$$

$$R_c = \sqrt{\frac{l^e}{c}}\,(1 + \delta) \tag{14}$$

where

$$2\delta = \frac{r}{\omega l^e} \qquad v_e \equiv \frac{1}{\sqrt{l^e c}} \tag{15}$$

Factors of Higher Order in the Parameters of a Line with Low Attenuation at High Frequencies. Although the formulas given in (6) to (10) are excellent approximations for most practical purposes using good transmission lines, it is of value in special instances to determine the first terms neglected in quantities such as R_c, β, v_p, and v_g which are not themselves small, as are α and ϕ_c. Thus, instead of (4),

$$f(h) \doteq \sqrt{1 + \frac{h^2}{4}}$$

so **that**, with Sec. 10, Eq. (16),

$$\beta \doteq \omega\sqrt{lc}\sqrt{\left(1 - \frac{rg}{\omega^2 lc}\right)\left(1 + \frac{h_\gamma^2}{4}\right)}$$

Using (2) and (9) and neglecting higher-order terms,

$$\beta \doteq \omega\sqrt{lc}\sqrt{1 + \frac{h_\gamma^2}{4} - \frac{rg}{\omega^2 lc}} \doteq \omega\sqrt{lc}\sqrt{1 + \frac{h_c^2}{4}} = \omega\sqrt{lc(1 + \phi_c^2)}$$

Accordingly

$$v_p = \frac{\omega}{\beta} = \frac{1}{\sqrt{lc(1 + \phi_c^2)}}$$

In order to determine v_g it is necessary to introduce the specific formula for l because it involves the frequency. Thus with

$$l = 2l^i + l^e \qquad \text{for a two-wire line}$$

$$l = l_a^i + l_b^i + l^e \qquad \text{for a coaxial line}$$

let

$$2\delta = \begin{cases} \dfrac{2l^i}{l^e} & \text{for a two-wire line} \\ \dfrac{l_a^i + l_b^i}{l^e} & \text{for a coaxial line} \end{cases}$$

Using Chap. I, Sec. 4, Eq. (34), and Chap. I, Sec. 6, Eq. (18), which are valid at high

frequencies,

$$2\delta = \frac{2\omega l^i}{\omega l^e} = \frac{2r^i}{\omega l^e} = \frac{r}{\omega l^e} \qquad \text{for the two-wire line}$$

$$2\delta = \frac{\omega(l_a^i + l_b^i)}{\omega l^e} = \frac{r_a^i + r_b^i}{\omega l^e} = \frac{r}{\omega l^e} \qquad \text{for the coaxial line}$$

Hence $$\delta = \frac{r}{2\omega l^e} \quad \text{and} \quad \delta^2 \ll 1$$

Clearly $\phi_c = \frac{1}{2\omega}\left(\frac{r}{l} - \frac{g}{c}\right)$ is never larger than δ, so that ϕ_c^2 is a term of higher order than ϕ_c or δ, subject to $\phi_c^2 \ll 1$ and $\delta_c^2 \ll 1$. Therefore

$$\beta \doteq \omega\sqrt{l^e c(1 + 2\delta)(1 + \phi_c^2)} \doteq \omega\sqrt{l^e c(1 + 2\delta)} \doteq \omega\sqrt{l^e c}\,(1 + \delta)$$

Accordingly $$v_p = \frac{\omega}{\beta} = \frac{1}{\sqrt{l^e c(1 + \delta)}} \doteq \frac{1 - \delta}{\sqrt{l^e c}} = v_e(1 - \delta)$$

where $$v_e \equiv \frac{1}{\sqrt{l^e c}} = \frac{v_0}{\sqrt{\mu_r \epsilon_r}} \doteq \frac{3 \times 10^8 \text{ m/sec}}{\sqrt{\mu_r \epsilon_r}}$$

and μ_r and ϵ_r are the relative permeability and dielectric constant. Also

$$v_g = \frac{1}{\partial\beta/\partial\omega} = \frac{v_e}{1 + \delta + \omega\partial\delta/\partial\omega}$$

But, since at high frequencies r varies as $\sqrt{\omega}$,

$$\delta \equiv \frac{r}{2\omega l^e} = \frac{P}{\sqrt{\omega}}$$

where P is independent of the frequency. Hence

$$\frac{\partial\delta}{\partial\omega} = -\frac{P}{2\omega^{\frac{3}{2}}} = -\frac{\delta}{2\omega}$$

so that $$v_g = \frac{v_e}{1 + \delta - \frac{1}{2}\delta} = \frac{v_e}{1 + \delta/2} \doteq v_e\left(1 - \frac{\delta}{2}\right)$$

It follows that both v_p and v_g are smaller than v_e but that v_g is greater than v_p, so that the dispersion is anomalous. Since δ is very small, the dispersion is also small.

Higher-order terms in R_c are obtained using (6) with $f(h_c) \doteq \sqrt{1 + h_c^2/4}$. Thus

$$R_c = \sqrt{\frac{l^e(1 + 2\delta)(1 + rg/\omega^2 lc)(1 + h_c^2/4)}{c(1 + g^2/\omega^2 c^2)}} = \sqrt{\frac{l^e}{c}}\sqrt{(1 + 2\delta)(1 + h_c^2)(1 - g^2/\omega^2 c^2)}$$

The leading higher-order term is the one in δ, so that

$$R_c \doteq \sqrt{\frac{l^e}{c}(1 + 2\delta)} = \sqrt{\frac{l}{c}} \doteq \sqrt{\frac{l^e}{c}}\,(1 + \delta)$$

Although δ is no smaller than ϕ_c, the error is usually insignificant if δ is neglected, whereas in at least one instance (to be described later) an error of 50 per cent is made if ϕ_c is neglected. This difference is due to the fact that $\phi_c R_c$ is the leading imaginary term in $\boldsymbol{Z}_c$, whereas δR_c is an extremely small fraction of the real part of R_c. It is always a good approximation at high frequencies to neglect δ in computing R_c, so that

$$R_c \doteq \sqrt{\frac{l^e}{c}}$$

The Line with Low Attenuation and Negligible Leakage Conductance per Unit Length. For most high-frequency lines the following condition applies in addition to (1):

$$\frac{g}{\omega c} \ll \frac{r}{\omega l} \tag{16}$$

and further simplification is possible. Thus

$$h_\gamma \doteq h_c \doteq \frac{r}{\omega l} \tag{17}$$

$$\alpha \doteq \frac{r}{2}\sqrt{\frac{c}{l}} = \frac{r}{2R_c} \tag{18}$$

$$\phi_c \doteq \frac{\alpha}{\beta} \doteq \frac{r}{2\omega l} \tag{19}$$

On the other hand, β, R_c, and v_p are as in (6), (8), and (10).

The Line without Attenuation. The extreme simplification afforded by neglecting the resistance of the line is attractive. The physically unrealizable conditions are

$$r \doteq 0 \qquad g \doteq 0 \tag{20}$$

so that

$$h_\gamma \doteq h_c \doteq 0 \tag{21}$$

$$\alpha \doteq 0 \doteq \phi_c \tag{22}$$

The expressions for β, v, and R_c *are the same as for low attenuation.* For this reason a limited number of important results involving sections of line of restricted length may be calculated quite accurately *apparently* by assuming (20). Great care must be exercised in the use of formulas that depend upon (20) and (21), since *correct* results are obtained only when the *same* results are obtained with (20) as with (1) and (16).

The Line with Low Distortion. A line with low distortion is one that need be restricted in *no other* manner except that ϕ_c is sufficiently small so that

$$\phi_c^2 \ll 1 \tag{23}$$

It has already been shown that (23) is equivalent to

$$h_c \leqq 0.45 \tag{24}$$

in which case

$$\phi_c^2 \leqq 0.05 \tag{25}$$

The Distortionless Line. The conditions defining a distortionless line are

$$\phi_c = 0 \qquad \text{or} \qquad \frac{r}{l} = \frac{g}{c} \tag{26}$$

In this case

$$\gamma = \alpha + j\beta = \sqrt{\frac{c}{l}}\,(r + j\omega l) \tag{27}$$

$$Z_c = R_c(1 - j\phi_c) = \sqrt{\frac{l}{c}} \tag{28}$$

Hence
$$\alpha = r\sqrt{\frac{c}{l}} = \frac{r}{R_c} \tag{29}$$
$$\beta = \omega\sqrt{lc} \tag{30}$$
$$R_c = \sqrt{\frac{l}{c}} \qquad \phi_c = 0 \tag{31}$$
$$v_p = \frac{1}{\sqrt{lc}} = v_g \tag{32}$$

If (26) is satisfied, these formulas are not approximate, as when (1) is satisfied, but exact. There would be no dispersion if l were not a function of frequency. At low frequencies in lines where r in ϕ_c affects the phase velocity, considerable improvement can be made by using loading coils to fulfill (26). At high frequencies the condition (26) can be fulfilled only with difficulty, and since the effect of r is smaller than that of l, little is gained. Most high-frequency transmission lines normally fulfill the conditions (1), so that large changes involving an increase in either l or g or both are required before (26) can be satisfied. At high frequencies this has not been found practicable.

Lines with High Attenuation: Attenuators.† The extreme case of high attenuation which leads to considerable simplification in the general formulas involves the following conditions:

$$\left(\frac{r}{\omega l}\right)^2 \gg 1 \qquad \left(\frac{g}{\omega c}\right)^2 \gg 1 \qquad \left(\frac{rg}{\omega^2 lc}\right)^2 \gg 1 \qquad \frac{r}{l} < \frac{g}{c} \tag{33}$$

Hence
$$h_\gamma \doteq \omega\left(\frac{l}{r} + \frac{c}{g}\right) \qquad h_c \doteq \omega\left(\frac{l}{r} - \frac{c}{g}\right) \tag{34}$$
$$h_\gamma^2 \ll 1 \qquad h_c^2 \ll 1 \tag{35}$$

so that
$$f(h) \doteq 1 \qquad g(h) \doteq \frac{h}{2} \tag{36}$$

for both h_γ and h_c. Hence
$$\gamma = \alpha + j\beta \tag{37}$$

with
$$\alpha = \sqrt{rg} \tag{38}$$
$$\beta \doteq rg\,\frac{h_\gamma}{2} \doteq \frac{\omega\sqrt{rg}}{2}\left(\frac{l}{r} + \frac{c}{g}\right) \tag{39}$$

Note that
$$\frac{\beta}{\alpha} = \frac{\omega}{2}\left(\frac{c}{g} + \frac{l}{r}\right) \qquad \frac{\beta^2}{\alpha^2} \ll 1 \tag{40}$$
$$v_p = \frac{\omega}{\beta} = \frac{2\sqrt{rg}}{lg + rc} \tag{41}$$

† Attenuators referred to here are *lossy* and not the beyond-cutoff type familiar in wave-guide theory.

Similarly
$$Z_c = R_c(1 + j\phi_c) \tag{42}$$
$$R_c = \sqrt{\frac{r}{g}} \tag{43}$$
with
$$\phi_c = \frac{h_c}{2} = \frac{\omega}{2}\left(\frac{l}{r} - \frac{c}{g}\right) \tag{44}$$

Line with Large Leakage Conductance and Negligible Resistance. A so-called lossy line may be constructed of very good conductors and a poor dielectric, so that a satisfactory approximation is

$$r \doteq 0 \qquad h_\gamma = h_c = \frac{g}{\omega c} \equiv h \tag{45a}$$

With Sec. 10, Eq. (14), and Sec. 11, Eq. (5), the propagation constant and characteristic impedance are

$$\gamma = \alpha + j\beta = j\omega\sqrt{lc}\,[f(h) - jg(h)] \tag{45b}$$
$$Z_c = R_c + jX_c = \sqrt{\frac{l}{c}}\sqrt{\frac{1}{1 + (g/\omega c)^2}}\,[f(h) + jg(h)] \tag{45c}$$

In two special cases simplification is possible. The first case assumes moderately low attenuation, as defined by

$$g^2 \ll \omega^2 c^2 \qquad h^2 \ll 1 \tag{46a}$$
so that
$$\alpha = \frac{g\sqrt{lc}}{2c} \qquad \beta = \omega\sqrt{lc} \qquad R_c = \sqrt{\frac{l}{c}} \qquad X_c = \frac{gR_c}{2\omega c} \tag{46b}$$

The second special case assumes very high attenuation, as defined by

$$\omega^2 c^2 \ll g^2 \qquad h^2 \gg 1 \tag{47a}$$
so that
$$\alpha \doteq \beta \doteq \sqrt{\frac{\omega lg}{2}} \qquad R_c \doteq X_c \doteq \sqrt{\frac{\omega l}{2g}} \tag{47b}$$

The Ocean Cable. An approximation that serves well for special types of cable, such as those used underwater, is

$$\frac{r}{\omega l} \gg 1 \qquad \frac{g}{\omega c} \ll 1 \tag{48}$$

The first condition is due to low frequencies and very small inductance, not to high resistance. In this case Sec. 10, Eq. (1), and Sec. 11, Eq. (1), give directly

$$\gamma = \alpha + j\beta \doteq \sqrt{j\omega rc} = (1 + j)\sqrt{\frac{\omega rc}{2}} \tag{49}$$
$$Z_c = R_c + jX_c = \sqrt{\frac{r}{j\omega c}} = (1 - j)\sqrt{\frac{r}{2\omega c}} \tag{50}$$

The phase velocity is

$$v_p = \frac{\omega}{\beta} = \sqrt{\frac{2\omega}{rc}} \tag{51}$$

Since v_p increases with frequency, the group velocity is larger than the phase velocity and can be computed using $r = P\sqrt{\omega}$, with P a constant. Then

$$\beta = \omega^{\frac{1}{2}}\sqrt{\frac{P_c}{2}} \qquad \frac{\partial\beta}{\partial\omega} = \tfrac{3}{4}\omega^{-\frac{1}{4}}\sqrt{\frac{P_c}{2}} = \frac{3\beta}{4\omega} \tag{52}$$

Hence
$$v_g = \frac{\delta\omega}{\delta\beta} = \frac{4\omega}{3\beta} = \tfrac{4}{3}v_p \tag{53}$$

Evidently dispersion is *anomalous* and quite large; higher frequencies travel more rapidly than lower frequencies. If the numerator and denominator of the expression under the radical in (51) are multiplied by l, the inductance per loop unit length of the cable, it becomes

$$v_p = \sqrt{\frac{2\omega l}{r}}\sqrt{\frac{1}{lc}} \tag{54}$$

Here the second square root gives the phase velocity (10) for a line with small attenuation. Since ωl is small compared with r, according to (48), it is clear that v_p for the cable is small compared with that along a conventional line. Lines for which (48) may be used are not encountered at high frequencies.

14. Relation between Reflection Coefficient and Terminal Functions. In the following sections a detailed study is made of the phase and attenuation functions Φ and ρ for various terminal impedances. Since the magnitude and angle of the reflection coefficient Γ are simply related to ρ and Φ, they may be obtained directly from ρ and Φ. The required relationships are readily deduced using

$$\Gamma = \Gamma e^{j\psi} \equiv \frac{Z - Z_c}{Z + Z_c} \qquad \Gamma' = \Gamma e^{j\psi'} = \frac{Y - Y_c}{Y + Y_c} = \frac{Z_c - Z}{Z_c + Z} \tag{1}$$

$$\theta = \rho + j\Phi = \coth^{-1}\frac{Z}{Z_c} \qquad \theta' = \rho + j\Phi' = \coth^{-1}\frac{Y}{Y_c} = \tanh^{-1}\frac{Z}{Z_c} \tag{2}$$

The division of (1) by Z_c and subsequent substitution from (2) give

$$\Gamma = \Gamma e^{j\psi} = \frac{\coth\theta - 1}{\coth\theta + 1} = e^{-2\theta} \tag{3}$$

Since $\theta = \rho + j\Phi$, the result is

$$\Gamma = \Gamma e^{j\psi} = e^{-2(\rho + j\Phi)} \tag{4}$$

so that $\Gamma = e^{-2\rho} = \dfrac{\coth\rho - 1}{\coth\rho + 1}$, or $\rho = \tfrac{1}{2}\ln\dfrac{1}{\Gamma} = \coth^{-1}\dfrac{1+\Gamma}{1-\Gamma}$ (5)

$$\psi = -2\Phi \text{ or } 2(\pi - \Phi) \tag{6a}$$

Similarly
$$\psi' = -2\Phi' \text{ or } 2(\pi - \Phi') \tag{6b}$$

It is clear that, when $\rho = 0$, $\Gamma = 1$; when $\rho = \infty$, $\Gamma = 0$. Using (5) and (6), Γ and ψ are obtained readily from ρ and Φ, and Γ and ψ' from ρ and Φ'.

15. The Phase and Attenuation Functions of the Terminations.[81] The general definition of the complex terminal function θ (or θ') of the impedance Z when used to terminate a line of characteristic impedance Z_c is given in Sec. 8. With $z_1 \equiv Z/Z_c$ and $y_1 \equiv Y/Y_c = Z_c/Z$, θ may be expressed as follows:

$$\theta = \rho + j\Phi = \coth^{-1} z_1 = \tanh^{-1} y_1 \tag{1}$$

Or, with

$$\Phi' = \Phi - \frac{\pi}{2} \tag{2}$$

$$\theta' = \rho + j\Phi' = \coth^{-1} y_1 = \tanh^{-1} z_1 \tag{3}$$

Explicit expressions for the terminal attenuation function ρ and the terminal phase function Φ are obtained readily. The normalized impedance $z_1 = r_1 + jx_1$ may be expanded as follows:

$$z_1 = \frac{Z}{Z_c} = \frac{R + jX}{R_c(1 - j\phi_c)} = \frac{R - \phi_c X + j(X + \phi_c R)}{R_c(1 + \phi_c^2)} \tag{4}$$

Hence

$$r_1 \equiv \frac{R - \phi_c X}{R_c(1 + \phi_c^2)} \doteq \frac{R}{R_c} \qquad x_1 \equiv \frac{X + \phi_c R}{R_c(1 + \phi_c^2)} \doteq \frac{X}{R_c} \tag{5}$$

The corresponding expansion of the hyperbolic cotangent is

$$\coth (\rho + j\Phi) = \frac{\sinh 2\rho - j \sin 2\Phi}{\cosh 2\rho - \cos 2\Phi} = r_1 + jx_1 \tag{6}$$

By equating the real and imaginary parts of (6), explicit formulas for the normalized resistance and reactance are obtained. They are

$$r_1 = \frac{\sinh 2\rho}{\cosh 2\rho - \cos 2\Phi} \tag{7}$$

$$x_1 = \frac{-\sin 2\Phi}{\cosh 2\rho - \cos 2\Phi} \tag{8}$$

With the aid of simple trigonometric and hyperbolic transformations, these formulas may be solved for the terminal functions. The results are

$$\rho = \tfrac{1}{2} \tanh^{-1} \frac{2r_1}{|z_1^2| + 1} \tag{9}$$

$$\Phi = \Phi' + \frac{\pi}{2} = \tfrac{1}{2} \tan^{-1} \frac{-2x_1}{|z_1^2| - 1} \tag{10}$$

For some purposes it is advantageous to express the terminal impedance in admittance form. Since

$$Y \equiv \frac{1}{Z} = G + jB \qquad y_1 = \frac{1}{z_1} = g_1 + jb_1 \tag{11}$$

with

$$G = \frac{R}{R^2 + X^2} \qquad g_1 = \frac{r_1}{r_1^2 + x_1^2} \tag{12a}$$

$$B = -X(R^2 + X^2) \qquad b_1 = -x_1(r_1^2 + x_1^2) \tag{12b}$$

it follows that, with $\boldsymbol{Y}_c = 1/\boldsymbol{Z}_c$,

$$\boldsymbol{y}_1 = g_1 + jb_1 = \frac{\boldsymbol{Y}}{\boldsymbol{Y}_c} = (G + jB)R_c(1 - j\phi_c) \tag{13}$$

so that

$$g_1 = R_c(G + \phi_c B) \doteq R_c G \tag{14a}$$

$$b_1 = R_c(B - \phi_c G) \doteq R_c B \tag{14b}$$

Since

$$\boldsymbol{y}_1 = \frac{\boldsymbol{Y}}{\boldsymbol{Y}_c} = \coth(\rho + j\Phi') \tag{15a}$$

whereas

$$\boldsymbol{z}_1 = \frac{\boldsymbol{Z}}{\boldsymbol{Z}_c} = \coth(\rho + j\Phi) \tag{15b}$$

it follows that ρ and Φ' are expressed in terms of g_1 and b_1 in exactly the same form as are ρ and Φ in terms of r_1 and x_1. Specifically

$$\rho = \tfrac{1}{2}\tanh^{-1}\frac{2g_1}{|\boldsymbol{y}_1^2| + 1} \tag{16}$$

$$\Phi' = \Phi - \frac{\pi}{2} = \tfrac{1}{2}\tan^{-1}\frac{-2b_1}{|\boldsymbol{y}_1^2| - 1} \tag{17}$$

The formulas for ρ, Φ, and Φ' apply to either termination. The subscript 0 or s may be used where required to distinguish between the terminal functions associated, respectively, with $\boldsymbol{Z}_0$ at $z = 0$ and $\boldsymbol{Z}_s$ at $z = s$.

In order to make the definition of the phase function Φ in (10) unique, it is necessary to specify the quadrants in which Φ is found for different types of termination. This information is obtained directly if the following conventions are adopted for $\tan 2\Phi = a/b$: 2Φ is in the *first* quadrant if a and b are *both positive*, in the *second* quadrant if a is *positive* and b is *negative*, in the *third* quadrant if a and b are *both negative*, and in the *fourth* quadrant if a is *negative* and b is *positive*. Obviously all these statements locating the angle 2Φ apply to the angle Φ if *octant* is written throughout for *quadrant*. Since trigonometric functions of 2Φ are in no way changed if this is increased by 2π, it follows that functions of Φ are not altered if Φ is increased by π. Accordingly whatever values x_1 and r_1 may have in the first, second, third, or fourth *octants*, respectively, are duplicated exactly in the fifth, sixth, seventh, and eighth octants. Thus, with $x_1 = (X + \phi_c R)/R_c(1 + \phi_c^2)$, the values indicated in Table 15.1 are determined. The corresponding values for Φ' are obtained by adding $\pi/2$ to Φ or by increasing the octant number by 2.

The following important characteristic of ρ may be noted in the general case: Whenever

$$\boldsymbol{z}_1 = 1 \qquad r_1 = 1 \qquad x_1 = 0 \tag{18}$$

it follows that

$$\rho = \tfrac{1}{2}\tanh^{-1} 1 = \infty \tag{19}$$

Evidently, when $\rho = \infty$, the termination has no effect on the incident train of traveling waves, so that no factor involving Φ can occur. The

mathematical limit for Φ as x_1 approaches zero, with $r_1 = 1$, is $\pi/4$ or $3\pi/4$.

TABLE 15.1

Reactance	x_1 (or b_1)	$\lvert z_1\rvert$ (or $\lvert y_1\rvert$)	$2\Phi = \tan^{-1}\dfrac{-2x_1}{\lvert z_1\rvert^2 - 1}$ or $\left(2\Phi' = \tan^{-1}\dfrac{-2b_1}{\lvert y_1\rvert^2 - 1}\right)$	Signs of a and b in $\tan^{-1}\dfrac{a}{b}$	Quadrant for 2Φ (or $2\Phi'$)	Octant for Φ (or Φ')
Capacitive: Large....	−	>1	$\tan^{-1}\dfrac{+2\lvert x_1\rvert}{\lvert\lvert z_1\rvert^2 - 1\rvert}$	$\dfrac{+}{+}$	I	I, V
	−	1	$\tan^{-1}\dfrac{\lvert 2x_1\rvert}{0}$	$\dfrac{+}{0}$	$\dfrac{\pi}{2}$	$\dfrac{\pi}{4}$ or $\dfrac{5\pi}{4}$
Small....	−	<1	$\tan^{-1}\dfrac{+2\lvert x_1\rvert}{-\lvert\lvert z_1\rvert^2 - 1\rvert}$	$\dfrac{+}{-}$	II	II, VI
	0	<1	.....	$\dfrac{0}{-}$	π	$\dfrac{\pi}{2}$ or $\dfrac{3\pi}{2}$
Inductive: Small....	+	<1	$\tan^{-1}\dfrac{-2\lvert x_1\rvert}{-\lvert\lvert z_1\rvert^2 - 1\rvert}$	$\dfrac{-}{-}$	III	III, VII
	+	1	$\tan^{-1}\dfrac{-\lvert 2x_1\rvert}{0}$	$\dfrac{-}{0}$	$\dfrac{3\pi}{2}$	$\dfrac{3\pi}{4}$ or $-\dfrac{\pi}{4}$
Large....	+	>1	$\tan^{-1}\dfrac{-2\lvert x_1\rvert}{+\lvert\lvert z_1\rvert^2 - 1\rvert}$	$\dfrac{-}{+}$	IV	IV, VIII
	0	>1	.....	$\dfrac{0}{+}$	0, 2π	0, π
	$\pm\infty$	>1	.....	$\dfrac{0}{+}$	0, 2π	0, π

16. Graphical Representation of the Terminal Functions in the Normalized Impedance or Admittance Plane; Circle Diagram.[11,47,81] Equations for curves of constant ρ and of constant Φ are readily derived in terms of r_1 and x_1, as given in Sec. 15, Eqs. (7) and (8). Thus curves of constant ρ are defined by

$$r_1^2 + x_1^2 - 2r_1 \coth 2\rho + 1 = 0 \tag{1}$$

or

$$(r_1 - \coth 2\rho)^2 + x_1^2 = \coth^2 2\rho - 1 = \frac{1}{\sinh^2 2\rho} \tag{2}$$

This gives a family of circles with origins at

$$r_1 = \coth 2\rho \qquad x_1 = 0 \tag{3}$$

and with radii equal to $1/\sinh 2\rho$. The same equation and family of circles are obtained in terms of g_1 and b_1.

Intercepts along the r_1 axis occur when $x_1 = 0$, that is, when

$$r_1^2 - 2r_1 \coth 2\rho + 1 = 0 \tag{4}$$

or
$$(r_1 - \tanh \rho)(r_1 - \coth \rho) = 0 \tag{5}$$

so that
$$r_1 = \coth \rho \text{ or } \tanh \rho \tag{6}$$

Note that $\coth \rho \geqq 1$, so that $x_1 = 0$, $r_1 > 1$ give intercepts associated with $\coth \rho$, and that $\tanh \rho \leqq 1$, so that $x_1 = 0$, $r_1 < 1$ give intercepts associated with $\tanh \rho$ when $x_1 = 0$, $r_1 = 1$, and $\rho = \infty$.

Similarly curves of constant Φ are defined by

$$x_1^2 + r_1^2 + 2x_1 \cot 2\Phi - 1 = 0 \tag{7}$$

or
$$(x_1 + \cot 2\Phi)^2 + r_1^2 = 1 + \cot^2 2\Phi = \frac{1}{\sin^2 2\Phi} \tag{8}$$

This equation defines a family of circles with origins at

$$r_1 = 0 \qquad x_1 = -\cot 2\Phi \tag{9}$$

and with radii equal to $1/|\sin 2\Phi|$. The intercepts along the x_1 axis occur at $r_1 = 0$. Thus

$$x_1^2 + 2x_1 \cot 2\Phi - 1 = 0 \tag{10}$$

or
$$(x_1 + \cot \Phi)(x_1 - \tan \Phi) = 0 \tag{11}$$

so that the roots are

$$x_1 = -\cot \Phi \text{ (or } \tan \Phi) \tag{12}$$

In order to be consistent with the assumed convention that x_1 is negative for $0 \leqq \Phi \leqq \pi/2$ and positive for $\pi/2 \leqq \Phi \leqq \pi$, only the root $x_1 = -\cot \Phi$ may be used to define the intercepts. The significance of this restriction is brought out by noting that, since

$$\cot (\pi + 2\Phi) = \cot 2\Phi \tag{13}$$

$$\sin^2 (\pi + 2\Phi) = \sin^2 2\Phi \tag{14}$$

it follows that the origins and radii of circles for Φ and $\Phi - \pi/2$ are the same, so that the families of circles for Φ and $\Phi - \pi/2$ coincide. This means that in the family of circles defined by (10) each circle represents two electrically different values of Φ in each range from zero to π, namely, Φ and $\Phi - \pi/2$. This ambiguity is resolved by the conditions imposed in Sec. 15 to make each pair of values r_1 and x_1 have a unique value of Φ. Since, by postulate,

$$x_1 \text{ is negative for } 0 \leqq \Phi \leqq \frac{\pi}{2} \tag{15a}$$

$$x_1 \text{ is positive for } \frac{\pi}{2} \leqq \Phi \leqq \pi \tag{15b}$$

it follows that to each circle of constant Φ, with its two possible values of Φ, is assigned only the value less than $\pi/2$ when x_1 is negative and only

the value greater than $\pi/2$ when x_1 is positive. This implies that the value of Φ assigned to each circle jumps by $\pi/2$ on crossing the r_1 axis, where $x_1 = 0$. However, since the intersections of the Φ circles with the r_1 axis satisfy Eq. (7) with $x_1 = 0$, that is, $r_1 = 1$, it follows that all Φ curves pass through the point $x_1 = 0, r_1 = 1$, where $\rho = \infty$, and are discontinuous by $\pi/2$ at this point. Thus, if $\Phi = 30°$ along a circle of constant Φ for x_1 negative, it equals 120° along the same circle for x_1 positive, the jump of 90° occurring at $x_1 = 0, r_1 = 1$. The limiting circle of infinite

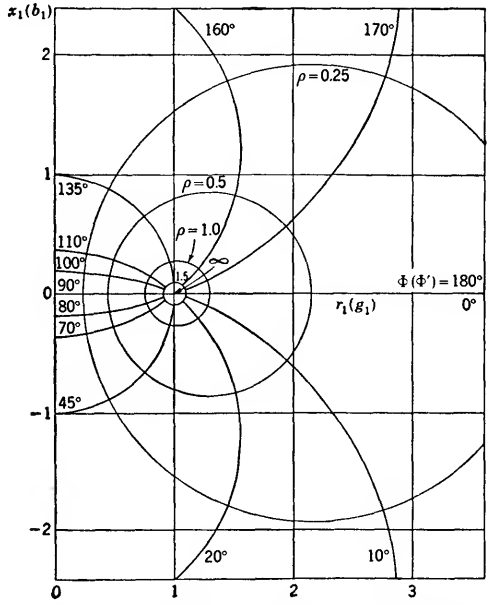


FIG. 16.1. Circle diagram—illustrative rectangular form.

radius that is the r_1 axis has the value 0 or 180° for $r_1 \geqq 1$ and the value 90° for $r \leqq 1$.

Since g_1 and b_1 satisfy exactly the same equations in terms of ρ and Φ' $(= \Phi - \pi/2)$, as do r_1 and x_1 in terms of ρ and Φ, it follows that the same families of circles are obtained in terms of g_1 and b_1, ρ and Φ'. Moreover the values of g_1 and b_1 which correspond to a given pair of values r_1 and x_1 have the *same* value of ρ and a value $\Phi' = \Phi - \pi/2$.

Families of circles plotted using x_1 (or b_1) and r_1 (or g_1) as rectangular coordinates are shown in Fig. 16.1. Circles of constant angle Φ (or Φ') have their centers along the positive and negative x_1 (or b_1) axis. They are scaled in degrees. Circles of constant ρ have their centers along the r_1 (or g_1) axis extending from $r_1 = 1$. They are scaled in nepers. Only a small number of circles are shown in Fig. 16.1, which is intended to

illustrate clearly the construction of the diagram. A more detailed diagram that may be used for determining approximate values of ρ and Φ or Φ' directly without computation is given in Fig. 16.2.

In terms of the reflection coefficient, circles of constant Φ (or Φ') are also circles of constant $\pi - \psi/2$ (or $\pi - \psi'/2$). This follows from the

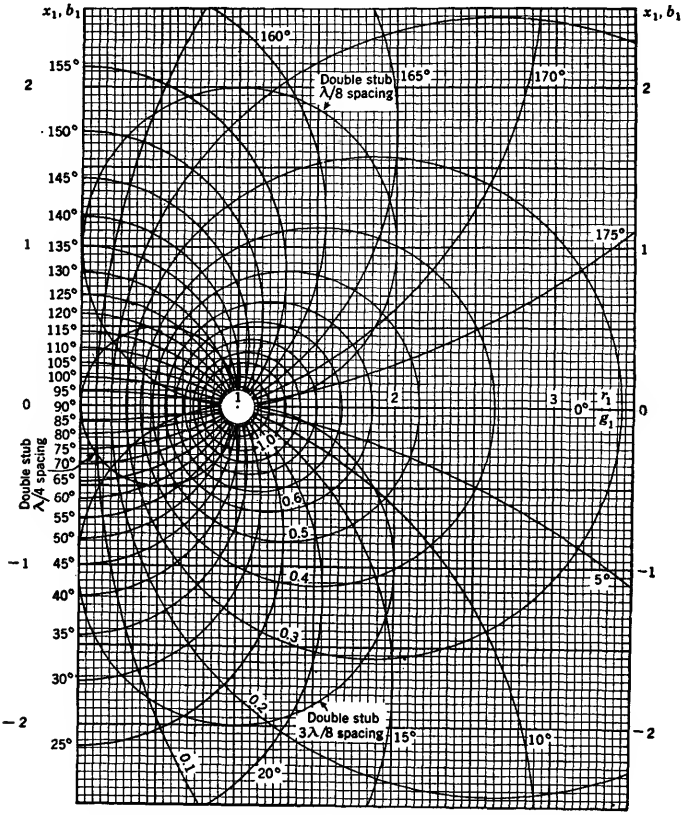


FIG. 16.2. Circle diagram—detailed rectangular form.

relation $\psi = 2(\pi - \Phi)$ or $\psi' = 2(\pi - \Phi')$. Similarly circles of constant ρ are also circles of constant Γ, since $\Gamma = e^{-2\rho}$.

The following applications of the circle diagram may be listed:

1. Determination of ρ and Φ from known values of r_1 and x_1 or of ρ and Φ' from known values of g_1 and b_1.

2. Determination of r_1 and x_1 from known (e.g., experimentally determined) values of ρ and Φ or of g_1 and b_1 from known values of ρ and Φ'.

3. Determination of $z_1 = r_1 + jx_1$ from given $y_1 = g_1 + jb_1$. This merely involves entering the circle diagram at the point g_1, b_1, noting the value of Φ', moving on a circle of constant ρ to $\Phi = \Phi' + 90°$, and reading

r_1 and x_1 appropriate to this point. The determination of y_1 with z_1 given is similar. Note that the circle diagram is actually being used to obtain the reciprocal of a complex number.

4. Determine ρ, given its intercept $S = \coth \rho$ on the axis of reals; determine $S = \coth \rho$, given ρ. (The quantity S is the standing-wave ratio, to be discussed later.)

17. Graphical Representation of the Normalized Impedance or Admittance in the Reflection-Coefficient Plane; Smith Chart.[58] The conventional circle diagram (Sec. 16) consists of circles of constant attenuation ρ and constant phase shift Φ (or Φ') in the complex $z_1 = r_1 + jx_1$ (or $y_1 = g_1 + jb_1$) plane. More generally it represents graphically the transformation from the complex values of $z_1 = r_1 + jx_1$ (or $y_1 = g_1 + jb_1$) to the complex values of $\theta = \rho + j\Phi$ (or $\theta' = \rho + j\Phi'$), according to the defining relations

$$z_1 = \coth \theta \qquad y_1 = \coth \theta' \tag{1}$$

Circles of constant ρ have centers on the r_1 axis and enclose the point $r_1 = 1$, $x_1 = 0$, which is the circle of zero radius for $\rho = \infty$. The axis of imaginaries $r_1 = 0$ is the circle of infinite radius for $\rho = 0$. Circles for all values of ρ from zero to infinity have intercepts with the r_1 axis between $r_1 = 0$ and $r_1 = 1$ and again between $r_1 = 0$ and $r_1 = \infty$. It is evident that any two circles for specified values of ρ lie relatively very close together as they cross the r_1 axis between 0 and 1, whereas they are relatively far apart as they again cross the r_1 axis between 1 and ∞.

Circles of constant Φ have their centers on the x_1 axis. All circles pass through the point $r_1 = 1$, $x_1 = 0$. It follows that two circles for different constant values of Φ lie close together near the point $r_1 = 1$, $x_1 = 0$ but are relatively far apart at values of r_1 and x_1 which are large compared with unity.

Since both r_1 and x_1 vary from zero to infinity, it is evident that a circle diagram of the type shown in Figs. 16.1 and 16.2 cannot be practical simultaneously in the range of small values *and* large values of r_1 and x_1. Either a number of circle diagrams drawn to different scales must be used or, if the convenience of a single diagram is desired, the scale must be transformed in a manner to compress the range of large values of r_1 and x_1 and expand the range of small values. This may be accomplished by the well-known bilinear transformation (Ref. 1, page 106) $z_1' = (az_1 + b)/(cz_1 + d)$, with $a = 2$, $b = 0$, and $c = d = 1$. This distorts the circle diagram in Fig. 16.1 in such a manner that the circles of constant ρ become concentric about the point $r_1 = r_1' = 1$, $x_1 = x_1' = 0$ with the x_1 axis ($\rho = 0$), a circle of *unit* radius, and the circles of constant Φ become radial lines. Simultaneously the simple straight lines (circles of infinite radius) $r_1 =$ constant and $x_1 =$ constant are distorted into more complicated families of circles with finite radii. These are nothing

else than the *representation of r_1 and x_1 in the complex plane of the reflection coefficient* $\Gamma = \Gamma e^{j\psi}$ in polar coordinates. This is shown more explicitly after the transformation has been carried out.

The desired transformation is achieved by requiring the new circles of constant ρ to have centers in the z_1' plane at $r_1' = 1$, $x_1' = 0$ and to have radii given by $|\exp(-2\theta)| = \exp(-2\rho) = \Gamma$. The equations of these circles are $(r_1' - 1)^2 + x_1'^2 = \exp(-4\rho)$. The circles of constant Φ in the z' plane are the radial lines defined by $2\Phi = -\tan^{-1}[x_1'/(r_1' - 1)]$. The equation of transformation is

$$e^{-2\theta} = e^{-2\rho}e^{-j2\Phi} = \sqrt{(r_1' - 1)^2 + x_2'^2}\, e^{j\tan^{-1}x_1'/(r_1'-1)} = z_1' - 1 \qquad (2)$$

where $z_1' = r_1' + jx_1'$ defines the rectangular coordinates of the new complex plane. With $z_1 = \coth\theta$, it is readily verified that (2) is a bilinear transformation from the complex z plane into the complex z_1' plane, according to

$$z_1' = \frac{2z_1}{z_1 + 1} \qquad (3)$$

The simple rectangular net of r_1 and x_1 in the z plane is distorted into more complicated families of circles in the z_1' plane. Their equations may be derived by solving (3) successively for r_1 and x_1 in terms of r_1' and x_1'. The results are

$$r_1 = \frac{r_1'(2 - r_1') - x_1'^2}{(r_1' - 2)^2 + x_1'^2} \qquad (4a)$$

$$x_1 = \frac{2x_1'}{(r_1' - 2)^2 + x_1'^2} \qquad (4b)$$

With considerable manipulation (4*a*) may be rearranged into the following form:

$$\left(r_1' - 1 - \frac{r_1}{r_1 + 1}\right)^2 + x_1'^2 = \frac{1}{(r_1 + 1)^2} \qquad (5)$$

This is the equation of a family of circles of constant r_1 in the z_1' plane. The circles have radii $1/(r_1 + 1)$ with centers at $r_1' = 1 + r_1/(r_1 + 1)$, $x_1' = 0$. The entire x axis defined by $r_1 = 0$ in the z_1 plane becomes a *circle of unit radius* with center at $r_1' = 1$, $x_1' = 0$ in the z' plane. Thus the entire half space $r_1 \geqq 0$ in the z_1 plane is mapped inside the unit circle in the z_1' plane. The line $r_1 = \infty$ maps into a circle of zero radius with center at $r_1' = 2$, $x_1' = 0$. The line $r_1 = 1$ maps into a circle of radius 0.5 with center at $r_1 = 1.5$, $x_1 = 0$. Thus the strip $0 \leqq r_1 \leqq 1$ in the z_1 plane maps into the region between the circles $r_1 = 0$ and $r_1 = 1$. The contours of constant r_1, which were straight lines in the z_1 plane, map into circles in the z_1' plane, as shown in Fig. 17.1. The intercepts $x_1 = 0$ on the r_1 axis in the z_1 plane transform into the points obtained

by setting $x_1 = 0$ in (4*b*). With $x_1 = 0$, $z_1 = r_1$ in (2) and

$$r_1' = \frac{2r_1}{r_1 - 1} \qquad x_1' = 0 \tag{6}$$

Eq. (4*b*) may be rearranged so that it becomes

$$(r_1' - 2)^2 + \left(x_1' - \frac{1}{x_1}\right)^2 = \frac{1}{x_1^2} \tag{7}$$

This equation defines a family of circles of constant x_1 in the z_1' plane with radii $1/|x_1|$ and with centers at $r_1' = 2$, $x_1' = 1/x_1$. The r_1 axis, defined by $x_1 = 0$ in the z_1 plane, becomes a section of a circle of infinite radius with center at $r_1' = 2$ and $x_1' = \infty$; this is the r_1' axis, defined by $x_1' = 0$. The intercepts on the r_1' axis, $x_1' = 0$, occur at the *single* point $r_1' = 2$. Hence all circles of constant x_1 pass through the point $r_1' = 2, x_1' = 0$. The circles of constant r_1 and x_1 in the z' plane (or g_1 and b_1 in the y' plane) are shown in Fig. 17.1. They correspond to the rectangular mesh of straight lines r_1 (or g_1) = constant and x_1 (or b_1) = constant in the z_1 plane (or y_1 plane). The concentric circles of constant ρ and radial lines of constant Φ (or Φ'), corresponding to the two families of circles in the z_1 plane (or y_1 plane), are shown in Fig. 17.2.

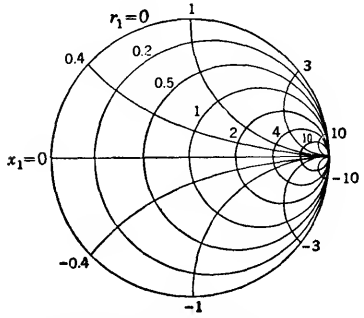


FIG. 17.1. Circles of constant r_1 and x_1 in transformed circle diagram.

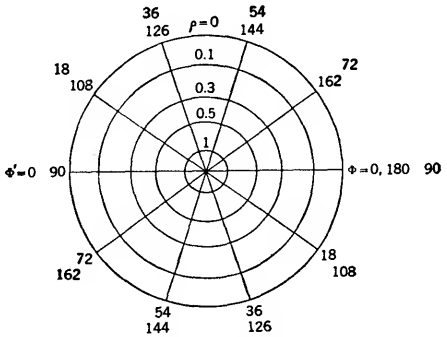


FIG. 17.2. Circles of constant ρ, Φ, and Φ' in transformed circle diagram.

Thus, whereas the original circle diagram for transforming from z_1 to θ (or from y_1 to θ') has a simple rectangular mesh for r_1 and x_1 (or g_1 and b_1) and two rather complicated families of circles for ρ and Φ (or Φ'), both of which extend to infinity, the transformed circle diagram (Fig. 17.3) (Smith chart) has complicated families of circles of constant r_1 and x_1 and simple

families of concentric circles and radial lines for ρ and Φ. Significantly *all* values of r_1 and x_1, including infinite values, are contained within or are on the unit circle $r_1 = 0$ or $\rho = 0$.

Since the circles of constant ρ in the z' plane are, in effect, circles of constant $\Gamma = e^{-2\rho}$, where, in the range $\rho = \infty$ to $\rho = 0$, Γ increases from

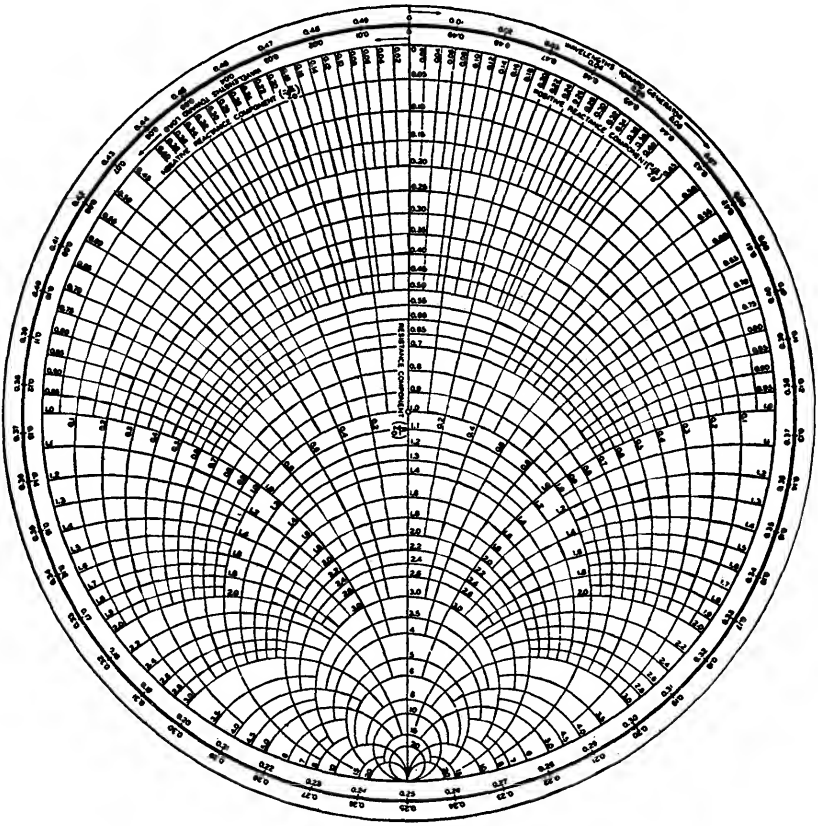


FIG. 17.3. Smith chart.

0 to 1, it is often convenient to use a linear scale of Γ as the parameter instead of the exponential scale for ρ. Thus Γ is simply the *radial distance* from the center of the diagram on a scale that has the value 1 for the bounding circle $r_1 = 0$. From symmetry, the circles of constant Φ can be scaled in terms of the angle of the complex reflection coefficient $\psi = 2(\pi - \Phi)$ [or $\psi' = 2(\pi - \Phi')$]. Thus, whereas Φ ranges from 0 to 180° clockwise around the circle, ψ ranges from 0 to 360° counterclockwise around the circle. The relation between the ρ and Φ scales and the Γ and ψ scales is indicated in Fig. 17.4.

It is evidently possible to use either circle diagram for converting from the terminal function $\theta = \rho + j\Phi$ (or $\theta' = \rho + j\Phi'$) to the normalized impedance $z_1 = r_1 + jx_1$ (or admittance $y_1 = g_1 + jb_1$), or vice versa. Alternatively the conversion may be from $\Gamma = \Gamma e^{j\psi}$ (or $\Gamma' = \Gamma e^{j\psi'}$) to z_1 (or y_1), or vice versa. Each has advantages for certain purposes.

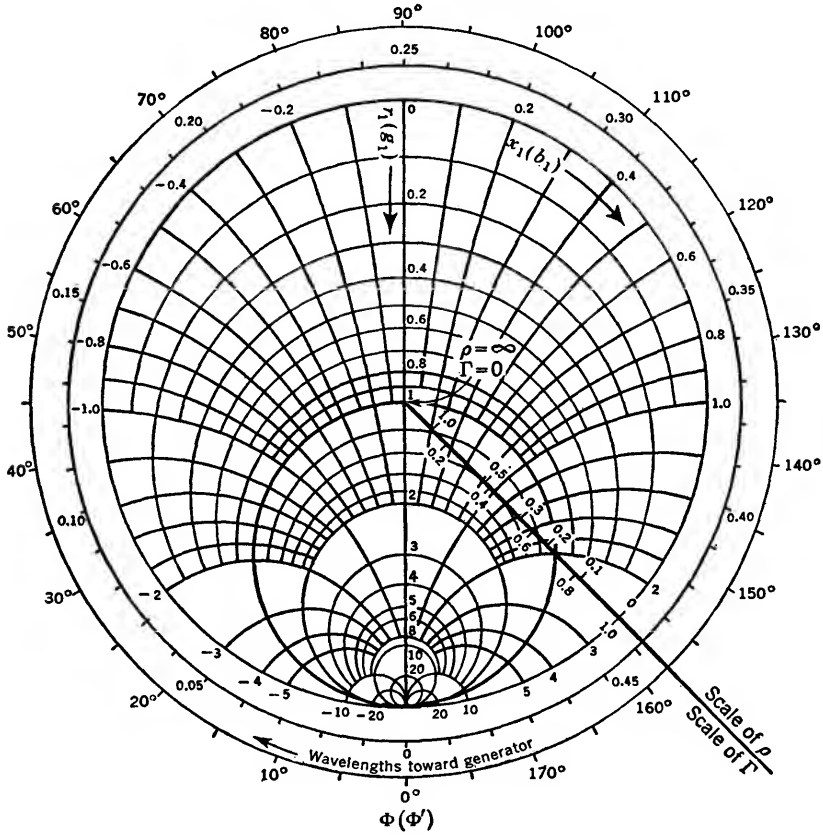


FIG. 17.4. Smith chart with scales for ρ, Γ, and Φ. Note that $\psi = 360° - 2\Phi$.

18. Special Forms of the Terminal Functions and of the Reflection Coefficient—Resistive Termination.[81] In order to obtain a clearer picture of the dependence of the terminal functions ρ and Φ upon the terminal impedance Z, consider a line with an essentially resistive termination such that $x_1 = (X + \phi_c R)/R_c(1 + \phi_c^2) = 0$. This is physically possible over a range of resistances extending from very small to enormous values. Note that very low values of resistance are usually associated with short pieces of copper wire which do not have zero reactance. In fact, their resistance is usually negligible compared with the inductive reactance.

Zero reactance with very small, although *never zero*, resistance, can be obtained with a series-resonant circuit.

The termination to be investigated is defined by

$$x_1 \equiv \frac{X + \phi_c R}{R_c(1 + \phi_c^2)} = 0 \tag{1}$$

It follows that

$$r_1 \equiv \frac{R - \phi_c X}{R_c(1 + \phi_c^2)} = \frac{R}{R_c} \tag{2}$$

without approximation. Similarly, with (1),

$$b_1 \equiv R_c(B - \phi_c G) = -\frac{R_c(X + \phi_c R)}{R^2 + X^2} = 0 \tag{3}$$

Also
$$g_1 \equiv R_c(G + \phi B) = \frac{R_c(R - \phi_c X)}{R^2 + X^2} = \frac{R_c}{R} \tag{4}$$

Note that
$$g_1 = \frac{R_c}{R} = \frac{1}{r_1} \tag{5}$$

The terminal functions are:

$$\rho = \tfrac{1}{2} \tanh^{-1} \frac{2r_1}{r_1^2 + 1} = \tfrac{1}{2} \tanh^{-1} \frac{2g_1}{g_1^2 + 1} \tag{6}$$

$$\Phi = \lim_{x_1 \to 0} \tfrac{1}{2} \tan^{-1} \frac{-2x_1}{r_1^2 + x_1^2 - 1} \tag{7a}$$

$$\Phi' = \lim_{b_1 \to 0} \tfrac{1}{2} \tan^{-1} \frac{-2b_1}{g_1^2 + b_1^2 - 1} \tag{7b}$$

Let ρ be investigated first using the trigonometric formula

$$\tanh 2\rho = \frac{2 \tanh \rho}{1 + \tanh^2 \rho} \tag{8}$$

with which (6) becomes

$$\frac{2 \tanh \rho}{1 + \tanh^2 \rho} = \frac{2r_1}{r_1^2 + 1} \tag{9}$$

This can be expressed in the form

$$(\tanh \rho - r_1)\left(\tanh \rho - \frac{1}{r_1}\right) = 0 \tag{10}$$

with roots
$$\tanh \rho = \begin{cases} r_1 \\ \dfrac{1}{r_1} \end{cases} \text{ or } \begin{cases} \dfrac{1}{g_1} \\ g_1 \end{cases} \tag{11}$$

Since the hyperbolic tangent can never exceed unity, it follows that

$$\rho = \tanh^{-1} r_1 \qquad r_1 \leqq 1 \tag{12}$$

$$\rho = \tanh^{-1} g_1 \qquad g_1 \leqq 1 \tag{13}$$

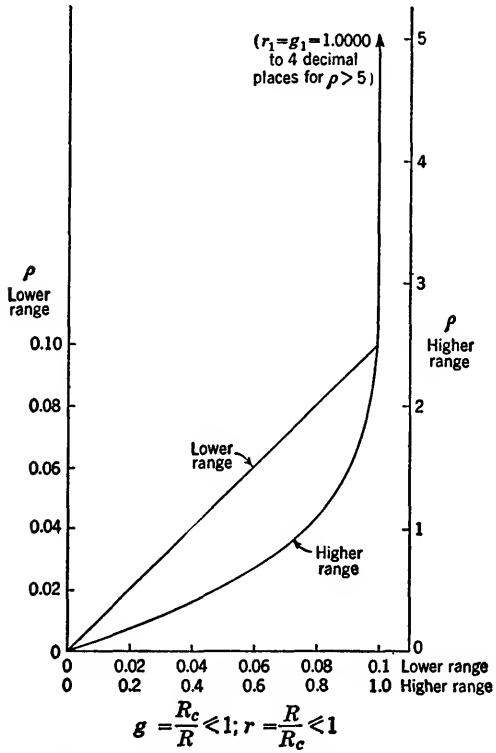


FIG. 18.1. The attenuation function $\rho = \tanh^{-1} r_1$, with $r_1 \leqq 1$, and $\rho = \tanh^{-1} g_1$, with $g_1 \leqq 1$, for a resistive termination, with $r_1 = 1/g_1$.

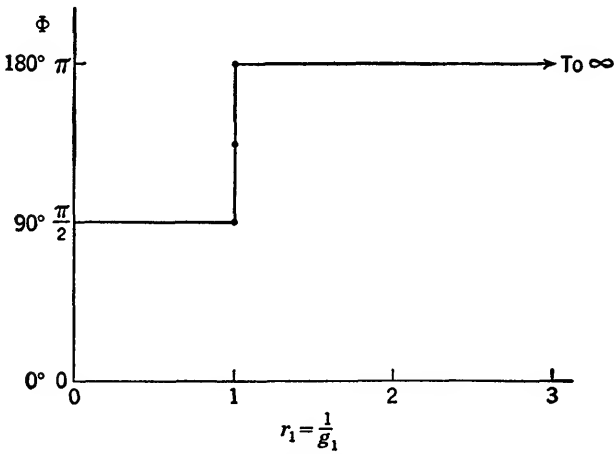


FIG. 18.2. The phase function Φ for a resistive termination, with $x_1 = 0$.

This includes the *entire* range of values of $r_1 = 1/g_1$ from zero to infinity. It is plotted in Fig. 18.1.

For small values of r_1 or small values of $g_1 = 1/r_1$ corresponding to very large values of r_1, the inverse hyperbolic tangent may be replaced by its argument. Thus

$$\rho \doteq r_1 \qquad \text{for } r_1^2 \ll 3 \tag{14}$$

$$\rho \doteq g_1 \qquad \text{for } g_1^2 \ll 3 \tag{15}$$

It is readily verified that the conditions

$$x_1 = 0 \qquad r_1 = 1 \tag{16a}$$

coincide with $z_1 = 1$ or $Z = Z_c = R_c(1 - j\phi_c)$ (16b)

for which $R = R_c \qquad X = -\phi_c R_c$ (17)

In this case $\rho = \infty$.

The phase functions Φ and Φ' as given by (7*a*,*b*) may be expressed as follows:

$$\Phi = \tfrac{1}{2} \tan^{-1} \frac{0}{r_1^2 - 1} \tag{18}$$

$$\Phi' = \tfrac{1}{2} \tan^{-1} \frac{0}{g_1^2 - 1} \tag{19}$$

For $r_1 = \dfrac{1}{g_1} < 1$,

$$\Phi = \tfrac{1}{2} \tan^{-1} \frac{0}{-} = \frac{\pi}{2} \text{ or } \frac{3\pi}{2} \tag{20a}$$

$$\Phi' = \Phi - \frac{\pi}{2} = 0 \text{ or } \pi \tag{20b}$$

For $g_1 = \dfrac{1}{r_1} < 1$,

$$\Phi' = \tfrac{1}{2} \tan^{-1} \frac{0}{-} = \frac{\pi}{2} \text{ or } \frac{3\pi}{2} \tag{21a}$$

$$\Phi = \Phi' + \frac{\pi}{2} = \pi \text{ or } 0 \tag{21b}$$

For $r_1 = 1$, Φ and Φ' are indeterminate because discontinuous. If r_1 or g_1 approaches 1 from small values, Φ or Φ' is $\pi/2$ or $3\pi/2$; if r_1 or g_1 approaches 1 from larger values, Φ or Φ' is 0 or π. On the other hand, if r_1 is set equal to unity *before* x_1 is made to vanish, the following result is obtained:

$$\Phi = \lim_{x_1 \to 0} \tfrac{1}{2} \tan^{-1} \frac{-2x_1}{x_1^2} = \lim_{x_1 \to 0} \tfrac{1}{2} \tan^{-1} \frac{-2}{|x_1|} = \tfrac{1}{2} \tan^{-1} \infty \tag{22a}$$

Since the argument becomes infinite with signs $-/0$, it must be at

$$\Phi = \frac{3\pi}{4} \text{ or } -\frac{\pi}{4} \qquad \Phi' = \Phi - \frac{\pi}{2} = \frac{\pi}{4} \tag{22b}$$

The phase function of a resistive termination is represented in Fig. 18.2.

The angle of the coefficient of reflection is given by

$$\psi = -2\Phi \text{ or } 2\pi - 2\Phi \tag{23a}$$

Hence

$$\begin{aligned} \psi &= 2\pi - \pi = \pi && \text{for } r_1 < 1 \text{ or } g_1 > 1 \\ \psi &= 2\pi - 2\pi = 0 && \text{for } r_1 > 1 \text{ or } g_1 < 1 \\ \psi &= 2\pi - \frac{3\pi}{2} = \frac{\pi}{2} && \text{for } r_1 = 1 = g_1 \end{aligned} \tag{23b}$$

Summarizing, if $x_1 = 0 = b_1$, $\Phi = 0$ and $\psi = 0$ for $g_1 < 1$ or $r_1 > 1$; $\Phi = \pi/2$ and $\psi = \pi$ for $r_1 < 1$ or $g_1 > 1$. With $r_1 = 1$, Φ and Φ' are $\pi/4$, and $\psi = \pi/2$.

If it is required that

$$X = 0 = B \tag{24}$$

instead of $x_1 = 0 = b_1$, then

$$r_1 = \frac{R - \phi_c X}{R_c(1 + \phi_c^2)} = \frac{R}{R_c(1 + \phi_c^2)} \doteq \frac{R}{R_c} \doteq \frac{1}{g_1} \tag{25a}$$

$$x_1 = \frac{X + \phi_c R}{R_c(1 + \phi_c^2)} = \frac{\phi_c R}{R_c(1 + \phi_c^2)} = \phi_c r_1 \tag{25b}$$

If ϕ_c^2 is neglected compared with unity, it follows that r_1 and hence ρ are the same for $X = 0$ as for $x_1 = 0$. On the other hand,

$$\Phi = \tfrac{1}{2} \tan^{-1} \frac{-2\phi_c r_1}{r_1^2 - 1} \tag{26}$$

With $r_1 > 1$, 2Φ is in the fourth quadrant $(-/+)$; for $r_1 < 1$, 2Φ is in the third quadrant $(-/-)$. Hence

$$\begin{aligned} \Phi &= \pi - \tfrac{1}{2} \tan^{-1} \frac{2\phi_c r_1}{|r_1^2 - 1|} && r_1 > 1 \\ \Phi &= \frac{\pi}{2} + \tfrac{1}{2} \tan^{-1} \frac{2\phi_c r_1}{|r_1^2 - 1|} && r_1 < 1 \end{aligned} \tag{27}$$

Also

$$\Phi = \tfrac{1}{2} \tan^{-1} \frac{-2\phi_c}{0} = \frac{3\pi}{4} \qquad r_1 = 1$$

Alternatively

$$\begin{aligned} \Phi' &= \Phi - \frac{\pi}{2} = \frac{\pi}{2} - \frac{1}{2} \tan^{-1} \frac{2\phi_c g_1}{|g_1^2 - 1|} && g_1 < 1 \\ \Phi' &= \Phi - \frac{\pi}{2} = \frac{1}{2} \tan^{-1} \frac{2\phi_c g_1}{|g_1^2 - 1|} && g_1 > 1 \\ \Phi' &= \frac{\pi}{4} && g_1 = 1 \end{aligned} \tag{28}$$

The principal range of Φ as a function of r_1 and g_1 with ϕ_c as parameter is shown in Fig. 18.3.

Summarizing the behavior of Φ and ρ for a resistive termination with $x_1 = 0$, the following simple picture may be described: As r_1 increases

from near zero to 1, ρ increases from near zero to infinity. Φ continues constant at $\pi/2$ until r_1 is exactly equal to 1. It then rises abruptly to $3\pi/4$. As r_1 increases further from 1 to very large values, ρ decreases from infinity to near zero. Φ rises abruptly from $3\pi/4$ to π as r_1 exceeds 1. Thus a normalized resistance r_1 that is smaller than 1 behaves like a zero resistance insofar as the phase function Φ is concerned; similarly a normalized resistance r_1 that is greater than 1 acts, insofar as Φ is concerned,

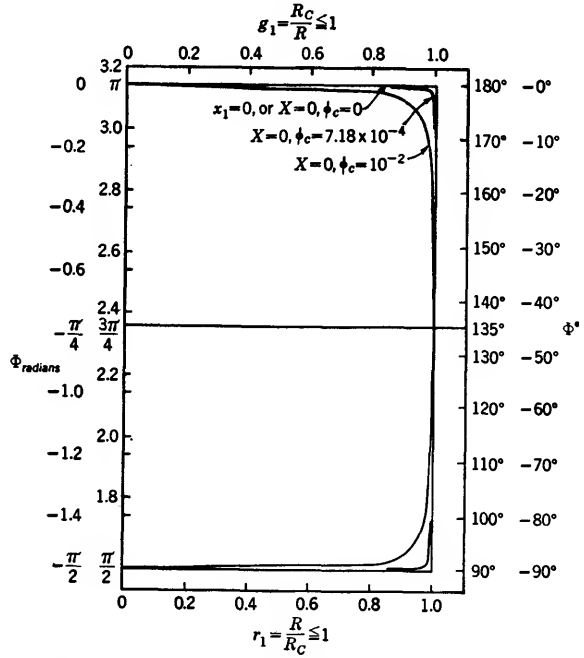


FIG. 18.3. The phase function Φ for a resistive termination, with $X = 0$ and $\phi_c^2 \ll 1$.

like an infinite resistance. If, instead of $x_1 = 0$, the condition is $X = 0$ on a line for which ϕ_c is small but not zero, so that $\phi_c^2 \ll 1$, the function ρ is just as for $x_1 = 0$, and the function Φ follows the same general behavior without quite such an abrupt change from $\Phi = \pi/2$ to $\Phi = \pi$ at $r_1 = 1$. The smaller ϕ_c is, the more rapid is the change.

19. Special Forms of the Terminal Functions—the Predominantly Reactive Termination.[81] It is not possible to construct a purely reactive termination. On the other hand, a terminal impedance with a resistive component that is negligible compared with the reactive component is easily obtained except for very small reactances and very large positive reactances. Negatively reactive impedances with extremely small resistance are easily constructed for a range of reactance which extends from practically negatively infinite to nearly zero. As the reactance

approaches zero, a point is reached where the resistance ceases to be small compared with the reactance, and ultimately as the reactance becomes still smaller, the resistance *always predominates*. In the case of positively reactive impedances exactly the same situation as for negative reactances obtains near zero values. Although it is a simple matter to provide positively reactive impedances with resistive components small compared with the reactive over a range of reactance extending from small values to extremely large ones, it is not possible to approach infinite values. This arises from the fact that very large values of inductive reactance usually must be obtained with parallel or antiresonant circuits. As the resonant frequency is approached from the positively reactive side, this latter increases to a large value before antiresonance is reached, but this is never infinite and always drops to zero at antiresonance while the resistance increases to a maximum. Thus a predominantly reactive termination is physically available in the range of X from negative infinity to nearly zero and from nearly zero on the positive side to extremely large but not infinite values. Near and at zero reactance the impedance is predominantly resistive.

Let the predominantly reactive termination be defined by the inequality

$$r_1^2 \ll |x_1^2 - 1| \tag{1}$$

For lines with low distortion (1) is equivalent to

$$\phi_c^2 \ll 1 \qquad R^2 \ll |X^2 - R_c^2| \tag{2}$$

Subject to (1) and (2), the general formulas for ρ and Φ become

$$\rho = \tfrac{1}{2} \tanh^{-1} \frac{2r_1}{x^2 + 1} \tag{3}$$

$$\Phi = \tfrac{1}{2} \tan^{-1} \frac{-2x_1}{x_1^2 - 1} \tag{4}$$

Since (1) includes $r_1^2 \ll x_1^2 + 1$, it follows that the argument of the inverse hyperbolic tangent in (3) is small. Hence

$$\rho \doteq \frac{r_1}{x_1^2 + 1} \tag{5}$$

The expressions for Φ may be simplified using the formula

$$\tan^{-1} x = \tfrac{1}{2} \tan^{-1} \frac{2x}{1 - x^2} \tag{6}$$

Thus

$$\Phi = \tfrac{1}{2} \tan^{-1} \frac{-2x_1}{x_1^2 - 1} = \tfrac{1}{2} \tan^{-1} \frac{-2x_1}{-(1 - x_1^2)} \tag{7}$$

Assuming x_1 positive and less than unity for the moment, the inverse

tangent in (7) is in the third quadrant. Hence

$$\Phi = \tfrac{1}{2}\left(\pi + \tan^{-1}\frac{2x_1}{1-x_1^2}\right) = \frac{\pi}{2} + \tan^{-1} x_1 = \pi + \tan^{-1} b_1 \qquad (8)$$

By replacing Φ with Φ' and x_1 with b_1 it follows that

$$\Phi' = \tfrac{1}{2}\left(\pi + \tan^{-1}\frac{2b_1}{1-b_1^2}\right) = \frac{\pi}{2} + \tan^{-1} b_1 = \pi + \tan^{-1} x_1 \qquad (9)$$

Also
$$\Phi' = \Phi - \frac{\pi}{2} = \tan^{-1} x_1 \qquad (10)$$

and
$$\Phi = \Phi' + \frac{\pi}{2} = \pi + \tan^{-1} b_1 \qquad (11)$$

It is clear from

$$\tan^{-1} x = \frac{\pi}{2} - \tan^{-1}\frac{1}{x} \qquad (12)$$

that
$$x_1 = \frac{1}{b_1} \qquad (13)$$

Useful formulas for x_1 are obtained from (8) and (9). Thus

$$x_1\left(\doteq \frac{X}{R_c}\right) = \tan\left(\Phi - \frac{\pi}{2}\right) = -\cot\Phi = \tan\Phi' \qquad (14)$$

$$b_1\ (\doteq BR_c) = -\cot\left(\Phi - \frac{\pi}{2}\right) = \tan\Phi = -\cot\Phi' \qquad (15)$$

The condition (1) defining a predominantly reactive termination includes the entire range of x_1 from zero to infinity except a range near $|x_1| = 1$. Insofar as ρ is concerned, the inequality (1) could be replaced by the much less restrictive conditions

$$r_1^2 \ll x_1^2 + 1 \qquad (16)$$

which is to be interpreted as a restriction on r_1 and not as limiting x_1. Accordingly formula (3) for ρ and others derived from it are valid for all values of x_1 if (16) is satisfied.

The condition (16) evidently is not sufficient for Φ or Φ', since

$$\text{For } |x_1| = 1, \qquad \Phi = \tfrac{1}{2}\tan^{-1}\frac{-2}{r_1^2} = \tfrac{1}{2}\left(2\pi - \tan^{-1}\frac{2}{r_1^2}\right) \qquad (17)$$

Using (12), it follows that

$$\Phi = \pi - \frac{1}{2}\left(\frac{\pi}{2} - \tan^{-1}\frac{r_1^2}{2}\right) \qquad (18)$$

or
$$\Phi = \frac{3\pi}{4} + \frac{1}{2}\tan^{-1}\frac{r_1^2}{2} \doteq \frac{3\pi}{4} + \frac{r_1^2}{4} \qquad (19)$$

Thus Φ as obtained from (4) is in error by $r_1^2/4$ in the extreme case $|x_1| = 1$. If (16) is satisfied instead of (1), it follows that

$$r_1^2 \ll 4 \qquad (20)$$

so that $r_1^2/4$ is negligible compared with $3\pi/4$. Accordingly (4) as well as (3) may be used subject to (16) instead of subject to (1). This means that, if

$$r_1^2 \ll 1 \tag{21}$$

x_1 may have all values.

For most purposes, therefore, the predominantly reactive termination may be defined by

$$r_1^2 \ll x_1^2 + 1 \tag{22}$$

A similar set of formulas may be obtained by writing b_1 for x_1, g_1 for r_1, and Φ' for Φ.

20. The Conducting Wire Bridge as a Termination; Resistive Wire.[81] Transmission-line measurements depend on the availability of a standard terminal impedance. The properties of such a standard necessarily

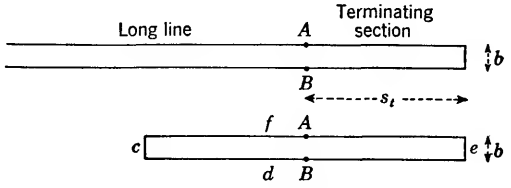


FIG. 20.1. Terminating section as half of a rectangle.

include terminal-zone effects. Whereas these are analyzed in general in Chap. V, it is advantageous to consider simple standards in this chapter. For the two-wire open line and the shielded-pair line a straight conducting wire bridge is useful. It is analyzed in this section. The conducting piston or disk for use in coaxial and other types of line is considered in the next section.

The impedance of a section of length s_t of a long line of length $s \gg s_t$, when terminated in a straight conducting bridge of length b equal to the spacing of the line, may be determined quite accurately if the following inequalities are satisfied:

$$s_t^2 \gg b^2 \gg a^2 \tag{1}$$

$$\beta_0^2 s_t^2 \ll 1 \tag{2}$$

where a is the radius of the conductors of the line and $\beta_0 = 2\pi/\lambda_0$. The method consists in treating the terminating section as one-half of a long and narrow rectangle of wire of length $2s_t$ and width b, as shown in Fig. 20.1. The impedance looking to the right from AB on the long line and on the rectangle is the same if the distance between the sides c and e of the rectangle is sufficiently great to make any coupling between them insignificant. This is ensured by (1).

Denoting the self-inductance of a typical side j of the rectangle by L_{jj} and the mutual inductance between sides i and j by L_{ij}, the total

inductance of the rectangle of wire is as follows (note that the mutual inductance of mutually perpendicular sides is zero):

$$L = L_{cc} + L_{ee} + L_{dd} + L_{ff} + L_{df} + L_{fd} + L_{ce} + L_{ec} \tag{3}$$

Subject to (1), the contribution to L by $L_{ce} + L_{ec}$ is negligible. By symmetry it follows that

$$L = 2(L_{ee} + L_{dd} + L_{df}) \tag{4}$$

The inductances in (4) are evaluated in Ref. 9, Chap. VI. Subject to (1), the final expression for L for wires in air is

$$L = \frac{1}{\pi\nu_0}\left[b\left(\sinh^{-1}\frac{b}{a_s} + \frac{a_s}{b} - \sqrt{1 + \frac{a_s^2}{b^2}}\right) + 2s_t \ln\frac{b}{a} + a - b\right] \tag{5}$$

where $\nu_0 = 1/\mu_0 = 10^7/4\pi$ m/henry, a is the radius of the wires of the long sides, and a_s is the radius of the short sides. The inductance per unit length of an ideal uniform line has been shown to be

$$l_0^e = \frac{1}{\pi\nu_0}\ln\frac{b}{a} \tag{6}$$

subject to the condition $b^2 \gg a^2$, which is included in (1). Strictly the square root occurring in (5) may be replaced by unity if (1) is imposed. However, by using the unrestricted formula

$$l_0^e = \frac{1}{\pi\nu_0}\cosh^{-1}\frac{b}{2a} \tag{7}$$

for the inductance per unit length of the line and retaining the term in a_s^2/b^2 in the radical in (5), this formula for L may be generalized to apply approximately to all values of b/a. With (6) or (7) the external inductance of the rectangle as given in (5) may be expressed as follows:

$$L^e = 2L_s + 2s_t l_0^e + 2L_T \tag{8}$$

where

$$L_s = \frac{b}{2\pi\nu_0}\left(\sinh^{-1}\frac{b}{a_s} + \frac{a_s}{b} - \sqrt{1 + \frac{a_s^2}{b^2}}\right) \tag{9}$$

and†

$$L_T = -\frac{b - a}{2\pi\nu_0} \tag{10}$$

The total external inductance L^e of the rectangle is made up of two parts: (1) the sum of the two inductances L_s of the short sides of the rectangle, and (2) the total inductance of the long sides treated as a transmission line and expressed in the form $2s_t \ln (b/a) + 2L_T$. The term $2s_t \ln (b/a)$ is the inductance of a uniform line with constant inductance per unit length, and L_T is the correction for the actual nonuniformity of the induc-

† The same formula for L_T is derived from the general integral [Sec. 4, Eq. (3)] in Chap. V, Sec. 12.

tance per unit length. The internal inductance L^i is negligible, so that $L = L^e + L^i \doteq L^e$.

Since the short ends c and e of the long rectangle in Fig. 20.1 are by postulate sufficiently far apart to be essentially uncoupled, a section of length s_t at the end of a long transmission line has an inductance given by one-half of (8), viz.,

$$L = L_s + s_t l_0^e + L_T \equiv L_{sa} + s_t l_0^e \tag{11}$$

where, by definition,

$$L_{sa} \equiv L_s + L_T \tag{12}$$

is the *apparent* impedance of the terminating wire bridge if the line is assumed to be uniform and L_s is the theoretical, isolated impedance of the bridge. Note that L_{sa} differs from L_s by a terminal-zone inductance L_T that is *negative*, indicating that the inductance per unit length is greater along a uniform line than near a terminating impedance at the end of the line. Note that the inductance of the bridge *apparently* terminating the line, as determined by measurement and calculation using (6) for the entire length of line, including the section of length s_t, is L_{sa}.

Since the resistance of the wire bridge is

$$R_s = br_s^i \tag{13}$$

where r_s^i is the internal resistance of a cylindrical conductor, it follows that the theoretical impedance of the bridge is

$$\boldsymbol{Z}_s = R_s + j\omega L_s \tag{14}$$

whereas the *apparent* terminal impedance of the bridge at the end of an assumed uniform line is

$$\boldsymbol{Z}_{sa} = R_s + j\omega L_{sa} \tag{15}$$

The terminal functions $\boldsymbol{\theta}_s = \rho_s + j\Phi_s$, corresponding to the theoretical impedance $\boldsymbol{Z}_s$, and $\boldsymbol{\theta}_{sa} = \rho_{sa} + j\Phi_{sa}$, corresponding to the apparent impedance $\boldsymbol{Z}_{sa}$, may be readily defined for the conducting wire bridge.

Highly Conducting Bridge. The normalized resistance and reactance of a highly conducting wire bridge may be assumed to satisfy the following conditions:

$$r_{1s}^2 \ll 1 \qquad x_{1s}^2 \ll 1 \tag{16}$$

where

$$r_{1s} = \frac{R_s - \phi_c X_s}{R_c(1 + \phi_c^2)} \doteq \frac{R_s}{R_c} - \phi_c \frac{X_s}{R_c} \tag{17a}$$

$$x_{1s} = \frac{X_s + \phi_c R_s}{R_c(1 + \phi_c^2)} \doteq \frac{X_s}{R_c} + \phi_c \frac{R_s}{R_c} \tag{17b}$$

In the approximate equalities in (17a,b) it is assumed that ϕ_c is sufficiently small so that $\phi_c^2 \ll 1$.

With (16)
$$\rho_s = \tfrac{1}{2}\tanh^{-1}\frac{2r_{1s}}{r_{1s}^2 + x_{1s}^2 + 1} \doteq r_{1s} \tag{18a}$$

$$\Phi_s = \tfrac{1}{2}\tan^{-1}\frac{-2|x_{1s}|}{-|r_{1s}^2 + x_{1s}^2 - 1|} \doteq \frac{\pi}{2} + \tan^{-1} x_{1s} \doteq \frac{\pi}{2} + x_{1s} \tag{18b}$$

Let
$$X_s = \omega L_s \qquad R_s = br_s^i \tag{19}$$

where r_s^i is the resistance per unit length of the conducting bridge of radius a_s.

For a low-loss line in air, $\phi_c \doteq r/2\omega l = \alpha/\beta$, where r is the resistance and l is the inductance per *loop* unit length. It follows that (18*a*), with (17*a*) and (19), may be expressed in the form

$$\rho_s \doteq \frac{R_s}{R_c} - \frac{r}{2\omega l}\frac{\omega L_s}{R_c} = \frac{r}{2R_c}\left(\frac{2R_s}{r} - \frac{L_s}{l}\right) \tag{20}$$

The following new symbols, which are dimensionally lengths in meters, are introduced conveniently for the ratios in (20):

$$m_s \equiv \frac{2R_s}{r} \qquad k_s \equiv \frac{L_s}{l} \tag{21}$$

Hence
$$\rho_s = \alpha(m_s - k_s) \tag{22}$$

Similarly
$$\Phi_s = \frac{\pi}{2} + \frac{X_s}{R_c} + \phi_c\frac{R_s}{R_c} = \frac{\pi}{2} + \frac{\omega l}{R_c}k_s + \frac{\alpha^2}{\beta}m \tag{23}$$

Since
$$\frac{R_c}{l} = \frac{1}{\sqrt{lc}} = v \qquad \frac{\omega}{v} \equiv \beta \tag{24}$$

it follows that, with $\alpha^2/\beta^2 \ll 1$,

$$\Phi_s = \frac{\pi}{2} + \beta\left(k_s + \frac{\alpha^2}{\beta^2}m_s\right) \doteq \frac{\pi}{2} + \beta k_s \tag{25}$$

The *apparent* terminal functions for the apparent terminal impedance $\boldsymbol{Z}_{sa} = R_{sa} + jX_{sa}$ are obtained in the same manner as (20) and (25). Since

$$X_{sa} = \omega L_{sa} = \omega(L_s + L_T) \tag{26}$$

it is necessary merely to define

$$k_{sa} \equiv \frac{L_{sa}}{l} = k_s + k_T = \frac{L_s}{l} + \frac{L_T}{l} \tag{27}$$

in order to obtain

$$\rho_{sa} = \alpha(m_s - k_{sa}) = \rho_s - \alpha k_T \tag{28}$$

$$\Phi_{sa} = \frac{\pi}{2} + \beta k_{sa} = \Phi_s + \beta k_T \tag{29}$$

It is convenient to represent the equivalent lengths k_s and k_{sa} as follows:

$$k_s = \frac{f_s b}{2} \qquad k_{sa} = \frac{f_{sa} b}{2} \tag{30}$$

where, with

$$y \equiv \frac{b}{a} \qquad y_s \equiv \frac{b}{a_s} \tag{31}$$

$$f_s = \frac{\sinh^{-1} y_s + y_s^{-1} - \sqrt{1 + y_s^{-2}}}{\cosh^{-1} (y/2)} \tag{32}$$

$$f_{sa} = \frac{\sinh^{-1} y_s + 2y_s^{-1} - 1 - \sqrt{1 + y_s^{-2}}}{\cosh^{-1} (y/2)} \tag{33}$$

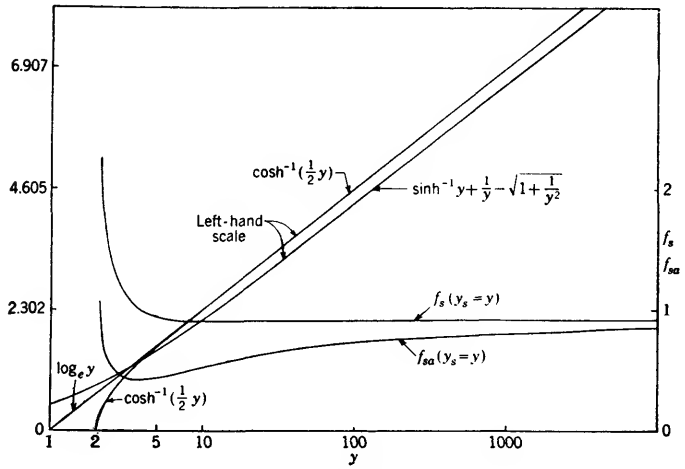


FIG. 20.2. The functions f_s and f_{sa} of $y = b/a$.

The functions f_s and f_{sa} are shown as functions of y in Fig. 20.2 in the special case where all wires are of the same size, so that $a_s = a$ and $y_s = y$. It is seen that

$$f_s \doteq 0.95 \qquad y \equiv \frac{b}{a} \geqq 5 \tag{34}$$

whereas f_{sa} is considerably smaller and much less constant when $y \geqq 5$. Evidently the theoretical, equivalent reactive length k_s of a straight conducting bridge made of wire of equal radius as the line is

$$k_s \doteq 0.475b \doteq \frac{b}{2} \tag{35}$$

However, since the inductance per unit length of the line is not constant near the terminating bridge, the apparent equivalent reactive length k_{sa}, as determined under the assumption that l is constant, is appreciably smaller than k_s.

If the bridge is not only equal in radius to the wires of the line but also made of the same material, it follows that

$$m_s = \frac{2R_s}{r} = b \tag{36}$$

so that, with (22),

$$\rho_s = \alpha b \left(1 - \frac{f_s}{2}\right) \qquad \rho_{sa} = \alpha b \left(1 - \frac{f_{sa}}{2}\right) \tag{37}$$

If (35) is a good approximation,

$$\rho_s \doteq \tfrac{1}{2}\alpha b \tag{38}$$

By choosing the radius a_s of the bridge somewhat smaller than the radius a of the line wires, f_s or f_{sa} may be made equal to unity for any particular value of b/a. The required value of a_s is obtained by setting (32) or (33) equal to unity and solving for $y_s = b/a_s$. For simplicity let y_s be quite large, so that the radical in (32) or (33) may be set equal to unity and y_s^{-1} neglected compared with 1. Specifically let

$$y_s \gg 1 \tag{39}$$

Then
$$f_s \doteq \frac{\sinh^{-1} y_s - 1}{\cosh^{-1} (y/2)} = 1 \qquad f_{sa} \doteq \frac{\sinh^{-1} y_s - 2}{\cosh^{-1} (y/2)} \tag{40}$$

For large arguments the inverse hyperbolic functions approach natural logarithms of twice the argument, so that (40) becomes

$$\ln 2y_s \doteq 1 + \ln y \qquad \ln 2y_s \doteq 2 + \ln y \tag{41}$$

or
$$\ln \frac{2y_s}{y} \doteq 1 \qquad \ln \frac{2y_s}{y} \doteq 2 \tag{42}$$

The results are

$$y_s \doteq 1.359y \qquad y_s \doteq 7.389y \tag{43}$$

Hence
$$a_s \doteq 0.736a \quad \text{for } f_s = 1$$
$$a_s \doteq 0.135a \quad \text{for } f_{sa} = 1 \tag{44}$$

If the radius of the termination is chosen to have one of these values and b/a is large, so that $b/a \geqq 5$,

$$f_s = 1 \qquad k_s = \frac{b}{2}$$
or
$$f_{sa} = 1 \qquad k_{sa} = \frac{b}{2} \tag{45}$$

If the terminating wire differs from the two-wire line in both diameter and material, the following formula is true, subject to the indicated condition:

$$a_s \sqrt{\frac{\omega\sigma_s}{\nu_s}} \geqq 10 \qquad R_s = \frac{b}{2\pi a_s} \sqrt{\frac{\omega}{2\sigma_s\nu_s}} \tag{46}$$

where σ_s and ν_s pertain to the material of the terminating wire. Similarly the comparable condition and the resistance per unit length of the line are

$$a\sqrt{\frac{\omega\sigma}{\nu}} \geqq 10 \qquad \frac{r}{2} = r^i = \frac{1}{2\pi a}\sqrt{\frac{\omega}{2\sigma\nu}} \tag{47}$$

Accordingly

$$\frac{m_s}{b} = \frac{2R_s}{rb} = \frac{a}{a_s}\sqrt{\frac{\sigma\nu}{\sigma_s\nu_s}} \tag{48}$$

The value of a_s to make $f_s = 1$ has been shown to be $a_s = 0.736a$; the value to make $f_{sa} = 1$ is $a_s = 0.139a$. With these values

$$\frac{m_s}{b} = 1.36\sqrt{\frac{\sigma\nu}{\sigma_s\nu_s}} \quad \text{or} \quad \frac{m_s}{b} = 7.4\sqrt{\frac{\sigma\nu}{\sigma_s\nu_s}} \tag{49}$$

Thus, if the materials can be so chosen that

$$\frac{\sigma\nu}{\sigma_s\nu_s} = 0.54 \quad \text{or} \quad \frac{\sigma\nu}{\sigma_s\nu_s} = 0.183 \tag{50}$$

it follows that

$$\frac{m_s}{b} = 1 \tag{51}$$

and

$$\rho_s = \tfrac{1}{2}\alpha b \quad \text{or} \quad \rho_{sa} = \tfrac{1}{2}\alpha b \tag{52}$$

It is to be noted that it is not possible for physical reasons to make $\rho_s = \frac{1}{2}\alpha b$ or $\rho_{sa} = \frac{1}{2}\alpha b$ if the two-wire line is copper, since a material with 1.85 or 5.45 times the conductivity of copper would be required for the terminating bridge. No such material is available.

By making use of the theory developed in this section, the apparent terminal functions of a conducting wire bridge may be determined. Note that the accuracy of these determinations involves errors of the order of magnitude of the radius of the wire in the measurement of lengths on the two-wire line.

In actual use a conducting bridge often must be movable along an extended section of two-wire line. As shown in Chap. VI, a conducting bridge may serve as an inductance common to the sections of line continuing in each direction whenever the bridge is not exactly at the end. In order to avoid the coupled-circuit effects and preserve the impedance of the bridge as a constant independent of its location along the line, it is often advantageous to use two bridges separated a distance $\lambda/4 - k_{sa}$ and connected so as to move together in tandem. This arrangement is illustrated in Fig. 20.3. As shown in Chap. III, Sec. 6, a section of line of this length which is terminated in a conducting bridge behaves essentially like an insulator of several hundred thousand ohms. Evidently the presence of such a high impedance that moves along and is always in parallel with the very low impedance bridge terminating the line has no

significant effect on the properties of this bridge, and these remain essentially unchanged as it is moved.

Resistive Bridge. If it is desired to terminate a two-wire line in its characteristic impedance in order to have a matched line that may be used, for example, for phase comparisons (Chap. IV, Sec. 13), a bridge consisting of a straight conductor made of resistance wire or a straight conductor with a small carbon resistor at its center may be used. Such a bridge has an inductive reactance that is essentially the same as if it were highly conducting. Since this is very small compared with the resistance, the condition of match is approximated closely when the resistance of the bridge is $R_s = R_c$.

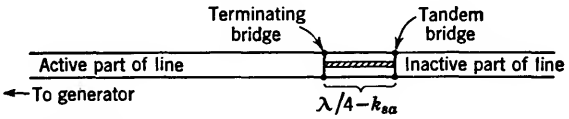


FIG. 20.3. Tandem-bridge section of line to form movable insulating support continuously in parallel with movable bridge.

21. Conducting Pistons and Disks as Terminations. A perfectly conducting piston in a coaxial line or a shielded-pair line and a perfectly conducting disk of infinite extent on an open-wire line are terminations that may be analyzed together using the theorem of images. In each case the electromagnetic field and the distributions of current and charge on the transmission line are unchanged if the conducting piston or disk at a point P along the line is removed and the line continued as a geometric image, including the generator with its polarity reversed. Since the potential difference across the line at P due to the image generator and line must always be equal and opposite to that maintained by the actual generator and line, it follows that the potential difference across the line at P is always zero. Hence the terminal function of the image line and of the equivalent conducting piston or infinite disk is $\theta_s = 0 + j\pi/2$. Accordingly a highly conducting piston for a coaxial line or shielded-pair line and an infinite disk for an open-wire line may be assumed to be represented by $\rho_s \doteq 0$ and $\Phi_s = \pi/2$. These are convenient for use as standard terminations.

In practice, a conducting disk of infinite extent is unavailable, and the question arises: How large must a disk be in order to approximate an infinite one as a termination? A suitable criterion may be obtained by investigating the rate of decrease of the magnetic field along, or of the surface current in, an infinite disk due to a pair of conductors separated a distance b and with equal and opposite currents. For simplicity, the conductors may be assumed infinitely long, since the contributions from sections of the line which are far from the disk compared with the spacing of the wires are negligible. In the plane that is equidistant from the two

conductors, the resultant magnetic field is radial and given approximately by

$$B_r(r) \doteq \frac{I_m}{2\pi\nu_0} \frac{b}{r^2 + b^2/4} \tag{1a}$$

In the plane containing the two conductors the field is approximately

$$B_\theta(r) \doteq \frac{I_m}{2\pi\nu_0} \left(\frac{1}{r - b/2} - \frac{1}{r + b/2} \right) = \frac{I_m}{2\pi\nu_0} \frac{b}{r^2 - b^2/4} \tag{1b}$$

I_m is the maximum of the sinusoidally distributed current along the transmission line and therefore the current entering and leaving the plane from the wires.

A suitable criterion of comparison is the magnetic field on the disk midway between its junction with the two conductors. This is given by (1*a*) with $r = 0$. It is

$$B_r\ (r = 0) = \frac{2I_m}{\pi\nu_0 b} \tag{2}$$

The ratio of the field at two locations at radius r to that at $r = 0$ is

$$\frac{B(r)}{B\ (r = 0)} \leqq \frac{b^2/4}{r^2 \pm b^2/4} \tag{3}$$

Let it be assumed that the magnetic field and the surface-current density at r are negligible compared with the field and surface-current density at $r = 0$ when the ratio in (3) is no greater than 0.01. Thus

$$\frac{b^2/4}{r^2 \pm b^2/4} \leqq 0.01 \tag{4}$$

This can be satisfied only when $b^2/4$ is small compared with r^2, so that (4) reduces to

$$\frac{b^2}{r^2} \leqq 0.04 \qquad \frac{b}{r} \leqq 0.2 \tag{5}$$

It follows that the maximum density of surface current on the infinite disk at a radial distance r from the center of the line is less than 1 per cent of the density halfway between the two conductors of the line if

$$r \geqq 5b \tag{6}$$

It may be assumed that, if the current density on an infinite disk at $r = 5b$ is only 1 per cent of that at its center, the effect of the part of the disk beyond $r = 5b$ is of no great significance and may be omitted. That is, (6) is a satisfactory criterion for determining the radius of a disk to terminate an open two-wire line with $\rho \doteq 0$ and $\Phi \doteq \pi/2$.

22. Terminations with Negative Attenuation Function or Reflection Coefficient Greater than Unity. An interesting special termination is that

for which the terminal attenuation function ρ_s becomes negative. Since the magnitude of the coefficient of reflection is $\Gamma_s = e^{-2\rho_s}$, it follows that negative values of ρ_s correspond to values of Γ_s *greater than unity.*†

The general formula for ρ_s is

$$\rho_s = \tfrac{1}{2} \tanh^{-1} \frac{2r_{1s}}{|z_{1s}|^2 + 1} \tag{1}$$

For ρ_s to be negative, r_{1s} must be negative. That is,

$$r_{1s} \equiv \frac{R_s - \phi_c X_s}{R_c(1 + \phi_c^2)} < 0 \tag{2}$$

Evidently this is possible only when X_s is positive and $\phi_c \neq 0$, that is,

$$X_s > 0 \qquad R_s < \phi_c X_s \tag{3}$$

(Note that $r_{1s} = 0$ means that $R_s = \phi_c X_s$, *not* that $R_s = 0$.) The second condition in (3) is equivalent to

$$\frac{R_s}{X_s} < \phi_c = \frac{X_c}{R_c} \tag{4}$$

For example, on a low-loss line with negligible leakage conductance, $\phi_c \doteq \alpha/\beta = r/2\omega l$, so that, since X is inductive,

$$\frac{R_s}{\omega L_s} < \frac{r}{2\omega l} \tag{5}$$

or

$$k_s = \frac{L_s}{l_s} > \frac{2R_s}{r} \left(= \frac{R_s}{r^i} \text{ for a two-wire line} \right) \tag{6}$$

† The possibility of coefficients of reflection that exceed unity even slightly may appear paradoxical to those accustomed to treat the characteristic impedance as a pure resistance. When $\boldsymbol{Z}_c = R_c$, so that it is a pure resistance, as for the distortionless or lossless line, for which $\phi_c = 0$, the coefficient of reflection can never exceed unity in magnitude, and it is possible to separate not only incident and reflected voltages and currents but also incident and reflected powers. When $\boldsymbol{Z}_c$ is complex, as in the lossy line, the current and voltage along an infinitely long or perfectly matched line are not exactly in phase. Although it is still possible to identify traveling waves of incident and reflected voltages and currents, a separation into incident and reflected powers is no longer possible owing to the appearance of cross-product terms. A termination with a reflection coefficient of unity reflects incident waves of current and voltage with the same phase difference. If the phase difference of the reflected current and voltage is *less* than for the incident waves, the reflection coefficient must exceed unity. The power factor for dissipation in the line has been improved. In the case of the usual low-loss lines, ϕ_c in $\boldsymbol{Z}_c = R_c(1 - j\phi_c)$ is very small, so that the incident voltage and current differ by the very small angle $\tan^{-1} \phi_c = \cos^{-1} (1/\sqrt{1 + \phi_c^2})$. It is readily verified from Sec. 5, Eq. (7), that, for a termination with $R_s = 0$ and $X_s = -X_c/2 = \phi_c R_c/2$, $\Gamma_s = \sqrt{1 + \phi_c^2}$, which exceeds unity slightly. Note that a change in power factor from $\cos \tan^{-1} \phi_c$ to unity corresponds to an increase in magnitude by a factor $\sqrt{1 + \phi_c^2}$. The contribution to the power by terms involving ϕ_c is referred to in Chap. IV, Sec. 6.

For a termination on an open-wire line consisting of a conducting wire bridge of the same radius as the wires of the line, Sec. 20, Eq. (22), gives

$$\rho_s = \alpha(m_s - k_s) \tag{7}$$

where $$k_s = \frac{L_s}{l} = \frac{f_s b}{2} \qquad m_s = \frac{R_s}{r^i} = \frac{b r_s^i}{r^i}$$

Note that r_s^i is the internal resistance per unit length of the bridge, and r^i is the internal resistance per unit length of each of the conductors of the line. Hence the requirement for negative ρ_s, namely,

$$m_s < k_s \tag{8}$$

reduces to

$$\frac{r_s^i}{r^i} < \frac{f_s}{2} \tag{9}$$

since f_s is slightly less than unity. That is, the resistance per unit length of each conductor of the two-wire line r^i must be at least double the resistance per unit length of the terminating bridge. Using

$$r^i = \frac{1}{2\pi a}\sqrt{\frac{\omega}{2\sigma\nu}} \tag{10}$$

the condition becomes

$$\frac{r_s^i}{r^i} = \sqrt{\frac{\sigma\nu}{\sigma_s\nu_s}} < \frac{f_s}{2} \leqq 0.5 \tag{11a}$$

or

$$\frac{\sigma\nu}{\sigma_s\nu_s} < \frac{f_s^2}{4} \leqq 0.25 \tag{11b}$$

Clearly, if the line is of copper immersed in air, no bridge with negative ρ_s is available. However, with a brass line and a copper termination,

$$m_s^2 = \left(\frac{r_s^i}{r^i}\right)^2 = \frac{\sigma\nu}{\sigma_s\nu_s} = \frac{1.2}{5.65} = 0.21 < 0.25 \tag{12}$$

so that

$$m_s \doteq 0.46b \tag{13}$$

and, with $f_s \doteq 0.96$,

$$\rho_s \doteq \alpha b(0.46 - 0.48) \doteq -0.02\alpha b \tag{14}$$

Evidently the higher the resistance of the line wires compared with the resistance of the conducting bridge, the more negative ρ_s may be. Note that, since f_{sa} is smaller than f_s, ρ_{sa} is always less negative than ρ_s for a given value of r_s^i/r^i. In particular, ρ_s may be negative, and ρ_{sa}, positive.

PROBLEMS

1. A section of transmission line is two wavelengths long and terminated in a load at $z = s$ equal to $Z_c/2$. The generator at $z = 0$ has an emf of 10 volts and an impedance equal to $2Z_c$. The losses in the relatively short line are negligible. Write out the first four terms in the infinite series for the voltage at a distance of one-quarter wavelength from the generator. Express the reflection coefficients numerically.

2. Express the voltage at the same point in the line described in the preceding problem as the sum of an incident and a reflected wave. Give numerical values.

3. Express the voltage on the line described in Prob. 1 in terms of a single wave traveling toward the load with variable phase velocity. Plot the amplitude of the voltage wave along the line; also plot the phase velocity.

4. Calculate the line constants r, l, and c (g is negligible) for a coaxial line consisting of a silver inner conductor of No. 20 wire and a tin outer conductor of inner radius 0.254 cm at a frequency of 3,000 Mc/sec. The dielectric is polystyrene ($\epsilon_r = 2.6$; $\mu_r = 1$). Use the following conductivities: σ (silver) $= 6.14 \times 10^7$ mhos/m; σ (tin) $= 0.87 \times 10^7$ mhos/m.

5. Determine the attenuation constant α, the phase constant β, the characteristic resistance R_c, the distortion factor ϕ_c, and the wavelength for the line in Prob. 4.

6. Calculate the line constants r, l, and c (g is negligible) for a two-conductor line made of brass with a conductivity of 1.22×10^7 mhos/m. The two conductors are identical and of radius 0.04 in. spaced 1 cm between centers in air. The frequency is 750 Mc/sec.

7. Calculate the attenuation constant, the phase constant, the characteristic resistance, and the distortion factor for the line in the preceding problem.

8. Determine the phase velocity and the group velocity for the line described in Prob. 6, using the more accurate formulas given in Sec. 13.

9. Calculate a few points and plot curves of $R_c \doteq \sqrt{l_0^e/c}$ for the following transmission lines for the indicated ranges of b/a. Use semilog paper. (For open-wire lines b is the distance between centers of adjacent wires, and a is the radius of each wire; for coaxial lines b is the inner radius of the outer conductor, and a the radius of the inner conductor.)

(a) Coaxial line with air as dielectric. Range, $1 \leqq b/a \leqq 600$.

(b) Coaxial line with polystyrene ($\epsilon_r = 2.6$) as dielectric. Range as in (a).

(c) Two-wire line with air as dielectric. Range as in (a). Note that the logarithmic formula is satisfactory only when $b^2 \gg a^2$.

(d) Four-wire line with diagonal conductors in parallel and with air as dielectric. Range, $5 \leqq b/a \leqq 600$.

10. Derive a formula for the minimum value of the attenuation constant α for a coaxial line with an outer conductor of fixed radius as the radius of the inner conductor is varied. Plot a curve of α as a function of the ratio of the radius of the outer to that of the inner conductor near the minimum to determine whether this is sharp or flat.

11. Determine the complex reflection coefficient Γ_s in polar form and the terminal functions ρ_s and Φ_s for the following impedances Z_s (ohms) terminating a low-loss line with $Z_c \doteq R_c = 300$ ohms: (a) $Z_s = 3{,}000 + j0$; (b) $Z_s = 0 + j3{,}000$; (c) $Z_s = 3{,}000(1 + j)$; (d) $Z_s = 0 + j300$; (e) $Z_s = 200 + j100$; (f) $Z_s = 0$; (g) $Z_s = \infty$.

12. An apparent impedance $Z_{sa} = 75 + j200$ ohms terminates a low-loss coaxial line of characteristic impedance $Z_c \doteq R_c = 50$ ohms. What are the corresponding values of the apparent reflection coefficient Γ_{sa}; the apparent terminal functions ρ_{sa}, Φ_{sa}, and Φ'_{sa}; and the apparent admittance Y_{sa}?

13. In an experimental determination of the impedance of an antenna, the following typical data were observed on a line for which $Z_c \doteq R_c = 50$ ohms:

Electrical length of antenna, radians.....	0.22	1.45	2.00	2.28
Measured ρ, nepers.....	0.001	0.870	0.230	0.147
Measured Φ, radians.....	0.17	1.57	3.00	3.14

Calculate R and X for the antenna at each length, and check with the circle diagram.

14. The capacitance of a capacitor is 15 $\mu\mu$f. It is connected as the terminal impedance of a line of characteristic impedance $\boldsymbol{Z}_c \doteq R_c = 400$ ohms. What are the terminal functions ρ and Φ at 150 Mc/sec? Assume the capacitor to be without loss.

15. A two-wire line is made of brass $\frac{1}{8}$ in. in diameter, with 2 cm between centers. A copper rod of the same diameter is used as a short-circuiting bar at the load end. Determine r_1, x_1, and Φ for this bar at 300 Mc/sec. (Use $\sigma = 1.5 \times 10^7$ mhos/m for brass and $\sigma = 5.65 \times 10^7$ mhos/m for copper.)

CHAPTER III

IMPEDANCE AND ADMITTANCE

1. Normalized Input Impedance and Admittance of a Terminated Section of Line. A transmission line extends from $z = 0$ to $z = s + s_t$, where $s_t^2 \gg b^2$. The impedance terminating the line at $z = s$ is $\boldsymbol{Z}_s = 1/\boldsymbol{Y}_s$. What is the impedance $\boldsymbol{Z}_z$ or admittance $\boldsymbol{Y}_z$ terminating the line at $z < s$? Alternatively, what is the impedance $\boldsymbol{Z}_{in} = \boldsymbol{Z}_z$ or admittance $\boldsymbol{Y}_{in} = \boldsymbol{Y}_z$ looking into the section of line to the right (Fig. 1.1) of the point z,

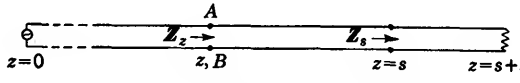


FIG. 1.1. Terminated transmission line.

expressed in terms of $\boldsymbol{Z}_s$ or $\boldsymbol{Y}_s$ and the length $s - z = w$ of the section? Note that this is not the same as the impedance $\boldsymbol{Z}_{in}$ of the isolated section of line of length w terminated in $\boldsymbol{Z}_s$ shown in Fig. 1.2. The absence of the line to the left of the points AB in Fig. 1.2 as compared with Fig. 1.1 involves an end effect and coupling effect in a terminal zone near AB.

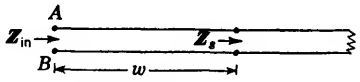


FIG. 1.2. Isolated section of transmission line. The impedance $\boldsymbol{Z}_{in}$ is not the same as $\boldsymbol{Z}_z$ in Fig. 1.1, owing to the end effect.

If a potential difference is maintained across AB in Fig. 1.1, equal and opposite currents are in the two conductors at z. Let phase be referred to the current in conductor 1 as heretofore. The input impedance or admittance of the line to the right of AB (which is equal to the load impedance or admittance terminating the line to the left of AB) is defined to be

$$\boldsymbol{Z}_{in} = R_{in} + jX_{in} \equiv \frac{\boldsymbol{V}_z}{\boldsymbol{I}_z} \qquad \boldsymbol{Y}_{in} = G_{in} + jB_{in} \equiv \frac{\boldsymbol{I}_z}{\boldsymbol{V}_z} \tag{1}$$

Note that, since AB is by definition far from both ends compared with the wavelength, the y component of the vector potential is zero or practically zero ($\boldsymbol{A}_y \doteq 0$) near AB, so that $\boldsymbol{E}_y = -\partial\phi/\partial y - j\omega\boldsymbol{A}_y \doteq -\partial\phi/\partial y$. Hence

$$\boldsymbol{V}_z \equiv \phi_{1z} - \phi_{2z} = 2\phi_{1z} \doteq \int_0^b \boldsymbol{E}_y \, dy \tag{2}$$

A number of formulas may be obtained for $\boldsymbol{Z}_{in}$ and $\boldsymbol{Y}_{in}$ corresponding to the several different representations of current and voltage along a transmission line. Each has certain advantages in special cases. Thus, for example, the exponential solutions [Chap. II, Sec. 5, Eqs. (10) and (11)] lead to the following formulas for the normalized input impedance and admittance:

$$\boldsymbol{z}_{1in} \equiv \frac{\boldsymbol{Z}_{in}}{\boldsymbol{Z}_c} = \frac{1 + \boldsymbol{\Gamma}_s e^{-2\gamma w}}{1 - \boldsymbol{\Gamma}_s e^{-2\gamma w}} \qquad \boldsymbol{y}_{1in} \equiv \frac{\boldsymbol{Y}_{in}}{\boldsymbol{Y}_c} = \frac{1 + \boldsymbol{\Gamma}'_s e^{-2\gamma w}}{1 - \boldsymbol{\Gamma}'_s e^{-2\gamma w}} \tag{3}$$

For a lossless line ($\alpha_s = 0$) these reduce to

$$\boldsymbol{z}_{1in} = \frac{\boldsymbol{Z}_{in}}{R_c} = \frac{1 + \Gamma_s e^{j(\psi_s - 2\beta w)}}{1 - \Gamma_s e^{j(\psi_s - 2\beta w)}} \qquad \boldsymbol{y}_{1in} = \frac{\boldsymbol{Y}_{in}}{G_c} = \frac{1 + \Gamma_s e^{j(\psi'_s - 2\beta w)}}{1 - \Gamma_s e^{j(\psi'_s - 2\beta w)}} \tag{4}$$

Note that

$$\boldsymbol{\Gamma}_s = \Gamma_s e^{j\psi} = \frac{\boldsymbol{z}_{1s} - 1}{\boldsymbol{z}_{1s} + 1} = -\frac{\boldsymbol{y}_{1s} - 1}{\boldsymbol{y}_{1s} + 1} = -\Gamma_s e^{j\psi'} = -\boldsymbol{\Gamma}'_s \tag{5}$$

where $\boldsymbol{z}_{1s} \equiv \boldsymbol{Z}_s/\boldsymbol{Z}_c$, $\boldsymbol{y}_{1s} \equiv \boldsymbol{Y}_s/\boldsymbol{Y}_c$, and

$$\boldsymbol{Z}_c = R_c(1 - j\phi_c) \qquad \boldsymbol{Y}_c = G_c(1 + j\phi_c) \tag{6}$$

The complex hyperbolic forms of the input impedance are obtained from Chap. II, Sec. 8, Eqs. (2) and (3). They are

$$\boldsymbol{z}_{1in} \equiv \frac{\boldsymbol{Z}_{in}}{\boldsymbol{Z}_c} = \frac{\boldsymbol{Z}_s \cosh \gamma w + \boldsymbol{Z}_c \sinh \gamma w}{\boldsymbol{Z}_s \sinh \gamma w + \boldsymbol{Z}_c \cosh \gamma w} \tag{7a}$$

$$\boldsymbol{y}_{1in} \equiv \frac{\boldsymbol{Y}_{in}}{\boldsymbol{Y}_c} = \frac{\boldsymbol{Y}_s \cosh \gamma w + \boldsymbol{Y}_c \sinh \gamma w}{\boldsymbol{Y}_s \sinh \gamma w + \boldsymbol{Y}_c \cosh \gamma w} \tag{7b}$$

Alternatively

$$\boldsymbol{z}_{1in} = \frac{\boldsymbol{z}_{1s} \coth \gamma w + 1}{\boldsymbol{z}_{1s} + \coth \gamma w} = \frac{\boldsymbol{z}_{1s} + \tanh \gamma w}{\boldsymbol{z}_{1s} \tanh \gamma w + 1} \tag{8a}$$

$$\boldsymbol{y}_{1in} = \frac{\boldsymbol{y}_{1s} \coth \gamma w + 1}{\boldsymbol{y}_{1s} + \coth \gamma w} = \frac{\boldsymbol{y}_{1s} + \tanh \gamma w}{\boldsymbol{y}_{1s} \tanh \gamma w + 1} \tag{8b}$$

For the lossless line ($\alpha_s = 0$)

$$\boldsymbol{z}_{1in} = \frac{\boldsymbol{Z}_{in}}{R_c} = \frac{1 - j\boldsymbol{z}_{1s} \cot \beta w}{\boldsymbol{z}_{1s} - j \cot \beta w} = \frac{\boldsymbol{z}_{1s} + j \tan \beta w}{1 + j\boldsymbol{z}_{1s} \tan \beta w} \tag{9a}$$

$$\boldsymbol{y}_{1in} = \frac{\boldsymbol{Y}_{in}}{G_c} = \frac{1 - j\boldsymbol{y}_{1s} \cot \beta w}{\boldsymbol{y}_{1s} - j \cot \beta w} = \frac{\boldsymbol{y}_{1s} + j \tan \beta w}{1 + j\boldsymbol{y}_{1s} \tan \beta w} \tag{9b}$$

For many purposes involving dissipative loads on low-loss lines, (9*a*,*b*) are adequate.

The completely hyperbolic form is simple and especially convenient for deriving explicit formulas for $\boldsymbol{R}_{in}$ and $\boldsymbol{X}_{in}$, $\boldsymbol{G}_{in}$ and $\boldsymbol{B}_{in}$. The desired formulas are obtained from Chap. II, Sec. 8, Eqs. (15) and (16). They are

$$\boldsymbol{z}_{1in} = \coth (\gamma w + \boldsymbol{\theta}_s) = \coth [(\alpha w + \rho_s) + j(\beta w + \Phi_s)] \tag{10a}$$

$$\boldsymbol{y}_{1in} = \coth (\gamma w + \boldsymbol{\theta}'_s) = \coth [(\alpha w + \rho_s) + j(\beta w + \Phi'_s)] \tag{10b}$$

For convenience, let the following notation be introduced:

$$A_w \equiv \alpha w + \rho_s \tag{11a}$$

$$F_w \equiv \beta w + \Phi_s \qquad F'_w \equiv \beta w + \Phi'_s \tag{11b}$$

$$\theta'_s = \theta_s - j\frac{\pi}{2} \qquad \Phi'_s = \Phi_s - \frac{\pi}{2} \tag{12}$$

Note that, with (11*a*,*b*), (10*a*) becomes

$$z_{1in} = \coth (A_w + jF_w) \qquad y_{1in} = \coth (A_w + jF'_w) \tag{13}$$

These formulas are like the expressions previously derived for the normalized terminal impedance z_{1s} and admittance y_{1s}, namely,

$$z_{1s} = \coth (\rho_s + j\Phi_s) \qquad y_{1s} = \coth (\rho_s + j\Phi'_s) \tag{14}$$

Obviously (11) must reduce to (12) whenever $w = 0$.

Since $$z_{1in} = r_{1in} + jx_{1in} \qquad y_{1in} = g_{1in} + jb_{1in} \tag{15}$$

it follows that the normalized input resistance and reactance, conductance and susceptance are

$$r_{1in} = \frac{\sinh 2A_w}{\cosh 2A_w - \cos 2F_w} = \frac{\sinh A_w \cosh A_w}{\sinh^2 A_w + \sin^2 F_w} \tag{16a}$$

$$g_{1in} = \frac{\sinh 2A_w}{\cosh 2A_w - \cos 2F'_w} = \frac{\sinh A_w \cosh A_w}{\sinh^2 A_w + \sin^2 F'_w} \tag{16b}$$

$$x_{1in} = \frac{-\sin 2F_w}{\cosh 2A_w - \cos 2F_w} = \frac{-\sin F_w \cos F_w}{\sinh^2 A_w + \sin^2 F_w} \tag{17a}$$

$$b_{1in} = \frac{-\sin 2F'_w}{\cosh 2A_w - \cos 2F'_w} = \frac{-\sin F'_w \cos F'_w}{\sinh^2 A_w + \sin^2 F'_w} \tag{17b}$$

Inverse relations are

$$A_w = \tfrac{1}{2}\tanh^{-1}\frac{2r_{1in}}{r_{1in}^2 + x_{1in}^2 + 1} = \tfrac{1}{2}\tanh^{-1}\frac{2g_{1in}}{g_{1in}^2 + b_{1in}^2 + 1} \tag{18}$$

$$F_w = \tfrac{1}{2}\tan^{-1}\frac{-2x_{1in}}{r_{1in}^2 + x_{1in}^2 - 1} \qquad F'_s = \tfrac{1}{2}\tan^{-1}\frac{-2b_{1in}}{g_{1in}^2 + b_{1in}^2 - 1} \tag{19}$$

These formulas have the same form and obey the same sign conventions as those derived previously for Z_s and Y_s. They differ only in the appearance of A_w instead of ρ_s and F_w or F'_w instead of Φ_s or Φ'_s. When $w = 0$, $A_w = \rho_s$, $F_w = \Phi_s$, and $F'_w = \Phi'_s$.

The normalized input resistance and reactance are expressed numerically in Tables 1.1 and 1.2 as functions of A_w and F_w. The input phase function F_w is represented as a function of the input attenuation function A_w in Fig. 1.3 with r_{1in} as parameter and in Fig. 1.4 with x_{1in} as parameter. With the substitution of the symbol Φ_s for F_w, ρ_s for A_w, r_{1s} for r_{1in}, and x_{1s} for x_{1in}, these tables and curves apply to the normalized terminal impedance $z_{1s} = r_{1s} + jx_{1s}$.

The analogous significance of A_s and F_s for the input impedance and ρ_s and Φ_s for the terminal impedance reveals the simple and fundamental parts played by the terminal functions. The attenuation function ρ_s plays the same role for the termination as does αs for the line. Indeed ρ_s/α is an *equivalent length* of line for the termination from the point of view of attenuation. Similarly the phase functions Φ_s and Φ'_s play the

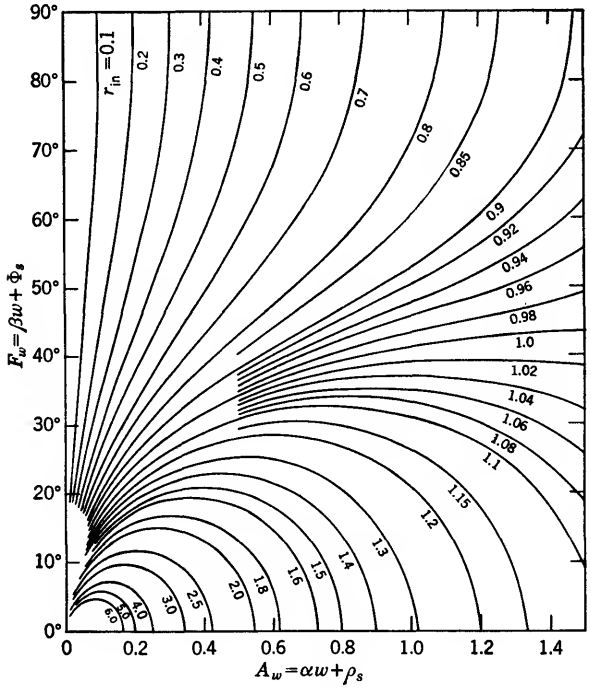


FIG. 1.3. Contours of constant r_{1in} with $F_w = \beta_w + \Phi_s$ and $A_w = \alpha w + \rho_s$ as variables.

same part in describing the effect of the termination as does βs for the line. The ratio Φ_s/β or Φ'_s/β is an equivalent length of line for the termination insofar as phase shift is concerned. The equivalent lengths for attenuation and for phase shift are not alike unless $\boldsymbol{Z}_s$ or $\boldsymbol{Y}_s$ is itself a section of transmission line or α for the section is modified so that $\rho_s/\alpha = \Phi_s/\beta$ or $\rho_s/\alpha = \Phi'_s/\beta$. In this special case it is possible to replace $\boldsymbol{Z}_s$ or $\boldsymbol{Y}_s$ by a section of transmission line which is its equivalent both in phase shift and in attenuation.

It is readily verified that, just as for ρ_s and Φ_s or Φ'_s in terms of r_{1s} and x_{1s} or g_{1s} and b_{1s}, the contours of constant A_s and the contours of constant F_w or F'_w are families of orthogonal circles. The intercepts, centers, and radii are as follows:

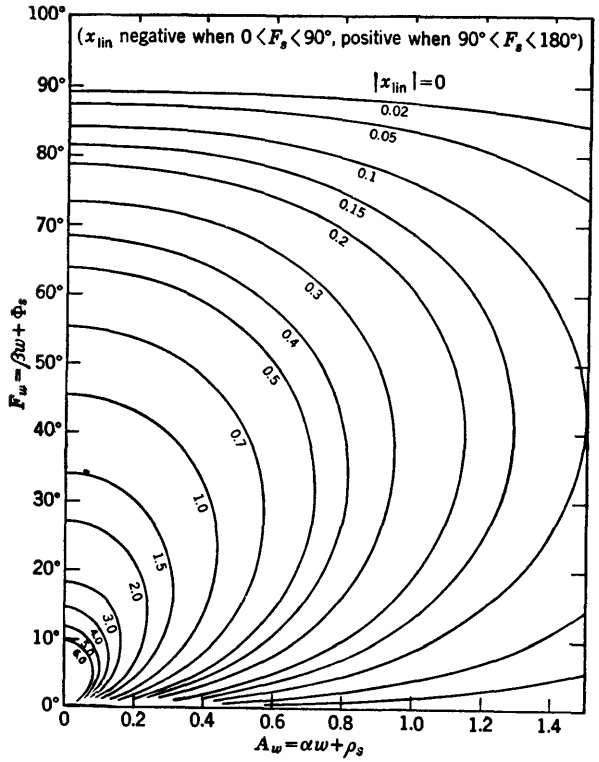


FIG. 1.4. Contours of constant x_{1in} with $F_w = \beta w + \Phi_s$ and $A_w = \alpha w + \rho_s$ as variables.

For circles of constant A_w:

$$\text{Intercepts are at } r_{1in} = \tanh A_w, \coth A_w \begin{cases} x_{1in} = 0 \\ b_{1in} = 0 \end{cases}$$

$$\text{Centers are at } r_{1in} = \coth 2A_w \begin{cases} x_{1in} = 0 \\ b_{1in} = 0 \end{cases}$$

Radii have magnitudes equal to $\operatorname{csch} 2A_w$

For circles of constant F_w and F'_w:

$$\text{Intercepts are at } r_{1in} = 0 \begin{cases} x_{1in} = -\cot F_w \text{ (or } \tan F_w) \\ b_{1in} = -\cot F'_w \text{ (or } \tan F'_w) \end{cases}$$

$$\text{Centers are at } r_{1in} = 0 \begin{cases} x_{1in} = -\cot 2F_w \\ b_{1in} = -\cot 2F'_w \end{cases}$$

$$\text{Radii have magnitudes equal to } \begin{cases} |\csc 2F_w| \\ |\csc 2F'_w| \end{cases}$$

The same circle diagrams previously constructed for ρ_s and Φ_s in terms of r_{1s} and x_{1s}, ρ_s and Φ'_s in terms of g_{1s} and b_{1s} may be used for $A_w = \alpha w + \rho_s$

TABLE 1.1

$$r_{1in} = \frac{\sinh 2A_w}{\cosh 2A_w - \cos 2F_w}$$

A_w \ F_w	0° 180°	0.5° 179.5°	1° 179°	2° 178°	3° 177°	4° 176°	5° 175°
0.0	.....	.....	0.000	0.000	0.000	0.000	0.000
0.003	.....	.....	9.524	2.441	1.091	0.6155	0.3945
0.004	.....	.....	12.50	3.236	1.451	0.8195	0.5256
0.005	.....	.....	15.15	4.016	1.808	1.022	0.6562
0.01	100.0	57.14	24.69	7.576	3.521	2.014	1.300
0.02	50.01	42.12	28.38	12.35	6.371	3.800	2.502
0.03	33.36	30.79	24.91	14.16	8.247	5.207	3.534
0.04	25.03	23.91	21.02	14.20	9.227	6.194	4.355
0.05	20.03	19.45	17.86	13.46	9.558	6.800	4.961
0.06	16.68	16.34	15.38	12.47	9.479	7.101	5.370
0.07	14.30	14.09	13.47	11.46	9.180	7.185	5.616
0.08	12.52	12.38	11.96	10.52	8.776	7.122	5.734
0.09	11.14	11.04	10.74	9.688	8.332	6.968	5.758
0.10	10.03	9.957	9.736	8.944	7.880	6.756	5.710
0.11	9.127	9.071	8.903	8.294	7.447	6.517	5.616
0.12	8.373	8.330	8.200	7.722	7.040	6.266	5.491
0.13	7.736	7.702	7.599	7.218	6.662	6.014	5.346
0.14	7.189	7.162	7.079	6.770	6.312	5.767	5.191
0.15	6.716	6.694	6.627	6.373	5.992	5.530	5.031
0.16	6.303	6.285	6.229	6.019	5.698	5.304	4.870
0.17	5.939	5.924	5.877	5.700	5.429	5.090	4.712
0.18	5.616	5.603	5.564	5.414	5.182	4.889	4.559
0.19	5.327	5.316	5.282	5.154	4.955	4.701	4.410
0.20	5.067	5.057	5.029	4.919	4.746	4.524	4.267
0.22	4.619	4.612	4.590	4.5069	4.3750	4.2030	4.001
0.24	4.246	4.241	4.224	4.1599	4.0570	3.9214	3.7600
0.26	3.933	3.928	3.915	3.8643	3.7826	3.6740	3.5433
0.28	3.664	3.661	3.650	3.6096	3.5436	3.4554	3.3483
0.30	3.433	3.430	3.421	3.3881	3.3341	3.2615	3.1728
0.32	3.231	3.2286	3.222	3.1941	3.1494	3.0890	3.0148
0.34	3.054	3.0517	3.046	3.0229	2.9855	2.9348	2.8720
0.36	2.897	2.8952	2.890	2.8709	2.8393	2.7962	2.7428
0.38	2.757	2.7557	2.751	2.7350	2.7081	2.6713	2.6254
0.40	2.632	2.6308	2.627	2.6131	2.5899	2.5582	2.5186
0.45	2.3702	2.3694	2.3669	2.3569	2.3406	2.3181	2.2899
0.50	2.1640	2.1634	2.1615	2.1543	2.1423	2.1259	2.1051
0.55	1.9979	1.9975	1.9960	1.9907	1.9817	1.9693	1.9535
0.60	1.8620	1.8617	1.8606	1.8564	1.8495	1.8399	1.8278
0.65	1.7493	1.7490	1.7482	1.7449	1.7394	1.7319	1.7223
0.70	1.6546	1.6544	1.6537	1.6511	1.6468	1.6407	1.6331
0.75	1.5744	1.5743	1.5737	1.5716	1.5681	1.5632	1.5569
0.90							
1.0	1.3130	1.3130	1.3127	1.3119	1.3104	1.3084	1.3059
1.2							
1.5	1.1048	1.1048	1.1047	1.1045	1.1041	1.1036	1.1029
2.0	1.0373	1.0373	1.0373	1.0372	1.0371	1.0369	1.0367

TABLE 1.1 (*Continued*)

$$r_{\text{lin}} = \frac{\sinh 2A_w}{\cosh 2A_w - \cos 2F_w}$$

A_w \ F_w	6° 174°	8° 172°	10° 170°	15° 165°	20° 160°	25° 155°	30° 150°
0.0	0.000	0.000	0.000	0.000	0.000	0.000	0.000
0.003							
0.004							
0.005	0.4566	0.2578	0.1657	0.07462	0.04273	0.02799	0.02000
0.01	0.9070	0.5136	0.3305	0.1491	0.08541	0.05596	0.03998
0.02	1.766	1.012	0.6547	0.2969	0.1704	0.1118	0.07989
0.03	2.539	1.481	0.9667	0.4422	0.2547	0.1672	0.1196
0.04	3.197	1.910	1.261	0.5839	0.3377	0.2222	0.1592
0.05	3.731	2.290	1.534	0.72080	0.41919	0.27655	0.19836
0.06	4.139	2.618	1.782	0.85203	0.49878	0.33009	0.23716
0.07	4.435	2.893	2.003	0.97684	0.57618	0.38269	0.27551
0.08	4.633	3.116	2.197	1.0946	0.65108	0.43422	0.31332
0.09	4.751	3.292	2.364	1.2048	0.72330	0.48459	0.35055
0.10	4.803	3.424	2.505	1.3071	0.79258	0.53366	0.38714
0.11	4.806	3.518	2.621	1.4013	0.85875	0.58132	0.42300
0.12	4.771	3.580	2.715	1.4874	0.92168	0.62750	0.45810
0.13	4.709	3.615	2.788	1.5655	0.98130	0.67214	0.49241
0.14	4.627	3.627	2.843	1.6356	1.0375	0.71513	0.52583
0.15	4.532	3.622	2.8823	1.6983	1.0903	0.75648	0.55840
0.16	4.429	3.601	2.9075	1.7536	1.1397	0.79611	0.59004
0.17	4.321	3.569	2.9206	1.8021	1.1857	0.83401	0.62073
0.18	4.211	3.5287	2.9237	1.8440	1.2283	0.87017	0.65045
0.19	4.100	3.4810	2.9181	1.8799	1.2677	0.90455	0.67917
0.20	3.9910	3.4283	2.9053	1.9101	1.3038	0.93719	0.70689
0.22	3.7792	3.3137	2.8632	1.9555	1.3671	0.99728	0.75930
0.24	3.5802	3.1930	2.8055	1.9835	1.4191	1.0506	0.80762
0.26	3.3959	3.0719	2.7382	1.9973	1.4608	1.0974	0.85191
0.28	3.2263	2.9534	2.6654	1.9997	1.4934	1.1381	0.89226
0.30	3.0709	2.8395	2.5903	1.9930	1.5179	1.1732	0.92878
0.32	2.9289	2.7315	2.5150	1.9794	1.5355	1.2029	0.96165
0.34	2.7990	2.6296	2.4409	1.9604	1.5471	1.2279	0.99106
0.36	2.6803	2.5340	2.3688	1.9375	1.5535	1.2486	1.0172
0.38	2.5716	2.4445	2.2993	1.9117	1.5557	1.2653	1.0403
0.40	2.4719	2.3609	2.2329	1.8840	1.5543	1.2785	1.0605
0.45	2.2564	2.1756	2.0805	1.8102	1.5389	1.2989	1.1001
0.50	2.0803	2.0199	1.9477	1.7358	1.5124	1.3054	1.1267
0.55	1.9347	1.8885	1.8326	1.6644	1.4800	1.3021	1.1430
0.60	1.8131	1.7771	1.7331	1.5979	1.4450	1.2925	1.1517
0.65	1.7108	1.6821	1.6470	1.5372	1.4096	1.2788	1.1546
0.70	1.6238	1.6007	1.5722	1.4821	1.3751	1.2627	1.1535
0.75	1.5494	1.5306	1.5072	1.4325	1.3422	1.2455	1.1495
0.90							
1.0	1.3027	1.2949	1.2850	1.2523	1.2105	1.1627	1.1118
1.2							
1.5	1.1021	1.1001	1.0975	1.0887	1.0770	1.0629	1.0471
2.0	1.0365	1.0357	1.0349	1.0321	1.0282	1.0234	1.0180

TABLE 1.1 (*Continued*)

$$r_{\text{lin}} = \frac{\sinh 2A_w}{\cosh 2A_w - \cos 2F_w}$$

A_w \ F_w	35° 145°	40° 140°	45° 135°	50° 130°	55° 125°	60° 120°
0.0	0.000	0.000	0.000	0.000	0.000	0.000
0.003						
0.004						
0.005	0.01520					
0.01	0.03039	0.02420	0.02000	0.01704	0.01490	0.01333
0.02	0.06073	0.04837	0.03998	0.03407	0.02980	0.02666
0.03	0.09100	0.07250	0.05994	0.05108	0.04468	0.03998
0.04	0.12115	0.09655	0.07983	0.06805	0.05954	0.05328
0.05	0.15109	0.12049	0.099672	0.084987	0.074364	0.066558
0.06	0.18084	0.14431	0.11943	0.10187	0.089155	0.079810
0.07	0.21033	0.16798	0.13909	0.11868	0.10390	0.093031
0.08	0.23953	0.19147	0.15864	0.13543	0.11860	0.10621
0.09	0.26841	0.21478	0.17808	0.15209	0.13324	0.11935
0.10	0.29694	0.23787	0.19738	0.16867	0.14782	0.13245
0.11	0.32506	0.26072	0.21652	0.18513	0.16232	0.14550
0.12	0.35275	0.28331	0.23549	0.20149	0.17674	0.15848
0.13	0.37999	0.30562	0.25430	0.21773	0.19109	0.17141
0.14	0.40673	0.32764	0.27290	0.23384	0.20534	0.18427
0.15	0.43298	0.34934	0.29131	0.24981	0.21950	0.19706
0.16	0.45868	0.37072	0.30951	0.26564	0.23355	0.20977
0.17	0.48383	0.39176	0.32748	0.28132	0.24750	0.22241
0.18	0.50842	0.41243	0.34522	0.29684	0.26133	0.23496
0.19	0.53240	0.43273	0.36271	0.31219	0.27504	0.24742
0.20	0.55578	0.45266	0.37995	0.32736	0.28863	0.25979
0.22	0.60070	0.49133	0.41365	0.35718	0.31543	0.28425
0.24	0.64308	0.52835	0.44625	0.38623	0.34167	0.30830
0.26	0.68289	0.56369	0.47770	0.41447	0.36733	0.33190
0.28	0.72013	0.59732	0.50798	0.44188	0.39238	0.35506
0.30	0.75482	0.62921	0.53704	0.46843	0.41679	0.37773
0.32	0.78700	0.65938	0.56489	0.49410	0.44056	0.39990
0.34	0.81675	0.68782	0.59152	0.51887	0.46366	0.42157
0.36	0.84414	0.71457	0.61691	0.54274	0.48607	0.44270
0.38	0.86924	0.73965	0.64107	0.56568	0.50778	0.46329
0.40	0.89221	0.76313	0.66404	0.58773	0.52881	0.48334
0.45	0.94084	0.81506	0.71630	0.63888	0.57829	0.53103
0.50	0.97847	0.85817	0.76159	0.68456	0.62342	0.57521
0.55	1.0069	0.89349	0.80050	0.72504	0.66432	0.61593
0.60	1.0278	0.92208	0.83365	0.76070	0.70120	0.65326
0.65	1.0427	0.94498	0.86172	0.79195	0.73430	0.68735
0.70	1.0528	0.96311	0.88535	0.81921	0.76388	0.71836
0.75	1.0591	0.97729	0.90515	0.84293	0.79025	0.74648
0.90	.....	1.0028	0.94681	0.89670	0.85293	0.81558
1.0	1.0604	1.0107	0.96403	0.92149	0.88369	0.85094
1.2	.....	1.0154	0.98368	0.95387	0.92664	0.90247
1.5	1.0300	1.0125	0.99505	0.97818	0.96236	0.94797
2.0	1.0120	1.0057	0.99933	0.99302	0.98697	0.98136

TABLE 1.1 (*Continued*)

$$r_{\text{lin}} = \frac{\sinh 2A_w}{\cosh 2A_w - \cos 2F_w}$$

A_w \ F_w	65° 115°	70° 110°	75° 105°	80° 100°	85° 95°	90°
0.0	0.000	0.000	0.000	0.000	0.000	0.000
0.003						
0.004						
0.005						
0.01	0.01217	0.01132	0.01072	0.01031	0.01008	0.009999
0.02	0.02434	0.02264	0.02143	0.02062	0.02015	0.02000
0.03	0.03651	0.03396	0.03214	0.03092	0.03022	0.02999
0.04	0.04866	0.04527	0.04285	0.04122	0.04029	0.03998
0.05	0.060791	0.056560	0.053537	0.051509	0.050341	0.049960
0.06	0.072903	0.067836	0.064215	0.061785	0.060386	0.059929
0.07	0.084993	0.079094	0.074878	0.072049	0.070419	0.069887
0.08	0.097051	0.090327	0.085520	0.082294	0.080435	0.079828
0.09	0.10908	0.10154	0.096145	0.092524	0.090438	0.089756
0.10	0.12108	0.11273	0.10675	0.10274	0.10042	0.099670
0.11	0.13303	0.12388	0.11732	0.11292	0.11039	0.10956
0.12	0.14495	0.13499	0.12787	0.12309	0.12033	0.11943
0.13	0.15681	0.14608	0.13839	0.13322	0.13025	0.12927
0.14	0.16863	0.15711	0.14887	0.14333	0.14013	0.13909
0.15	0.18039	0.16811	0.15932	0.15341	0.15000	0.14888
0.16	0.19209	0.17907	0.16973	0.16345	0.15983	0.15865
0.17	0.20374	0.18997	0.18010	0.17346	0.16963	0.16838
0.18	0.21532	0.20083	0.19043	0.18344	0.17940	0.17808
0.19	0.22683	0.21163	0.20072	0.19337	0.18913	0.18775
0.20	0.23827	0.22237	0.21095	0.20327	0.19883	0.19737
0.22	0.26094	0.24369	0.23129	0.22293	0.21810	0.21652
0.24	0.28329	0.26475	0.25140	0.24240	0.23720	0.23550
0.26	0.30530	0.28554	0.27129	0.26167	0.25611	0.25429
0.28	0.32695	0.30604	0.29094	0.28074	0.27484	0.27290
0.30	0.34823	0.32623	0.31033	0.29958	0.29335	0.29131
0.32	0.36911	0.34611	0.32946	0.31818	0.31164	0.30950
0.34	0.38960	0.36566	0.34831	0.33654	0.32971	0.32748
0.36	0.40966	0.38493	0.36686	0.35463	0.34754	0.34521
0.38	0.42929	0.40372	0.38511	0.37246	0.36511	0.36271
0.40	0.44849	0.42221	0.40305	0.39001	0.38244	0.37995
0.45	0.49450	0.46678	0.44648	0.43262	0.42455	0.42190
0.50	0.53763	0.50894	0.48782	0.47334	0.46489	0.46212
0.55	0.57788	0.54862	0.52698	0.51209	0.50339	0.50052
0.60	0.61524	0.58581	0.56393	0.54882	0.53997	0.53705
0.65	0.64980	0.62054	0.59867	0.58352	0.57461	0.57167
0.70	0.68164	0.65284	0.63120	0.61616	0.60729	0.60437
0.75	0.71090	0.68280	0.66159	0.64678	0.63804	0.63515
0.90	0.78453	0.75956	0.74045	0.72697	0.71895	0.71630
1.0	0.82335	0.80094	0.78364	0.77136	0.76403	0.76159
1.2	0.88169	0.86450	0.85104	0.84140	0.83559	0.83366
1.5	0.93534	0.92469	0.91624	0.91011	0.90639	0.90515
2.0	0.97635	0.97206	0.96861	0.96609	0.96455	0.96403

TABLE 1.2

$$x_{1in} = \frac{-\sin 2F_w}{\cosh 2A_w - \cos 2F_w}\dagger$$

A_w \ F_w	0 180°	0.5° 179.5°	1° 179°	2° 178°	3° 177°
0.0	..	.....	−57.21	−28.59	−19.07
0.003	..	.....	−55.40	−28.38	−19.01
0.004	..	.....	−54.53	−28.22	−18.96
0.005	..	.....	−52.88	−28.02	−18.90
0.01	0	−49.86	−43.09	−26.42	−18.40
0.02	0	−18.37	−24.75	−21.53	−16.64
0.03	0	−8.95	−14.48	−16.45	−14.36
0.04	0	−5.21	−9.160	−12.37	−12.04
0.05	0	−3.39	−6.221	−9.376	−9.974
0.06	0	−2.371	−4.463	−7.229	−8.237
0.07	0	−1.750	−3.346	−5.690	−6.832
0.08	0	−1.344	−2.597	−4.568	−5.709
0.09	0	−1.065	−2.071	−3.734	−4.813
0.10	0	−0.8630	−1.688	−3.099	−4.091
0.11	0	−0.7137	−1.401	−2.609	−3.510
0.12	0	−0.5999	−1.181	−2.223	−3.037
0.13	0	−0.5111	−1.009	−1.915	−2.648
0.14	0	−0.4405	−0.8710	−1.665	−2.326
0.15	0	−0.3836	−0.7595	−1.460	−2.057
0.16	0	−0.3369	−0.6679	−1.290	−1.830
0.17	0	−0.2982	−0.5918	−1.147	−1.637
0.18	0	−0.2658	−0.5279	−1.027	−1.473
0.19	0	−0.2383	−0.4737	−0.9239	−1.331
0.20	0	−0.2148	−0.4273	−0.8353	−1.208
0.22	0	−0.1771	−0.3526	−0.69199	−1.0065
0.24	0	−0.1484	−0.2957	−0.58196	−0.85046
0.26	0	−0.1261	−0.2513	−0.49577	−0.72717
0.28	0	−0.1083	−0.2160	−0.42698	−0.62811
0.30	0	−0.09401	−0.1876	−0.37124	−0.54742
0.32	0	−0.08230	−0.1642	−0.32548	−0.48089
0.34	0	−0.07259	−0.1449	−0.28744	−0.42539
0.36	0	−0.06445	−0.1287	−0.25550	−0.37864
0.38	0	−0.05757	−0.1150	−0.22841	−0.33889
0.40	0	−0.05169	−0.1032	−0.20525	−0.30483
0.45	0	−0.04028	−0.08047	−0.16017	−0.23834
0.50	0	−0.03212	−0.06419	−0.12788	−0.19055
0.55	0	−0.02612	−0.05216	−0.10397	−0.15509
0.60	0	−0.02152	−0.04302	−0.085795	−0.12808
0.65	0	−0.01797	−0.03592	−0.071670	−0.10706
0.70	0	−0.01516	−0.03031	−0.060485	−0.090394
0.75	0	−0.01290	−0.02579	−0.051489	−0.076980
0.90					
1.0	0	−0.006317	−0.01263	−0.025233	−0.037768
1.2					
1.5	0	−0.001924	−0.003849	−0.0076912	−0.011521
2.0	0	−0.0006633	−0.001327	−0.0026514	−0.0039725

† x_{1in} is negative for $0° < F_s < 90°$ and positive for $180° > F_s > 90°$.

TABLE 1.2 (*Continued*)

$$x_{1in} = \frac{-\sin 2F_w}{\cosh 2A_w - \cos 2F_w}$$

A_w \ F_w	4° 176°	5° 175°	6° 174°	8° 172°	10° 170°
0.0	−14.30	−11.43	−9.515	−7.115	−5.671
0.003	−14.28	−11.42			
0.004	−14.26	−11.41			
0.005	−14.23	−11.39	−9.494	−7.106	−5.666
0.01	−14.02	−11.28	−9.429	−7.079	−5.652
0.02	−13.22	−10.86	−9.179	−6.971	−5.597
0.03	−12.07	−10.22	−8.791	−6.799	−5.507
0.04	−10.76	−9.443	−8.300	−6.572	−5.385
0.05	−9.448	−8.601	−7.743	−6.302	−5.237
0.06	−8.215	−7.752	−7.155	−5.999	−5.065
0.07	−7.119	−6.943	−6.565	−5.676	−4.877
0.08	−6.169	−6.197	−5.995	−5.345	−4.676
0.09	−5.359	−5.525	−5.458	−5.013	−4.468
0.10	−4.670	−4.925	−4.960	−4.687	−4.255
0.11	−4.090	−4.397	−4.505	−4.372	−4.042
0.12	−3.599	−3.935	−4.094	−4.073	−3.832
0.13	−3.183	−3.531	−3.723	−3.790	−3.627
0.14	−2.829	−3.177	−3.391	−3.525	−3.428
0.15	−2.527	−2.869	−3.094	−3.278	−3.2373
0.16	−2.268	−2.598	−2.829	−3.050	−3.0551
0.17	−2.044	−2.361	−2.592	−2.839	−2.8821
0.18	−1.850	−2.152	−2.380	−2.6443	−2.7185
0.19	−1.681	−1.967	−2.190	−2.4653	−2.5643
0.20	−1.533	−1.804	−2.0201	−2.3006	−2.4192
0.22	−1.2874	−1.5291	−1.7294	−2.0104	−2.1554
0.24	−1.0944	−1.3094	−1.4927	−1.7650	−1.9243
0.26	−0.94034	−1.1316	−1.2985	−1.5572	−1.7223
0.28	−0.81543	−0.98592	−1.1374	−1.3804	−1.5459
0.30	−0.71296	−0.86539	−1.0028	−1.2294	−1.3916
0.32	−0.62797	−0.76471	−0.88949	−1.0998	−1.2565
0.34	−0.55672	−0.67981	−0.79325	−0.98799	−1.1379
0.36	−0.49647	−0.60763	−0.71095	−0.89109	−1.0336
0.38	−0.44506	−0.54579	−0.64008	−0.80665	−0.94148
0.40	−0.40088	−0.49246	−0.57869	−0.73275	−0.85991
0.45	−0.31428	−0.38737	−0.45700	−0.58419	−0.69319
0.50	−0.25175	−0.31105	−0.36803	−0.47375	−0.56683
0.55	−0.20519	−0.25398	−0.30116	−0.38973	−0.46927
0.60	−0.16964	−0.21027	−0.24974	−0.32451	−0.39269
0.65	−0.14192	−0.17610	−0.20943	−0.27301	−0.33167
0.70	−0.11991	−0.14892	−0.17728	−0.23170	−0.28238
0.75	−0.10217	−0.12697	−0.15129	−0.19814	−0.24210
0.90					
1.0	−0.050207	−0.062523	−0.074679	−0.098410	−0.12118
1.2					
1.5	−0.015331	−0.019118	−0.022873	−0.030269	−0.037469
2.0	−0.0052880	−0.006597	−0.0078963	−0.010461	−0.012971

TABLE 1.2 (*Continued*)

$$x_{1in} = \frac{-\sin 2F_w}{\cosh 2A_w - \cos 2F_w}$$

A_w \ F_w	15° 165°	20° 160°	25° 155°	30° 150°	35° 145°
0.0	−3.7322	−2.7474	−2.1445	−1.7321	−1.4281
0.003					
0.004					
0.005	−3.7308	−2.7468	−2.1439	−1.7319	−1.4280
0.01	−3.7266	−2.7451	−2.1433	−1.7314	−1.4277
0.02	−3.7100	−2.7381	−2.1397	−1.7293	−1.4264
0.03	−3.6827	−2.7265	−2.1338	−1.7258	−1.4242
0.04	−3.6451	−2.7104	−2.1255	−1.7210	−1.4212
0.05	−3.5979	−2.6899	−2.1149	−1.7149	−1.4174
0.06	−3.5416	−2.6653	−2.1021	−1.7074	−1.4127
0.07	−3.4773	−2.6368	−2.0871	−1.6987	−1.4071
0.08	−3.4060	−2.6046	−2.0702	−1.6887	−1.4008
0.09	−3.3287	−2.5691	−2.0513	−1.6776	−1.3937
0.10	−3.2459	−2.5304	−2.0304	−1.6652	−1.3859
0.11	−3.1592	−2.4889	−2.0079	−1.6518	−1.3773
0.12	−3.0692	−2.4450	−1.9838	−1.6373	−1.3680
0.13	−2.9769	−2.3989	−1.9582	−1.6218	−1.3580
0.14	−2.8830	−2.3509	−1.9312	−1.6054	−1.3473
0.15	−2.7885	−2.3014	−1.9030	−1.5881	−1.3361
0.16	−2.6938	−2.2507	−1.8736	−1.5699	−1.3242
0.17	−2.5996	−2.1989	−1.8433	−1.5510	−1.3118
0.18	−2.5066	−2.1465	−1.8122	−1.5314	−1.2988
0.19	−2.4150	−2.0936	−1.7803	−1.5112	−1.2854
0.20	−2.3251	−2.0404	−1.7478	−1.4904	−1.2715
0.22	−2.1520	−1.9342	−1.6815	−1.4473	−1.2424
0.24	−1.9889	−1.8293	−1.6139	−1.4026	−1.2119
0.26	−1.8366	−1.7269	−1.5461	−1.3568	−1.1801
0.28	−1.6954	−1.6277	−1.4784	−1.3103	−1.1475
0.30	−1.5652	−1.5325	−1.4116	−1.2634	−1.1141
0.32	−1.4457	−1.4417	−1.3461	−1.2165	−1.0803
0.34	−1.3361	−1.3555	−1.2822	−1.1699	−1.0462
0.36	−1.2359	−1.2740	−1.2202	−1.1239	−1.0120
0.38	−1.1443	−1.1972	−1.1604	−1.0785	−0.97788
0.40	−1.0607	−1.1250	−1.1028	−1.0342	−0.94402
0.45	−0.88174	−0.96363	−0.96930	−0.92813	−0.86126
0.50	−0.73850	−0.82723	−0.85088	−0.83026	−0.78238
0.55	−0.62306	−0.71225	−0.74682	−0.74113	−0.70840
0.60	−0.52931	−0.61533	−0.65593	−0.66076	−0.63984
0.65	−0.45254	−0.53349	−0.57679	−0.58877	−0.57689
0.70	−0.38914	−0.46416	−0.50795	−0.52458	−0.51949
0.75	−0.33639	−0.40520	−0.44808	−0.46752	−0.46742
0.90					
1.0	−0.17264	−0.21454	−0.24557	−0.26547	−0.27475
1.2					
1.5	−0.054338	−0.069105	−0.081278	−0.090516	−0.096619
2.0	−0.018909	−0.024218	−0.028728	−0.032305	−0.034847

TABLE 1.2 (*Continued*)

$$x_{1in} = \frac{-\sin 2F_w}{\cosh 2A_w - \cos 2F_w}$$

A_w \ F_w	40° 140°	45° 135°	50° 130°	55° 125°	60° 120°
0.0	−1.1918	−1.0000	−0.83910	−0.70021	−0.57735
0.003					
0.004					
0.005					
0.01	−1.1915	−0.99980	−0.83896	−0.70010	−0.57728
0.02	−1.1906	−0.99920	−0.83853	−0.69979	−0.57705
0.03	−1.1892	−0.99820	−0.83782	−0.69927	−0.57666
0.04	−1.1872	−0.99681	−0.83682	−0.69854	−0.57612
0.05	−1.1846	−0.99502	−0.83554	−0.69761	−0.57544
0.06	−1.1815	−0.99284	−0.83398	−0.69646	−0.57459
0.07	−1.1778	−0.99028	−0.83214	−0.69512	−0.57360
0.08	−1.1735	−0.98733	−0.83003	−0.69357	−0.57246
0.09	−1.1688	−0.98402	−0.82765	−0.69183	−0.57117
0.10	−1.1635	−0.98032	−0.82499	−0.68989	−0.56973
0.11	−1.1577	−0.97628	−0.82208	−0.68775	−0.56815
0.12	−1.1514	−0.97187	−0.81891	−0.68542	−0.56643
0.13	−1.1447	−0.96713	−0.81548	−0.68291	−0.56456
0.14	−1.1374	−0.96204	−0.81181	−0.68021	−0.56255
0.15	−1.1298	−0.95663	−0.80789	−0.67732	−0.56041
0.16	−1.1217	−0.95090	−0.80374	−0.67426	−0.55814
0.17	−1.1131	−0.94486	−0.79935	−0.67103	−0.55573
0.18	−1.1042	−0.93853	−0.79475	−0.66762	−0.55320
0.19	−1.0949	−0.93191	−0.78992	−0.66405	−0.55053
0.20	−1.0853	−0.92501	−0.78488	−0.66032	−0.54775
0.22	−1.0650	−0.91044	−0.77421	−0.65239	−0.54182
0.24	−1.0435	−0.89491	−0.76278	−0.64387	−0.53544
0.26	−1.0209	−0.87853	−0.75066	−0.63480	−0.52862
0.28	−0.99749	−0.86137	−0.73791	−0.62523	−0.52141
0.30	−0.97331	−0.84355	−0.72459	−0.61519	−0.51382
0.32	−0.94854	−0.82516	−0.71078	−0.60473	−0.50589
0.34	−0.92332	−0.80629	−0.69652	−0.59389	−0.49765
0.36	−0.89778	−0.78704	−0.68189	−0.58271	−0.48912
0.38	−0.87204	−0.76748	−0.66694	−0.57124	−0.48034
0.40	−0.84622	−0.74770	−0.65173	−0.55952	−0.47133
0.45	−0.78194	−0.69779	−0.61292	−0.52937	−0.44800
0.50	−0.71914	−0.64805	−0.57365	−0.49848	−0.42388
0.55	−0.65879	−0.59933	−0.53459	−0.46738	−0.39936
0.60	−0.60159	−0.55228	−0.49630	−0.43652	−0.37480
0.65	−0.54795	−0.50738	−0.45921	−0.40628	−0.35049
0.70	−0.49807	−0.46492	−0.42366	−0.37694	−0.32669
0.75	−0.45200	−0.42510	−0.38986	−0.34875	−0.30361
0.90	−0.33567	−0.32180	−0.30014	−0.27241	−0.24006
1.0	−0.27443	−0.26580	−0.25022	−0.22896	−0.20319
1.2	−0.18294	−0.17996	−0.17185	−0.15930	−0.14298
1.5	−0.099536	−0.099328	−0.096160	−0.090270	−0.081951
2.0	−0.036294	−0.036619	−0.035835	−0.033985	−0.031143

TABLE 1.2 (*Continued*)

$$x_{1in} = \frac{-\sin 2F_w}{\cosh 2A_w - \cos 2F_w}$$

A_w \ F_w	65° 115°	70° 110°	75° 105°	80° 100°	85° 95°	90°
0.0	−0.46631	−0.36397	−0.26795	−0.17633	−0.087489	0
0.003						
0.004						
0.005						
0.01	−0.46625	−0.36393	−0.26792	−0.17631	−0.087481	0
0.02	−0.46608	−0.36381	−0.26783	−0.17625	−0.087454	0
0.03	−0.46579	−0.36360	−0.26769	−0.17616	−0.087410	0
0.04	−0.46540	−0.36331	−0.26749	−0.17604	−0.087349	0
0.05	−0.46489	−0.36294	−0.26723	−0.17587	−0.087270	0
0.06	−0.46427	−0.36249	−0.26692	−0.17567	−0.087173	0
0.07	−0.46353	−0.36196	−0.26655	−0.17544	−0.087059	0
0.08	−0.46269	−0.36135	−0.26612	−0.17517	−0.086928	0
0.09	−0.46174	−0.36066	−0.26564	−0.17486	−0.086779	0
0.10	−0.46068	−0.35988	−0.26510	−0.17452	−0.086614	0
0.11	−0.45951	−0.35903	−0.26450	−0.17415	−0.086431	0
0.12	−0.45823	−0.35810	−0.26386	−0.17374	−0.086232	0
0.13	−0.45685	−0.35710	−0.26316	−0.17329	−0.086016	0
0.14	−0.45537	−0.35602	−0.26240	−0.17281	−0.085784	0
0.15	−0.45378	−0.35486	−0.26159	−0.17230	−0.085536	0
0.16	−0.45209	−0.35363	−0.26073	−0.17175	−0.085270	0
0.17	−0.45031	−0.35233	−0.25982	−0.17118	−0.084990	0
0.18	−0.44843	−0.35096	−0.25886	−0.17057	−0.084695	0
0.19	−0.44645	−0.34951	−0.25785	−0.16993	−0.084383	0
0.20	−0.44437	−0.34800	−0.25679	−0.16925	−0.084056	0
0.22	−0.43996	−0.34477	−0.25453	−0.16782	−0.083358	0
0.24	−0.43520	−0.34128	−0.25208	−0.16626	−0.082602	0
0.26	−0.43010	−0.33754	−0.24946	−0.16459	−0.081792	0
0.28	−0.42470	−0.33357	−0.24667	−0.16282	−0.080927	0
0.30	−0.41900	−0.32938	−0.24372	−0.16094	−0.080013	0
0.32	−0.41303	−0.32498	−0.24063	−0.15896	−0.079050	0
0.34	−0.40681	−0.32039	−0.23739	−0.15689	−0.078043	0
0.36	−0.40036	−0.31561	−0.23401	−0.15474	−0.076993	0
0.38	−0.39370	−0.31068	−0.23052	−0.15251	−0.075903	0
0.40	−0.38685	−0.30559	−0.22692	−0.15020	−0.074777	0
0.45	−0.36902	−0.29229	−0.21747	−0.14414	−0.071819	0
0.50	−0.35045	−0.27837	−0.20755	−0.13776	−0.068694	0
0.55	−0.33143	−0.26403	−0.19727	−0.13113	−0.065446	0
0.60	−0.31223	−0.24946	−0.18680	−0.12436	−0.062118	0
0.65	−0.29309	−0.23486	−0.17625	−0.11751	−0.058750	0
0.70	−0.27420	−0.22036	−0.16573	−0.11066	−0.055378	0
0.75	−0.25576	−0.20612	−0.15535	−0.10389	−0.052034	0
0.90	−0.20426	−0.16594	−0.12583	−0.084508	−0.042433	0
1.0	−0.17390	−0.14195	−0.10803	−0.072741	−0.036581	0
1.2	−0.12356	−0.10166	−0.077846	−0.052646	−0.026545	0
1.5	−0.071522	−0.059332	−0.045730	−0.031072	−0.015711	0
2.0	−0.027407	−0.022896	−0.017747	−0.012108	−0.0061376	0

and $F_w = \beta w + \Phi_s$ in terms of r_{1in} and x_{1in} or for $A_w = \alpha w + \rho_s$ and $F'_w = \beta w + \Phi'_s$ in terms of g_{1in} and b_{1in}.

In Chap. II, Sec. 16, several applications of the circle diagram are listed in terms of the functions ρ, Φ, r_1, x_1 and ρ, Φ', g_1, b_1. Evidently these apply equally if A is substituted for ρ and F for Φ and if a subscript *in* is added to r_1, x_1, g_1, and b_1. Additional applications include the following:

1. From known values of ρ_s and Φ_s (or Φ'_s) and of αw and βw, values of $A_w = \alpha w + \rho_s$ and $F_w = \beta w + \Phi_s$ (or $F'_w = \beta w + \Phi'_s$) may be determined from the circle diagram, and from these r_{1in} and x_{1in} (or g_{1in} and b_{1in}) may be obtained.

2. From known values of r_{1in} and x_{1in} (or g_{1in} and b_{1in}), A_w and F_w (or F'_w) may be determined from the circle diagram, and from these and known values of αw and βw, ρ_s and Φ_s (or Φ'_s) may be obtained. From these, in turn, r_{1s} and x_{1s} (or g_{1s} and b_{1s}) may be found from the circle diagram.

2. Input Impedance and Admittance. The formulas relating input impedance and admittance to normalized input impedance and admittance are

$$r_{1in} = \frac{R_{in} - \phi_c X_{in}}{R_c(1 + \phi_c^2)} \qquad g_{1in} = \frac{G_{in} + \phi_c B_{in}}{G_c(1 + \phi_c^2)} \tag{1}$$

$$x_{1in} = \frac{X_{in} + \phi_c R_{in}}{R_c(1 + \phi_c^2)} \qquad b_{1in} = \frac{B_{in} - \phi_c R_{in}}{G_c(1 + \phi_c^2)} \tag{2}$$

The inverse relations are

$$R_{in} = R_c(r_{1in} + \phi_c x_{1in}) \qquad G_{in} = G_c(g_{1in} - \phi_c b_{1in}) \tag{3}$$

$$X_{in} = R_c(x_{1in} - \phi_c r_{1in}) \qquad B_{in} = G_c(b_{1in} + \phi_c g_{1in}) \tag{4}$$

Note that

$$R_c G_c = \frac{1}{1 + \phi_c^2} \tag{5}$$

The formulas involving the phase and attenuation functions are

$$R_{in} = R_c \frac{\sinh 2A_w - \phi_c \sin 2F_w}{\cosh 2A_w - \cos 2F_w} \tag{6a}$$

$$G_{in} = G_c \frac{\sinh 2A_w + \phi_c \sin 2F'_w}{\cosh 2A_w - \cos 2F'_w} \tag{6b}$$

$$X_{in} = -R_c \frac{\sin 2F_w + \phi_c \sinh 2A_w}{\cosh 2A_w - \cos 2F_w} \tag{7a}$$

$$B_{in} = -G_c \frac{\sin 2F'_w - \phi_c \sinh 2A_w}{\cosh 2A_w - \cos 2F'_w} \tag{7b}$$

Note that

$$A_w = \alpha w + \rho_s \qquad F_w = \beta w + \Phi_s \qquad F'_w = \beta w + \Phi'_s \tag{8}$$

and also

$$\cosh 2A_w - \cos 2F_w = 2(\sinh^2 A_w + \sin^2 F_w) \tag{9}$$

The formulas (6) and (7) are general and involve no restrictions or

approximations other than those implied in the derivation of the differential equations and their application to terminated sections of line.

The impedance and admittance given by (6) and (7) are studied conveniently in two forms. The criterion distinguishing them is whether the input reactance can be made to vanish or not by varying the phase function $F_w = \Phi_s + \beta w$ over a range from zero to π. The condition of zero input reactance characterizes a section of line with an input impedance that is tuned to resonance or antiresonance. Any section of line for which the input reactance can be made to vanish by varying F_w is *potentially resonant.* A section in which the input reactance cannot be made zero by varying F_w is *nonresonant.*

An examination of (7*a*,*b*) shows that the input reactance or susceptance is zero when

$$\sin 2F_w = -\phi_c \sinh 2A_w \tag{10a}$$

$$\sin 2F'_w = \phi_c \sinh 2A_w \tag{10b}$$

Since the sine cannot exceed unity in magnitude, it is essential that the following condition be satisfied:

$$\phi_c \sinh 2A_w \leqq 1 \tag{11}$$

This is the condition characterizing all potentially resonant sections of line. Correspondingly the condition for nonresonance is

$$\phi_c \sinh 2A_w > 1 \tag{12}$$

Nonresonant Section of Line. Subject to (12), X_{in} *is always negative.* Since ϕ_c is very small on a low-loss line, the condition (12) implies that A_w is quite large. Clearly, if (12) is satisfied together with $\phi_c^2 \ll 1$, it follows that

$$\sinh 2A_w \gg 1 \tag{13}$$

so that, from (6) and (7),

$$R_{in} = R_c \tanh 2A_w \qquad G_{in} = G_c \tanh 2A_w \tag{14}$$

$$\begin{aligned} X_{in} &= -R_c(\tanh 2A_w)\left(\phi_c + \frac{\sin 2F_w}{\sinh 2A_w}\right) \\ B_{in} &= G_c(\tanh 2A_w)\left(\phi_c - \frac{\sin 2F'_w}{\sinh 2A_w}\right) \end{aligned} \tag{15}$$

where the large parentheses are always positive subject to (12). Moreover for $A_w \geqq 2$, $\sinh 2A_w \geqq 27$ and $1 \geqq \tanh 2A_w \geqq 0.9993$. Hence

$$\boldsymbol{Z}_{in} \doteq R_c\left[1 - j\left(\phi_c + \frac{\sin 2F_w}{\sinh 2A_w}\right)\right] \tag{16}$$

$$\boldsymbol{Y}_{in} \doteq G_c\left[1 + j\left(\phi_c - \frac{\sin 2F'_w}{\sinh 2A_w}\right)\right] \tag{17}$$

The imaginary parts of (16) and (17) are very small, so that $\boldsymbol{Z}_{in}$ and $\boldsymbol{Y}_{in}$ are *essentially real* and the line is matched for all practical purposes. The *perfectly nonresonant* or *exactly matched* line is defined by

$$A_w = \alpha w + \rho_s = \infty \tag{18}$$

$$\boldsymbol{Z}_{in} = R_c(1 - j\phi_c) = \boldsymbol{Z}_c \qquad \boldsymbol{z}_{1in} = 1 \tag{19a}$$

$$\boldsymbol{Y}_{in} = G_c(1 + j\phi_c) = \boldsymbol{Y}_c \qquad \boldsymbol{y}_{1in} = 1 \tag{19b}$$

Resonant Section of Line. The potentially resonant sections of line may have zero input reactance and susceptance when one of two possible conditions is satisfied. The two possibilities are distinguished as *input resonance* and *input antiresonance*, as follows:

Input Resonance

$$F_w - \frac{n\pi}{2} = F'_w - \frac{(n-1)\pi}{2} = \tfrac{1}{2}\sin^{-1}(\phi_c \sinh 2A_w)$$

$$= \tfrac{1}{2}\cos^{-1}\sqrt{1 - \phi_c^2 \sinh^2 2A_w} \qquad n \text{ odd} \tag{20a}$$

$$X_{in} = 0 \qquad (R_{in})_{res} = \frac{R_c(1 + \phi_c^2)\sinh 2A_w}{\cosh 2A_w + \sqrt{1 - \phi_c^2 \sinh^2 2A_w}} \tag{20b}$$

$$B_{in} = 0 \qquad (G_{in})_{res} = \frac{G_c(1 + \phi_c^2)\sinh 2A_w}{\cosh 2A_w - \sqrt{1 - \phi_c^2 \sinh^2 2A_w}} \tag{20c}$$

Input Antiresonance

$$F_w - \frac{n\pi}{2} = F'_w - \frac{(n-1)\pi}{2} = \pi - \tfrac{1}{2}\sin^{-1}(\phi_c \sinh 2A_w)$$

$$= \pi - \tfrac{1}{2}\cos^{-1}\sqrt{1 - \phi_c^2 \sinh^2 2A_w} \qquad n \text{ even} \tag{21a}$$

$$X_{in} = 0 \qquad (R_{in})_{antires} = \frac{R_c(1 + \phi_c^2)\sinh 2A_w}{\cosh 2A_w - \sqrt{1 - \phi_c^2 \sinh^2 2A_w}} \tag{21b}$$

$$B_{in} = 0 \qquad (G_{in})_{antires} = \frac{G_c(1 + \phi_c^2)\sinh 2A_w}{\cosh 2A_w + \sqrt{1 - \phi_c^2 \sinh^2 2A_w}} \tag{21c}$$

For a low-loss line and a termination that satisfy the following inequalities:

$$\phi_c^2 \ll 1 \qquad \phi_c^2 \sinh^2 2A_w \ll 1 \tag{22}$$

(20) and (21) may be readily simplified. Since ϕ_c is very small on a good line, (22) is not a severe restriction on ρ_s in A_w. Most terminations that are not adjusted to be matched satisfy (22).

Input Resonance

$$F_w - \frac{n\pi}{2} = F'_w - \frac{(n-1)\pi}{2} \doteq 0 \qquad n = 1, 3, 5, \ldots \tag{23a}$$

$$X_{in} = 0 \qquad (R_{in})_{res} \doteq R_c \tanh A_w \tag{23b}$$

$$B_{in} = 0 \qquad (G_{in})_{res} \doteq G_c \coth A_w \tag{23c}$$

Input Antiresonance

$$F_w - \frac{n\pi}{2} = F'_w - \frac{(n-1)\pi}{2} \doteq \pi \qquad n = 0, 2, 4, 6, \ldots \tag{24a}$$

$$X_{in} = 0 \qquad (R_{in})_{antires} \doteq R_c \coth A_w \tag{24b}$$

$$B_{in} = 0 \qquad (G_{in})_{antires} \doteq R_c \tanh A_w \tag{24c}$$

For a low-loss line and a low-loss termination that satisfy the following inequalities:

$$\phi_c^2 \ll 1 \qquad A_w^2 \ll 1 \tag{25}$$

conditions of resonance and antiresonance are as follows:

Input Resonance

$$F_w - \frac{n\pi}{2} = F'_w - \frac{(n-1)\pi}{2} = \phi_c A_w \doteq 0 \qquad n = 1, 3, 5, \ldots \tag{26a}$$

$$X_{in} = 0 \qquad (R_{in})_{res} \doteq R_c A_w \tag{26b}$$

$$B_{in} = 0 \qquad (G_{in})_{res} \doteq \frac{G_c}{A_w} \tag{26c}$$

Input Antiresonance

$$F_w - \frac{n\pi}{2} = F'_w - \frac{(n-1)\pi}{2}$$

$$= \pi - \phi_c A_w \doteq \pi \qquad n = 0, 2, 4, 6, \ldots \tag{27a}$$

$$X_{in} = 0 \qquad (R_{in})_{antires} \doteq \frac{R_c}{A_w} \tag{27b}$$

$$B_{in} = 0 \qquad (G_{in})_{antires} \doteq G_c A_w \tag{27c}$$

Note that in (20) to (27)

$$A_w = \alpha w + \rho_s \qquad F_w = \beta w + \Phi_s \qquad F'_w = \beta w + \Phi'_s \tag{28}$$

It is well to note that, subject to (22), the approximate formulas for input resonance and antiresonance coincide with the exact formulas for *normalized* input resonance and antiresonance, defined as follows:

Normalized Input Resonance

$$F_w - \frac{n\pi}{2} = F'_w - \frac{(n-1)\pi}{2} = 0 \qquad n = 1, 3, 5, \ldots \tag{29a}$$

$$x_{1in} = 0 \qquad (r_{1in})_{res} = \frac{(R_{in})_{res}}{R_c} = \tanh A_w \tag{29b}$$

$$b_{1in} = 0 \qquad (g_{1in})_{res} = \frac{(G_{in})_{res}}{G_c} = \coth A_w \tag{29c}$$

Normalized Input Antiresonance

$$F_w - \frac{n\pi}{2} = F'_w - \frac{(n-1)\pi}{2} = \pi \qquad n = 0, 2, 4, 6, \ldots \tag{30a}$$

$$x_{1in} = 0 \qquad (r_{1in})_{antires} = \frac{(R_{in})_{antires}}{R_c} = \coth A_w \tag{30b}$$

$$b_{1in} = 0 \qquad (g_{1in})_{antires} = \frac{(G_{in})_{antires}}{G_c} = \tanh A_w \tag{30c}$$

The general formulas for input resistance and reactance are considered conveniently in two ranges.

Range of Impedance Including Input Resonance. This range is defined by the condition

$$\sin^2 F_w \gg \sinh^2 A_w \tag{31}$$

so that F_w is not near $n\pi/2$, with n even. It follows that the normalized input resistance and reactance are

$$r_{1in} = \frac{\sinh A_w \cosh A_w}{\sin^2 F_w} = \tfrac{1}{2} \sinh 2A_w \csc^2 F_w \tag{32a}$$

$$x_{1in} = -\cot F_w \tag{32b}$$

If A_w is small compared with unity, this is the principal range. Note that $\frac{1}{2} \sinh 2A_w \doteq A_w$ if A_w is small. The input resistance and reactance are

$$R_{in} = R_c(r_{1in} + \phi_c x_{1in}) = R_c(\tfrac{1}{2} \sinh 2A_w \csc^2 F_s - \phi_c \cot F_w) \tag{33a}$$

$$X_{in} = R_c(x_{1in} - \phi_c r_{1in}) = -R_c(\cot F_w - \tfrac{1}{2} \phi_c \sinh 2A_w \csc^2 F_w) \tag{33b}$$

The terms with ϕ_c as a factor are usually negligible except in determining R_{in} for short sections of line with terminations for which ρ_s is very small. For example, if the following conditions are satisfied:

$$A_w^2 = (\alpha w + \rho_s)^2 \ll 1 \qquad F_w = \beta w + \Phi_s \qquad (\beta w)^2 \ll 1 \qquad \phi_c = \frac{\alpha}{\beta} \tag{34}$$

it follows that

$$R_{in} = R_c \csc^2 F_w \left(\alpha w + \rho_s - \frac{\alpha}{\beta} \sin F_w \cos F_w\right) \tag{35}$$

If $\Phi_s \doteq 0$, $\sin F_w \doteq \sin \beta w \doteq \beta w$ and $\cos F_w \doteq 1$, so that

$$R_{in} \doteq \frac{R_c \rho_s}{\beta^2 w^2} \tag{36a}$$

If the term with $\phi_c = \alpha/\beta$ as a coefficient is neglected, the result is

$$R_{in} \doteq \frac{R_c(\alpha w + \rho_s)}{\beta^2 w^2} \tag{36b}$$

This is comparable with (36*a*) only if αw is negligible compared with ρ_s.

Similarly, if $\Phi_{sa} = \pi/2 + \beta k_{sa}$, $\rho_s = \alpha(b - k_{sa})$, as for a conducting bridge, $\sin F_w \doteq 1$, and $\cos F_w \doteq -\beta(w + k_{sa})$, so that

$$R_{in} \doteq R_c \left[\alpha(w + b - k_{sa}) + \frac{\alpha}{\beta} \beta(w + k_{sa}) \right] \doteq R_c \alpha(2w + b) \quad (37a)$$

where it is implied that $\beta^2 w^2 \ll 1$. If ϕ_c is neglected, $\rho_s = \alpha b$, and the term in α/β is missing. That is,

$$R_{in} \doteq R_c \alpha(w + b) \quad (37b)$$

Clearly the contribution from the conductors of the line is 50 per cent in error if the term in ϕ_c is omitted.

Range of Impedance Including Input Antiresonance. This range is defined by

$$\sin^2 F_w \ll \sinh^2 A_w \quad (38)$$

so that the normalized input resistance and reactance are

$$r_{1in} = \coth A_w \quad (39a)$$

$$x_{1in} = -\frac{\sin F_w \cos F_w}{\sinh^2 A_w} = -\tfrac{1}{2} \sin 2F_w \operatorname{csch}^2 A_w \quad (39b)$$

If A_w is large compared with unity, as for a line that is almost matched, this is the principal range. Evidently r_{1in} is near unity, and x_{1in} is very small. On the other hand, if A_w is small compared with unity, this range includes only narrow bands near $F_w = n\pi/2$, with n even.

The input resistance and reactance are

$$R_{in} = R_c(r_{1in} + \phi_c x_{1in}) = R_c(\coth A_w - \tfrac{1}{2}\phi_c \sin 2F_w \operatorname{csch}^2 A_w) \quad (40a)$$

$$X_{in} = R_c(x_{1in} - \phi_c r_{1in}) = -R_c(\tfrac{1}{2} \sin 2F_w \operatorname{csch}^2 A_w + \phi_c \coth A_w) \quad (40b)$$

The general formulas for the input admittance Y_{in} may be referred in a similar manner to two principal ranges. However, these ranges do not correspond to those of the input impedance.

Range of Admittance Including Input Antiresonance. This range is defined by the condition

$$\sin^2 F'_w \gg \sinh^2 A_w \quad (41)$$

so that F'_w is not near $(n - 1)\pi/2$, with n odd. The normalized input conductance and susceptance are

$$g_{1in} = \tfrac{1}{2} \sinh 2A_w \csc^2 F'_w \quad (42a)$$

$$b_{1in} = -\cot F'_w \quad (42b)$$

If A_w is small compared with unity, this is the principal range. The input conductance and susceptance in $Y_{in} = G_{in} + jB_{in}$ are

$$G_{in} = G_c(g_{1in} - \phi_c b_{1in}) = G_c(\tfrac{1}{2} \sinh 2A_w \csc^2 F'_w + \phi_c \cot F'_w) \quad (43a)$$

$$B_{in} = G_c(b_{1in} + \phi_c g_{1in}) = -G_c(\cot F'_w + \tfrac{1}{2}\phi_c \sinh 2A_w \csc^2 F'_w) \quad (43b)$$

The terms with ϕ_c are usually negligible except in determining the input conductance of short sections of line with terminations for which ρ_s is small. The situation parallels that discussed in conjunction with (34) to (37).

Range of Admittance Including Input Resonance. The condition for this range is

$$\sin^2 F'_w \ll \sinh^2 A_w \tag{44}$$

The normalized admittance is given by

$$g_{1in} = \coth A_w \qquad b_{1in} = -\tfrac{1}{2} \sin 2F'_w \operatorname{csch}^2 A_w \tag{45}$$

If A_w is large compared with unity, as for a line that is matched or nearly matched, this is the principal range with g_{1in} near unity and b_{1in} small. If A_w is small compared with unity, this range is very narrow and near $F'_w = (n - 1)\pi/2$, with n odd.

The input conductance and susceptance are

$$G_{in} = G_c(g_{1in} - \phi_c b_{1in}) = G_c(\coth A_w + \tfrac{1}{2}\phi_c \sin 2F'_w \operatorname{csch}^2 A_w) \tag{46a}$$
$$B_{in} = G_c(b_{1in} + \phi_c g_{1in}) = -G_c(\tfrac{1}{2} \sin 2F'_w \operatorname{csch}^2 A_w - \phi_c \coth A_w) \tag{46b}$$

3. Extreme Values of the Input Resistance and Conductance. Sections of transmission line can be so designed that the input resistance or the input conductance is extremely small or extremely great. Many of the most useful applications of sections of line arise from these two properties. The conditions under which R_{in} or G_{in} may assume extreme values by suitably adjusting the length w of the section with a given terminal impedance must be determined by equating the derivative of R_{in} or G_{in} with respect to w to zero. Differentiation of Sec. 2, Eq. (6*a*), leads to the following equation:

$$(\cosh 2A_w - \cos 2F_w)(\alpha \cosh 2A_w - \phi_c\beta \cos 2F_w) - (\sinh 2A_w - \phi_c \sin 2F_w)(\alpha \sinh 2A_w + \beta \sin^2 2F_w) = 0 \tag{1a}$$

Similarly differentiation of (6*b*) gives the following equation:

$$(\cosh 2A_w - \cos 2F'_w)(\alpha \cosh 2A_w + \phi_c\beta \cos 2F'_w) - (\sinh 2A_w + \phi_c \sin 2F'_w)(\alpha \sinh 2A_w + \beta \sin^2 2F'_w) = 0 \tag{1b}$$

This second equation, (1*b*), differs from (1*a*) only in having F'_w in place of F_w and $-\phi_c$ in place of ϕ_c. By suitable rearrangement these equations may be expressed as follows:

$$\frac{\sinh 2A_w \sin 2F_w}{1 - \cosh 2A_w \cos 2F_w} = \frac{\alpha + \phi_c\beta}{\beta - \phi_c\alpha} = \frac{\alpha(1 + \phi_c\beta/\alpha)}{\beta(1 - \phi_c\alpha/\beta)} \equiv 2\delta \tag{2a}$$

$$\frac{\sinh 2A_w \sin 2F'_w}{1 - \cosh 2A_w \cos 2F'_w} = \frac{\alpha - \phi_c\beta}{\beta + \phi_c\alpha} = \frac{\alpha(1 - \phi_c\beta/\alpha)}{\beta(1 + \phi_c\alpha/\beta)} \equiv 2\delta' \tag{2b}$$

where δ and δ' are as defined in (2*a*) and (2*b*) for temporary use. For a

low-loss line with negligible leakage conductance, for which

$$\phi_c = \frac{\alpha}{\beta} \qquad \phi_c^2 \ll 1 \tag{3}$$

it follows that

$$\delta = \phi_c = \frac{\alpha}{\beta} \qquad \delta' = 0 \tag{4}$$

Thus the behavior of resistance and conductance near their extreme values differs unless, as in a dissipationless line, $\phi_c = 0$.

Since (2*a*) and (2*b*) are formally alike, the analysis may be continued using (2*a*). The parallel result for (2*b*) is obtained by adding primes on F_w and δ. The following rearrangement of (2*a*) is convenient:

$$\sinh 2A_w \sin 2F_w + 2\delta \cosh 2A_w \cos 2F_w = 2\delta \tag{5}$$

Let
$$D \equiv \sqrt{\sinh^2 2A_w + 4\delta^2 \cosh^2 2A_w} \tag{6}$$

Then (5) can be expressed as follows:

$$\frac{\sinh 2A_w}{D} \sin 2F_w + \frac{2\delta \cosh 2A_w}{D} \cos 2F_w = \frac{2\delta}{D} \tag{7}$$

Now let

$$\frac{\sinh 2A_w}{D} = \cos 2\psi \qquad \frac{2\delta \cosh 2A_w}{D} = \sin 2\psi \qquad 2\delta \coth 2A_w = \tan 2\psi \tag{8}$$

so that (7) becomes

$$\sin 2(F_w + \psi) = \frac{2\delta}{D} \tag{9}$$

Since the right side in (9) is essentially positive, the argument of the sine must be in the first or second quadrants. That is,

$$F_w = \frac{n\pi}{2} - \psi + \frac{1}{2} \sin^{-1} \frac{2\delta}{D} \qquad n = 0, 2, 4, 6, \ldots \tag{10}$$

$$F_w = \frac{n\pi}{2} - \psi - \frac{1}{2} \sin^{-1} \frac{2\delta}{D} \qquad n = 1, 3, 5, \ldots \tag{11}$$

These formulas may be put into more convenient forms. Note that, with (6),

$$\sin^{-1} \frac{2\delta}{D} = \tan^{-1} \frac{2\delta}{\sqrt{1 + 4\delta^2 \sinh 2A_w}} \tag{12}$$

The substitution of (12) in (10) and (11), using (8), yields

$$F_w = \frac{n\pi}{2} - \frac{1}{2} \left(\tan^{-1} \frac{2\delta}{\tanh 2A_w} - \tan^{-1} \frac{2\delta}{\sqrt{1 + 4\delta^2 \sinh 2A_w}} \right) \qquad n \text{ even} \tag{13}$$

$$F_w = \frac{n\pi}{2} - \frac{1}{2} \left(\tan^{-1} \frac{2\delta}{\tanh 2A_w} + \tan^{-1} \frac{2\delta}{\sqrt{1 + 4\delta^2 \sinh 2A_w}} \right) \qquad n \text{ odd} \tag{14}$$

The formula $$\tan^{-1} x \pm \tan^{-1} y = \tan^{-1} \frac{x \pm y}{1 \mp xy} \tag{15}$$

permits the expression of (13) and (14) in the following forms:

$$F_w = \frac{n\pi}{2} - \frac{1}{2} \tan^{-1} 2\delta \frac{\sqrt{1 + 4\delta^2} \sinh 2A_w - \tanh 2A_w}{4\delta^2 + \sqrt{1 + 4\delta^2} \sinh 2A_w \tanh 2A_w} \qquad n \text{ even} \tag{16}$$

$$F_w = \frac{n\pi}{2} - \frac{1}{2} \tan^{-1} 2\delta \frac{\sqrt{1 + 4\delta^2} \sinh 2A_w + \tanh 2A_w}{\sqrt{1 + 4\delta^2} \sinh 2A_w \tanh 2A_w - 4\delta^2} \qquad n \text{ odd} \tag{17}$$

These are the *general formulas giving extremizing values of* F_w.

Restriction to Low-loss Lines. The low-loss line with low over-all attenuation is defined by

$$4\delta^2 \ll 1 \qquad 4A_w^2 \ll 1 \tag{18}$$

Subject to (18), the hyperbolic functions may be expanded in series to obtain

$$F_w = \frac{n\pi}{2} - \frac{1}{2} \tan^{-1} 2\delta \frac{(2A_w)^3(\frac{1}{6} + \frac{1}{3})}{4(\delta^2 + A_w^2)} \doteq \frac{n\pi}{2} - \frac{A_w^3 \delta}{\delta^2 + A_w^2} \qquad n \text{ even} \tag{19}$$

Similarly (17) becomes

$$F_w = \frac{n\pi}{2} - \frac{1}{2} \tan^{-1} \frac{2A_w\delta}{A_w^2 - \delta^2} \qquad n \text{ odd} \tag{20}$$

The argument in (19) is sufficiently small so that it may replace the inverse trigonometric function. This is not necessarily the case in (20), since the difference in the denominator may be small. For simplicity in interpreting (19) and (20), let the line be required to have negligible leakage conductance, so that

$$\frac{g}{\omega c} \ll \frac{r}{\omega l} \qquad \phi_c = \frac{\alpha}{\beta} = \delta \tag{21}$$

With (21), (19) becomes

$$F_w = \frac{n\pi}{2} - \frac{(\alpha/\beta)(\alpha w + \rho_s)^3}{\alpha^2/\beta^2 + (\alpha w + \rho_s)^2} = \frac{n\pi}{2} - \frac{\alpha^2 w_\rho^2 \beta w_\rho}{1 + \beta^2 w_\rho^2} \qquad n \text{ even} \tag{22}$$

where $$w_\rho \equiv w + \frac{\rho_s}{\alpha} \tag{23}$$

Since $F_w = \beta w + \Phi_s = \beta w_\rho - \beta\rho_s/\alpha + \Phi_s$, (22) may be solved for βw_ρ. Thus

$$\beta w_\rho \left(1 + \frac{\alpha^2 w_\rho^2}{1 + \beta^2 w_\rho^2}\right) = \frac{n\pi}{2} - \Phi_s + \frac{\beta\rho_s}{\alpha} \qquad n \text{ even} \tag{24}$$

Since it has been assumed that

$$A_w^2 = (\alpha w + \rho_s)^2 = (\alpha w_\rho)^2 \ll 1 \qquad \left(\frac{\alpha}{\beta}\right)^2 \ll 1 \tag{25}$$

it follows that (24) reduces to

$$F_w = \beta w + \Phi_s = \frac{n\pi}{2} \qquad n \text{ even} \tag{26}$$

The value of βw defined by (26) locates the *maximum* value of R_{in}, as is shown later.

Subject to (21), (20) becomes

$$F_w = \frac{n\pi}{2} - \frac{1}{2}\tan^{-1}\frac{2(\alpha/\beta)(\alpha w + \rho_s)}{(\alpha w + \rho_s)^2 - \alpha^2/\beta^2} \qquad n \text{ odd} \tag{27a}$$

With (23), this is equivalent to

$$F_w = \frac{n\pi}{2} - \frac{1}{2}\tan^{-1}\frac{2/\beta w_\rho}{1 - (1/\beta w_\rho)^2} \qquad n \text{ odd} \tag{27b}$$

The use of the trigonometric identity $\tan^{-1} x = \frac{1}{2}\tan^{-1}[2x/(1 - x^2)]$ in (27*b*) reduces this to

$$F_w = \frac{n\pi}{2} - \tan^{-1}\frac{1}{\beta w_\rho} = \frac{(n-1)\pi}{2} + \tan^{-1}\beta w_\rho \qquad n \text{ odd} \tag{28}$$

Hence

$$\tan F_w = \tan(\beta w + \Phi_s) = \beta\left(w + \frac{\rho_s}{\alpha}\right) \tag{29}$$

This relation gives the values of βw which locate the *minimum* values of input resistance.

Formulas corresponding to (26) and (28) for the extreme values of the input conductance are obtained directly from (19) and (20) by adding a prime on F_w and on δ and noting that $\delta' = 0$. Thus (19) gives

$$F'_w = \beta w + \Phi'_s = \frac{n\pi}{2} \qquad n \text{ even} \tag{30}$$

Similarly (20) gives

$$F'_w = \beta w + \Phi'_s = \frac{n\pi}{2} \qquad n \text{ odd} \tag{31}$$

It will be shown that (30) locates the maxima of G_{in} and (31) locates the minima of G_{in}.

Substitution of (26) in Sec. 2, Eq. (6*a*), using (21) and (25) gives

$$R_{in} = (R_{in})_{\max} = \frac{R_c}{\alpha w + \rho_s} \qquad F_w = \beta w + \Phi_s = \frac{n\pi}{2} \qquad n = 0, 2, 4, \ldots \tag{32}$$

In order to substitute (27*b*) in Sec. 2, Eq. (6*a*), note that, with n odd,

$$\sin 2F_w = \sin\left(n\pi - \tan^{-1}\frac{2\beta w_\rho}{\beta^2 w_\rho^2 - 1}\right) = \sin\tan^{-1}\frac{2\beta w_\rho}{\beta^2 w_\rho^2 - 1} = \frac{2\beta w_\rho}{\beta^2 w_\rho^2 + 1} \tag{33a}$$

$$\cos 2F_w = \cos\left(n\pi - \tan^{-1}\frac{2\beta w_\rho}{\beta^2 w_\rho^2 - 1}\right) = -\cos\tan^{-1}\frac{2\beta w_\rho}{\beta^2 w_\rho^2 - 1} = -\frac{\beta^2 w_\rho^2 - 1}{\beta^2 w_\rho^2 + 1} \tag{33b}$$

Hence $$R_{in} = R_c\frac{2\alpha w_\rho(\beta^2 w_\rho^2 + 1) - 2\alpha w_\rho}{\beta^2 w_\rho^2 + 1 + \beta^2 w_\rho^2 - 1} = R_c\alpha w_\rho \tag{34}$$

so that finally

$$R_{in} = (R_{in})_{\min} = R_c(\alpha w + \rho_s) \qquad \tan(\beta w + \Phi_s) = \beta\left(w + \frac{\rho_s}{\alpha}\right) \tag{35}$$

Substitution of (30) and (31) in Sec. 2, Eq. (6*b*), leads directly to

$$G_{in} = (G_{in})_{\max} = \frac{G_c}{\alpha w + \rho_s} \qquad \beta w + \Phi_s' = \frac{n\pi}{2} \qquad n \text{ even} \tag{36}$$

$$G_{in} = (G_{in})_{\min} = G_c(\alpha w + \rho_s) \qquad \beta w + \Phi_s' = \frac{n\pi}{2} \qquad n \text{ odd} \tag{37}$$

Note that $(R_{in})_{\max}$ and $(G_{in})_{\min}$ occur at the *same* values of βw, but that $(R_{in})_{\min}$ and $(G_{in})_{\max}$ do *not*.

4. Extreme Values of the Input Reactance and Susceptance. Extreme values of X_{in} and B_{in} are obtained by differentiating Sec. 2, Eqs. (7*a*,*b*), with respect to w and equating the derivatives to zero. The resulting equation for $dX_{in}/dw = 0$ is

$$\begin{aligned}(\cosh 2A_w - \cos 2F_w)(\beta\cos 2F_w + \alpha\phi_c\cosh 2A_w)\\ - (\sin 2F_w + \phi_c\sinh 2A_w)(\alpha\sinh 2A_w + \beta\sin 2F_w) = 0\end{aligned} \tag{1}$$

Collecting terms and rearranging give

$$\cosh 2A_w\cos 2F_w - 2\delta\sinh 2A_w\sin 2F_w = 1 \tag{2}$$

where $$2\delta \equiv \frac{\beta\phi_c + \alpha}{\beta - \alpha\phi_c} \tag{3}$$

Aside from constant factors the expression [Sec. 2, Eq. (7*b*)] for B_{in} differs from Sec. 2, Eq. (7*a*), for X_{in} only in having F_w' appear in place of F_w and $-\phi_c$ in place of ϕ_c. Hence the equation corresponding to (2) is

$$\cosh 2A_w\cos 2F_w' - 2\delta'\sinh 2A_w\sin 2F_w' = 1 \tag{4}$$

where $$2\delta' \equiv \frac{\alpha - \beta\phi_c}{\beta + \alpha\phi_c} \tag{5}$$

Note that, for the line with negligible leakage conductance, for which

$\phi_c^2 = \alpha^2/\beta^2 \ll 1$, it follows that

$$\delta = \frac{\alpha}{\beta} \qquad \delta' = 0 \tag{6}$$

The solution of (2) is readily carried out by dividing through by

$$D' \equiv \sqrt{\cosh^2 2A_w + 4\delta^2 \sinh 2A_w} \tag{7}$$

and setting

$$\frac{\cosh 2A_w}{D'} = \cos 2\psi' \qquad \frac{2\delta \sinh 2A_w}{D'} = \sin 2\psi' \qquad 2\delta \tanh 2A_w = \tan 2\psi' \tag{8}$$

The result is

$$F_w = \frac{n\pi}{2} - \psi' \pm \cos^{-1}\frac{1}{D'} \qquad n \text{ even} \tag{9}$$

However, with (7),

$$\cos^{-1}\frac{1}{D'} = \tan^{-1}\sqrt{D'^2 - 1} = \tan^{-1}(\sqrt{1 + 4\delta^2}\sinh 2A_w) \tag{10}$$

so that, with (8) and (10), (9) becomes

$$F_w = \frac{n\pi}{2} - \frac{1}{2}\tan^{-1}(2\delta \tan 2A_w) \pm \frac{1}{2}\tan^{-1}(\sqrt{1 + 4\delta^2}\sinh 2A_w) \qquad n \text{ even} \tag{11}$$

The arctangents may be combined into

$$F_w = \frac{n\pi}{2} - \frac{1}{2}\tan^{-1}\frac{2\delta \tanh 2A_w \mp \sqrt{1 + 4\delta^2}\sinh 2A_w}{1 - 2\delta\sqrt{1 + 4\delta^2}\tanh 2A_w \sinh 2A_w} \qquad n \text{ even} \tag{12}$$

This is the *general formula.*

Restriction to Low-loss Line. Subject to the conditions

$$(2A_w)^2 \ll 1 \qquad (2\delta)^2 \ll 1 \tag{13}$$

(12) reduces to

$$F_w = \frac{n\pi}{2} + A_w(2\delta \mp 1) \qquad n \text{ even} \tag{14}$$

With (6) and the notation $w_\rho = w + \rho/\alpha$, (14) becomes

$$\beta w_\rho - \frac{\beta\rho_s}{\alpha} + \Phi_s = \frac{n\pi}{2} \mp \alpha w_\rho \qquad n \text{ even} \tag{15}$$

where the term $2\delta A_w$ has been neglected compared with unity as a result of (13). The solution of (15) for βw_ρ gives

$$\beta w_\rho = \frac{n\pi/2 - \Phi_s + \beta\rho_s/\alpha}{1 \pm \alpha/\beta} \tag{16}$$

Hence $$\beta w = \left(\frac{n\pi}{2} - \Phi_s + \frac{\beta\rho_s}{\alpha}\right)\left(1 \mp \frac{\alpha}{\beta}\right) - \frac{\beta\rho_s}{\alpha} \qquad n \text{ even} \tag{17}$$

Finally $$\beta w = \left(\frac{n\pi}{2} - \Phi_s\right)\left(1 \mp \frac{\alpha}{\beta}\right) \mp \rho_s \qquad n \text{ even} \tag{18}$$

This is the *final formula* for the length w giving *extreme values* of X_{in}.

The corresponding formula for extreme values of B_{in} is obtained from (14), with F'_w written for F_w and $\delta' = 0$ for δ. Since the term in δ was neglected, the same formula is obtained, viz.,

$$\beta w = \left(\frac{n\pi}{2} - \Phi'_s\right)\left(1 \mp \frac{\alpha}{\beta}\right) \mp \rho_s \qquad n \text{ even} \tag{19}$$

The extreme values of X_{in} and B_{in} are obtained by substituting the equivalent of (18) and (19) in Sec. 2, Eqs. (7*a*,*b*), using (6) and (13). That is,

$$\begin{aligned} F_w &= \left(\frac{n\pi}{2} \mp A_w\right) \qquad n \text{ even} \\ F'_w &= \left(\frac{n\pi}{2} \mp A_w\right) \qquad n \text{ even} \end{aligned} \tag{20}$$

are substituted in

$$X_{in} = -R_c \frac{\sin 2F_w + 2A_w\alpha/\beta}{1 + 2A_w^2 - \cos 2F_w} \qquad B_{in} = -G_c \frac{\sin 2F'_w - 2A_w\alpha/\beta}{1 + 2A_w^2 - \cos 2F'_w} \tag{21}$$

Since $$\sin (n\pi \mp 2A_w) \doteq \mp 2A_w \qquad n \text{ even}$$
$$\cos (n\pi \mp 2A_w) = \cos 2A_w \doteq 1 - 2A_w^2 \qquad n \text{ even} \tag{22}$$

it follows that

$$X_{in} = -R_c \frac{\mp 2A_w + 2A_w\alpha/\beta}{1 + 2A_w^2 - 1 + 2A_w^2} \tag{23a}$$

$$B_{in} = -G_c \frac{\mp 2A_w - 2A_w\alpha/\beta}{1 + 2A_w^2 - 1 + 2A_w^2} \tag{23b}$$

$$X_{in} = \pm \frac{R_c}{2A_w}\left(1 \mp \frac{\alpha}{\beta}\right) \tag{24a}$$

$$B_{in} = \pm \frac{G_c}{2A_w}\left(1 \pm \frac{\alpha}{\beta}\right) \tag{24b}$$

where the upper signs go together and the lower signs go together in (23) and (24). Specifically

$$(X_{in})_{\max} = \frac{R_c}{2A_w}\left(1 - \frac{\alpha}{\beta}\right) \qquad \beta w = \left(\frac{n\pi}{2} - \Phi_s\right)\left(1 - \frac{\alpha}{\beta}\right) - \rho_s \qquad n \text{ even} \tag{25a}$$

$$(X_{in})_{\min} = -\frac{R_c}{2A_w}\left(1 + \frac{\alpha}{\beta}\right) \qquad \beta w = \left(\frac{n\pi}{2} - \Phi_s\right)\left(1 + \frac{\alpha}{\beta}\right) + \rho_s \qquad n \text{ even} \tag{25b}$$

$$(B_{in})_{\max} = \frac{G_c}{2A_w}\left(1 + \frac{\alpha}{\beta}\right) \qquad \beta w = \left(\frac{n\pi}{2} - \Phi_s'\right)\left(1 - \frac{\alpha}{\beta}\right) - \rho_s \qquad n \text{ even} \tag{26a}$$

$$(B_{in})_{\min} = -\frac{G_c}{2A_w}\left(1 - \frac{\alpha}{\beta}\right) \qquad \beta w = \left(\frac{n\pi}{2} - \Phi_s'\right)\left(1 + \frac{\alpha}{\beta}\right) + \rho_s \qquad n \text{ even} \tag{26b}$$

5. Summary of Critical Values of Input Impedance and Admittance for a Section of Low-loss Line.

Conditions Assumed

$$\phi_c^2 = \left(\frac{\alpha}{\beta}\right)^2 \ll 1 \tag{1a}$$

$$A_w^2 = (\alpha w + \rho_s)^2 \ll 1 \tag{1b}$$

Input Resonance, n Odd

$$\beta w = \frac{n\pi}{2} - \Phi_s \qquad X_{in} = 0 \qquad R_{in} = (R_{in})_{res} = R_c(\alpha w + \rho_s) \tag{2a}$$

$$\beta w = \frac{(n-1)\pi}{2} - \Phi_s' \qquad B_{in} = 0 \qquad G_{in} = (G_{in})_{res} = (G_{in})_{\max} = \frac{G_c}{\alpha w + \rho_s} \tag{2b}$$

Input Antiresonance, n Even

$$\beta w = \frac{n\pi}{2} - \Phi_s \qquad X_{in} = 0 \qquad R_{in} = (R_{in})_{antires} = (R_{in})_{\max} = \frac{R_c}{\alpha w + \rho_s} \tag{3a}$$

$$\beta w = \frac{(n-1)\pi}{2} - \Phi_s' \qquad B_{in} = 0 \qquad G_{in} = (G_{in})_{antires} = (G_{in})_{\min} = G_c(\alpha w + \rho_s) \tag{3b}$$

Minimum Input Resistance

$$\tan(\beta w + \Phi_s) = \beta\left(w + \frac{\rho_s}{\alpha}\right) \qquad R_{in} = (R_{in})_{\min} = R_c(\alpha w + \rho_s) \tag{4}$$

For $\Phi_s = 0$ and $\rho_s = 0$,

$\beta w = 0$	4.49	7.72	10.90	for $(R_{in})_{\min}$
$\beta w = 1.57$	4.71	7.85	10.99	for $(R_{in})_{res}$

Extreme Values of Input Reactance and Susceptance, n Even

$$(\boldsymbol{Z}_{in} = R_{in} + jX_{in} \qquad \boldsymbol{Y}_{in} = G_{in} + jB_{in})$$

$$\beta w = \left(\frac{n\pi}{2} - \Phi_s\right)\left(1 - \frac{\alpha}{\beta}\right) - \rho_s$$

$$X_{in} = (X_{in})_{\max} = \frac{R_c}{2}\frac{1 - \alpha/\beta}{\alpha w + \rho_s} \doteq \tfrac{1}{2}(R_{in})_{\max}\left(1 - \frac{\alpha}{\beta}\right) \tag{5a}$$

$$\beta w = \left(\frac{n\pi}{2} - \Phi_s\right)\left(1 + \frac{\alpha}{\beta}\right) + \rho_s$$

$$X_{in} = (X_{in})_{\min} = -\frac{R_c}{2}\frac{1 + \alpha/\beta}{\alpha w + \rho_s} \doteq -\tfrac{1}{2}(R_{in})_{\max}\left(1 + \frac{\alpha}{\beta}\right) \tag{5b}$$

$$\beta w = \left(\frac{n\pi}{2} - \Phi_s'\right)\left(1 - \frac{\alpha}{\beta}\right) - \rho_s$$
$$B_{in} = (B_{in})_{\max} = \frac{G_c}{2}\frac{1 + \alpha/\beta}{\alpha w + \rho_s} \doteq \tfrac{1}{2}(G_{in})_{\max}\left(1 + \frac{\alpha}{\beta}\right) \tag{5c}$$

$$\beta w = \left(\frac{n\pi}{2} - \Phi_s'\right)\left(1 + \frac{\alpha}{\beta}\right) + \rho_s$$
$$B_{in} = (B_{in})_{\min} = -\frac{G_c}{2}\frac{1 - \alpha/\beta}{\alpha w + \rho_s} \doteq -\tfrac{1}{2}(G_{in})_{\max}\left(1 - \frac{\alpha}{\beta}\right) \tag{5d}$$

Relations between Extreme Values

$$(R_{in})^2_{\max} \doteq 4|(X_{in})_{\max}(X_{in})_{\min}| \qquad (R_{in})_{\max} = (X_{in})_{\max} - (X_{in})_{\min} \tag{6a}$$
$$(G_{in})^2_{\max} \doteq 4|(B_{in})_{\max}(B_{in})_{\min}| \qquad (G_{in})_{\max} = (B_{in})_{\max} - (B_{in})_{\min} \tag{6b}$$

It is interesting to study graphically the general behavior of the input impedance $\boldsymbol{Z}_{in}$ and input admittance $\boldsymbol{Y}_{in}$ of a low-loss section of

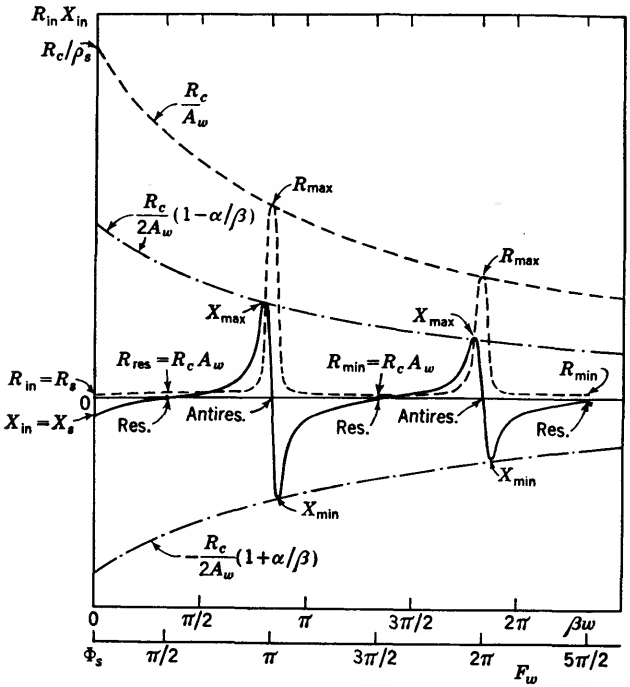


FIG. 5.1. Schematic diagram of R_{in} and X_{in} for section of line of electrical length βw.

transmission line of length s, line spacing b, characteristic impedance $\boldsymbol{Z}_c = R_c(1 - j\phi_c)$, and propagation constant $\gamma = \alpha + j\beta$ when terminated in an arbitrary impedance $\boldsymbol{Z}_s = R_s + jX_s$ with complex terminal function $\boldsymbol{\theta}_s = \rho_s + j\Phi_s$. It is assumed that this termination consists of

a section of line of length s_t ($s_t^2 \gg b^2$) with an arbitrary impedance at its end, so that end effects do not exist at the location of Z_s.

A schematic diagram of the input resistance and reactance of a line with low over-all attenuation is shown in Fig. 5.1. Actually the peaks should be very many times higher and narrower in order to represent correctly a low-loss line. For the present the distorted curves in Fig. 5.1 are convenient to describe the salient properties of the impedance.

The curves shown in Fig. 5.1 apply to a section of line of electrical length βw terminated in an impedance Z_s that includes a rather low

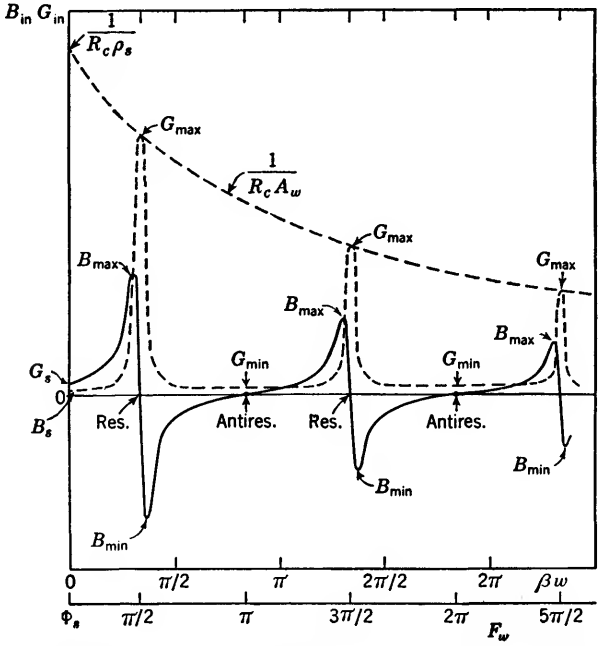


FIG. 5.2. Schematic diagram of G_{in} and B_{in} for section of line of electrical length βw.

resistance R_s and a somewhat greater capacitive reactance X_s. The appropriate values are indicated at $\beta w = 0$ or $F_w = \beta w + \Phi_s = \Phi_s$. As the length βw is increased from zero, the input reactance X_{in} rises from X_s to zero at $F_w = \pi/2$, which defines input resonance as given in (2a). At this length the resonant input resistance is quite small, namely, $(R_{in})_{res} = R_c(\alpha w + \rho_s)$. As βw is increased further, the input resistance rises first slowly, then very rapidly to a maximum value of

$$(R_{in})_{max} = \frac{R_c}{(\alpha w + \rho_s)}$$

at $F_w = \pi$. This is the antiresonant value. Beyond $\beta w = \pi - \Phi_s$ the

resistance drops first rapidly, then slowly until it reaches a minimum $(R_{in})_{\min} = R_c(\alpha w + \rho_s)$ at a value of βw defined by (4). Correspondingly the input reactance rises to a maximum $(X_{in})_{\max}$ at a value of βw [specified accurately in (5a)] which lies very slightly to the left of $F_w = \pi$. It drops abruptly through antiresonance with $X_{in} = 0$ at $F_w = \pi$ and then decreases to a negative extreme value $(X_{in})_{\min}$; it then rises to pass through zero again at resonance. The entire cycle is then repeated. The maximum values of resistance are on the curve $R_c/(\alpha w + \rho_s)$ at $F_w = n\pi$. The extreme positive values of the reactance are on the curve $\dfrac{R_c}{2(\alpha w + \rho_s)}\left(1 - \dfrac{\alpha}{\beta}\right)$; the negative values are on the curve $\dfrac{-R_c}{\alpha w + \rho_s}\left(1 + \dfrac{\alpha}{\beta}\right)$. Note that in magnitude a negative extreme is always greater than the associated positive extreme. Corresponding curves for input susceptance and conductance are shown in Fig. 5.2.

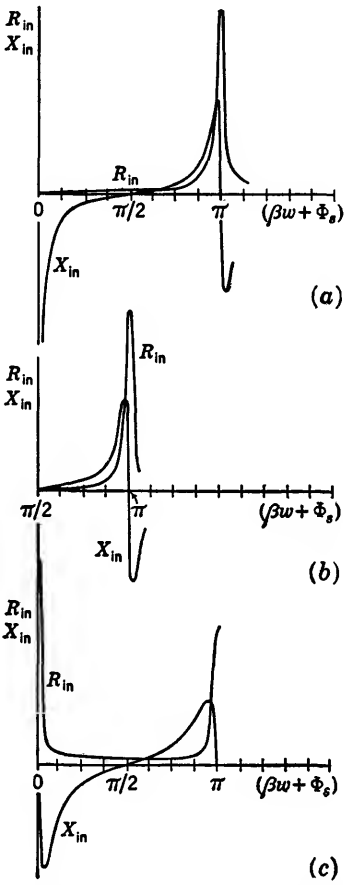


FIG. 5.3. Schematic diagram of R_{in} and X_{in} for a transmission line of electrical length βw with different terminations. (*a*) Ideal open end, $\Phi_s = 0$, $\rho_s = 0$, $R_s = 0$, $X_s = -\infty$. (*b*) Ideal short circuit, $\Phi_s = \pi/2$, $\rho_s = 0$, $R_s = 0$, $X_s = 0$. (*c*) Parallel resonant circuit, $\Phi_s = 0$, ρ_s small, R_s large, $X_s = 0$.

If the impedance $\boldsymbol{Z}_s$ of the termination at $w = 0$ is changed, the general shape of the curves is unaffected, but they are moved bodily toward shorter or longer lengths depending on the nature of the impedance. Let a few special cases be considered:

1. $R_s = 0$, $X_s = -\infty$. These conditions correspond to an *ideal* open end with $\rho_s = 0$, $\Phi_s = 0$. The impedance curve has the shape illustrated in Fig. 5.3*a*.

2. $R_s = 0$, $X_s = 0$. These conditions define a perfect short circuit such as given by an infinite perfectly conducting disk on an open-wire line or a perfectly conducting piston in a coaxial line. The corresponding terminal functions are $\rho_s = 0$, $\Phi_s = \pi/2$. The behavior of R_{in} and X_{in} for such a termination is shown in Fig. 5.3*b*.

3. R_s very large, $X_s = 0$. These conditions apply to a tuned parallel

resonant current. The corresponding terminal functions are ρ_s very small, $\Phi_s = 0$. The impedance curves behave as shown in Fig. 5.3c.

Complete sets of curves of the input impedance of a particular section of two-wire line terminated in an ideal open end with $R_s = 0$, $X_s = -\infty$ and in a perfect short circuit with $R_s = 0$, $X_s = 0$ are shown in Fig. 5.4 as functions of the length w of the section. Similar curves for a particular coaxial line are given in Fig. 5.5. Note that in both sets of curves

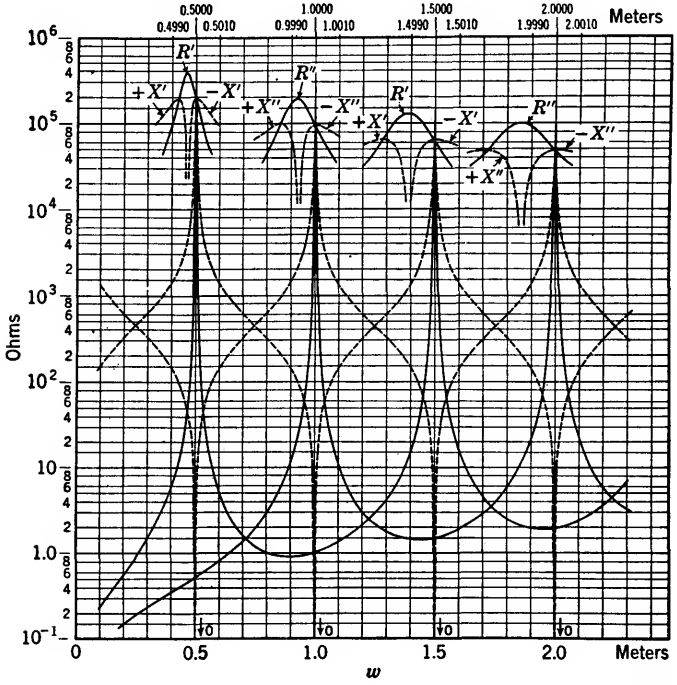


FIG. 5.4. Z_{in} for two-wire line. $R_c = 439.8$ ohms, $\phi_c = 7.183 \times 10^{-4}$, $\alpha = 2.258 \times 10^{-3}$ neper/m, $\beta = 3.144$ radians/m, $a = 5.118 \times 10^{-4}$ m, $b = 0.02$ m, $\lambda_{air} = 2$ m, $\lambda_{line} = 1.992$ m. $Z'_{in} = R'_{in} + jX'_{in}$ for an ideal short circuit. $Z''_{in} = R''_{in} + jX''_{in}$ for ideal open end.

antiresonances occur at $\beta w = n\pi/2$, where n is odd for the short-circuited end and even for the ideal open end. Corresponding curves of the input admittance are shown in Figs. 5.6 and 5.7.

The input impedances and admittances of the same sections of line terminated in pure resistance of $R_s = 60$ and 2,500 ohms are shown in Figs. 5.8 to 5.11.

6. Section of Transmission Line as an Insulator.[70,81,99] One of the most interesting practical applications of terminated sections of transmission line makes use of the very high values of resistance which can be obtained at antiresonance. The formula for maximum input resistance

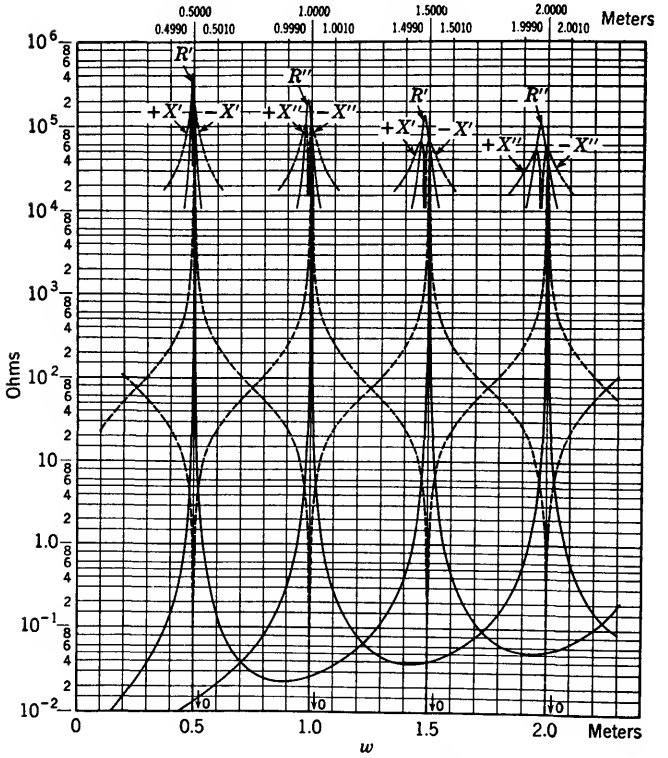


FIG. 5.5. Z_{in} for coaxial line. $R_c = 75.13$ ohms, $\phi_c = 1.384 \times 10^{-4}$, $\alpha = 3.577 \times 10^{-4}$ neper/m, $\beta = 3.142$ radians/m, $a = 0.01$ m, $b = 0.035$ m, $\lambda_{air} = 2$ m, $\lambda_{line} = 1.992$ m. $Z'_{in} = R'_{in} + jX'_{in}$ for ideal short circuit. $Z''_{in} = R''_{in} + jX'_{in}$ for ideal open end.

of a section of low-loss line for which

$$\alpha = \frac{r}{2R_c} \tag{1}$$

is

$$(R_{in})_{max} = \frac{R_c}{A_s} = \frac{R_c^2}{\frac{1}{2}r(s + \rho_{sa}/\alpha)} \tag{2}$$

at

$$s = \frac{n\lambda}{2} - \frac{\Phi_s}{\beta} \qquad n = 0, 1, 2, \ldots \tag{3}$$

For a two-wire line terminated in a bridge of length b and made of the same wire as the line, the apparent terminal functions are

$$\Phi_{sa} = \frac{\pi}{2} + \beta k_{sa} \qquad \rho_{sa} = \alpha(m_s - k_{sa}) \doteq \tfrac{1}{2}\alpha b \tag{4}$$

where k_{sa} and m_s are as defined and evaluated in Chap. II, Sec. 20. For

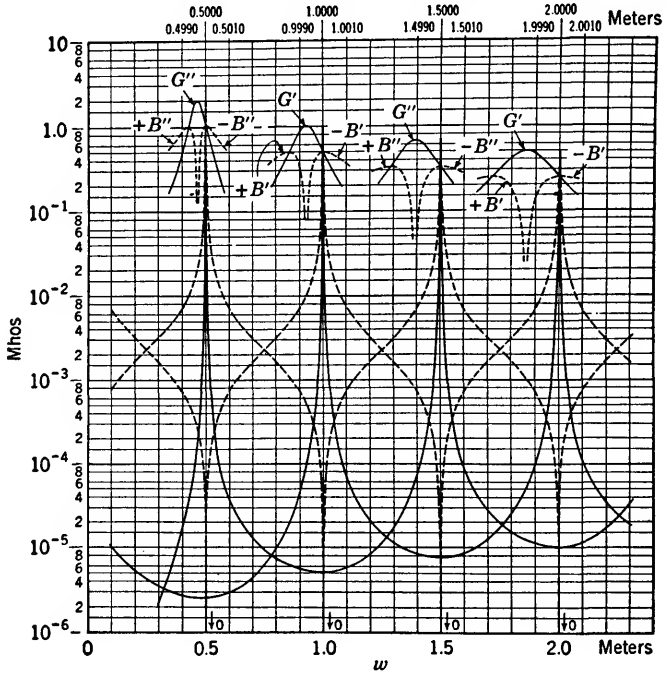


FIG. 5.6. Y_{in} for two-wire line. Constants of the line are the same as in Fig. 5.4. $Y'_{in} = G'_{in} + jB'_{in}$ for ideal short circuit. $Y''_{in} = G''_{in} + jB''_{in}$ for ideal open end.

the coaxial line

$$\Phi_s = \Phi_{sa} \doteq \frac{\pi}{2} \qquad \rho_s = \rho_{sa} \doteq 0 \tag{5}$$

The appropriate conditions for antiresonance with n integral are

$$s = \frac{n\lambda}{2} - \frac{\Phi_{sa}}{\beta} = \frac{n\lambda}{2} - \frac{\lambda}{4} - k_{sa} \qquad \text{for the two-wire line} \tag{6a}$$

$$s = \frac{n\lambda}{2} - \frac{\lambda}{4} \qquad \text{for the coaxial line} \tag{6b}$$

and the corresponding antiresonant resistances are

$$(R_{in})_{\max} = \frac{R_c}{\alpha s + \rho_{sa}} = \frac{R_c}{\alpha(s + b/2)} = \frac{2R_c^2}{r(s + b/2)} \qquad \text{for the two-wire line} \tag{7a}$$

and

$$(R_{in})_{\max} = \frac{R_c}{\alpha s} = \frac{2R_c^2}{rs} \qquad \text{for the coaxial line} \tag{7b}$$

For convenience let

$$s' = s + \frac{\rho_{sa}}{\alpha} \doteq s + \frac{b}{2} \qquad \text{for the two-wire line} \tag{8}$$

$$s' = s \qquad \text{for the coaxial line} \tag{9}$$

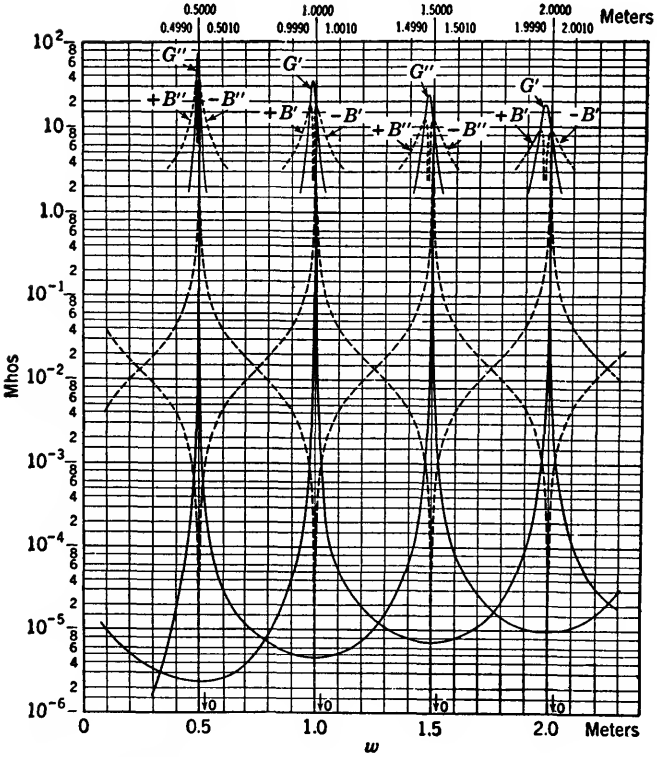


FIG. 5.7. Y_{in} for coaxial line. Constants of the line are the same as in Fig. 5.5. $Y'_{in} = G'_{in} + jB'_{in}$ for ideal short circuit. $Y''_{in} = G''_{in} + jB''_{in}$ for ideal open end.

The shortest possible lengths and the greatest resistance are obtained with $n = 1$, so that $s' = \lambda/4$ and

$$(R_{in})_{max} = \frac{4R_c}{\alpha\lambda} = \frac{8R_c^2}{r\lambda} \tag{10}$$

For a line with low attenuation per unit length when operated at sufficiently high frequencies, the following simple formulas are good approximations:

For the two-wire line

$$R_c = \frac{\zeta}{\pi} \cosh^{-1} \frac{b}{2a} \qquad r = \frac{m}{a}\sqrt{\omega} \qquad m \equiv \frac{1}{\pi}\sqrt{\frac{1}{2\sigma\nu}} \tag{11}$$

For the coaxial line

$$R_c = \frac{\zeta}{2\pi} \ln \frac{b}{a} \qquad r = \frac{m\sqrt{\omega}}{2b}\left(1 + \frac{b}{a}\right) \qquad m = \frac{1}{\pi}\sqrt{\frac{1}{2\sigma\nu}} \tag{12}$$

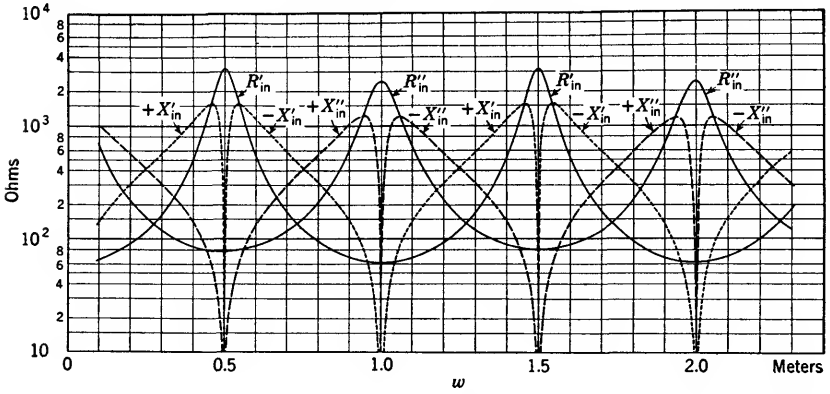


FIG. 5.8. Z_{in} for two-wire line. Constants of the line are as in Fig. 5.4. R'_{in} and X'_{in} for $R_s = 60$ ohms, $X_s = 0$; R''_{in} and X''_{in} for $R_s = 2500$ ohms, $X_s = 0$.

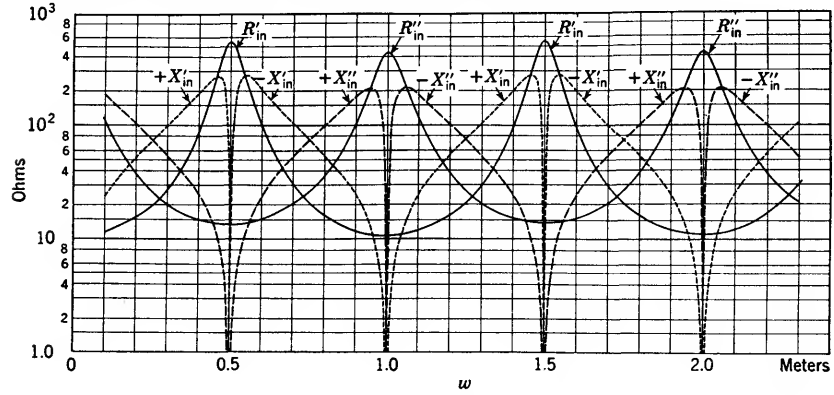


FIG. 5.9. Z_{in} for coaxial line. Constants of the line are as in Fig. 5.5. R'_{in} and X'_{in} for $R_s = 60$ ohms, $X_s = 0$; R''_{in} and X''_{in} for $R_s = 2500$ ohms, $X_s = 0$.

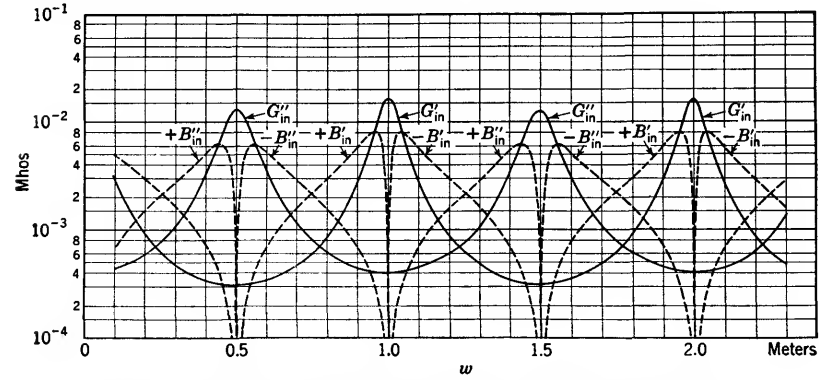


FIG. 5.10. Y_{in} for two-wire line under same conditions as in Fig. 5.8.

In the above

$$\zeta \equiv \frac{1}{\sqrt{\epsilon_d \nu_d}} = \frac{\zeta_0}{\sqrt{\epsilon_{rd} \nu_{rd}}} = \frac{120\pi}{\sqrt{\epsilon_{rd} \nu_{rd}}} \quad \text{ohms} \tag{13}$$

Using

$$\lambda = \frac{v_p}{f} = \frac{2\pi v_p}{\omega} \qquad v_p = \sqrt{\frac{\nu_d}{\epsilon_d}} = v_0 \sqrt{\frac{\nu_{rd}}{\epsilon_{rd}}} \doteq 3 \times 10^8 \sqrt{\frac{\nu_{rd}}{\epsilon_{rd}}} \quad \text{m/sec} \tag{14}$$

the following formulas are obtained:

For the two-wire line

$$\frac{8R_c^2}{r\lambda} = \frac{4b}{m} \frac{\sqrt{\omega}}{2\pi v_p} \frac{\zeta^2}{\pi^2} \frac{2a}{b} \left(\cosh^{-1} \frac{b}{2a} \right)^2 \tag{15}$$

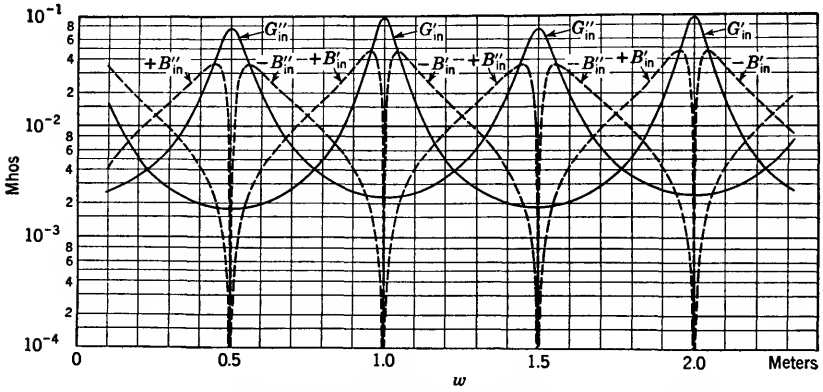


FIG. 5.11. Y_{in} for coaxial line under same conditions as in Fig. 5.9.

For the coaxial line

$$\frac{8R_c^2}{r\lambda} = \frac{4b}{m} \frac{\sqrt{\omega}}{2\pi v_p} \frac{\zeta^2}{\pi^2} \frac{[\ln (b/a)]^2}{1 + b/a} \tag{16}$$

Let

$$K \equiv \frac{4}{m} \frac{1}{2\pi v_p} \frac{\zeta^2}{\pi^2} \tag{17}$$

Then for the two-wire line

$$(R_{in})_{\max} = \frac{8R_c^2}{r\lambda} = bK \sqrt{\omega} \frac{2a}{b} \left(\cosh^{-1} \frac{b}{2a} \right)^2 \tag{18}$$

and for the coaxial line

$$(R_{in})_{\max} = \frac{8R_c^2}{r\lambda} = bK \sqrt{\omega} \frac{[\ln (b/a)]^2}{1 + (b/a)} \tag{19}$$

The numerical value of K is

$$K \equiv \frac{0.121}{\nu_{rd}} \sqrt{\frac{\sigma \nu_r}{\epsilon_{rd} \nu_{rd}}} \tag{20}$$

For copper in air $\sigma = 5.65 \times 10^7$, $\nu_r = 1$, $\epsilon_{rd} = 1$, and $\nu_{rd} = 1$, so that $K = 0.121 \times \sqrt{56.5} \times 10^3 = 0.91 \times 10^3$.

It is to be noted that $(R_{in})_{\max,\max}$ increases indefinitely with frequency and with b. However, for a given value of b the functions $(2a/b)[\cosh^{-1}(b/2a)]^2$ and $[\ln(b/a)]^2/(1 + b/a)$ can be maximized by suitably adjusting a. Let $y = b/2a$. The maximum value of $(1/y)(\cosh^{-1} y)^2$ is obtained by differentiating and equating to zero.

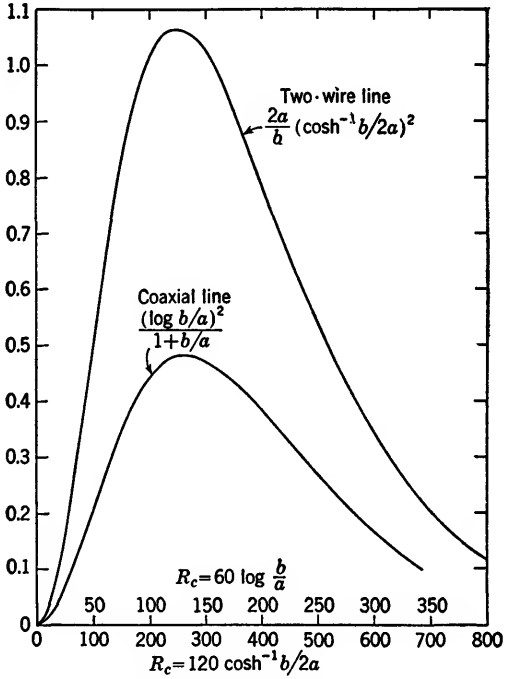


FIG. 6.1. Functions of separation determining extreme values of $(R_{in})_{\max}$.

The result is $y = b/2a = 3.95$, so that for maximum $(R_{in})_{\max}$, with b fixed, the wire radius should be

$$a = \frac{b}{7.90} \tag{21}$$

The function $(1/y)(\cosh^{-1} y)^2$ is plotted in Fig. 6.1. It is seen that its maximum value is 1.064. Similarly, with $x = b/a$, the function $(\ln x)^2/(1 + x)$ may be shown to have the maximum $x = b/a = 9.2$, so that, for given b, the radius of the inner conductor of the coaxial line should be

$$a = \frac{b}{9.2} \tag{22}$$

The function $(\ln x)^2/(1 + x)$ is plotted in Fig. 6.1 as a function of x. Its maximum value is 0.481.

The characteristic resistances corresponding to these extremizing values of a are as follows:

For the two-wire line
$$R_c = \frac{246}{\sqrt{\epsilon_{rd}\nu_{rd}}} \tag{23}$$

For the coaxial line
$$R_c = \frac{133.1}{\sqrt{\epsilon_{rd}\nu_{rd}}} \tag{24}$$

The corresponding extreme values of $(R_{in})_{max}$ are as follows:

For the two-wire line
$$\begin{aligned}(R_{in})_{max,max} &= \frac{246}{\alpha s\sqrt{\nu_{dr}\epsilon_{dr}}} \qquad \frac{b}{a} = 7.9 \\ &= bK\sqrt{\omega} \times 1.064\end{aligned} \tag{25}$$

For the coaxial line
$$\begin{aligned}(R_{in})_{max,max} &= \frac{133.1}{\alpha s\sqrt{\nu_{dr}\epsilon_{dr}}} \qquad \frac{b}{a} = 9.2 \\ &= bK\sqrt{\omega} \times 0.481\end{aligned} \tag{26}$$

For copper in air $K = 0.91 \times 10^3$, so that

For the two-wire line
$$(R_{in})_{max,max} = 0.97b\sqrt{\omega} \times 10^3 = 2.43b\sqrt{f} \times 10^3 \tag{27}$$

For the coaxial line
$$(R_{in})_{max,max} = 0.438b\sqrt{\omega} \times 10^3 = 1.098b\sqrt{f} \times 10^3 \tag{28}$$

In the case of the two-wire line described in Fig. 5.4, for which $b = 2$ cm and $a = 5.118 \times 10^{-2}$ cm at $f = 1.5 \times 10^8$ Mc/sec, the maximum value of R_{in} is
$$(R_{in})_{max} = \frac{R_c}{\alpha s} = \frac{439.8}{2.258 \times 10^{-3} \times 0.50} = 397{,}000 \text{ ohms} \tag{29}$$

If the radius of the wires is changed from 5.118×10^{-2} cm to the optimum value, $a = b/7.9 = 2/7.9 = 0.253$ cm, so that $R_c = 246$ ohms and $\alpha = 0.828 \times 10^{-3}$ neper/m,
$$(R_{in})_{max,max} = 0.02 \times 2.43 \times 1.225 \times 10^4 = 595{,}000 \text{ ohms} \tag{30}$$

For the coaxial line described in Fig. 5.5, for which $b = 3.5$ cm and $a = 1$ cm, the maximum value is $(R_{in})_{max} = R_c/\alpha s = 420{,}000$ ohms. By adjusting the radius to be $a = b/9.2 = 3.5/9.2 = 0.38$ cm, so that $R_c = 133.1$ ohms,
$$(R_{in})_{max,max} = 1.098 \times 0.035 \times 1.225 \times 10^4 = 471{,}000 \text{ ohms} \tag{31}$$

Since it is not difficult to obtain resistances of the order of magnitude of half a megohm or more using antiresonant sections of transmission

line at high frequencies, such sections serve admirably as insulators for supporting transmission lines or circuit elements whenever these are to be designed for *single-frequency* operation. Because the shortest length of a section designed for this purpose is about one-quarter of a wavelength, such insulating stubs are useful only at ultrahigh and microwave frequencies. Since the maximum input resistance increases with frequency (because the length decreases more rapidly than the resistance increases), the insulating properties of quarter-wave stubs improve as the frequency becomes higher. At sufficiently high frequencies they are superior to most insulators (and often more rugged). In Fig. 6.2 schematic diagrams are shown of parallel- and coaxial-line stubs arranged to support both wires in the case of the parallel line and the inner conductor of the coaxial line. The proper location and spacing of supporting insulators, whether constructed of stubs or of dielectric material, are discussed in a subsequent section. The question of end effects is also considered later.

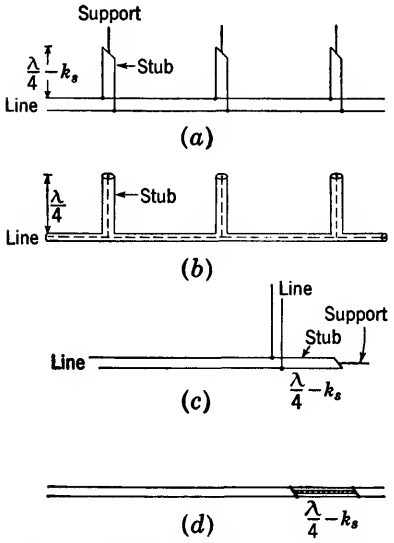


FIG. 6.2. High-impedance stubs used as insulators. (*a*) Stub supports for two-wire line. (*b*) Closed-end supports for inner conductor of coaxial line. (*c*) Stub support at right-angle bend in two-wire line. (*d*) Quarter-wave high-impedance stub in tandem with movable bridge.

7. Impedance Transformation Using a Network of Transmission-line Sections—General Formulation. In order to reduce the power losses in transmission over long distances to a minimum, a transmission line must be terminated in its characteristic impedance Z_c. Such a termination is shown in a later section to lead to minimum losses in the line. Schematic circuit diagrams for two-wire and coaxial lines with matching networks are shown in Fig. 7.1. In Fig. 7.2 a very general matching network is inserted between the end of the long line and the load impedance Z_s. In order to distinguish quantities associated with the long line from those used to describe the matching section, the latter are designated with a subscript m. Thus Z_c is the characteristic impedance of the long line; Z_{cm} is that of the matching section.

The condition that must be satisfied is

$$Z_{in} = Z_c \qquad \text{or} \qquad R_{in} = R_c \qquad X_{in} = -\phi_c R_c \tag{1}$$

where Z_{in} is the input impedance of the matching section of length s,

with the load Z_s as its termination. In Fig. 7.2 Z_{in} is the impedance at AA. The general relations (1) for the input resistance and reactance of a terminated section of transmission line may be expressed in admittance form as follows:

$$Y_A = Y_{Ax} + Y_{Ay} = Y_c \tag{2}$$

where $Y_A = 1/Z_A$ is the input admittance of the entire matching network at AA as seen from the feeding line and Y_{Ax} and Y_{Ay} are, respectively, the admittance at AA of the part of the matching network of length x with its termination and of the length y with its termination. $Y_c = 1/Z_c$ is the characteristic admittance of the feeding line; $Y_{cm} = 1/Z_{cm}$ is the characteristic admittance of the matching sections.

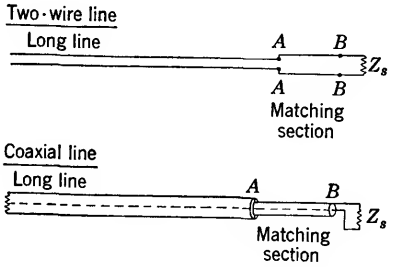


FIG. 7.1. Circuit for matching a load to a long line.

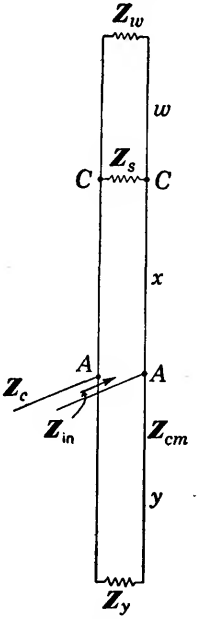


FIG. 7.2. General matching section.

Division of (2) by Y_{cm} gives the normalized values *referred to the matching line.* Thus

$$y_{1Ax} + y_{1Ay} = y_{1c} \tag{3}$$

The separation of real and imaginary parts gives

$$g_{1Ax} + g_{1Ay} = g_{1c} \qquad b_{1Ax} + b_{1Ay} = b_{1c} \tag{4}$$

Since

$$y_{1c} \equiv \frac{Y_c}{Y_{cm}} = \frac{Z_{cm}}{Z_c} = \frac{R_{cm}(1 - j\phi_{cm})}{R_c(1 - j\phi_c)} = \frac{R_{cm}}{R_c}\frac{(1 - \phi_{cm}\phi_c) - j(\phi_{cm} - \phi_c)}{1 + \phi_c^2} \tag{5a}$$

it follows that for a low-loss line, with $\phi_c^2 \ll 1$ and $\phi_c\phi_{cm} \ll 1$,

$$g_{1c} = \frac{R_{cm}}{R_c}\frac{1 - \phi_{cm}\phi_c}{1 + \phi_c^2} \doteq \frac{R_{cm}}{R_c} \tag{5b}$$

$$b_{1c} = \frac{R_{cm}}{R_c}\frac{\phi_{cm} - \phi_c}{1 + \phi_c^2} \doteq 0 \tag{5c}$$

For a low-loss line it is correct to assume $\phi_c^2 \doteq (\alpha/\beta)^2 \ll 1$. Since β is

the same and α is very small on both lines, the difference $\phi_{cm} - \phi_c$ is negligible compared with $b_{1Ax} + b_{1Ay}$ in (4).

Since the matching section of length y may be constructed to have an extremely small input conductance by making it essentially reactive, the following condition is easily satisfied:

$$g_{1Ax} \gg g_{1Ay} \tag{6}$$

With (5c) and (6), (4) becomes simply

$$g_{1Ax} = g_{1c} \doteq \frac{R_{cm}}{R_c} \qquad b_{1Ax} + b_{1Ay} = 0 \tag{7}$$

These are the fundamental conditions for matching the load with its matching network to the long line. The introduction of the terminal functions defined in Sec. 1 into (7) permits these to be expressed as follows:

$$\frac{\sinh 2A_x}{\cosh 2A_x - \cos 2F'_x} = \frac{R_{cm}}{R_c} \tag{8a}$$

$$\frac{\sin 2F'_x}{\cosh 2A_x - \cos 2F'_x} + \frac{\sin 2F'_y}{1 - \cos 2F'_y} = 0 \tag{8b}$$

where $A_x \equiv \alpha x + \rho_x$, $F'_x \equiv \beta x + \Phi'_x$, and $F'_y = \beta y + \Phi'_y$. Note that ρ_x and Φ'_x are the terminal functions of $\boldsymbol{Z}_x$ consisting of $\boldsymbol{Z}_s$ in parallel with the stub of length x. Equation (8b) may be written as follows:

$$\frac{\sin F'_x \cos F'_x}{\sinh^2 A_x + \sin^2 F'_x} + \cot F'_y = 0 \tag{8c}$$

In general, two variables are necessary to satisfy both (8a) and (8c). Depending on the choice of these variables, the matching network may be simplified in any one of several ways. In its complete form the following arbitrarily adjustable quantities are available:

1. The lengths w, x, and y, with the restriction that the attenuation $\alpha(w + x + y)$ must be small compared with ρ_s.
2. The terminating impedances $\boldsymbol{Z}_x$ and $\boldsymbol{Z}_y$, with the restriction that their attenuation functions ρ_x and ρ_y must be negligible compared with the attenuation function ρ_s of the load.
3. The characteristic impedance of the matching line

$$\boldsymbol{Z}_{cm} = R_{cm}(1 - j\phi_{cm})$$

within somewhat narrow practical limits. The condition that ϕ_{cm} be as small as possible must be observed.

8. The Series Transformer.[81,97,101] A simple form of the general matching network is shown in Fig. 7.1. It is derived by removing the sections of line of length w and y and selecting x and R_c as the variables.

This means that $F'_y = \pi/2$ and $\cot F'_y = 0$. Also $Z_s = Z_x$ is the entire impedance terminating the section of length x. The general Eqs. (8*a*) and (8*c*) reduce to the following:

$$\frac{\sinh 2A_x}{\cosh 2A_x - \cos 2F'_x} = \frac{R_{cm}}{R_c} \tag{1}$$

$$\sin 2F'_x = 0 \tag{2}$$

There are two infinite sets of solutions. From these the solution with the smallest physically possible value of $n = 0, 1, 2, \ldots$ should be chosen. The sets are

$$F'_x = (2n + 1)\frac{\pi}{2} \qquad \tanh A_x = \frac{R_{cm}}{R_c} \tag{3}$$

$$F'_x = n\pi \qquad \coth A_x = \frac{R_{cm}}{R_c} \tag{4}$$

Since $\tanh A_x \leqq 1$ and $\coth A_x \geqq 1$, it follows that, with n an integer,

$$R_c = R_{cm} \coth A_x \qquad F'_x = (2n + 1)\frac{\pi}{2} \qquad R_c > R_{cm} \tag{5a}$$

$$R_c = R_{cm} \tanh A_x \qquad F'_x = n\pi \qquad R_c < R_{cm} \tag{5b}$$

For a properly designed matching section, x is sufficiently short and α sufficiently small so that it is correct to set $\alpha x \ll \rho_x$. Hence

$$A_x = \alpha x + \rho_x \doteq \rho_x \tag{6}$$

It is shown in a later section that, when the condition $\alpha x \ll \rho_x$ is satisfied, the quantity $\coth \rho_x$ is equal to the standing-wave ratio S_x on the matching section of line of length x. Thus

$$S_x = \coth \rho_x \tag{7}$$

With this notation the conditions for match are

$$R_c = R_{cm}S_x \qquad F'_x = (2n + 1)\frac{\pi}{2} \qquad R_c > R_{cm} \tag{8}$$

$$R_c = \frac{R_{cm}}{S_x} \qquad F'_x = n\pi \qquad R_c < R_{cm} \tag{9}$$

where n is an integer.

Although simple in form, (8) and (9) are convenient only if R_{cm} is given and R_c is to be determined. Usually the reverse is true. In this case R_{cm} is not directly available from (8) or (9), since it is involved in ρ_x through the relation

$$\tanh 2\rho_x = \frac{2r_{1xm}}{r_{1xm}^2 + x_{1xm}^2 + 1} \tag{10}$$

where

$$r_{1xm} = \frac{R_{1x}}{R_{cm}} \qquad x_{1xm} = \frac{X_{1x}}{R_{cm}} \tag{11}$$

An explicit formula for R_{cm} is readily derived using

$$\tanh 2\rho_x = \frac{2 \tanh \rho_x}{1 + \tanh^2 \rho_x} \tag{12}$$

$$\text{together with} \quad \tanh \rho_x = \begin{cases} \dfrac{R_c}{R_{cm}} & \text{for } F'_x = n\pi \\ \dfrac{R_{cm}}{R_c} & \text{for } F'_x = (2n+1)\dfrac{\pi}{2} \end{cases} \tag{13}$$

If (10) and (12) are equated using either of the two forms of (13) in succession, the following relation may be derived:

$$R_{cm} = \sqrt{\frac{R_c(R_x^2 + X_x^2) - R_c^2 R_x}{R_x - R_c}} = R_c \sqrt{\frac{r_{1x}^2 + x_{1x}^2 - r_{1x}}{r_{1x} - 1}} \tag{14}$$

where $r_{1x} \equiv R_x/R_c$ and $x_{1x} \equiv X_x/R_c$.

$$\begin{aligned} &\text{If } R_c > R_{cm}, && F'_x = \frac{2n+1}{2}\pi \\ &\text{If } R_c < R_{cm}, && F'_x = n\pi \end{aligned} \tag{15}$$

In the special case of a purely resistive termination $X_x = 0$, $\Phi'_x = 0$ for $R_{cm} > R_x$, and $\Phi'_x = \pi/2$ for $R_{cm} < R_x$. Hence

$$R_{cm} = \sqrt{R_c R_x} \qquad \beta x = \begin{Bmatrix} F'_x - 0 \\ F'_x - \dfrac{\pi}{2} \end{Bmatrix} = \begin{Bmatrix} \dfrac{2n+1}{2}\pi \\ n\pi - \dfrac{\pi}{2} \end{Bmatrix} = \frac{2n+1}{2}\pi$$

$$\text{for} \begin{cases} R_c > R_{cm} > R_x \\ R_c < R_{cm} < R_x \end{cases} \tag{16}$$

From (1) it follows that, if $R_{cm} = R_c$, a match is possible only if

$$A_x = \infty \tag{17}$$

Clearly it is not possible to achieve a match for all values of R_x and X_x, since the radical in (14) *must remain real.* This is true subject to one of the following sets of conditions:

$$\text{For } R_x > R_c, \qquad R_x^2 + X_x^2 > R_c R_x \tag{18}$$

$$\text{For } R_x < R_c, \qquad R_x^2 + X_x^2 < R_c R_x \tag{19}$$

Evidently (18) is always true, whereas in (19) the values of R_x and X_x are limited.

The regions in the r_{1x}, x_{1x} plane in which a match is possible are bounded by the following curves:

$$r_{1x} = 1 \tag{20}$$

$$r_{1x}^2 + x_{1x}^2 - r_{1x} = 0 \quad \text{or} \quad (r_{1x} - \tfrac{1}{2})^2 + x_{1x}^2 = \tfrac{1}{4} \tag{21}$$

Evidently (20) is the equation of a straight line; on the other hand, (21) is the equation of a circle with center at $r_{1x} = \frac{1}{2}$, $x_{1x} = 0$ and with radius $\frac{1}{2}$. This circle is shown in Fig. 8.1. *A match is possible only if r_{1x} and x_{1x} have values that lie to the right of the line $r_{1x} = 1$ or within the circle.* Matching is impossible if r_{1x} and x_{1x} lie both to the left of the line $r_{1x} = 1$ and outside the circle.

The complete solution for R_{cm} and x can be expressed as follows (normalization is with respect to R_c, and g_c is by definition the ratio R_{cm}/R_c):

$$R_{cm} \equiv g_c R_c = R_c \sqrt{\frac{r_{1x}^2 + x_{1x}^2 - r_{1x}}{r_{1x} - 1}} \qquad (22)$$

For $g_c < 1$,

$$\begin{aligned} \beta x &= n\pi - \Phi_x' \\ &= n\pi - \tfrac{1}{2} \tan^{-1} \frac{-2g_c x_{1x}}{r_{1x}^2 + x_{1x}^2 - g_c^2} \end{aligned} \qquad (23)$$

For $g_c > 1$,

$$\beta x = \frac{2n+1}{2}\pi - \Phi_x' = \frac{2n+1}{2}\pi - \tfrac{1}{2} \tan^{-1} \frac{-2g_c x_{1x}}{r_{1x}^2 + x_{1x}^2 - g_c^2} \qquad (24)$$

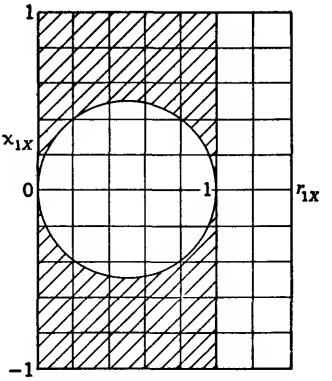


FIG. 8.1. Loci of match for series sections; match possible for $r_{1x} > 1$ or within circle for $r_{1x} < 1$.

9. Matching Section with a Single Movable Stub.[81,109] A widely used form of the general network described in Sec. 7 dispenses with the section of length w but retains the stub of length y (see Figs. 9.1 and 9.2). The points of connection AA' are made movable, so that both x and y

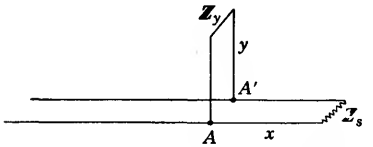


FIG. 9.1. Single stub on two-wire line.

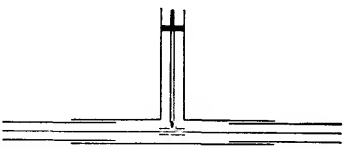


FIG. 9.2. Movable adjustable stub on coaxial line.

may be adjusted, or, in any case, βx and $(\beta y + \Phi_y)$ are made available. It is convenient to use lines of the same characteristic impedance throughout. That is, $\boldsymbol{Z}_c = \boldsymbol{Z}_{cm}$, so that $g_{1c} = \boldsymbol{Z}_{cm}/\boldsymbol{Z}_c = 1$. Accordingly Sec. 7, Eqs. (7), become

$$g_{1Ay} \ll 1 \qquad g_{1Ax} = 1 \qquad b_{1Ax} + b_{1Ay} = 0 \qquad (1)$$

Note that $\boldsymbol{Z}_s = \boldsymbol{Z}_x$. After the terminal functions $A_x \equiv \alpha x + \rho_x$ and

$F'_x \equiv \beta x + \Phi'_x$ are introduced, the following equations are obtained:

$$g_{1A} \doteq g_{1Ax} = \frac{\sinh 2A_x}{\cosh 2A_x - \cos 2F'_x} = 1 \tag{2a}$$

$$b_{1A} = b_{1Ax} + b_{1Ay} = \frac{\sin 2F'_x}{\cosh 2A_x - \cos 2F'_x} + \cot F'_y = 0 \tag{2b}$$

The first of these, (2a), may be solved for F'_x. Thus, after combining terms,

$$\cos 2F'_x = (\cosh A_x - \sinh A_x)^2 \tag{3}$$

The second, (2b), gives

$$\cot F'_y = -\frac{\sin 2F'_x}{\sinh 2A_x} \tag{4}$$

These two equations, (3) and (4), may be rearranged as follows, using $\cot \frac{1}{2} u = \sqrt{(1 + \cos u)/(1 - \cos u)}$:

$$\cot F'_x = \sqrt{\frac{1 + \cos 2F'_x}{1 - \cos 2F'_x}} = \sqrt{\frac{1 + \cosh 2A_x - \sinh 2A_x}{1 - \cosh 2A_x + \sinh 2A_x}} \tag{5}$$

But with

$$\cosh 2u + 1 = 2 \cosh^2 u \qquad \cosh 2u - 1 = 2 \sinh^2 u \tag{6}$$

and with $\alpha x \ll \rho_x$ it is readily shown that

$$\cot (\beta x + \Phi'_x) \doteq \pm \sqrt{\coth \rho_x} \doteq \pm \sqrt{S} \tag{7}$$

or, with $\Phi_x = \Phi'_x \pm \pi/2$,

$$\tan (\beta x + \Phi_x) \doteq \mp \sqrt{\coth \rho_x} \doteq \mp \sqrt{S} \tag{8}$$

Similarly, since $\cos u = \cot u/\sqrt{1 + \cot^2 u}$ and $\sin u = 1/\sqrt{1 + \cot^2 u}$,

$$\cot F'_y = -\frac{2 \sin F'_x \cos F'_x}{\sinh 2A_x} = -\frac{2 \cot F'_x}{(1 + \cot^2 F'_x) \sinh 2A_x}$$

$$= -\frac{\pm 2 \sqrt{\coth A_x}}{(1 + \coth A_x) \sinh 2A_x} \tag{9}$$

But since

$$\sinh 2u = \frac{2 \coth u}{\coth^2 u - 1} \tag{10}$$

it follows that

$$\cot F'_y = \mp \frac{\sqrt{\coth A_x}}{1 + \coth A_x} \frac{\coth^2 A_x - 1}{\coth A_x} = \mp \frac{\coth A_x - 1}{\sqrt{\coth A_x}} \tag{11}$$

Finally, setting $F'_y = \beta y + \Phi'_y$ and $A_x = \alpha x + \rho_x$, the following formulas are obtained:

$$\cot (\beta y + \Phi'_y) = \mp [\sqrt{\coth (\alpha x + \rho_x)} - \sqrt{\tanh (\alpha x + \rho_x)}] \tag{12}$$

Since αx is small compared with ρ_x,

$$\begin{aligned}\cot(\beta y + \Phi_y') &\doteq \mp(\sqrt{\coth \rho_x} - \sqrt{\tanh \rho_x}) \\ &= \mp\left(\sqrt{S} - \frac{1}{\sqrt{S}}\right) = \mp\frac{S-1}{\sqrt{S}}\end{aligned} \tag{13}$$

An alternative form is obtained using $\Phi_y' = \Phi_y - \pi/2$. It is

$$\tan(\beta y + \Phi_y) = \pm\frac{S-1}{\sqrt{S}} \tag{14}$$

It is possible to combine (7) and (12) using the relation

$$\cot(\alpha + \beta) = \frac{\cot\alpha \cot\beta - 1}{\cot\beta + \cot\alpha} \tag{15}$$

The resulting formula is

$$\cot(\beta x + \beta y + \Phi_x' + \Phi_y') = \mp[\coth(\alpha x + \rho_x)]^{\frac{1}{2}} \doteq \mp(\coth\rho_x)^{\frac{1}{2}} = \mp S^{\frac{1}{2}} \tag{16}$$

or

$$\cot(\beta x + \beta y + \Phi_x + \Phi_y) = \mp S^{\frac{1}{2}} \tag{17}$$

For a *purely resistive termination* $\boldsymbol{Z}_s = R_s = R_x$, the following relations obtain:

$$\begin{aligned}&\text{For } r_{1x} < 1, \quad \rho_x = \tanh^{-1} r_{1x} \qquad \Phi_x = \frac{\pi}{2}, \text{ or } \Phi_x' = \pi \text{ or } 0 \\ &\text{For } g_{1x} < 1, \quad \rho_x = \tanh^{-1} g_{1x} \qquad \Phi_x = 0 \text{ or } \pi, \text{ or } \Phi_x' = \frac{\pi}{2}\end{aligned} \tag{18}$$

Alternatively, since $r_{1x} = 1/g_{1x}$,

$$\begin{aligned}&\text{For } r_{1x} < 1, \qquad \rho_x = \coth^{-1} g_{1x} \qquad \Phi_x' = 0 \\ &\text{For } g_{1x} < 1, \qquad \rho_x = \coth^{-1} r_{1x} \qquad \Phi_x' = \frac{\pi}{2}\end{aligned} \tag{19}$$

The following formulas follow directly:

For $g_{1x} > 1$ or $r_{1x} < 1$:

$$\begin{aligned}\cot(\beta x + \Phi_x') &= \cot\beta x = \pm\sqrt{g_{1x}} \\ \cot(\beta x + \beta y + \Phi_x' + \Phi_y') &= \cot[\beta(x+y) + \Phi_y'] = \mp g_{1x}^{\frac{1}{2}}\end{aligned} \tag{20}$$

For $r_{1x} > 1$:

$$\begin{aligned}\cot(\beta x + \Phi_x') &= -\tan\beta x = \pm\sqrt{r_{1x}} \\ \cot(\beta x + \beta y + \Phi_x' + \Phi_y') &= -\tan[\beta(x+y) + \Phi_y'] = \mp r_{1x}^{\frac{1}{2}}\end{aligned} \tag{21}$$

The following specifications are usually convenient:

a. Choose an *open* stub ($\Phi_y' \doteq \pi/2$) for $r_{1x} < 1$ so that

$$\tan\beta x = \pm\sqrt{r_{1x}} \qquad \text{with } + \text{ sign for shortest length} \tag{22}$$

$$-\cot\left[\beta(x+y) + \frac{\pi}{2}\right] = \tan[\beta(x+y)] = g_{1x}^{\frac{1}{2}} \tag{23}$$

The final formulas for the circuit in Fig. 9.1 are

$$\begin{aligned} \beta x &= \tan^{-1} \frac{R_x}{R_c} = \tan^{-1} r_{1x} \\ \beta(x + y) &= \tan^{-1} \left(\frac{R_c}{R_x}\right)^{\frac{1}{2}} = \tan^{-1} \left(\frac{1}{r_{1x}}\right)^{\frac{1}{2}} \end{aligned} \tag{24}$$

b. Choose a *closed* stub ($\Phi_y' = \beta k_y$) for $r_{1x} > 1$ so that

$$\begin{aligned} \tan \beta x &= \mp \sqrt{r_{1x}} \qquad \text{with + sign for shortest length} \\ \tan \beta(x + y + k_y) &= -r_{1x}^{\frac{1}{2}} \\ \tan [\pi - \beta(x + y + k_y)] &= r_{1x}^{\frac{1}{2}} \\ \beta(x + y + k_y) &= \pi - \tan^{-1} r_{1x}^{\frac{1}{2}} = \frac{\pi}{2} + \tan^{-1} g_{1x}^{\frac{1}{2}} \end{aligned}$$

since $\tan^{-1} x = \pi/2 - \tan^{-1} (1/x)$. The final formulas for the circuit of Fig. 9.2 are

$$\begin{aligned} \beta x &= \tan^{-1} \frac{R_x}{R_c} = \tan^{-1} r_{1x} \\ \beta(x + y + k_y) &= \pi - \tan^{-1} \left(\frac{R_c}{R_x}\right)^{\frac{1}{2}} = \frac{\pi}{2} + \tan^{-1} r_{1x}^{\frac{1}{2}} \end{aligned} \tag{25}$$

where k_y is the equivalent length of the terminating bridge. If this is a piston in a coaxial line, $k_y = 0$; if it is a conducting bridge on an open-wire line, $k_y = k_{sa}$, with k_{sa} as defined in Chap. II, Sec. 20.

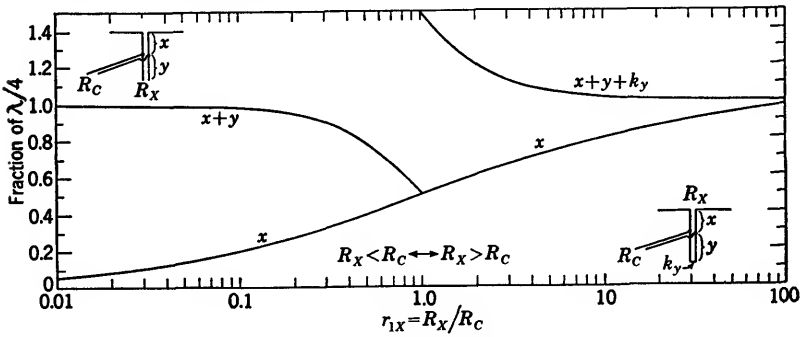


FIG. 9.3. Stub matching with pure resistance termination.

Cases *a* and *b* for a purely resistive termination are illustrated in Fig. 9.3. Numerical and graphical solutions are described below for a particular problem.

Illustrative Example 1 for Single-stub Matching

Given. A load impedance $\boldsymbol{Z}_s = \boldsymbol{Z}_x = 1{,}600 + j800$ ohms to be matched to a line with characteristic resistance $R_c = 400$ ohms.

Problem. To determine the lengths x and y as fractions of a wavelength for a stub with an ideal closed end.

Analytical Solution

1. Determination of normalized resistance and reactance:

$$r_{1x} = \frac{R_x}{R_c} = 4 \qquad x_{1x} = \frac{X_x}{R_c} = 2$$

2. Determination of terminal functions:

$$\rho_x = \tfrac{1}{2} \tanh^{-1} \frac{2r_{1x}}{r_{1x}^2 + x_{1x}^2 + 1} = 0.2$$

$$\Phi_x = \tfrac{1}{2} \tan^{-1} \frac{-2x_{1x}}{r_{1x}^2 + x_{1x}^2 - 1} = 174.1° \qquad \Phi_x' = 84.1°$$

3. Determination of the length x using (8):

$$\tan (\beta x + \Phi_x) = \pm \sqrt{\coth \rho_x} = \pm 2.26$$
$$\beta x = 180° \pm \tan^{-1} 2.26 - 174.1° = 72°$$
$$x = 0.20\lambda$$

4. Determination of the length y using (14):

$$\tan (\beta y + \Phi_y) = \mp (\sqrt{\coth \rho_x} - \sqrt{\tanh \rho_x}) = \mp 1.814$$
$$\beta y + \Phi_y = 180 \mp 61.2° = 118.8° \text{ (or } 241.2°)$$

For the shortest length y choose an ideal closed end with $\Phi_y = 90°$. Then

$$\beta y = 28.8°$$
$$y = 0.080\lambda$$
$$x + y = 0.280\lambda$$

Graphical Solution on the Circle Diagram (*Fig.* 9.4). To change to normalized admittance,

1. Compute $r_{1x} = 4$; $x_{1x} = 2$.
2. Locate $r_{1x} = 4$ and $x_{1x} = 2$ on the chart, and note that this is at $\rho_x = 0.2$ and $\Phi_x = 174°$.
3. Move on circle of constant ρ_x through 90° to locate $\Phi_x' = 84°$ for use with g_{1x} and b_{1x}.

To obtain match,

4. First condition for match: $g_{1x} = 1$. Move along circle of constant $\rho_x = 0.2$ to $\beta x + \Phi_x' = 156°$ at $g_{1x} = 1$. (Note that $b_{1x} = +1.8$.) Then $\beta x = 72°$ and $x = 0.201\lambda$.
5. Second condition for match: $b_{1x} = -b_{1y}$. Locate

$$b_{1y} = -b_{1x} = -1.8$$

on the axis of b. Read off $\beta y + \Phi_y' = 29°$. For the shortest length y choose an ideal short circuit with $\Phi_y' = 0$ ($\Phi_y = \pi/2$) so that $\beta y = 29°$ and $y = 0.080\lambda$; $x + y = 0.28\lambda$.

Illustrative Example 2 for Single-stub Matching

Given. A load impedance $Z_s = Z_x = 3{,}200 + j1{,}600$ ohms to be matched to a two-wire line with characteristic resistance $R_c = 400$ ohms.

Problem. To determine the lengths x and y as fractions of a wavelength for a stub with an ideal open end or closed end.

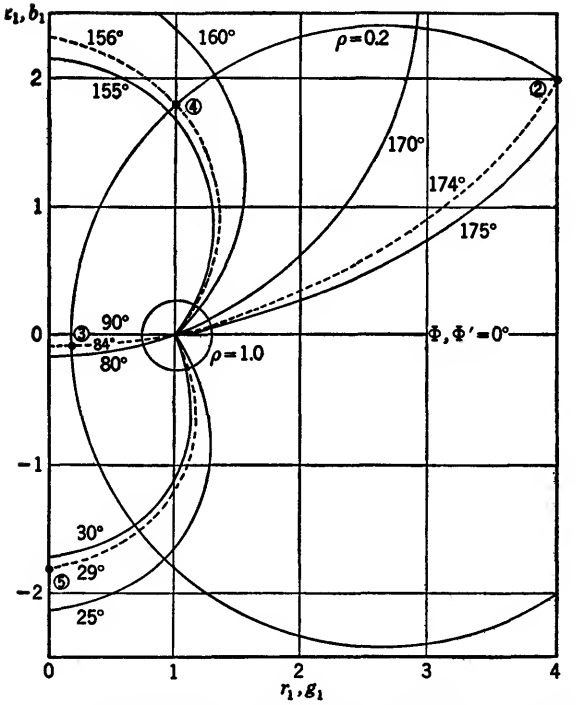


FIG. 9.4. Graphical solution of single-stub matching (Example 1).

Analytical Solution

1. Determination of normalized resistance and reactance:

$$r_{1x} = \frac{R_x}{R_c} = 8 \qquad x_{1x} = \frac{X_x}{R_c} = 4$$

2. Determination of terminal functions:

$$\rho_x = \tfrac{1}{2} \tanh^{-1} \frac{2r_{1x}}{r_{1x}^2 + x_{1x}^2 + 1} = 0.1$$

$$\Phi_x = \tfrac{1}{2} \tan^{-1} \frac{-2x_{1x}}{r_{1x}^2 + x_{1x}^2 - 1} = 177.1° \qquad \Phi_x' = 87.1°$$

3. Determination of the length x using (8):

$$\tan (\beta x + \Phi_x) = \pm \sqrt{\coth \rho_x} = \pm 3.16$$
$$\beta x = 180° \pm \tan^{-1} 3.16 - 177.1° = 75.4°$$
$$x = 0.21\lambda$$

4. Determination of the length y using (14):

$$\tan (\beta y + \Phi_y) = \mp (\sqrt{\coth \rho_x} - \sqrt{\tanh \rho_x}) = \mp 2.844$$
$$\beta y + \Phi_y = 180° \mp 70.6° = 109.4° \text{ (or } 250.6°)$$

For the shortest length y choose an ideal closed end with $\Phi_y = 90°$. Then

$$\beta y = 19.4°$$
$$y = 0.054\lambda$$
$$x + y = 0.264\lambda$$

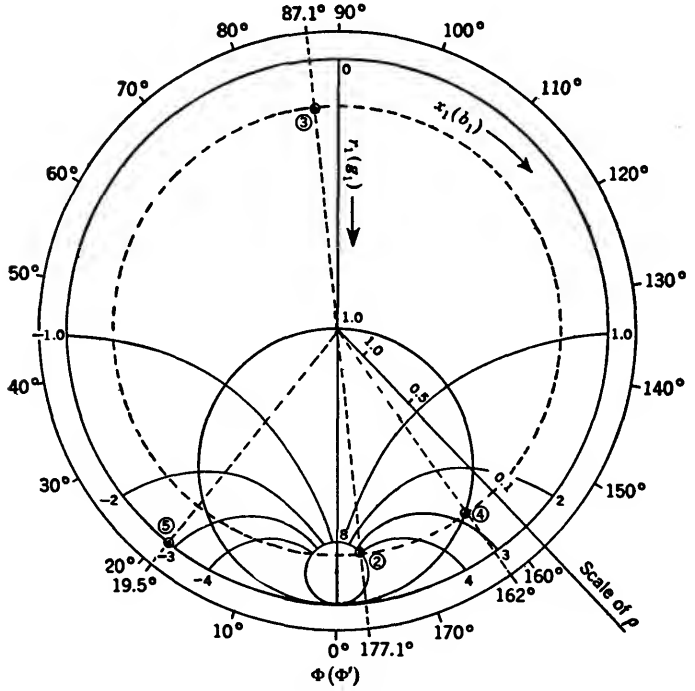


FIG. 9.5. Graphical solution of single-stub matching (Example 2).

Graphical Solution on the Circle Diagram (*Fig.* 9.5). To change to normalized admittance,

1. As before, $r_{1z} = 8$; $x_{1z} = 4$.
2. Locate $r_{1z} = 8$ and $x_{1z} = 4$ on the chart. Note that this occurs at $\rho_z = 0.1$ and $\Phi_z = 177.1°$.
3. Move on circle of constant ρ_z through 90° to locate $\Phi'_z = 87.1°$ for use with g_{1z} and b_{1z}.

To obtain match,

4. First condition for match: $g_{1z} = 1$. Move from $\rho_z = 0.1, \Phi'_z = 87.1°$ to $\rho_z = 0.1$, $\beta x + \Phi'_z = 162°$ at $g_{1z} = 1$. (Note that $b_{1z} = +2.85$.) Then $\beta x = 75°$ and $x = 0.21\lambda$.

5. Second condition for match: $b_{1x} = -b_{1y}$. Hence locate

$$b_{1y} = -b_{1x} = -2.85 \ (g_{1x} = 0)$$

on the axis of b. Read off $\beta y + \Phi_y' = 19.5°$. Choose $\Phi_y' = 0$ ($\Phi_y = \pi/2$) so that $\beta y = 19.5°$ and $y = 0.054\lambda$; $x + y = 0.264\lambda$.

10. Matching Section Consisting of a Double-stub Tuner.[11,109] For the double-stub tuner the lengths w and y are adjustable, whereas x, Φ_w, and Φ_y are fixed but arbitrary. All sections have the same characteristic impedance $\boldsymbol{Z}_c$ as the long line. The lengths w and y may be so chosen that

$$g_{1Cw} \ll 1 \qquad b_{1Cw} = -\cot(\beta w + \Phi_w') \tag{1}$$

$$g_{1Ay} \ll 1 \qquad b_{1Ay} = -\cot(\beta y + \Phi_y') \tag{2}$$

where the notation is that of Sec. 7. Circuits for open and coaxial lines are shown in Figs. 10.1 and 10.2. The conditions for match are

$$g_{1A} = g_{1Ax} = 1 \tag{3}$$

$$b_{1A} = b_{1Ax} + b_{1Ay} = 0 \tag{4}$$

Because the termination of the section of length x consists of the load $\boldsymbol{Z}_s = R_s + jX_s$ or $\boldsymbol{Y}_s = G_s + jB_s$ *in parallel* with the section of length w, it is not convenient to represent their combined impedance by terminal

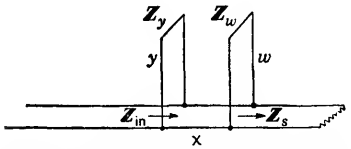


FIG. 10.1. Double-stub matching network for two-wire line.

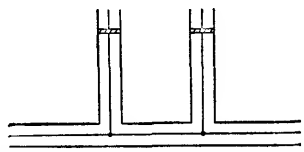


FIG. 10.2. Double-stub matching network for coaxial line.

functions. If $\boldsymbol{Z}_x = R_x + jX_x$ applies to $\boldsymbol{Z}_s$ in parallel with the stub of length w, the hyperbolic form of the admittance $\boldsymbol{Y}_{Ax}$ looking into the line of length x is

$$\boldsymbol{y}_{1Ax} = \frac{\sinh \gamma x + \boldsymbol{y}_{1x} \cosh \gamma x}{\cosh \gamma x + \boldsymbol{y}_{1x} \sinh \gamma x} = \frac{1 + \boldsymbol{y}_{1x} \coth \gamma x}{\coth \gamma x + \boldsymbol{y}_{1x}} \tag{5}$$

where $\boldsymbol{y}_{1Ax} = \boldsymbol{Y}_{Ax}/\boldsymbol{Y}_c$ and $\boldsymbol{y}_{1x} = \boldsymbol{Y}_x/\boldsymbol{Y}_c$. Since the length x is to be kept small and its termination includes the load, it is a good approximation to set $\alpha x \ll \rho_x$ and $\beta x \neq n\pi$. Then $\coth \gamma x \doteq -j \cot \beta x$, so that

$$\boldsymbol{y}_{1Ax} = \frac{1 - j\boldsymbol{y}_{1x} \cot \beta x}{\boldsymbol{y}_{1x} - j \cot \beta x} \tag{6}$$

where

$$\boldsymbol{y}_{1x} = g_{1x} + jb_{1x} = g_{1Cw} + g_{1s} + j(b_{1Cw} + b_{1s}) \doteq g_{1s} + j(b_{1Cw} + b_{1s}) \tag{7}$$

and

$$b_{1Cw} = -\cot(\beta w + \Phi_w') \qquad g_{1Cw} \ll g_{1s} \tag{8}$$

It follows that

$$y_{1Ax} = g_{1Ax} + jb_{1Ax} = \frac{1 - j(g_{1x} + jb_{1x}) \cot \beta x}{g_{1x} + jb_{1x} - j \cot \beta x} \tag{9}$$

The separation of real and imaginary parts leads to

$$g_{1Ax} = \frac{g_{1x} \csc^2 \beta x}{g_{1x}^2 + (\cot \beta x - b_{1x})^2} \tag{10}$$

$$b_{1Ax} = \frac{g_{1x}^2 \cot \beta x - (\cot \beta x - b_{1x})(1 + b_{1x} \cot \beta x)}{g_{1x}^2 + (\cot \beta x - b_{1x})^2} \tag{11}$$

Application of the condition for match (3) gives

$$g_{1x} \csc^2 \beta x = g_{1x}^2 + (\cot \beta x - b_{1x})^2 \tag{12}$$

This equation may be rearranged as follows:

$$(g_{1x} - \tfrac{1}{2} \sec^2 \beta x)^2 + (\cot \beta x - b_{1x})^2 = (\tfrac{1}{2} \csc^2 \beta x)^2 \tag{13}$$

This is the equation of a circle with center at

$$g_{1x} = \frac{1}{2 \sin^2 \beta x} \qquad b_{1x} = \cot \beta x \tag{14}$$

and with radius

$$R = \frac{1}{2 \sin^2 \beta x} \tag{15}$$

The circle (13) passes through the point $b_{1x} = 0$, $g_{1x} = 1$. As is shown later, especially useful values of βx are $\pi/4$, $\pi/2$, $3\pi/4$. For these the following table applies:

βx	$\frac{\pi}{4}$	$\frac{\pi}{2}$	$\frac{3\pi}{4}$
Center at	$g_{1x} = 1 \quad b_{1x} = 1$	$\frac{1}{2}, 0$	$1, -1$
Radius	1	$\frac{1}{2}$	1

(16)

The associated circles are shown in Chap. II, Fig. 16.2. For a fixed value of x a match is possible only if g_{1x} and b_{1x} lie on the appropriate circle. Since $g_{1x} = g_{1s}$ is not adjustable, whereas $b_{1x} = b_{1s} + b_{1Cw}$ is adjustable in b_{1Cw}, a match cannot always be achieved with a given value of impedance and a given value of x.

The two quantities to be determined, $F_w' = \beta w + \Phi_w'$ and $F_y' = \beta y + \Phi_y'$, are readily evaluated from b_{1Cw} and b_{1Ay}. In order to determine b_{1Cw} it is possible to solve the equation $g_{1Ax} = 1$ for $b_{1x} = b_{1Cw} + b_{1s}$. Thus

$$g_{1x} \csc^2 \beta x = g_{1x}^2 + (\cot \beta x - b_{1x})^2 \tag{17}$$

$$\cot \beta x - b_{1x} = \pm g_{1x} \sqrt{\frac{1}{g_{1x} \sin^2 \beta x} - 1} \tag{18}$$

$$b_{1Cw} = -b_{1s} + \cot \beta x \mp g_{1x} \sqrt{\frac{1}{g_{1x} \sin^2 \beta x} - 1} \tag{19}$$

Accordingly, with

$$g_{1x} = g_{1s} \qquad \text{and} \qquad b_{1Cw} = -\cot(\beta w + \Phi'_w) \tag{20}$$

it follows that

$$\cot(\beta w + \Phi'_w) = b_{1s} - \cot \beta x + g_{1s}\sqrt{\frac{1}{g_{1s}\sin^2 \beta x} - 1} \tag{21}$$

In order to determine $b_{1Ay} = -b_{1Ax}$, (11) may be rearranged. Thus, using (12),

$$b_{1Ay} = -b_{1Ax} = \frac{(\cot \beta x - b_{1x})(1 + b_{1x}\cot \beta x) - g_{1x}^2 \cot \beta x}{g_{1x}\csc^2 \beta x} \tag{22}$$

The elimination of b_{1x} from (22), using $b_{1x} = b_{1Cw} + b_{1s}$ and $g_{1x} = g_{1s}$, gives, after considerable rearrangement,

$$-b_{1Ay} = -\cot \beta x \pm \sqrt{\frac{1}{g_{1s}\sin^2 \beta x} - 1} \tag{23}$$

Since, in general,

$$b_{1Cw} = -\cot(\beta w + \Phi'_y) \tag{24}$$

it follows that (19) is equivalent to

$$-b_{1Cw} = \cot(\beta w + \Phi'_y) = b_{1s} - \cot \beta x \pm g_{1s}\sqrt{\frac{1}{g_{1s}\sin^2 \beta x} - 1} \tag{25}$$

Similarly, for (23),

$$-b_{1Ay} = \cot(\beta y + \Phi'_y) = -\cot \beta x \pm \sqrt{\frac{1}{g_{1s}\sin^2 \beta x} - 1} \tag{26}$$

In these formulas the upper signs go together, as do the lower signs. Since the *radical must be real*, the restriction on g_{1s} is

$$g_{1s}\sin^2 \beta x \leqq 1 \tag{27}$$

This is greatest for $\beta x = \pi/2$ and least for $\beta x = \pi$. However, no adjustment in b_{1Ay} is possible for $\beta x = \pi$, and the adjustment is extremely delicate for βx near π; furthermore $\beta x = n\pi$ was excluded when attenuation was neglected. A good compromise, which provides a reasonable range and accurate adjustment, is $\beta x = \pi/4$ or $3\pi/4$. Note that $\beta x = \pi/2$ gives the smallest range. For pistons in coaxial stubs $\Phi'_y = 0 = \Phi'_w$; for bridged two-wire lines $\Phi'_y = \beta k_{ya}$; $\Phi'_w = \beta k_{wa}$ where k_{ya} or k_{wa} can be made small. These three important cases give

(*a*)
$$\beta x = \frac{\pi}{4} \qquad \sin^2 \beta x = \tfrac{1}{2} \qquad \cot \beta x = 1 \tag{28}$$

$$\cot(\beta w + \Phi'_w) = -1 + b_{1s} \pm g_{1s}\sqrt{\frac{2}{g_{1s}} - 1} \tag{29}$$

$$\cot(\beta y + \Phi'_y) = -1 \pm \sqrt{\frac{2}{g_{1s}} - 1} \tag{30}$$

Since the radical must be real, it follows that

$$g_{1s} < 2 \tag{31}$$

(*b*) $$\beta x = \frac{3\pi}{4} \qquad \sin^2 \beta x = \tfrac{1}{2} \qquad \cot \beta x = -1 \tag{32}$$

$$\cot (\beta w + \Phi'_w) = 1 + b_{1s} \pm g_{1s} \sqrt{\frac{2}{g_{1s}} - 1} \tag{33}$$

$$\cot (\beta y + \Phi'_y) = 1 \pm \sqrt{\frac{2}{g_{1s}} - 1} \tag{34}$$

As before, $$g_{1s} < 2 \tag{35}$$

(*c*) $$\beta x = \frac{\pi}{2} \qquad \sin^2 \beta x = 1 \qquad \cot \beta x = 0 \tag{36}$$

$$\cot (\beta w + \Phi'_w) = b_{1s} \pm g_{1s} \sqrt{\frac{1}{g_{1s}} - 1} \tag{37}$$

$$\cot (\beta y + \Phi'_y) = \pm \sqrt{\frac{1}{g_{1s}} - 1} \tag{38}$$

$$g_{1s} < 1 \tag{39}$$

For ideal pistons $\Phi' = 0$. As usual, upper signs go together, and lower signs go together.

Instead of calculating the lengths w and y of the double-stub tuner using the appropriate formulas derived above, a circle diagram may be used. This is especially convenient if the $\lambda/8$ and $3\lambda/8$ matching circles are provided as in Chap. II, Fig. 16.2. The general procedure follows:

1. Enter circle diagram at given values of g_{1s} and b_{1s} of load.
2. Adjust length w of stub in parallel with load so that its susceptance b_{1Cw} makes the combined admittance g_{1s} and $b_{1s} + b_{1Cw} = b_{1x}$ fall on the circle appropriate to the given value of βx, say, at P. This determines w. The point P has coordinates $\rho_x = \rho_s$ and Φ'_x.
3. Add βx to Φ'_x to give $\beta x + \Phi'_x$. Then $\beta x + \Phi'_x$ and $\rho_x = \rho_s$ are the terminal functions looking toward load at junction with second stub. These values of $\beta x + \Phi'_x$ and ρ_x occur at $g_{1Ax} = 1$ and the same value of b_{1Ax}.
4. Adjust length y of second stub so that $b_{1Ay} = -b_{1Ax}$; that is, $b_{1Ay} + b_{1Ax} = 0$. (The second stub is used to tune the input susceptance to zero. The first stub has been adjusted to give an input conductance of unity.) This determines y.

Numerical and graphical solutions are described below for a given problem.

Illustrative Example for Double-stub Matching

Given. A load impedance $Z_s = 1{,}600 + j800$ ohms to be matched to a two-wire line with characteristic resistance $R_c = 400$ ohms.

Problem. With length x fixed but arbitrary, to determine lengths y and z as fractions of the wavelength for stubs with ideal closed ends.

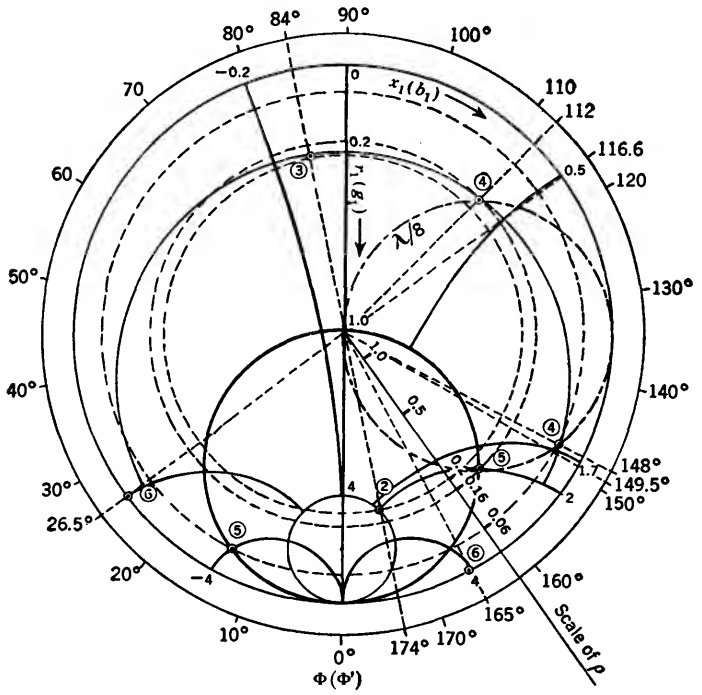


FIG. 10.3. Graphical solution of double-stub matching using Smith chart.

Analytical Solution

1. Determination of normalized impedance and admittance:

$$r_{1s} = \frac{R_s}{R_c} = 4 \qquad x_{1s} = \frac{X_s}{R_c} = 2$$

$$g_{1s} = \frac{r_{1s}}{r_{1s}^2 + x_{1s}^2} = 0.2 \qquad b_{1s} = \frac{-x_{1s}}{r_{1s}^2 + x_{1s}^2} = -0.1$$

2. Determination of the length w using (19) and (20) with x fixed. (For $\lambda/8$ double-stub spacing, $\beta x = \pi/4$.) First condition for match: $g_{1A} = g_{1Ax} = 1$.

$$g_{1x} = g_{1s} = 0.2$$

$$b_{1C_w} = -b_{1s} + \cot \beta x \mp g_{1x}\sqrt{\frac{1}{g_{1x}\sin^2 \beta x} - 1} = \begin{cases} 0.5 \\ 1.7 \end{cases}$$

$$b_{1x} = b_{1s} + b_{1C_w} = -0.1 + \begin{cases} 0.5 \\ 1.7 \end{cases} = \begin{cases} 0.4 \\ 1.6 \end{cases}$$

$$b_{1C_w} = -\cot(\beta w + \Phi'_w) \qquad \Phi'_w = 0$$

$$\beta w = 116.6° \qquad w = 0.324\lambda$$

or

$$\beta w = 149.5° \qquad w = 0.415\lambda$$

3. Determination of the length y using (23) and (26). Second condition for match: $b_{1A} = b_{1Ax} + b_{1Ay} = 0$.

$$b_{1Ax} = -b_{1Ay} = -\cot \beta x \pm \sqrt{\frac{1}{g_{1s} \sin^2 \beta x} - 1} = \begin{cases} 2.00 \\ -4.00 \end{cases}$$

$$-b_{1Ax} = \cot (\beta y + \Phi_y') \qquad \Phi_y' = 0$$

$$\beta y = 26.6° \qquad y = 0.074\lambda$$

or

$$\beta y = 165° \qquad y = 0.458\lambda$$

Graphical Solution on the Circle Diagram (*Figs.* 10.3 *and* 10.4). To change to normalized admittance,

1. Compute $r_{1s} = 4$; $x_{1s} = 2$.
2. Locate $r_{1s} = 4$ and $x_{1s} = 2$ on the chart, and note that this occurs at $\rho_s = 0.2$ and $\Phi_s = 174°$.
3. Move on circle of constant ρ_s through 90° to locate $\Phi_s' = 84°$ for use with $g_{1s} = 0.2$ and $b_{1s} = -0.1$.

To obtain match,

4. First condition for match: $g_{1A} = g_{1Ax} = 1$. Add b_{1Cw} to b_{1s} to make $b_{1Cw} + b_{1s} = b_{1x}$

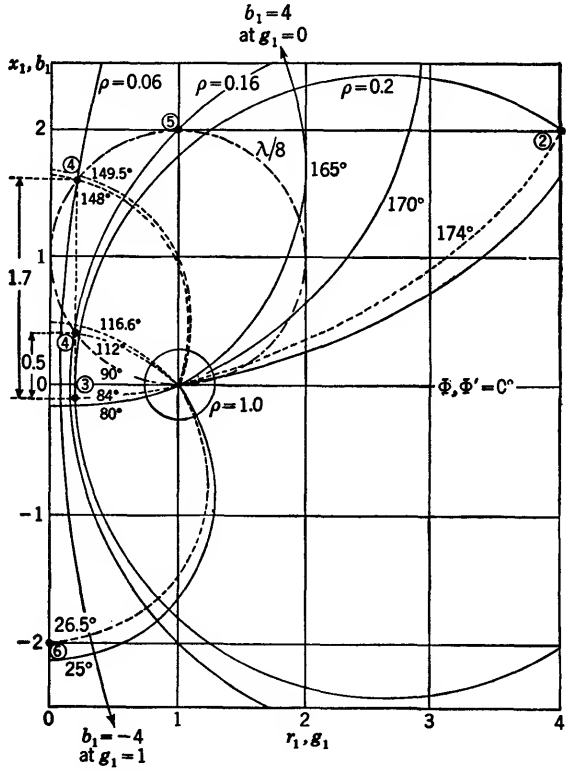


FIG. 10.4. Graphical solution of double-stub matching using circle diagram.

intersect the $\lambda/8$ circle at $\rho = 0.16$ (or 0.06), $\Phi'_{Cw} = 112°$ (or 148°), giving $b_{1Cw} = 0.5$ (or 1.7), corresponding to $\beta w = 116.6°$ (or 149.5°); $w = 0.324\lambda$ (or 0.415λ).

5. Second condition for match: $b_{1A} = b_{1Ax} + b_{1Ay} = 0$. Add 45° to $\Phi'_{Cw} = 112°$ (148°) on circle of constant $\rho = 0.16$ (or $\rho = 0.06$) to reach the $g_{1A} = 1$ line, where $b_{1Ax} = 2.00$ (or -4.00).

6. Locate $b_{1Ay} = -b_{1Ax} = -2.00$ (or 4.00); $g_{1A} = 0$. Read off $\beta y + \Phi'_y = 26.5°$ (or 165°). For the shortest length y choose an ideal short circuit with $\Phi'_y = 0$ so that $\beta y = 26.5°$ for $b_{1Ay} = -2.00$ ($\beta y = 165°$ for $b_{1Ay} = 4.00$); $y = 0.074\lambda$ (or $y = 0.458\lambda$). (If an ideal open circuit with $\Phi' = 90°$ is chosen when $\beta y + \Phi'_y = 165°$, it follows that $\beta y = 75°$ and $y = 0.208\lambda$.)

11. Matching with a Shunt Section.† A less widely used circuit for matching consists of a section of line of length s_2 which is connected in parallel with a length s_1, forming part of a long line that is terminated in an impedance Z_s, as shown in Fig. 11.1. Z_s may be the input impedance of an additional section of line terminated in an arbitrary impedance.

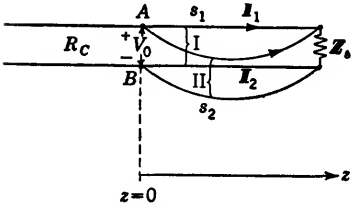


FIG. 11.1. Shunt sections of transmission line for impedance matching.

An exact analysis of the shunt matching network involves the coupling between the two parallel sections in addition to the usual terminal-zone and junction effects. In the present analysis it is assumed that the coupling between the two shunt sections is negligible. For open-wire lines this may be approximated by sufficiently small line spacing compared with the separation of the two sections; for coaxial or shielded-pair lines it is satisfied automatically.

The first step in determining the conditions for match in the circuit of Fig. 11.1 is to derive an expression for the impedance looking to the right at AB. This is accomplished by applying Chap. II, Sec. 8, Eqs. (6) and (7), to each of the shunt sections that are assumed to have the same line constants. Let the voltage and current in the undivided line at AB be V_0 and I_0, and at the load, V_s and I_s. It follows that

$$I_0 = I_{10} + I_{20} \qquad I_s = I_{1s} + I_{2s} \tag{1}$$

Also

$$V_0 = V_s \cosh \gamma s_1 + I_{s1} Z_c \sinh \gamma s_1 = V_s \cosh \gamma s_2 + I_{s2} Z_c \sinh \gamma s_2 \tag{2}$$

$$I_{10} Z_c = V_s \sinh \gamma s_1 + I_{s1} Z_c \cosh \gamma s_1 \tag{3a}$$

$$I_{20} Z_c = V_s \sinh \gamma s_2 + I_{s2} Z_c \cosh \gamma s_2 = V_s \sinh \gamma s_2 + (I_s - I_{s1}) Z_c \cosh \gamma s_2 \tag{3b}$$

The addition of (3a) and (3b) and the elimination of I_{s1} using (1) and

† Parts of this section follow the work of Tai.[101]

(2) give

$$I_0 Z_c = \frac{2V_s[\cosh \gamma(s_1 + s_2) - 1] + I_s Z_c[\sinh \gamma(s_1 + s_2)]}{\sinh \gamma s_1 + \sinh \gamma s_2} \tag{4}$$

The elimination of I_{s1} from the left side of (2) gives

$$V_0 = \frac{V_s \sinh \gamma(s_1 + s_2) + I_s Z_c \sinh \gamma s_1 \sinh \gamma s_2}{\sinh \gamma s_1 + \sinh \gamma s_2} \tag{5}$$

The normalized impedance looking to the right at AB in Fig. 11.1 is

$$z_{10} \equiv \frac{Z_0}{Z_c} = \frac{V_0}{I_0 Z_c} = \frac{z_{1s} \sinh \gamma(s_1 + s_2) + \sinh \gamma s_1 \sinh \gamma s_2}{2z_{1s}[\cosh \gamma(s_1 + s_2) - 1] + \sinh \gamma(s_1 + s_2)} \tag{6}$$

The normalized terminating impedance $z_{1s} \equiv Z_{1s}/Z_c = V_s/I_s Z_c$ may be expressed as

$$z_{1s} = \coth \theta_s \tag{7}$$

where $\theta_s = \rho_s + j\Phi_s$ is the complex terminal function. If (7) is substituted in (6) and this is rearranged, the expression below may be obtained. Since the sections of line are assumed to be highly conducting and quite short, it is satisfactory to neglect $\alpha(s_1 + s_2)$ as compared with ρ_s if Z_s is a dissipative load, as is assumed. It follows that $\gamma = \alpha + j\beta \doteq j\beta$. The desired expression is

$$z_{10} = \frac{\cosh^2 \theta_s \cos \beta s_1 \cos \beta s_2 - \cosh(\theta_s + j\beta s_1) \cosh(\theta_s + j\beta s_2)}{\sinh 2\theta_s - \sinh[2\theta_s + j\beta(s_1 + s_2)] + j \cosh^2 \theta_s \sin \beta(s_1 + s_2)} \tag{8}$$

The condition for match $z_{10} = 1$ may now be imposed, and the following solutions of the resulting pair of equations obtained:

$$\tan \tfrac{1}{2}\beta(s_1 + s_2) = \frac{\cos 2\Phi_s - e^{-2\rho_s}}{2 \sin 2\Phi_s} \tag{9}$$

$$\tan \tfrac{1}{2}\beta(s_1 - s_2) = \left[\frac{(5e^{-2\rho_s} + 3 \cos 2\Phi_s)(e^{-2\rho_s} - \cos 2\Phi_s)}{4(1 - e^{-4\rho_s})}\right]^{\frac{1}{2}} \tag{10}$$

These equations define the lengths s_1 and s_2 of the two shunt sections for different values of the terminal function $\theta_s = \rho_s + j\Phi_s$. Note that a physically meaningful solution requires real and positive values of both s_1 and s_2.

Since the right side of (9) is always real, there is no restriction on $s_1 + s_2$. A positive real value of $s_1 + s_2$ can always be found. On the other hand, $s_1 - s_2$ is real only when ρ_s and Φ_s satisfy the following equation:

$$\frac{(5e^{-2\rho_s} + 3 \cos 2\Phi_s)(e^{-2\rho_s} - \cos 2\Phi_s)}{1 - e^{-4\rho_s}} \geqq 0 \tag{11}$$

It follows that a normalized impedance z_{10} can be matched by a pair of

shunt sections with their junction at the terminal impedance only if ρ_s and Φ_s corresponding to z_{1s} in (7) satisfy (11). The corresponding equations are

$$r_{1s} = 1 \tag{12a}$$

$$4(r_{1s}^2 + x_{1s}^2) - 5r_{1s} + 1 = 0 \tag{12b}$$

Evidently (12a) is the equation of a vertical line in the $r_{1s}x_{1s}$ plane, and (12b) is the equation of a circle of radius $\frac{3}{8}$ with center at $r_{1s} = \frac{5}{8}$, $x_{1s} = 0$. These curves (Fig. 11.2) define two regions. A match is possible only for values of r_{1s} and x_{1s} to the left of the line $r_{1s} = 1$, but *not* including the circle of radius $\frac{3}{8}$. A match is not possible if r_{1s} and x_{1s} are to the right of the line $r_{1s} = 1$ or in the circle to the left of this line.

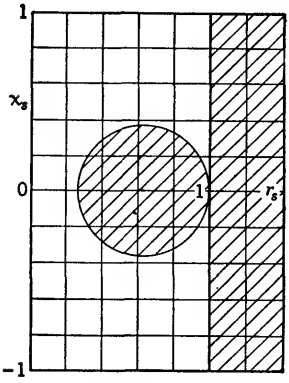


FIG. 11.2. Loci of match for shunt sections; match possible only outside cross-hatched area.

Explicit expressions for βs_1 and βs_2 may be obtained by solving (9) and (10). They are

$$\frac{2\pi s_1}{\lambda} = \beta s_1 = \tan^{-1} A + \tan^{-1} B \tag{13a}$$

$$\frac{2\pi s_2}{\lambda} = \beta s_2 = \tan^{-1} A - \tan^{-1} B \tag{13b}$$

where A is the quantity on the right in (9) and B is the quantity on the right in (10). A plot of s_1/λ and s_2/λ is given in Fig. 11.3, with Φ_s as variable and ρ_s as parameter. The range of Φ_s is limited to $0 \leqq \Phi_s \leqq 90°$, since it is clear from (9) and (10) that $180° - \Phi_s$ for $180° \geqq \Phi_s \geqq 90°$ gives exactly the same values of A and B for use in (13a,b).

Illustrative Example 1 for Matching with Shunt Sections

Given. A load impedance $\boldsymbol{Z}_s = 200 - j400$ ohms to be matched to a two-wire line with characteristic resistance $R_c = 400$ ohms.

Problem. To determine the lengths s_1 and s_2 as fractions of a wavelength using the same type of line throughout.

Solution

1. Determination of normalized resistance and reactance:

$$r_{1s} = \frac{R_s}{R_c} = 0.5 \qquad x_{1s} = \frac{X_s}{R_c} = -1$$

2. Referring to Fig. 11.2, it is seen that this point lies within the region of possible match. From the circle diagram or by computation, the values of ρ_s and Φ_s corresponding to the given values of r_{1s} and x_{1s} are found to be 0.24 neper and 41.5°, respectively.

3. From Fig. 11.3 the required values of s_1/λ and s_2/λ are 0.572 and 0.350.

Illustrative Example 2 for Matching with Shunt Sections

If a match is not possible with shunt sections terminated directly in the load, an additional section of line of appropriate length s_3 may be inserted between the junction of the shunt sections and the load Z_s.

Given. $Z_s = 800 + j0$ ohms to be matched to a two-wire line with $R_c = 400$.

Problem. To determine the lengths s_1/λ and s_2/λ as fractions of a wavelength and s_3/λ if the additional section is required.

Solution

1. The normalized impedances are $r_{1s} = 2$ and $x_{1s} = 0$. The corresponding terminal functions are $\rho_s = 0.55$ and $\Phi_s = 0$.

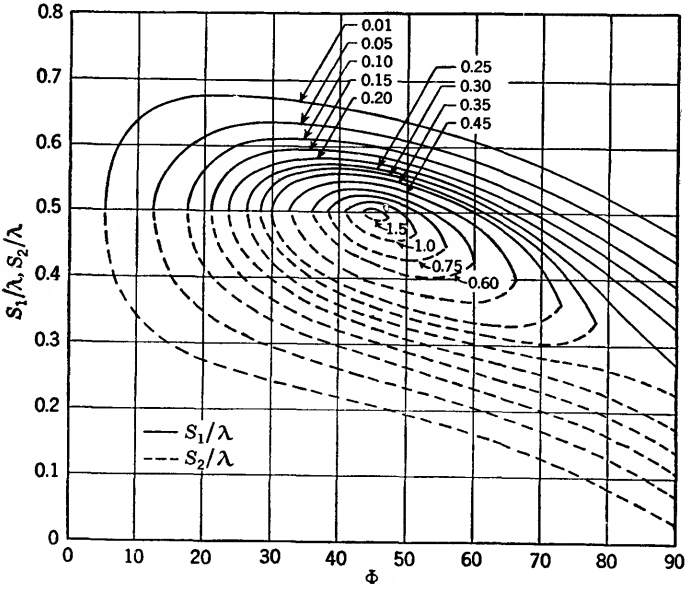


FIG. 11.3. Contours of constant s_1/λ and s_2/λ as functions of ρ and Φ for use in impedance matching with shunt sections.

2. Referring to Fig. 11.2, it is seen that the point in question lies outside the range of possible match. Let an additional section of length $s_3 = \lambda/8$ or $\beta s_3 = 45°$ be inserted.

3. The values of ρ and Φ terminating the shunt sections at their junction at a distance $\lambda/8$ from the load are $\rho = \rho_s + \alpha s_3 = 0.55$ and $\Phi = \Phi_s + \beta s_3 = 45°$. (Line losses are neglected.)

4. The new values of ρ and Φ are within the range of match. From Fig. 11.3, $s_1/\lambda = 0.535$ and $s_2/\lambda = 0.414$.

It is to be noted that junction, coupling, and terminal-zone effects have been neglected in this section, so that the quantitative accuracy of the formulas in any particular application depends on the degree to which these effects are significant. Corrections for them when they are not negligible are considered in Chap. V.

12. Representation of a Section of Transmission Line by Lumped Equivalents; Impedance, Admittance, and Scattering Matrices.[15] The "lumped equivalent" of the section of transmission line to the right of the points 11′ in Fig. 12.1*a* is any combination of lumped elements which, when connected across 11′ in place of the section of line as in Fig. 12.1*b*, leaves all distributions of current and voltage at all points along the line to the left of 11′ unaltered. Actually no such network can be provided in practice in any general sense, since even approximately lumped elements do not exist independent of frequency. Even in the restricted sense of the response to a *single frequency*, which is usually implied when an "equivalent lumped" network is to be substituted for a section of line, it is not possible to provide such a network owing to the change in the coupling between the line and the network—distributed or lumped—to the right of 11′. End effects and coupling effects in the vicinity of 11′ in the circuit of Fig. 12.1*a* differ from those in the circuit of Fig. 12.1*b*. It follows that it is not actually possible to maintain the same distribution of current and charge along the *entire* line to the left of 11′ in the change from Fig. 12.1*a* to Fig. 12.1*b*. The best that can be achieved is to keep the distribution to the left of a junction zone of length near 10 times the line spacing from 11′ unchanged, whereas the distribution in the junction zone may be quite different. This means that the *apparent* impedance terminating the line at 11′ *as seen from a sufficient distance* to the left of 11′ is the same in the two cases.

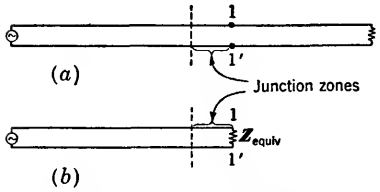


FIG. 12.1. Lumped equivalent of two-terminal section of transmission line.

A more general problem is the substitution of a lumped equivalent for a piece of line *between two* sets of points, 11′ and 22′ in Fig. 12.2*a*, so that excluding short junction regions all currents and voltages to the left of 11′ and to the right of 22′ are unchanged. It is assumed that the equivalence is to apply only at a single frequency.

The voltage and current in any cross-sectional plane $w = s - z$ along a transmission line may be expressed in terms of the voltage and current at another plane s (where $s \geqq z$) in the following form, as obtained from Chap. II, Sec. 8, Eqs. (6) and (7):

$$V(w) = V(0) \cosh \gamma w + I(0) Z_c \sinh \gamma w \tag{1a}$$

$$I(w) = V(0) Y_c \sinh \gamma w + I(0) \cosh \gamma w \tag{1b}$$

Alternatively

$$V(w) = V(0)\boldsymbol{A} + I(0)\boldsymbol{B} \tag{1c}$$

$$I(w) = V(0)\boldsymbol{C} + I(0)\boldsymbol{D} \tag{1d}$$

where $$\boldsymbol{A} = \boldsymbol{D} = \cosh \gamma w \qquad \boldsymbol{B} = Z_c^2 \boldsymbol{C} = Z_c \sinh \gamma w \tag{1e}$$

Z_c is the characteristic impedance, and $Y_c = 1/Z_c$ is the characteristic admittance of the line; $w = s - z$ is the distance measured from the point s toward z, as shown in Fig. 12.2.

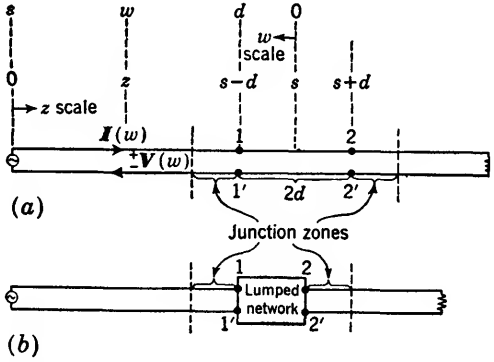


FIG. 12.2. Lumped equivalent of four-terminal section of transmission line.

Consider the problem of representing the length of line $2d$ between the terminal pairs $11'$ and $22'$ by an electrically equivalent four-terminal network of lumped elements, as in Fig. 12.3. The problem is readily analyzed using symmetry and the odd and even components of current and voltage referred to the cross-sectional plane $z = s$ or $w = 0$ at the center of the length $2d$. Thus let the actual currents and voltages along the line be separated into symmetrical and antisymmetrical combinations such that

$$V(w) = V^{(s)}(w) + V^{(a)}(w) \quad (2a)$$
$$I(w) = I^{(s)}(w) + I^{(a)}(w) \quad (2b)$$

where the symmetrical combination consists of that part of the voltage which is *odd* and that part of the current which is *even* with respect to the plane $w = 0$, and the antisymmetrical combination consists of the corresponding even part of the voltage and the odd part of the current. This pairing of the components is necessary, since $I(w) \sim \partial V(w)/\partial(w)$. The following explicit formulas are derived from (1a,b):

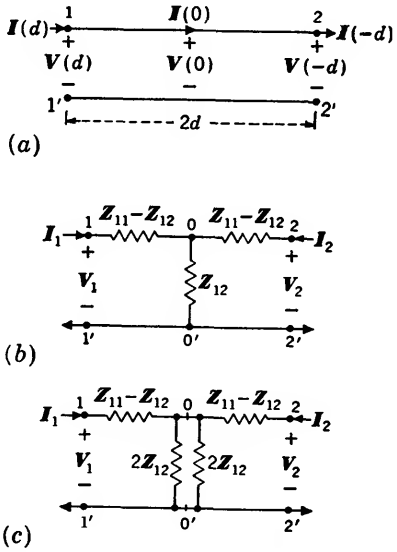


FIG. 12.3. Equivalent T network of section of transmission line.

Symmetrical Combination

For even current:

$$I^{(s)}(w) = \tfrac{1}{2}[I(w) + I(-w)] = I(0) \cosh \gamma w \tag{3a}$$

For odd voltage:

$$V^{(s)}(w) = \tfrac{1}{2}[V(w) - V(-w)] = I(0) Z_c \sinh \gamma w \tag{3b}$$

For symmetrical admittance:

$$Y_{in}^{(s)}(w) \equiv \frac{I^{(s)}(w)}{V^{(s)}(w)} = Y_c \coth \gamma w \tag{3c}$$

Antisymmetrical Combination

For odd current:

$$I^{(a)}(w) = \tfrac{1}{2}[I(w) - I(-w)] = V(0) Y_c \sinh \gamma w \tag{4a}$$

For even voltage:

$$V^{(a)}(w) = \tfrac{1}{2}[V(w) + V(-w)] = V(0) \cosh \gamma w \tag{4b}$$

For antisymmetrical impedance:

$$Z_{in}^{(a)}(w) = \frac{V^{(a)}(w)}{I^{(a)}(w)} = Z_c \coth \gamma w \tag{4c}$$

Note that

$$V(-w) = V^{(a)}(w) - V^{(s)}(w) \tag{5a}$$

$$I(-w) = -I^{(a)}(w) + I^{(s)}(w) \tag{5b}$$

It is now interesting to note that the normalized symmetrical admittance looking to the right at the terminals $11'$ at $w = d$ in Fig. 12.3*a*, viz.,

$$y_{1in}^{(s)}(d) = \coth \gamma d \tag{6a}$$

is precisely the normalized input admittance of a section of line of length d when its end is an *ideal short circuit*. This follows from Sec. 1, Eq. (10*b*), with $w = d$ and $\theta_s' = 0$. Similarly the normalized antisymmetrical impedance, viz.,

$$z_{1in}^{(a)}(d) = \coth \gamma d \tag{6b}$$

is the normalized input impedance of a section of line of length d when its end is an *ideal open circuit*. This follows from Sec. 1, Eq. (10*a*), with $w = d$ and $\theta_s = 0$. Accordingly the current $I(d) = I^{(s)}(d) + I^{(a)}(d)$ and the voltage $V(d) = V^{(s)}(d) + V^{(a)}(d)$ at the terminals $11'$ of the line section are the sums of the currents and voltages that would be obtained if the line section were provided *successively* with perfect short circuits and perfect open circuits at $w = 0$ in Fig. 12.3*a*. The symmetrical combination is the solution of the short-circuited line of length d; the antisymmetrical combination is the solution of the open-circuited line of length d. In each case the section of line is equivalent to a single lumped admittance or impedance, given by (3*c*) or (4*c*).

In order to obtain the equivalent circuit of the original section of line, let the symmetrical (short-circuit) impedance and the antisymmetrical (open-circuit) impedance be represented as follows:

$$Z_{in}^{(s)}(d) \equiv Z_{11} - Z_{12} = Z_c \tanh \gamma d \tag{7a}$$
$$Z_{in}^{(a)}(d) \equiv Z_{11} + Z_{12} = Z_c \coth \gamma d \tag{7b}$$

where the newly introduced impedances Z_{11} and Z_{12} are *defined* by (7*a*) and (7*b*). Thus

$$Z_{11} \equiv \tfrac{1}{2}[Z_{in}^{(s)}(d) + Z_{in}^{(a)}(d)] = \frac{Z_c}{2}(\tanh \gamma d + \coth \gamma d) \tag{7c}$$

$$Z_{12} \equiv \tfrac{1}{2}[Z_{in}^{(a)}(d) - Z_{in}^{(s)}(d)] = \frac{Z_c}{2}(\coth \gamma d - \tanh \gamma d) = Z_c \operatorname{csch} 2\gamma d \tag{7d}$$

It is now readily verified that the equivalent circuit of the transmission-line section of length $2d$ in Fig. 12.3*a* is the T network in Fig. 12.3*b* or its more symmetrical equivalent in Fig. 12.3*c*. Since the general case is the superposition of the symmetrical and antisymmetrical cases when the network is short-circuited and open-circuited at its center, it is necessary merely to demonstrate that Fig. 12.3*c* yields the correct short-circuit and open-circuit impedances. That this is true is seen by inspection. It follows that the four-terminal network in Fig. 12.3*b* or in Fig. 12.3*c* is the equivalent of a section of transmission line of length d if the impedances are assigned the values specified in (7*c*,*d*).

The Impedance Matrix. If conventions regarding the signs of the voltages and the directions of the currents are adopted to conform with Fig. 12.3*c*, it follows that, with (2*a*,*b*) and (5*a*,*b*),

$$V_1 = V(d) = V(0) \cosh \gamma d + I(0) Z_c \sinh \gamma d \tag{8a}$$
$$V_2 = V(-d) = V(0) \cosh \gamma d - I(0) Z_c \sinh \gamma d \tag{8b}$$
$$I_1 = I(d) = V(0) Y_c \sinh \gamma d + I(0) \cosh \gamma d \tag{9a}$$
$$I_2 = -I(-d) = V(0) Y_c \sinh \gamma d - I(0) \cosh \gamma d \tag{9b}$$

Note that the positive direction of the current at terminals 22′ is chosen opposite in the lumped network to conform with convention. By solving (9*a*) and (9*b*) for $I(0)$ and $V(0)$ and substituting these values in (8*a*,*b*), the following well-known equations are obtained for the T network:

$$V_1 = I_1 Z_{11} + I_2 Z_{12} \tag{10a}$$
$$V_2 = I_1 Z_{21} + I_2 Z_{22} \tag{10b}$$

where $Z_{21} = Z_{12}$ for all reciprocal elements and $Z_{22} = Z_{11}$ in this particular case, since the network is symmetrical with identical sides.

The two Eqs. (10*a*,*b*) may be expressed in the following matrix† form:

$$\mathbf{V} = \mathbf{ZI} \tag{11a}$$

† See Ref. 6 for a brief discussion of matrices.

where **V** and **I** are the column matrices given by

$$\mathbf{V} \equiv \begin{bmatrix} V_1 \\ V_2 \end{bmatrix} \qquad \mathbf{I} \equiv \begin{bmatrix} I_1 \\ I_2 \end{bmatrix} \tag{11b}$$

and **Z** is the square impedance matrix

$$\mathbf{Z} \equiv \begin{bmatrix} Z_{11} & Z_{12} \\ Z_{21} & Z_{22} \end{bmatrix} \tag{11c}$$

In this representation, using an impedance matrix, a point of view is implied in which currents are treated as fundamental or given quantities and the voltages are calculated from them using the matrix.

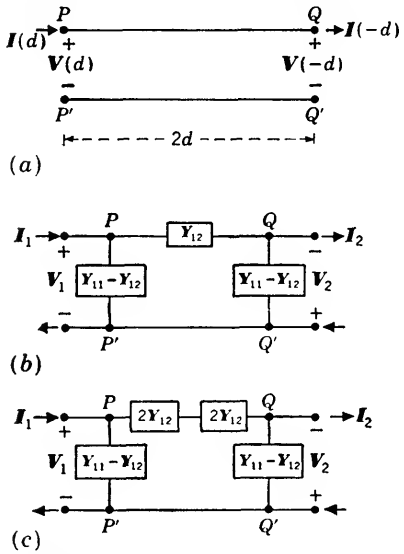


FIG. 12.4. Equivalent Π network of section of transmission line.

The Admittance Matrix. If desired, the point of view may be changed, the voltages may be treated as fundamental or given, and the currents may be calculated from them using an *admittance matrix*. For this purpose the Π network in Fig. 12.4*b* or its symmetrically drawn equivalent in Fig. 12.4*c* is convenient. It is evident that (8*a*,*b*) and (9*a*,*b*) apply directly if the sign of V_2 in (8*b*) and of I_2 in (9*b*) are reversed to conform with the conventions of Fig. 12.4. It is readily verified with (6*a*,*b*) that the symmetrical or short-circuit admittance $Y_{in}^{(s)}(d) = 1/Z_{in}^{(s)}(d)$ and the antisymmetrical or open-circuit admittance $Y_{in}^{(a)}(d) = 1/Z_{in}^{(a)}(d)$ are given by

$$Y_{in}^{(s)}(d) = Y_c \coth \gamma d \equiv Y_{11} + Y_{12} \tag{12a}$$

$$Y_{in}^{(a)}(d) = Y_c \tanh \gamma d \equiv Y_{11} - Y_{12} \tag{12b}$$

where Y_{11} and Y_{12} are defined in (12*a*,*b*). They are

$$Y_{11} = \frac{Y_c}{2} (\tanh \gamma d + \coth \gamma d) \tag{13a}$$

$$Y_{12} = \frac{Y_c}{2} (\coth \gamma d - \tanh \gamma d) \tag{13b}$$

The corresponding equations are obtained from Fig. 12.4 or from (9*a*,*b*), with $I(0)$ and $V(0)$ eliminated using (8*a*,*b*) (with signs of V_2 and I_2 reversed). They are

$$I_1 = V_1 Y_{11} + V_2 Y_{12} \tag{14a}$$

$$I_2 = V_1 Y_{21} + V_2 Y_{22} \tag{14b}$$

where $Y_{21} = Y_{12}$ from reciprocity and $Y_{22} = Y_{11}$ from symmetry. The direction of the current and the sign of the voltage at terminals 2 have been reversed in Figs. 12.4*b* and 12.4*c* as compared with those in Figs. 12.3*b* and 12.3*c* (the current is now in the same direction as in the transmission-line section in Fig. 12.4*a*, but the voltage is reversed) in order that the final equations may be in the form (14*a*,*b*), and Y_{12} (rather than $-Y_{12}$) is the series element in the circuits of Figs. 12.4*b* and 12.4*c*.

The current equations in matrix form are

$$\mathbf{I} = \mathbf{YV} \tag{15}$$

where $$\mathbf{I} \equiv \begin{bmatrix} I_1 \\ I_2 \end{bmatrix} \qquad \mathbf{V} \equiv \begin{bmatrix} V_1 \\ V_2 \end{bmatrix}$$

and where the admittance matrix is

$$\mathbf{Y} = \begin{bmatrix} Y_{11} & Y_{12} \\ Y_{21} & Y_{22} \end{bmatrix} \tag{16}$$

If the sign conventions used for the impedance matrix are adopted,

$$\mathbf{Y} = \begin{bmatrix} Y_{11} & -Y_{12} \\ -Y_{21} & Y_{22} \end{bmatrix} \tag{17}$$

The Scattering Matrix. Instead of representing a section of line by equivalent lumped impedances or admittances, it is advantageous for some applications to introduce its reflecting and transmitting properties. This is accomplished by expressing current and voltage in the exponential form given in Chap. I, Sec. 13. With slight changes in the notation to suit present requirements, the solution is as given in Chap. I, Sec. 13, Eqs. (13) and (14), namely:

$$V(z) = \sqrt{Z_c}\,(Ae^{-\gamma z} + Be^{\gamma z}) \tag{18a}$$

$$I(z) = \sqrt{Y_c}\,(Ae^{-\gamma z} - Be^{\gamma z}) \tag{18b}$$

where A and B are arbitrary constants to be evaluated from the boundary conditions, γ is the complex propagation constant, Z_c is the characteristic impedance, and Y_c is the characteristic admittance. As discussed in Chap. I, the first term in (18*a*) and (18*b*) represents a wave traveling in the positive z direction, and the second term represents a wave traveling in the negative z direction.

From the point of view of the traveling-wave description given in Chap. II, Secs. 6 and 7, the section of line between terminals 11′ and 22′ in Fig. 12.2 may be regarded as receiving a traveling wave of different amplitude and phase approaching from each side. A part of each incident wave may be reflected and a part transmitted into the section.

Let the complex amplitudes of the incident wave reaching terminals 11′ from the left be A_1, and let those of the wave reaching terminals 22′

from the right be A_2. Let the wave leaving 11′ and moving toward the left have an amplitude B_1, and let that leaving 22′ and moving toward the right have an amplitude B_2. A portion of the wave leaving 11′, namely, $S_{11}A_1$, is the reflected part of the incident wave A_1; the rest is the wave that has traveled from 22′ to 11′, where it emerges with amplitude $S_{12}A_2$. Owing to the linearity of the equations these two parts combine linearly. Thus

$$B_1 = S_{11}A_1 + S_{12}A_2 \tag{19a}$$

Similarly, on the other side,

$$B_2 = S_{21}A_1 + S_{22}A_2 \tag{19b}$$

In these two equations the S's are complex coefficients that characterize the network between terminals 11′ and 22′.

In the simple case under discussion the section between 11′ and 22′ is like the rest of the line. Therefore it is possible to write down formulas for the S's directly. Owing to the fact that at 11′ the line continues smoothly, there is no reflection of the incident A_1, so that the entire outgoing wave is the emerging wave that had the amplitude A_2 at 22′ and must be equal to

$$B_1 = e^{-2\gamma d}A_2 \tag{20a}$$

at 11′. Similarly

$$B_2 = e^{-2\gamma d}A_1 \tag{20b}$$

It follows that, for the smooth line between 11′ and 22′,

$$S_{11} = 0 \qquad S_{12} = S_{21} = e^{-2\gamma d} \qquad S_{22} = 0 \tag{21}$$

The general case of (19a,b) may be expressed in matrix form. Thus the scattering relation is

$$\mathbf{B} = \mathbf{SA} \tag{22}$$

where

$$\mathbf{B} \equiv \begin{bmatrix} B_1 \\ B_2 \end{bmatrix} \qquad \mathbf{A} \equiv \begin{bmatrix} A_1 \\ A_2 \end{bmatrix} \tag{23}$$

and where the scattering matrix is defined by

$$\mathbf{S} \equiv \begin{bmatrix} S_{11} & S_{12} \\ S_{21} & S_{22} \end{bmatrix} \tag{24}$$

(Note that this matrix has been defined in terms of the sign and direction convention for voltage and current which agrees with that used in defining the impedance matrix.) In the simple case at hand

$$\mathbf{S} = \begin{bmatrix} 0 & e^{-2\gamma d} \\ e^{-2\gamma d} & 0 \end{bmatrix} \tag{25}$$

The matrix elements in the general matrix (24) may be interpreted as foliows:

S_{11} is the complex amplitude of the wave that is reflected (or scattered) at the terminals 11′ when a wave of unit amplitude is incident on these terminals.

S_{12} is the complex amplitude of the wave emerging at 11′ when a wave of unit amplitude is incident on the terminals 22′.

S_{22} is the complex amplitude of the wave that is reflected (or scattered) at the terminals 22′ when a wave of unit amplitude is incident on these same terminals.

S_{21} is the complex amplitude of the wave emerging at 22′ when a wave of unit amplitude is incident on the terminals 11′.

For reciprocal elements $S_{21} = S_{12}$. For nonreciprocal elements such as gyrators, $S_{21} \neq S_{12}$. The ideal gyrator is characterized by $S_{21} = -S_{12}$, $S_{11} = S_{22} = 0$. The notation $\mathbf{T} \equiv S_{12}$ is common, and this quantity is called the *transmission coefficient.* Evidently S_{11} and S_{22} are *reflection coefficients.* Note that in the simple special case described by (25) the reflection coefficients are zero.

Although in the simple case at hand the characteristic impedances of the lines to the right and left of the junction are the same, the definition of the scattering matrix (24) is valid when they are different. This more general case is considered in Chap. V, Sec. 4.

Relations between Impedance, Admittance, and Scattering Matrices. The terminals 11′ are located at $z = s - d$, and the terminals 22′ at $z = s + d$. It follows from (18a,b) that

$$V_1 = V(s-d) = \sqrt{Z_c}\,[Ae^{-\gamma(s-d)} + Be^{\gamma(s-d)}] = \sqrt{Z_c}\,(A_1 + B_1) \tag{26a}$$

$$V_2 = V(s+d) = \sqrt{Z_c}\,[Ae^{-\gamma(s+d)} + Be^{\gamma(s+d)}] = \sqrt{Z_c}\,(A_2 + B_2) \tag{26b}$$

$$I_1 = I(s-d) = \sqrt{Y_c}\,[Ae^{-\gamma(s-d)} - Be^{\gamma(s-d)}] = \sqrt{Y_c}\,(A_1 - B_1) \tag{27a}$$

$$I_2 = -I(s+d) = -\sqrt{Y_c}\,[Ae^{-\gamma(s+d)} - Be^{\gamma(s+d)}] = \sqrt{Y_c}\,(A_2 - B_2) \tag{27b}$$

where $A_1 = Ae^{-\gamma(s-d)}$, $B_1 = Be^{\gamma(s-d)}$, $A_2 = Be^{\gamma(s+d)}$, $B_2 = Ae^{-\gamma(s+d)}$.

With (19a,b) the B's may be eliminated, and the following equations obtained:

$$V_1 = \sqrt{Z_c}\,[(1 + S_{11})A_1 + S_{12}A_2] \tag{28a}$$

$$V_2 = \sqrt{Z_c}\,[S_{21}A_1 + (1 + S_{22})A_2] \tag{28b}$$

$$I_1 = \sqrt{Y_c}\,[(1 - S_{11})A_1 - S_{12}A_2] \tag{29a}$$

$$I_2 = \sqrt{Y_c}\,[-S_{21}A_1 + (1 - S_{22})A_2] \tag{29b}$$

By solving (29a,b) for A_1 and A_2 and substituting these values in (28a,b), the following equations are obtained:

$$V_1 = I_1Z_{11} + I_2Z_{12} \tag{30a}$$

$$V_2 = I_1Z_{21} + I_2Z_{22} \tag{30b}$$

where $Z_{11} = \frac{Z_c}{D}[(1 + S_{11})(1 - S_{22}) + S_{12}S_{21}]$ $Z_{12} = \frac{2Z_cS_{12}}{D}$ (31*a*)

$Z_{22} = \frac{Z_c}{D}[(1 - S_{11})(1 + S_{22}) + S_{12}S_{21}]$ $Z_{21} = \frac{2Z_cS_{21}}{D}$ (31*b*)

where $D = (1 - S_{11})(1 - S_{22}) - S_{12}S_{21}$ (31*c*)

If the section is symmetrical, $S_{22} = S_{11}$ and $S_{21} = S_{12}$, so that

$$Z_{22} = Z_{11} = Z_c \frac{1 - S_{11}^2 + S_{12}^2}{(1 - S_{11})^2 - S_{12}^2} \tag{32a}$$

$$Z_{21} = Z_{12} = Z_c \frac{2S_{12}}{(1 - S_{11})^2 - S_{12}^2} \tag{32b}$$

The series elements of the equivalent symmetrical T section are

$$Z_{11} - Z_{12} = Z_c \frac{1 + S_{11} - S_{12}}{1 - (S_{11} - S_{12})} \tag{33}$$

The shunt element is Z_{12} in (32*b*).

By solving (28*a*,*b*) for A_1 and A_2 and substituting these values in (29*a*,*b*), the currents are expressed as functions of the voltages and admittances, with the latter expressed in terms of the elements of the scattering matrix.

The impedance and admittance matrices may be formulated directly in terms of the scattering matrix. As a first step, the matrix equivalents of (28*a*,*b*) and (29*a*,*b*) are

$$\mathbf{V} = \sqrt{Z_c}\,(\mathbf{U} + \mathbf{S})\mathbf{A} \tag{34a}$$

$$\mathbf{I} = \sqrt{Y_c}\,(\mathbf{U} - \mathbf{S})\mathbf{A} \tag{34b}$$

where the unit matrix is

$$\mathbf{U} \equiv \begin{bmatrix} 1 & 0 \\ 0 & 1 \end{bmatrix} \tag{35}$$

and where **V**, **I**, and **A** are column matrices:

$$\mathbf{V} = \begin{bmatrix} V_1 \\ V_2 \end{bmatrix} \qquad \mathbf{I} = \begin{bmatrix} I_1 \\ I_2 \end{bmatrix} \qquad \mathbf{A} = \begin{bmatrix} A_1 \\ A_2 \end{bmatrix} \tag{36}$$

By premultiplying both sides of (34*b*) by $\sqrt{Z_c}\,(\mathbf{U} - \mathbf{S})^{-1}$ and substituting the expression so obtained for **A** in (34*a*), it follows from the defining equation $\mathbf{V} = \mathbf{ZI}$ for the impedance matrix **Z** that

$$\mathbf{Z} = Z_c(\mathbf{U} + \mathbf{S})(\mathbf{U} - \mathbf{S})^{-1} \tag{37a}$$

Similarly

$$\mathbf{Y} = Y_c(\mathbf{U} - \mathbf{S})(\mathbf{U} + \mathbf{S})^{-1} \tag{37b}$$

The relations between the impedance, admittance, and scattering matrices have thus been established. Evidently a knowledge of **S** permits the direct evaluation of **Z** or **Y**. Conversely a knowledge of **Z** or **Y** permits

the evaluation of S using the following easily verified relations:

$$\mathbf{S} = (\mathbf{z}_1 - \mathbf{U})(\mathbf{z}_1 + \mathbf{U})^{-1} \tag{38a}$$
$$\mathbf{S} = (\mathbf{U} - \mathbf{y}_1)(\mathbf{U} + \mathbf{y}_1)^{-1} \tag{38b}$$

where $\mathbf{z}_1 = \mathbf{Z}/Z_c$ and $\mathbf{y}_1 = \mathbf{Y}/Y_c$.

13. Unbalanced Load Terminating a Symmetrically Driven Shielded-pair Line.[72,105] The load terminating a shielded-pair line of length s (Fig. 13.1) consists of two impedances, Z_{s1} and Z_{s2}, in series. Their junction is connected to the shield through an impedance Z_p. If Z_{s1} and Z_{s2} are unequal, the load $Z_s = Z_{s1} + Z_{s2}$ is unbalanced. In this case it

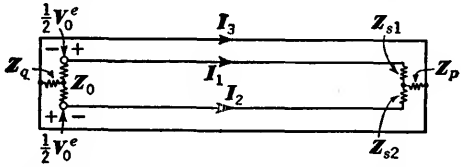


FIG. 13.1. Shielded-pair line with unbalanced load when $Z_{s1} \neq Z_{s2}$.

is convenient to introduce the difference impedance Z_d, defined by

$$Z_d = Z_{s1} - \tfrac{1}{2}Z_s = \tfrac{1}{2}Z_s - Z_{s2} = \tfrac{1}{2}(Z_{s1} - Z_{s2}) \tag{1a}$$

so that

$$Z_{s1} = \tfrac{1}{2}Z_s + Z_d \qquad Z_{s2} = \tfrac{1}{2}Z_s - Z_d \tag{1b}$$

Let the currents in the two inner conductors 1 and 2 of the line be separated into symmetrical (codirectional) and antisymmetrical (equal and opposite) parts as follows:†

$$I_1^s = I_2^s = \tfrac{1}{2}(I_1 + I_2) = \tfrac{1}{2}I^s \tag{2a}$$
$$I_1^a = -I_2^a = \tfrac{1}{2}(I_1 - I_2) = I^a \tag{2b}$$

Note that each of the inner conductors carries only one-half of the total symmetrical current I^s, which is equal and opposite to the current $-I^s$ in the shield (conductor 3). The factor $\frac{1}{2}$ on the right in (2a) is introduced for this reason. The total currents in each conductor are

$$I_1 = I^a + \tfrac{1}{2}I^s \qquad I_2 = -I^a + \tfrac{1}{2}I^s \qquad I_3 = -(I_1^s + I_2^s) = -I^s \tag{3}$$

The voltage drops across the two parts, Z_{s1} and Z_{s2}, of the load are

$$V_1(s) = I_1(s)Z_{s1} \qquad V_2(s) = -I_2(s)Z_{s2} \tag{4}$$

where the sign conventions of Fig. 13.2 are assumed.

If use is made of (1) and (3), the voltage drops may be expressed as follows:

$$V_1(s) = \tfrac{1}{2}I^a(s)Z_s + \tfrac{1}{4}I^s(s)Z_s + I^a(s)Z_d + \tfrac{1}{2}I^s(s)Z_d \tag{5a}$$
$$V_2(s) = \tfrac{1}{2}I^a(s)Z_s - \tfrac{1}{4}I^s(s)Z_s - I^a(s)Z_d + \tfrac{1}{2}I^s(s)Z_d \tag{5b}$$

† Note that the symmetrical and antisymmetrical currents in this section are not the same as those in Sec. 12.

Now let the voltage drops across Z_d be represented by equivalent generators with appropriately defined emfs. Specifically let

$$V_s^e \equiv -I^a(s)Z_d \qquad V_s^a \equiv -I^s(s)Z_d \tag{6}$$

so that

$$V_1(s) = \tfrac{1}{2}I^a(s)Z_s + \tfrac{1}{4}I^s(s)Z_s - V_s^s - \tfrac{1}{2}V_s^a \tag{7a}$$

$$V_2(s) = \tfrac{1}{2}I^a(s)Z_s - \tfrac{1}{4}I^s(s)Z_s + V_s^s - \tfrac{1}{2}V_s^a \tag{7b}$$

The equivalent generators with emfs V_s^s and $\frac{1}{2}V_s^a$ are shown in Fig. 13.2.

The currents I_1, I_2, and I_3 at any point along the shielded-pair line may be formulated in terms of the circuit of Fig. 13.2 if use is made of the principle of superposition to determine separately the currents maintained by each of the three pairs of emfs $\frac{1}{2}V_0^e$, $\frac{1}{2}V_s^a$, and V_s^s. Since the impedances of the network are balanced, the two pairs of emfs $\frac{1}{2}V_0^e$ and $\frac{1}{2}V_s^a$ when operating alone can maintain only antisymmetrical (equal and opposite) currents; the two emfs V_s^s when operating alone maintain only symmetrical (codirectional) currents in the inner conductors of the line.

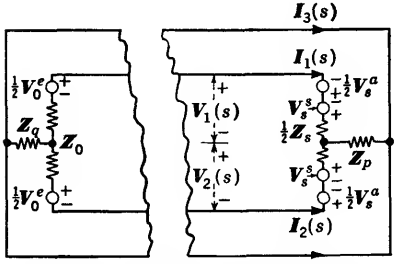


FIG. 13.2. Equivalent circuit for Fig. 13.1.

The antisymmetrical (equal and opposite) currents maintained at any point at a distance z from Z_0 (or $w = s - z$ from Z_s) in the inner conductors by the emfs V_0^e and V_s^a are given by

$$I_1^a(z) = -I_2^a(z) = I^a(z) = V_0^e F(w,s) + V_s^a G(z,s) \tag{8}$$

where

$$F(w,s) \equiv Y_{ca} \frac{\sinh \theta_0 \sinh (\gamma_a w + \theta_s)}{\sinh (\gamma_a s + \theta_0 + \theta_s)} \tag{9a}$$

$$G(z,s) \equiv Y_{ca} \frac{\sinh \theta_s \sinh (\gamma_a z + \theta_0)}{\sinh (\gamma_a s + \theta_0 + \theta_s)} \tag{9b}$$

As usual, $\theta_0 = \coth^{-1}(Z_0/Z_{ca})$ and $\theta_s = \coth^{-1}(Z_s/Z_{ca})$; $Z_{ca} = 1/Y_{ca}$ is the characteristic impedance, and γ_a is the propagation constant† of the shielded-pair line when driven antisymmetrically with equal and opposite currents in its inner conductors and no current in the shield.

The symmetrical (codirectional) currents maintained by the generators V_s^s are divided equally between conductors 1 and 2, which are in parallel. The entire equal and opposite current is in the shield. The sum of the codirectional currents in the inner conductors is given by

$$I_1^s(z) + I_2^s(z) = -I_3(z) = I^s(z) = V_s^s H(z,s) \tag{10}$$

† Note that except for the small effect of l^i the phase constants β_a and β_s are equal if the line is filled with a homogeneous dielectric. On the other hand, β_s and β_a may differ greatly if the dielectric between the two inner conductors differs from that between them and the shield.

where
$$H(z,s) \equiv Y_{cs} \frac{\sinh \theta_p \sinh (\gamma_s z + \theta_q)}{\sinh (\gamma_s s + \theta_p + \theta_q)} \tag{11}$$

where
$$\theta_p = \coth^{-1} \frac{Z_p + Z_s/4}{Z_{cs}} \qquad \theta_q = \coth^{-1} \frac{Z_q + Z_0/4}{Z_{cs}}$$

Z_0 is the impedance in series with the generators. It is center-tapped to the shield through an impedance Z_q. $Z_{cs} = 1/Y_{cs}$ is the characteristic impedance, and γ_s is the propagation constant of the shielded-pair line when driven symmetrically with the inner conductors in parallel.

With (6) in (8) and (10), currents at $z = s$ or $w = 0$ are

$$I^a(s) = V_0^e F(0,s) - I^s(s) Z_d G(s,s) \tag{12}$$
$$I^s(s) = -I^a(s) Z_d H(s,s) \tag{13}$$

where $F(0,s)$ is given by (9a) with $w = 0$, $G(s,s)$ is given by (9b) with $z = s$, and $H(s,s)$ is given by (11) with $z = s$. The substitution of (13) in (12) permits the determination of $I^a(s)$. Thus

$$I^a(s) = \frac{V_0^e F(0,s)}{1 - Z_d^2 G(s,s) H(s,s)} \tag{14}$$

Similarly, with (14) in (13),

$$I^s(s) = -\frac{V_0^e Z_d F(0,s) H(s,s)}{1 - Z_d^2 G(s,s) H(s,s)} \tag{15}$$

It is now possible to substitute (14) and (15) in (8) and (10) using (6) and in this manner to obtain expressions for the antisymmetrical and symmetrical currents at any point along the line in terms of V_0^e. The results are

$$I^a(z) = V_0^e [F(w,s) + N Z_d H(s,s) G(z,s)] \tag{16}$$
$$I^s(z) = -V_0^e N H(z,s) \tag{17}$$

where $w = s - z$ and the dimensionless factor N is defined by

$$N \equiv \frac{Z_d F(0,s)}{1 - Z_d^2 G(s,s) H(s,s)} \tag{18}$$

The total currents in each conductor are defined in (3). With (16) and (17) they are

$$I_1(z) = V_0^e \{F(w,s) + N[Z_d H(s,s) G(z,s) - \tfrac{1}{2} H(z,s)]\} \tag{19}$$
$$I_2(z) = -V_0^e \{F(w,s) + N[Z_d H(s,s) G(z,s) + \tfrac{1}{2} H(z,s)]\} \tag{20}$$
$$I_3(z) = -V_0^e N H(z,s) \tag{21}$$

The ratio of the total unbalanced current to the principal part of the balanced current is $NH(z,s)/F(w,s)$.

It is seen that, when $Z_d = 0$, so that the load is balanced, $N = 0$, and the entire line is balanced with

$$I_1(z) = -I_2(z) = V_0^e F(w,s) \tag{22}$$

The same result is obtained when the impedance $\boldsymbol{Z}_p$ joining the load to the shield is removed or made infinite. With $\boldsymbol{Z}_p = \infty$, $\theta_p = 0$ and $\boldsymbol{H}(z,s) = \boldsymbol{H}(s,s) = 0$.

The power dissipated by the symmetrical current is the real part of the complex power

$$\boldsymbol{P}^s = \tfrac{1}{2}\boldsymbol{V}_s^s\boldsymbol{I}^{s*}(s) = -\tfrac{1}{2}\boldsymbol{Z}_d\boldsymbol{I}^a(s)\boldsymbol{I}^{s*}(s) \tag{23}$$

The last step in (23) is made using (6). With (14) and (15) it is seen that (23) is equivalent to

$$\boldsymbol{P}^s = \tfrac{1}{2}\left|\frac{\boldsymbol{V}_0^e\boldsymbol{F}(0,s)\boldsymbol{Z}_d}{1 - \boldsymbol{Z}_d^2\boldsymbol{G}(s,s)\boldsymbol{H}(s,s)}\right|^2 \boldsymbol{H}^*(s,s) \tag{24}$$

The real part of $\boldsymbol{P}^s$ in (24) can be reduced by making the real part of $\boldsymbol{H}^*(s,s)$ as small as possible. This is given by (11) with $z = s$. Thus

$$\boldsymbol{H}(s,s) = \boldsymbol{Y}_{cs}\frac{\sinh\theta_p\sinh(\gamma_s s + \theta_q)}{\sinh(\gamma_s s + \theta_p + \theta_q)} = \frac{\boldsymbol{Y}_{cs}}{\coth(\gamma_s s + \theta_q) + \coth\theta_p} \tag{25}$$

The last step follows after expanding the denominator and dividing through by the numerator. Since $\coth\theta_p = (\boldsymbol{Z}_p + \boldsymbol{Z}_s/4)/\boldsymbol{Z}_{cs}$ and $\coth(\gamma_s s + \theta_q) = \boldsymbol{Z}_{ins}^s/\boldsymbol{Z}_{cs}$, where $\boldsymbol{Z}_{ins}^s$ is the symmetrical or coaxial-mode input impedance of the line looking from the load toward the generator, it follows that

$$\begin{aligned}\boldsymbol{H}^*(s,s) &= \frac{1}{\boldsymbol{Z}_{ins}^{s*} + \boldsymbol{Z}_p^* + \boldsymbol{Z}_s^*/2} \\ &= \frac{R_{ins}^s + R_p + R_s/4 - j(X_{ins} + X_p + X_s/4)}{(R_{ins}^s + R_p + R_s/4)^2 + (X_{ins} + X_p + X_s/4)^2}\end{aligned} \tag{26}$$

Evidently $\boldsymbol{H}^*(s,s)$ (and with it the power dissipated by the symmetrical currents) vanishes when $\boldsymbol{Z}_p$ is made infinite, i.e., when the lumped load is not connected to the shield. Since there are cases when $\boldsymbol{Z}_p$ is small or even zero, this method of eliminating unbalanced currents may not be available. However, even when $\boldsymbol{Z}_p = 0$, the real part of $\boldsymbol{H}(s,s)$ can be made very small by making R_{ins}^s sufficiently great.

The input resistance R_{ins}^s is given by Sec. 2, Eq. (6a), viz.,

$$R_{ins}^s = R_{cs}\frac{\sinh 2(\alpha_s s + \rho_q)}{\cosh 2(\alpha_s s + \rho_q) - \cos 2(\beta_s s + \Phi_q)} \tag{27}$$

where the term with ϕ_c as a factor has been omitted as negligible. Its maximum value occurs when $\beta_s s + \Phi_q = \pi$, for which

$$R_{ins}^s = R_{cs}\coth(\alpha_s s + \rho_q) \tag{28}$$

Since (28) involves the attenuation $\alpha_s s$ of the entire length of line and, in addition, the attenuation function ρ_q of the impedances $\boldsymbol{Z}_q + \boldsymbol{Z}_0/2$, a very great value of R_{ins}^s is unavailable, in general. Fortunately this difficulty can be removed by a simple expedient.

Coaxial-mode Suppressor; Unbalance Squelcher. In order to obtain a high input resistance R^s_{ins} for the coaxial mode when looking toward the generator from the load, it is possible to connect at a quarter wavelength from the load a double-stub reactive network that has little or no effect on the antisymmetrical currents but is essentially equivalent to a short circuit for the symmetrical currents. Such a network, originally introduced by Tomiyasu[106] and called by him an "unbalance squelcher," is illustrated in Fig. 13.3.

Insofar as the antisymmetrical (equal and opposite) currents are concerned, the circuit in Fig. 13.3 consists of two insulating stubs connected across the line at AA' and BB'. The lengths AC and BD from the twin line to the bridges CC' and DD' are $\lambda_a/4 - k$, where k is the equivalent length of the bridge and λ_a is the wavelength for the antisymmetrical

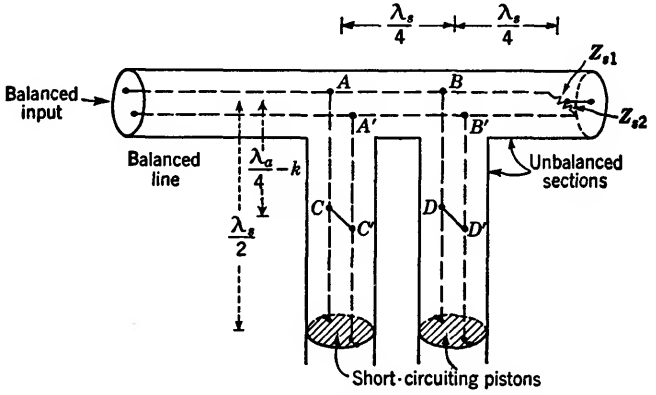


FIG. 13.3. Tomiyasu's unbalance squelcher; λ_a is the wavelength for the balanced currents, and λ_s is the wavelength for the unbalanced currents.

mode. Therefore the impedance looking into each stub at AA' and BB' is very high—several hundred thousand ohms if the adjustment is carefully made. It follows that these stubs have a negligible effect on the balanced currents on the line if this is terminated in a dissipative load.

The unbalanced (codirectional) currents are generated at the asymmetrical load by the generators V^s_s in Fig. 13.1. These are located on the right toward the output in Fig. 13.3. For codirectional currents the line and the two stubs behave like coaxial lines with the two inner conductors in parallel. The bridges CC' and DD' contribute nothing, since they join equipotential points. Therefore, if the stub at AA' is $\lambda_s/2$ in length and is terminated in a short-circuiting piston, its input impedance is extremely low—a few tenths of an ohm at most—so that the shielded-pair line is effectively short-circuited in the plane containing AA' for all symmetrical-mode currents on the shielded-pair line. For such currents

the impedance looking toward AA' from the cross section at BB' is the very high value of a quarter-wavelength line terminated in a short circuit. On the other hand, the parallel impedance at BB' looking toward DD' in the stub is the extremely low value for a half-wave closed-end stub. It follows that the line is effectively terminated in a very low resistance at BB' insofar as coaxial-mode currents generated on the output side are concerned.

The input resistance as seen from the load a quarter wavelength from BB' is the very large value

$$R^s_{ins} = R_{cs} \coth \frac{3\alpha\lambda}{4} \doteq \frac{4R_{cs}}{3\alpha\lambda} \tag{29}$$

If $Z_p = 0$ and $(R^s_{ins} + R_s/2)^2$ is very much greater than $(X_s/2)^2$, it follows from (26) that

$$\text{Re } \boldsymbol{H}(s,s) \doteq \frac{1}{R^s_{ins} + R_s/2} \tag{30}$$

Accordingly, if R^s_{ins} is sufficiently great, the power dissipated by the symmetrical currents is small, and these currents are confined essentially to the section of line and the stubs to the right of AA' in Fig. 13.3.

It has been shown that an asymmetrical load is equivalent to a symmetrical load in series with generators that maintain both balanced and unbalanced currents. In particular, the emf V^a_s of the generator of balanced (antisymmetrical) currents is proportional to the codirectional (symmetrical) currents in the load. This follows from (6). Accordingly, if the amplitude of the symmetrical currents in the unbalanced load is large, these will generate a correspondingly large balanced voltage. If, as in some types of precision measurements on shielded-pair lines, it is undesirable to have an effective generator of balanced currents in the load, it is not sufficient merely to localize the symmetrical currents by means of an unbalance squelcher. It is necessary also to reduce the amplitude of the symmetrical currents. This may be accomplished by modifying the unbalance squelcher, as shown in Fig. 13.4, where one of the stubs is terminated in Z_{cs}, the characteristic impedance of the line for the symmetrical mode. The symmetrical currents are thus dissipated without reflection, and their amplitude is kept small. Note that the terminated stub is the one adjacent to the unbalanced line. The symmetrical impedance looking into this stub from the line is Z_{cs}, and this is still very small compared with the very great impedance looking into the line toward the other stub.

If an unbalanced current is excited in a shielded-pair line by an asymmetrical or unbalanced generator, the coaxial mode may be confined to a section of line near the generator by inserting the circuit of Fig. 13.3 or Fig. 13.4 close to the generator.

Once the symmetrical currents have been suppressed from the principal part of a shielded-pair line, this may be replaced by an open two-wire line if desired.

Instead of eliminating unbalanced currents from the main line by locating an unbalance squelcher near an unbalanced load or generator, it is adequate for some types of measurements merely to construct a detector that responds only to the balanced currents. In such cases it is desirable to terminate the line in its characteristic impedance insofar as the symmetrical currents are concerned. A double bridge that permits the separation of balanced and unbalanced currents on a shielded-pair line has been constructed by Matthews.[86] By connecting the two inner conductors and bringing a center tap out through the shield as the inner conductor of a coaxial line, only the unbalanced mode is obtained. By placing a tubular bridge with a gap at its center a quarter wavelength nearer the generator, the balanced voltage maintained across the gap

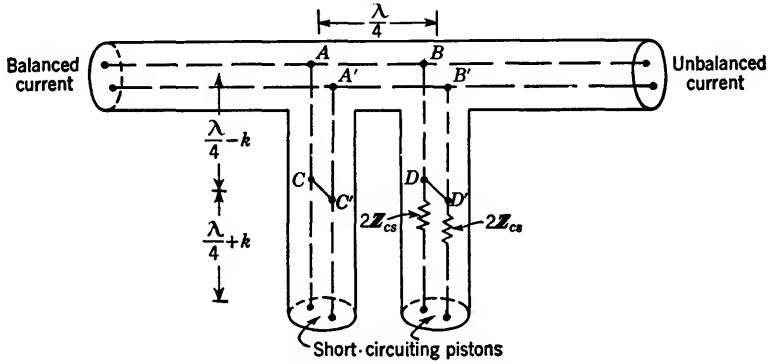


FIG. 13.4. Coaxial-mode suppressor for shielded-pair line.

may be used to drive a coaxial line placed inside one side of the bridge, provided its inner conductor crosses the gap and is connected to the other side of the bridge. The coaxial line for the balanced mode may be contained inside one of the inner conductors of the shielded-pair line and brought out to a detector.

14. Series Stubs and Unbalanced Sections of Line; Folded Dipole; Balun; Shielded Loop. Sections of transmission line serve many purposes when connected in parallel with the line. Some useful properties may be realized by connecting sections of transmission line in series.

Consider first an open two-wire line. If this is cut at any point along *one* of its conductors and the two terminals so created are connected to an auxiliary two-wire line as in Fig. 14.1*a*, the auxiliary line is in series with *one* of the conductors of the main line, and this, quite obviously, is unbalanced. The codirectional currents in an unbalanced open-wire line do not differ from the radiating currents in an *antenna*. Since any cir-

cuit that radiates significantly is not useful as a transmission line, further study of the circuit in Fig. 14.1*a* is of no interest to transmission-line theory and cannot be analyzed by transmission-line methods.

The *main* transmission line in Fig. 14.1*a* may be balanced by the expedient of connecting another auxiliary two-wire line identical with the first one in series with the second conductor of the main line, as shown in Fig. 14.1*b*. However, the fact that the entire circuit is now geometrically symmetrical with respect to a plane perpendicular to and bisecting the distance between the lines does not ensure that the auxiliary transmission lines are balanced. Actually they may be unbalanced so completely as to constitute one of the most useful types of antenna, the

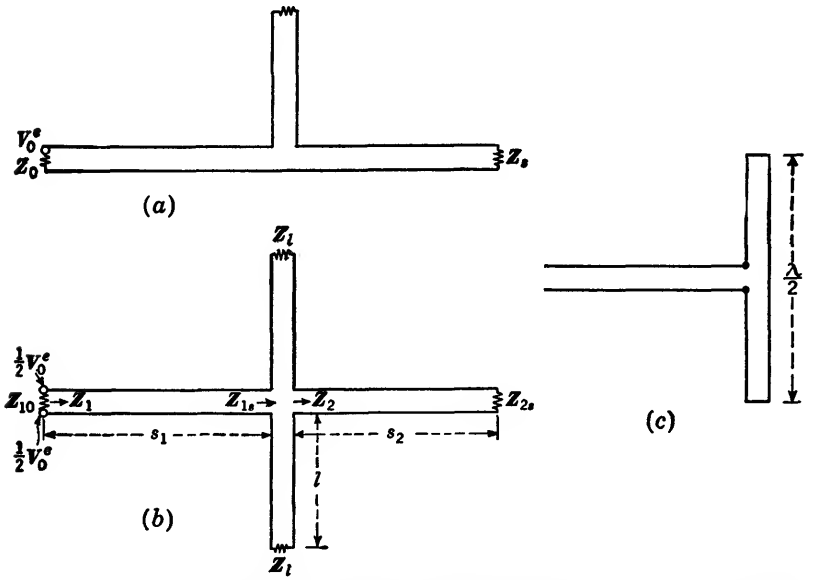


FIG. 14.1. (*a*) Two-wire line with unbalanced series section. (*b*) Balanced two-wire line with balanced series sections. (*c*) Folded-dipole antenna.

so-called folded dipole. This is achieved when the auxiliary sections are each about a quarter wavelength long when terminated in a wire bridge and when the impedance Z_2 looking into the length s_2 of the main line is as low as possible. In the usual arrangement (Fig. 14.1*c*) $s_2 = 0$, and Z_{2s} is the impedance of a short straight conductor.† Alternatively the series sections of line behave like transmission lines with virtually balanced currents when Z_2 is very great, for example, when $Z_2 = \infty$. In general, series sections of *open-wire* line are useful primarily as antennas.

An interesting modification of Fig. 14.1*b* is shown in Fig. 14.2*a*, where

† The folded dipole is analyzed in Refs. 10 and 11.

all lines are shielded pairs. This does not alter the fact that the main line is balanced and the auxiliary lines in general are unbalanced. However, the metallically enclosed unbalanced lines do not radiate and can be analyzed by transmission-line methods as in the preceding section. In Fig. 14.2*a* the symmetrical generator with emf V_0^e in series with an internal impedance Z_0 is shown center-tapped and connected to the shield. The same is true of the terminating impedance Z_{2s} of the main line. Since the main line (including load and generator) is balanced, there is no net flow of charge along the shield and no current in the center taps to the load and generator. Evidently these may be removed if desired insofar

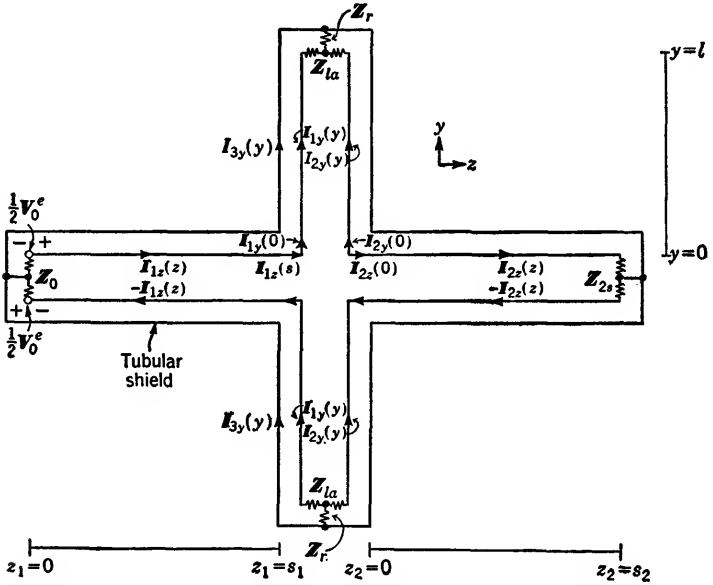


FIG. 14.2*a*. Cross section of balanced shielded-pair line with series sections.

as balanced currents are concerned. The impedance Z_{la} terminating each of the auxiliary series sections of line of length l is symmetrical and connected to the shield at its center through an arbitrary impedance Z_r, so that the effective terminating impedance for the symmetrical mode is $Z_{ls} = \frac{1}{2}Z_{la} + Z_r$. Z_r may be a lumped impedance, as in Fig. 14.2*a*, including a short circuit $Z_{ls} = 0$ and an open circuit $Z_{ls} = \infty$, or the input impedance of a section of coaxial line of arbitrary length, as in Fig. 14.2*b*.

The analysis of the circuit in Fig. 14.2*a* involves the determination of the currents in both branches of the main line and in the series sections. The current $I_{1z}(z)$ in the left-hand part of the main line is balanced and readily determined from conventional transmission-line for-

mulas as soon as the terminating impedance

$$Z_{1s} = \frac{V_1(s)}{I_{1z}(s)} = \frac{V_1(s)}{I_{1y}(0)} \tag{1a}$$

is known. Correspondingly the current $I_{2z}(z)$ in the right-hand part of the main line is also balanced and is easily evaluated if the voltage

$$V_2(0) = I_{2z}(0)Z_2 \tag{1b}$$

across its input terminals is known. Z_2 is the input impedance of the right-hand section of the main line of length s_2. The currents $I_{1y}(y)$ and $I_{2y}(y)$ in the two conductors of the twin line in the series sections are not

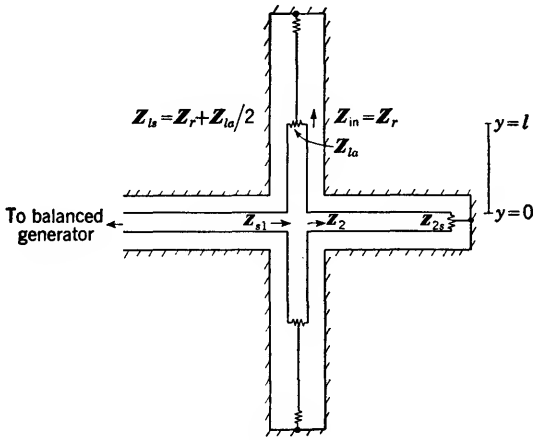


FIG. 14.2b. Cross section of balanced shielded-pair line with series sections ending in coaxial lines.

necessarily equal and opposite. If they are unbalanced, there must be a current $I_{3y}(y)$ in the shield, as indicated in Fig. 14.2a.

For simplicity it is assumed in the present analysis that the line spacings are sufficiently small compared with the wavelength so that junction and coupling effects may be ignored. If this is not the case, account may be taken of them using methods described in Chap. V.

In order to determine the currents $I_{1y}(y)$ and $I_{2y}(y)$ in the two conductors of each of the series lines, it is convenient to separate them into antisymmetrical and symmetrical components. The former are, by definition, the equal and opposite currents of the balanced twin line with zero current in the shield, namely,

$$I^a_{2y}(y) = -I^a_{1y}(y) \equiv -I^a_y(y) \qquad I^a_{3y}(y) = 0$$

The latter are the equal codirectional currents $I^s_{2y}(y) = I^s_{1y}(y)$. The total

symmetrical current in the conductors is

$$I_y^s(y) \equiv I_{1y}^s(y) + I_{2y}^s(y) = 2I_{1y}^s(y) = -I_{3y}(y)$$

where $I_{3y}(y)$ is the current in the shield and $I_y^s(y)$ is the sum of the equal symmetrical currents in the two inner conductors.

The total currents in each of the two inner conductors are

$$I_{1y}(y) = I_{1y}^s(y) + I_{1y}^a(y) = \tfrac{1}{2}I_y^s(y) + I_y^a(y) \tag{2a}$$
$$I_{2y}(y) = I_{1y}^s(y) - I_{1y}^a(y) = \tfrac{1}{2}I_y^s(y) - I_y^a(y) \tag{2b}$$

These expressions may be solved for the symmetrical and antisymmetrical currents as follows:

$$I_y^s(y) = I_{1y}(y) + I_{2y}(y) \qquad I_y^a(y) = \tfrac{1}{2}[I_{1y}(y) - I_{2y}(y)] \tag{2c}$$

The equal codirectional or symmetrical currents may be represented as if maintained by equal in-phase emfs V^s; the equal and opposite or antisymmetrical currents may be represented as if maintained by equal and opposite emfs V^a and $-V^a$. Thus the effective emfs in the two conductors are

$$V_1(s) = V^s + V^a \qquad V_2(0) = V^s - V^a \tag{3a}$$

so that

$$V^s = \tfrac{1}{2}[V_1(s) + V_2(0)] \qquad V^a = \tfrac{1}{2}[V_1(s) - V_2(0)] \tag{3b}$$

Since there is no actual generator at the center of conductor 2, but an impedance Z_2 is connected in series with it at $y = 0$, the Compensation Theorem states that

$$V_2(0) = -I_{2y}(0)Z_2 = I_{2z}(0)Z_2 \tag{4}$$

and therefore

$$V^s = \tfrac{1}{2}[V_1(s) - I_{2y}(0)Z_2] \tag{5a}$$
$$V^a = \tfrac{1}{2}[V_1(s) + I_{2y}(0)Z_2] \tag{5b}$$

Let the complex propagation constant and characteristic impedance of all parts of the shielded twin line be γ_a and Z_{ca}, respectively, when the line is operated antisymmetrically with currents and charges in the two inner conductors equal and opposite and no current or charge on the shield. These constants may be evaluated in any particular case using Chap. I, Sec. 9, Eqs. (10). Similarly let the propagation constant and characteristic impedance of the shielded twin line be γ_s and Z_{cs} when the line is operated symmetrically with equal and codirectional currents in the two inner conductors and with the shield carrying current equal in magnitude to the sum of the currents in the inner conductors but opposite in direction. These constants may be evaluated using Chap. I, Sec. 9, Eqs. (23*a*,*b*).

The antisymmetrical or twin-mode currents in the identical series sections of line may be determined with the aid of Fig. 14.3, in which two equal and opposite generators each with emf V^a are connected in series with two identical sections of line each of length l and terminated in an

arbitrary impedance Z_{la}. The antisymmetrical currents in the upper section are given by Chap. II, Sec. 8, Eq. (16), with $l - y$ substituted for w, θ_{la} substituted for θ_s, and θ_0 set equal to $j\pi/2$. (This last substitution depends on the equivalence of the lower series section and one-

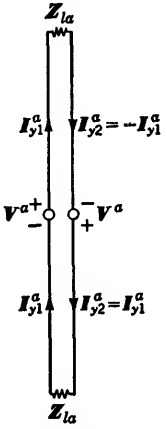


FIG. 14.3. Antisymmetrical problem in the analysis of the series sections.

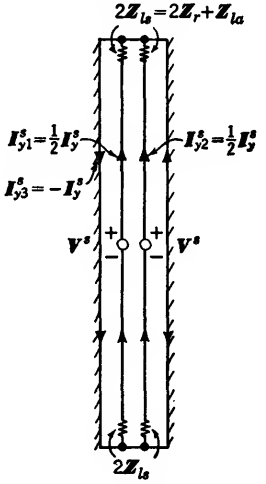


FIG. 14.4. Symmetrical problem in the analysis of the series sections.

half of each generator to a perfectly conducting infinite image plane.) Thus the normalized current is

$$\frac{I^a_y(y)}{V^a} = \frac{I^a_{y1}(y)}{V^a} = Y_{ca}\frac{\sinh\left[\gamma_a(l-y)+\theta_{la}\right]}{\cosh\left(\gamma_a l+\theta_{la}\right)} \tag{6a}$$

The antisymmetrical input admittance is defined by

$$\frac{I^a_{1y}(0)}{V^a} = \frac{I^a_y(0)}{V^a} = Y^a = Y_{ca}\tanh\left(\gamma_a l+\theta_{la}\right) = \frac{1}{Z^a} \tag{6b}$$

With (6b) the antisymmetrical current is

$$I^a_y(y) = I^a_y(0)\frac{\sinh\left[\gamma_a(l-y)+\theta_{la}\right]}{\sinh\left(\gamma_a l+\theta_{la}\right)} \qquad I^a_y(0) = Y^a V^a \tag{6c}$$

The antisymmetrical currents in the lower series section in Fig. 14.3 are equal to and codirectional with those in the upper section. That is, $I^a_y(-y) = I^a_y(y)$.

The symmetrical or coaxial-mode currents in the upper series section are derived using Fig. 14.4. Since the two inner conductors are in parallel with equal and codirectional currents, it follows that

$$I^s_{1y}(y) = I^s_{2y}(y) = \tfrac{1}{2}I^s_y(y) = -\tfrac{1}{2}I_{3y}(y) \tag{7}$$

where $I_y^s(y)$ is the sum of the currents in the inner conductors and the negative of the current $I_{3y}(y)$ in the shield. [Note that, since $I_{3y}^a(y) = 0$, $I_{3y}(y) = I_{3y}^s(y)$.] With appropriate changes in the notation, the normalized symmetrical current $I_y^s(y) = I_{1y}^s(y) + I_{2y}^s(y) = -I_{3y}^s(y)$ is given by

$$\frac{I_y^s(y)}{V^s} = \tfrac{1}{2}Y_{cs}\frac{\sinh\left[\gamma_s(l-y)+\theta_{ls}\right]}{\cosh\left(\gamma_s l+\theta_{ls}\right)} \tag{8a}$$

The factor $\frac{1}{2}$ occurs as a consequence of the fact that the parallel generators are driving identical sections of line in series. The symmetrical input admittance seen by each emf V^s is defined by

$$\frac{I_{1y}^s(0)}{V^s} = \frac{I_y^s(0)}{2V^s} \equiv Y^s = \tfrac{1}{4}Y_{cs}\tanh\left(\gamma_s l+\theta_{ls}\right) = \frac{1}{Z^s} \tag{8b}$$

Since Z^s is the impedance of two identical sections of line in series defined in terms of one-half of the total current, the input impedance Z_{inc} of the upper or lower section, when driven in the symmetrical mode and referred to the total symmetrical current, is

$$\frac{V^s}{2I_y(0)} = Z_{inc} = \tfrac{1}{4}Z^s = Z_{cs}\coth\left(\gamma_s l+\theta_{ls}\right) \tag{8c}$$

$$I_y^s(y) = I_y^s(0)\frac{\sinh\left[\gamma_s(l-y)+\theta_{ls}\right]}{\sinh\left(\gamma_s l+\theta_{ls}\right)} \qquad I_y^s(0) = 2Y^sV^s \tag{8d}$$

The symmetrical currents in the lower series section are the same as those in the upper section, since $I_y(-y) = I_y(y)$.

The total current in each conductor is given by (2c). It follows that

$$I_y^s(0) = I_{1y}(0) + I_{2y}(0) = I_{1z}(s) - I_{2z}(0) \tag{9a}$$

$$I_y^a(0) = \tfrac{1}{2}[I_{1y}(0) - I_{2y}(0)] = \tfrac{1}{2}[I_{1z}(s) + I_{2z}(0)] \tag{9b}$$

Hence the amplitude factors in (6c) and (8c) are expressed in terms of the currents $I_{1y}(0) = I_{1z}(s)$ and $I_{2y}(0) = -I_{2z}(0)$, which enter the series sections from the main lines on the left and right. It follows that the total currents in the conductors of the series sections may be determined as soon as $I_{1z}(s)$ and $I_{2z}(0)$ are available.

The currents $I_{1y}(0) = I_{1z}(s)$ and $I_{2y}(0) = -I_{2z}(0)$ may be obtained using (3a) in the following equivalent form:

$$V_1(s) = I_{1y}^s(0)Z^s + I_{1y}^a(0)Z^a = \tfrac{1}{2}I_y^s(0)Z^s + I_y^a(0)Z^a \tag{10a}$$

$$V_2(0) = I_{1y}^s(0)Z^s - I_{1y}^a(0)Z^a = \tfrac{1}{2}I_y^s(0)Z^s - I_y^s(0)Z^a \tag{10b}$$

The symmetrical and antisymmetrical currents may be eliminated from (10a,b) with (9a,b). Thus

$$V_1(s) = I_{1y}(0)\tfrac{1}{2}(Z^s + Z^a) + I_{2y}(0)\tfrac{1}{2}(Z^s - Z^a) \tag{11a}$$

$$V_2(0) = I_{1y}(0)\tfrac{1}{2}(Z^s - Z^a) + I_{2y}(0)\tfrac{1}{2}(Z^s + Z^a) \tag{11b}$$

Now let $V_2(0)$ be replaced by the voltage drop across the input impedance Z_2 of the right-hand section of line, as in (4). Also let the following definitions be made:

$$Z_{11} \equiv \tfrac{1}{2}(Z^s + Z^a) \qquad Z_{22} \equiv \tfrac{1}{2}(Z^s + Z^a) + Z_2 \tag{12a}$$

$$Z_{21} \equiv Z_{12} \equiv \tfrac{1}{2}(Z^s - Z^a) \tag{12b}$$

It follows that (11a,b) may be expressed in the form

$$V_1(s) = I_{1y}(0)Z_{11} + I_{2y}(0)Z_{12} = I_{1z}(s)Z_{11} - I_{2z}(0)Z_{12} \tag{13a}$$

$$0 = I_{1y}(0)Z_{21} + I_{2y}(0)Z_{22} = I_{1z}(s)Z_{21} - I_{2z}(0)Z_{22} \tag{13b}$$

These equations are solved readily for the total current $I_{1y}(0) = I_{1z}(s)$ entering the series sections from the main line on the left. Thus

$$I_{1y}(0) = I_{1z}(s) = V_1(s)Y_{1s} = \frac{V_1(0)}{Z_{1s}} \tag{14a}$$

where

$$Z_{1s} = Z_{11} - \frac{Z_{12}Z_{21}}{Z_{22}} = \frac{2Z^sZ^a + Z_2(Z^s + Z^a)}{Z^s + Z^a + 2Z_2} \tag{14b}$$

is the input impedance of the series section as a load on the main line. Similarly, from (13b),

$$-I_{2y}(0) = I_{2z}(0) = I_{1z}(s)\frac{Z_{21}}{Z_{22}} \equiv \frac{V_1(s)}{Z_t} \tag{15}$$

where

$$Z_t = \frac{Z_{11}Z_{22} - Z_{12}Z_{22}}{Z_{12}} = \frac{2Z^sZ^a + Z_2(Z^s + Z^a)}{Z^s - Z^a} \tag{16}$$

is the transfer impedance.

The voltage $V_1(z)$ and the current $I_{1z}(z)$ at any point in the left-hand part of the main line may be evaluated using Chap. II, Sec. 8, Eqs. (17) and (18), or their equivalents, since the terminal impedance Z_{1s} is given by (14) using (6b) and (8b). The voltage $V_2(z)$ and the current $I_{2z}(z)$ at any point in the right-hand part of the main line are also given by Chap. II, Sec. 8, Eqs. (17) and (18), with V_0^s replaced by

$$V_2(0) = I_{2z}(0)Z_2 = \frac{V_1(s)Z_2}{Z_t}$$

where $V_1(s)$ is the voltage across the load of the left-hand part of the main line, Z_2 is the input impedance of the right-hand part of the main line, and Z_t is obtained from (16) with (6b) and (8b).

The antisymmetrical and symmetrical parts of the current in the series sections are given by (6c) and (8d), with $I_y^s(0)$ and $I_y^a(0)$ obtained from (9a) and (9b) using the values of $I_{1z}(s)$ and $I_{2z}(0)$ as determined in the preceding paragraph. The total currents in each conductor, $I_{1y}(y)$ and $I_{2y}(y)$, are given by (2a) and (2b). The current in the shield is $I_3^s(y) = -I_y^s(y)$. Thus the currents in all conductors of the network in Fig. 14.2a have been determined.

Three special cases are significant:

a. Series Sections Excited in Twin Mode Alone. If the symmetrical impedance Z^s is made sufficiently great so that the inequality

$$|Z^s| \gg |Z^a + 2Z_2| \tag{17}$$

is satisfied, the input impedance Z_{1s} in (14*b*) becomes

$$Z_{1s} = \frac{2Z^a + Z_2(1 + Z^a/Z^s)}{1 + (Z^a + 2Z_2)/Z^s} \doteq 2Z^a + Z_2 \tag{18}$$

The transfer impedance Z_t in (16) becomes

$$Z_t = \frac{2Z^a + Z_2(1 + Z^a/Z^s)}{1 - Z^a/Z^s} \doteq 2Z^a + Z_2 \tag{19}$$

Since the transfer impedance is practically equal to the input impedance, it follows that $I_{2s}(0) = I_{1s}(s)$, or

$$I_{2y}(0) = -I_{1y}(0) \tag{20}$$

This means that the series sections behave like ordinary sections of shielded-pair line with balanced currents. This is indicated by the form of the input impedance (18), which is the sum of three impedances.

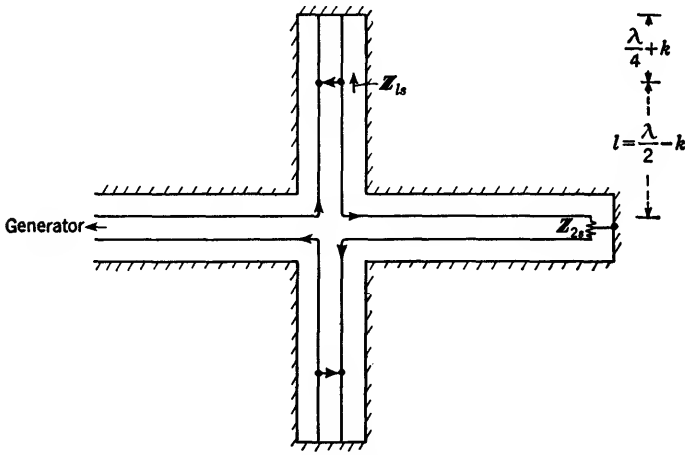


FIG. 14.5. Series sections excited in twin mode alone.

The condition (17) may be satisfied by selecting the length l occurring in (8*b*) to be near an integral, even multiple of a quarter wavelength, with Z_{la} very small and Z_{ls} very great, as for a $\lambda/4$ closed-end stub. This is accomplished in Fig. 14.5 by having the series stub, *including* its termination Z_{ls}, a $3\lambda/4$ closed-end stub. In this way Z^s is the very high input impedance of the $3\lambda/4$ closed-end stub, whereas Z^a is the very low input impedance of a $\lambda/2$ closed-end stub. The length s_2 and the load

Z_{2s} must also be so chosen that Z_2 is not too large. A possible circuit is shown in Fig. 14.5.

b. Series Sections Excited in Coaxial Mode Alone. If the antisymmetrical impedance Z^a is made sufficiently great so that the inequality

$$|Z^a| \gg |Z^s + 2Z_2| \tag{21}$$

is satisfied, the terminating impedance Z_{1s} in (14*b*) and the transfer impedance Z_t in (16) become

$$Z_{1s} = \frac{2Z^s + Z_2(1 + Z^s/Z^a)}{1 + (Z^s + 2Z_2)/Z^a} \doteq 2Z^s + Z_2 \tag{22}$$

$$Z_t = \frac{2Z^s + Z_2(1 + Z^s/Z^a)}{Z^s/Z^a - 1} \doteq -(2Z^s + Z_2) \tag{23}$$

Since the transfer impedance is the negative of the input impedance, it follows that $I_{2s}(0) = -I_{1s}(s)$, or

$$I_{2y}(0) = I_{1y}(0) \tag{24}$$

Therefore the series sections behave like sections of coaxial line with a double inner conductor. This means that, instead of a termination Z_{1s}

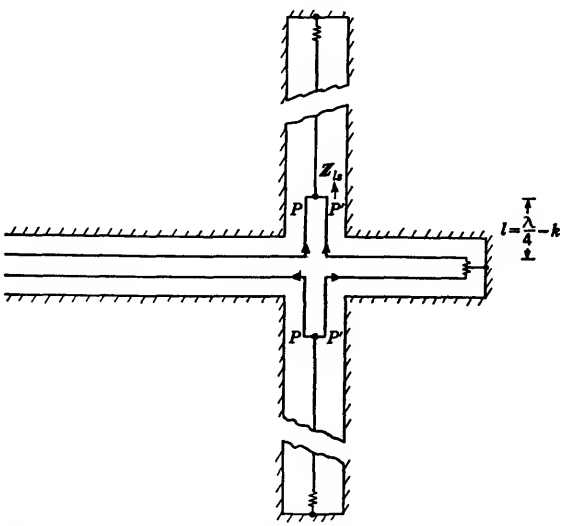


FIG. 14.6. Series sections with codirectional currents converted to coaxial lines.

equivalent to a series combination of three sections of balanced shielded-pair line, as in case *a*, the termination is equivalent to a series combination of two identical sections of line, with currents in the coaxial mode and combined impedance $2Z^s$, and a single section of balanced shielded-pair line with impedance Z_2. When $Z_2 = 0$, this structure is the shielded-

pair transmission-line analogue of the folded-dipole antenna for the open two-wire line.

A circuit arrangement in which the series sections conduct only the coaxial mode is shown in Fig. 14.6. It is assumed that the input impedance Z_{ls} of each coaxial line at PP' has a value such that the input impedance of each series section at its junction with the main line is very much smaller for the symmetrical (coaxial) mode than for the antisymmetrical (twin-line) mode, as required by (21). This is accomplished, for example, if $Z_{la} \doteq 0$, $l \doteq \lambda/4 - k$, and Z_{ls} does not exceed the characteristic impedance Z_{cs}.

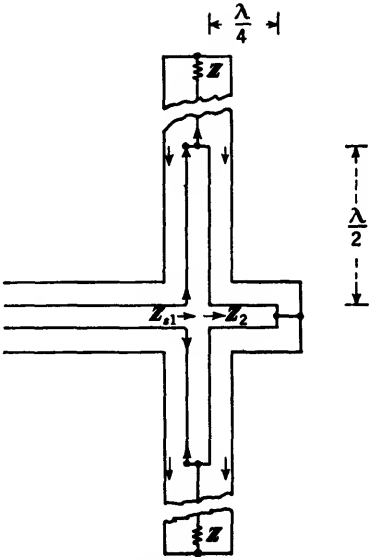


FIG. 14.7. Balanced twin line feeding series sections in which the twin and coaxial modes are equal.

c. Series Sections Excited with Equal Twin-mode and Coaxial-mode Currents. Let the following conditions be imposed on (14*b*) and (16):

$$Z^a = 0 \qquad 2|Z_2| \gg |Z^s| \tag{25}$$

As a consequence

$$Z_{1s} = \frac{Z^s}{2 + Z^s/Z_2} \doteq \tfrac{1}{2}Z^s = 2Z_{inc} \tag{26a}$$

$$Z_{1t} = Z_2 \tag{26b}$$

where Z_{inc} is the input impedance of each of the two identical series sections driven in the coaxial mode. The currents entering the two inner conductors of the series sections are

$$I_{1y}(0) = I_{1z}(s) = \frac{2V_1(s)}{Z^s} \tag{27a}$$

$$-I_{2y}(0) = I_{2z}(0) = \frac{V_1(s)}{Z_2} \qquad |I_{2y}(0)| \ll |I_{1y}(0)| \tag{27b}$$

A circuit that satisfies (25) is shown in Fig. 14.7.

By making Z_2 sufficiently great compared with Z^s, the current in the second conductor may be made as small as desired compared with the current in the first conductor. This means that the codirectional currents are practically equal to the oppositely directed currents, so that they add to twice the value of one in the first conductor and cancel in the second conductor. Under these conditions the second conductor may be dispensed with, and the circuit arranged as in Fig. 14.8*a* or as in Fig. 14.8*b*, where Z_2 is infinite. The series sections are now coaxial lines instead of twin lines in which one conductor carries all the current.

Evidently, from (26*a*),

$$Z_{1s} = 2Z_{inc} \tag{27c}$$

where Z_{inc} is the input impedance of each of the coaxial lines. Thus the two sections of coaxial line are simply in series, and Z_{inc} in (27*c*) is the input impedance of each coaxial-line section.

Baluns.[19] It is often necessary to connect a balanced line, such as a shielded-pair line or a two-wire line, to a coaxial line that is inherently unbalanced. Balanced-to-unbalanced converters, or baluns, may be derived from some of the special circuits involving series sections of line.

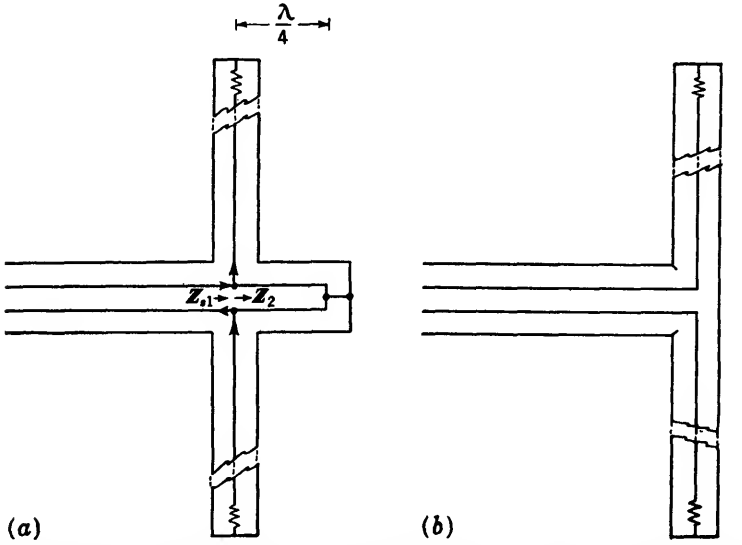


FIG. 14.8. Balanced shielded-pair lines feeding identical matched coaxial lines using two different circuits.

Consider first case *b* with its defining condition (21). Evidently this latter may be satisfied equally well with $Z_2 = 0$. Suppose that the terminations for the series sections in the circuit of Fig. 14.2*b* are $Z_{la} = 0$ and $Z_{ls} = Z_r = Z_c$, where Z_c is the characteristic impedance of the coaxial line. The resultant circuit is shown in Fig. 14.9. For it

$$Z_{1s} \doteq 2Z^s \qquad Z_l = -2Z^s \tag{28}$$

This circuit converts from a balanced shielded-pair line to two coaxial lines.

In general, interest is in converting to a single coaxial line. Since the two lines are in series, it might be supposed that it is merely necessary to replace one of them by a short, unloaded section, as shown in Fig. 14.10, provided the requirement (21), that is, $|Z^a| \gg |Z^s|$, is maintained. This

could be accomplished by making the section a closed-end half-wave stub for the coaxial mode and a closed-end quarter-wave section for the twin mode. However, this provides a completely unbalanced load which, as described in Sec. 13, generates an unbalanced codirectional current on the main shielded-pair line. Note that, even though no connection is shown in Fig. 14.10 from the point L to the shield, this does not mean that Z_p in Fig. 14.1 is infinite. Evidently a very appreciable fraction of the power would be dissipated by the currents in the symmetrical mode in the main shielded-pair line unless an unbalance squelcher, such as

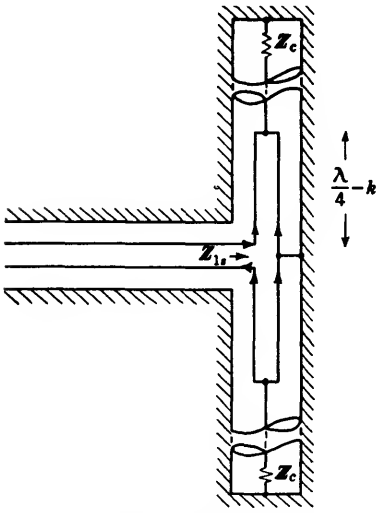


FIG. 14.9. Balanced twin line feeding two matched coaxial lines.

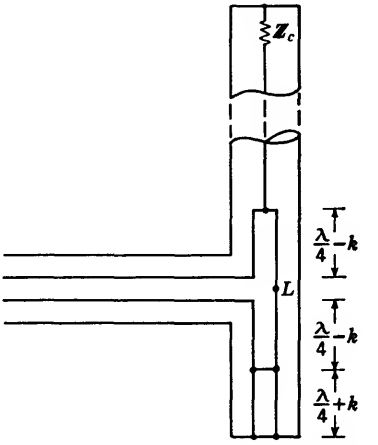


FIG. 14.10. Shielded-pair line feeding one matched coaxial line.

shown in Fig. 14.3, were inserted in the shielded-pair line near its junction with the coaxial line. If such a symmetrical-mode suppressor were used in the circuit of Fig. 14.10, this would constitute an effective, albeit constructionally somewhat complicated, balun.

Without an unbalance squelcher a balanced shielded-pair line can be maintained only when the load is equally divided between the two series sections, as in Fig. 14.9. This suggests the possibility of continuing the balanced shielded-pair line as *two* coaxial lines, each terminated in Z_c. This is illustrated in Fig. 14.11. As a consequence of symmetry it is immaterial whether the two series sections are divided by a metal wall at SS' or not.

Although the circuit of Fig. 14.11 provides a completely balanced conversion from a shielded-pair line to a load in a coaxial line, it has the undesirable feature of requiring two coaxial lines to the load. Fortunately this may be avoided by arranging the outputs of the two coaxial

lines *in parallel* and then connecting the load, as is shown in Fig. 14.12. Since the two lines carry currents exactly 180° out of phase at points that are equidistant from the junction with the shielded-pair line, it is necessary to insert an extra half wavelength of line in one of the lines in

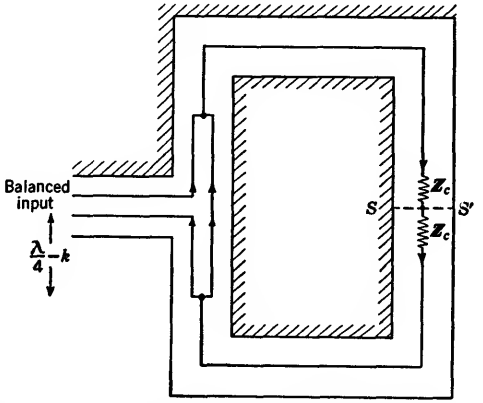


FIG. 14.11. Shielded-pair line with balanced load consisting of two identical, matched coaxial lines folded so that their loads are in series.

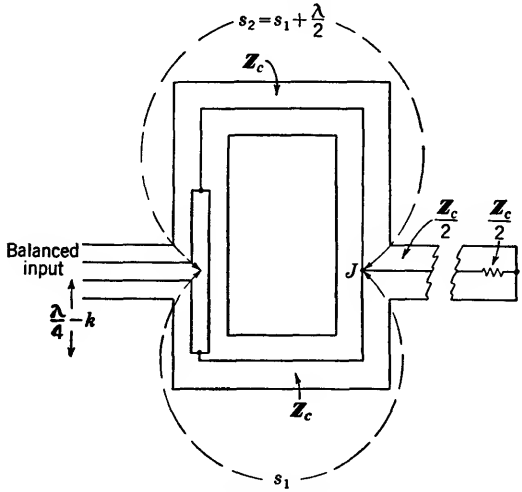


FIG. 14.12. Balun for connecting from shielded-pair line to coaxial line (based on Fig. 14.9).

order to have the outputs from the two lines in phase. With this half-wavelength section an effective balun is achieved which does not require the use of an unbalance squelcher.

The circuit in Fig. 14.8*b* which converts from a balanced shielded-pair line to two identical coaxial lines may be used as a balun in either of the

two connections shown in Figs. 14.11 and 14.12. In this case the section of shielded-pair line extending for the first quarter wavelength of the series lines is absent. As a consequence the length s_1 in the circuit corresponding to Fig. 14.12 may be reduced to as small a length as is physically practicable, including zero. The result is the simple circuit shown in Fig. 14.13. This provides an effective balun.

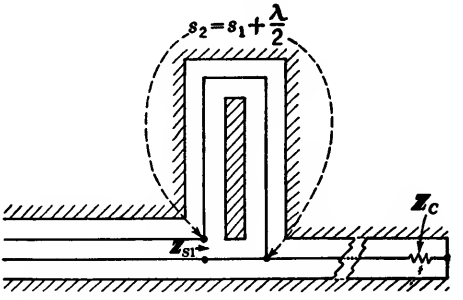


FIG. 14.13. Balun (based on Fig. 14.8*b*).

As a consequence of the reciprocal theorem, the baluns described in the preceding paragraphs may be used to convert from a coaxial line to a balanced shielded-pair line.

Since many of the circuits described depend on an inequality that requires a certain impedance to be very large or very small compared

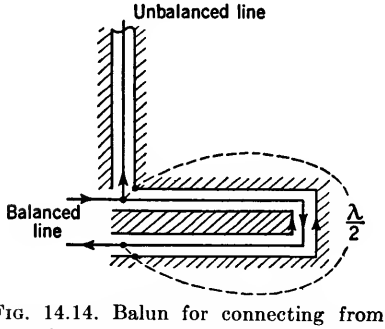


FIG. 14.14. Balun for connecting from two-wire line to coaxial line.

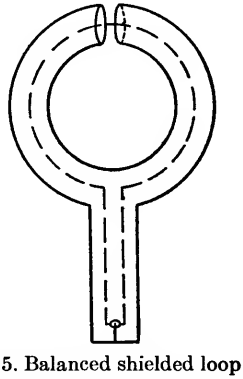


FIG. 14.15. Balanced shielded loop driven from shielded-pair line.

with another impedance, the operation of the circuits is frequency-sensitive. In practice, the significant impedances can be made adjustable to permit their use with any *one* of a range of frequencies, but this does not imply broadband operation.

It is to be noted that the entire discussion in this chapter has assumed that the cross-sectional dimensions of all shielded-pair and coaxial lines

are so small that junction effects are negligible. In general, this is not necessarily the case. For example, in Fig. 14.13 the fact that series line 2 branches off at right angles, whereas series line 1 does not, involves a different terminal-zone correction, so that the shielded-pair line may be slightly unbalanced.

Application to Two-wire Open Line. Whenever the unbalanced current on the main shielded-pair line is vanishingly small, this line may be replaced by a two-wire line with appropriate changes in constants without modifying the formulas. In particular, the baluns described in the preceding paragraphs may be used for converting from an open two-wire line to a coaxial line. This is illustrated in Fig. 14.14. If the unbalanced currents on the shielded-pair line are not insignificant, the corresponding currents on a two-wire line cannot be determined from transmission-line theory.

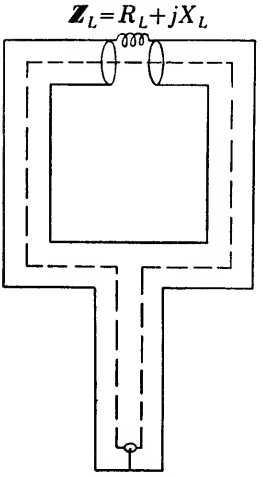


FIG. 14.16. Square shielded loop with outer surface replaced schematically by a coil of equal impedance. R_L is equal to the radiation resistance.

Shielded Loop Antenna.[11] An important type of antenna (especially for direction finding and exploring electromagnetic fields in the form of a probe) is the shielded loop. This consists of a section of coaxial line which is bent into a closed loop and driven from a shielded-pair line, as shown in Fig. 14.15. A section of the shield is removed opposite the junction of the two types of line, so that the outer surface of the coaxial line constitutes a loop antenna. For present purposes it is equivalent to a lumped load $Z_L = R_L + jX_L$ connected in series with the shield of the coaxial line, as shown in Fig. 14.16 for a square instead of a circular loop.†

The circuit of Fig. 14.15 or 14.16 satisfies the symmetry condition presupposed in conjunction with (27*c*), so that the load terminating the shielded-pair line is two identical coaxial lines each terminated in $Z_L/2$. It follows that the load terminating the shielded-pair line is

$$Z_{1s} = 2Z_c \coth (\gamma s + \theta_L) \tag{29a}$$

where

$$\theta_L = \coth^{-1} \frac{Z_L}{2Z_c} \tag{29b}$$

and s is the length of each line. Referring to Figs. 14.15 and 14.16, s is one-half the length of the inner conductor in the loop. The two sections of coaxial line with characteristic impedance Z_c and propagation constant γ are seen to be in series.

† Formulas for R_L and X_L for circular and square loops are given in Ref. 9, Chap. VI.

15. The Hybrid Junction for Transmission Lines.[8,13,15,90] A useful circuit element for coaxial, shielded-pair, and two-wire lines is the hybrid junction. This consists of a combination of shunt and series sections connected at the same cross section in a transmission line. It is advantageous first to analyze the circuit that is simplest in form and then to consider other possibilities.

In Fig. 15.1 is shown a hybrid-junction circuit for use with two-wire or shielded-pair lines. It consists of four transmission lines, each extending from a pair of generators with emfs $\frac{1}{2}V_0^e$ and impedances Z_0 toward a common junction region. Lines 1 and 2 extend continuously from A

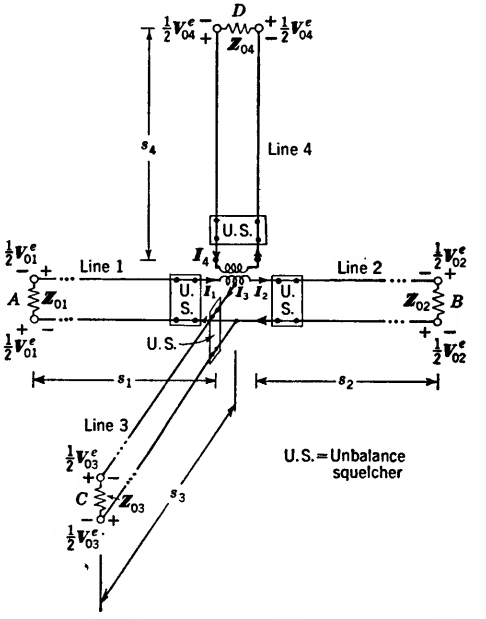


FIG. 15.1. Hybrid junction for shielded-pair or two-wire line.

to B. At their junction line 3 is connected in parallel and extends at right angles to C. Lines 1 and 2 are coupled by ideal transformers to line 4, which extends to D. Since line 4 in the simple circuit of Fig. 15.1 is coupled to only one of the conductors of lines 1 and 2, it constitutes an asymmetrical load that generates unbalanced currents, and these in turn can excite unbalanced currents in lines 3 and 4. Therefore an "unbalance squelcher" (preferably of the terminated type shown in Fig. 13.4) is connected in each line near the junction region, as described in the preceding section. Note that the four unbalance squelchers have little or no effect on the balanced currents. Owing to the presence of unbalanced currents on all four lines between the unbalance squelchers

and the common junction, these sections as well as the squelchers themselves must be constructed of shielded-pair line. Between the squelcher and the generator only balanced currents exist, so that in this range each line may be constructed either of shielded-pair cable or of two open wires. Since codirectional currents are relatively small and are excluded from the four transmission lines, they may be ignored without serious error in the analysis of the equal and opposite currents. To include them would add great complications without significantly altering the results.†

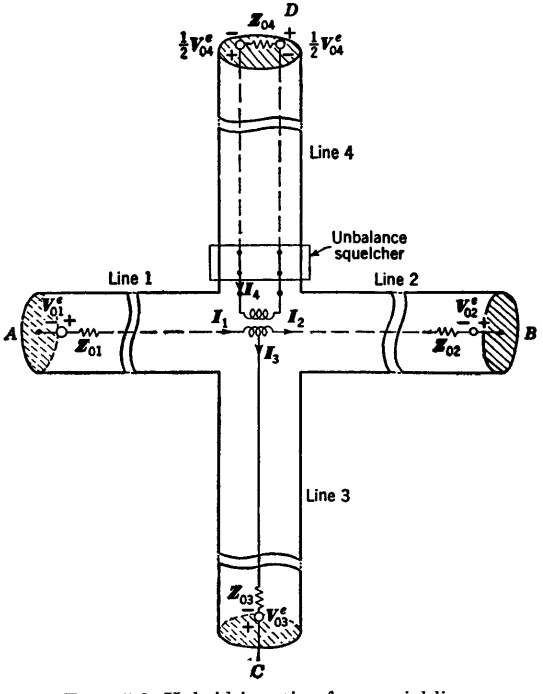


FIG. 15.2. Hybrid junction for coaxial line.

The circuit of Fig. 15.2 is a coaxial-line equivalent of Fig. 15.1. Actually it consists of only three coaxial lines—the collinear lines 1 and 2 and the shunt line 3. The series line 4 is a shielded-pair line. Since each of the three coaxial lines can support only a single mode, an unbalance squelcher is required only in line 4.

The essential characteristics of the hybrid junction may be determined by inspection. It is clear from Fig. 15.1 or 15.2 that currents maintained by V_{03}^e divide equally between lines 1 and 2 at the junction and induce no voltage in line 4. Similarly currents maintained by V_{04}^e are

† An analysis of both codirectional and equal and opposite currents is given in Ref. 86.

limited to lines 4, 1, and 2. Evidently there is no coupling between lines 3 and 4.

In order to facilitate the analysis of the hybrid junction, let the transmission-line problems be eliminated by introducing lumped circuits that are their equivalents insofar as the junction is concerned. This is accomplished by applying Thévenin's theorem at the cross sections where the lines join. Let the open-circuit voltages across these terminals be V_1, V_2, V_3, and V_4. Also let the impedances looking back into the lines with the driving generators short-circuited be Z_1, Z_2, Z_3, and Z_4. Then each line at the junction is equivalent to its open-circuit voltage in series with its input impedance and the junction, as shown in Fig. 15.3. The four currents $I_1 \equiv I_1(s_1)$, $I_2 \equiv I_2(s_2)$, $I_3 \equiv I_3(s_3)$, and $I_4 \equiv I_4(s_4)$ in Fig. 15.3 are the same as in Figs. 15.1 and 15.2. In the former and in line 4 of the latter the indicated currents are only the antisymmetrical parts of the total current in the junction region.

Let it be assumed that the number of turns on the transformer windings in lines 1 and 2 is the same and given by $n_2 = n_1$. Let the number of turns on the winding in line 4 be n_4. The general current and voltage equations for an ideal transformer with three windings are

$$n_1 I_1 + n_2 I_2 + n_4 I_4 = 0 \qquad (1a)$$

$$\frac{e_1}{n_1} = \frac{e_2}{n_2} = \frac{e_4}{n_4} \qquad (1b)$$

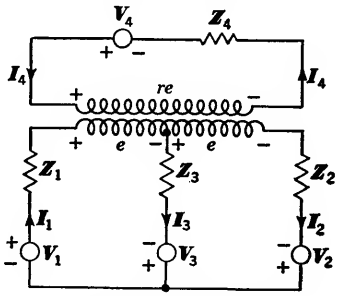


FIG. 15.3. Equivalent circuit for hybrid junction.

where $e_1 = e_2 = e$ is the voltage across the windings in lines 1 and 2 and e_4 is the voltage across the winding in line 4. I_1, I_2, and I_4 are the currents through the three windings. For the case at hand,

$$n_4 = rn_1 = rn_2 \qquad (2a)$$

so that

$$I_1 + I_2 + rI_4 = 0 \qquad (2b)$$

$$e_1 = e_2 = \frac{e_4}{r} \equiv e \qquad (2c)$$

The following mesh equations are obtained directly using Fig. 15.3 and (2*b*,*c*):

$$V_4 = re + I_4 Z_4 = re - \frac{Z_4}{r}(I_1 + I_2) \qquad (3a)$$

$$V_1 + V_3 = e + I_1 Z_1 + I_3 Z_3 = e + I_1(Z_1 + Z_3) - I_2 Z_3 \qquad (3b)$$

$$V_2 - V_3 = e + I_2 Z_2 - I_3 Z_3 = e + I_2(Z_2 + Z_3) - I_1 Z_3 \qquad (3c)$$

In (3*b*,*c*) use is made of the equation

$$I_3 = I_1 - I_2 \qquad (4)$$

By solving (3*a*) for e and substituting this in (3*b*,*c*), the following equations are obtained:

$$I_1A + I_2B = V_a \tag{5a}$$
$$I_1B + I_2C = V_b \tag{5b}$$

where

$$A \equiv Z_1 + Z_3 + \frac{Z_4}{r^2} \qquad B \equiv -Z_3 + \frac{Z_4}{r^2} \qquad C \equiv Z_2 + Z_3 + \frac{Z_4}{r^2} \tag{6a}$$

$$V_a \equiv V_1 + V_3 - \frac{V_4}{r} \qquad V_b \equiv V_2 - V_3 - \frac{V_4}{r} \tag{6b}$$

The solutions for I_1 and I_2 are obtained directly. They are

$$I_1 = V_1Y_{11} + V_2Y_{12} + V_3Y_{13} + V_4Y_{14} \tag{7a}$$
$$I_2 = V_1Y_{21} + V_2Y_{22} + V_3Y_{23} + V_4Y_{24} \tag{7b}$$

where $$Y_{11} = \frac{Z_2 + Z_3 + Z_4/r^2}{D} \qquad Y_{12} = \frac{Z_3 - Z_4/r^2}{D} \tag{7c}$$

$$Y_{13} = \frac{Z_2 + 2Z_4/r^2}{D} \qquad Y_{14} = -(Z_2 + 2Z_3)(rD)^{-1} \tag{7d}$$

$$Y_{21} = Y_{12} \qquad Y_{22} = \frac{Z_1 + Z_2 + Z_4/r^2}{D} \tag{7e}$$

$$Y_{23} = -\frac{Z_1 + 2Z_4/r^2}{D} \qquad Y_{24} = -(Z_1 + 2Z_3)(rD)^{-1} \tag{7f}$$

where $$D \equiv AC - B^2 = Z_1Z_2 + Z_2Z_3 + Z_3Z_1 + \frac{Z_4}{r^2}(Z_1 + Z_2 + 4Z_3) \tag{8}$$

With I_1 and I_2 determined, the other two currents are readily found from (4) and (2*b*). The expressions are as follows:

$$I_3 = I_1 - I_2 = V_1Y_{31} + V_2Y_{32} + V_3Y_{33} + V_4Y_{34} \tag{9a}$$
$$I_4 = -\frac{I_1 + I_2}{r} = V_1Y_{41} + V_2Y_{42} + V_3Y_{43} + V_4Y_{44} \tag{9b}$$

where

$$Y_{31} = Y_{13} \qquad Y_{32} = Y_{23} \tag{9c}$$
$$Y_{33} = \frac{Z_1 + Z_2 + 4Z_4/r^2}{D} \qquad Y_{34} = (Z_1 - Z_2)(rD)^{-1} \tag{9d}$$
$$Y_{41} = Y_{14} \qquad Y_{42} = Y_{24} \tag{9e}$$
$$Y_{43} = Y_{34} \qquad Y_{44} = (Z_1 + Z_2 + 4Z_3)(r^2D)^{-1} \tag{9f}$$

The four equations (7*a*,*b*) and (9*a*,*b*) may be expressed in matrix form as follows:

$$\mathbf{I} = \mathbf{YV} \tag{10}$$

where $$\mathbf{I} \equiv \begin{bmatrix} I_1 \\ I_2 \\ I_3 \\ I_4 \end{bmatrix} \qquad \mathbf{V} \equiv \begin{bmatrix} V_1 \\ V_2 \\ V_3 \\ V_4 \end{bmatrix} \tag{11a}$$

and the admittance matrix is

$$\mathbf{Y} \equiv \begin{bmatrix} Y_{11} & Y_{12} & Y_{13} & Y_{14} \\ Y_{21} & Y_{22} & Y_{23} & Y_{24} \\ Y_{31} & Y_{32} & Y_{33} & Y_{34} \\ Y_{41} & Y_{42} & Y_{43} & Y_{44} \end{bmatrix} \tag{11b}$$

Important applications of the hybrid junction involve the use of only *one* of the four generators.

Special Case A

$$V_1 = V_2 = V_3 = 0 \qquad V_4 \neq 0 \tag{12a}$$

$$I_1 = -\frac{V_4(Z_2 + 2Z_3)}{rD} \tag{12b}$$

$$I_2 = -\frac{V_4(Z_1 + 2Z_3)}{rD} \tag{12c}$$

$$I_3 = \frac{V_4(Z_1 - Z_2)}{rD} \tag{12d}$$

$$I_4 = \frac{V_4(Z_1 + Z_2 + 4Z_3)}{r^2D} \tag{12e}$$

Special Case B

$$V_1 = V_2 = V_4 = 0 \qquad V_3 \neq 0 \tag{13a}$$

$$I_1 = \frac{V_3(Z_2 + 2Z_4/r^2)}{D} \tag{13b}$$

$$I_2 = -\frac{V_3(Z_1 + 2Z_4/r^2)}{D} \tag{13c}$$

$$I_3 = \frac{V_3(Z_1 + Z_2 + 4Z_4/r^2)}{D} \tag{13d}$$

$$I_4 = \frac{V_3(Z_1 - Z_2)}{rD} \tag{13e}$$

Special Case C

$$V_1 = V_3 = V_4 = 0 \qquad V_2 \neq 0 \tag{14a}$$

$$I_1 = \frac{V_2(Z_3 - Z_4/r^2)}{D} \tag{14b}$$

$$I_2 = \frac{V_2(Z_1 + Z_3 + Z_4/r^2)}{D} \tag{14c}$$

$$I_3 = \frac{-V_2(Z_1 + 2Z_4/r^2)}{D} \tag{14d}$$

$$I_4 = \frac{-V_2(Z_1 + 2Z_3)}{rD} \tag{14e}$$

Special Case D

$$V_2 = V_3 = V_4 = 0 \qquad V_1 \neq 0 \tag{15a}$$

$$I_1 = \frac{V_1(Z_2 + Z_3 + Z_4/r^2)}{D} \tag{15b}$$

$$I_2 = \frac{V_1(Z_3 - Z_4/r^2)}{D} \tag{15c}$$

$$I_3 = \frac{V_1(Z_2 + 2Z_4/r^2)}{D} \tag{15d}$$

$$I_4 = \frac{-V_1(Z_2 + 2Z_3)}{rD} \tag{15e}$$

The Hybrid Junction as a Bridge. The relations (12*d*) and (13*e*) lead to the following important conclusions:

$$V_4 \neq 0;\ I_3 = 0 \qquad \text{when } Z_1 = Z_2 \tag{16a}$$

$$V_3 \neq 0;\ I_4 = 0 \qquad \text{when } Z_1 = Z_2 \tag{16b}$$

The condition $Z_1 = Z_2$ requires that the impedances looking back into lines 1 and 2 from the junction be the same. If the two sections of line are identical in cross section and length, this condition can be satisfied only if

$$Z_{01} = Z_{02} \tag{17}$$

Clearly the sufficient evidence that (17) is satisfied is the vanishing of I_3 if V_{04}^e (Figs. 15.1 and 15.2) is the only emf or the vanishing of I_4 if V_{03}^e is the only emf. Accordingly it is possible to compare two impedances Z_{01} and Z_{02} by a null method.

If Z_{01} is a variable standard impedance and Z_{02} is an unknown impedance that is to be measured, these impedances can be connected as terminations of the identical line sections 1 and 2. By inserting a generator in line 4 and a detector in line 3 (or vice versa), the current in the detector vanishes when the variable standard impedance is adjusted to equal the unknown impedance. Thus, when $I_3 = 0$ (or $I_4 = 0$), $Z_{02} = Z_{01}$.

The Hybrid Junction as a Line Stretcher. A linear shift in phase can be introduced in a matched transmission line by changing its length with the aid of a telescoping section known as a line stretcher. The hybrid junction makes possible the accomplishment of the same result without changing the physical length of the line. This is achieved by selecting lines 1 and 2 as the continuous line in which a shift in phase is to be produced. Let V_{01}^e be the only active generator emf, and let both lines 1 and 2 be terminated in their characteristic impedance $Z_c \doteq R_c$. That is,

$$\frac{V_1}{I_1} = Z_1 + R_c \qquad Z_{02} = Z_2 = Z_c \doteq R_c \tag{18a}$$

With (7) and (8), these requirements are equivalent to the following:

$$\frac{V_1}{I_1} = \frac{1}{Y_{11}} = \frac{D}{R_c + Z_3 + Z_4/r^2} = Z_1 + R_c \tag{18b}$$

It is readily verified using (8) and (18*a*) that (18*b*) is satisfied if

$$\frac{4Z_3Z_4}{r^2} = R_c^2 \tag{19}$$

This is satisfied when lines 3 and 4 are terminated in movable highly conducting pistons, so that $\boldsymbol{Z}_{03} = \boldsymbol{Z}_{04} \doteq 0$ and $\boldsymbol{\theta}_{03} \doteq \boldsymbol{\theta}_{04} \doteq j\pi/2$. Furthermore let line 4 be maintained exactly a quarter wavelength longer than line 3. In practice, this may be realized by having the two pistons ganged together so that

$$\beta s_4 = \beta s_3 + \frac{\pi}{2} \tag{20}$$

(It is assumed that the phase constants of the lines are all the same.) Since the line sections can be kept short, their losses may be neglected. As seen from the hybrid junction, the impedances are

$$\boldsymbol{Z}_3 = jR_{c3} \tan \beta s_3 \qquad \boldsymbol{Z}_4 = -jR_{c4} \cot \beta s_3 \tag{21}$$

The condition (19) requires that

$$R_{c3}R_{c4} = \frac{r^2R_c^2}{4} \tag{22}$$

The ratio of the current $\boldsymbol{I}_2$ entering line 2 to the current $\boldsymbol{I}_1$ leaving line 1 is obtained from (7a,b). Thus

$$\frac{\boldsymbol{I}_2}{\boldsymbol{I}_1} = \frac{\boldsymbol{Y}_{21}}{\boldsymbol{Y}_{11}} = \frac{\boldsymbol{Z}_3 - \boldsymbol{Z}_4/r^2}{R_c + \boldsymbol{Z}_3 + \boldsymbol{Z}_4/r^2} = \frac{j[R_{c3} \tan \beta s_3 + (R_{c4}/r^2) \cot \beta s_3]}{R_c + j[R_{c3} \tan \beta s_3 - (R_{c4}/r^2) \cot \beta s_3]} \tag{23}$$

This expression is reduced to very simple form if the dimensions of lines 3 and 4 can be so chosen that their characteristic resistances have the following values:

$$R_{c3} = \frac{R_c}{2} \qquad \frac{R_{c4}}{r^2} = \frac{R_c}{2} \tag{24a}$$

where R_c is the characteristic resistance of lines 1 and 2. With this choice it follows directly that

$$\frac{\boldsymbol{I}_2}{\boldsymbol{I}_1} = e^{j\psi} \qquad \psi = \pi - 2\beta s_3 \tag{24b}$$

By varying βs_3 (with $\beta s_4 = \beta s_3 + \pi/2$) between $\pi/2$ and π, the phase ψ of the current entering line 2 may be shifted linearly from 0 to π, whereas both lines 1 and 2 remain terminated in their characteristic impedance R_c.

As described later in this section, important types of hybrid junctions have $r = 2$, so that (22) requires $R_{c3} = R_{c4} = R_c$. In this case (23) becomes

$$\frac{\boldsymbol{I}_2}{\boldsymbol{I}_1} = \frac{1 + \frac{1}{4} \cot^2 \beta s_3}{1 + j \cot \beta s_3 - \frac{1}{4} \cot^2 \beta s_3} = \frac{1 - (j/2) \cot \beta s_3}{1 + (j/2) \cot \beta s_3} = e^{j\psi} \tag{25a}$$

where $$\psi = -2 \tan^{-1} (\tfrac{1}{2} \cot \beta s_3) = 2 \tan^{-1} (\tfrac{1}{2} \tan \beta s_4) \tag{25b}$$

This formula also provides a range of ψ from 0 to π as βs_3 is varied from $\pi/2$ to π, but the variation of ψ is not linear in βs_3 as with (24*b*).

The Measurement of Phase with the Hybrid Junction. The phase difference ψ between two voltages may be determined with the hybrid junction by applying these voltages to lines 1 and 2 and observing the currents I_3 and I_4. With $V_1 \neq 0$, $V_2 \neq 0$, $V_3 = 0$, and $V_4 = 0$, the general expressions (9*a*,*b*) reduce to

$$I_3 = V_1 Y_{31} + V_2 Y_{32} \tag{26a}$$

$$I_4 = V_1 Y_{41} + V_2 Y_{42} \tag{26b}$$

In these equations V_1 and V_2 are the open-circuit voltages at the ends of the lines when these are disconnected at terminals 1 and 2. In a phase comparison the significant voltages are those maintained across terminals 1 and 2 when the lines are connected. These are

$$V_1' = V_1 - I_1 Z_1 \qquad V_2' = V_2 - I_2 Z_2 \tag{27}$$

where Z_1 and Z_2 are the impedances looking back into lines 1 and 2. If the values of V_1 and V_2 in (27) are substituted in (3*b*,*c*), it is seen that the terms involving Z_1 and Z_2 cancel. Evidently the general expressions for I_3 and I_4 may be expressed in terms of V_1' and V_2' instead of V_1 and V_2 simply by setting Z_1 and Z_2 equal to zero. Hence

$$I_3 = V_1' Y_{31}' + V_2' Y_{32}' \tag{28a}$$

$$I_4 = V_1' Y_{41}' + V_2 Y_{42}' \tag{28b}$$

where Y_{ij}' is obtained from Y_{ij} by setting Z_1 and Z_2 equal to zero. With (7*c*–*f*) and (9*c*,*d*) it is found that

$$Y_{31}' = Y_{32}' = \frac{1}{2Z_3} \tag{29a}$$

$$Y_{41}' = Y_{42}' = -\frac{r}{2Z_4} \tag{29b}$$

If (28*a*) and (28*b*) are solved for the currents using (29*a*,*b*), the results are

$$I_3 = \frac{V_1' - V_2'}{2Z_3} = \frac{V_1'}{2Z_3}(1 - ve^{i\psi}) \tag{30a}$$

$$I_4 = -\frac{V_1' + V_2'}{2Z_4/r} = -\frac{V_1' r}{2Z_4}(1 + ve^{i\psi}) \tag{30b}$$

with the complex ratio factor v defined as follows:

$$v = ve^{i\psi} \equiv \frac{V_2'}{V_1'} \tag{31}$$

The formulas (30*a*,*b*) may be rearranged in two ways that lead to different methods of measuring the phase ψ. They are considered in turn.

Ratio Method for Measuring Phase of Voltages of Equal Amplitude. If an attenuator is available so that the magnitudes of the two voltages

V_1' and V_2' maintained across terminals 1 and 2 of the hybrid junction can be kept equal, it follows that $v = 1$, so that the magnitudes of the currents in (30*a*) and (30*b*) are given by

$$|I_3| = \left|\frac{V_1'}{2Z_3}\right| \sqrt{2(1 - \cos\psi)} = \left|\frac{V_1'}{2Z_3}\right| \sin\frac{\psi}{2} \tag{32a}$$

$$|I_4| = \left|\frac{V_1'r}{2Z_4}\right| \sqrt{2(1 + \cos\psi)} = \left|\frac{V_1'r}{2Z_4}\right| \cos\frac{\psi}{2} \tag{32b}$$

These currents may be normalized by noting the following conditions:

$$\text{For } \psi = 0, \qquad I_3 = 0 \qquad |I_4| = |I_{4\max}| = \left|\frac{V_1'r}{2Z_4}\right| \tag{33a}$$

$$\text{For } \psi = \pi, \qquad I_4 = 0 \qquad |I_3| = |I_{3\max}| = \left|\frac{V_1'}{2Z_3}\right| \tag{33b}$$

By introducing normalized currents the following relations are obtained:

$$i_3 \equiv \left|\frac{I_3}{I_{3\max}}\right| = \sin\frac{\psi}{2} \tag{34a}$$

$$i_4 \equiv \left|\frac{I_4}{I_{4\max}}\right| = \cos\frac{\psi}{2} \tag{34b}$$

From these equations an explicit expression for the phase difference is obtained:

$$\psi = 2 \tan^{-1}\frac{i_3}{i_4} \tag{34c}$$

If one of the voltages V_{01}^s or V_{02}^s applied at the input terminals of lines 1 and 2 is variable in phase, this can be varied until $I_3 = 0$ is observed and $|I_{4\max}|$ is determined. By again varying the phase until $I_4 = 0$ is observed and $|I_{3\max}|$ is determined, the circuit is standardized for phase comparison. By applying a standard reference signal to line 1 and the signal of unknown phase to line 2, the phase difference is obtained directly from the ratio of the normalized currents in lines 3 and 4 using (34*c*). Note that this method requires the two voltages V_1' and V_2' to be equal in amplitude.

Balanced-detector Method for Comparing Phase of Unequal Voltages. If the two voltages are not equal in magnitude, a convenient alternative method of phase comparison is available. Although it can be directly based on (30*a*,*b*), it is advantageous to obtain the corresponding expressions when the voltages are applied to arms 3 and 4 instead of arms 1 and 2, since, in general, lines 1 and 2 can be made alike more readily than 3 and 4.

Let the voltages applied across lines 3 and 4 be V_3' and V_4', where these are related to the open-circuit voltages V_3 and V_4 by the formulas $V_3 = V_3' + I_3Z_3$ and $V_4 = V_4' + I_4Z_4$. If these are used in (3*a*,*b*,*c*) to

eliminate V_3 and V_4, the terms in Z_3 and Z_4 cancel, so that (7a,b) may be expressed as follows:

$$I_1 = V'_3 Y'_{13} + V'_4 Y'_{14} \tag{35a}$$

$$I_2 = V'_3 Y'_{23} + V'_4 Y'_{24} \tag{35b}$$

where

$$Y'_{13} = \frac{1}{Z_1} \qquad Y'_{23} = -\frac{1}{Z_2} \tag{35c}$$

$$Y'_{14} = -\frac{1}{rZ_1} \qquad Y'_{24} = -\frac{1}{rZ_2} \tag{35d}$$

By now requiring that the impedances looking into lines 1 and 2 be equal, i.e.,

$$Z_1 = Z_2 \tag{36}$$

and by setting

$$v = ve^{i\psi} \equiv \frac{V'_4}{rV'_3}$$

Eqs. (35) become

$$I_1 = \frac{V'_3}{Z_1}(1 - ve^{i\psi}) \qquad I_2 = -\frac{V'_3}{Z_1}(1 + ve^{i\psi}) \tag{37}$$

These equations correspond to (30a,b) if Z_3 is made equal to Z_4/r. Since it is more convenient to satisfy $Z_1 = Z_2$ than $Z_3 = Z_4/r$, Eqs. (37) are preferred to (30a) and (30b).

The magnitudes of the currents entering the two lines are

$$|I_1| = \left|\frac{V'_3}{Z_1}\right| (1 + v^2 - 2v \cos \psi)^{\frac{1}{2}} \tag{38a}$$

$$|I_2| = \left|\frac{V'_3}{Z_1}\right| (1 + v^2 + 2v \cos \psi)^{\frac{1}{2}} \tag{38b}$$

It is now clear that any quantity that involves the difference between an arbitrary power n of the two currents, that is,

$$|I_2|^n - |I_1|^n = \left|\frac{V'_3}{Z_1}\right|^n [(1 + v^2 + 2v \cos \psi)^{n/2} - (1 + v^2 - 2v \cos \psi)^{n/2}] \tag{39}$$

vanishes when $\psi = \pi/2$. Evidently, if a circuit can be provided which measures a quantity proportional to the difference current in (39), a null reading indicates that the two voltages are 90° out of phase. If a reference voltage with known variable phase is available, the phase of an unknown voltage is readily determined by varying the phase of the reference signal until it is 90° out of phase with the unknown.

In Fig. 15.4 an arrangement is shown for determining the relative phase distribution of the electromagnetic field near an antenna system. Two balanced detectors are used to rectify individually the currents I_1 and I_2. The rectified output of each of the two identical detectors is

proportional to some power of the radio-frequency current. The difference of these outputs is applied to the receiver.

The Hybrid Junction as a Directional Coupler. The function of a directional coupler is to permit the separate and independent determination of the currents maintained by generators (or their equivalents) at opposite ends of a matched transmission line. In particular, if in Fig. 15.1 lines 1 and 3 together constitute a continuous transmission line with V_{01}^e and V_{03}^e as active emfs while $V_{02}^e = V_{04}^e = 0$, the hybrid junction

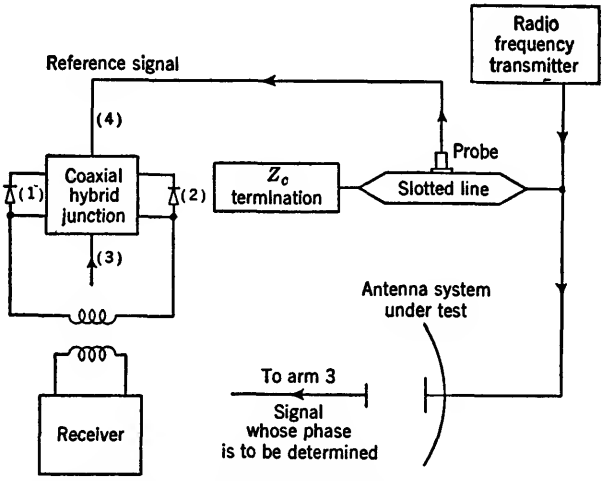


FIG. 15.4. Balanced-detector method of relative phase measurement with a hybrid junction.

acts as a directional coupler if I_4 is a measure of that part of the current in lines 1 and 3 which is maintained by V_{01}^e, and I_2 is a measure of the part of the current maintained by V_{03}^e. Evidently this means that I_2 must vanish when V_{01}^e is the only active emf and that I_4 must vanish when V_{03}^e is the only active emf. It follows from (15*c*) and (13*e*) that the necessary conditions are

$$Z_2 = Z_1 \qquad \frac{Z_4}{r^2} = Z_3 \tag{40}$$

If (40) is satisfied, it follows from special cases D and B, using (8), that the currents are

Case D:

$$V_2 = V_3 = V_4 = 0 \qquad V_1 \neq 0 \tag{41a}$$

$$I_1 = I_3 = \frac{V_1}{Z_1 + 2Z_3} \tag{41b}$$

$$I_2 = 0 \tag{41c}$$

$$I_4 = \frac{-V_1}{r(Z_1 + 2Z_3)} \tag{41d}$$

Case B: $$V_1 = V_2 = V_4 = 0 \qquad V_3 \neq 0 \tag{42a}$$

$$I_1 = -I_2 = \frac{V_3}{Z_1 + 2Z_3} \tag{42b}$$

$$I_3 = \frac{2V_3}{Z_1 + 2Z_3} \tag{42c}$$

$$I_4 = 0 \tag{42d}$$

Now let it be required that lines 1 and 3 be matched at the junction, so that

$$\frac{V_1}{I_1} = Z_1 + Z_{c1} = Z_1 + 2Z_3 \tag{43a}$$

$$\frac{V_3}{I_3} = Z_3 + Z_{c3} = Z_3 + \frac{Z_1}{2} \tag{43b}$$

These equations require the following:

$$Z_3 = Z_{c3} = \frac{Z_{c1}}{2} = \frac{Z_1}{2} \tag{44}$$

Evidently each line must be terminated in its characteristic impedance at the end remote from the junction. With (40) and (44) these relations must be satisfied:

$$Z_{01} = Z_1 = Z_{c1} \qquad Z_{02} = Z_2 = Z_{c2} = Z_{c1} \tag{45a}$$

$$Z_{03} = Z_3 = Z_{c3} = \frac{Z_{c1}}{2} \qquad Z_{04} = Z_4 = Z_{c4} = r^2 Z_{c3} = \frac{r^2 Z_{c1}}{2} \tag{45b}$$

The currents maintained by V_{01}^e are given by

$$I_1 = I_3 = \frac{V_1}{2Z_{c1}} \qquad I_2 = 0 \qquad I_4 = \frac{-V_1}{2rZ_{c1}} \tag{46}$$

The currents maintained by V_{03}^e are

$$I_1 = -I_2 = \frac{V_3}{2Z_{c1}} \qquad I_3 = \frac{V_3}{Z_{c1}} \qquad I_4 = 0 \tag{47}$$

If V_{01}^e is the only emf and line 3 is terminated in its characteristic impedance, I_2 is zero. If line 3 is not terminated in its characteristic impedance but in $Z_{03} = Z_{c3} + Z'_{03}$, it is possible to replace Z'_{03} by an emf $V_{03} = -I_{03}Z'_{03}$. The current I_2 is then a measure of this voltage and therefore of the reflected wave from the termination. Thus I_4 measures the direct wave, and I_2 measures the reflected wave.

Various types of directional couplers are in common use. In principle their operation corresponds to that of the hybrid junction as described above, but different constructions are involved. Some types consist of two lines coupled by holes at one or two points. The theory of transmission-line directional couplers is formulated in Chap. VI, Sec. 5.

Hybrid Junctions without Transformers. In the circuits of Figs. 15.1 and 15.2 transformers are used to couple line 4 to lines 1 and 2 and to provide the center tap leading to line 3. In actual practice at high frequencies it is possible to eliminate the coils in Fig. 15.2 by letting the

inner conductors of lines 1 and 2 continue smoothly to a junction and substituting a straight conductor for the coil at the end of line 4. This in no way alters the analysis. If a coaxial output is desired for line 4, the coupling loop may be the equivalent of a shielded loop, as described in conjunction with Figs. 14.14 and 14.15. A simple circuit of this type is illustrated in Fig. 15.5; useful modifications are shown in Figs. 15.6 and 15.7.†

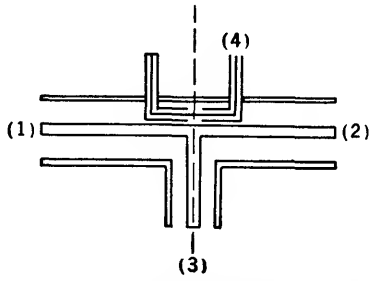


FIG. 15.5. Coaxial hybrid junction with shielded coupling loop.

Instead of coupling line 4 to lines 1 and 2, as in Figs. 15.1 and 15.2, it may be joined directly, provided line 3 begins with a high-impedance stub, as shown in Figs. 15.8 and 15.9. In this case the antisymmetrical currents at the junctions satisfy the following equations:

$$I_1 + I_4 = \tfrac{1}{2}I_3 \qquad I_2 + I_4 = -\tfrac{1}{2}I_3 \tag{48}$$

so that

$$I_1 + I_2 + 2I_4 = 0 \qquad I_1 - I_2 = I_3 \tag{49}$$

If the two equations in (49) are compared with (2*b*) and (4), it is seen

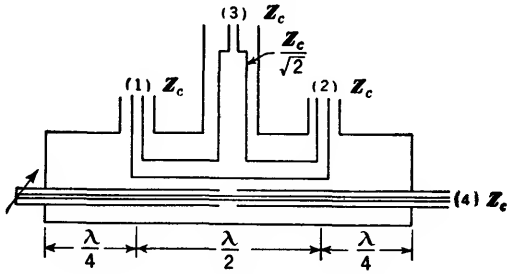


FIG. 15.6. Modified coaxial hybrid junction.

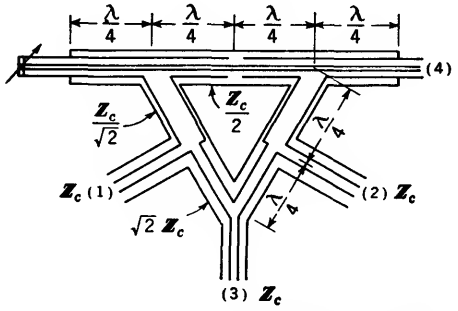


FIG. 15.7. Modified coaxial hybrid junction.

† These are due to Morita and Sheingold.[90]

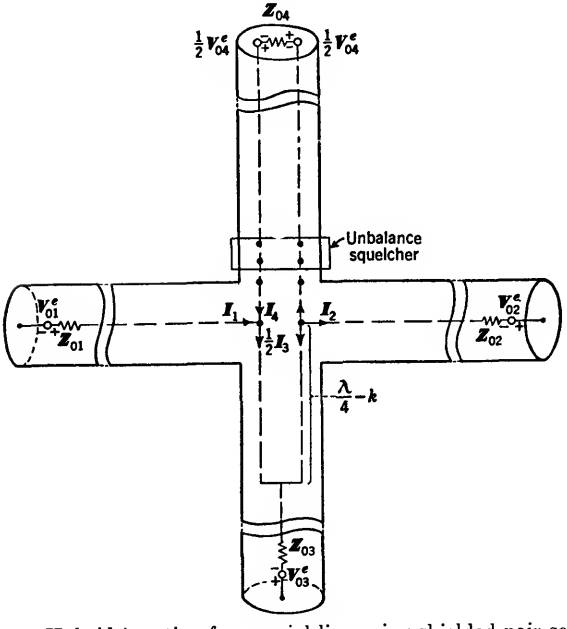


FIG. 15.8. Hybrid junction for coaxial line using shielded-pair section.

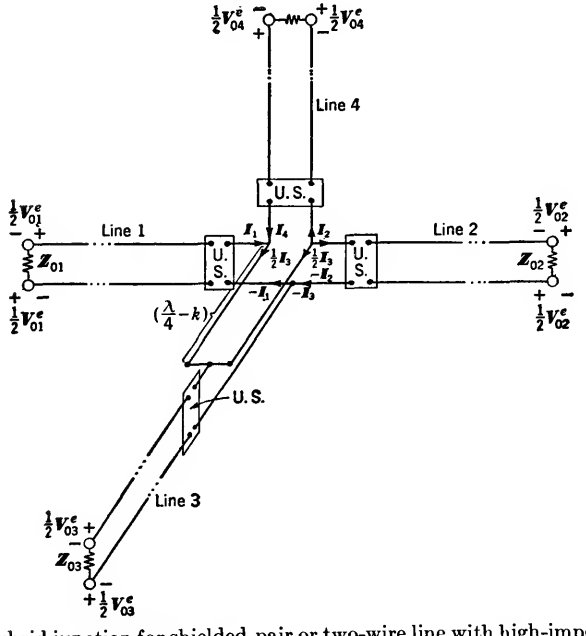


FIG. 15.9. Hybrid junction for shielded-pair or two-wire line with high-impedance stub.

that they correspond exactly if the transformer ratio r is set equal to 2. It follows that all the results derived for the transformer-coupled lines apply if r is replaced by 2.

The hybrid junctions for shielded-pair and two-wire lines in Figs. 15.1 and 15.9 are unbalanced in all four lines instead of only in line 4 (in which codirectional currents must be suppressed with an unbalance squelcher). This is a consequence of the insertion of a series section of line in only

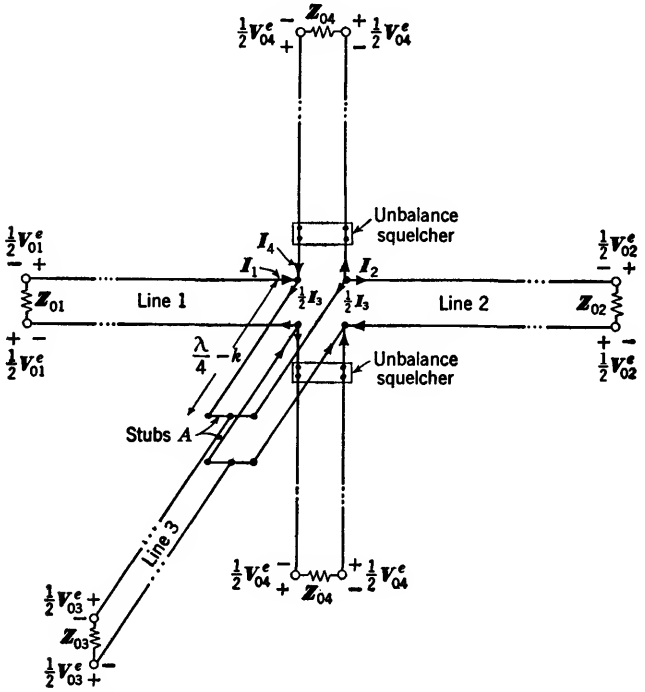


FIG. 15.10. Hybrid junction for shielded-pair or two-wire line in completely symmetrical form with high-impedance stubs.

one of the two conductors. Evidently the unbalance on lines 1, 2, and 3 can be eliminated by using two complete and identical lines 4, as in Fig. 15.10. Alternatively the load and generators in the lower line 4 may be omitted, and the line fixed in length at $y + \lambda/4$. The open ends of the lower line 4 are then connected to the upper line 4 at a distance y from the junction. The length y may be kept as short as practical convenience dictates.

It is readily verified that the analysis of the balanced circuit of Fig. 15.10 differs in no essential manner from that of Fig. 15.9.

Ring Circuit. An alternative method of constructing a hybrid junction for use with coaxial lines is the ring circuit shown in Fig. 15.11.

It is readily verified by inspection that it has the essential properties of the hybrid junction if the lines are treated as lossless. Thus, if a voltage is applied to line 4, the resulting current divides equally between lines 1 and 2, and no voltage is maintained across line 3. Similarly, if a voltage is maintained across line 3, equal voltages are established across lines

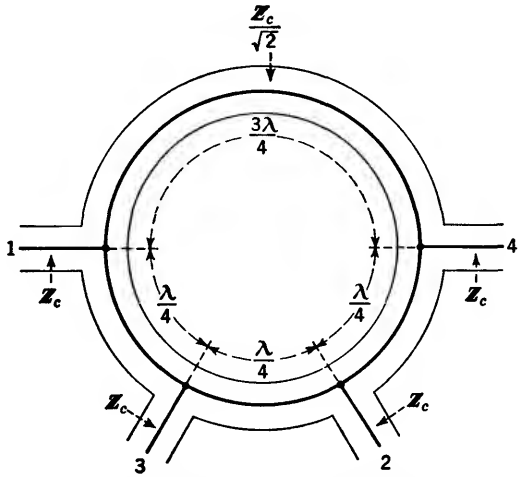


FIG. 15.11. Hybrid junction in form of ring circuit, or "rat race."

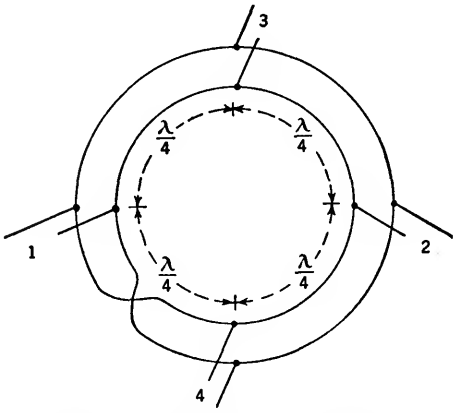


FIG. 15.12. Modified ring circuit with reversed connections.

1 and 2, and the voltage across line 4 is zero. Clearly lines 3 and 4 are not coupled. Unlike the transformer-coupled circuit of Fig. 15.2, the ring, or "rat race," is highly frequency-sensitive, since its operation depends on the spacing of the four lines around the ring specified in Fig. 15.11.

A ring circuit of different construction is shown in Fig. 15.12. It consists of a ring that is one wavelength rather than one and one-half wavelengths in circumference. The four transmission-line connections are uniformly spaced around the ring. However, one of the four quarter wavelengths between connections is spiraled through 180°, so that the connections at one end are reversed. It is readily verified that this ring also has the essential properties of the hybrid junction and is much less frequency-sensitive than the more conventional ring in Fig. 15.11. On the other hand, it is difficult to adapt the ring in Fig. 15.12 for use with coaxial lines.

PROBLEMS

1. Determine the input impedance of a section of line of length 20.2 m for which $Z_c = 400(1 - j\alpha/\beta)$ and $\alpha = 2 \times 10^{-3}$ neper/m at a frequency of 300 Mc/sec. The line is terminated in an apparent impedance $Z_{sa} = 100 - j800$ ohms.

2. What would be the input impedance of the line described in Prob. 1 if it were lossless?

3. A section of coaxial line is to be designed to provide a maximum possible input impedance. It is specified that the inner radius of the shield must be 1.5 cm. Determine other specifications using the best physically available materials. What is the maximum input impedance?

4. Design a transmission system using a series transformer to match an impedance $Z_{sa} = 40 + j20$ to a 50-ohm coaxial cable so that the line is terminated in its characteristic impedance.

5. Design a single-stub matching network for a load $Z_{sa} = 20 - j500$ ohms so that the line is terminated in its characteristic impedance $Z_c \doteq R_c = 440$ ohms. Do this analytically and also graphically using both types of circle diagram. Explain the graphical solutions in detail with the aid of construction lines.

6. Design a double-stub matching network for a load $Z_{sa} = 800 + j600$ ohms on a line for which $Z_c \doteq R_c = 72$ ohms. The input impedance of the network and load is to be 72 ohms. Use analytical and graphical methods.

7. Investigate the broadband properties of the series transformer by determining the standing-wave ratio as a function of the frequency if the line is matched at a given fixed frequency f_0. Use appropriate constants. The standing-wave ratio is given by $S = \coth \rho_s$.

8. Repeat the preceding problem for the single-stub matching network.

9. Investigate the impedance-matching properties of a triple-stub tuner consisting of three shunt stubs appropriately spaced at fixed distances along a transmission line.

10. An impedance $Z_s = 20 - j500$ ohms terminates a line with $R_c = 440$ ohms, $\alpha = 2.26 \times 10^{-3}$ neper/m, and $\phi_c = \alpha/\beta$. The frequency is 150 Mc/sec.

(*a*) Determine ρ_s and Φ_s by calculation and by circle diagram.

(*b*) Determine the shortest distance from the load along the line at which the impedance looking toward the load is a pure resistance. What is this resistance? What are the associated values of ρ_s and Φ_s? What is the standing-wave ratio as defined by $S = \coth \rho_s$?

(*c*) Repeat part (*b*) for the next shortest distance for which the impedance is a pure resistance.

11. A coaxial line is constructed of an aluminum tube with inner diameter of 1 in. and wall thickness of $\frac{1}{8}$ in. The inner conductor is steel drill rod $\frac{1}{4}$ in. in diameter that is silver-plated for a distance of exactly one-half wavelength from the terminating piston. Determine the values of the terminal functions and the reflection coefficients

terminating the line at the *beginning* of the silvered section. Assume the piston to be perfectly conducting. The frequency is 300 Mc/sec.

12. An apparent impedance $Z_{sa} = 616 - j2{,}096$ ohms terminates a two-wire line with characteristic impedance $Z_c = 400$ ohms and an attenuation constant $\alpha = 10^{-3}$ neper/m at a frequency for which the phase constant is $\beta = 0.30$ radian/m. Determine (*a*) the apparent terminal functions; (*b*) the apparent reflection coefficient; (*c*) the input impedance of a 20-m length of line when terminated in Z_{sa}; (*d*) the length of line required in addition to the 20 m in (*c*) so that the line is characterized by input resonance. What is the input impedance at input resonance?

CHAPTER IV

GENERAL AMPLITUDE RELATIONS FOR CURRENT AND VOLTAGE

1. The Distribution of Current and Voltage and the Transfer of Power along a Nonresonant Line. The distribution of voltage along an infinitely long line is described in Chap. I, Sec. 14, and illustrated in Chap. I, Fig. 14.1. The description involves traveling waves of constant phase. The distributions of voltage and current along a line of length s that is terminated in $\boldsymbol{Z}_c$ are the same as those along the first s meters of an infinitely long line. From Chap. II, Sec. 5, Eq. (12), they are given by

$$\boldsymbol{V}_z = \boldsymbol{I}_z\boldsymbol{Z}_c = \frac{V_0^e\boldsymbol{Z}_c}{\boldsymbol{Z}_0 + \boldsymbol{Z}_c}\, e^{-(\alpha+j\beta)z} \tag{1}$$

where z is the distance from $z = 0$ along a line of length s, $\boldsymbol{Z}_0$ is the impedance of the generator, and V_0^e is its electromotive force. Since $\boldsymbol{Z}_c = R_c(1 - j\phi_c)$, it is evident that the current and voltage at the cross section z satisfy the relation

$$\boldsymbol{V}_z = \boldsymbol{I}_z R_c e^{-j\tan^{-1}\phi_c} \tag{2}$$

Thus the voltage leads the current in phase by the usually very small angle $\tan^{-1}\phi_c$. For a line with low distortion defined by $\phi_c^2 \ll 1$, (2) becomes simply

$$\boldsymbol{V}_z \doteq \boldsymbol{I}_z R_c e^{-j\phi_c} \doteq \boldsymbol{I}_z R_c \tag{3}$$

The losses on many lines are sufficiently low so that ϕ_c is very small (10^{-3} or less), and the exponential in (3) may be replaced by its leading term of unity, as on the right in (3).

The power supplied to the nonresonant line at its input terminals at $z = 0$ is the real part of $\frac{1}{2}\boldsymbol{V}_0\boldsymbol{I}_0^*$. That is,

$$P_0 = \tfrac{1}{2}|\boldsymbol{I}_0^2|R_{\text{in}} = \tfrac{1}{2}|\boldsymbol{I}_0|^2 R_c \tag{4}$$

where $\boldsymbol{I}_0$ is the peak value. The power dissipated in the matched load at the end of a line of length s is

$$P_s = \tfrac{1}{2}|\boldsymbol{I}_s|^2 R_s = \tfrac{1}{2}|\boldsymbol{I}_s|^2 R_c = \tfrac{1}{2}|\boldsymbol{I}_0^2|R_c e^{-2\alpha s} \tag{5}$$

This follows since, by definition of a nonresonant line, $\boldsymbol{Z}_s = \boldsymbol{Z}_c$.

The efficiency of transmission is

$$W = \frac{P_s}{P_0} = \frac{|I_s|^2}{|I_0|^2} = e^{-2\alpha s} \tag{6}$$

The transmission loss is usually expressed by the power ratio P_0/P_s. Thus the loss in decibels is defined by

$$L \text{ (db)} = 10 \log \frac{P_0}{P_s} = 4.3429 \ln \frac{P_0}{P_s} \tag{7}$$

Using (6)

$$L \text{ (db)} = 8.6858 \alpha s \tag{8}$$

where α is measured in nepers per meter and s is in meters.

The power dissipated in heating the line is

$$P_l = P_0 - P_s = R_c(|I_0'| - |I_s|^2) = R_c|I_0|^2(1 - e^{-2\alpha s}) \tag{9}$$

It is interesting to note at this point that the forms [Chap. I, Sec. 13, Eqs. (13) and (14)] reduce to

$$V_z = \sqrt{Z_c}\, Ae^{-\gamma z} \tag{10}$$

$$I_z = \sqrt{Y_c}\, Ae^{-\gamma z} \tag{11}$$

for the infinite line, so that the input power at $z = 0$ is

$$P_0 = \text{Re } \tfrac{1}{2} V_z^* I_z = \tfrac{1}{2} AA^* = \tfrac{1}{2} A^2 \tag{12}$$

2. General Expressions for Current and Voltage for an Arbitrarily Terminated Line When Driven by a Single Pair of Equal and Opposite Point Generators (or Their Equivalent) Anywhere along the Line.[80,81] General formulas for the current and voltage at any cross section z' of a transmission line extending from $z' = 0$ to $z' = s'$ are given in Chap. II,

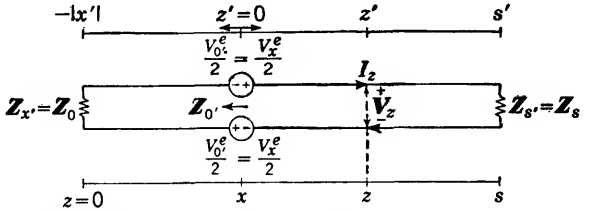


FIG. 2.1. Transmission line driven by one pair of equal and opposite point generators at an arbitrary distance x from one end of the line.

Sec. 8, Eqs. (15) and (16). No restrictions are implied on the impedance of either the load at $z' = s'$ or the generator at $z' = 0'$. It follows that, if the circuit of Chap. II, Fig. 5.1*a*, in the modification of Fig. 2.1 (upper scale) is used, in which the emf is equivalent to a pair of equal and opposite point generators† each of magnitude $\frac{1}{2}V_{0'}^e$, the generator imped-

† A point generator is an impedanceless, extensionless emf. Its physical realization is discussed in Chap. VI.

ance $\boldsymbol{Z}_{0'}$ is the input impedance of a section of line of arbitrary length x' terminated in an equally arbitrary impedance $\boldsymbol{Z}_{x'}$. Using Chap. II, Sec. 8, Eq. (16), with all coordinates primed, the current at z' is

$$\boldsymbol{I}_{z'} = \frac{V_{0'}^{e}}{\boldsymbol{Z}_c} \frac{\sinh \theta_{0'} \sinh (\gamma w' + \theta_{s'})}{\sinh (\gamma s' + \theta_{0'} + \theta_{s'})} \tag{1}$$

where $w' \equiv s' - z'$, $\theta_{0'}$ is the complex terminal function of the impedance $\boldsymbol{Z}_{0'}$ looking to the left from the generators, and $\theta_{s'}$ is the complex terminal function of the load $\boldsymbol{Z}_{s'}$. The impedance $\boldsymbol{Z}_{0'}$ may be expressed as follows:

$$\boldsymbol{Z}_{0'} = \boldsymbol{Z}_c \coth (\gamma x' + \theta_{x'}) \tag{2}$$

where $\theta_{x'}$ is the complex terminal function of $\boldsymbol{Z}_{x'}$. By definition

$$\theta_{0'} \equiv \coth^{-1} \frac{\boldsymbol{Z}_{0'}}{\boldsymbol{Z}_c} = \gamma x' + \theta_{x'} \tag{3}$$

If (3) is substituted in (1), the result is

$$\boldsymbol{I}_{z'} = \frac{V_{0'}^{e}}{\boldsymbol{Z}_c} \frac{\sinh (\gamma x' + \theta_{x'}) \sinh (\gamma w' + \theta_{s'})}{\sinh (\gamma s' + \gamma x' + \theta_{x'} + \theta_{s'})} \tag{4}$$

Now let the origin be transferred from 0′ at the generators to the actual left end of the line where the terminating impedance $\boldsymbol{Z}_{x'}$ is located. Let z be measured from this end; let the total length of line be $s = s' + x'$. The distance from the new and unprimed origin to the primed origin locating the generators is $x = x'$; also $\theta_{x'} = \theta_0$, $\theta_{s'} = \theta_s$, $w' = s' - z'$, $w = s - z$, and $V_{0'}^{e} = V_x^e$. With this notation (4) may be expressed as follows:

$$\boldsymbol{I}_z = \frac{V_x^e}{\boldsymbol{Z}_c} \frac{\sinh (\gamma x + \theta_0) \sinh (\gamma w + \theta_s)}{\sinh (\gamma s + \theta_0 + \theta_s)} \qquad x \leqq z \leqq s \tag{5}$$

Similarly

$$\boldsymbol{V}_z = V_x^e \frac{\sinh (\gamma x + \theta_0) \cosh (\gamma w + \theta_s)}{\sinh (\gamma s + \theta_0 + \theta_s)} \qquad x \leqq z \leqq s \tag{6}$$

These relations give current and voltage at any cross section z along a line which is terminated in $\boldsymbol{Z}_0$ at $z = 0$ and in $\boldsymbol{Z}_s$ at $z = s$ and which is driven by a pair of equal and opposite point generators, each of emf $\frac{1}{2}V_x^e$, at $z = x$. The circuit is shown in Fig. 2.1, using the lower scale.

In order to express $\boldsymbol{I}_z$ and $\boldsymbol{V}_z$ at points between $z = 0$ and the generator at $z = x$, it is necessary merely to interchange ends, i.e., substitute $-\boldsymbol{I}_z$ for $\boldsymbol{I}_z$ and $-V_x^e$ for V_x^e. This is equivalent to measuring distances from $\boldsymbol{Z}_s$ instead of from $\boldsymbol{Z}_0$. It also involves a change in subscripts from 0 to s and vice versa in (5) and (6) and the substitution of $y \equiv s - x$ for x and of z for $w \equiv s - z$. (Note that the generators are in series with the

conductors of the line.) The resulting formulas are

$$I_z = \frac{V_x^e}{Z_c} \frac{\sinh(\gamma y + \theta_s)\sinh(\gamma z + \theta_0)}{\sinh(\gamma s + \theta_0 + \theta_s)} \qquad 0 \leqq z \leqq x \tag{7}$$

$$V_z = -V_x^e \frac{\sinh(\gamma y + \theta_s)\cosh(\gamma z + \theta_0)}{\sinh(\gamma s + \theta_0 + \theta_s)} \qquad 0 \leqq z \leqq x \tag{8}$$

Evidently (7) and (8) are formally like (5) and (6). Together with (5) and (6) they define the complex current and voltage at an arbitrary cross section along a line terminated at *both* ends in unrestricted impedances. The line is driven at any cross section x by a pair of equal and opposite point generators or their equivalent, as described in Chap. VI, Sec. 3.

In using (5) and (6) or (7) and (8), note that I_z and V_z depend on *three* independent variables. In (5) and (6) these are the distance x from Z_0 to the generators, the distance $w \equiv s - z$ from Z_s to the point where I_z and V_z are evaluated, and the over-all length s of the line. In (7) and (8), on the other hand, the three variables are the distance $y \equiv s - x$ from Z_s to the generators, the distance z from Z_0 to the point where I_z and V_z are calculated, and the length s of the line.

3. General Expressions for Current and Voltage for an Arbitrarily Terminated Line When Driven by Two Pairs of Equal and Opposite Point Generators (or Their Equivalent) Anywhere along the Line.[80,81] In order to treat various methods of driving a transmission line by driving units coupled anywhere along the line, it is necessary to obtain expressions for I_z and V_z for a line that has two equal and opposite point generators in each line, with the two separated a small distance. The circuit

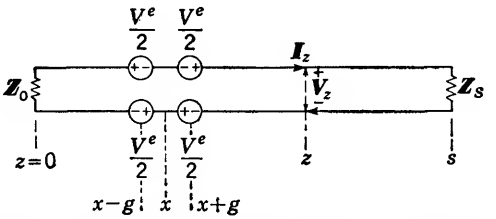


FIG. 3.1. Transmission line driven by two pairs of equal and opposite point generators symmetrically located with respect to an arbitrary point at a distance x from one end of the line.

arrangement is shown in Fig. 3.1. Let the distance from Z_0 to a point on each conductor halfway between each pair of generators be x. Let the distance from this point to each generator be g, so that the coordinates of the generators are $z = x - g$ and $z = x + g$. Each generator is impedanceless and has an emf $\frac{1}{2}V^e$, as in Fig. 3.1.

The current at any point z due to the pair of generators at $x + g$ is given by Sec. 2, Eq. (5), with $x + g$ substituted for x; similarly the cur-

rent due to the pair of generators at $x - g$ is given by Sec. 2, Eq. (5), with $x - g$ substituted for x. The current due to both generators operating simultaneously is the algebraic sum of the currents obtained for each one separately. Using Sec. 2, Eq. (5), and the polarities for the generators shown in Fig. 3.1, the following current is obtained:

$$I_z = \frac{V_x^e}{Z_c} \frac{\sinh(\gamma w + \theta_s)}{\sinh(\gamma s + \theta_0 + \theta_s)} \{\sinh[\gamma(x + g) + \theta_0] - \sinh[\gamma(x - g) + \theta_0]\} \tag{1}$$

After the hyperbolic sines in the braces are expanded using the combinations $\gamma x + \theta_0$ and γg, the following formula is obtained:

$$I_z = \frac{W_x^e}{Z_c} \frac{\cosh(\gamma x + \theta_0) \sinh(\gamma w + \theta_s)}{\sinh(\gamma s + \theta_0 + \theta_s)} \qquad x + g \leqq z \leqq s \tag{2}$$

where

$$W_x^e \equiv 2V^e \sinh \gamma g \tag{3}$$

The corresponding formula for the voltage from Sec. 2, Eq. (6), is

$$V_z = W_x^e \frac{\cosh(\gamma x + \theta_0) \cosh(\gamma w + \theta_s)}{\sinh(\gamma s + \theta_0 + \theta_s)} \qquad x + g \leqq z \leqq s \tag{4}$$

If the same combination is carried out with Sec. 2, Eqs. (7) and (8), the following results are readily derived (note that $x + g$ corresponds to $y - g$ and that $x - g$ corresponds to $y + g$, since by definition $y \equiv s - x$):

$$I_z = -\frac{W_x^e}{Z_c} \frac{\cosh(\gamma y + \theta_s) \sinh(\gamma z + \theta_0)}{\sinh(\gamma s + \theta_0 + \theta_s)} \qquad 0 \leqq z \leqq x - g \tag{5}$$

$$V_z = W_x^e \frac{\cosh(\gamma y + \theta_s) \cosh(\gamma z + \theta_0)}{\sinh(\gamma s + \theta_0 + \theta_s)} \qquad 0 \leqq z \leqq x - g \tag{6}$$

Actually no restrictions have been imposed on the distance $2g$ between the point generators in each conductor. However, the currents and voltages are defined only at points outside the distance $2g$ in (2) and (4) and in (5) and (6). Note that, if g is sufficiently small to satisfy the inequality $|\gamma g|^2 \ll 1$, (3) reduces to

$$W_x^e \doteq 2V^e \gamma g \doteq j2V^e \beta g \tag{7}$$

The last step in (7) implies the inequality $\alpha \ll \beta$. If $2g$ is allowed to become infinitesimally small while V^e is made correspondingly great, W_x^e remains finite.

The general relations (2), (4) and (5), (6) give the current and voltage at any point z along a terminated line that is driven by two pairs of equal and opposite point generators (or their equivalents) symmetrically placed on each side of the point x along the line.

The nature of the discontinuity at the point x in the limit as $2g$ approaches zero, while V^e becomes infinite and W_x^e remains finite, is inter-

esting. As z approaches x from above, (2) and (4) reduce to

$$I_z = \frac{W_x^e}{Z_c} \frac{\cosh(\gamma x + \theta_0) \sinh(\gamma y + \theta_s)}{\sinh(\gamma s + \theta_0 + \theta_s)} \tag{8}$$

$$V_z = W_x^e \frac{\cosh(\gamma x + \theta_0) \cosh(\gamma y + \theta_s)}{\sinh(\gamma s + \theta_0 + \theta_s)} \tag{9}$$

As z approaches x from below, (5) and (6) reduce to

$$I_z = -\frac{W_x^e}{Z_c} \frac{\cosh(\gamma y + \theta_s) \sinh(\gamma x + \theta_0)}{\sinh(\gamma s + \theta_0 + \theta_s)} \tag{10}$$

$$V_z = W_x^e \frac{\cosh(\gamma y + \theta_s) \cosh(\gamma x + \theta_0)}{\sinh(\gamma s + \theta_0 + \theta_s)} \tag{11}$$

It is seen that V_z is continuous while I_z jumps from I_z to $-I_z$ at $z = x$. The discontinuity is readily evaluated to be

$$I_z\ (z \to x \text{ from above}) - I_z\ (z \to x \text{ from below}) = \frac{W_x^e}{Z_c} \tag{12}$$

Thus a discontinuity in V_z by V^e at $x + g$ and by $-V^e$ at $x - g$ with continuous I_z is equivalent, in the limit as g approaches zero, to a continuous V_z and a discontinuity in I_z by W_x^e/Z_c at $z = x$. Physically these mathematical results may be interpreted as follows: The two pairs of equal and opposite point generators tend to set up equal and opposite currents in the conductors of length $2g$ between them. Depending on the impedances in the two directions, one or the other pair may produce a larger current. In this case the equal and opposite generators at the ends of the infinitesimal distance $2g$ are equivalent to a current generator at the center or a line driven by a shunt generator at $z = x$.

4. General Expressions for Current and Voltage for an Arbitrarily Terminated Line When Driven by Three Pairs of Generators (or Their Equivalent) Anywhere along the Line.[80,81] In order to represent analytically asymmetrical driving units coupled to a transmission line, it is necessary to consider a line driven by three pairs of equal and opposite generators symmetrically oriented with respect to the point x, as shown in Fig. 4.1. The total current and voltage maintained by the three pairs

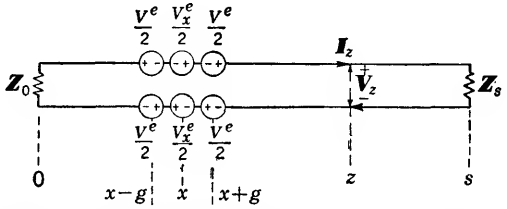


FIG. 4.1. Transmission line driven by three pairs of equal and opposite point generators symmetrically located with respect to an arbitrary point at a distance x from one end of the line.

of generators are obtained by superimposing the solutions obtained in Secs. 2 and 3. The resulting expressions are compactly written using the following shorthand notation:

$$S_m \equiv \sinh(\gamma m + \theta_0) \qquad S_n \equiv \sinh(\gamma n + \theta_s) \tag{1}$$

$$C_m \equiv \cosh(\gamma m + \theta_0) \qquad C_n \equiv \cosh(\gamma n + \theta_s) \tag{2}$$

$$S_s \equiv \sinh(\gamma s + \theta_0 + \theta_s) \tag{3}$$

$$C_s \equiv \cosh(\gamma s + \theta_0 + \theta_s) \tag{4}$$

In (1) and (2) m may stand for x or z, and n stands for y or w. With this notation the expressions for the current and voltage at any point along a transmission line that is driven by three pairs of point generators arranged as in Fig. 4.1 are

$$I_z = \frac{1}{Z_c}\frac{(V_x^e S_x + W_x^e C_x)S_w}{S_s} \qquad x + g \leqq z \leqq s \tag{5}$$

$$V_z = \frac{(V_x^e S_x + W_x^e C_x)C_w}{S_s} \qquad x + g \leqq z \leqq s \tag{6}$$

$$I_z = \frac{1}{Z_c}\frac{(V_x^e S_y - W_x^e C_y)S_z}{S_s} \qquad 0 \leqq z \leqq x - g \tag{7}$$

$$V_z = \frac{(-V_x^e S_y + W_x^e C_y)C_z}{S_s} \qquad 0 \leqq z \leqq x - g \tag{8}$$

As before, z is the distance from Z_0 to the point at which current and voltage are measured; $w \equiv s - z$ is the distance from Z_s at the other end of the line to the same point; x is the distance from Z_0 to the mid-point of the three generators; and $y \equiv s - x$ is the distance from Z_s to the same point. The pair of generators maintaining V_x^e is at x, and the two pairs maintaining W_x^e are located at $x \pm g$.

5. Polar Form of the General Expressions for Current and Voltage. The general expressions for the complex current or voltage at any point along a transmission line when driven by one, two, or three pairs of point generators may be expressed conveniently in polar form introduced in Chap. II, Sec. 9. With $\gamma = \alpha + j\beta$ and $\theta = \rho + j\Phi$, the hyperbolic functions are easily separated into real and imaginary parts. If all phases are referred to V_x^e (which is thus assumed to be real), the formulas for the current and voltage due to *one* pair of generators may be expressed as follows:

$$I_z = \frac{V_x^e}{R_c}\frac{S_x S_w}{S_s}\, e^{j(\sigma_x - \sigma_s + \sigma_w + \phi_c)} \qquad x \leqq z \leqq s \tag{1}$$

$$V_z = V_x^e \frac{S_x C_w}{S_s}\, e^{j(\sigma_x - \sigma_s + \epsilon_w)} \qquad x \leqq z \leqq s \tag{2}$$

$$I_z = \frac{V_x^e}{R_c}\frac{S_y S_z}{S_s}\, e^{j(\sigma_y - \sigma_s + \sigma_z + \phi_c)} \qquad 0 \leqq z \leqq x \tag{3}$$

$$V_z = V_x^e \frac{S_y C_z}{S_s}\, e^{j(\sigma_y - \sigma_s + \epsilon_z + \pi)} \qquad 0 \leqq z \leqq x \tag{4}$$

where

$$S_x = [\sinh^2(\alpha x + \rho_0) + \sin^2(\beta x + \Phi_0)]^{\frac{1}{2}}$$
$$\sigma_x = \tan^{-1}[\tan(\beta x + \Phi_0)\coth(\alpha x + \rho_0)] \tag{5a}$$

$$S_y = [\sinh^2(\alpha y + \rho_s) + \sin^2(\beta y + \Phi_s)]^{\frac{1}{2}}$$
$$\sigma_y = \tan^{-1}[\tan(\beta y + \Phi_s)\coth(\alpha y + \rho_s)] \tag{5b}$$

$$S_w = [\sinh^2(\alpha w + \rho_s) + \sin^2(\beta w + \Phi_s)]^{\frac{1}{2}}$$
$$\sigma_w = \tan^{-1}[\tan(\beta w + \Phi_s)\coth(\alpha w + \rho_s)] \tag{5c}$$

$$S_s = [\sinh^2(\alpha s + \rho_0 + \rho_s) + \sin^2(\beta s + \Phi_0 + \Phi_s)]^{\frac{1}{2}}$$
$$\sigma_s = \tan^{-1}[\tan(\beta s + \Phi_0 + \Phi_s)\coth(\alpha s + \rho_0 + \rho_s)] \tag{5d}$$

$$C_w = [\sinh^2(\alpha w + \rho_s) + \cos^2(\beta w + \Phi_s)]^{\frac{1}{2}}$$
$$\epsilon_w = \tan^{-1}[\tan(\beta w + \Phi_s)\tanh(\alpha w + \rho_s)] \tag{6a}$$

$$C_z = [\sinh^2(\alpha z + \rho_0) + \cos^2(\beta z + \Phi_0)]^{\frac{1}{2}}$$
$$\epsilon_z = \tan^{-1}[\tan(\beta z + \Phi_0)\tanh(\alpha z + \rho_0)] \tag{6b}$$

Note that the subscript on S or C always refers to the variable. The characteristic impedance is

$$\boldsymbol{Z}_c = R_c(1 - j\phi_c) \doteq R_c e^{-j\phi_c} \tag{7}$$

since it is assumed that $\phi_c^2 \ll 1$.

The corresponding expressions for two pairs of point generators are

$$\boldsymbol{I}_z = \frac{\boldsymbol{W}_x^s}{R_c}\frac{C_x S_w}{S_s} e^{j(\epsilon_x - \sigma_s + \sigma_w + \phi_c)} \qquad x + g \leqq z \leqq s \tag{8}$$

$$\boldsymbol{V}_z = \boldsymbol{W}_x^s \frac{C_x C_w}{S_s} e^{j(\epsilon_x - \sigma_s + \epsilon_w)} \qquad x + g \leqq z \leqq s \tag{9}$$

$$\boldsymbol{I}_z = \frac{\boldsymbol{W}_x^s}{R_c}\frac{C_y S_z}{S_s} e^{j(\epsilon_y - \sigma_s + \sigma_z + \phi_c)} \qquad 0 \leqq z \leqq x - g \tag{10}$$

$$\boldsymbol{V}_z = \boldsymbol{W}_x^s \frac{C_y C_z}{S_s} e^{j(\epsilon_y - \sigma_s + \epsilon_z)} \qquad 0 \leqq z \leqq x - g \tag{11}$$

where, in addition to (5*a*,*b*,*c*,*d*) and (6*a*,*b*), the following shorthand symbols are used:

$$C_x = [\sinh^2(\alpha x + \rho_0) + \cos^2(\beta x + \Phi_0)]^{\frac{1}{2}}$$
$$\epsilon_x = \tan^{-1}[\tan(\beta x + \Phi_0)\tanh(\alpha x + \rho_0)] \tag{12}$$

$$C_y = [\sinh^2(\alpha y + \rho_s) + \cos^2(\beta y + \Phi_s)]^{\frac{1}{2}}$$
$$\epsilon_y = \tan^{-1}[\tan(\beta y + \Phi_s)\tanh(\alpha y + \rho_s)] \tag{13}$$

$$S_z = [\sinh^2(\alpha z + \rho_0) + \sin^2(\beta z + \Phi_0)]^{\frac{1}{2}}$$
$$\sigma_z = \tan^{-1}[\tan(\beta z + \Phi_0)\coth(\alpha z + \rho_0)] \tag{14}$$

The polar formulas for current and voltage in a line driven by three pairs of point generators are complicated. They are obtained by adding (1) and (8), (2) and (9), (3) and (10), and (4) and (11) with appropriate phase relations between W_x^s and V_x^s and reducing to polar form. Note that any of the formulas (5), (6), (12), (13), or (14) may be expressed in terms of double arguments using Chap. II, Sec. 9, Eq. (3) or (4), viz.,

$$S = \sqrt{\tfrac{1}{2}(\cosh 2u - \cos 2v)} = \sqrt{\sinh^2 u + \sin^2 v} \tag{15}$$

$$C = \sqrt{\tfrac{1}{2}(\cosh 2u + \cos 2v)} = \sqrt{\sinh^2 u + \cos^2 v} \tag{16}$$

If, in the expressions for $|\boldsymbol{V}_z|$ and $|\boldsymbol{I}_z|$, the over-all length s of a transmission line is varied in such a manner that S_s is the *only* variable factor, the resulting variations in $|\boldsymbol{V}_z|$ and $|\boldsymbol{I}_z|$ are called *resonance curves.* If the single variable is w or z locating the point where $\boldsymbol{V}_z$ and $\boldsymbol{I}_z$ are measured, the resulting variations in $|\boldsymbol{V}_z|$ and $|\boldsymbol{I}_z|$ are called *voltage* or *current distribution curves.* If the location of the driving point x or y is varied with all else constant, the resulting variation in $|\boldsymbol{V}_z|$ or $|\boldsymbol{I}_z|$ at an arbitrary fixed point z is called a *driving-point distribution curve.* These three types of curves, corresponding to variations in s alone, w or z alone, and x or y alone, are considered in Sec. 7. Note that $w \equiv s - z$ and $y \equiv s - x$.

6. The Transfer of Power along a Transmission Line.[81] One of the principal functions of a transmission line is to transfer power from a generator to a load. Let it be assumed that the source of power is equivalent to one pair of point generators at a point $z = x$ on a transmission line that is terminated in a load impedance† $\boldsymbol{Z}_s$ at $z = s$. The time-average power transferred to the section of line of length $s - z$ and its termination $\boldsymbol{Z}_s$ is

$$P_z = \text{Re } \tfrac{1}{2}\boldsymbol{V}_z\boldsymbol{I}_z^* \tag{1}$$

where $\boldsymbol{V}_z$ is the complex (peak) voltage and $\boldsymbol{I}_z^*$ is the complex conjugate of the (peak) current at the point z on the line. These quantities are given by Sec. 2, Eqs. (5) and (6), or by Sec. 5, Eqs. (1) and (2). The desired formula for power is obtained from (1) using Sec. 2, Eqs. (5) and (6), by expressing the hyperbolic functions involving the variables x and s in polar form, as in Sec. 5. The desired forms are

$$\boldsymbol{I}_z = \frac{\boldsymbol{V}_x^e S_x}{\boldsymbol{Z}_c S_s}[\sinh(\gamma w + \boldsymbol{\theta}_s)]e^{j(\sigma_x - \sigma_s)} \tag{2}$$

$$\boldsymbol{V}_z = \boldsymbol{V}_x^e \frac{S_z}{S_s}[\cosh(\gamma w + \boldsymbol{\theta}_s)]e^{j(\sigma_x - \sigma_s)} \tag{3}$$

The substitution of (2) and (3) in (1) gives

$$\frac{1}{2}\boldsymbol{V}_z\boldsymbol{I}_z^* = \frac{1}{2}\frac{(\boldsymbol{V}_x^e)^2 S_x^2}{\boldsymbol{Z}_c^* S_s^2}\sinh(A_w - jF_w)\cosh(A_w + jF_w) \tag{4}$$

where $A_w \equiv \alpha w + \rho_s$ and $F_w \equiv \beta w + \Phi_s$. Since $\boldsymbol{Z}_c = R_c(1 - j\phi_c)$ and

$$\sinh(A_w - jF_w)\cosh(A_w + jF_w) = \tfrac{1}{2}(\sinh 2A_w - j \sin 2F_w) \tag{5}$$

the time-average power transferred to the line at a distance w from the load is

$$P_z = \frac{(\boldsymbol{V}_x^e)^2}{4R_c}\frac{S_x^2}{S_s^2}[\sinh 2(\alpha w + \rho_s) - \phi_c \sin 2(\beta w + \Phi_s)] \tag{6}$$

† Terminal-zone effects are assumed negligible for the sake of simplicity. If they are significant, the apparent terminal impedance $\boldsymbol{Z}_{sa}$ must replace $\boldsymbol{Z}_s$.

The power in the load at $z = s$ is given by (6) with $w = 0$. It is†

$$P_s = \frac{(V_x^e)^2}{4R_c}\frac{S_x^2}{S_s^2}(\sinh 2\rho_s - \phi_c \sin 2\Phi_s) \tag{7}$$

The power in the line and load is given by (6) with $z = x$ or $w = s - x$. It is

$$P_x = \frac{(V_x^e)^2}{4R_c}\frac{S_x^2}{S_s^2}[\sinh 2(\alpha s - \alpha x + \rho_s) - \phi_c \sin 2(\beta s - \beta x + \Phi_s)] \tag{8}$$

The ratio of the power in the load to the power in the line and load is the efficiency. It is

$$W = \frac{P_s}{P_x} = \frac{\sinh 2\rho_s - \phi_c \sin 2\Phi_s}{\sinh 2(\alpha s - \alpha x + \rho_s) - \phi_c \sin 2(\beta s - \beta x + \Phi_s)} \tag{9}$$

When the generator is at the end of the line ($x = 0$), as is usual, the power ratio is

$$W = \frac{P_s}{P_0} = \frac{\sinh 2\rho_s - \phi_c \sin 2\Phi_s}{\sinh 2(\alpha s + \rho_s) - \phi_c \sin 2(\beta s + \Phi_s)} \tag{10}$$

On low-loss lines ϕ_c is of the order of magnitude of 10^{-3} or 10^{-4}. If $\sinh 2\rho_s$ is large compared with this value, as is usual if $\boldsymbol{Z}_s$ is a dissipative impedance, the ratio reduces to the simple form

$$W = \frac{P_s}{P_0} \doteq \frac{\sinh 2\rho_s}{\sinh 2(\alpha s + \rho_s)} \tag{11}$$

The ratio of the power P_L dissipated in the line to the total power transferred to the line is

$$\frac{P_L}{P_0} = 1 - \frac{P_s}{P_0} \doteq 1 - \frac{\sinh 2\rho_s}{\sinh 2(\alpha s + \rho_s)} \tag{12}$$

The *insertion loss* in the line is defined in terms of the ratio of the power

† Note that in order to dissipate no power in the load, $P_s = 0$, it is necessary that $\sinh 2\rho_s = \phi_c \sin 2\Phi_s$. Suppose the termination consists of a small inductive impedance $R_s + j\omega L_s$ such as a wire bridge with $\Phi_s = \beta k_s + \pi/2$ and $\rho_s = \alpha(m_s - k_s)$, where $k_s = L_s/l$ and $m_s = R_s/r^i = 0$ for no dissipation. Since ρ_s is small, $P_s = 0$ in (7) reduces to $\rho_s = -\alpha k_s$; also $\Gamma_s = e^{-2\rho_s} = e^{2\alpha k_s}$. Note that ρ_s is negative and that Γ_s is *greater* than 1. Even if m_s is not zero but sufficiently small so that it is less than k_s, ρ_s is still negative and Γ_s greater than 1, as discussed in Chap. II, Sec. 22. Alternatively, if $\rho_s = 0$ and $\Gamma_s = 1$, $k_s = m_s$ and the power to the load is

$$P_s = \frac{(V_x^e)^2 S_x^2}{4R_c S_s^2}\frac{2\alpha R_s}{r^i}$$

Thus a reflection coefficient of unity is strictly not possible with an ideal dissipationless termination if this is a small inductive reactance and the line itself is dissipative. On most low-loss lines ϕ_c is sufficiently small so that the reflection coefficient can exceed unity by only an extremely small amount.

to the load without the line ($s = 0$) to the power to the load with the line.

$$L \text{ (db)} = 10 \log \frac{P_0}{P_s} \doteq 10 \log \frac{\sinh 2(\alpha s + \rho_s)}{\sinh 2\rho_s} \tag{13}$$

The convenience and obvious significance of the terminal function ρ_s are evident in (9) to (13).

Optimum Termination. The optimum termination *minimizes* the losses on the line and maximizes the efficiency. The condition for maximum efficiency is

$$\frac{\partial W}{\partial \rho_s} = 0 \tag{14}$$

If this differentiation is carried out using (11), the resulting condition is

$$\tanh 2(\alpha s + \rho_s) = \tanh 2\rho_s \tag{15}$$

For a line that is not lossless, $\alpha s > 0$, so that (15) can be satisfied only when

$$\rho_s = \infty \qquad \boldsymbol{Z}_s = \boldsymbol{Z}_c \tag{16}$$

This is the condition for maximum efficiency. With (16), (11) becomes

$$W\ (\rho_s = \infty) = \lim_{\rho_s \to \infty} \frac{\sinh 2\rho_s}{\sinh 2(\alpha s + \rho_s)} = \lim_{\rho_s \to \infty} \frac{e^{2\rho_s}}{e^{2(\alpha s + \rho_s)}} = e^{-2\alpha s} \tag{17}$$

The corresponding minimum insertion loss is

$$L \text{ (db)} = 10 \log e^{2\alpha s} = 8.686 \alpha s \tag{18}$$

where α is the attenuation constant in nepers per meter. Note that (16) is the condition for a matched line, so that (17) and (18) coincide with Sec. 1, Eqs. (6) and (8).

If the impedance $\boldsymbol{Z}_s$ terminating the line is predominantly resistive and, in addition, differs considerably from the characteristic resistance R_c of the line, it is shown in Chap. II, Sec. 18, that

For $R_s < R_c$, $\qquad \rho_s \doteq \dfrac{R_s}{R_c} \qquad \rho_s^2 \ll 3$ (19*a*)

For $R_s > R_c$, $\qquad \rho_s \doteq \dfrac{R_c}{R_s} \qquad \rho_s^2 \ll 3$ (19*b*)

If the over-all attenuation is no greater than ρ_s in (19*a*,*b*), the following condition is satisfied:

$$(\alpha s + \rho_s)^2 \ll 3 \tag{20}$$

so that the hyperbolic sines in (11) may be replaced by their arguments. With (20) and (19*a*,*b*), (11) becomes

$$W = \frac{P_s}{P_0} \doteq \frac{\rho_s}{\alpha s + \rho_s} = \begin{cases} \left(1 + \dfrac{R_s}{R_c}\,\alpha s\right)^{-1} & R_s < R_c \\ \left(1 + \dfrac{R_c}{R_s}\,\alpha s\right)^{-1} & R_c < R_s \end{cases} \tag{21}$$

so that the power (insertion) loss in decibels subject to (19*a*,*b*) and (20) is

$$L \text{ (db)} \doteq 10 \log \left(1 + \frac{R_s}{R_c} \alpha s\right) \qquad R_s < R_c \tag{22a}$$

$$L \text{ (db)} \doteq 10 \log \left(1 + \frac{R_c}{R_s} \alpha s\right) \qquad R_c < R_s \tag{22b}$$

A graphical representation is given in Fig. 6.1 of the power loss L (db) as a function of line length in a typical transmission line when matched and when terminated in a pure resistance that is considerably smaller

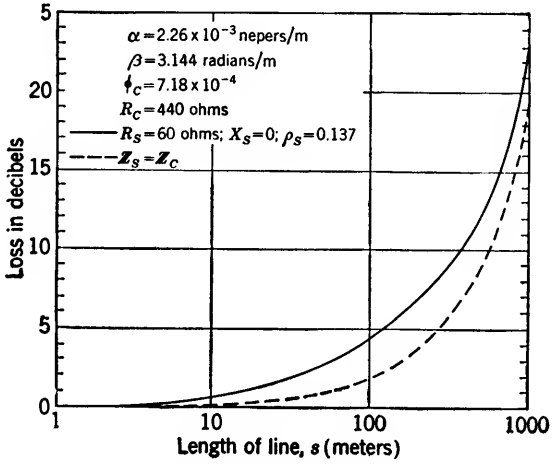


FIG. 6.1. Power loss in a matched line and in a line that is not matched.

than the characteristic resistance. For the case represented, it is evident that, if the line is short (5 m or less), the line loss is negligible, so that little is gained by using a matching network. On the other hand, for a line that is long enough so that line loss is significant, it is essential to match the load with an appropriate network if good efficiency is to be maintained.

7. Resonance Curves and the Condition for Resonance.[8,78,81] The magnitudes of the voltage and current at a distance w from an impedance $\boldsymbol{Z}_s$ at $z = s$ or $w = 0$ due to generators located at a distance x from $\boldsymbol{Z}_0$ at $z = 0$ are given by the following expressions:

$$V_z = V_x^e \frac{S_x C_w}{S_s} \qquad I_z = \frac{V_x^e}{R_c} \frac{S_x S_w}{S_s} \tag{1}$$

If the length s of the line is the only variable, while the distance w of the detector from $\boldsymbol{Z}_s$ and the distance x of the generators from $\boldsymbol{Z}_0$ are kept

constant,†

$$V_s(s) \sim I_s(s) \sim S_s^{-1} = [\sinh^2(\alpha s + \rho_0 + \rho_s) + \sin^2(\beta s + \Phi_0 + \Phi_s)]^{-\frac{1}{2}} \quad (2)$$

Thus the function S_s^{-1} characterizes the dependence of both V_s and I_s on the length of the line. This function, when plotted against βs, is called a *resonance curve.* A transmission line with its two terminations Z_0 and Z_s is said to be *resonant* when S_s^{-1} has its maximum value.

With the notation

$$A_s \equiv \alpha s + \rho_0 + \rho_s \qquad F_s \equiv \beta s + \Phi_0 + \Phi_s \quad (3)$$

the conditions determining the extreme values of S_s^{-1} with respect to changes in s are obtained by differentiating (2) with respect to s and equating the result to zero. The following equation is obtained:

$$(\cosh 2A_s - \cos 2F_s)^{-\frac{3}{2}}(\alpha \sinh 2A_s + \beta \sin 2F_s) = 0 \quad (4a)$$

Since $\cosh 2A_s$ always exceeds unity, the only possible roots are defined by

$$-\sin 2F_s = \frac{\alpha}{\beta} \sinh 2A_s \quad (4b)$$

This leads to the following extremizing values of F_s:

$$F_s = \frac{2n+1}{2}\pi + \tfrac{1}{2}\sin^{-1}\left(\frac{\alpha}{\beta}\sinh 2A_s\right)$$
for minimum S_s^{-1} and $n = 0, 1, 2, \ldots$ (5a)

$$F_s = n\pi - \tfrac{1}{2}\sin^{-1}\left(\frac{\alpha}{\beta}\sinh 2A_s\right)$$
for maximum S_s^{-1} and $n = 0, 1, 2, \ldots$ (5b)

These cannot be solved readily for s unless A_s is small. However, if A_s is small, so that

$$A_s^2 \ll 1 \qquad \sinh 2A_s \doteq 2A_s \quad (6)$$

it follows that

$$\tfrac{1}{2}\sin^{-1}\left(\frac{\alpha}{\beta}\sinh 2A_s\right) \doteq \frac{\alpha}{\beta} A_s \ll 1 \quad (7)$$

With (7), (5a) becomes

$$F_s \equiv \beta s + \Phi_0 + \Phi_s = \frac{2n+1}{2}\pi + \frac{\alpha}{\beta}(\alpha s + \rho_0 + \rho_s)$$
for minimum S_s^{-1} (8a)

A similar expression is obtained for (5b). Since it is assumed that the

† Note that changing s by moving Z_s (or Z_0) requires that the detector (or the generator) be moved in tandem.

condition $\alpha^2/\beta^2 \ll 1$ is satisfied, it follows that (5*a*) and (5*b*) become

$$F_s \equiv \beta s + \Phi_0 + \Phi_s = \frac{2n+1}{2}\pi + \frac{\alpha}{\beta}(\rho_0 + \rho_s) \qquad \text{for minimum } S_s^{-1} \quad (8b)$$

$$F_s \equiv \beta s + \Phi_0 + \Phi_s = n\pi - \frac{\alpha}{\beta}(\rho_0 + \rho_s) \qquad \text{for maximum } S_s^{-1} \quad (8c)$$

Whenever the condition

$$\frac{\alpha}{\beta}(\rho_0 + \rho_s) \ll 1 \tag{9}$$

is satisfied, the following expressions are valid:

$$F_s \equiv \beta s + \Phi_0 + \Phi_s \doteq \frac{2n+1}{2}\pi$$

for $n = 0, 1, 2, \ldots$ and S_s^{-1} a minimum (10*a*)

$$F_s \equiv \beta s + \Phi_0 + \Phi_s \doteq n\pi$$

for $n = 0, 1, 2, \ldots$ and S_s^{-1} a maximum (10*b*)

The condition (10*b*) maximizing S_{si}^{-1} is called the *condition for resonance.*

Note that the angle σ_s in $\boldsymbol{S}_s = S_s e^{j\sigma_s}$ has the following values:

$$\sigma_s \equiv \tan^{-1}(\tan F_s \coth A_s) = \begin{cases} \dfrac{\pi}{2} & \text{for minimum } S_s^{-1} \\ 0 & \text{for maximum } S_s^{-1} \end{cases} \tag{11}$$

The extreme values of S_s^{-1} are

$$(S_s^{-1})_{\min} = \frac{1}{\cosh A_s} = \frac{1}{\cosh(\alpha s + \rho_0 + \rho_s)} \qquad \beta s_{\min} + \Phi_0 + \Phi_s = \frac{2n+1}{2}\pi$$

$$n = 0, 1, 2, \ldots \quad (12a)$$

$$(S_s^{-1})_{\max} = \frac{1}{\sinh A_s} = \frac{1}{\sinh(\alpha s + \rho_0 + \rho_s)} \qquad \beta s_{\max} + \Phi_0 + \Phi_s = n\pi$$

$$n = 0, 1, 2, \ldots \quad (12b)$$

Among the special cases the following are important:

$$(\alpha s + \rho_0 + \rho_s)^2 \ll 1 \qquad (S_s^{-1})_{\min} \doteq 1 \qquad (S_s^{-1})_{\max} \doteq \frac{1}{\alpha s_{\max} + \rho_0 + \rho_s} \tag{13}$$

$$\rho_0 + \rho_s \gg \alpha s \qquad (S_s^{-1})_{\min} \doteq \frac{1}{\cosh(\rho_0 + \rho_s)} \qquad (S_s^{-1})_{\max} \doteq \frac{1}{\sinh(\rho_0 + \rho_s)} \tag{14}$$

Note that in (14) the extreme values are independent of s.

The general shape of the resonance curves for low over-all attenuation ($A_s^2 \ll 1$) is obtained readily from (2) if it is noted that, except near resonance where $F_s \equiv \beta s + \Phi_0 + \Phi_s = n\pi$,

$$S_s^{-1} \doteq |\csc F_s| \qquad \sinh^2 A_s \ll \sin^2 F_s \tag{15}$$

It follows that the resonance curve is a cosecant curve limited by the bounding curves csch A and sech A, as shown in Fig. 7.1 for a line with

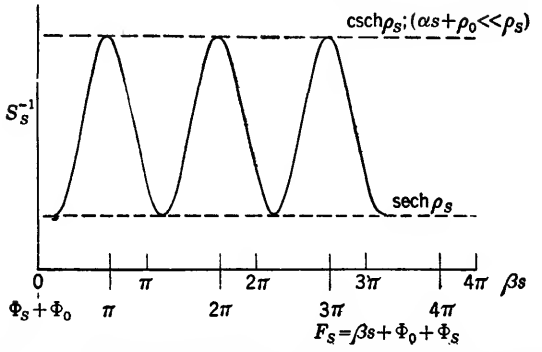


FIG. 7.1. Resonance curves (qualitative) for a line with negligible losses in the line and in the generator; $\alpha s + \rho_0 \ll \rho_s$.

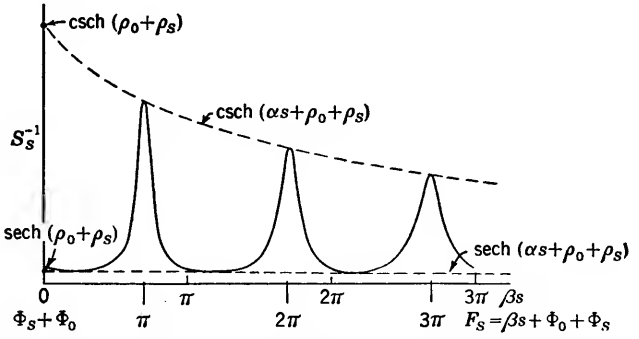


FIG. 7.2. Resonance curves (qualitative) for a moderately damped line.

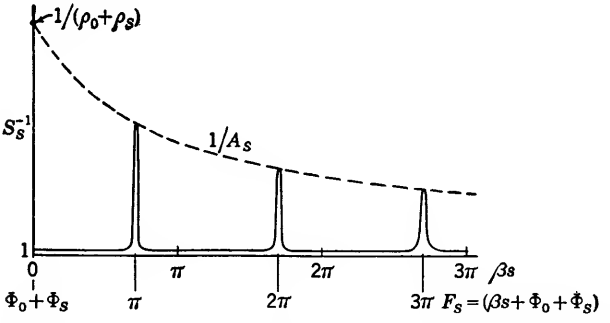


FIG. 7.3. Resonance curves (qualitative) for a line with low over-all attenuation.

negligible losses in the line and generator, in Fig. 7.2 for a line with moderate over-all attenuation, and in Fig. 7.3 for a line in which the over-all attenuation is small.

8. Distribution Curves.[8,78,81] The variation of the voltage and current along a fixed transmission line may be expressed as a function of the distance $w \equiv s - z$ from the load impedance Z_s. The formulas for

the magnitudes of the voltage and current distribution functions are

$$V_z(w) \sim C_w = [\sinh^2 (\alpha w + \rho_s) + \cos^2 (\beta w + \Phi_s)]^{\frac{1}{2}} \quad (1)$$
$$I_z(w) \sim S_w = [\sinh^2 (\alpha w + \rho_s) + \sin^2 (\beta w + \Phi_s)]^{\frac{1}{2}} \quad (2)$$

An alternative formula for $V_z(w)$ which is like that for $I_z(w)$ is readily obtained if the terminal function $\Phi'_s = \Phi_s - \pi/2$ is introduced in (1). The result is

$$V_z(w) \sim S'_w = [\sinh^2 (\alpha w + \rho_s) + \sin^2 (\beta w + \Phi'_s)]^{\frac{1}{2}} \quad (3)$$

Evidently the voltage varies in just the same manner as the current, but the distribution is shifted along the line an electrical distance $\pi/2$ with respect to the current. Distributions of the voltage and current as defined by (1) and (2) or (3) and (2) may be observed in practice by moving a loosely coupled voltage or current detector along the line while all other quantities are kept constant.

The variations of the magnitudes of the voltage and current at a given *fixed* point z along a transmission line, as the location x of one pair of equal and opposite point generators (or their equivalent) is changed, are expressed as follows, using Sec. 5, Eqs. (1) and (2):

$$V_z(x) \sim I_z(x) \sim S_x = [\sinh^2 (\alpha x + \rho_0) + \sin^2 (\beta x + \Phi_0)]^{\frac{1}{2}} \quad (4)$$

Note that (4) implies $x \leqq z \leqq s$ and that x is the only variable, with all other quantities constant. This may be accomplished in practice by moving a loosely coupled oscillator or coupling unit parallel to the line while the voltage or current is read from a stationary detector.

If two pairs of equal and opposite generators symmetrically located with respect to the point x are moved, the voltage and current at the fixed point z (with $x \leqq z \leqq s$) vary as follows, using Sec. 5, Eqs. (8) and (9):

$$V_z(x) \sim I_z(x) \sim C_x = [\sinh^2 (\alpha x + \rho_0) + \cos^2 (\beta x + \Phi_0)]^{\frac{1}{2}} \quad (5)$$

Alternatively, in terms of $\Phi'_0 = \Phi_0 - \pi/2$,

$$V_z(x) \sim I_z(x) \sim S'_x = [\sinh^2 (\alpha x + \rho_0) + \sin^2 (\beta x + \Phi'_0)]^{\frac{1}{2}} \quad (6)$$

Plots of the functions S_w and $C_w = S'_w$ against βw or of S_x and $C_x = S'_x$ against βx are called *distribution curves.*

With appropriate changes in variables and parameters, the functions S_w, S'_w, S_x, and S'_x are essentially the reciprocals of S_s^{-1}. Therefore the extreme values are obtained directly from the analysis of S_s^{-1} in Sec. 7. For current and voltage they are

$$[I_z(w)]_{\max} \sim (S_w)_{\max} = \cosh (\alpha w + \rho_s) \quad \text{when } \beta w + \Phi_s = \frac{2n+1}{2}\pi \quad (7a)$$
$$[I_z(w)]_{\min} \sim (S_w)_{\min} = \sinh (\alpha w + \rho_s) \quad \text{when } \beta w + \Phi_s = n\pi \quad (7b)$$

$$[V_z(w)]_{\max} \sim (S'_w)_{\max} = \cosh(\alpha w + \rho_s) \quad \text{when } \beta w + \Phi'_s = \frac{2n+1}{2}\pi \tag{8a}$$

$$[V_z(w)]_{\min} \sim (S'_w)_{\min} = \sinh(\alpha w + \rho_s) \quad \text{when } \beta w + \Phi'_s = n\pi \tag{8b}$$

where $n = 0, 1, 2, \ldots$.

For one pair of point generators at x,

$$[I_z(x)]_{\max} \sim [V_z(x)]_{\max} \sim (S_x)_{\max} = \cosh(\alpha x + \rho_0) \quad \text{when } \beta x + \Phi_0 = \frac{2n+1}{2}\pi \tag{9a}$$

$$[I_z(x)]_{\min} \sim [V_z(x)]_{\min} \sim (S_x)_{\min} = \sinh(\alpha x + \rho_0) \quad \text{when } \beta x + \Phi_0 = n\pi \tag{9b}$$

For two pairs of point generators symmetrically spaced about x,

$$[I_z(x)]_{\max} \sim [V_z(x)]_{\max} \sim (S'_x)_{\max} = \cosh(\alpha x + \rho_0) \quad \text{when } \beta x + \Phi'_0 = \frac{2n+1}{2}\pi \tag{10a}$$

$$[I_z(x)]_{\min} \sim [V_z(x)]_{\min} \sim (S'_x)_{\min} = \sinh(\alpha x + \rho_0) \quad \text{when } \beta x + \Phi'_0 = n\pi \tag{10b}$$

The general shapes of the distribution curves for low over-all attenuation are given by

$$C_w = S'_w \doteq |\sin(\beta w + \Phi'_s)| \quad \sinh^2(\alpha w + \rho_s) \ll \sin^2(\beta w + \Phi'_s) \tag{11a}$$

$$S_w \doteq |\sin(\beta w + \Phi_s)| \quad \sinh^2(\alpha w + \rho_s) \ll \sin^2(\beta w + \Phi_s) \tag{11b}$$

$$C_x = S'_x \doteq |\sin(\beta x + \Phi'_0)| \quad \sinh^2(\alpha x + \rho_0) \ll \sin^2(\beta x + \Phi'_0) \tag{12a}$$

$$S_x \doteq |\sin(\beta x + \Phi_0)| \quad \sinh^2(\alpha x + \rho_0) \ll \sin^2(\beta x + \Phi_0) \tag{12b}$$

The nature of the distribution curves S_w and $C_w = S'_w$ for the current and voltage may be seen in Fig. 8.1. Note that $\beta w = \beta(s - z)$ is scaled to increase from left to right.

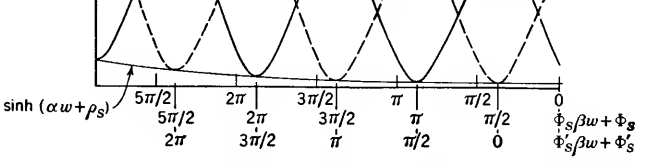


FIG. 8.1. Current and voltage distributions along a transmission line.

9. Resonance-curve and Distribution-curve Ratios; the Standing-wave Ratio.[8,78,81] Quantities that are useful in various transmission-line measurements are the ratios of maximum values of resonance or distribution curves to adjacent minima. For lines with low over-all attenuation

the maxima of resonance curves and the minima of distribution curves are very sharp, whereas the minima of resonance curves and the maxima of distribution curves are broad. This behavior is readily understood if it is recalled that the expression for distribution curves is formally the reciprocal of the expression for resonance curves in terms of the appropriate variables. For lines with a dissipative load both resonance-curve maxima and distribution-curve minima are broad.

The ratio of the maximum of a resonance curve to an adjacent minimum is obtained directly from Sec. 7, Eqs. (12*a*,*b*). Thus

$$R = \frac{(S_s^{-1})_{\max}}{(S_s^{-1})_{\min}} = \frac{\cosh(\alpha s_{\min} + \rho_0 + \rho_s)}{\sinh(\alpha s_{\max} + \rho_0 + \rho_s)} \tag{1}$$

where

$$s_{\max} = \frac{n\pi - \Phi_0 - \Phi_s}{\beta} \qquad n = 0, 1, 2, \ldots \tag{2a}$$

$$s_{\min} = s_{\max} \pm \frac{\lambda}{4} \tag{2b}$$

If the attenuation constant α of the line is sufficiently small so that

$$\frac{\alpha\lambda}{4} \ll \alpha s_{\max} + \rho_0 + \rho_s \tag{3}$$

(1) reduces to

$$R = \frac{(S_s^{-1})_{\max}}{(S_s^{-1})_{\min}} \doteq \coth(\alpha s_{\max} + \rho_0 + \rho_s) \tag{4}$$

If $\alpha s_{\max}$ is small compared with ρ_s, as is usual, it follows that

$$\alpha s_{\max} \ll \rho_0 + \rho_s \tag{5}$$

so that

$$\frac{(S_s^{-1})_{\max}}{(S_s^{-1})_{\min}} \doteq \coth(\rho_0 + \rho_s) \tag{6}$$

Finally, if it is correct to set

$$\rho_0 \ll \rho_s \tag{7}$$

it follows that

$$\frac{(S_s^{-1})_{\max}}{(S_s^{-1})_{\min}} \doteq \coth \rho_s \equiv S = SWR \tag{8}$$

The quantity $S \equiv \coth \rho_s$ is known as the *standing-wave ratio.*† It is customarily defined in terms of the distribution curves of current and voltage rather than in terms of resonance curves. This is carried out in the following.

The ratio of any given current maximum along a transmission line to an adjacent minimum is obtained directly from Sec. 8, Eqs. (7*a*,*b*). It is

$$\frac{[I_z(w)]_{\max}}{[I_z(w)]_{\min}} = \frac{(S_w)_{\max}}{(S_w)_{\min}} = \frac{\cosh(\alpha w_{\max} + \rho_s)}{\sinh(\alpha w_{\min} + \rho_s)} \tag{9}$$

† The letter S without subscript or with subscript V or I is used for the standing-wave ratio. S with subscript s, w, x, etc., is an amplitude as in Sec. 8, Eq. (2).

where $$w_{max} = \frac{[(2n + 1)/2]\pi - \Phi_s}{\beta} \qquad n = 0, 1, \ldots \tag{10a}$$

$$w_{min} = w_{max} \pm \frac{\lambda}{4} \tag{10b}$$

Subject to the condition

$$\frac{\alpha\lambda}{4} \ll \alpha w_{max} + \rho_s \tag{11a}$$

it follows that (9) may be expressed in the form

$$\frac{[I_z(w)]_{max}}{[I_z(w)]_{min}} = \frac{(S_w)_{max}}{(S_w)_{min}} \doteq \coth\ (\alpha w_{max} + \rho_s) \tag{11b}$$

The attenuation constant of most low-loss lines is sufficiently small so that, when the line is loaded, the following conditions are satisfied:

$$\rho_s \gg \alpha w_{max} \qquad \rho_s \gg \alpha w_{min} \tag{12}$$

In this case the ratio in (11*b*) reduces to a constant. Thus

$$\frac{[I_z(w)]_{max}}{[I_z(w)]_{min}} \doteq \coth \rho_s \equiv S_I \tag{13}$$

where the quantity S_I is the current *standing-wave ratio* for the section of line between the generator and $\boldsymbol{Z}_s$. The voltage standing-wave ratio is obtained in the same manner. Subject to (13) it is

$$\frac{[V_z(w)]_{max}}{[V_z(w)]_{min}} = \frac{(S'_w)_{max}}{(S'_w)_{min}} = \coth \rho_s \equiv S_V \tag{14}$$

Note that subject to (12) the standing-wave ratio of the current and voltage distribution curves depends only on the terminal function ρ_s, so that

$$S_V = S_I = S \tag{15}$$

The ratio of the maximum current at z to the minimum current at the *same* point, as obtained by moving the generators, has the following value for *one pair* of equal and opposite point generators at x:

$$\frac{[I_z(x)]_{max}}{[I_z(x)]_{min}} = \frac{(S_x)_{max}}{(S_x)_{min}} = \frac{\cosh\ (\alpha x_{max} + \rho_0)}{\sinh\ (\alpha x_{min} + \rho_0)} \tag{16}$$

Subject to the condition

$$\rho_0 \gg \alpha x_{max} \qquad \rho_0 \gg \alpha x_{min} \tag{17}$$

which requires that the attenuation of the section of line of length x_{max} or x_{min} be negligibly small compared with the attenuation of the generator, (16) reduces to

$$\frac{[V_z(x)]_{max}}{[V_z(x)]_{min}} = \frac{[I_z(x)]_{max}}{[I_z(x)]_{min}} = \frac{(S_w)_{max}}{(S_w)_{min}} \doteq \coth \rho_0 \equiv S_1 \tag{18}$$

For two pairs of equal and opposite generators, the corresponding ratio is

$$\frac{[V_z(x)]_{\max}}{[V_z(x)]_{\min}} = \frac{[I_z(x)]_{\max}}{[I_z(x)]_{\min}} = \coth \rho_0 \equiv S_2 \tag{19}$$

Evidently (18) and (19) are the standing-wave ratios for the section of line between the generators symmetrically placed with respect to x and Z_0.

The standing-wave ratio usually is most easily measured from the current or voltage distribution curves using (13) or (14). But the other methods also serve their purposes in special circumstances. A curve of the standing-wave ratio as a function of the terminal attenuation ρ_s is shown in Fig. 9.1.

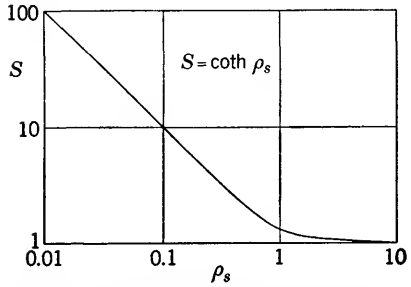


FIG. 9.1. Standing-wave ratio as a function of the terminal function ρ_s.

The standing-wave ratio has a particularly simple form if the terminal impedance $\boldsymbol{Z}_s$ is predominantly resistive, so that, as defined in Chap. II, Sec. 18, $x_{1s} = 0$ and

$$\rho_s = \tanh^{-1} r_{1s} \qquad \text{for } r_{1s} \leqq 1 \tag{20a}$$

$$\rho_s = \tanh^{-1} g_{1s} \qquad \text{for } g_{1s} \leqq 1 \tag{20b}$$

where $g_{1s} = 1/r_{1s} = R_c/R_s$. Since $\rho_s = \coth^{-1} S$, it follows that

$$r_{1s} = \tanh \rho_s = \tanh (\coth^{-1} S) \tag{21a}$$

$$g_{1s} = \frac{1}{r_{1s}} = S \qquad \text{for } r_1 \leqq 1 \tag{21b}$$

Similarly

$$g_{1s} = \tanh \rho_s = \tanh (\coth^{-1} S) \tag{22a}$$

$$r_{1s} = \frac{1}{g_{1s}} = S \qquad \text{for } r_1 \geqq 1 \tag{22b}$$

For lines with low attenuation, so that terms with the distortion factor ϕ_c as coefficient are negligible,

$$r_{1s} \doteq \frac{R_s}{R_c} \doteq S \qquad \text{for } R_s \geqq R_c \tag{23a}$$

$$g_{1s} \doteq \frac{R_c}{R_s} \doteq S \qquad \text{for } R_s \leqq R_c \tag{23b}$$

These are simple and useful formulas.

10. Distributions of Current and Voltage in a Resonant Line; Components of Current and Voltage. The distribution curves discussed in Sec. 8 and pictured in Fig. 8.1 represent the *magnitude* of the current and voltage. Also of interest are the *components* that are in phase with the

emf of the generator and in phase quadrature with it. For simplicity let the line be driven by a single pair of point generators (or their equivalent) at $z = 0$, so that $x = 0$ in the general formulas of Sec. 2. The expressions for current and voltage are

$$V_z = V_0^e \frac{\sinh \theta_0 \cosh (\gamma w + \theta_s)}{\sinh (\gamma s + \theta_0 + \theta_s)} \equiv \bar{V}_s \cosh (\gamma w + \theta_s) \tag{1}$$

$$I_z = \frac{V_0^e}{Z_c} \frac{\sinh \theta_0 \sinh (\gamma w + \theta_s)}{\sinh (\gamma s + \theta_0 + \theta_s)} \equiv \frac{\bar{V}_s}{Z_c} \sinh (\gamma w + \theta_s) \tag{2}$$

where $\bar{V}_s$ is as defined in (1) and (2). For convenience let it be assumed that the impedance of the generator is a pure resistance $Z_0 = R_0$, which is much smaller than R_c. Then

$$R_0 \ll R_c \qquad \rho_0 \doteq \frac{R_0}{R_c} \ll 1 \qquad \Phi_0 = \frac{\pi}{2} \tag{3}$$

and

$$\sinh \theta_0 = \sinh (\rho_0 + j\Phi_0) = j \cosh \rho_0 \tag{4}$$

Let the circuit be tuned to resonance so that

$$\beta s + \Phi_0 + \Phi_s = n\pi \qquad n \text{ odd} \tag{5}$$

Then

$$\sinh (\gamma s + \theta_0 + \theta_s) = -\sinh (\alpha s + \rho_0 + \rho_s) \tag{6}$$

Hence, expanding $\cosh (\gamma w + \theta_s)$ and $\sinh (\gamma w + \theta_s)$,

$$V_z = V_0^e \frac{-j \cosh \rho_0}{\sinh (\alpha s + \rho_0 + \rho_s)} [\cosh (\alpha w + \rho_s) \cos (\beta w + \Phi_s) + j \sinh (\alpha w + \rho_s) \sin (\beta w + \Phi_s)] \tag{7}$$

$$I_z = \frac{V_0^e}{R_c(1 - j\phi_c)} \frac{-j \cosh \rho_0}{\sinh (\alpha s + \rho_0 + \rho_s)} [\sinh (\alpha w + \rho_s) \cos (\beta w + \Phi_s) + j \cosh (\alpha w + \rho_s) \sin (\beta w + \Phi_s)] \tag{8}$$

Let the following notation be introduced:

$$A_w \equiv \alpha w + \rho_s \qquad F_w \equiv \beta w + \Phi_s \tag{9}$$

From (1) and (2) and with (4) and (6) it follows that

$$\bar{V}_s \equiv V_0^e \frac{\sinh \theta_0}{\sinh (\gamma s + \theta_0 + \theta_s)} = V_0^e \frac{-j \cosh \rho_0}{\sinh (\alpha s + \rho_0 + \rho_s)} \tag{10}$$

Then, since $\bar{V}_s$ in (10) is equal to $-j\bar{V}_s$, it follows that

$$V_z = \bar{V}_s(\sinh A_w \sin F_w - j \cosh A_w \cos F_w) \tag{11}$$

$$I_z = \frac{\bar{V}_s}{R_c} (1 + j\phi_c)(\cosh A_w \sin F_w - j \sinh A_w \cos F_w) \tag{12}$$

It is readily verified that the terms with ϕ_c as coefficient contribute nothing of significance in practically important cases. Thus

$$I_z = \frac{\bar{V}_s}{R_c} [\cosh A_w \sin F_w + \phi_c \sinh A_w \cos F_w - j(\sinh A_w \cos F_w - \phi_c \cosh A_w \sin F_w)] \tag{13}$$

Using the formulas

$$A \sin x + B \cos x = \sqrt{A^2 + B^2} \cos \left(x - \tan^{-1} \frac{A}{B}\right) \tag{14a}$$

$$= \sqrt{A^2 + B^2} \sin \left(x + \tan^{-1} \frac{B}{A}\right) \tag{14b}$$

and neglecting terms multiplied by ϕ_c^2,

$$I_z = \frac{\bar{V}_s}{R_c} \{\cosh A_w \sin [F_w + \tan^{-1} (\phi_c \tanh A_w)] - j \sinh A_w \cos [F_w + \tan^{-1} (\phi_c \coth A_w)]\} \tag{15}$$

Since $\tanh A_w$ can never exceed unity, the angle

$$\tan^{-1} (\phi_c \tanh A_w) \doteq \phi_c \tanh A_w \tag{16}$$

is of magnitude ϕ_c, which is of order 10^{-3} on a low-loss line. In practical application angles are not usually measured to the nearest thousandth of a radian, so that no observable error is introduced by assuming $\phi_c \tanh A_w \doteq 0$. The angle $\tan^{-1} (\phi_c \coth A_w)$ in (15) is negligibly small so long as $\coth A_w$ does not become large. It becomes large only when A_w becomes small, that is, when $\coth A_w \doteq 1/A_w$. In this case

$$\tan^{-1} (\phi_c \coth A_w) \doteq \tan^{-1} \frac{\phi_c}{A_w} \doteq \tan^{-1} \frac{1}{\beta(w + \rho_s/\alpha)} \tag{17}$$

Clearly, if ρ_s is large compared with α, this angle is very small. On the other hand, if $\rho_s \doteq 0$, the angle defined in (17) is small only when βw is sufficiently large; as $\beta w \to 0$, the angle approaches $\pi/2$. Thus the angle is important only when $\rho_s \doteq 0$ and βw becomes small. However, when w becomes small, $\sinh A_w \doteq A_w = \alpha w$ likewise becomes extremely small. Thus, when the phase of the cosine in (15) is significantly affected by the term in ϕ_c, the amplitude of the entire term becomes vanishingly small. Hence no significant error is made if the terms in ϕ_c are omitted, so that

$$\boldsymbol{V}_z = V_z'' + jV_z' \doteq \bar{V}_s(\sinh A_w \sin F_w - j \cosh A_w \cos F_w) \tag{18}$$

$$\boldsymbol{I}_z = I_z'' + jI_z' \doteq \frac{\bar{V}_s}{R_c} (\cosh A_w \sin F_w - j \sinh A_w \cos F_w) \tag{19}$$

The voltage and current for the load are obtained with $w = 0$. They are

$$\boldsymbol{V}_s = V_s'' + jV_s' \doteq \bar{V}_s(\sinh \rho_s \cos \Phi_s - j \cosh \rho_s \sin \Phi_s) \tag{20}$$

$$\boldsymbol{I}_s = I_s'' + jI_s' \doteq \frac{\bar{V}_s}{R_c} (\cosh \rho_s \sin \Phi_s - j \sinh \rho_s \cos \Phi_s) \tag{21}$$

The functions V_z'', V_z', and $|\boldsymbol{V}_z|$ are shown graphically in Fig. 10.1, and I_z'', I_z', and $|\boldsymbol{I}_z|$ in Fig. 10.2. The magnitudes $|\boldsymbol{V}_z|$ and $|\boldsymbol{I}_z|$ are, of course, identical with distribution curves for the voltage and current in Sec. 8.

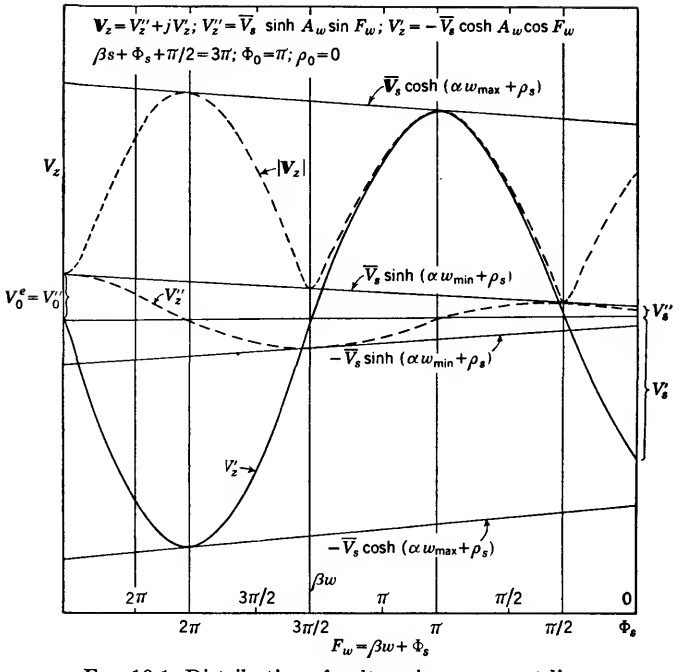


FIG. 10.1. Distribution of voltage in a resonant line.

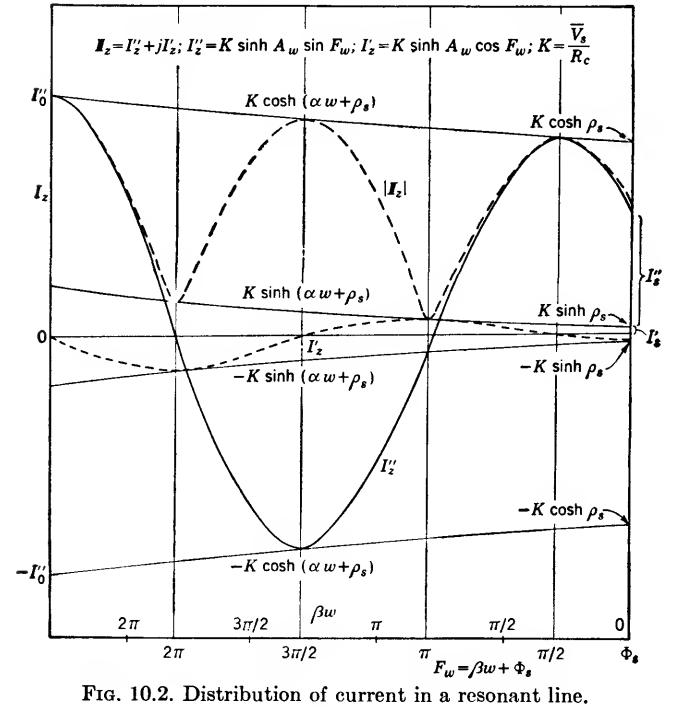


FIG. 10.2. Distribution of current in a resonant line.

11. The Widths of Resonance and Distribution Curves.[11,78,81] The greater the over-all attenuation of a transmission line, as defined by the function $\alpha s + \rho_0 + \rho_s$, where αs is the attenuation of the line, ρ_0 that of the generator, and ρ_s that of the load, the lower and broader are the maxima of the resonance curves described in Sec. 7. Similarly, the greater the attenuation of the terminated section of line between that point z where the current and voltage are measured and the load at $z = s$, as characterized by the function $\alpha w + \rho_s$, where $w = s - z$, the higher and broader are the minima of the distribution curves for current and voltage described in Sec. 8. The same is true of the distribution curves obtained by moving the point of coupling x of the emf in terms of the function $\alpha x + \rho_0$. It may be concluded that the ratio of maximum to minimum and the width at a specified fraction of the maximum or minimum of the resonance or distribution curves are useful in transmission-line measurements of attenuation.

Width of Resonance Curve. The square of the amplitude of a resonance curve is shown in Sec. 8 to be proportional to the function

$$S_s^{-2} = (\sinh^2 A_s + \sin^2 F_s)^{-1} \tag{1}$$

where the shorthand notation

$$A_s \equiv \alpha s + \rho_0 + \rho_s \qquad F_s \equiv \beta s + \Phi_0 + \Phi_s \tag{2}$$

is used. As usual, α is the attenuation constant, β is the phase constant, and s is the length of the line between the impedances $\boldsymbol{Z}_0$ at $z = 0$ and $\boldsymbol{Z}_s$ at $z = s$. The phase functions of these impedances are Φ_0 and Φ_s; the corresponding attenuation functions are ρ_0 and ρ_s.

The maximum amplitude squared is defined by (1) when the condition of resonance

$$F_s = \beta s + \Phi_0 + \Phi_s = n\pi \qquad n = 0, 1, 2, \ldots, s \geqq 0 \tag{3}$$

is satisfied. It is

$$(S_s^{-2})_{\max} = \operatorname{csch}^2 A_s \tag{4}$$

The square of the amplitude (1) is reduced to an arbitrary fraction $1/p^2$ of the maximum when F_s is changed from (3) to one of the two values

$$F_{s1} = F_s - \delta F_1 \qquad F_{s2} = F_s + \delta F_2 \tag{5}$$

Note that the required change in F_s may be made by varying (a) the length of the line s, (b) the frequency, so that $\beta = \omega/v$ changes, or (c) $\boldsymbol{Z}_0$ or $\boldsymbol{Z}_s$, so that Φ_0 or Φ_s is changed. In any one of these cases A_s is also affected so that, paralleling (5),

$$A_{s1} = A_s - \delta A_1 \qquad A_{s2} = A_s + \delta A_2 \tag{6}$$

Thus
$$S_s^{-2} = \frac{(S_s^{-2})_{\max}}{p^2} = \frac{1}{\sinh^2 (A_s \mp \delta A) + \sin^2 (F_s \mp \delta F)} \tag{7}$$

where the upper sign is for F_{s1}, with subscript 1 on δA and δF, and the lower sign is for F_{s2}, with subscript 2 on δA and δF. Note that, if the amplitude is reduced entirely by changing the length of the line from s to

$$s_1 = s - \delta s_1 \qquad \text{or} \qquad s_2 = s + \delta s_2 \tag{8}$$

it follows that

$$\delta F_1 = \beta \delta s_1 \qquad \delta F_2 = \beta \delta s_2 \tag{9a}$$

$$\delta A_1 = \alpha \delta s_1 \qquad \delta A_2 = \alpha \delta s_2 \tag{9b}$$

The substitution of (4) in the middle term in (7), using the condition for resonance (3), gives

$$p^2 \sinh^2 A_s = \sinh^2 (A_s \mp \delta A) + \sin^2 (n\pi \mp \delta F) \tag{10}$$

where the subscript 1 is used on δA and δF with the upper sign, and the subscript 2 with the lower sign. By expanding the hyperbolic and circular sines the following transformed expression may be derived:

$$(p^2 - \cosh^2 \delta A) \sinh^2 A_s + 2 \sinh A_s \cosh A_s \sinh \delta A \cosh \delta A - \sinh^2 \delta A \cosh^2 A_s = \sin^2 \delta F \tag{11}$$

So long as the change in F_s is made by varying either the length s or the frequency, the associated change in A_s is very small if, as is assumed, a low-loss line is involved. That is,

$$(\delta A)^2 \ll 1 \qquad \sinh \delta A \doteq \delta A \qquad \cosh \delta A \doteq 1 \tag{12}$$

With (12), (11) may be approximated by

$$\left(\sqrt{p^2 - 1} \sinh A_s \pm \frac{\delta A \cosh A_s}{\sqrt{p^2 - 1}}\right)^2 = \sin^2 \delta F \tag{13}$$

The two equations from (13) are

$$\sqrt{p^2 - 1} \sinh A_s + \frac{\delta A_1 \cosh A_s}{\sqrt{p^2 - 1}} = |\sin \delta F_1| \tag{14}$$

$$\sqrt{p^2 - 1} \sinh A_s - \frac{\delta A_2 \cosh A_s}{\sqrt{p^2 - 1}} = |\sin \delta F_2| \tag{15}$$

Let (14) be added to (15) to give

$$|\sin \delta F_1| + |\sin \delta F_2| = 2\sqrt{p^2 - 1} \sinh A_s \left(1 + \frac{\delta A_1 - \delta A_2}{2\sqrt{p^2 - 1} \tanh A_s}\right) \tag{16}$$

Since δA_1 and δA_2 are both small and nearly equal, the condition

$$|\delta A_1 - \delta A_2| \ll 2\sqrt{p^2 - 1} \tanh A_s \tag{17}$$

usually can be satisfied easily. Subject to (17), (16) can be solved for A_s as follows:

$$A_s \doteq \sinh^{-1} \frac{|\sin \delta F_1| + |\sin \delta F_2|}{2\sqrt{p^2 - 1}} \tag{18}$$

This is the fundamental equation relating the over-all damping factor $A_s = \alpha s + \rho_0 + \rho_s$ to the changes δF_1 and δF_2 required to reduce the resonance curve to $1/p$ of its maximum value in both directions.

Note that the resonance curve is symmetrical if $\delta F_1 = \delta F_2$ and $\delta A_1 = \delta A_2$. *For a symmetrical curve* (17) *is satisfied automatically*, so that (18) is a good approximation. It is evident from (14) and (15) that δF_1 and δF_2 approach equality as the terms in δA become smaller. Hence satisfactory conditions for an approximately symmetrical resonance curve are

$$\delta A_1 \ll (p^2 - 1) \tanh A_s \qquad \delta A_2 \ll (p^2 - 1) \tanh A_s \tag{19}$$

With (19),
$$\delta F_1 \doteq \delta F_2 \doteq \delta F \tag{20}$$

so that (18) reduces to

$$A_s \doteq \sinh^{-1} \frac{|\sin \delta F|}{\sqrt{p^2 - 1}} \tag{21}$$

If the over-all damping is sufficiently small so that

$$\sin^2 \delta F_1 \doteq \sin^2 \delta F_2 \doteq (p^2 - 1) \sinh^2 A_s \ll 1 \tag{22}$$

it follows that $\sin \delta F_1 \doteq \delta F_1$ and $\sin \delta F_2 \doteq \delta F_2$, so that (18) reduces to

$$A_s \doteq \frac{\delta F_1 + \delta F_2}{2\sqrt{p^2 - 1}} = \frac{\Delta F_s}{2\sqrt{p^2 - 1}} \tag{23}$$

where
$$\Delta F_s \equiv \delta F_1 + \delta F_2 \tag{24}$$

is the angular width of the resonance curve at a level $1/p$ of maximum. By setting $p^2 = 2$ and thus defining the so-called *half-power level*, the following very simple relation is obtained:

$$A_s \doteq \frac{\Delta F_s}{2} \tag{25}$$

That is, the over-all attenuation factor is one-half the width of the resonance curve at a level $1/p = 0.707$.

If the only variable is the length s of the line, so that $\delta F = \beta\, \delta s$ and $\Delta F_s = \Delta s = \beta(\delta s_1 + \delta s_2)$, (23) reduces to the following:

$$A_s = \alpha s + \rho_0 + \rho_s \doteq \frac{\beta\, \Delta s}{2\sqrt{p^2 - 1}} \tag{26a}$$

With $p^2 = 2$,
$$A_s = \alpha s + \rho_0 + \rho_s \doteq \frac{\beta\, \Delta s}{2} \tag{26b}$$

Note that Δs is the width of the resonance curve at power level $1/p$ when the line is resonant at the length s defined by (3). The conditions implied in (26*a*,*b*) are

$$\alpha\, \delta s \doteq \frac{\alpha\, \Delta s}{2} \ll 1 \qquad (\delta s)^2 \ll \left(\frac{\lambda}{2\pi}\right)^2 \tag{27}$$

Width of Distribution Curve. Let the distribution curve obtained by moving a current or voltage probe along the line be examined. (The distribution curve obtained by moving the point of coupling of the generator may be obtained by a simple change in notation.) The square of the *minimum* amplitude is

$$S_w^2 = \sinh^2 A_w \tag{28}$$

where $A_w = \alpha w + \rho_s$. The minimum current amplitude occurs when

$$F_w = \beta w + \Phi_s = n\pi \qquad w \geqq 0 \tag{29}$$

The square of the amplitude increases to p^2 times the minimum at two values of F_w, one located on each side of the minimum as defined in (28). These values are

$$F_{w1} = F_w - \delta F_1 \qquad F_{w2} = F_w + \delta F_2 \tag{30a}$$

If w is the only variable, the locations of the two values defined in (30*a*) are

$$w_1 = w - \delta w_1 \qquad w_2 = w + \delta w_2 \tag{30b}$$

The values of A corresponding to (30*a*) are

$$A_{w1} = A_w - \delta A_1 \qquad A_{w2} = A_w + \delta A_2 \tag{30c}$$

The values of S_w^2 at F_{w1} and F_{w2} must satisfy the equations

$$p^2 \sinh^2 A_w = \sinh^2 (A_w \mp \delta A) + \sin^2 (n\pi \mp \delta F) \tag{31}$$

where the upper sign is for δF_1 and δA_1 and the lower sign is for δF_2 and δA_2. Since (31) is like (10), with a subscript w instead of s, it follows that the same solutions are obtained subject to corresponding conditions. The fundamental relation is (18), with the subscript s replaced by w; δF_1 and δF_2 are the changes in F_w which increase the amplitude to the level p. The relation corresponding to (26*a*) is

$$A_w = \alpha w + \rho_s \doteq \frac{\beta \Delta w}{2\sqrt{p^2 - 1}} \tag{32a}$$

With $p^2 = 2$, this reduces to

$$A_w = \alpha w + \rho_s \doteq \frac{\beta \Delta w}{2} \tag{32b}$$

In (32*a*,*b*) Δw is the distance between half-power points on each side of the dip in the distribution curve which occurs at w. Conditions corresponding to (27), with w substituted for s, must be satisfied if (32*a*,*b*) are used. The conditions for a symmetrical distribution-curve dip are like (19), with subscript w substituted for s.

12. The "Q" of a Transmission Line. A quality factor Q may be defined for a complete transmission-line circuit consisting of a length of line s, a load impedance $\boldsymbol{Z}_s$, and a generator impedance $\boldsymbol{Z}_0$ or for a termi-

nated section consisting of a length of line w and a load impedance $\boldsymbol{Z}_s$. In both cases the definition for the reciprocal of the Q is

$$\frac{1}{Q} \equiv \frac{\delta f' + \delta f''}{f} = \frac{\delta\omega' + \delta\omega''}{\omega} = \frac{\delta\beta' + \delta\beta''}{\beta} \tag{1}$$

where $f + \delta f'$ and $f - \delta f''$ are the "half-power frequencies" at which the square of the current or voltage at an arbitrary point along the line is reduced to one-half the maximum value at the *fundamental* frequency f.† Experimentally Q may be obtained from a resonance curve by varying the frequency in order to determine f, $f + \delta f'$, and $f - \delta f''$. In the frequency range $f - \delta f'$ to $f + \delta f'$ let the following condition be a good approximation:

$$\delta A_s \ll A_s \equiv \alpha s + \rho_0 + \rho_s \tag{2}$$

Also
$$\delta F_s = \delta(\beta s + \Phi_0 + \Phi_s) \tag{3}$$

It is understood in (2) and (3) that δA_s stands for either $\delta A_s'$ or $\delta A_s''$ and δF_s for $\delta F_s'$ or $\delta F_s''$, where $A_s + \delta A_s'$ and $F_s + \delta F_s'$ correspond to $\omega + \delta\omega'$ and $A_s - \delta A_s''$ and $F_s - \delta F_s''$ correspond to $\omega - \delta\omega''$, where ω is the fundamental resonant frequency.

If interest is in a terminated *section* of line of length w with load $\boldsymbol{Z}_s$, (2) and (3) are replaced by the following:

$$\delta A_w \ll A_w \qquad A_w = \alpha w + \rho_s \tag{4}$$

$$\delta F_w = \delta(\beta w + \Phi_s) \tag{5}$$

Since with (3) the condition implied in Sec. 11, Eq. (23), is fulfilled, it follows that, with $p = 2$,

$$A_s = \tfrac{1}{2}(\delta F_s' + \delta F_s'') \doteq \frac{s}{2}(\delta\beta' + \delta\beta'') + \tfrac{1}{2}(\delta\Phi_0' + \delta\Phi_0'') + \tfrac{1}{2}(\delta\Phi_s' + \delta\Phi_s'') \tag{6}$$

Similarly
$$A_w = \tfrac{1}{2}(\delta F_w' + \delta F_w'') \doteq \frac{w}{2}(\delta\beta' + \delta\beta'') + \tfrac{1}{2}(\delta\Phi_s' + \delta\Phi_s'') \tag{7}$$

If (6) is substituted in (1), an expression is obtained for the loaded total Q of the entire resonant transmission-line circuit including the line, the load, and the generator. It is

$$Q = Q_t = \frac{\beta s}{2[\alpha s + \rho_0 + \rho_s - (\delta\Phi_0' + \delta\Phi_0'' + \delta\Phi_s' + \delta\Phi_s'')]} \tag{8}$$

where s is the length of line at the lowest resonant frequency. It is given by

$$\beta s + \Phi_0 + \Phi_s = n\pi \tag{9}$$

where n is the smallest integer for which βs is positive.

† A Q factor for a given circuit at each of an unlimited number of harmonic frequencies can be defined if desired. In this section only the Q at the fundamental frequency is introduced.

Alternatively, if (7) is substituted in (1), an expression is obtained for the *loaded* Q at input resonance of a *section* of line of length w terminated in the load $\boldsymbol{Z}_s$. It is

$$Q = Q_L = \frac{\beta w}{2[\alpha w + \rho_s - (\delta\Phi_s' + \delta\Phi_s'')]} \tag{10}$$

The resonant length w is defined by

$$\beta w + \Phi_s = n\pi \tag{11}$$

where n is the smallest integer for which βw is positive.

If the ends of the line are either open- or short-circuited,

$$\rho_0 \doteq \rho_s \doteq 0 \qquad \delta\Phi_s \doteq \delta\Phi_s \doteq 0 \tag{12}$$

and (8) and (10) reduce to the simple form characteristic of the line alone. The unloaded Q is

$$Q = Q_0 = \frac{\beta}{2\alpha} \tag{13}$$

Note that Q_0 is independent of the length of the line. Since

$$\frac{\alpha}{\beta} = \frac{1}{2\omega}\left(\frac{r}{l} + \frac{g}{c}\right) \tag{14}$$

it follows that

$$\frac{1}{Q_0} = \frac{r}{\omega l} + \frac{g}{\omega c} \tag{15}$$

For a low-loss line the condition $(\alpha/\beta)^2 \ll 1$ is satisfied, so that

$$Q_0^2 \gg 4 \tag{16}$$

The external Q's of the resonant circuit of length s and the resonant section of line of length w, respectively, may be defined by

$$Q_E = \frac{\beta s}{2[\rho_0 + \rho_s - (\delta\Phi_0' + \delta\Phi_0'' + \delta\Phi_s' + \delta\Phi_s'')]} \tag{17a}$$

$$Q_E = \frac{\beta w}{2(\rho_s - \delta\Phi_s' - \delta\Phi_s'')} \tag{17b}$$

so that

$$\frac{1}{Q_t} = \frac{1}{Q_0} + \frac{1}{Q_E} \tag{18a}$$

$$\frac{1}{Q_L} = \frac{1}{Q_0} + \frac{1}{Q_E} \tag{18b}$$

It is significant that, if $\delta F_s = \delta(\beta s)$ and $\delta\Phi = 0$, the effect of varying the frequency with s fixed (so that $\delta F_s = s\ \delta\beta$) is essentially equivalent to varying the length with the frequency fixed (so that $\delta F_s = \beta\ \delta s$). In this latter case Q_t is given by

$$\frac{1}{Q_t} = \frac{\delta s' + \delta s''}{s} \tag{19}$$

where $s + \delta s'$ and $s - \delta s''$ are the lengths of line at a fixed frequency for which the square of the current or voltage at an arbitrary point along the line is reduced to one-half of the maximum value at the resonant length s. Similarly, with $\delta F_w = \delta(\beta w)$ and $\delta\Phi_s = 0$,

$$\frac{1}{Q_L} = \frac{\delta w' + \delta w''}{w} \tag{20}$$

where w is the length of the section for *input* resonance and $w + \delta w'$ and $w - \delta w''$ are the half-power lengths.

It may be concluded that, when $\delta\Phi = 0$, the Q of the transmission-line circuit may be determined from resonance curves using either the frequency or the length of line as the variable.

13. Theory of Transmission-line Measurements.[8,14,62–64,66–68,71–73,76–79,81,88,89,91,98,103] Although in some respects the transmission line is not convenient for making electrical measurements, it is both versatile and valuable at frequencies that are sufficiently high to make bridge circuits with lumped elements unavailable. If the distance between the conductors of the transmission line is sufficiently small compared with the wavelength to make higher propagating modes impossible and to keep radiation from open-wire lines negligible, transmission-line theory provides a highly accurate analogue of experimentally observable and measurable conditions. This is true except near the terminations or discontinuities along the line where appropriate corrections usually must be made to take account of end effects in the line and coupling effects between the line and the termination, as discussed in Chap. II, Secs. 3 and 4. Let it be assumed in the following that account has been taken of such effects and that the actual transmission line with nonuniform properties near its ends has been replaced analytically by an equivalent uniform line terminated in measurable *apparent* impedances. The actual determination of an apparent impedance $\boldsymbol{Z}_{0a}$ or $\boldsymbol{Z}_{sa}$ from the theoretical ideal impedance $\boldsymbol{Z}_0$ or $\boldsymbol{Z}_s$ is considered in Chap. V.

A general transmission-line system consists of a section of line extending from $z = 0$ to $z = s$ and terminated at $z = 0$ in $\boldsymbol{Z}_0$ and at $z = s$ in $\boldsymbol{Z}_s$. Owing to terminal-zone effects this system is equivalent to an ideal *uniform* line of length s terminated in the apparent impedances $\boldsymbol{Z}_{0a}$ and $\boldsymbol{Z}_{sa}$ at $z = 0$ and $z = s$, respectively. The line is driven by the equivalent of one *or* two pairs of equal and opposite point generators symmetrically placed with respect to an arbitrary and movable point x. Experimentally available equivalents of such generators are described in Chap. VI.

A number of quantities that can be measured on such a transmission line are described in the following. The purpose is to outline the theoretical foundations, not to discuss the experimental technique.[8] Note

that bridge and phase measurements using the hybrid junction are discussed in Chap. III, Sec. 15.

The Measurement of Phase Constant and Wavelength. The phase constant β and the wavelength $\lambda = 2\pi/\beta$ may be determined using either resonance or distribution curves.

a. Resonance-curve Method. The particular lengths of line s_n for which the maximum of a resonance curve (obtained by changing the over-all length of the line with everything else constant) may be observed are defined by the condition

$$\beta s_n + \Phi_{0a} + \Phi_{sa} = n\pi \qquad n = 0, 1, 2, \ldots, s_n > 0 \tag{1a}$$

If two such lengths s_n and s_{n-1} are determined experimentally by varying the length s of the line, it follows from (1*a*) that

$$\beta = \frac{\pi}{s_n - s_{n-1}} \qquad \lambda = 2(s_n - s_{n-1}) \tag{1b}$$

In order to obtain sharp resonance curves, both terminations $\boldsymbol{Z}_{0a}$ and $\boldsymbol{Z}_{sa}$ should be reactive and preferably should be pistons in shielded lines (as in Fig. 13.1) and metal disks or conducting bridges on open-wire lines. High precision in determining β and λ may be achieved by plotting the vicinity of each resonance peak and drawing mid-point lines to locate the peak accurately.

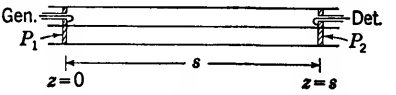


FIG. 13.1. Coaxial line with pistons and coupling loops for measuring wavelength and phase constant by the resonance-curve method.

Since it has been assumed that s is the *only* variable, neither the distance $w = s - z$ from the current or voltage probe to $\boldsymbol{Z}_{sa}$ nor the distance x from $\boldsymbol{Z}_{0a}$ to the center of the configuration of point generators must be changed as s is varied. A possible procedure is to couple the generator or the detector to the line by means of a loop which is attached directly to a movable piston, as in Fig. 13.1, or to a movable disk or wire bridge.

If both the point of coupling of the generators and the location of the current or voltage probe are fixed at distances x and z, respectively, from the impedance $\boldsymbol{Z}_0$, whereas the length s of the line is varied by moving $\boldsymbol{Z}_s$ (usually in the form of a piston with $\boldsymbol{Z}_s \doteq 0$), it is clear that $w = s - z$ varies linearly with s. In this case the magnitude of the current at z is proportional to

$$|I_z| \sim \sqrt{\frac{\sinh^2(\alpha w + \rho_s) + \sin^2(\beta w + \Phi_s)}{\sinh^2(\alpha s + \rho_0 + \rho_s) + \sin^2(\beta s + \Phi_0 + \Phi_s)}} \tag{2a}$$

If the location z of the current-detector probe is fixed so that

$$\beta(s - w) + \Phi_0 = \frac{2n + 1}{2}\pi$$

with n integral, this expression becomes

$$|I_z| \sim \sqrt{\frac{\sinh^2(\alpha w + \rho_s) + \cos^2(\beta s + \Phi_0 + \Phi_s)}{\sinh^2(\alpha s + \rho_0 + \rho_s) + \sin^2(\beta s + \Phi_0 + \Phi_s)}} \tag{2b}$$

For small over-all attenuation $|I_z|$ varies as $|\cot(\beta s + \Phi_0 + \Phi_s)|$ [instead of as $|\sec(\beta s + \Phi_0 + \Phi_s)|$ when the detector is moved with Z_s, so that w is constant]. The locations and amplitudes of the extreme values are given by

$$\begin{aligned} \beta s + \Phi_0 + \Phi_s &= \frac{2n+1}{2}\pi \\ \beta w + \Phi_s &= m\pi \\ |I_z|_{\min} &= \frac{\sinh(\alpha w + \rho_s)}{\cosh(\alpha s + \rho_0 + \rho_s)} \end{aligned} \tag{2c}$$

$$\begin{aligned} \beta s + \Phi_0 + \Phi_s &= n\pi \\ \beta w + \Phi_s &= \frac{2m+1}{2}\pi \\ |I_z|_{\max} &= \frac{\cosh(\alpha w + \rho_s)}{\sinh(\alpha s + \rho_0 + \rho_s)} \end{aligned} \tag{2d}$$

Since the distances between maxima are the same as when s alone is varied, with w fixed, and the resonance maxima are almost as sharp, β and λ may be determined equally well if only a terminating piston is moved, with detector and generator fixed, provided the detector is placed exactly where it gives maximum deflection. Note that the above formulas apply to V_z if Φ_s is replaced by Φ'_s.

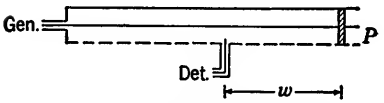


FIG. 13.2. Slotted coaxial line with movable detector probe for measuring wavelength and phase constant using the voltage-distribution curve. If a loop is substituted for a straight probe, the current distribution curve replaces the voltage distribution curve.

It is shown in Chap. VI that the condition for the driving source to be equivalent to a configuration of point generators along the line requires that this be coupled loosely to the line.

b. Distribution-curve Methods—Current and Voltage. Since distribution curves as functions of w or x are reciprocals of resonance curves as functions of s, the same procedure in measuring λ may be followed using *minima* of distribution curves as using *maxima* of resonance curves.

If a current or voltage probe is moved along the line, as in the circuit of Fig. 13.2, to obtain a current or voltage distribution curve and, in particular, to locate its minima at w_n, the equations that these satisfy are as follows:

$$[I_z(w)]_{\min} \text{ occurs at } \beta w_n + \Phi_{sa} = n\pi \tag{3a}$$

$$[V_z(w)]_{\min} \text{ occurs at } \beta w_n + \Phi'_{sa} = n\pi \tag{3b}$$

where $n = 0, 1, 2, \ldots$ and $w_n > 0$. Evidently

$$\beta = \frac{\pi}{w_n - w_{n-1}} \qquad \lambda = 2(w_n - w_{n-1}) \tag{4}$$

The distribution-curve minima are sharp only if Z_{sa} is essentially reactive. If required, a plot of the curves may be made, and mid-point lines drawn to locate each minimum more accurately.

Since the current or voltage probe is not included in the analysis, it must be coupled sufficiently loosely to provide no significant reaction on the generator.

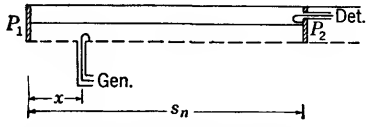


FIG. 13.3. Slotted coaxial line with movable generator loop for measuring wavelength and phase constant using the distribution curve of the point of excitation.

c. Distribution-curve Methods—Point of Excitation. If a distribution curve is obtained as a function of x by moving the generators (as by moving a loosely coupled oscillator or coupling unit, as in Fig. 13.3) relative to the line, minima in the curve occur when

For one pair of point generators:

$$\beta x_n + \Phi_{0a} = n\pi \tag{5a}$$

For two pairs of point generators:

$$\beta x_n + \Phi'_{0a} = n\pi \tag{5b}$$

where $n = 0, 1, 2, \ldots$ and $x > 0$. Evidently

$$\beta = \frac{\pi}{x_n - x_{n-1}} \qquad \lambda = 2(x_n - x_{n-1}) \tag{6}$$

The Measurement of Frequency or Phase Velocity. The transmission line permits the measurement of frequency only indirectly. Since

$$f = \frac{v}{\lambda} = \frac{\beta v}{2\pi} \tag{7}$$

it is clear that, if the velocity v is known, f can be evaluated from (7) if β or λ is measured. Alternatively, if the frequency is known, the phase velocity v may be determined using (7). Theoretical values of v are given in Chap. II, Sec. 12.

The Measurement of the Attenuation Constant. The attenuation constant α of a low-loss line is usually so small as to make its experimental determination difficult. Although methods based on the use of Sec. 9, formulas (1), (9), or (16), are theoretically possible, the ratios of maximum to minimum amplitude in a resonance curve or a distribution curve are very great if the only attenuation is that of a section of line. The measurement of such large ratios involves serious difficulties. These include the problem of a detector accurately calibrated over a range from very low to very high levels and sufficiently sensitive to permit very loose

coupling. Note that the losses introduced by the detector must be negligible compared with the small losses in the line itself.

Other formulas upon which the measurement of α may be based are Sec. 11, Eqs. (26*b*) and (32*b*). These involve the half-power widths Δs_n of resonance curves with maxima at s_n or the half-power widths Δw_n of distribution curves with minima at w_n. The appropriate formulas are

$$\alpha s_n + \rho_{0a} + \rho_{sa} = \frac{\beta \, \Delta s_n}{2} \tag{8}$$

$$\alpha w_n + \rho_{sa} = \frac{\beta \, \Delta w_n}{2} \tag{9}$$

In order to make use of (8), the length of the line is varied by moving one of the terminations, as in Fig. 13.1, and the locations s_n and s_{n+m} of two resonance curves and their respective widths Δs_n and Δs_{n+m} at 0.707 of maximum amplitude are measured. The quantities so determined are related by the formula

$$\alpha = \frac{\beta}{2} \frac{\Delta s_n - \Delta s_{n+m}}{s_n - s_{n+m}} \tag{10}$$

In order to use (9), the current or voltage probe is moved to locate two distribution-curve minima using Fig. 13.2 at distances w_n and w_{n+m} from the terminating piston or bridge at $z = s$. The half-power width of each is then measured by determining $w + \delta w'$ and $w - \delta w''$ and setting $\Delta w = \delta w' + \delta w''$. The formula for α obtained from (9) when written for w_n and w_{n+m} is

$$\alpha = \frac{\beta}{2} \frac{\Delta w_n - \Delta w_{n+m}}{w_n - w_{n+m}} \tag{11}$$

Since the several distances and widths in (10) and (11) must be measured with great accuracy, it is often necessary to plot resonance or extended sections of distribution curves.

The Measurement of the Apparent Phase Function of a Termination. The apparent phase function Φ_{sa} for an unknown impedance may be determined using the same methods described for the measurement of β. Note that resonance-curve methods may be used to determine the phase function of the generator impedance as well as that of the load; distribution-curve methods using voltage and current probes are useful only for the load.

a. Resonance-curve Method. The measurement of Φ_a (either Φ_{sa} or Φ_{0a}) depends on the availability of a standard termination such as a short-circuiting piston in a shielded line or a sufficiently large conducting disk in an open line. For both of these $\Phi_a = \Phi = \pi/2$. An alternative for an open line is a conducting bridge for which $\Phi_a = \pi/2 + \beta k_{sa}$ (see Chap. II, Sec. 20).

If the phase function of the standard impedance is $\Phi_{sa} = \pi/2$, the

shortest resonant length s_{n1} of line is given by

$$\beta s_{n1} + \Phi_{0a} + \frac{\pi}{2} = \pi \tag{12a}$$

Alternatively, if the standard is $\Phi_{0a} = \pi/2$,

$$\beta s_{n1} + \frac{\pi}{2} + \Phi_{sa} = \pi \tag{12b}$$

The shortest resonant length with the unknown impedance [Z_{sa} for use with (12a) and Z_{0a} for use with (12b)] is s_{n2}, given by

$$\beta s_{n2} + \Phi_{0a} + \Phi_{sa} = \pi \tag{13}$$

Subtraction of (13) from (12a) leads to

$$\Phi_{sa} = \frac{\pi}{2} + \beta(s_{n1} - s_{n2}) \tag{14a}$$

Subtraction of (13) from (12b) gives

$$\Phi_{0a} = \frac{\pi}{2} + \beta(s_{n1} - s_{n2}) \tag{14b}$$

The two resonant lengths s_{n1} for the short circuit and s_{n2} for the unknown impedance may be determined experimentally by changing the length of the line as in the determination of β and subject to the same conditions. Two cases are illustrated in Figs. 13.4 and 13.5. The latter shows an

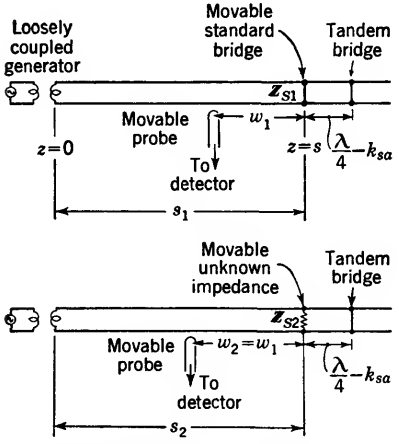


FIG. 13.4. Circuits for the two steps in the measurement of the apparent phase function and attenuation function of an unknown load impedance Z_{s2} using the resonance-curve method and a two-wire line.

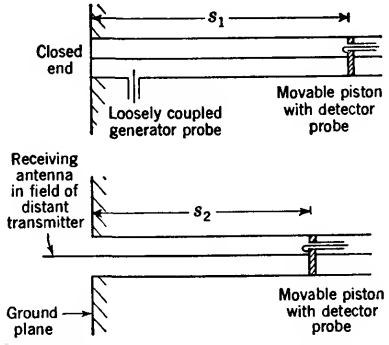


FIG. 13.5. Circuits for the two steps in the measurement of the apparent phase function and attenuation function of a receiving antenna using the resonance-curve method and a coaxial line.

important application of this method to the measurement of the impedance of a receiving antenna while used for reception. In this case the antenna is the generator for the attached transmission line, so that distribution-curve methods are not applicable.

b. Distribution-curve Method. The function Φ_{sa} may be determined using a movable probe with a line of fixed length. By locating the minimum of the current or voltage distribution curve for the unknown impedance at a distance w_n from the end of the line, the following equations are obtained, respectively, from (3*a*) and (3*b*):

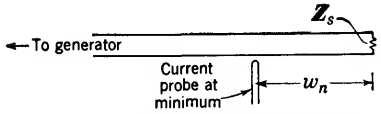


FIG. 13.6. Measurement of the apparent phase function Φ_{sa} using a movable current probe.

$$\Phi_{sa} = \pi - \beta w_n \qquad (15a)$$

$$\Phi'_{sa} = \pi - \beta w_n \qquad (15b)$$

The apparent phase function is thus determined using a movable current probe (as in Fig. 13.6) with (15*a*) and a movable voltage probe with (15*b*). Note that $\Phi'_{sa} = \Phi_{sa} - \pi/2$.

An alternative procedure that permits the measurement of a difference in lengths instead of the actual length w_n and makes use of a standard termination such as a short-circuiting piston or disk is to apply (3*a*) or (3*b*) to the standard termination and then to the unknown. If the minimum using the standard termination is at w_{n1} and the minimum with the unknown is at w_{n2}, the following equation applies for a current probe as derived from (3*a*), assuming the standard termination to be a perfect short circuit (this is illustrated in Fig. 13.7):

$$\Phi_{sa} = \frac{\pi}{2} + \beta(w_{n1} - w_{n2}) \qquad (16a)$$

Similarly for (3*b*) and a voltage probe

$$\Phi'_{sa} = \frac{\pi}{2} + \beta(w_{n1} - w_{n2}) \qquad (16b)$$

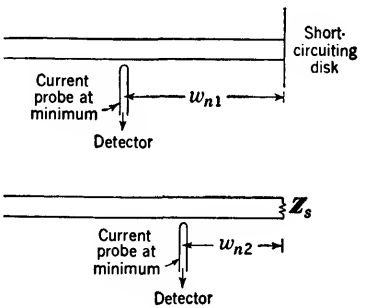


FIG. 13.7. Two steps in the measurement of the apparent phase function Φ_{sa} using a movable current probe.

This is the distribution-curve analogue of the resonance-curve formula (14). It has an advantage over (15) in that it involves only the difference between the scale readings for the two minima with the two terminations instead of the actual distance of one minimum from the end of the line.

A distribution-curve method of measuring Φ_0 using a movable source may be based on a formula like (15) or (16) with x substituted for w and Φ_0 for Φ_s.

The Measurement of the Apparent Attenuation Function of a Termination. The function ρ_{sa} of an unknown impedance may be determined using one of several methods. Since ρ_{sa} for the termination is usually quite large compared with the attenuation of the line, ratio methods as well as half-power-width methods may be used.

a. Resonance- and Distribution-curve-ratio Methods. By varying the over-all length of a terminated line the ratio of maximum to minimum along a resonance curve may be obtained. The general formula for this ratio is Sec. 9, Eq. (1). Since the attenuation of a quarter wavelength of the line is usually negligible compared with the attenuation of the load, Sec. 9, Eq. (4), is satisfactory. If the ratio R_2 of the maximum to the minimum of a resonance curve is determined for Z_{sa} and again as R_1 for a standard termination such as a perfect short circuit ($\rho_{sa} = 0$), the following two equations are obtained:

$$\alpha s_{2\max} + \rho_{0a} + \rho_{sa} = \coth^{-1} R_1 \tag{17a}$$

$$\alpha s_{1\max} + \rho_{0a} = \coth^{-1} R_2 \tag{17b}$$

The circuits of Fig. 13.4 may be used. It follows that

$$\rho_{sa} = \coth^{-1} R_2 - \coth^{-1} R_1 \tag{18}$$

since with $|s_{2\max} - s_{1\max}| \leqq \lambda/4$ the term $\alpha(s_{2\max} - s_{1\max})$ is negligible. Note that the attenuation of a detector may be included in ρ_{0a}, so that the only error involved in (18) is the neglect of a quantity of the order of magnitude of $\alpha\lambda/4$.

If a movable probe is used with the circuit of Fig. 13.6 to determine the ratio of the maximum to the minimum of a distribution curve for current or voltage—the so-called current or voltage standing-wave ratio—the general equation [Sec. 9, Eq. (11*b*)] is applicable. Since the attenuation of the line is usually negligible, Sec. 9, Eqs. (13) and (14), are valid. That is,

$$\rho_{sa} = \coth^{-1} S \tag{19}$$

where S is the current or voltage standing-wave ratio. The most convenient method of determining ρ_{sa} is usually from the current or voltage standing-wave ratio, as given in (19). It is well to note, however, that the reactive and resistive loading of the probe is neglected.

The apparent attenuation function ρ_{0a} of the apparent impedance Z_{0a} at the other end of the line may be determined in a similar manner from the ratio of the maximum to the minimum of the distribution curve obtained by moving the generators.

b. Resonance- and Distribution-curve-width Methods. By varying the length s of a terminated line on both sides of a resonant length s_{n2} for an unknown Z_{sa} in order to determine the half-power width Δs_{n2} and repeating this procedure to determine the half-power width Δs_{n1} of a resonance curve with maximum at s_{n1} for a standard termination for which $\rho_{sa} = 0$,

the following equations are obtained using (8):

$$\alpha s_{n2} + \rho_{0a} + \rho_{sa} = \frac{\beta \Delta s_{n2}}{2} \tag{20a}$$

$$\alpha s_{n1} + \rho_{0a} = \frac{\beta \Delta s_{n1}}{2} \tag{20b}$$

By subtraction the following formula for ρ_{sa} is obtained:

$$\rho_{sa} = \frac{\beta}{2}(\Delta s_{n2} - \Delta s_{n1}) - \alpha(s_{n2} - s_{n1}) \tag{21}$$

If s_{n2} and s_{n1} are chosen as close together as possible, the last term in (21) with α as a factor is usually negligible, so that

$$\rho_{sa} \doteq \frac{\beta}{2}(\Delta s_{n2} - \Delta s_{n1}) \tag{22}$$

Note that the contribution to the attenuation by a detector may be included in ρ_{0a} and that its effect is subtracted if it remains constant.

By moving a current or voltage probe along the line on both sides of a distribution-curve minimum at w_n in order to determine the half-power width Δw_n, the right side of (9) is determined if β is known. If α is also known, ρ_{sa} may be obtained directly. Alternatively, if the attenuation due to the line is negligible, so that $\alpha w_n \ll \rho_{sa}$, a satisfactory approximation is

$$\rho_{sa} \doteq \frac{\beta \Delta w_n}{2} \tag{23}$$

Determination of Reflection Coefficient. The apparent reflection coefficient $\mathbf{\Gamma}_{sa} = \Gamma_{sa} e^{j\psi_{sa}}$ is determined directly from values of ρ_{sa} and Φ_{sa} using the relations

$$\Gamma_{sa} = e^{-2\rho_{sa}} \qquad \psi_{sa} = -2\Phi_{sa} \tag{24}$$

The terminal functions ρ_{sa} and Φ_{sa} may be obtained using any of the several methods. If the standing-wave-ratio method is used, a convenient formula relates Γ_{sa} directly to the standing-wave ratio. Thus, since

$$e^{-2\rho_{sa}} = \frac{\coth \rho_{sa} - 1}{\coth \rho_{sa} + 1}$$

when $\rho_{sa} \gg \alpha w$ and $S = \coth \rho_{sa}$, it follows that

$$\Gamma_{sa} = \frac{S - 1}{S + 1} \tag{25}$$

Determination of Apparent Impedance. Once the apparent terminal functions ρ_{sa} and Φ_{sa} have been determined for a given termination, the apparent normalized impedance $z_{1sa} = r_{1sa} + jx_{1sa}$ may be calculated

directly using Chap. II, Sec. 15, Eqs. (7) and (8). If the actual impedance $\boldsymbol{Z}_{sa}$ is required, the characteristic impedance $\boldsymbol{Z}_c$ of the line must be known.

If resistance and reactance curves for a given termination are to be determined as functions of the frequency or some variable characteristic of the termination, it is usually more accurate to plot smooth curves through the experimentally determined values of ρ_{sa} and Φ_{sa} and then compute r_{1sa} and x_{1sa} from the curves rather than first to compute r_{1sa} and x_{1sa} directly. This is due to the fact that ρ_{sa} and Φ_{sa} are smoother, more slowly varying quantities than r_{1sa} and x_{1sa}.

Three-probe Method of Measuring Apparent Impedance. Impedance may be measured using three fixed voltage or current probes instead of a single movable one as in the standing-wave-ratio method. The measured quantities required are the relative voltages (or currents) at three fixed points along the line near the unknown terminating impedance.[63,64,71]

Suppose that the apparent impedance $\boldsymbol{Z}_{sa} = R_{sa} + jX_{sa}$ is at $z = s$ or $w = 0$. The voltage at a distance w from the termination is given by Sec. 2, Eq. (6), or Sec. 5, Eq. (2). Its magnitude is

$$V_z = \frac{V_x^e S_x}{S_s} C_w \tag{26a}$$

where
$$\begin{aligned} C_w^2 &= \sinh^2(\alpha w + \rho_{sa}) + \cos^2(\beta w + \Phi_{sa}) \\ &= \tfrac{1}{2}[\cosh 2(\alpha w + \rho_{sa}) + \cos 2(\beta w + \Phi_{sa})] \end{aligned} \tag{26b}$$

Let the three voltage probes be located at βw_1, $\beta w_2 = \beta w_1 + \pi/4$, and $\beta w_3 = \beta w_1 + \pi/2$. The relative voltages are given by

$$C_{w1}^2 = \tfrac{1}{2}[\cosh 2(\alpha w_1 + \rho_{sa}) + \cos 2(\beta w_1 + \Phi_{sa})] \tag{27a}$$

$$\begin{aligned} C_{w2}^2 &= \tfrac{1}{2}[\cosh 2(\alpha w_2 + \rho_{sa}) + \cos 2(\beta w_2 + \Phi_{sa})] \\ &= \tfrac{1}{2}[\cosh 2(\alpha w_2 + \rho_{sa}) - \sin 2(\beta w_1 + \Phi_{sa})] \end{aligned} \tag{27b}$$

$$\begin{aligned} C_{w3}^2 &= \tfrac{1}{2}[\cosh 2(\alpha w_3 + \rho_{sa}) + \cos 2(\beta w_3 + \Phi_{sa})] \\ &= \tfrac{1}{2}[\cosh 2(\alpha w_2 + \rho_{sa}) - \cos 2(\beta w_1 + \Phi_{sa})] \end{aligned} \tag{27c}$$

It is now easily verified that, subject to the condition

$$\cosh \alpha(w_1 - w_3) \doteq 1 \qquad \text{or} \qquad \left(\frac{\alpha\lambda}{4}\right)^2 \ll 1 \tag{28}$$

the following expressions are valid:

$$\frac{V_1^2 + V_3^2 - V_2^2}{V_2^2} = \frac{\sinh^2 2(\alpha w_2 + \rho_{sa}) + \cos^2 2(\beta w_1 + \Phi_{sa})}{[\cosh 2(\alpha w_2 + \rho_{sa}) - \sin 2(\beta w_1 + \Phi_{sa})]^2} \tag{29a}$$

$$\frac{V_1^2 - V_3^2}{2V_2^2} = \frac{\sinh 2(\alpha w_2 + \rho_{sa}) \sinh \alpha(w_1 - w_3) + \cos 2(\beta w_1 + \Phi_{sa})}{\cosh 2(\alpha w_2 + \rho_{sa}) - \sin 2(\beta w_1 + \Phi_{sa})} \tag{29b}$$

If the first of the three probes is located at

$$\beta w_1 = \frac{\pi}{4} \qquad \text{so that } \beta w_2 = \frac{\pi}{2} \text{ and } \beta w_3 = \frac{3\pi}{4} \tag{30}$$

the above formulas reduce to

$$\frac{V_1^2 + V_3^2 - V_2^2}{V_2^2} = \frac{\sinh^2 2(\alpha\lambda/4 + \rho_{sa}) + \sin^2 2\Phi_{sa}}{[\cosh 2(\alpha\lambda/4 + \rho_{sa}) - \cos 2\Phi_{sa}]^2} \tag{31a}$$

$$\frac{V_1^2 - V_3^2}{2V_2^2} = \frac{\sinh 2(\alpha\lambda/4 + \rho_{sa}) \sinh \alpha\lambda/4 - \sin 2\Phi_{sa}}{\cosh 2(\alpha\lambda/4 + \rho_{sa}) - \cos 2\Phi_{sa}} \tag{31b}$$

Subject to the following conditions (which are readily satisfied for a wide range of impedances terminating a low-loss line):

$$\frac{\alpha\lambda}{4} \ll \rho_{sa} \tag{32a}$$

$$\left|\sinh 2\left(\frac{\alpha\lambda}{4} + \rho_{sa}\right) \sinh \frac{\alpha\lambda}{4}\right| \ll |\sin 2\Phi_{sa}| \tag{32b}$$

these may be reduced further. The results are

$$\frac{V_1^2 + V_3^2 - V_2^2}{V_2^2} \doteq \frac{\sinh^2 2\rho_{sa} + \sin^2 2\Phi_{sa}}{(\cosh 2\rho_{sa} - \cos 2\Phi_{sa})^2} = r_{1sa}^2 + x_{1sa}^2 \tag{33a}$$

$$\frac{V_1^2 - V_3^2}{2V_2^2} \doteq \frac{-\sin 2\Phi_{sa}}{\cosh 2\rho_{sa} - \cos 2\Phi_{sa}} = x_{1sa} \tag{33b}$$

where r_{1sa} and x_{1sa} are the normalized apparent terminal resistance and reactance, as defined in Chap. III, Sec. 2. Only if terminal-zone effects are negligible may the subscripts a be omitted.

It is seen that, by measuring the voltage amplitude at three fixed points located at exactly $\lambda/8$, $\lambda/4$, and $3\lambda/8$ from the load, the impedance of the load may be determined. Note that the three probes are assumed to be so tuned and so loosely coupled as to have no significant effect on the line and on one another. If desired, the probes may be located at other distances than those specified in (30), with corresponding changes in the formulas.

Determination of the Characteristic Impedance of the Line. The characteristic impedance of a transmission line is a scale factor relating current and voltage. It is the normalizing factor in the impedance. It can be computed directly from the dimensions of the line using the theoretical formula, but in general it cannot be measured on the line itself, since there is no absolute standard for impedance.

The characteristic impedance of one transmission line is readily measured using another line with a known characteristic impedance. This is accomplished by measuring the apparent impedance of a section of the line when used as a termination for the measuring line. The usual procedure is to select a section of line of length s and measure its input impedance $\boldsymbol{Z}_{ic}$ when it is short-circuited with a piston or a disk and $\boldsymbol{Z}_{io}$ when it is open-circuited. In the first case $\rho_s = 0$ and $\Phi_s = \pi/2$; in the second case $\rho_s = 0$ and $\Phi_s = 0$. The two input impedances are

$$\boldsymbol{Z}_{io} = \boldsymbol{Z}_c \coth \boldsymbol{\gamma} s \qquad \boldsymbol{Z}_{ic} = \boldsymbol{Z}_c \tanh \boldsymbol{\gamma} s \tag{34}$$

The product of these expressions is

$$Z_c^2 = Z_{io}Z_{ic} \tag{35}$$

If Z_{io} and Z_{ic} are measured, Z_c may be computed from (35).

Note that, where two transmission lines with different cross sections are connected, a discontinuity exists of which no account is taken in the above procedure. Moreover an ideal open circuit such as is presumed in (34) does not exist owing to the capacitive end effect that characterizes every practically available transmission line. An analysis of junction and end effects is given in Chap. V. But for many purposes, especially with lines of sufficiently small cross-sectional dimensions, they are relatively unimportant, and (35) with (34) is adequate. In this section (35) is considered without correction.

By separating the real and imaginary parts of (35) using

$$Z_{io} = R_{io} + jX_{io},\ Z_{ic} = R_{ic} + jX_{ic}, \text{ and } Z_c = R_c(1 - j\phi_c)$$

the following two equations are obtained:

$$R_c^2(1 - \phi_c^2) = R_{io}R_{ic} - X_{io}X_{ic} \tag{36a}$$

$$-2\phi_c R_c^2 = X_{io}R_{ic} + X_{ic}R_{io} \tag{36b}$$

It follows from these equations or from the typical curves of the input reactance of a section of transmission line that either X_{io} or X_{ic} is negative and the other is positive. Since on all low-loss lines the inequality $\phi_c^2 \ll 1$ is a good approximation, (36a) may be used to evaluate R_c and (36b) to evaluate ϕ_c. Thus, with $\phi_c^2 \ll 1$,

$$R_c \doteq \sqrt{R_{io}R_{ic} - X_{io}X_{ic}} \tag{37a}$$

$$\phi_c \doteq -\frac{1}{2}\frac{X_{io}R_{ic} + X_{ic}R_{io}}{R_{io}R_{ic} - X_{io}X_{ic}} \tag{37b}$$

If the lengths s of the section of line of unknown characteristic impedance Z_c may be assigned freely, great simplification is achieved by selecting a length for which the inequalities

$$R_{io}^2 \ll |X_{io}|^2 \qquad R_{ic}^2 \ll |X_{ic}|^2 \tag{38}$$

are satisfied. This is true when the electrical length is near one of the following: $\beta s = \pi/4,\ 3\pi/4, \ldots$. With such a choice of βs (37a,b) reduce to

$$R_c = \sqrt{-X_{io}X_{ic}} \tag{39a}$$

$$\phi_c = \frac{1}{2}\left(\frac{R_{ic}}{X_{ic}} + \frac{R_{io}}{X_{io}}\right) \tag{39b}$$

In this case R_c can be determined from a measurement of reactances only.

Typical numerical values illustrating the order of magnitude of X_{io} and X_{ic} compared with R_{io} and R_{ic} when $\beta s = \pi/4$ and $3\pi/4$ are listed in Table 13.1.

TABLE 13.1

Type of line	βs	R_{ic}	R_{io}	$-X_{io} = X_{ic}$	$(R_{ic}/X_{ic})^2$	$(R_{io}/X_{io})^2$
Two-wire.....	$\frac{\pi}{4}$	0.9	0.2	440	4.2×10^{-6}	2.1×10^{-7}
Two-wire.....	$\frac{3\pi}{4}$	1.3	2.0	440	8.3×10^{-6}	2.1×10^{-5}
Coaxial.....	$\frac{\pi}{4}$	0.02	0.005	75	7.1×10^{-8}	4.5×10^{-9}
Coaxial.....	$\frac{3\pi}{4}$	0.3	0.5	75	1.6×10^{-5}	4.5×10^{-5}

In most cases the calculation of R_c from (39*a*) is convenient and reasonably accurate. On the other hand, the very small quantity ϕ_c is usually more easily determined from the approximate relation $\phi_c \doteq \alpha/\beta$ and the measured values of α and β.

Comparison of Phases. If a transmission line is terminated in its characteristic impedance, the current and voltage vary progressively and uniformly in phase along the line. Use of this fact may be made for comparing relative phases at different points in a circuit or in another

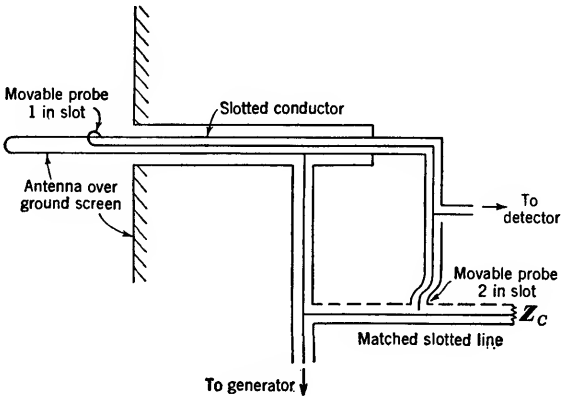


FIG. 13.8. Circuit for comparing phases (attenuators, line stretchers, etc., are not shown).

transmission line or for determining the complete relative distribution of phase along a line or an antenna.

The procedure is illustrated in Fig. 13.8 for determining the phase along an antenna. It consists simply in coupling a fraction of the power supplied to the circuit in which measurements of phase are contemplated into an auxiliary transmission line that is terminated in its characteristic impedance Z_c. Two movable probes, each connected to a transmission line and both joined to a mixer and detector, are provided. One of the

probes serves to explore the circuit under test (the antenna in Fig. 13.8), whereas the other must travel along the auxiliary matched line. A convenient but arbitrary reference point for phase is selected in the circuit under test, and the first probe is moved to this point and there coupled to the circuit. The second probe is now moved along the matched line until a minimum (or, if the outputs are correctly adjusted with attenuators, a null) is observed in the detector. The location of the probe along the line is marked; it is the reference point in the line. In this adjustment the signals reaching the mixer from the circuit and from the matched line are in phase opposition.

The first probe is now moved to a position at which phase is to be determined in the circuit under test, or it is moved progressively from point to point. At each location the traveling probe is moved along the matched line until a minimum (or null) is observed in the detector. From the distance in the matched line between the reference point and the location of the probe, the relative phase at the particular point or succession of points may be determined.

Measurement of Dielectric Constants, Permeabilities, and Conductivities of Poorly Conducting Media: Drude's Method. A theoretically simple method of measuring the dielectric constant ϵ and the conductivity σ of solids and liquids uses the material in question as the dielectric in a transmission line of coaxial or shielded-pair type. By determining the phase constant β and the attenuation constant α using methods described earlier in this chapter, formulas of Chap. II, Sec. 10, may be used to compute ϵ and σ. If good conductors are used for the transmission line, the condition $\omega^2 lc \gg rg$ is easily satisfied by the line constants l, c, r, and g. It follows from Chap. II, Sec. 10, Eq. (16), that

$$\beta = \omega \sqrt{lc}\, f(h_\gamma) \qquad \alpha = \omega \sqrt{lc}\, g(h_\gamma) \tag{40}$$

where, from Chap. II, Sec. 10, Eq. (8),

$$h_\gamma \doteq \frac{g}{\omega c} + \frac{r}{\omega l} = \frac{\sigma}{\omega \epsilon} + \frac{r}{\omega l} \tag{41}$$

For a low-loss line (as is here assumed) the following inequality must be satisfied:

$$h_\gamma^2 \ll 1 \tag{42}$$

so that

$$f(h_\gamma) \doteq 1 \qquad g(h_\gamma) \doteq \frac{h_\gamma}{2} \tag{43}$$

After the substitution of (43) in (40) and the use of (42), the following expressions are obtained for the phase and attenuation constants of the line with a low-loss dielectric medium with real effective dielectric constant $\epsilon_e = \epsilon_0 \epsilon_{er}$, conductivity σ_e, and permeability $\mu = \mu_0 \mu_r$:

$$\beta_e = \omega \sqrt{\mu \epsilon_e} \qquad \alpha_e = \frac{\sqrt{\mu \epsilon_e}}{2} \left(\frac{\sigma_e}{\epsilon_e} + \frac{r}{\mu_r l_0^e} \right) \tag{44}$$

where $\mu_r l_0^e \equiv l^e$ is the inductance per unit length of the line. If the same line is evacuated so that $\sigma_e = 0$, $\mu_r = 1$, and $\epsilon_{er} = 1$, the constants are

$$\beta = \omega \sqrt{\mu_0 \epsilon_0} \qquad \alpha = \frac{\sqrt{\mu_0 \epsilon_0}}{2} \frac{r}{l_0^e} \tag{45}$$

The combination of (44) and (45) gives

$$\mu_r \epsilon_{er} = \frac{\beta_e^2}{\beta^2} \qquad \sigma_e = 2 \sqrt{\frac{\epsilon_0 \epsilon_{er}}{\mu_0 \mu_r}} \left(\alpha_e - \alpha \sqrt{\frac{\epsilon_{er}}{\mu_r}} \right) \tag{46}$$

If the medium is a dielectric with $\mu_r = 1$, (46) reduces to

$$\epsilon_{er} = \frac{\beta_e^2}{\beta^2} \qquad \sigma_e = 2 \sqrt{\frac{\epsilon_0 \epsilon_{er}}{\mu_0}} \left(\alpha_e - \alpha \sqrt{\epsilon_{er}} \right) \tag{47}$$

If β_e and β are measured, ϵ_{er} may be determined; if, in addition, α_e and α are measured, σ_e may be evaluated.

If the medium is a magnetic material with $\epsilon_{er} \doteq 1$,

$$\mu_r = \frac{\beta_e^2}{\beta^2} \qquad \sigma_e = 2 \sqrt{\frac{\epsilon_0}{\mu_0 \mu_r}} \left(\alpha_e - \frac{\alpha}{\sqrt{\mu_r}} \right) \tag{48}$$

so that μ_r and σ_e may be determined if β_e, β, α_e, and α are known.

Although theoretically simple, the method referred to above for measuring dielectric constants, permeabilities, and conductivities is not always convenient from the experimental point of view. This is primarily due to the large sample of dielectric required to fill the entire line and the high over-all attenuation with an even slightly conducting medium. It may be added that transmission-line measurements in a dielectric-filled line are often awkward. Other methods without these difficulties are described in Chap. V.

PROBLEMS

1. A low-loss transmission line ($R_c = 300$ ohms, $\phi_c = \alpha/\beta = 10^{-3}$, $s = 4.2$ m) connects a generator ($\mathbf{Z}_{0a} = 10 + j0$ ohms, $V_0^e = 100$ volts, $f = 300$ Mc/sec) to a load ($\mathbf{Z}_{sa} = 4{,}000 + j0$ ohms). Determine the following:

(*a*) The currents in the generator and the load.

(*b*) The current and the voltage on the line halfway between the generator and the load.

(*c*) The location and magnitude of each maximum and minimum of current along the line.

(*d*) The standing-wave ratio.

(*e*) The efficiency of power transmission to the load.

2. A two-wire line of characteristic impedance $\mathbf{Z}_c \doteq R_c = 300$ ohms is loaded at one end by an antenna with impedance $\mathbf{Z}_s = 90 + j45$ ohms. At a distance of one-half wavelength from the load a second, identical antenna is connected across the line. Determine the standing-wave ratio and the distribution of current on the main line and on the section between the two antennas. Neglect losses in the line and assume terminal-zone effects to be negligible.

3. An impedance of $800 - j50$ ohms is measured on a transmission line for which $Z_c \doteq R_c = 400$ ohms and $\alpha = 10^{-3}$ neper/m. The frequency is 100 Mc/sec.

(*a*) Where is the voltage minimum nearest the load? What is the standing-wave ratio?

(*b*) What is the width of the resonance curve obtained by varying the length of the line about the peak occurring at the next to the shortest length of line?

4. An apparent impedance $Z_{sa} = 100 - j40$ ohms is to be measured by the distribution-curve-dip method on a low-loss line for which $Z_c \doteq R_c = 50$ ohms. Neglecting line losses, predict the distance from the load and the half-power width of the current distribution-curve dip.

5. The frequency of a generator is determined accurately to six significant figures at a value near 300 Mc/sec. Describe a method for determining experimentally the phase velocity of propagation along a coaxial line. Select practical values for the line constants and determine the accuracy with which such a measurement might be made.

6. A coaxial line is terminated in its characteristic impedance $Z_c \doteq R_c = 50$ ohms by a series transformer connected between the end of the line and a resistive load of 800 ohms. Neglecting losses in the line and junction effects, determine and plot the distribution of the magnitude of the normalized current along the line and along the transformer.

7. A two-wire line is terminated in its characteristic impedance $Z_c \doteq R_c = 400$ ohms by a single-stub matching network inserted between the line and a resistive load of 50 ohms. Determine the normalized currents on the line and in the two parts of the matching circuit. Neglect losses in the line and in the matching section, and assume junction effects to be negligible. Use a closed or open stub, whichever is shorter.

8. A copper two-wire line is placed symmetrically in a brass pipe to form a shielded-pair line. The pipe is to be filled with water in order to measure the dielectric constant by moving a copper-wire bridge along the two-wire line to determine the location of successive resonances. The wires are No. 9 separated 2 cm between centers; the pipe is 8 cm in diameter. Investigate the accuracy of the results to be expected by determining the sharpness of two successive resonance curves. This may be done by comparing the half-power widths when the pipe is filled successively with air and with water. Use $\sigma = 2 \times 10^{-4}$ mho/m ($\epsilon_r = 81$) for distilled water, $\sigma = 5.65 \times 10^7$ mhos/m for copper, and $\sigma = 1.5 \times 10^7$ mhos/m for brass.

9. Repeat Prob. 8 for lake water with $\sigma = 10^{-2}$ mho/m and $\epsilon_r = 81$.

CHAPTER V

DISCONTINUITIES AND NONUNIFORMITIES IN TRANSMISSION LINES

1. Two-terminal-pair Networks in Transmission Lines.[15] The continuity of a uniform transmission line may be interrupted in numerous ways. In earlier chapters shunt and series sections of line and combinations of these are considered under the ideal conditions in which

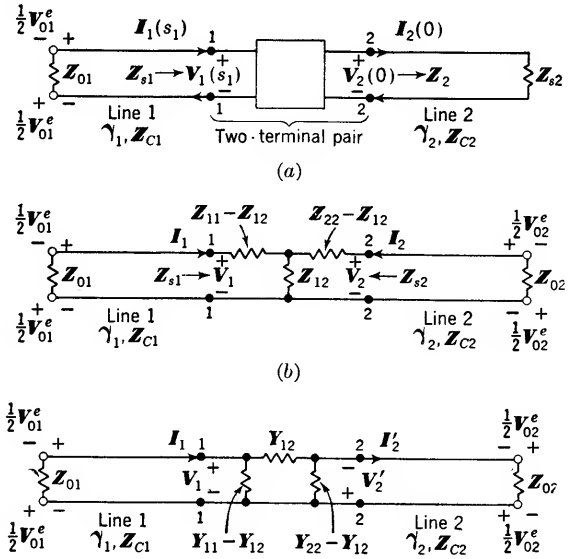


FIG. 1.1. (*a*) Two-terminal pair joining two lines. (*b*) T network as common load for two lines. (*c*) Π network as common load for two lines.

terminal-zone and junction-zone effects are negligible, so that the formulation of uniform-line theory may be applied to each section as if isolated. In general, the uniformity of a transmission line may be interrupted by an arbitrary network that has two pairs of terminals. Such a network is a special case of a general four-terminal network; it may be called a two-terminal pair or a transducer. Three independent parameters are required to describe its electrical properties provided nonreciprocal cir-

cuit elements such as gyrators are excluded. In its most general form it connects two different but individually uniform lines, as illustrated in Fig. 1.1*a*. The properties of such a network may be represented by the input and output currents and voltages associated with the two pairs of terminals, as in Fig. 1.1*a*; by an equivalent T section, as in Fig. 1.1*b*; or by an equivalent Π section, as in Fig. 1.1*c*. In each case the sign and direction conventions for voltages and currents are different. The choice in Fig. 1.1*a* is that characteristic of a continuing transmission line. In Fig. 1.1*b* the currents and voltages are those characteristic of two lines for which the two pairs of terminals of the T section constitute the load. Note that this choice makes the currents maintained by the two generators codirectional in the mutual element $\boldsymbol{Z}_{12}$. In Fig. 1.1*c* the currents and voltages at terminals 2 are reversed as compared with Fig. 1.1*b*, so that the currents maintained by the two generators are codirectional in the mutual element $\boldsymbol{Y}_{12}$. Note that

$$\boldsymbol{I}_2(0) = -\boldsymbol{I}_2 = \boldsymbol{I}_2' \qquad \text{and} \qquad \boldsymbol{V}_2(0) = \boldsymbol{V}_2 = -\boldsymbol{V}_2'$$

Balanced T and Π networks for use with balanced lines are shown in

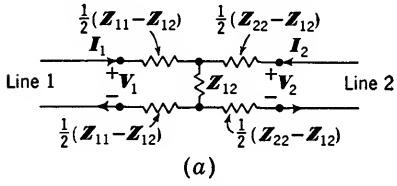


FIG. 1.2*a*. Balanced T network as common load for two balanced lines.

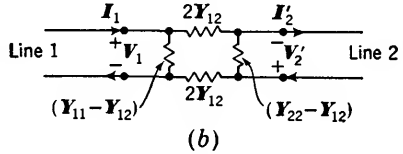


FIG. 1.2*b*. Balanced Π network as common load for two balanced lines.

Fig. 1.2*a* and *b*. The same equations apply to these figures as to Fig. 1.1*b* and *c*.

Input-Output Current-Voltage Equations. The input and output currents and voltages in Fig. 1.1*a* and *b* are related as follows:

$$\boldsymbol{V}_1(s) = \boldsymbol{V}_1 = \boldsymbol{V}_2(0)\boldsymbol{A} + \boldsymbol{I}_2(0)\boldsymbol{B} = \boldsymbol{V}_2\boldsymbol{A} - \boldsymbol{I}_2\boldsymbol{B} = -\boldsymbol{V}_2'\boldsymbol{A} + \boldsymbol{I}_2'\boldsymbol{B} \quad (1a)$$

$$\boldsymbol{I}_1(s) = \boldsymbol{I}_1 = \boldsymbol{V}_2(0)\boldsymbol{C} + \boldsymbol{I}_2(0)\boldsymbol{D} = \boldsymbol{V}_2\boldsymbol{C} - \boldsymbol{I}_2\boldsymbol{D} = -\boldsymbol{V}_2'\boldsymbol{C} + \boldsymbol{I}_2'\boldsymbol{D} \quad (1b)$$

These equations may be inverted and solved for $\boldsymbol{V}_2$ and $\boldsymbol{I}_2$. With the relation

$$\boldsymbol{AD} - \boldsymbol{BC} = 1 \qquad (2)$$

(which applies to all reciprocal circuits and is derived very readily by application of the reciprocal theorem to the circuit of Fig. 1.1*a*) the results are

$$\boldsymbol{V}_2(0) = \boldsymbol{V}_2 = -\boldsymbol{V}_2' = \boldsymbol{DV}_1 - \boldsymbol{BI}_1 \qquad (3a)$$

$$\boldsymbol{I}_2(0) = -\boldsymbol{I}_2 = \boldsymbol{I}_2' = -\boldsymbol{CV}_1 + \boldsymbol{AI}_1 \qquad (3b)$$

These expressions may be written in matrix form as follows [only formulas for $\boldsymbol{V}_2$ and $\boldsymbol{I}_2$ for use in Fig. 1.1*b* are given, but the substitutions $\boldsymbol{V}_2(0) = \boldsymbol{V}_2$ and $\boldsymbol{I}_2(0) = -\boldsymbol{I}_2$ or $\boldsymbol{V}_2' = -\boldsymbol{V}_2$ and $\boldsymbol{I}_2 = -\boldsymbol{I}_2'$ may be made

to adapt the formulation to Fig. 1.1*a* or *c*]:

$$\begin{bmatrix} V_1 \\ I_1 \end{bmatrix} = \begin{bmatrix} A & B \\ C & D \end{bmatrix} \begin{bmatrix} V_2 \\ -I_2 \end{bmatrix} \tag{4}$$

$$\begin{bmatrix} V_2 \\ I_2 \end{bmatrix} = \begin{bmatrix} D & B \\ C & A \end{bmatrix} \begin{bmatrix} V_1 \\ -I_1 \end{bmatrix} \tag{5}$$

As given in (2), it is necessary that the determinant

$$\begin{vmatrix} A & B \\ C & D \end{vmatrix} = \begin{vmatrix} D & B \\ C & A \end{vmatrix} = 1 \tag{6}$$

if the reciprocal theorem is to be satisfied.

It is clear from (4) and (5) that a symmetrical four-terminal network is defined by

$$D = A \tag{7}$$

An ideal transformer of N turns connected to step up the voltage by a factor N and step down the current by a factor $1/N$ from terminals 1 to terminals 2 is given by

$$\begin{bmatrix} A & B \\ C & D \end{bmatrix} = \begin{bmatrix} \frac{1}{N} & 0 \\ 0 & N \end{bmatrix} \tag{8a}$$

so that

$$V_1 = \frac{V_2}{N} \qquad I_1 = NI_2 \tag{8b}$$

This is illustrated in Fig. 1.3.

The T network of Fig. 1.1*b* is conveniently represented by the voltage equations

$$V_1 = I_1Z_{11} + I_2Z_{12} \tag{9a}$$

$$V_2 = I_1Z_{21} + I_2Z_{22} \tag{9b}$$

where the relation corresponding to (6) and defining a reciprocal circuit is

$$Z_{12} = Z_{21} \tag{10}$$

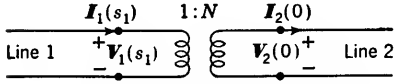


FIG. 1.3. Ideal step-up transformer.

The matrix equivalent is

$$\begin{bmatrix} V_1 \\ V_2 \end{bmatrix} = \begin{bmatrix} Z_{11} & Z_{12} \\ Z_{21} & Z_{22} \end{bmatrix} \begin{bmatrix} I_1 \\ I_2 \end{bmatrix} \tag{11}$$

If (9*a*,*b*) or (11) is solved for the currents, the results are

$$I_1 = V_1Y_{11} - V_2Y_{12} \tag{12a}$$

$$I_2 = -V_1Y_{21} + V_2Y_{22} \tag{12b}$$

where

$$Y_{11} = \frac{Z_{22}}{Z_{11}Z_{22} - Z_{12}Z_{21}} \tag{13a}$$

$$Y_{12} = \frac{Z_{12}}{Z_{11}Z_{22} - Z_{12}Z_{21}} \tag{13b}$$

$$Y_{22} = \frac{Z_{11}}{Z_{11}Z_{22} - Z_{12}Z_{21}} \tag{13c}$$

Note that (12*a*,*b*) may be written with all plus signs, if the sign of Y_{12} in (13*b*) is reversed. Alternatively, if the sign convention is changed from that of Fig. 1.1*b* to that of Fig. 1.1*c* by substituting $V_2' = -V_2$ and $I_2' = -I_2$ in (12*a*,*b*), only plus signs appear with Y_{12}, as defined in (13*b*). In this case the Z's are defined for the conventions of Fig. 1.1*b*, and the Y's for the conventions of Fig. 1.1*c*.

The Π network of Fig. 1.1*c* may be represented by the following current equations:

$$I_1 = V_1 Y_{11} + V_2' Y_{12} \tag{14a}$$
$$I_2' = V_1 Y_{21} + V_2' Y_{22} \tag{14b}$$

where
$$Y_{21} = Y_{12} \tag{15}$$

The matrix equivalent is

$$\begin{bmatrix} I_1 \\ I_2' \end{bmatrix} = \begin{bmatrix} Y_{11} & Y_{12} \\ Y_{21} & Y_{22} \end{bmatrix} \begin{bmatrix} V_1 \\ V_2' \end{bmatrix} \tag{16}$$

If (14*a*,*b*) are solved for V_1 and V_2', the results are

$$V_1 = I_1 Z_{11} - I_2' Z_{12} \tag{17a}$$
$$V_2' = -I_1 Z_{21} + I_2' Z_{21} \tag{17b}$$

where
$$Z_{11} = \frac{Y_{22}}{Y_{11}Y_{22} - Y_{12}Y_{21}} \tag{18a}$$
$$Z_{12} = \frac{Y_{12}}{Y_{11}Y_{22} - Y_{12}Y_{21}} \tag{18b}$$
$$Z_{22} = \frac{Y_{11}}{Y_{11}Y_{22} - Y_{12}Y_{21}} \tag{18c}$$

Note that (17*a*,*b*) may be made formally like (9*a*,*b*) if Z_{12} is changed to the negative of the value defined in (18*b*). Alternatively the sign convention may be changed from that in Fig. 1.1*c* to that in Fig. 1.1*b* by introducing $V_2 = -V_2'$ and $I_2 = -I_2'$, which changes (17*a*,*b*) into (9*a*,*b*) and leaves (18*b*) unchanged. In this case, however, the Y's are all defined using the conventions of Fig. 1.1*c*, the Z's using the convention of Fig. 1.1*b*.

The relations between the elements of the impedance and admittance matrices and the *ABCD* coefficients are obtained by substituting (9*a*,*b*) and (14*a*,*b*) in the appropriate forms of (1*a*,*b*). The results are

$$\frac{Z_{11}}{Z_{12}} = A = \frac{Y_{22}}{Y_{12}} \tag{19a}$$
$$\frac{Z_{11}Z_{22} - Z_{12}^2}{Z_{12}} = B = \frac{1}{Y_{12}} \tag{19b}$$
$$\frac{1}{Z_{12}} = -C = \frac{Y_{11}Y_{22} - Y_{12}^2}{Y_{12}} \tag{19c}$$
$$\frac{Z_{22}}{Z_{12}} = -D = \frac{Y_{11}}{Y_{12}} \tag{19d}$$

Note that the equations on the left imply the "impedance" sign conventions of Fig. 1.1*b*, and those on the right, the "admittance" sign conventions of Fig. 1.1*c*. If the "impedance" conventions are to be used throughout and (12*a*,*b*) are to be written with the plus signs, negative signs must be attached to $\boldsymbol{Y}_{12}$ in (19*b*,*c*). Similarly, if the "admittance" convention is to be used throughout and (17*a*,*b*) are to be written with plus signs, negative signs must be attached to $\boldsymbol{Z}_{12}$ in (19*b*,*c*).

As a consequence of the reciprocal relations (2), (10), and (15), only three instead of four parameters are required in order to specify the properties of the two-terminal-pair network. These may be any three of the ***ABCD*** coefficients—usually $\boldsymbol{A}$, $\boldsymbol{D}$, and $\boldsymbol{B}$ or $\boldsymbol{C}$; $\boldsymbol{Z}_{11}$, $\boldsymbol{Z}_{12}$, and $\boldsymbol{Z}_{22}$; or $\boldsymbol{Y}_{11}$, $\boldsymbol{Y}_{12}$, and $\boldsymbol{Y}_{22}$.

The impedance or admittance looking into the network at terminals 11 when terminals 22 are connected to an arbitrary load $\boldsymbol{Z}_L = 1/\boldsymbol{Y}_L$ (or vice versa) may be expressed in terms of the ***ABCD*** coefficients, the impedance coefficients, or the admittance coefficients.

Proceeding from (1*a*,*b*) using the "impedance" or "admittance" conventions of Fig. 1.1*b* or 1.1*c* and setting

$$\boldsymbol{V}_2 = -\boldsymbol{I}_2\boldsymbol{Z}_L \qquad \text{or} \qquad \boldsymbol{I}_2' = -\boldsymbol{V}_2'\boldsymbol{Y}_L \tag{20}$$

the input impedance and admittance at terminals 11 are

$$\boldsymbol{Z}_{1in} \equiv \frac{\boldsymbol{V}_1}{\boldsymbol{I}_1} = \frac{\boldsymbol{A}\boldsymbol{Z}_L - \boldsymbol{B}}{\boldsymbol{C}\boldsymbol{Z}_L - \boldsymbol{D}} = \frac{1}{\boldsymbol{Y}_{1in}} \tag{21}$$

The ***ABCD*** coefficients may be expressed in terms of the impedance or admittance coefficients using (19*a*,*b*,*c*,*d*), or (9*a*,*b*) and (14*a*,*b*) may be solved directly to obtain the following equivalent formulas:

$$\boldsymbol{Z}_{1in} = \boldsymbol{Z}_{11} - \frac{\boldsymbol{Z}_{12}\boldsymbol{Z}_{21}}{\boldsymbol{Z}_{22} + \boldsymbol{Z}_L} \tag{22}$$

$$\boldsymbol{Y}_{1in} = \boldsymbol{Y}_{11} - \frac{\boldsymbol{Y}_{12}\boldsymbol{Y}_{21}}{\boldsymbol{Y}_{22} + \boldsymbol{Y}_L} \tag{23}$$

$\boldsymbol{Z}_{1in}$ and $\boldsymbol{Y}_{1in}$ are, of course, independent of the convention adopted for the directions of the currents and voltages.

If the two-terminal-pair network is driven from terminals 22 and the load $\boldsymbol{Z}_L$ is connected across terminals 11, the input impedance and admittance are

$$\boldsymbol{Z}_{2in} = \frac{\boldsymbol{D}\boldsymbol{Z}_L - \boldsymbol{B}}{\boldsymbol{C}\boldsymbol{Z}_L - \boldsymbol{A}} = \frac{1}{\boldsymbol{Y}_{2in}} \tag{24}$$

$$\boldsymbol{Z}_{2in} = \boldsymbol{Z}_{22} - \frac{\boldsymbol{Z}_{12}\boldsymbol{Z}_{21}}{\boldsymbol{Z}_{11} + \boldsymbol{Z}_L} \tag{25}$$

$$\boldsymbol{Y}_{2in} = \boldsymbol{Y}_{22} - \frac{\boldsymbol{Y}_{12}\boldsymbol{Y}_{21}}{\boldsymbol{Y}_{11} + \boldsymbol{Y}_L} \tag{26}$$

In order to determine three coefficients using (21) and (24), (22) and (25), or (23) and (26), convenient values of the arbitrary load Z_L may be selected. In general, these are the short- and open-circuit values $Z_L = 0$ and $Z_L = \infty$, although any other values may be selected. Consider the following values:

For $Z_L = \infty$ and $Y_L = 0$:

$$Z_{1in} \equiv Z_{1oc} = \frac{A}{C} = Z_{11} \qquad Y_{1in} = Y_{1oc} = \frac{Y_{11}Y_{22} - Y_{12}^2}{Y_{22}} \tag{27a}$$

$$Z_{2in} \equiv Z_{2oc} = \frac{D}{C} = Z_{22} \qquad Y_{2in} = Y_{2oc} = \frac{Y_{11}Y_{22} - Y_{12}^2}{Y_{11}} \tag{27b}$$

For $Z_L = 0$ and $Y_L = \infty$:

$$Z_{1in} \equiv Z_{1sc} = \frac{B}{D} = \frac{Z_{11}Z_{22} - Z_{12}^2}{Z_{22}} \qquad Y_{1in} = Y_{1sc} = Y_{11} \tag{28a}$$

$$Z_{2in} \equiv Z_{2sc} = \frac{B}{A} = \frac{Z_{11}Z_{22} - Z_{12}^2}{Z_{11}} \qquad Y_{2in} = Y_{2sc} = Y_{22} \tag{28b}$$

With (2) it follows that

$$\frac{Z_{1sc}}{Z_{1oc}} = \frac{BC}{AD} = \frac{Z_{2sc}}{Z_{2oc}} \tag{29}$$

Also

$$\frac{Y_{1sc}}{Y_{1oc}} = \frac{Y_{2sc}}{Y_{2oc}} \tag{30}$$

It is clear that, if any *three* of the four quantities Z_{1oc}, Z_{2oc}, Z_{1sc}, and Z_{2sc} are determined, the $ABCD$ coefficients, the impedance coefficients, and the admittance coefficients can be evaluated, and with these the input impedance and admittance of reciprocal networks.

If the network is purely reactive, it follows from (19*a*,*b*,*c*,*d*) that A and D must be real, B and C imaginary.

Symmetrical Networks. The representation of two-terminal-pair networks is readily specialized to the important case of *symmetrical* networks by setting, in addition to $Z_{21} = Z_{12}$ and $Y_{21} = Y_{12}$,

$$A = D \qquad Z_{11} = Z_{22} \qquad Y_{11} = Y_{22} \tag{31}$$

An alternative representation of a symmetrical network makes use of the resolution of the total currents and voltages into symmetrical and antisymmetrical combinations referred to the plane through the *center* of the network. It has already been shown in Chap. III, Sec. 12, that the elements of the impedance matrix of a symmetrical T section may be expressed as follows:

$$Z_{11} = \tfrac{1}{2}[Z_{in}^{(s)} + Z_{in}^{(a)}] \tag{32a}$$

$$Z_{12} = -\tfrac{1}{2}[Z_{in}^{(s)} - Z_{in}^{(a)}] \tag{32b}$$

$Z_{in}^{(s)}$ is the input impedance at either pair of terminals when (*a*) equal voltages in phase are applied simultaneously across both pairs of termi-

nals, as in Fig. 1.4*a*, or (*b*) the T section is short-circuited across its center, as in Fig. 1.4*b*. $Z_{in}^{(a)}$ is the input impedance at either pair of terminals when (*a*) equal voltages in phase opposition are applied simultaneously across both pairs of terminals, as in Fig. 1.4*c*, or (*b*) the T section is open-circuited across its center, as in Fig. 1.4*d*.

In Chap. III, Sec. 12, the elements of the T section were calculated to represent a length $2d$ of smooth line. Obviously the same procedure and

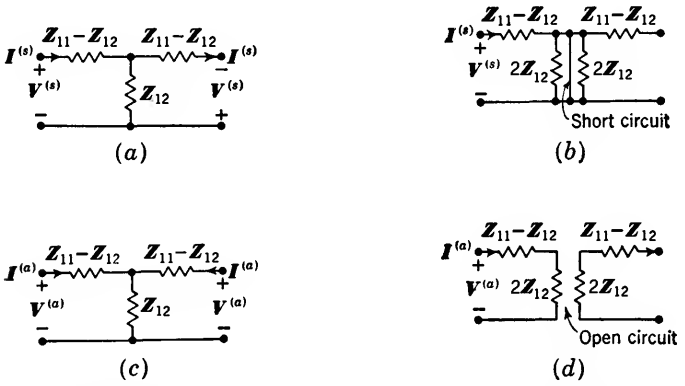


FIG. 1.4. (*a*) Circuit for determining $Z^{(s)}$. (*b*) Equivalent circuit for determining $Z^{(s)}$. (*c*) Circuit for determining $Z^{(a)}$. (*d*) Equivalent circuit for determining $Z^{(a)}$.

set of formulas apply to any symmetrical network for which an equivalent T section is to be determined.

The corresponding formulas for the elements of a symmetrical Π section are

$$Y_{11} = \tfrac{1}{2}[Y_{in}^{(s)} + Y_{in}^{(a)}] \tag{33a}$$

$$Y_{12} = -\tfrac{1}{2}[Y_{in}^{(s)} - Y_{in}^{(a)}] \tag{33b}$$

where $Y_{in}^{(s)} = 1/Z_{in}^{(s)}$ and $Y_{in}^{(a)} = 1/Z_{in}^{(a)}$.

2. Equivalent Transformer for Two-terminal-pair Network that Includes Sections of Transmission Line. Weissfloch Tangent Relation.[15,33,137] A simple and useful transformation of the general formula [Sec. 1, Eq. (21)] for the input impedance of a two-terminal-pair network may be carried out if this network includes sections of transmission line of adequate length. Consider the circuit in Fig. 2.1, in which an arbitrary two-terminal-pair network is connected between two transmission lines that may have different characteristics. Let the input terminals 11 be located in line 1 at an adequate but arbitrary distance from the network; let the output terminals be at 22 in line 2, also at an adequate distance from the network. The input impedance is given by

Sec. 1, Eq. (21), in the form

$$Z_{1in} = \frac{AZ_L - B}{CZ_L - D} = \frac{(A/C)Z_L - B/C}{Z_L - D/C} \tag{1}$$

where the output impedance Z_L is the impedance looking into a line of length S terminated in an arbitrary impedance Z_T. The characteristic

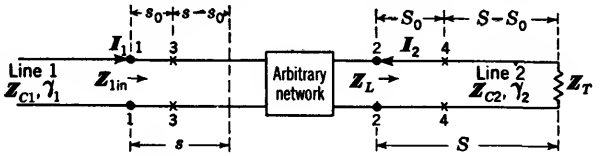


FIG. 2.1. Arbitrary two-terminal-pair network connecting two transmission lines.

impedances and propagation constants of the two lines are Z_{c1}, Z_{c2} and γ_1, γ_2. It follows that

$$Z_L = Z_{c2} \coth (\gamma_2 S + \theta_T) = Z_{c2} \tanh (\gamma_2 S + \theta_T') \tag{2}$$

where $\theta_T' = \tanh^{-1} (Z_T/Z_{c2})$. For convenience let

$$a = \frac{A}{CZ_{c1}} \qquad b = \frac{B}{CZ_{c1}Z_{c2}} \qquad c = \frac{D}{CZ_{c2}} \tag{3}$$

Also let

$$Z_{1in} = Z_{c1} \coth \left(\gamma_1 s + \rho_1 + j\frac{\pi}{2}\right) = Z_{c1} \tanh (\gamma_1 s + \rho_1) \tag{4}$$

where s is the distance from the input terminals 11 to the point between these terminals and the network at which the *current* has its *maximum*. The impedance looking to the right at this point is characterized by $\theta_1 = \rho_1 + j\pi/2$.

If (2), (3), and (4) are substituted in (1), this becomes

$$\tanh (\gamma_1 s + \rho_1) = \frac{a \tanh (\gamma_2 S + \theta_T') - b}{\tanh (\gamma_2 S + \theta_T') - c} \tag{5}$$

Now let the reference plane in line 1 be shifted from 11 to 33, a distance s_0 nearer the current maximum. The input impedance looking toward the load at 33 is given by

$$Z_{3in} = Z_{c1} \tanh [\gamma_1(s - s_0) + \rho_1] = Z_{c1} \frac{\tanh (\gamma_1 s + \rho_1) - \tanh \gamma_1 s_0}{1 - \tanh (\gamma_1 s + \rho_1) \tanh \gamma_1 s_0} \tag{6}$$

The substitution of (5) in (6) leads to the equation

$$\tanh [\gamma_1(s - s_0) + \rho_1] = \frac{(a - f_0) \tanh (\gamma_2 S + \theta_T') - (b - cf_0)}{bf_0 - c - (af_0 - 1) \tanh (\gamma_2 S + \theta_T')} \tag{7}$$

where

$$f_0 \equiv \tanh \gamma_1 s_0 \tag{8}$$

This expression may be rearranged as follows:

$$\tanh [\gamma_1(s - s_0) + \rho_1] = \frac{a - f_0}{bf_0 - c} \frac{\tanh (\gamma_2 S + \theta_T') - \tanh \gamma_2 S_0}{1 - \tanh \gamma_2 S_0 \tanh (\gamma_2 S + \theta_T')} \tag{9}$$

where the substitutions

$$\tanh \gamma_2 S_0 = \frac{b - cf_0}{a - f_0} = \frac{af_0 - 1}{bf_0 - c} \equiv p_0 \tag{10}$$

have been made as a definition of the complex distance S_0. The complex quantity p_0 is defined in (10). It is assumed that s_0 and S_0 can be so determined that (10) may be satisfied. For convenience let

$$k \equiv \frac{a - f_0}{bf_0 - c} \tag{11}$$

With (10) and (11), (9) reduces to the simple form

$$\tanh [\gamma_1(s - s_0) + \rho_1] = k \tanh [\gamma_2(S - S_0) + \theta_T'] \tag{12}$$

If the three new coefficients f_0, p_0, and k are determined experimentally, the three parameters a, b, and c in the original Eq. (5) may be obtained by solving the following three equations simultaneously [these are obtained from (10) and (11)]:

$$\begin{aligned} af_0 - bf_0p_0 + cp_0 &= 1 \\ ap_0 - b + cf_0 &= f_0p_0 \\ a - bf_0k + ck &= f_0 \end{aligned} \tag{13}$$

The solutions are

$$a = \frac{f_0p_0 - k}{p_0 - f_0k} \qquad b = \frac{f_0 - p_0k}{p_0 - f_0k} \qquad c = \frac{f_0p_0k - 1}{p_0 - f_0k} \tag{14}$$

Alternatively, if a, b, and c are given, the three parameters f_0, p_0, and k may be evaluated. The parameter f_0 is easily obtained from the middle equation in (10). This reduces to

$$f_0^2 - f_0 \frac{1 + a^2 - c^2 - b^2}{a - bc} + 1 = 0 \tag{15a}$$

so that

$$f_0 = \frac{1 + a^2 - b^2 - c^2}{2(a - bc)} \pm \left\{ \left[\frac{1 + a^2 - b^2 - c^2}{2(a - bc)} \right]^2 - 1 \right\}^{\frac{1}{2}} \tag{15b}$$

With f_0 obtained from (15b), p_0 and k can be evaluated directly from (10) and (11). Note that, in general, f_0, p_0, and k are complex and whereas s_0 is a real distance, S_0 is complex and not a physically meaningful distance. The $\pm$ sign in (15b) indicates two possible values of f_0 and hence of k and p_0.

The coefficients a, b, and c can be expressed directly in terms of the impedance elements of a T section or the admittance elements of a Π section using Sec. 1, Eqs. (19a,b,c,d), together with (3). Thus, for the T section,

$$\begin{aligned} a &= \frac{Z_{11}}{Z_{c1}} \qquad b = \frac{Z_{11}Z_{22} - Z_{12}^2}{Z_{c1}Z_{c2}} \qquad c = \frac{Z_{22}}{Z_{c2}} \\ f_0 &= \tanh \gamma_1 s_0 \qquad p_0 = \tanh \gamma_2 S_0 \qquad k = \frac{a - f_0}{bf_0 - c} \end{aligned} \tag{16}$$

The corresponding relations for the π section are easily derived. They are

$$\begin{aligned} \boldsymbol{a} &= \frac{Y_{11}}{Y_{c1}} \qquad \boldsymbol{b} = \frac{Y_{11}Y_{22} - Y_{12}^2}{Y_{c1}Y_{c2}} \qquad \boldsymbol{c} = \frac{Y_{22}}{Y_{c2}} \\ \boldsymbol{f}_0 &= \coth \gamma_1 s_0 \qquad \boldsymbol{p}_0 = \coth \gamma_2 S_0 \qquad \boldsymbol{k} = \frac{\boldsymbol{a} - \boldsymbol{f}_0}{\boldsymbol{b}\boldsymbol{f}_0 - \boldsymbol{c}} \end{aligned} \tag{17}$$

Reactive Network. The most important special case is that of a purely reactive two-terminal-pair network connected between two essentially lossless transmission lines. The following simplifications apply:

$$\begin{aligned} \boldsymbol{Z}_{11} &= jX_{11} \qquad \boldsymbol{Z}_{12} = jX_{12} \qquad \boldsymbol{Z}_{22} = jX_{22} \qquad \rho_1 = 0 \\ \boldsymbol{Z}_{c1} &\doteq R_{c1} \qquad \boldsymbol{Z}_{c2} \doteq R_{c2} \qquad \gamma_1 = j\beta_1 \qquad \gamma_2 = j\beta_2 \qquad \boldsymbol{\theta}_T' = j\Phi_T' \end{aligned} \tag{18}$$

With (18), the fundamental Eq. (12) reduces to the Weissfloch tangent relation:[33,137]

$$\tan \beta_1(s - s_0) = k \tan [\beta_2(S - S_0) + \Phi_T'] \tag{19}$$

In the original Weissfloch form $\Phi_T' = 0$, since a perfect short circuit is assumed to be the termination of line 2. For the tangent relation (19), which involves only real quantities, the general formulas (16) reduce to

$$\begin{aligned} \boldsymbol{a} = ja = j\frac{X_{11}}{R_{c1}} \qquad \boldsymbol{b} = b = \frac{X_{11}X_{22} - X_{12}^2}{R_{c1}R_{c2}} \qquad \boldsymbol{c} = jc = j\frac{X_{22}}{R_{c2}} \\ \boldsymbol{f}_0 = jf_0 = j \tan \beta_1 s_0 \qquad \boldsymbol{p}_0 = jp_0 = j \tan \beta_2 S_0 \qquad \boldsymbol{k} = k = \frac{a - f_0}{bf_0 - c} \end{aligned} \tag{20}$$

The real quantities a, b, and c may be expressed in terms of the real parameters f_0, p_0, and k as follows:

$$a = \frac{f_0p_0 + k}{p_0 - f_0k} \qquad b = \frac{f_0 - p_0k}{p_0 - f_0k} \qquad c = \frac{1 + f_0p_0k}{p_0 - f_0k} \tag{21}$$

The relation corresponding to (15b) is

$$-f_0 = \frac{1 - a^2 - b^2 + c^2}{2(a - bc)} \pm \left\{\left[\frac{1 - a^2 - b^2 + c^2}{2(a - bc)}\right]^2 + 1\right\}^{\frac{1}{2}} \tag{22a}$$

With f_0 determined from a, b, and c in (22a), k may be determined from (20), and p_0 from†

$$p_0 = \frac{af_0 + 1}{bf_0 - c} = \frac{b + cf_0}{f_0 - a} \tag{22b}$$

Note that the $\pm$ sign indicates two possible values of $\boldsymbol{f}_0$ and hence of $\boldsymbol{k}$ and $\boldsymbol{p}_0$. Since $\boldsymbol{p}_0 = jp_0$ is a pure imaginary, $S_0 = S_0$ *is real.*

The significance of the tangent relation (19) is that its left side is the normalized input impedance at terminals 3 looking toward the network

† Note that b and c are the negative of the corresponding parameters in the original paper of Weissfloch.

on the right (Fig. 2.1), whereas the right side is k times the normalized impedance looking toward the right at terminals 4. That is,

$$\boldsymbol{Z}_{in3} = jX_{in3} = jR_{c1} \tan \beta_1(s - s_0) \tag{23a}$$

$$\boldsymbol{Z}_{L4} = jX_{L4} = jR_{c2} \tan [\beta_2(S - S_0) + \Phi_T'] \tag{23b}$$

It follows that the input impedance at terminals 33 is a constant n^2 times the output impedance at terminals 4:

$$\frac{\boldsymbol{Z}_{in3}}{\boldsymbol{Z}_{L4}} = \frac{X_{in3}}{X_{L4}} = k\frac{R_{c1}}{R_{c2}} \equiv n^2 \tag{24}$$

Accordingly the entire network between terminals 33 in line 1 and terminals 44 in line 2 is equivalent to an ideal transformer with ratio of turns n. This is illustrated in Fig. 2.2.

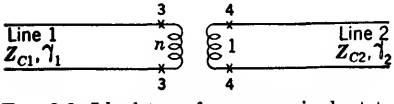


FIG. 2.2. Ideal transformer equivalent to network between terminals 33 and 44 of Fig. 2.1.

Owing to the fact that S_0 in (12) is complex and not a physically measurable distance, a dissipative network cannot be represented by a simple transformer, and no simple interpretation of (12) is available. Since there are other more convenient procedures for determining the equivalent T or Π of a dissipative two-terminal-pair network than using (12), only the simple relation (19) for reactive networks is considered.

The theoretical results obtained for the reactive network may be summarized as follows: Given an arbitrary reactive network with two pairs of terminals to which are connected uniform transmission lines, it is always possible to locate input and output terminals so as to include with the original network sections of the transmission lines of appropriate lengths, so that the thus augmented network can be replaced in its entirety by an equivalent ideal transformer. Moreover for each network there are two possible combinations of added sections of line and transformer ratios. This is Weissfloch's transformer theorem. The practical importance of the theorem depends on the experimental or theoretical determination of the three essential parameters, namely, the locations of the input and output terminals along the feeding and loading lines (which permits the replacement of the included network by a transformer) and the factor k that determines the transformer ratio.

3. Experimental Determination of an Equivalent Ideal Transformer for a Reactive Network.[15,33,137] In order to combine suitable sections of transmission line with an arbitrary reactive network so that the properties of the combination are those of an ideal transformer, it is necessary to locate the new input and output terminals (33 and 44 in Figs. 2.1 and 2.2) and determine the ratio n of the equivalent transformer. The experimental determination of these unknowns depends on certain simple

properties of the functional relationship between the variables S and s. As illustrated in Fig. 2.1, S is the distance between the arbitrary output terminals 22 in line 2 and the reactive termination $\boldsymbol{Z}_T = jX_T$, which has the phase constant Φ'_T; s is the distance between the arbitrary input terminals 11 and the location of a voltage minimum or current maximum between these terminals and the reactive network under test.

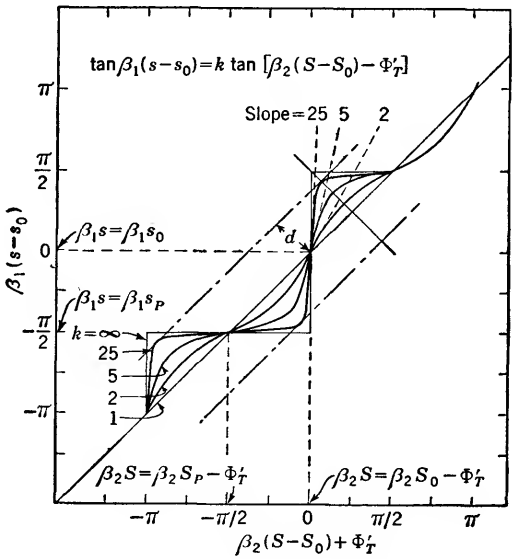


FIG. 3.1. Plot of $\beta(s - s_0)$ as a function of $\beta(S - S_0) - \Phi'_T$.

If the electrical length $\beta_1(s - s_0)$ is plotted as a function of $\beta_2(S - S_0) + \Phi'_T$ according to the fundamental relation [Sec. 2, Eq. (19)], viz.,

$$\tan \beta_1(s - s_0) = k \tan [\beta_2(S - S_0) + \Phi'_T] \tag{1}$$

where $\beta_1 s_0$, $\beta_2 S_0$, and Φ'_T are constants, the curves in Fig. 3.1 are obtained for arbitrarily chosen values of the constant parameter k ranging from 1 to infinity. For $k = 1$ the curve is the straight 45° line; for $k = \infty$ it is a series of vertical and horizontal lines zigzagging across the 45° line. For all intermediate values of k the curve oscillates symmetrically along the 45° line.

It is now easily proved that the origin of coordinates in Fig. 3.1, viz., the points where $\beta_2 S = \beta_2 S_0 - \Phi'_T$ and $\beta_1 s = \beta_1 s_0$, occurs at the point of *maximum slope* and that this maximum slope is precisely k. This is accomplished by writing (1) in the more compact form

$$\tan (y - y_0) = k \tan (x - x_0) \tag{2}$$

where $y = \beta_1 s$, $y_0 = \beta_1 s_0$, $x = \beta_2 S$, and $x_0 = \beta_2 S_0 - \Phi'_T$, and differenti-

ating with respect to x in order to obtain the slope of the curve. The result is

$$\frac{dy}{dx} = k\frac{\cos^2(y - y_0)}{\cos^2(x - x_0)} = k\frac{1 + \tan^2(x - x_0)}{1 + k^2\tan^2(x - x_0)}$$
$$= k\frac{1 + k^{-1}\tan^2(y - y_0)}{1 + \tan^2(y - y_0)} \tag{3}$$

The several forms in (3) are obtained by elimination of $y - y_0$ or $x - x_0$ using (2). The extreme values of this slope are obtained by equating d^2y/dx^2 to zero. The results are

$$\left(\frac{dy}{dx}\right)_{\max} = k \qquad \text{when } x = x_0 \text{ and } y = y_0 \tag{4a}$$

$$\left(\frac{dy}{dx}\right)_{\min} = \frac{1}{k} \qquad \text{when } x = x_0 + \frac{\pi}{2} \text{ and } y = y_0 + \frac{\pi}{2} \tag{4b}$$

where it is assumed that $k \geqq 1$. (If $k < 1$, the maximum and minimum values are interchanged.) The minimum value is obtained using the second and third forms of (3).

The following significant conclusions may be drawn: If S is varied experimentally with respect to arbitrarily selected output terminals (22 in Fig. 2.1) by moving a reactive termination of known and constant Φ_T' (preferably a short circuit for which $\Phi_T' = 0$) and if the corresponding distances s from the arbitrary input terminals (11 in Fig. 2.1) to a voltage minimum are determined, s may be plotted as a function of S. The resulting curve must fall between the limiting curves $k = 1$ and $k = \infty$ in Fig. 3.1. By locating the point of *maximum* slope, values of $\beta_1 s_0$ and $\beta_2 S_0 - \Phi_T'$ are determined. Since β_1 and β_2 as well as Φ_T' are known, s_0 and S_0 are determined. By measuring the maximum slope of the curve through the point $\beta_1 s = \beta_1 s_0$, $\beta_2 S = \beta_2 S_0 - \Phi_T'$, k is determined. It follows that, by locating the input terminals 33 at $s = s_0$ along line 1 and the output terminals 44 at $S = S_0$ along line 2, the two sections of line and the reactive network lying between these pairs of terminals may be replaced by an ideal transformer with $n^2 = kR_{c1}/R_{c2}$. The characteristic resistances R_{c1} and R_{c2} of the two lines are assumed to be known.

Since the determination of the maximum slope k directly from the oscillating curve cannot always be achieved with sufficient accuracy, especially if k is large, an alternative and more accurate procedure is desirable. This depends on the determination of the amplitude and location of the maximum excursion of the oscillating curve from the 45° line. Referring to Fig. 3.2 (which shows an enlarged and simplified section of Fig. 3.1), the point of maximum excursion is located by the coordinates (in radians) $\beta_1 s_m$ and $\beta_2 S_m - \Phi_T'$ along the two axes. The distance (in radians) between lines through the maximum and minimum excursions

from the parallel to the 45° line is D. It follows by plane geometry that

$$\beta_2(S_m - S_0) = \frac{\pi}{4} - \frac{D}{2}\cos 45° = \frac{\pi - D\sqrt{2}}{4} \tag{5}$$

Since the slope of the oscillating curve at the point of maximum excursion is 1, it follows from (3) that

$$\frac{dy}{dx} = k\,\frac{1 + \tan^2(x_m - x_0)}{1 + k^2\tan^2(x_m - x_0)} = 1 \tag{6}$$

where $x_m = \beta_2 S_m - \Phi'_T$ and $x_0 = \beta_2 S_0 - \Phi'_T$. This equation may be solved for k to give

$$k = \cot^2(x_m - x_0) = \cot^2\left(\frac{\pi}{4} - \frac{D\sqrt{2}}{4}\right) \tag{7}$$

Thus, by determining the distance D from the measured curve, it is possible to calculate k using (7). Usually D is more easily determined accurately than is the maximum slope k directly.

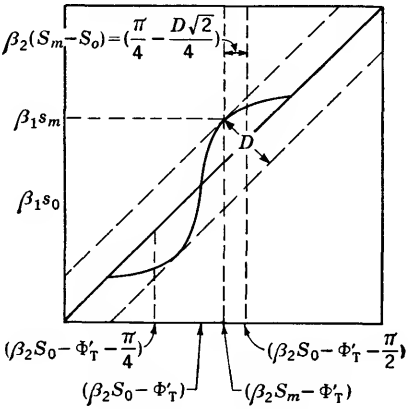


FIG. 3.2. Section of Fig. 3.1.

If the reference point is shifted from the point of *maximum* slope $\beta_1 s_0$, $\beta_2 S_0 - \Phi'_T$ to the point of *minimum* slope $\beta_1 s_p \equiv \beta_1 s_0 + \pi/2$, $\beta_2 S_p - \Phi'_T = \beta_2 S_0 - \Phi'_T + \pi/2$, the fundamental Eq. (1) becomes

$$\tan \beta_1(s - s_p) = \frac{1}{k}\tan[\beta_2(S - S_p) + \Phi'_T] \tag{8}$$

which is like (1) except that the minimum slope $1/k$ replaces the maximum slope k. It follows that the input impedance at the terminals defined by $\beta_1 s_p$ (at a distance $\lambda_0/4$ from 33) is n^2 times the output impedance at the terminals defined by $\beta_2 S_p$ (at a distance $\lambda_0/4$ from 44), where now

$$n^2 = \frac{R_{c1}}{kR_{c2}} \tag{9}$$

Thus, if the input and output terminals are at the points $\beta_1 s_0$ and $\beta_2 S_0$ locating a *maximum* slope in the $\beta_1 s$ vs. $\beta_2 S$ curve, the equivalent transformer for the lines and network between these terminals must have $n^2 = R_{c1}k/R_{c2}$, where k is the maximum slope. Alternatively, if the input and output terminals are at the points $\beta_1 s_p$ and $\beta_2 S_p$ locating a minimum slope, the equivalent transformer must have $n^2 = R_{c1}/kR_{c2}$, where $1/k$ is the minimum slope.

Alternative Procedure for Movable Reactive Network. If the reactive network under test is movable along a uniform line and the terminating reactance X_T and the arbitrary input terminals 11 (Fig. 2.1) are fixed in position, a slightly different formula is convenient. In addition to the obvious simplifications resulting from the fact that both sections of line are alike, so that $\beta_2 = \beta_1 = \beta$ and $\boldsymbol{Z}_{c2} = \boldsymbol{Z}_{c1} = \boldsymbol{Z}_c$, the dependent variable in the input line is not s, as previously defined, but

$$l = s - S \tag{10}$$

Evidently, as the entire reactive network is moved toward the input terminals 11, the output terminals 22 move along with the network, so that S is increased. Insofar as the output line is concerned, it makes no difference whether S is varied by moving the terminating reactance X_T with the reactive network fixed or by moving the reactive network with X_T fixed. However, if S is increased by moving the reactive network toward the input terminals 11 instead of by moving X_T away from the reactive network, a voltage maximum occurs at a distance $l = s - S$ instead of s from terminals 11. Also the point corresponding to $\beta s = \beta s_0$ when $\beta S = \beta S_0 - \Phi'_T$ occurs at $\beta l = \beta l_0 = \beta(s_0 - S_0) + \Phi'_T$.

The relationship between l and S is readily established using the well-known formula for the tangent of the difference of two quantities—in this case $\beta(s - s_0)$ and $\beta(S - S_0) + \Phi'_T$. Thus

$$\begin{aligned} \tan \beta(l - l_0) &= \frac{\tan \beta(s - s_0) - \tan [\beta(S - S_0) + \Phi'_T]}{1 - \tan \beta(s - s_0) \tan [\beta(S - S_0) + \Phi'_T]} \\ &= \frac{(1 - k) \tan [\beta(S - S_0) + \Phi'_T]}{1 - k \tan^2 [\beta(S - S_0) + \Phi'_T]} \end{aligned} \tag{11}$$

The second step in (11) follows when $\tan \beta(s - s_0)$ is eliminated using (1) with $\beta_2 = \beta_1 = \beta$ and $\boldsymbol{Z}_{c2} = \boldsymbol{Z}_{c1} = \boldsymbol{Z}_c$.

If $\beta(l - l_0)$ is plotted as a function of $\beta(S - S_0) + \Phi'_T$, as defined in (11), the curve in Fig. 3.3 is obtained. It is seen that this is a curve that oscillates about the horizontal $\beta(l - l_0) = 0$ axis instead of about the 45° line. Since the values of $\beta(S - S_0) + \Phi'_T$ are the same as in Fig. 3.1, the location of the point of maximum slope is still at $\beta(S - S_0) + \Phi'_T = 0$. This occurs when $\beta(l - l_0) = 0$. It is readily verified by differentiation that the slope of the curve defined by (11) is given by

$$\frac{dy}{dx} = (1 - k)(\sec^2 x) \frac{1 - k \tan^2 x}{(1 + k \tan^2 x)^2} \tag{12}$$

where $y \equiv \beta(l - l_0)$ and $x \equiv \beta(S - S_0) + \Phi'_T$. Since it is known that the maximum slope is at $l = 0$, $x = 0$ and the minimum slope at $l = 0$, $x = \pm\pi/2$, formulas for these extreme values are obtained directly from

(12). They are

$$m_1 = \left(\frac{dy}{dx}\right)_{\max} = 1 - k \qquad \text{at } y = 0,\ x = 0 \tag{13a}$$

$$m_2 = \left(\frac{dy}{dx}\right)_{\min} = \frac{k-1}{k} \qquad \text{at } y = 0,\ x = \frac{\pi}{2} \tag{13b}$$

These values are illustrated in Fig. 3.3.

The equivalent ideal transformer of a reactive network which can be moved along a uniform line may be determined as follows: First, input terminals 11 are fixed at an arbitrary point, and a reactive termination

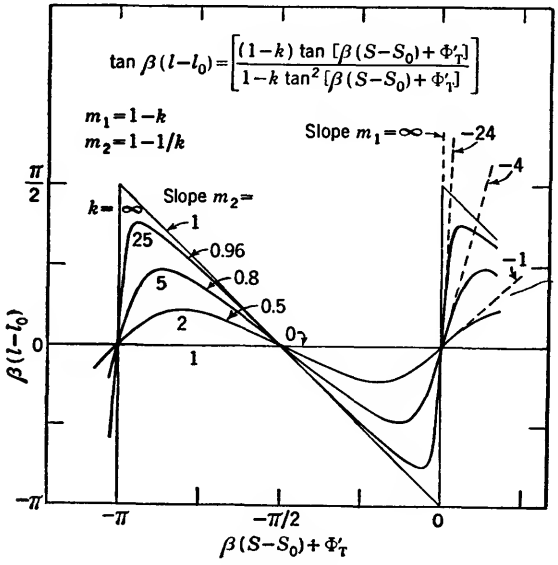


FIG. 3.3. Plot of $\beta(l - l_0) = \beta(s - s_0) - \beta(S - S_0) - \Phi_T'$ against $\beta(S - S_0) + \Phi_T'$.

X_T is located at a convenient fixed point. Output terminals 22 are specified at an arbitrary distance from the reactive network and are imagined to move with the network. The distance from the movable output terminals 22 to the termination X_T is S. The distance from the fixed input terminals 11 to a voltage minimum or current maximum is l. S is next varied in steps by moving the reactive network, and the distance l from the input terminals to a voltage minimum is determined. A curve of βl as a function of βS is plotted. The point of maximum slope locates $\beta l = \beta l_0$ and $\beta S = \beta S_0 - \Phi_T'$. Since Φ_T' is assumed known, βS_0 is determined. The terminals of the ideal transformer are at s_0 and S_0. The transformer ratio is $n^2 = k = 1 - m_1$, where m_1 is the maximum slope determined from the curve.

The point of minimum slope also may be used to determine an alternative ideal transformer.

The method of moving the reactive network is convenient, especially when this consists of a piece of dielectric for which an equivalent ideal transformer is required.

4. Deschamps's Graphical Method for Determining the Scattering Matrix and Equivalent Circuit of a Junction. A graphical method for determining the electrical behavior of a two-terminal-pair network has been described by Deschamps.[116,135] Consider the arbitrary passive network connected between two pairs of terminals, as shown in Fig. 1.1*a* or 4.1. The input terminals 11 are driven from transmission line 1 with

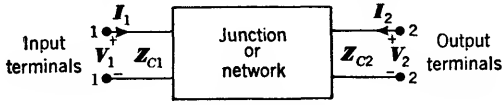


FIG. 4.1. Junction or network connecting two transmission lines.

characteristic impedance Z_{c1}; the output terminals 22 are connected to the loaded transmission line 2 with characteristic impedance Z_{c2}. As discussed in Sec. 1, the complete specification of the electrical properties of the network at a given frequency involves a knowledge of the relations between the input current and voltage (I_1 and V_1) and the output current and voltage (I_2 and V_2). If the network is represented by an equivalent T section, these relations are contained in the simultaneous equations

$$V_1 = I_1 Z_{11} + I_2 Z_{12} \tag{1a}$$

$$V_2 = I_1 Z_{21} + I_2 Z_{22} \tag{1b}$$

or in the equivalent matrix equation

$$\mathbf{V} = \mathbf{IZ} \tag{2a}$$

where

$$\mathbf{V} = \begin{bmatrix} V_1 \\ V_2 \end{bmatrix} \qquad \mathbf{Z} = \begin{bmatrix} Z_{11} & Z_{12} \\ Z_{21} & Z_{22} \end{bmatrix} \qquad \mathbf{I} = \begin{bmatrix} I_1 \\ I_2 \end{bmatrix} \tag{2b}$$

The series elements of the T section are $Z_{11} - Z_{12}$ and $Z_{22} - Z_{12}$; the shunt element is $Z_{21} = Z_{12}$.

It is shown in Chap. III, Sec. 12, that a section of transmission line may be represented by an equivalent T section using an impedance representation, by an equivalent II section using an admittance representation, or in terms of reflection and transmission coefficients in a traveling-wave representation. This is also true of an arbitrary two-terminal-pair network. In Chap. III, Sec. 12, a traveling wave of complex amplitude A_1 reaching terminals 11 from the left and a similar wave of amplitude A_2 reaching terminals 22 from the right were related to the outgoing traveling waves of complex amplitudes B_1 leaving terminals 11 toward the left and B_2 leaving terminals 22 toward the right. The appropriate equations are Chap. III, Sec. 12, Eqs. (19*a*,*b*), or

$$B_1 = S_{11} A_1 + S_{12} A_2 \tag{3a}$$

$$B_2 = S_{21} A_1 + S_{22} A_2 \tag{3b}$$

The matrix equivalent is

$$\mathbf{B} = \mathbf{SA} \tag{4a}$$

where $$\mathbf{B} = \begin{bmatrix} B_1 \\ B_2 \end{bmatrix} \qquad \mathbf{S} = \begin{bmatrix} S_{11} & S_{12} \\ S_{21} & S_{22} \end{bmatrix} \qquad \mathbf{A} = \begin{bmatrix} A_1 \\ A_2 \end{bmatrix} \tag{4b}$$

The matrix elements may be interpreted as in Chap. III, Sec. 12. S_{11} (S_{22}) is the complex amplitude of the reflected wave at terminals 11 (22) due to a wave of unit amplitude incident on terminals 11 (22). The equation $S_{22} = S_{11}$ is true only if the network is symmetrical. S_{12} (S_{21}) is the complex amplitude of the transmitted wave at terminals 11 (22) due to a wave of unit amplitude incident on terminals 22 (11). The relation $S_{21} = S_{12}$ is true for all reciprocal networks. S_{12} is often denoted by T and called the *transmission coefficient* of the junction or network.

The relations between the complex amplitudes A_1 and A_2 of the traveling wave and the input and output voltages and currents are like those given in Chap. III, Sec. 12, except that the characteristic impedances of the two lines are now not necessarily equal. The appropriately generalized formulas for two different transmission lines are

$$V_1 = \sqrt{Z_{c1}}\,[(1 + S_{11})A_1 + S_{12}A_2] \tag{5a}$$
$$V_2 = \sqrt{Z_{c2}}\,[S_{21}A_1 + (1 + S_{22})A_2] \tag{5b}$$
$$I_1 = \sqrt{Y_{c1}}\,[(1 - S_{11})A_1 - S_{12}A_2] \tag{6a}$$
$$I_2 = \sqrt{Y_{c2}}\,[-S_{21}A_1 + (1 - S_{22})A_2] \tag{6b}$$

If (6a) and (6b) are solved for A_1 and A_2 and the values so obtained are substituted in (5a,b), the voltage Eqs. (1a) and (1b) are obtained with

$$Z_{11} = \frac{Z_{c1}}{D}\,[(1 + S_{11})(1 - S_{22}) + S_{12}S_{21}] \qquad Z_{12} = \frac{2\sqrt{Z_{c1}Z_{c2}}}{D}\,S_{12} \tag{7}$$

$$Z_{22} = \frac{Z_{c2}}{D}\,[(1 - S_{11})(1 + S_{22}) + S_{12}S_{21}] \qquad Z_{21} = \frac{2\sqrt{Z_{c1}Z_{c2}}}{D}\,S_{21} \tag{8}$$

where $$D = (1 - S_{11})(1 - S_{22}) - S_{12}S_{21} \tag{9}$$

The matrix form of these equations is readily derived. First let the following diagonal matrices be defined:

$$\mathbf{Z}_c^{\frac{1}{2}} \equiv \begin{bmatrix} Z_{c1}^{\frac{1}{2}} & 0 \\ 0 & Z_{c2}^{\frac{1}{2}} \end{bmatrix} \qquad \mathbf{Y}_c^{\frac{1}{2}} \equiv \begin{bmatrix} Y_{c1}^{\frac{1}{2}} & 0 \\ 0 & Y_{c2}^{\frac{1}{2}} \end{bmatrix} = \mathbf{Z}_c^{-\frac{1}{2}} \tag{10}$$

With (10) the matrix forms of (5a,b) and (6a,b) are

$$\mathbf{V} = \mathbf{Z}_c^{\frac{1}{2}}(\mathbf{U} + \mathbf{S})\mathbf{A} \tag{11}$$
$$\mathbf{I} = \mathbf{Y}_c^{\frac{1}{2}}(\mathbf{U} - \mathbf{S})\mathbf{A} \tag{12}$$

where $\mathbf{U}$ is the unit matrix; $\mathbf{V}$, $\mathbf{I}$, and $\mathbf{A}$ are column matrices, as defined in Chap. III, Sec. 12, Eq. (36); and $\mathbf{S}$ is the scattering matrix

$$\mathbf{S} = \begin{bmatrix} S_{11} & S_{12} \\ S_{21} & S_{22} \end{bmatrix} \tag{13}$$

By premultiplying both sides of (12), first with $\mathbf{Z}_c^{\frac{1}{2}}$ and then with

$(\mathbf{U} - \mathbf{S})^{-1}$, and substituting the expression so obtained for $\mathbf{A}$ in (11), the matrix equation corresponding to (1*a*,*b*) is obtained. It relates the impedance matrix

$$\mathbf{Z} = \begin{bmatrix} Z_{11} & Z_{12} \\ Z_{21} & Z_{22} \end{bmatrix} \tag{14}$$

in $\mathbf{V} = \mathbf{ZI}$ to the scattering matrix:

$$\mathbf{Z} = \mathbf{Z}_c^{\frac{1}{2}}(\mathbf{U} + \mathbf{S})(\mathbf{U} - \mathbf{S})^{-1}\,\mathbf{Z}_c^{\frac{1}{2}} \tag{15a}$$

The inverse relation is

$$\mathbf{S} = (\mathbf{Y}_c^{\frac{1}{2}}\mathbf{Z}\mathbf{Y}_c^{\frac{1}{2}} - \mathbf{U})(\mathbf{Y}_c^{\frac{1}{2}}\mathbf{Z}\mathbf{Y}_c^{\frac{1}{2}} + \mathbf{U})^{-1} \tag{15b}$$

An alternative formulation of the general relations (5*a*,*b*) and (6*a*,*b*) is obtained by introducing the following transformed voltage and current at the output terminals 22:

$$V_2' = \frac{V_2}{N} \qquad I_2' = I_2 N \tag{16}$$

where

$$N \equiv \sqrt{\frac{Z_{c2}}{Z_{c1}}} \doteq \sqrt{\frac{R_{c2}}{R_{c1}}} \tag{17}$$

If (5*b*) is divided by N and (6*b*) is multiplied by N, they become

$$V_2' = \sqrt{Z_{c1}}\,[S_{21}A_1 + (1 + S_{22})A_2] \tag{18}$$

$$I_2' = \sqrt{Y_{c1}}\,[-S_{21}A_1 + (1 - S_{22})A_2] \tag{19}$$

These are the equations for the network connected between two *identical lines* with characteristic impedance Z_{c1}. On the other hand, the relations (16) coincide with Sec. 1, Eq. (8*b*), for an ideal transformer for which N is real. Since ϕ_c in $Z_c = R_c(1 - j\phi_c)$ is an extremely small quantity in low-loss lines, N may be taken to be real. It follows that the circuit of Fig. 4.1 may be replaced by that of Fig. 4.2, where the

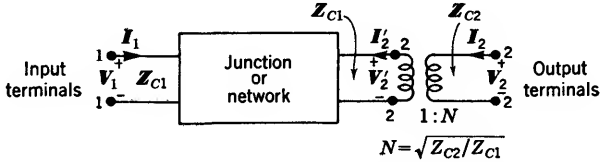


FIG. 4.2. Junction or network together with an ideal transformer connecting two transmission lines.

same unknown junction or network is now connected between lines of equal characteristic impedance.

The method of Deschamps is based on the measurement of the complex reflection coefficient $\Gamma_s = \Gamma_s e^{j\psi_s}$ at the terminals 11 in Fig. 4.1 when terminals 22 are connected to a line of variable length l terminated in a short circuit. The effective load impedance across 22 is Z_L, and this is also the input impedance of the short-circuited line. (If a perfect short circuit is not available, any reactive termination of known reactance may

be used, since it is equivalent to a short circuit at a known distance from it.)

Referring to Fig. 4.3 and Eqs. (3*a*,*b*), consider a wave of complex amplitude A_1 incident on the terminals 11 from the left. The complex

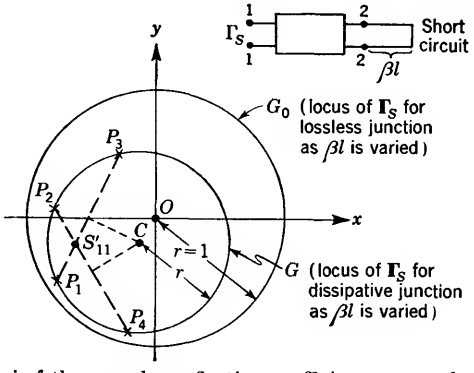


FIG. 4.3. Loci of the complex reflection coefficient Γ_s as a function of βl.

amplitude of the outgoing wave traveling toward the right at terminals 22 is given by (3*b*), viz.,

$$B_2 = S_{21}A_1 + S_{22}A_2 \tag{20}$$

where A_2 is the complex amplitude of the wave reaching the terminals 22 from the right, i.e., reflected from the input impedance Z_L of line 2. By definition of Γ_L,

$$A_2 = \Gamma_L B_2 \tag{21}$$

If (21) is substituted in (20) and this is solved for B_2, the result is

$$\frac{B_2}{A_1} = \frac{S_{21}}{1 - S_{22}\Gamma_L} \tag{22}$$

The complex amplitude of the wave traveling to the left from terminals 11 is given by (3*a*). It is

$$B_1 = S_{11}A_1 + S_{12}A_2 \tag{23}$$

With (21) and (22), (23) may be expressed as follows:

$$\Gamma_s \equiv \frac{B_1}{A_1} = S_{11} + S_{21}\Gamma_L \frac{B_2}{A_1} = S_{11} + \frac{S_{12}S_{21}\Gamma_L}{1 - S_{22}\Gamma_L} \tag{24}$$

For a reciprocal junction this may be rearranged into

$$\Gamma_s = \frac{(S_{12}^2 - S_{11}S_{22})\Gamma_L + S_{11}}{-S_{22}\Gamma_L + 1} \tag{25}$$

which is the well-known bilinear form usually expressed as follows:

$$w = \frac{Az + B}{Cz + D} \tag{26}$$

When $R_L = 0$, the magnitude Γ_L of the reflection coefficient Γ_L is unity,

so that, as its angle ψ_L is varied, Γ_L describes a circle of unit radius in the complex plane. It is a fundamental property of the bilinear transformation that circles in the z plane (Γ_L plane) are mapped into circles in the w plane (Γ_s plane). Therefore the locus of Γ_s as Γ_L is varied (by changing l) is also a circle such as G_0 (Fig. 4.3) if the junction is lossless and $|\Gamma_s| = 1$, or a displaced and smaller circle such as G if the junction is dissipative.

Using theorems of non-Euclidean geometry and the well-known properties of the bilinear transformation, Deschamps has derived[116] graphical procedures for determining the magnitude and angle of the three matrix elements S_{11}, S_{22}, and S_{12} in (25). Simplified proofs based on plane geometry have also been derived,[135] together with modified procedures. Since the details of the proof and interpretation of the geometrical constructions are long and not directly related to transmission-line theory, they are omitted. The steps in the application of Deschamps's method are as follows:

a. Determination of Reflection Coefficients. The output terminals 22 (Fig. 4.1) of the network or junction under test are connected to a short-circuited line 2 of electrical length βl. The complex coefficient of reflection Γ_s of the terminal impedance Z_s presented to the driving line 1 by the network at its input terminals 11 is measured for each of four electrical lengths βl_i of the line. These electrical lengths are chosen in pairs to have the following values: βl_1, βl_2, $\beta l_3 = \beta l_1 + \pi/2$, $\beta l_4 = \beta l_2 + \pi/2$. Although the values of βl_1 and βl_2 are arbitrary, it is advisable to select βl_2 so that $\beta l_2 = \beta l_1 + \pi/4$. In this manner the four lengths are equally spaced along a half wavelength of line 2. The reflection coefficients are measured using a method described in Chap. IV, Sec. 13, e.g., by determining the standing-wave ratio and the locations of current or voltage minima relative to the terminals 11.

b. Construction of Circle. The four complex reflection coefficients Γ_{si}, with $i = 1, 2, 3, 4$, are plotted at P_i in the complex plane, as shown in Fig. 4.3. The center C of the circle G upon which the four points must lie is obtained by drawing the line P_1P_3 and P_2P_4 and erecting their perpendicular bisectors. The desired center is the point of intersection of these bisectors. With C located, the circle G with radius r may be drawn. If the junction is lossless, the four points must lie on G_0, and C is at 0.

c. Graphical Determination of S_{11}. The point of intersection S'_{11} of the lines P_1P_3 and P_2P_4 is called the *crossover point.* In order to determine S_{11}, the following construction is made: The line $S'_{11}C$ is drawn (Fig. 4.4). On opposite sides of this line, beginning at S'_{11} and C, perpendiculars are erected which intersect the circle G at A and B. The line AB is drawn. Its intersection with $S'_{11}C$ at S_{11} is known as the *iconocenter.* The complex number corresponding to this point in the complex plane is the coefficient S_{11} of the scattering matrix.

d. Graphical Determination of S_{12} and S_{22}. The determination of S_{12} and S_{22} is facilitated if one of the points P_i corresponds to an electrical length βl, which locates the short circuit exactly a quarter wavelength from the output terminals 22 (this is equivalent to an open circuit at

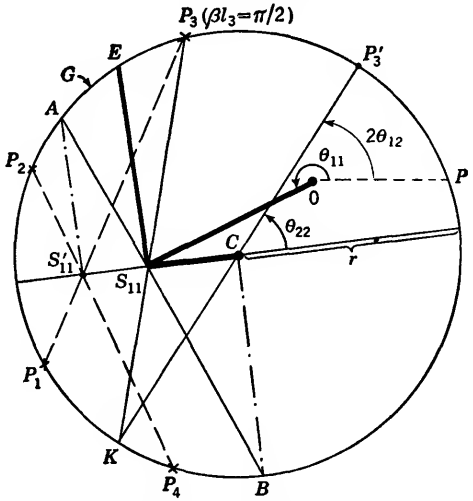


FIG. 4.4. Constructions in the determination of the elements of the scattering matrix.

these terminals). If βl_1 is chosen to be zero, so that point P_1 corresponds to a short circuit directly across the terminals 22, P_3 at $\beta l_3 = \beta l_1 + \pi/2$ is the desired particular point. Referring to Fig. 4.4, let the line P_3S_{11} be drawn and extended to intersect the circle G at K. From K the diameter KCP_3' may be drawn. Next the perpendicular to the line $S_{11}'C$ at S_{11} is drawn; it intersects the circle G at E near P_3. Using the known radius r of the measured circle G, the following values are true. For the sake of completeness the value of S_{11} is also included. Let $S = |S|e^{j\theta}$ with appropriate subscripts. Then, referring to Fig. 4.4, the elements of the scattering matrix are

$$
\begin{aligned}
S_{11}: &\qquad |S_{11}| = \overline{OS}_{11} &&\qquad \theta_{11} = \angle(\overline{OP},\overline{OS}_{11}) \\
S_{12}: &\qquad |S_{12}| = \frac{\overline{S_{11}E}}{\sqrt{r}} &&\qquad \theta_{12} = \tfrac{1}{2}\angle(\overline{OP},\overline{CP}_3') \\
S_{22}: &\qquad |S_{22}| = \frac{\overline{S_{11}C}}{r} &&\qquad \theta_{22} = \angle(\overline{S_{11}C},\overline{CP}_3')
\end{aligned}
\tag{27}
$$

Each of the angles defined in (27) is that through which the first line segment in the parentheses must be turned in order to make it coincide with the second line segment in the parentheses. The sign is positive if the rotation is counterclockwise and negative if the rotation is clockwise. The angle θ_{12} of S_{12} is indeterminate by π.

With the scattering matrix S known, the impedance or admittance matrix and the elements of a T or Π section that is electrically equivalent to the unknown junction or network may be determined.

If the movable impedance Z_L terminating line 2 is not a perfect short circuit, as has been assumed, and the construction to determine the matrix elements is carried out as for $Z_L = 0$, the values determined are S''_{11}, S''_{12}, and S''_{22}. These are related to the correct values as follows:

$$S''_{11} = S_{11} \qquad (S''_{12})^2 = -\Gamma_L S_{12}^2 \qquad S''_{22} = -\Gamma_L S_{22} \tag{28}$$

where Γ_L is the complex reflection coefficient of Z_L. Evidently a knowledge of Γ_L is required if S_{12} and S_{22} are to be determined from S''_{12} and S''_{22}. On the other hand, the ratio

$$\frac{S_{12}^2}{S_{22}} = \frac{(S''_{12})^2}{S''_{22}} \tag{29}$$

is available without a knowledge of Γ_L, and this makes the determination of S_{12} and S_{22} possible without Γ_L in two special cases: (*a*) Symmetrical junction: If the junction or network is symmetrical, $S_{22} = S_{11}$, so that (29) can be solved for S_{12}. (*b*) Reversible junction: If the junction or network can be reversed so that terminals 22 are the input and terminals 11 are the output, both S_{11} and S_{22} can be determined successively together with the ratio (29). In this case two independent values of S_{12} may be obtained, the one serving as a check on the other.

If a junction or network is not reciprocal, so that $S_{21} \neq S_{12}$, the entire Deschamps technique is still valid except that $\sqrt{S_{21}S_{12}}$ is determined instead of $S_{21} = S_{12}$. In order to determine S_{12} and S_{21} it is necessary to perform at least one additional measurement, and this *cannot* be carried out on just one side of the junction since any measurement that involves the transmission through a junction in both directions successively is incapable of resolving the effect of its nonreciprocal property. Possible measurements include the determination of the magnitude and phase of the voltage or the current on *both* sides of the junction when driven from one side. An alternative procedure makes use of symmetrical and identical generators on each side of the junction. A voltage measurement (magnitude and phase) is made on one side or preferably on both sides of the junction. In this case it follows from (3*a*,*b*), with $A_2 = A_1$ equal incident voltages on each side, that

$$\frac{B_1}{A_1} = S_{11} + S_{12} \qquad \frac{B_2}{A_2} = S_{21} + S_{22}$$

By measuring these two reflection coefficients of the junction when driven simultaneously and equally from both sides, S_{12} and S_{21} may be evalu-

ated, since S_{11} and S_{22} are assumed known. Evidently one of the measurements is sufficient if $\sqrt{S_{12}S_{21}}$ is also known. However, since S_{12} and S_{21} may be quite different in order of magnitude—for some devices involving ferrites S_{21} may be extremely small whereas S_{12} is near unity—independent determinations of S_{21} and S_{12} may be preferred.

A valuable feature of the Deschamps method is the opportunity it provides for estimating errors in the experimental data. This is illustrated in the following example:

Illustrative Example.† The experimental data in this example are derived from standing-wave measurements obtained using a dissipative junction in the circuit of Fig. 4.5. In the example to be described the junction is symmetrical, but this does not need to be the case in order that the method may be applied.

The reflection coefficients Γ_s at the input terminals were determined experimentally, with the short-circuiting piston at the following values of βl: 0, $\pi/8$, $\pi/4$, $3\pi/8$, $\pi/2$,

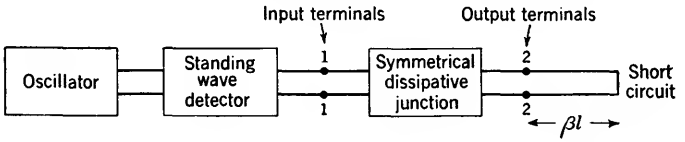


FIG. 4.5. Circuit for measuring the reflection coefficient of a junction.

$5\pi/8$, $3\pi/4$, $7\pi/8$. The value $\beta l = 0$ corresponds to a short circuit, and the value $\beta l = \pi/2$ corresponds to an open circuit across 22. Eight points rather than four were used in order to estimate the experimental errors involved. The eight experimentally determined reflection coefficients are shown plotted in Fig. 4.6. (If a Smith chart with superimposed reflection-coefficient circles is available, the impedance Z_s may be determined experimentally and plotted as such using the RX coordinates of the chart. These plotted points are the desired reflection coefficients using the Γ,ψ coordinates.) Since the accuracy of the elements of the scattering matrix which are to be determined depends on the accuracy of the graphical constructions, it is advantageous to use a large-scale chart of the reflection coefficient. Since only concentric circles and radial lines are involved, an appropriate chart is readily constructed.

Following the procedure outlined in general earlier in this section, the pairs of points for which $\beta l = 0$, $\pi/2$; $\pi/8$, $5\pi/8$; $\pi/4$, $3\pi/4$; and $3\pi/8$, $7\pi/8$ are joined by straight lines. Theoretically these chords should intersect at the crossover point S'_{11}. Owing to possible experimental error they may not, and the degree to which their intersections define a point is a measure of the consistency of the experimental data. For the experimental data under study the enlarged view of the crossover region in Fig. 4.7 indicates that the chord defined by the points $\pi/8$, $5\pi/8$ is not consistent with the other three, which satisfactorily locate the point S'_{11} at the center of a very small triangle. The center C of the circle G that should be the locus of the eight reflection coefficients is readily determined as the point of intersection of the perpendicular bisectors of the three chords that virtually intersect at S''. It is found that a circle can be drawn through seven of the eight points by using as radius the average of the distances from C to the plotted points. It may be concluded that the point for $\beta l = \pi/8$, which alone lies off the circle G, is in error and is responsible for the failure of the fourth chord to intersect the other three at S'_{11} in Fig. 4.7. Since two extra pairs of points have been determined, this point may be disregarded.

† This example is adapted from Ref. 135.

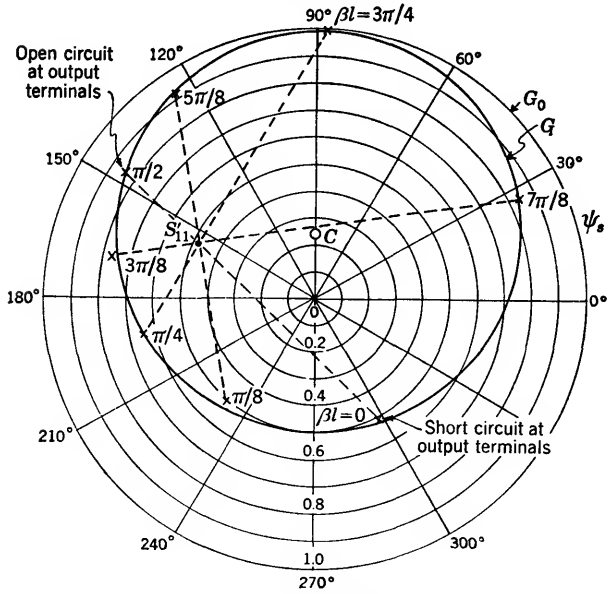


FIG. 4.6. Locus of experimentally determined reflection coefficients $\Gamma_s = \Gamma_s e^{i\psi_s}$.

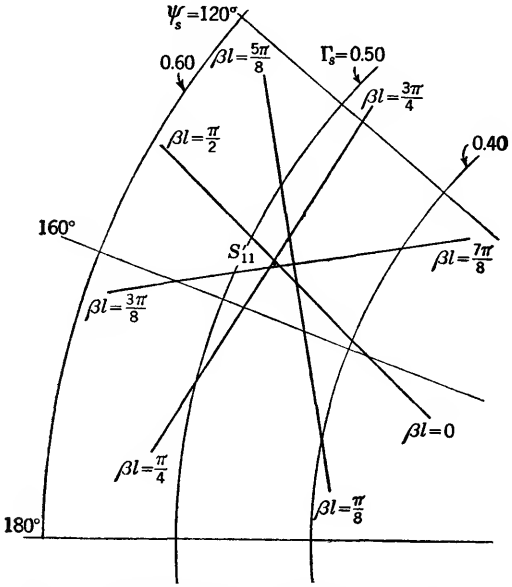


FIG. 4.7. Enlarged section of the crossover region.

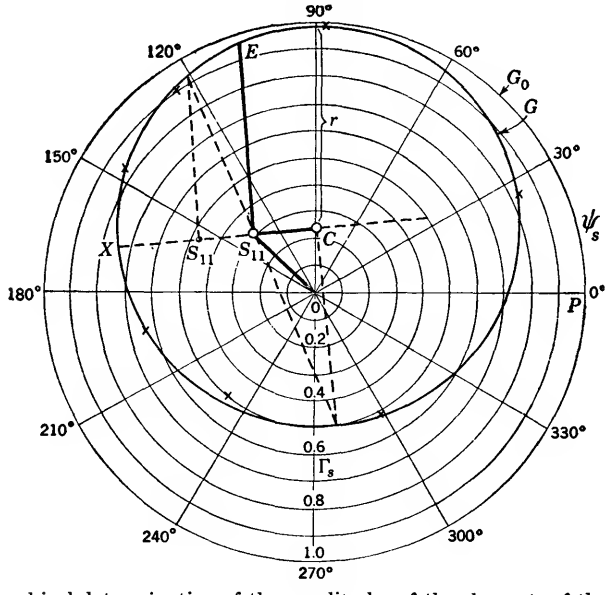


FIG. 4.8. Graphical determination of the amplitudes of the elements of the scattering matrix.

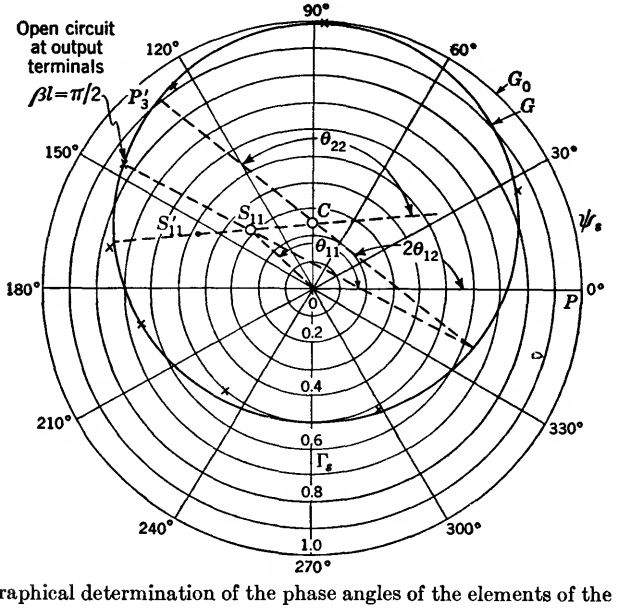


FIG. 4.9. Graphical determination of the phase angles of the elements of the scattering matrix.

With S'_{11} and C located and the circle G drawn, the graphical constructions previously described may be performed to determine the magnitudes and angles of the scattering-matrix elements. For three-place accuracy a reflection-coefficient chart 1 m in diameter was used. The constructions are shown in Figs. 4.8 and 4.9. The values obtained for the matrix elements $\boldsymbol{S} = Se^{j\theta}$ are

$$S_{11} = \overline{OS}_{11} = 0.331 \qquad \theta_{11} = \angle(\overline{OP},\overline{OS}_{11}) = 135° \tag{30a}$$

$$S_{12} = \frac{\overline{S_{11}E}}{\sqrt{r}} = 0.808 \qquad \theta_{12} = \tfrac{1}{2}\angle(\overline{OP},\overline{CP}'_3) = 70.6° \text{ or } 109.4° \tag{30b}$$

$$S_{22} = \frac{\overline{S_{11}C}}{r} = 0.328 \qquad \theta_{22} = \angle(\overline{S_{11}C},\overline{CP}'_3) = 132.8° \tag{30c}$$

The angle θ_{12} of S_{12} is indeterminate by 180°, so that there are two possible values.

Since the junction is known to be symmetrical, S_{11} and S_{22} should be equal. The results obtained are in good agreement in view of the fact that the distances required are measurable only within 0.001 unit.

In most cases only the magnitudes S_{11}, S_{12}, and S_{22} are necessary. The angles are not required in order to calculate the division of power due to the junction. Since the power reflected at the input terminals 11 is proportional to S_{11}^2 and the transmitted power is proportional to S_{12}^2, the following results are obtained:

Power reflected: $S_{11}^2 \times 100\,\% = 11.0\,\%$ (31a)
Power transmitted to matched load: $S_{12}^2 \times 100\,\% = 65.3\,\%$ (31b)
Power dissipated in the junction: $(1 - S_{11}^2 - S_{21}^2) \times 100\,\% = 23.7\,\%$ (31c)

If it is desired to design a matching network to eliminate the reflected power, the angle θ_{11} of S_{11} must be known. All three angles are required in order to calculate the equivalent impedance matrix and the elements of an equivalent T section (Chap. III, Fig. 12.3). Formulas for the latter are given in Chap. III, Sec. 12. For the symmetrical case the normalized series and shunt impedances are obtained from Chap. III, Sec. 12, Eqs. (32*b*) and (33). They are

$$z_1 = \frac{Z_{11} - Z_{12}}{Z_{1c}} = \frac{1 + S_{11} - S_{12}}{1 - S_{11} + S_{12}} \tag{32a}$$

$$z_2 = \frac{Z_{12}}{Z_{1c}} = \frac{2S_{12}}{(1 - S_{11})^2 - S_{12}^2} \tag{32b}$$

Since there is an indeterminacy of 180° in θ_{12}, two equally valid T sections are obtained. It is usually advantageous to select the representation in which the resistive elements of the impedances are positive. The two possible sets of values are

$$z_1 = \begin{cases} 0.190 - j0.414 \\ 0 + j1.0197 \end{cases} \qquad z_2 = \begin{cases} -0.095 + j0.729 \\ 0.095 - j0.729 \end{cases} \tag{33}$$

where the upper values belong together, as do the lower ones.

5. Measurement of Impedance and Reflection Coefficient through a Junction.† If an unknown impedance is connected to a measuring line through an adapting section or other junction, the problem arises to determine this impedance or its reflection coefficient from observations made on the measuring line. That is, measurements are to be made

† This section is based on Ref. 135.

through a junction. This is possible by an extension of the graphical method of Deschamps described in the preceding section.

Consider the circuit represented schematically in Fig. 5.1. The adapting section or junction is between terminals 11 and 22. The measuring line 1 is attached at the left of 11, so that the impedance Z_s looking into the junction at 11 is the load terminating the measuring line. Its coefficient of reflection is $\Gamma_s = \Gamma_s e^{j\psi_s}$. On the right an unknown impedance is connected to the output terminals 22; it presents an impedance Z_L with reflection coefficient $\Gamma_L = \Gamma_L e^{j\psi_L}$. The problem is to determine Z_L or Γ_L from measurements on line 1.

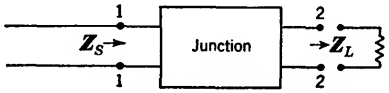


FIG. 5.1. Junction terminated in an unknown load.

The first part of the measurement consists in replacing Z_L by a lossless line terminated in a movable short circuit and proceeding as if to determine the scattering matrix of the junction, just as described in the preceding section. The steps include the measurement of the four reflection coefficients and from them the determination of the crossover point S'_{11}, the center C of the circle G, and the iconocenter S_{11}, just as in Figs. 4.6 to 4.8. These points and the circle are shown in Fig. 5.2.

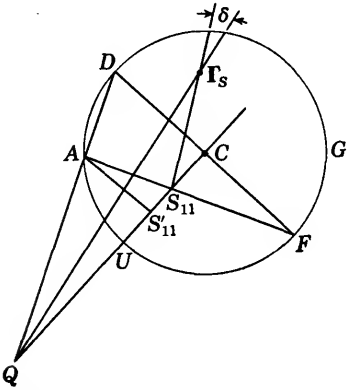


FIG. 5.2. Construction for determining Γ_s.

The next step is to reconnect the unknown impedance Z_L across terminals 22 and measure the reflection coefficient $\Gamma_s = \Gamma_s e^{j\psi_s}$ now terminating line 1 at terminals 11. This is plotted on the complex reflection-coefficient plane, as shown in Fig. 5.2. Referring to this figure, the following constructions are now carried out: Draw $S'_{11}A$ perpendicular to $S'_{11}C$. Draw CD perpendicular to $S'_{11}C$. Draw DA extended to meet CS_{11} (extended) at Q. Draw $Q\Gamma_s$ and $S_{11}\Gamma_s$. It then follows that $\Gamma_L = \Gamma_L e^{j\psi_L}$ is given by

$$\Gamma_L = \frac{\overline{S_{11}\Gamma_s}}{(\overline{Q\Gamma_s})S_{22}} \qquad \psi_L = \delta - \theta_{22} \tag{1}$$

where $S_{22} = S_{22}e^{j\theta_{22}}$ is the element of the scattering matrix determined in Sec. 4 and the angle δ is as shown in Fig. 5.2.

It is to be noted that this method requires the previous determination of S_{22}. Note also that, as S'_{11} approaches C, the point Q moves farther and farther away. If for a certain junction and a certain load the point

Q is too far away for practical use, an alternative construction is available. This construction may be used in all cases.

Referring to Fig. 5.3, the lines $D\Gamma_s$ and $C\Gamma_s$ are drawn. From the point U where QC intersects the circle G, a line is drawn parallel to AD, intersecting CD at V. Through V another line is drawn parallel to $D\Gamma_s$ and intersecting $C\Gamma_s$ at Y.

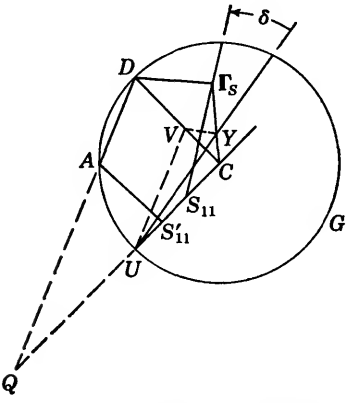


FIG. 5.3. Alternative construction for determining Γ_s.

It can be shown that

$$(\overline{Q\Gamma_s})S_{22} = \overline{UY} \qquad (2)$$

$$\delta \equiv \angle(\overline{Q\Gamma_s},\overline{S_{11}\Gamma_s}) = \angle(\overline{UY},\overline{S_{11}\Gamma_s}) \qquad (3)$$

so that

$$\Gamma_L = \frac{\overline{S_{11}\Gamma_s}}{\overline{UY}} \qquad \psi_L = \delta - \theta_{22} \qquad (4)$$

Illustrative Example. Let the junction be that investigated in the numerical example in Sec. 4. After its properties have been determined using a variable length of short-circuited line, let an unknown impedance Z_L be attached to its output terminals 22. The reflection coefficient $\Gamma_s = 0.70e^{j60°}$ is measured at the input terminals and plotted in Fig. 5.4. After the construction outlined in the second method described above and indicated in Fig. 5.4 is performed, the

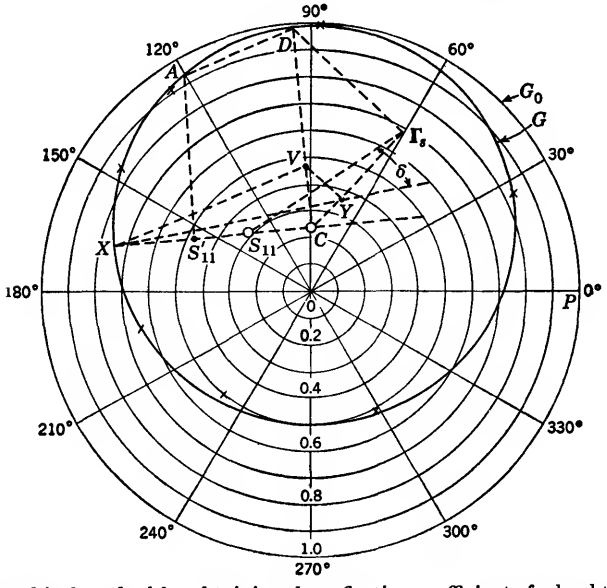


FIG. 5.4. Graphical method for obtaining the reflection coefficient of a load terminating a symmetrical junction.

reflection coefficient $\Gamma_L = \Gamma_L e^{j\psi}$ is found to be

$$\Gamma_L = \frac{\overline{S_{11}\Gamma_s}}{\overline{UY}} = 0.787 \qquad \psi_L = \delta - \theta_{22} = -115.8° \tag{5}$$

where $\delta = \angle(\overline{UY}, \overline{S_{11}\Gamma_s})$. The normalized impedance is given by

$$z_{1L} = \frac{Z_L}{Z_c} = \frac{1 + \Gamma_L}{1 - \Gamma_L} = 0.165 - j0.615 \tag{6}$$

6. Theory of a Dielectric and Magnetic Slab or Bead in a Transmission Line.† In most applications transmission lines are not uniform along their entire length. Usually junctions, connectors, or supports occur at intervals. It follows that the analysis of a line in which a length d is characterized by parameters that differ from those along the rest of the line is of practical importance. The modified section may continue from a given point all the way to the load, or it may be a short piece inserted between the generator and the load. As shown in Fig. 6.1, such a section may differ from the rest of the line in various ways: (*a*) The metallic conductors in the section are identical with those outside but are immersed in a different dielectric medium. (*b*) The dielectric medium in the section is the same as for the rest of the line, but the cross-sectional dimensions and spacing of the conductors are different. (*c*) Both the dielectric and the conductors in the section of length d differ from those elsewhere along the line. (*d*) The section consists of a symmetrical recurrent network of approximately lumped reactive elements distributed uniformly along the length d.

The principal and common characteristic of these four types of circuit is that the parameters of the line in the length d (region 1) are not the same as elsewhere along the line, so that the propagation constant $\gamma_1 = \alpha_1 + j\beta_1$ and the characteristic impedance $Z_{c1} = R_{c1}(1 - j\phi_{c1})$ differ from the values $\gamma = \alpha + j\beta$ and $Z_c = R_c(1 - j\phi_c)$ in the rest of the line. Owing to end and coupling effects it is to be expected that the behavior of a smooth line that is interrupted by a section of length d with physical properties such as those described in (*a*) to (*d*) *may not be represented completely* and accurately simply by assuming *uniform* but different line constants on the main line and in the section of length d. In general, junction effects resulting from the nonuniformity of line parameters and from transverse conducting surfaces at the junctions actually obtain except in case *a*. However, since such effects can be represented by equivalent lumped elements at the junctions, account may be taken of them after the effect of changes in γ and Z_c has been determined. It

† It is implicit in the analysis in this section that the TEM mode is the only propagating mode. For the coaxial line this means that the inner circumference of the outer conductor is less than the TEM wavelength *in* the line. Note that $\lambda_{TEM} = 2\pi/\beta = 2\pi/\omega\sqrt{\mu\epsilon}$.

follows that, although the complete analysis of Fig. 6.1*a* is the specific purpose of this section, the results of such an analysis may be generalized to apply to Fig. 6.1*b*, *c*, and *d* by substituting appropriate values of γ_1 and Z_{c1} and supplementing these later with the analyses of the junction problems.

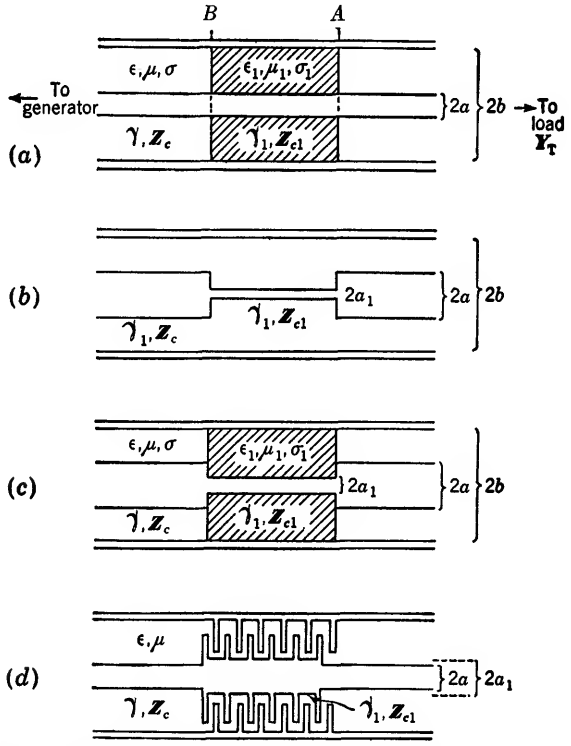


FIG. 6.1. Section of a coaxial line involving changes in the parameters. (*a*) Dielectric slab in a uniform line. (*b*) Section with inner conductor of reduced size. (*c*) Undercut section with dielectric. (*d*) Section with added capacitance and change in size of inner conductor. The left-hand boundary B is at $z' = 0$, the right-hand boundary A at $z' = d$.

Consider a long transmission line that has air (any other good dielectric may be used with small changes in notation) as its dielectric everywhere except in a section (region 1) between A and B (Fig. 6.1) which contains a homogeneous medium of thickness d which may be characterized by a complex dielectric factor:

$$\xi_1 \equiv \epsilon_1 - \frac{j\sigma_1}{\omega} = \epsilon_1(1 - jh_e) \tag{1a}$$

and a complex reluctivity ν_1 (or permeability $\mu_1 = 1/\nu_1$):

$$\nu_1 \doteq \nu_1(1 + jh_m) \qquad \mu_1 \doteq \mu_1(1 - jh_m) \tag{1b}$$

It is assumed that the medium in region 1 involves only small losses, so that the dielectric factor and the reluctivity are predominantly real. Since ϵ_1 and σ_1 in (1*a*) may stand for the real effective dielectric constant and conductivity, ohmic losses arising from time lags in polarization response as well as from actual conduction are included. The imaginary part of (1*b*) represents ohmic losses arising from time lags in magnetization. The assumed restrictions

$$h_m^2 \ll 1 \qquad h_e^2 \ll 1 \tag{1c}$$

although not necessary in the analysis, lead to considerable algebraic simplification.

The sides of the slab of material of thickness d are plane, parallel, and perpendicular to the conductors of the transmission line. In the case of Fig. 6.1*a* the conductors pierce the slab of material without change in cross-sectional size or shape. Let it be assumed that they are so highly conducting that the electromagnetic field in the surrounding medium differs negligibly from that with perfect conductors. This implies that the axial component of the electric field is negligible, that is, $E_z \doteq 0$, in the determination of the transverse field. It can be shown that under these assumptions the boundary conditions for the electromagnetic field are satisfied when the inductance, capacitance, and leakage conductance of *each section* of line are assumed to be the same as if the entire line were like that section. For example, in the case of a coaxial line, the constants of the air-filled parts are given in Chap. I, Sec. 6. To avoid confusion with regions 1 and 2, the radii of the conductors of the coaxial line are a and b instead of a_1 and a_2:

$$l^e = \frac{\mu_0}{2\pi} \ln \frac{b}{a} \qquad c = \frac{2\pi\epsilon_0}{\ln (b/a)} \qquad g = 0 \tag{2}$$

For the dielectric-filled section in which $\mu_1 = \mu_r\mu_0$ and $\epsilon_1 = \epsilon_r\epsilon_0$,

$$l_1^e = \mu_r l^e \qquad c_1 = \epsilon_r c \qquad g_1 = \frac{2\pi\sigma_1}{\ln (b/a)} \tag{3a}$$

With Chap. I, Sec. 4, Eqs. (38*a*) to (40), it follows that

$$l_1^e = \mu_r l^e(1 - jh_m) \qquad l_1^e = \mu_r l^e \qquad r_1 = r^i + \omega l^e h_m \tag{3b}$$

Since the conductors themselves are uniform, the small internal impedance per unit length $z^i = r^i + j\omega l^i$ is the same in all sections of the line.

The proof that the boundary conditions for the electric and magnetic fields are satisfied is readily given. Consider the coaxial line as a typical example. The fields in a homogeneous dielectric-filled line are given in Chap. I, Sec. 3. For determining the transverse field they may be

assumed to consist of the following two components:

$$E_{r1} = \frac{q_1}{2\pi\xi_1 r} \qquad B_{\theta 1} = \frac{I_1}{2\pi\nu_1 r} \tag{4}$$

For an air-filled line the fields are

$$E_r = \frac{q}{2\pi\epsilon_0 r} \qquad B_\theta = \frac{I}{2\pi\nu_0 r} \tag{5}$$

The boundary conditions on the electromagnetic field between the air and the imperfect dielectric (region 1), on the one hand, and between each of these and the conductors (assumed perfect for this purpose), on the other hand, are as follows: The surface density of charge is described by $\mathfrak{n}$; the surface density of current on a perfect conductor is denoted by l; the charge per unit length is q; the total axial current is I. Between the two dielectric media the tangential electric field is continuous; the tangential magnetic B-field is discontinuous:

$$z' = 0, d \qquad a \leqq r \leqq b \qquad E_r = E_{r1} \qquad \nu_0 B_\theta = \nu_1 B_{\theta 1} \tag{6a}$$

Between the air and the conductors the normal electric field is discontinuous; the tangential magnetic field is discontinuous:

$$z' \leqq 0 \qquad r = a \qquad \epsilon_0 E_r = \mathfrak{n}_a = \frac{q}{2\pi a} \qquad \nu_0 B_\theta = l_a = \frac{I}{2\pi a} \tag{6b}$$

$$z' \leqq 0 \qquad r = b \qquad \epsilon_0 E_r = -\mathfrak{n}_b = \frac{-q}{2\pi b} \qquad \nu_0 B_\theta = -l_b = \frac{-I}{2\pi b} \tag{6c}$$

Between the dielectric medium and the conductors the normal electric field is discontinuous, as is the tangential magnetic field:

$$0 \leqq z' \leqq d \qquad r = a \qquad \xi_1 E_{r1} = \mathfrak{n}_{a1} = \frac{q_1}{2\pi a} \qquad \nu_1 B_\theta = l_{a1} = \frac{I_1}{2\pi a} \tag{6d}$$

$$0 \leqq z' \leqq d \qquad r = b \qquad \xi_1 E_{r1} = -\mathfrak{n}_{b1} = \frac{-q_1}{2\pi b} \qquad \nu_1 B_\theta = -l_{b1} = \frac{-I_1}{2\pi b} \tag{6e}$$

The substitution of (4) and (5) in (6*a*) leads to the following relations between the charge per unit length q_1 and current I_1 in the conductors when in the dielectric medium and the corresponding values q and I when the conductors are in air:

$$q_1 = \frac{q\xi_1}{\epsilon_0} \qquad I_1 = I \tag{7}$$

If these values are substituted in (6*b*) to (6*e*), *all equations are found to be consistent with* (6*a*). Since, from Chap. I, Sec. 10, Eqs. (10) and (11),

$$\phi = \frac{q}{2\pi\xi} \ln \frac{b}{r} \qquad A_z = \frac{I}{2\pi\nu} \ln \frac{b}{r} \tag{8}$$

it follows that, with (7),

$$\phi_1 = \phi \qquad \nu_1 A_{1z} = \nu_0 A_z \tag{9a}$$

so that

$$V_1 = (\phi_a - \phi_b)_1 = V = \phi_a - \phi_b$$
$$\nu_1 W_{1z} = \nu_1 (A_{za} - A_{zb})_1 = \nu_0 W_z = \nu_0 (A_{za} - A_{zb}) \tag{9b}$$

Significantly both V and I are continuous across the boundaries at $z' = 0$ and $z' = d$, whereas both q and W_z are discontinuous.

Since the boundary conditions are satisfied if the line constants l^e, c, and $g = 0$ are used outside the slab and l_1^e, c_1, and g_1, as given in (3), are used inside the slab, it follows that the conventional line equations may be used throughout, with V and I continuous at $z' = 0$ and d, with $\gamma = \alpha + j\beta$ and $Z_c = R_c(1 - j\phi_c)$ as the propagation constant and characteristic impedance outside the slab, and with $\gamma_1 = \alpha_1 + j\beta_1$ and $Z_{c1} = R_{c1}(1 - j\phi_{c1})$ as the corresponding quantities inside the slab.

Referring to Fig. 6.1, the admittance looking to the right into the line at its junction with region 1 at A is $Y_A = Y_c \coth \theta'_A$, where

$$\theta'_A = \rho_A + j\Phi'_A = \gamma s + \theta'_T = \alpha s + \rho_T + j(\beta s + \Phi'_T)$$

The admittance terminating the line at a distance s from the nearest point of the slab is $Y_T = G_T + jB_T$; its terminal function is

$$\theta'_T = \rho_T + j\Phi'_T = \coth^{-1} \frac{Y_T}{Y_c} \tag{10}$$

The characteristic admittance and propagation constant of the air-filled sections are $Y_c = G_c(1 + j\phi_c)$ and $\gamma = \alpha + j\beta$.

At the same junction but with reference to the characteristic admittance of the dielectric-filled line, the admittance terminating the dielectric-filled line is

$$Y_A = Y_{c1} \coth \theta'_{A1} \tag{11a}$$

where $\theta'_{A1} = \rho_{A1} + j\Phi'_{A1}$ is defined by (11a) in the form

$$\theta'_{A1} = \coth^{-1} \frac{Y_A}{Y_{c1}} = \coth^{-1} \left(\frac{Y_A}{Y_c} \frac{Y_c}{Y_{c1}} \right) = \coth^{-1} (r_c \coth \theta'_A) \tag{11b}$$

where the ratio of characteristic admittances is

$$r_c \equiv \frac{Y_{c1}}{Y_c} = \frac{Z_c}{Z_{c1}} = \frac{R_c}{R_{c1}} \frac{1 - j\Phi_c}{1 - j\phi_{c1}} \doteq r_c(1 + j\phi_r) \tag{11c}$$

$$r_c \equiv \frac{R_c}{R_{c1}} = \frac{G_{c1}}{G_c} \doteq \sqrt{\frac{l^e c_1}{c l_1^e}} \qquad \phi_r = \phi_{c1} - \phi_c \doteq \frac{1}{2\omega} \left[\frac{r_1}{l_1^e} - \frac{r}{l^e} - \left(\frac{g_1}{c_1} - \frac{g}{c} \right) \right] \tag{11d}$$

In most cases the dielectric materials are sufficiently poor conductors to permit the neglect of ϕ_c and ϕ_{c1}. That is, $\phi_c \ll 1$, $\phi_{c1} \ll 1$, and $\phi_c \phi_{c1} \ll 1$.

The important ratio r_c has the following significance for the coaxial line illustrated in Fig. 6.1c:

$$r_c = \frac{\sqrt{\epsilon_{1r}} \ln (b/a)}{\sqrt{\mu_{1r}} \ln (b/a_1)} \tag{12a}$$

For Fig. 6.1a, $a_1 = a$, so that $r_c = \sqrt{\epsilon_{1r}/\mu_{1r}}$. For Fig. 6.1b, $\epsilon_{1r} = \mu_{1r} = 1$, so that r_c is simply the ratio of the logarithms. It is significant to note that

$$r_c = 1 \qquad \text{for } \sqrt{\mu_{1r}} \ln \frac{b}{a_1} = \sqrt{\epsilon_{1r}} \ln \frac{b}{a} \tag{12b}$$

or

$$a_1 = b\left(\frac{a}{b}\right)^k \qquad k = \sqrt{\epsilon_{1r}\nu_{1r}} = \sqrt{\frac{\epsilon_{1r}}{\mu_{1r}}} \tag{12c}$$

If, as in Fig. 6.1a, $a_1 = a$, then $r_c = 1$ when $\mu_{1r} = \epsilon_{1r}$; also $r_c > 1$ when $\epsilon_{1r} > \mu_{1r}$, and $r_c < 1$ when $\epsilon_{1r} < \mu_{1r}$. If $\mu_{1r} = 1$ and the dielectric is an undercut slab or bead, as in Fig. 6.1c, $r_c = 1$ when $a_1 = b(a/b)^k$ and $k = \sqrt{\epsilon_{1r}}$. Junction effects owing to the change in size of the inner conductor are neglected.

The admittance looking to the right into the dielectric slab of thickness d at its input junction with the line at B in Fig. 6.1 is

$$Y_B = Y_{c1} \coth (\gamma_1 d + \theta'_{A1}) = r_c Y_c \coth (\gamma_1 d + \theta'_{A1}) \tag{13a}$$

The same admittance viewed as the termination of the air-filled line to the left of the dielectric slab and referred to the characteristic admittance of the line in air is

$$Y_B = Y_c \coth \theta'_B \tag{13b}$$

By equating (13a) to (13b) and using (11b), it follows that

$$\theta'_B = \coth^{-1} \{r_c \coth [\gamma_1 d + \coth^{-1} (r_c^{-1} \coth \theta'_A)]\} \tag{14}$$

Use is now made of the identity

$$\coth (x + y) = \frac{1 + \coth x \coth y}{\coth x + \coth y} \tag{15}$$

in order to transform (14) into

$$\theta'_B = \coth^{-1} \frac{\coth \theta'_A + r_c \tanh \gamma_1 d}{1 + r_c^{-1} \coth \theta'_A \tanh \gamma_1 d} \tag{16}$$

In logarithmic form using the identity

$$\coth^{-1} x = \tfrac{1}{2} \ln \frac{x + 1}{x - 1} \tag{17}$$

(16) is

$$\theta'_B = \tfrac{1}{2} \ln \frac{\coth \theta'_A + 1 + (r_c^{-1} \coth \theta'_A + r_c) \tanh \gamma_1 d}{\coth \theta'_A - 1 - (r_c^{-1} \coth \theta'_A - r_c) \tanh \gamma_1 d} \tag{18}$$

By separating the real and imaginary parts of the expression on the right in (18), formulas for ρ_B and Φ'_B may be obtained. Since these are long in the general case, they are not written out.

Matched Line with Dielectric and Magnetic Slab. Considerable simplification results if the line is matched at its final termination and the distortion factors ϕ_{c1} of the dielectric and ϕ_c of the air-filled line are sufficiently small. Let these conditions be expressed as follows:

$$\boldsymbol{Y}_T = \boldsymbol{Y}_c \qquad \text{so that } \boldsymbol{\theta}'_T = \infty,\ \boldsymbol{\theta}'_A = \infty, \text{ and } \coth \boldsymbol{\theta}'_A = \mathbf{1} \tag{19a}$$

$$\phi_r = \phi_{c1} - \phi_c \ll 1 \qquad \text{so that } r_c \doteq r_c \tag{19b}$$

Subject to these conditions, (18) may be reduced to

$$\boldsymbol{\theta}'_B = \rho_B + j\Phi'_B = \tfrac{1}{2} \ln \frac{2 + (r_c + r_c^{-1}) \tanh \gamma_1 d}{(r_c - r_c^{-1}) \tanh \gamma_1 d} \tag{20}$$

The real and imaginary parts of the logarithm may be separated using the identity

$$\tanh (x + jy) = \frac{\tanh x + j \tan y}{1 + j \tanh x \tan y} \tag{21}$$

The final results for the matched line are

$$\rho_B = \tfrac{1}{2} \ln A \qquad A = \sqrt{\frac{(2 + k_1 T)^2 + (k_1 + 2T)^2 t^2}{k_2^2 (T^2 + t^2)}} \tag{22a}$$

$$\Phi'_B = \frac{n\pi}{4} + \frac{1}{2} \tan^{-1} \left(\frac{k_1 + 2T}{2 + k_1 T} t \right) + \frac{1}{2} \tan^{-1} \frac{T}{t} \tag{22b}$$

where $n = 1$ for $r_c < 1$ and $n = 3$ for $r_c > 1$. The following abbreviations have been used:

$$k_1 \equiv r_c + r_c^{-1} \qquad k_2 \equiv r_c - r_c^{-1} \tag{22c}$$

$$T \equiv \tanh \alpha_1 d \qquad t = \tan \beta_1 d \tag{22d}$$

The corresponding formulas for the reflection coefficient

$$\boldsymbol{\Gamma}'_B = \Gamma_B e^{j\psi'_B} = \frac{(\boldsymbol{Y}_B - \boldsymbol{Y}_c)}{(\boldsymbol{Y}_B + \boldsymbol{Y}_c)}$$

are obtained directly. They are

$$\Gamma_B = e^{-2\rho_B} = \frac{1}{A} \qquad \psi'_B = -2\Phi'_B \tag{22e}$$

The voltage or current standing-wave ratio is

$$S = \coth \rho_B = \coth (\tfrac{1}{2} \ln A) = \frac{A + 1}{A - 1} \tag{22f}$$

The power standing-wave ratio is S^2.

Matched Line Unaffected by Dielectric Slab. An important special case of (22*a*,*b*) is obtained when $r_c = 1$. This occurs under conditions specified in (12*a*,*b*,*c*). Of these, the most practical is the undercut dielectric bead. In this case $k_1 = 2$ and $k_2 = 0$, so that $\rho_B = \infty$, $\Gamma_B = e^{-2\rho_B} = 0$, and $S = 1$. Since there is no reflection, the phase function Φ'_B and the phase angle $\psi'_B = -2\Phi'_B$ of the complex reflection coefficient are meaningless.

Matched Low-loss Line with Dielectric and Magnetic Slab. If the attenuation constant α_1 of the dielectric medium is sufficiently small so that the following inequalities are good approximations:

$$T \equiv \tanh \alpha_1 d \doteq \alpha_1 d \ll \frac{r_c + r_c^{-1}}{2} \equiv \frac{k_1}{2} \tag{23}$$

(22*a*) and (22*b*) reduce to simpler forms. These are

$$\rho_B \doteq \tfrac{1}{2} \ln \frac{[4 + (r_c + r_c^{-1})^2 \tan^2 \beta_1 d]^{\frac{1}{2}}}{|(r_c - r_c^{-1}) \tan \beta_1 d|} \tag{24a}$$

$$\Phi_B' \doteq \frac{\pi}{4} + \frac{1}{2} \tan^{-1} \left[\frac{1}{2} (r_c + r_c^{-1}) \tan \beta_1 d \right] \quad \begin{cases} n = 1, r_c < 1 \\ n = 3, r_c > 1 \end{cases} \tag{24b}$$

$$\Gamma_B = \frac{|(r_c - r_c^{-1}) \tan \beta_1 d|}{[4 + (r_c + r_c^{-1})^2 \tan^2 \beta_1 d]^{\frac{1}{2}}} \tag{24c}$$

The power standing-wave ratio $S^2 = \coth^2 \rho_B$, with ρ_B obtained from (24*a*), is plotted in Fig. 6.2 as a function of $\beta_1 d/2\pi$ for a nonmagnetic

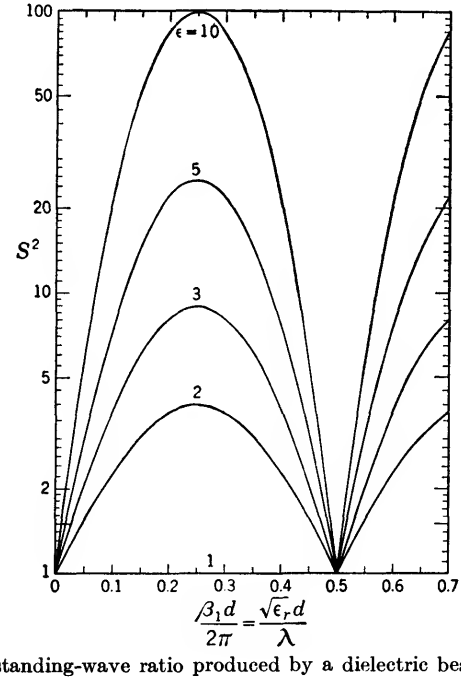


FIG. 6.2. Power standing-wave ratio produced by a dielectric bead of length d in a coaxial line.

dielectric bead. With $\mu_r = 1$ it follows that $r_c = \sqrt{\epsilon_r}$ and $\beta_1 = \sqrt{\epsilon_r}\beta$, so that $\beta_1 d/2\pi = \sqrt{\epsilon_r}\, d/\lambda$. The parameter in Fig. 6.2 is the relative dielectric constant ϵ_r. It is seen that the maximum effect of the bead occurs when its electrical length is an integral odd multiple of a quarter

wavelength, and that the minimum effect (actually zero effect for a lossless dielectric) occurs when its electrical length is an integral multiple of a half wavelength.

a. Thin Slab in Matched Line. In the case of an *electrically short* low-loss bead defined by

$$(\beta_1 d)^2 \ll 1 \qquad (r_c + r_c^{-1})^2 \beta_1^2 d^2 \ll 4 \qquad \left(\frac{\alpha_1}{\beta_1}\right)^2 \ll 1 \tag{25}$$

the following expressions are good approximations:

$$\rho_B = \tfrac{1}{2} \ln \frac{2}{|r_c - r_c^{-1}|\beta_1 d}$$

$$= \begin{cases} \tfrac{1}{2} \ln \dfrac{2}{(\epsilon_r - 1)\beta d} & \text{for } \mu_r = 1 \text{ and } r_c = \sqrt{\epsilon_r} \\ \tfrac{1}{2} \ln \dfrac{2}{(\mu_r - 1)\beta d} & \text{for } \epsilon_r = 1 \text{ and } r_c = \dfrac{1}{\sqrt{\mu_r}} \\ \infty & \text{for } r_c = 1 \end{cases} \tag{26a}$$

$$\Phi_B' \doteq \frac{n\pi}{4} + \frac{1}{4}(r_c + r_c^{-1})\beta_1 d$$

$$= \begin{cases} \dfrac{3\pi}{4} + \dfrac{1}{4}(\epsilon_r + 1)\beta d & \text{for } \mu_r = 1 \text{ and } r_c = \sqrt{\epsilon_r} \\ \dfrac{\pi}{4} + \dfrac{1}{4}(\mu_r + 1)\beta d & \text{for } \epsilon_r = 1 \text{ and } r_c = \dfrac{1}{\sqrt{\mu_r}} \end{cases} \tag{26b}$$

(where $n = 1$ for $r_c < 1$ and $n = 3$ for $r_c > 1$)

$$\Gamma \doteq \tfrac{1}{2}|r_c - r_c^{-1}|\beta_1 d = \begin{cases} \tfrac{1}{2}(\epsilon_r - 1)\beta d & \text{for } \mu_r = 1 \text{ and } r_c = \sqrt{\epsilon_r} \\ \tfrac{1}{2}(\mu_r - 1)\beta d & \text{for } \epsilon_r = 1 \text{ and } r_c = \dfrac{1}{\sqrt{\mu_r}} \\ 0 & \text{for } r_c = 1 \end{cases} \tag{26c}$$

b. Quarter-wave Slab in Matched Line. In the special case of a low-loss bead or slab having an electrical length of exactly *a quarter wavelength*, that is, $\beta_1 d = \pi/2$ and $t = \tan \beta_1 d = \infty$, the following formulas may be obtained from the general relations (22*a*,*b*) [it is assumed that (23) is satisfied]:

$$\rho_B = \tfrac{1}{2} \ln \left| \frac{r_c + r_c^{-1}}{r_c - r_c^{-1}} \right|$$

$$= \begin{cases} \tfrac{1}{2} \ln \dfrac{\epsilon_r + 1}{\epsilon_r - 1} \doteq \coth^{-1} \epsilon_r & \text{for } \mu_r = 1 \text{ and } r_c = \sqrt{\epsilon_r} \\ \tfrac{1}{2} \ln \dfrac{\mu_r + 1}{\mu_r - 1} = \coth^{-1} \mu_r & \text{for } \epsilon_r = 1 \text{ and } r_c = \dfrac{1}{\sqrt{\mu_r}} \\ \infty & \text{for } r_c = 1 \end{cases} \tag{27a}$$

$$\Phi_B' = \begin{cases} \pi & \text{for } r_c > 1 \\ \dfrac{\pi}{2} & \text{for } r_c < 1 \end{cases} \tag{27b}$$

$$\Gamma'_B = \left|\frac{r_c - r_c^{-1}}{r_c + r_c^{-1}}\right| = \begin{cases} \dfrac{\epsilon_r - 1}{\epsilon_r + 1} & \text{for } \mu_r = 1 \text{ and } r_c = \sqrt{\epsilon_r} \\ \dfrac{\mu_r - 1}{\mu_r + 1} & \text{for } \epsilon_r = 1 \text{ and } r_c = \dfrac{1}{\sqrt{\mu_r}} \\ 0 & \text{for } r_c = 1 \end{cases} \tag{27c}$$

$$S = \coth \rho_B = r_c = \begin{cases} \sqrt{\epsilon_r} & \text{for } \mu_r = 1 \text{ and } r_c = \sqrt{\epsilon_r} \\ \sqrt{\mu_r} & \text{for } \epsilon_r = 1 \text{ and } r_c = \dfrac{1}{\sqrt{\mu_r}} \\ 1 & \text{for } r_c = 1 \end{cases} \tag{27d}$$

c. Half-wave Slab in Matched Line. The formulas for a low-loss slab that has an electrical length of exactly a half wavelength, that is, $\beta_1 d = \pi$, so that $t = \tan \beta_1 d = 0$, are obtained from the general formulas (22*a*,*b*). They are

$$\rho_B = \tfrac{1}{2} \ln \frac{2}{|r_c - r_c^{-1}|\alpha_1 d} \doteq \infty \qquad \text{for } \alpha_1 d \text{ small} \tag{28a}$$

$$\Phi'_B = \begin{cases} \pi & \text{for } r_c > 1 \\ \dfrac{\pi}{2} & \text{for } r_c < 1 \end{cases} \tag{28b}$$

$$\Gamma' = \tfrac{1}{2}|r_c - r_c^{-1}|\alpha_1 d \doteq 0 \qquad \text{for } \alpha_1 d \text{ small} \tag{28c}$$

Since $\rho_B \doteq \infty$ and $\Gamma \doteq 0$, it follows that the dielectric slab has no significant effect and the line remains matched.

Ideal Open Circuit at End of Dielectric and Magnetic Slab. If the section of line to the right of the slab in Fig. 6.1 is adjusted to make the impedance looking into it at A extremely great, so that it is approximately equivalent to an ideal open circuit for which $\theta'_A = 0 + j\pi/2$ and $\coth \theta'_A = 0$, the general expression (18) for the terminal function θ'_B reduces to the following much simpler form:

$$\theta'_{BO} = \tfrac{1}{2} \ln \left(\frac{1 + r_c \tanh \gamma_1 d}{1 - r_c \tanh \gamma_1 d} e^{j\pi} \right) \tag{29}$$

Using standard identities, it follows that

$$\tanh \gamma_1 d = \frac{\tanh \alpha_1 d \sec^2 \beta_1 d + j \tan \beta_1 d \operatorname{sech}^2 \alpha_1 d}{1 + \tanh^2 \alpha_1 d \tan^2 \beta_1 d} \tag{30}$$

If the losses in the dielectric slab are at least moderately low, so that the following inequality is a good approximation:

$$(\alpha_1 d)^2 \ll 1 \tag{31}$$

the relation (30) reduces approximately to

$$\tanh \gamma_1 d \doteq \alpha_1 d \sec^2 \beta_1 d + j \tan \beta_1 d \tag{32a}$$

provided $\beta_1 d$ is *not* near an odd multiple of $\pi/2$. When $\beta_1 d = \pi/2$, (30) reduces to

$$\tanh \gamma_1 d = \frac{1}{\tanh \alpha_1 d} \doteq \frac{1}{\alpha_1 d} \tag{32b}$$

With (32*a*) and (11*c*), together with the shorthand notation

$$H_0 \equiv \alpha_1 d \sec^2 \beta_1 d - \phi_r \tan \beta_1 d \tag{33}$$

$\theta'_{BO} = \rho_{BO} + j\Phi'_{BO}$ in (29) becomes

$$\begin{aligned} \theta'_{BO} &= \tfrac{1}{2} \ln \frac{r_c^{-1} + H_0 + j \tan \beta_1 d}{r_c^{-1} - H_0 - j \tan \beta_1 d} + j \frac{\pi}{2} \\ &= \tfrac{1}{4} \ln \frac{1 + \delta_0}{1 - \delta_0} + j\Phi'_{BO} \end{aligned} \tag{34}$$

Since δ_0 as defined in (34) is small compared with unity, the logarithm may be expanded in series to give

$$\rho_{BO} \doteq \frac{\delta_0}{2} = \frac{r_c H_0}{1 + r_c^2 \tan^2 \beta_1 d} \tag{35a}$$

$$\begin{aligned} \Phi'_{BO} &= \frac{1}{2} \left(\tan^{-1} \frac{\tan \beta_1 d}{r_c + H_0} + \tan^{-1} \frac{\tan \beta_1 d}{r_c - H_0} \right) + \frac{\pi}{2} \\ &= \tan^{-1} (r_c^{-1} \tan \beta_1 d) + \frac{\pi}{2} \end{aligned} \tag{35b}$$

Interesting special cases are summarized as follows:

For $(\beta_1 d)^2 \ll 1$:

$$\rho_{BO} \doteq r_c^{-1} H_0 = \frac{\beta_1 d}{r_c} \left(\frac{\alpha_1}{\beta_1} - \phi_r \right) \tag{36a}$$

$$\Phi'_{BO} \doteq \frac{\beta_1 d}{r_c} + \frac{\pi}{2} \tag{36b}$$

For $\beta_1 d = \pi$:

$$\rho_{BO} \doteq \frac{\alpha_1 d}{r_c} \qquad \Phi'_{BO} = \frac{\pi}{2} \tag{37}$$

For $\beta_1 d = \frac{\pi}{2}$:

$$\rho_{BO} \doteq \frac{\alpha_1 d}{r_c} \qquad \Phi'_{BO} = \pi \tag{38}$$

Ideal Short Circuit at End of Dielectric. If the section of line to the right of the slab in Fig. 6.1 is adjusted to make the impedance looking into it at A extremely small, so that it approximates an ideal short circuit (in a coaxial line the dielectric slab may be placed in contact with the short-circuiting piston), it follows that $\theta'_A = 0$ and $\coth \theta'_A = \infty$, and (18) reduces to

$$\theta'_{BS} = \tfrac{1}{2} \ln \frac{1 + r_c^{-1} \tanh \gamma_1 d}{1 - r_c^{-1} \tanh \gamma_1 d} \tag{39}$$

Since $r_c = r_c(1 + j\phi_r)$ and $r_c^{-1} \doteq r_c^{-1}(1 - j\phi_r)$, it follows that, aside from the added term $j\pi/2$, (39) is like (29) except that r_c^{-1} occurs in place of

r_c and $-\phi_r$ in place of ϕ_r. With these changes (35*a*) and (35*b*) apply to (39). The results are

$$\rho_{BS} \doteq \frac{r_c H_S}{r_c^2 + \tan^2 \beta_1 d} \tag{40a}$$

$$\Phi'_{BS} = \tfrac{1}{2}\left(\tan^{-1}\frac{\tan \beta_1 d}{r_c^{-1} + H_S} + \tan^{-1}\frac{\tan \beta_1 d}{r_c^{-1} + H_S}\right) \doteq \tan^{-1}(r_c \tan \beta_1 d) \tag{40b}$$

where
$$H_S \equiv \alpha_1 d \sec^2 \beta_1 d + \phi_r \tan \beta_1 d \tag{40c}$$

For the special cases the following are obtained:

For $(\beta_1 d)^2 \ll 1$: $\rho_{BS} \doteq r_c \beta_1 d\left(\frac{\alpha_1}{\beta_1} + \phi_r\right)$ $\Phi'_{BS} = r_c \beta_1 d$ (41)

For $\beta_1 d = \pi$: $\rho_{BS} = \alpha_1 d r_c$ $\Phi'_{BS} = 0$ (42)

For $\beta_1 d = \frac{\pi}{2}$: $\rho_{BS} = \alpha_1 d r_c$ $\Phi'_{BS} = \frac{\pi}{2}$ (43)

Lumped Capacitance in Matched Line. The particular values of ρ_B and Φ'_B when a lumped capacitance C is connected across the transmission line at B may be derived from the formulas for the dielectric slab by taking the limit as the thickness d approaches zero. If c is the capacitance per unit length of the air-filled line and $c_1 = \epsilon_r c$ is that of the dielectric-filled line, the capacitance per unit length added by the dielectric is

$$C = (c_1 - c)d = cd(\epsilon_r - 1) \tag{44}$$

Any derived lumped constant may be represented in this equation as the assigned constant value of C in the limit as $d \to 0$ and $\epsilon_r \to \infty$.

Consider the value of

$$\omega C R_c = \omega c d(\epsilon_r - 1) R_c = \omega d(\epsilon_r - 1)\sqrt{lc} = \beta d(\epsilon_r - 1) \tag{45}$$

In the limit as $d \to 0$ and $\epsilon_r \to \infty$ this becomes

$$\omega C R_c \to \beta d \epsilon_r = \beta_1 d \sqrt{\epsilon_r} \tag{46}$$

Thus the values of ρ_B and Φ_B may be obtained from the general ones for a dielectric slab by substituting $\omega C R_c$ for $\beta_1 d \sqrt{\epsilon_r}$ and then letting $\delta \to 0$ and $\epsilon_r \to \infty$. This procedure is illustrated below, beginning with (22*a*) specialized for a lossless line:

$$\rho_B = \tfrac{1}{2} \ln \sqrt{\frac{4 + (r_c + r_c^{-1})^2 \tan^2 \beta_1 d}{(r_c - r_c^{-1})^2 \tan^2 \beta_1 d}} \tag{47}$$

where
$$r_c + r_c^{-1} = \sqrt{\epsilon_r} + \frac{1}{\sqrt{\epsilon_r}} \to \sqrt{\epsilon_r} \text{ as } \epsilon_r \to \infty \tag{48a}$$

$$r_c - r_c^{-1} = \sqrt{\epsilon_r} - \frac{1}{\sqrt{\epsilon_r}} \to \sqrt{\epsilon_r} \text{ as } \epsilon_r \to \infty \tag{48b}$$

$$\beta_1 d = \frac{\omega C R_c}{\sqrt{\epsilon_r}} \tag{48c}$$

Note that

$$\lim_{\epsilon_r \to \infty} (r_c + r_c^{-1})^2 \tan^2 \beta_1 d = \lim_{\epsilon_r \to \infty} \sqrt{\epsilon_r} \tan^2 \frac{\omega C R_c}{\sqrt{\epsilon_r}} = \omega^2 C^2 R_c^2 \quad (49)$$

Hence

$$\rho_B = \tfrac{1}{2} \ln \sqrt{\frac{4 + \omega^2 C^2 R_c^2}{\omega^2 C^2 R_c^2}} = \tfrac{1}{4} \ln \left[1 + \left(\frac{2}{\omega C R_c} \right)^2 \right] \quad (50a)$$

$$\Phi'_B = \frac{3\pi}{4} + \frac{1}{2} \tan^{-1} \left(\frac{1}{2} \sqrt{\epsilon_r} \tan \beta_1 d \right) = \frac{3\pi}{4} + \frac{1}{2} \tan^{-1} \frac{\omega C R_c}{2} \quad (50b)$$

If the condition $(\omega C R_c)^2 \ll 1$ is satisfied, the following simpler formulas give the phase and attenuation functions introduced into a matched line by a simple lumped capacitance:

$$\rho_B \doteq \tfrac{1}{2} \ln \frac{2}{\omega C R_c} \qquad \Phi'_B = \frac{3\pi}{4} + \frac{\omega C R_c}{4} \quad (51)$$

Line Loaded with Uniformly Distributed Lumped Capacitances or Inductances. If N approximately lumped shunt capacitances C_1 or series inductances L_1 are connected in a line in a section of length d (Fig. 6.1*d*), the line may be analyzed by assuming that the effective capacitance and inductance per unit length of line are augmented by the amounts NC_1/d and NL_1/d, so that the effective capacitance and inductance per unit length between A and B in Fig. 6.1*d* are

$$c_1 = c'_1 + \frac{NC_1}{d} \qquad l_1 = l'_1 + \frac{NL_1}{d} \quad (52)$$

where c'_1 and l'_1 are the values with the lumped elements absent. The characteristic impedance Z_{c1} and propagation constant γ_1 for the length d are defined as usual. By proper choice of C_1 or L_1 or both, a loaded line with various properties can be obtained. For example, at sufficiently low frequencies l may be increased sufficiently by lumped series inductances L_1 so that $r/l = g/c$ and the distortion factor ϕ_c vanishes. At high frequencies variable reactive tuners may be constructed for use on open-wire or shielded-pair lines by providing small capacitor plates that may be rotated from closely meshed positions to widely separated ones.[125] Alternatively the reactance of ordinary variable capacitors may be determined at high frequencies by analyzing them as sections of capacitively loaded transmission line in which the stack and rotor rods are the parallel conductors.[125]

7. The Maximum-Minimum-shift Method for Determining Dielectric Constants and Permeabilities of Solids and Liquids and Equivalent Sections of Transmission Line for Symmetrical Two-terminal-pair Networks.[123,129,130] A simple direct procedure for determining both the dielectric constant and the permeability of a slab of material of con-

venient thickness is available in the maximum-minimum-shift method.† In its original form it was described only for measuring relative dielectric constants. However, it is extended without difficulty to the determination of the relative permeability.

The fundamental principle of the method is simple. In effect, it involves the successive measurement of the impedance of a section of transmission line when immersed in the material under test when terminated in an open and a short circuit. Since the sample to be used may be chosen to be symmetrical, it is convenient to make use of the symmetrical and antisymmetrical combinations involving, respectively, an open circuit and a short circuit in the plane through the *center* of the slab (see Chap. III, Sec. 12).

A location in which a voltage maximum and a current *null* are at the center of the slab is symmetrical with respect to the voltage and antisymmetrical with respect to the current. It is equivalent to an open circuit at the center. A location in which a voltage *null* and a current maximum are at the center of the slab is antisymmetrical with respect to the voltage and symmetrical with respect to the current. It is equivalent to a short circuit at the center. Actually, completely symmetrical distributions of current and voltage (in which current or voltage *nulls* rather than minima occur at the center of the slab) are achieved only if the slab itself is exactly at the center of a resonant symmetrical section of line that is driven by identical generators loosely coupled at *both* ends. If the generators are in phase, there is a voltage null at the center of the slab; if they are 180° out of phase, there is a current null at the center of the slab. In practice, the slab may be placed with its center at a voltage or current maximum, with sections of low-loss line on each side. Only one of these sections need be driven by a loosely coupled generator if the material in the slab is not highly dissipative, as indicated by the sharpness of the resonance curves. Preferably the detector should be coupled to the same section as the generator.

Mathematical Formulation. The first step in deriving the tangent relation on which the maximum-minimum-shift method depends is to compare the input admittance of two sections of transmission line. Of these, the first (Fig. 7.1*a*) has only air (vacuum) as the dielectric from the arbitrarily located input terminals at $z' = 0$ to the reactive termination with admittance $Y_T = jB_T$ at $z' = s'$. The second section of line (Fig. 7.1*b*) is immersed in a medium with complex dielectric factor ξ_1 and complex permeability μ_1 from $z' = 0$ (plane B in Fig. 6.1*a*) to $z' = d$

† It is implicit in the analysis given in this section that the TEM mode is the only propagating mode. For the coaxial line this means that the inner circumference of the outer conductor is less than the TEM wavelength *in* the line. Note that $\lambda_{TEM} = 2\pi/\beta = 2\pi/\omega\sqrt{\mu\epsilon}$. If $\mu = \mu_0\mu_r$ or $\epsilon = \epsilon_0\epsilon_r$ differs greatly from μ_0 or ϵ_0, the cross-sectional size of the line may have to be very small.

(plane A in Fig. 6.1a) and in air from $z' = d$ to $z' = d + s$, where it is terminated in $\boldsymbol{Y}_T \doteq jB_T$. The material parameters have the properties discussed in conjunction with Sec. 6, Eqs. (1a,b,c). It is assumed that the two sections of line are identical except for the added presence of the dielectric medium in the second section. (In practice the measurements are made successively on the same section of line with and without the slab.) Both lines are highly conducting, and the conductivity of the dielectric or magnetic sample is sufficiently small so that Sec. 6, condition (1c), is satisfied. If the medium is a liquid, retaining walls are required. These may be ignored if made of a material like Polyfoam which has a relative dielectric constant and a relative permeability differing negligibly from 1. If they are made of a solid dielectric, they may be sufficiently thin to permit their analytical representation as small lumped admittances

$$\boldsymbol{Y}_w = jB_w = -j\omega C_w$$

at $z' = 0$ and $z' = d$ (Fig. 7.1c). In the following the more general problem involving a liquid enclosed in thin, solid retaining walls is formulated, since the results are readily specialized to the simpler and more important cases involving liquids with Polyfoam walls or a solid dielectric with no additional walls by setting $B_w = 0$.

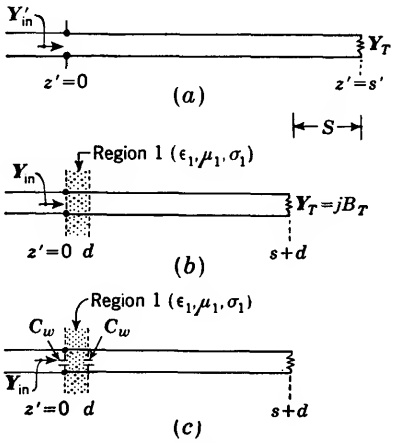


FIG. 7.1. Sections of transmission line. (a) Uniform section. (b) Slab of dielectric of length d along otherwise uniform line. (c) Slab of fluid dielectric between thin walls represented by lumped capacitances along otherwise uniform line.

The input admittance $\boldsymbol{Y}'$ for the section of line in Fig. 7.1a is

$$\boldsymbol{Y}' = G' + jB' = \boldsymbol{Y}_c \coth (\boldsymbol{\gamma}s' + \boldsymbol{\theta}'_T) \doteq -jG_c \cot (\beta s' + \Phi'_T) \qquad (1)$$

The characteristic admittance of the line is $\boldsymbol{Y}_c \doteq G_c = 1/R_c$; the propagation constant is $\boldsymbol{\gamma} = \alpha + j\beta$. The terminal function of $\boldsymbol{Y}_T$ is

$$\boldsymbol{\theta}'_T = \rho_T + j\Phi'_T \doteq j\Phi'_T$$

for an ideal short-circuit $\boldsymbol{\theta}'_T = 0$. The values following the approximately equal sign in (1) and the related definitions apply only if the attenuation of the line is neglected and the termination is a pure reactance.

The input admittance $\boldsymbol{Y}_2$ of the section of line of length s in Fig. 7.1c in parallel with the lumped admittance $\boldsymbol{Y}_w \doteq jB_w$ of the right-hand

retaining wall is

$$\boldsymbol{Y}_2 = G_2 + jB_2 = \boldsymbol{Y}_w + \boldsymbol{Y}_c \coth (\boldsymbol{\gamma} s + \boldsymbol{\theta}'_T) \doteq j[B_w - G_c \cot (\beta s + \Phi'_T)] \quad (2)$$

The input admittance $\boldsymbol{Y}$ of the entire line in Fig. 7.1c is

$$\boldsymbol{Y} = G + jB = \boldsymbol{Y}_w + \boldsymbol{Y}_{c1} \frac{\boldsymbol{Y}_2 \coth \boldsymbol{\gamma}_1 d + \boldsymbol{Y}_{c1}}{\boldsymbol{Y}_2 + \boldsymbol{Y}_{c1} \coth \boldsymbol{\gamma}_1 d} \quad (3)$$

where $\boldsymbol{Y}_{c1} = G_{c1}(1 + j\phi_{c1})$ is the characteristic admittance and

$$\boldsymbol{\gamma}_1 = \alpha_1 + j\beta_1$$

is the propagation constant of the line when immersed in the slab of material medium between $z = 0$ and $z = d$.

The fundamental step in the derivation of the desired equation is to require the lengths s' and s to be so related that the input susceptances B and B' are equal. Thus

$$B = B' \qquad \text{or} \qquad \operatorname{Im} \boldsymbol{Y} = \operatorname{Im} \boldsymbol{Y}' \quad (4)$$

The properties of the dielectric material are represented by $\boldsymbol{\gamma}_1$ and $\boldsymbol{Z}_{c1}$; its thickness d is arbitrary.

It is readily verified, using (1) and (3) with (2), that (4) may be transformed into the following general equation:

$$\operatorname{Re} \{\boldsymbol{C}_1[\coth (\boldsymbol{\gamma} s' + \boldsymbol{\theta}'_T) - \coth (\boldsymbol{\gamma} s + \boldsymbol{\theta}'_T)] + \coth (\boldsymbol{\gamma} s' + \boldsymbol{\theta}'_T) \coth (\boldsymbol{\gamma} s + \boldsymbol{\theta}'_T) - \boldsymbol{C}_2\} = 0 \quad (5)$$

where
$$\boldsymbol{C}_1 = C_{1r} + jC_{1i} \equiv \boldsymbol{r}_c \coth \boldsymbol{\gamma}_1 d + \boldsymbol{Y}_w \boldsymbol{Z}_c \quad (6a)$$

$$\boldsymbol{C}_2 = C_{2r} + jC_{2i} \equiv \boldsymbol{r}_c^2 + 2\boldsymbol{r}_c \boldsymbol{Y}_w \boldsymbol{Z}_c \coth \boldsymbol{\gamma}_1 d + \boldsymbol{Y}_w^2 \boldsymbol{Z}_c^2 \quad (6b)$$

with
$$\boldsymbol{r}_c \equiv \frac{\boldsymbol{Z}_c}{\boldsymbol{Z}_{c1}} \quad (7)$$

With these definitions of $\boldsymbol{C}_1$ and $\boldsymbol{C}_2$, it is the real part of (5) which is derived from the susceptance. It is readily verified that (5) with $\boldsymbol{Y}_w = 0$ is obtained directly by equating Sec. 6, Eq. (13b), with Sec. 6, Eq. (16), to (3) with $\boldsymbol{Y}_w = 0$. Equation (5) expresses the relationship between all values of s' and s for which the input susceptances of the two sections (the one of length s' in air, the other of length d in the dielectric or magnetic medium and length s in air) are equal. In the complete absence of the material medium ($d = 0$, $B_w = 0$) the input admittances are equal when $s' = s_1$. If a dielectric or magnetic medium is present, $d + s$ is taken to be less than s'.

The greatest effect on the input susceptance B_{in} is produced by the material medium when it is so situated that the values of s' and s which satisfy (5) are such that $s' - s$ is a maximum. With this combination of s' and s the circuit reaches its greatest sensitivity to the reactive effect of a dielectric or magnetic sample, so that it represents the optimum condition for the precise measurement of ϵ_r or μ_r.

The particular forms of Eq. (5) for which $s' - s$ has its extreme values are obtained by setting the derivative of $s' - s$ with respect to s' equal to zero or, what is equivalent, by setting

$$\frac{ds}{ds'} = \frac{d(\gamma s)}{d(\gamma s')} = 1 \tag{8}$$

Using familiar formulas, let (5) be transformed into the following equivalent expression:

$$\text{Re}\left\{-\boldsymbol{C}_1 \sinh \gamma(s' - s) + \frac{1 + \boldsymbol{C}_2}{2} \cosh \gamma(s' - s) + \frac{1 - \boldsymbol{C}_2}{2} \cosh [\gamma(s' + s) + 2\theta_T]\right\} = 0 \tag{9}$$

If (9) is differentiated with respect to s' and (8) is imposed, the following condition is obtained:

$$(\boldsymbol{C}_2 - 1) \sinh [\gamma(s' + s) + 2\theta'_T] = 0 \tag{10}$$

Since $\boldsymbol{C}_2$ is not equal to unity, in general, (10) is equivalent to the following:

$$\sinh [\alpha(s' + s) + 2\rho_T] \cos [\beta(s' + s) + 2\Phi'_T] + j \cosh [\alpha(s' + s) + 2\rho_T] \sin [\beta(s' + s) + 2\Phi'_T] = 0 \tag{11}$$

where only the imaginary part is relevant for the condition (4). This part of (11) is satisfied when

$$\beta(s' + s) + 2\Phi'_T = k\pi \qquad k = 0, 1, 2, \ldots \tag{12}$$

Using (12) in (9), the following equation is obtained for the maximum and minimum values of $s' - s$ (indicated by the subscript m):

$$C_{1i} \sin \beta(s' - s)_m + \tfrac{1}{2}(1 + C_{2r}) \cos \beta(s' - s)_m \pm \tfrac{1}{2}(1 - C_{2r}) = 0 \tag{13a}$$

where the upper sign is for k even and the lower sign is for k odd in (12), and where C_{1i} and C_{2r} are the imaginary part of $\boldsymbol{C}_1$ and the real part of $\boldsymbol{C}_2$, respectively. In deriving (13a) it is assumed that the following inequalities are good approximations:

$$|C_{1i}| \gg |C_{2i}\alpha(s' - s)| \qquad [\alpha(s' + s) + \rho_T]^2 \ll 1 \tag{13b}$$

Equation (13a) is readily transformed into the following two equations:

$$\cot^2 \Delta + 2C_{1i} \cot \Delta - C_{2r} = 0 \qquad k \text{ even in (12)} \tag{14a}$$

$$\tan^2 \Delta - 2C_{1i} \tan \Delta - C_{2r} = 0 \qquad k \text{ odd in (12)} \tag{14b}$$

where the notation

$$\Delta \equiv \tfrac{1}{2}\beta(s' - s)_m = \tfrac{1}{2}\beta(d + S_m) \tag{15}$$

is introduced. In (15) S_m is the *maximum* or *minimum* shift in the position of the termination when adjusted for resonance successively

without and with the material medium. The shift S is shown in Fig. 7.1. The solutions of (14a) and (14b) are

$$\cot \Delta = -C_{1i} \pm \sqrt{C_{1i}^2 + C_{2r}} \tag{16}$$

$$\tan \Delta = C_{1i} \pm \sqrt{C_{1i}^2 + C_{2r}} \tag{17}$$

where, for $2\Delta = \beta(s' - s)$ positive and less than π, only the upper signs are relevant. The complex constants $\boldsymbol{C}_1 = C_{1r} + jC_{1i}$ and $\boldsymbol{C}_2 = C_{2r} + jC_{2i}$ are defined in (6a,b). Although the real and imaginary parts of $\boldsymbol{C}_1$ and $\boldsymbol{C}_2$ are separable, in general, without restricting the properties of the material in the slab under investigation, resonance curves are sharp only for materials that are not very good conductors. Accordingly it is convenient to obtain the simpler formulas that apply to samples of moderately low effective conductivity. This is in agreement with Sec. 6, conditions (1c). Therefore let the following restrictions be imposed on the propagation constant $\gamma_1 = \alpha_1 + j\beta_1$ and the characteristic impedance $\boldsymbol{Z}_{c1} = R_{c1}(1 - j\phi_{c1})$:

$$(\alpha_1 d)^2 \ll 1 \qquad \left(\frac{\alpha_1}{\beta_1}\right)^2 \ll 1 \qquad \phi_{c1}^2 \ll 1 \tag{18}$$

Subject to these conditions,

$$\coth \gamma_1 d \doteq -j \cot \beta_1 d + \alpha_1 d \csc^2 \beta_1 d \tag{19}$$

provided the additional requirement

$$\tan^2 \beta_1 d \gg \alpha_1^2 d^2 \tag{20}$$

is satisfied. With (7) and (18) it follows [as in Sec. 6, Eqs. (11c,d)] that

$$\boldsymbol{r}_c \equiv \frac{R_c(1 - j\phi_c)}{R_{c1}(1 - j\phi_{c1})} \doteq r_c(1 + j\phi_r) \qquad r_c \equiv \frac{R_c}{R_{c1}} = \sqrt{\frac{\epsilon_r}{\mu_r}} \qquad \phi_r \doteq \phi_{c1} - \phi_c \tag{21}$$

where ϵ_r and μ_r are the relative dielectric constant and permeability of the material medium. Note that

$$\beta_1 = n\beta \qquad n \equiv \sqrt{\epsilon_r \mu_r} \tag{22}$$

where n is the index of refraction. In a nonmagnetic dielectric material $\mu_r = 1$ and $r_c = n = \sqrt{\epsilon_r}$; in a nondielectric magnetic material $\epsilon_r = 1$ and $r_c = 1/\sqrt{\mu_r} = 1/n$.

With (18) to (22) it follows from (6a,b) that

$$C_{1i} = B_w R_c - r_c \cot n\beta d \tag{23}$$

$$C_{2r} = r_c^2 + 2r_c B_w R_c \cot n\beta d - B_w^2 R_c^2 \tag{24}$$

so that

$$-C_{1i} + \sqrt{C_{1i}^2 + C_{2r}} = -B_w R_c + r_c \cot \tfrac{1}{2} n\beta d \tag{25}$$

$$C_{1i} + \sqrt{C_{1i}^2 + C_{2r}} = B_w R_c + r_c \tan \tfrac{1}{2} n\beta d \tag{26}$$

If (25) and (26) are substituted in (16) and (17), these may be expressed as follows:

$$\cot \Delta_i + B_w R_c = r_c \cot \tfrac{1}{2} n\beta d \qquad k \text{ even in (12)} \qquad (27a)$$

$$\tan \Delta_v - B_w R_c = r_c \tan \tfrac{1}{2} n\beta d \qquad k \text{ odd in (12)} \qquad (27b)$$

It is readily verified that condition (12), $\beta(s' + s) + 2\Phi'_T = k\pi$, with $k = 0, 1, 2, \ldots$, ensures that the extreme values $\Delta_i = \frac{1}{2}\beta(s - s')_{mi}$ and $\Delta_v = \frac{1}{2}\beta(s - s')_{mv}$ occur when the current and voltage distribution patterns are symmetrical with respect to the center of the slab. With (12) the part of the susceptance B_2 in (2) due to the line is given by

$$B_{2in} \equiv B_2 - B_w = -G_c \cot [k\pi - (\beta s' + \Phi'_T)] = G_c \cot (\beta s' + \Phi'_T) \qquad (28a)$$

Since the susceptance B' in (1) is equal to the susceptance B in (3) and since B_{2in} in (28*a*) is the negative of B' in (1), it follows that, when located for extreme shift, $B_{2in} = -B$. However, since the entire circuit is adjusted for resonance, the susceptance B looking into the slab must be the negative of the susceptance at the same points but looking away from the slab back into the line:

$$B_{2in} = -B = B_L \qquad (28b)$$

That is, the susceptances looking into the line in both directions from the edges of the dielectric slab are the *same*. This is possible only when the current and voltage distributions are symmetrical with respect to the center of the slab. In particular, the extreme value Δ_i defined in (27*a*) always occurs when the largest number of current maxima consistent with the electrical thickness $n\beta d$ of the sample are contained within it. When $n\beta d$ is less than π, this means a current maximum at the center of the slab. (When $n\beta d$ is between π and 2π, it means voltage maximum at the center, with two symmetrically placed current maxima within the slab.) Alternatively the extreme value Δ_v defined in (27*b*) occurs when the largest number of voltage or charge maxima are contained within the sample. For $n\beta d$ less than π, this means a voltage maximum at the center of the slab. The question as to which of the two extreme values Δ_i and Δ_v is a maximum and which is a minimum depends on the relative magnitudes of ϵ_r and μ_r. If $\mu_r = 1$ and $\epsilon_r > 1$, Δ_v is the maximum and Δ_i is the minimum. If $\epsilon_r = 1$ and $\mu_r > 1$, Δ_i is the maximum and Δ_v is the minimum. If $\epsilon_r = \mu_r$, there is only one value of $s' - s$ for all positions of the slab, so that Δ_v and Δ_i are equal.

Equations (27*a*) and (27*b*) may be solved for $r_c = \sqrt{\epsilon_r/\mu_r}$ and $n = \sqrt{\mu_r \epsilon_r}$. The square root of the product of (27*a*) and (27*b*) is

$$\sqrt{\frac{\epsilon_r}{\mu_r}} = r_c = [\cot \Delta_i \tan \Delta_v + B_w R_c(\tan \Delta_i - \cot \Delta_v) - B_w^2 R_c^2]^{\frac{1}{2}} \qquad (29a)$$

The ratio of (27*b*) to (27*a*) yields

$$\sqrt{\mu_r\epsilon_r} = n = \frac{2}{\beta d}\tan^{-1}\left(\frac{\tan\Delta_v - B_wR_c}{\cot\Delta_i + B_wR_c}\right)^{\frac{1}{2}} \tag{29b}$$

If the sample includes no solid retaining walls, $B_w = 0$, and the following simpler expressions are obtained:

$$\sqrt{\frac{\epsilon_r}{\mu_r}} = r_c = (\cot\Delta_i \tan\Delta_v)^{\frac{1}{2}} \tag{30a}$$

$$\sqrt{\epsilon_r\mu_r} = n = \frac{2}{\beta d}\tan^{-1}(\tan\Delta_i \tan\Delta_v)^{\frac{1}{2}} \tag{30b}$$

It follows that

$$\epsilon_r = r_c n = \frac{2}{\beta d}(\cot\Delta_i \tan\Delta_v)^{\frac{1}{2}}\tan^{-1}(\tan\Delta_i \tan\Delta_v)^{\frac{1}{2}} \tag{31a}$$

$$\mu_r = \frac{n}{r_c} = \frac{2\tan^{-1}(\tan\Delta_i \tan\Delta_v)^{\frac{1}{2}}}{\beta d \cot\Delta_i \tan\Delta_v} \tag{31b}$$

If the two extreme values $(s' - s)_i$ and $(s' - s)_v$ in Δ_i and Δ_v are determined experimentally, the relative dielectric constant ϵ_r *and* the relative permeability μ_r of the sample may be determined from (29*a*,*b*) or from (31*a*,*b*). The only other quantities required are the thickness d of the sample and the wavelength λ in $\beta = 2\pi/\lambda$ for the line in air. Thus, since only four length measurements are involved, an *absolute* method for the determination of ϵ_r and μ_r is available.

If a liquid material is contained between solid retaining walls for which B_w is not zero, B_wR_c may be determined experimentally using (27*a*) or (27*b*) with the cell empty. In this case $r_c = n = 1$, so that

$$B_wR_c = \tan\Delta_{ve} - \tan\tfrac{1}{2}\beta d = \cot\tfrac{1}{2}\beta d - \cot\Delta_{ie} \tag{32a}$$

where $\Delta_{ve} = \frac{1}{2}\beta(s' - s)_{mv}$ and $\Delta_{ie} = \frac{1}{2}\beta(s' - s)_{mi}$ for the cell empty. Alternatively the susceptance B_w of the walls may be eliminated by subtracting the equations for the empty cell from those for the full cell. For (27*b*), for example, the result is

$$\tan\Delta_v - \tan\Delta_{ve} + \tan\tfrac{1}{2}\beta d = r_c\tan\tfrac{1}{2}n\beta d \tag{32b}$$

Important and very simple special forms of (31*a*) and (31*b*) are obtained for a sufficiently thin sample. Subject to the condition $(n\beta d)^2 \ll 1$ and with $B_w = 0$, (27*a*) and (27*b*) reduce to

$$\frac{n}{r_c} = \mu_r = \frac{(s' - s)_{mi}}{d} \qquad \beta(s' + s) + 2\Phi_T' = k\pi \qquad k \text{ even} \tag{33a}$$

$$nr_c = \epsilon_r = \frac{(s' - s)_{mv}}{d} \qquad \beta(s' + s) + 2\Phi_T' = k\pi \qquad k \text{ odd} \tag{33b}$$

It follows that for an electrically thin sample μ_r can be determined directly from the one extreme shift, and ϵ_r from the other. The extreme shift for

determining μ_r from (33a) occurs when the center of the sample is at a current maximum; that for determining ϵ_r from (33b) occurs when the center of the sample is at a voltage maximum.

If $\mu_r = \epsilon_r$, the general Eq. (5) reduces to

$$n = \sqrt{\mu_r \epsilon_r} = \mu_r = \epsilon_r = \frac{s' - s}{d} \tag{34}$$

In this case the shift $S = s' - s - d$ is constant for all locations of the cell.

The locus of the extreme values $(s' - s)_m$ as a function of s' may be determined using the extremizing condition (12). The result is

$$\frac{\beta(s' - s)_m}{\beta s' + \Phi_T' - k\pi/2} = 2 \tag{35}$$

Accordingly, if values of $\beta(s' - s)_m$ for a range of possible values of n, r_c, and d are plotted as a function of $\beta s' + \Phi_T' - k\pi/2$, all points must be on a line of slope 2. This applies to both $\beta(s' - s)_{mv}$ and $\beta(s' - s)_{mi}$.

Experimental Procedure. In order to measure dielectric constants and permeabilities by the extreme-shift method, a sample of the material of

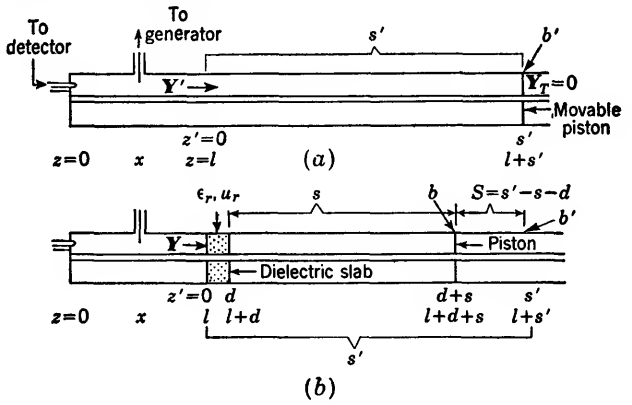


FIG. 7.2. (a) Location of piston at b' for resonance with no dielectric slab. (b) Location of piston at b for resonance with dielectric slab between $z = l$ and $z = l + d$.

thickness d must be moved along a transmission line that has a loosely coupled generator and a loosely coupled detector fixed near one end and a movable reactive termination (e.g., a piston) $\boldsymbol{Y}_T = jB_T$ at the other, as shown in Fig. 7.2, with $Y_T = 0$.† The first operation is to locate the position b' (Fig. 7.2a) of the reactive termination at which the circuit *without* dielectric is tuned to resonance, as indicated by a maximum deflection of the detector.

† If preferred, the dielectric may be fixed, and the detector, generator, and piston moved relative to it. For simplicity the procedure is described only for a movable dielectric slab.

The second operation is to move the slab of material (or the cell containing the liquid) from the point b' toward the detector step by step, thus increasing the distance s' between b' and the left-hand surface of the dielectric. For each position of the dielectric the reactive termination is moved toward the dielectric to b, where the circuit is again tuned to resonance, as indicated by a maximum deflection of the detector. The distance between the termination at the resonant position b and the

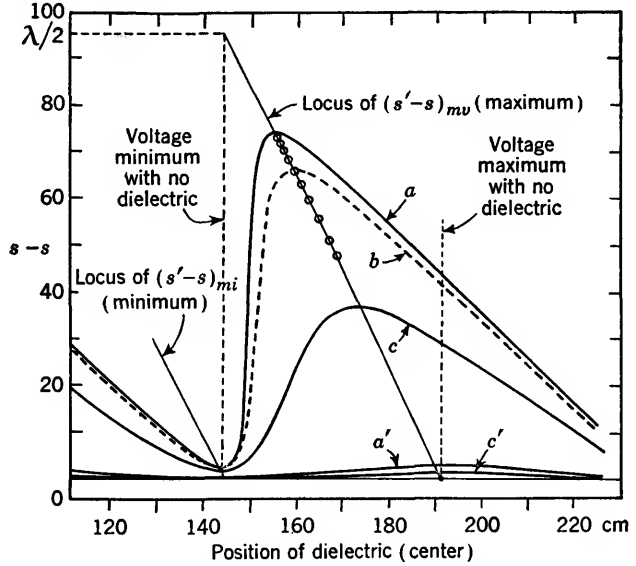


FIG. 7.3. Shift curves: a—distilled water in cell of thickness 2.08 cm; a'—the same cell empty; c—distilled water in cell of thickness 0.52 cm; c'—the same cell empty. The large circles locate the maxima of the shift curves of water solutions of ethyl alcohol; b is one of these completely plotted; $\lambda = 188.8$ cm.

right side of the dielectric is s. As s' and s are increased step by step but, in general, at different rates, a "shift curve" may be plotted of the difference $s' - s$ as a function of the location along the line of the center of the slab. The origin of the linear scale along the line is arbitrary. Typical "shift curves" for water solutions of ethyl alcohol for which $\epsilon_r > 1$, with $\mu_r = 1$, are shown in Fig. 7.3.

As s' is increased by moving the sample toward the detector, a point is reached where the reactive termination must be moved *away from* rather than *toward* the dielectric in order to tune the circuit to resonance. At this point a further *increase* in s' results in a decrease in $s' - s$—evidently the maximum value $(s' - s)_{mv}$ of $s' - s$ has been reached. For a certain range beyond this maximum, $s' - s$ decreases as s' is increased. Then $s' - s$ reaches a minimum $(s' - s)_{mi}$ and again starts increasing with

continually increasing s'. As indicated in Fig. 7.3, the center of the dielectric slab is at a voltage minimum when $s' - s$ is a minimum. If the reactive termination is a perfect short circuit (e.g., a piston) and the slab is electrically thin, the center of the dielectric is $\lambda/2$ from b' when $s' - s$ is a minimum.

In order to determine the dielectric constant of a material with $\mu_r = 1$, it is sufficient to measure the maximum value $(s' - s)_{mv}$ of $s' - s$; it is *not* necessary to plot a complete shift curve like those in Fig. 7.3. Several experimentally determined maximum values (without the rest of the associated shift curves) are also shown in Fig. 7.3. Note also that they

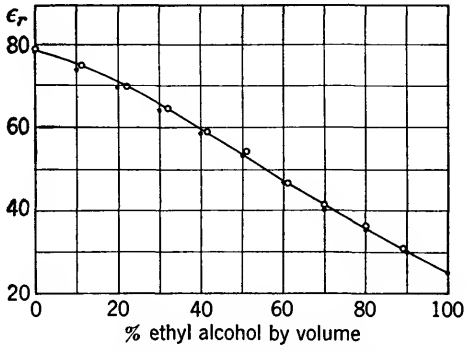


FIG. 7.4. Dielectric constant of water solutions of ethyl alcohol referred to water at 15.5°C. The circles are experimental points obtained using the cell of thickness 2.08 cm. Solid dots are from data given by Wyman [*J. Am. Chem. Soc.*, 53: 3297 (1931)]. Room temperatures.

all lie on the straight line of slope 2, as required by (35) (in Fig. 7.3 s' increases from left to right).

With $(s' - s_2)_{mv}$ measured and $\beta = 2\pi/\lambda$ known (or measured), $n = r_c = \sqrt{\epsilon_r}$ may be evaluated from (27*b*) with $B_w = 0$ or from (34) if there are solid retaining walls. The values of ϵ_r obtained from the measurements represented in Fig. 7.3 are given in Fig. 7.4.

The Size of the Sample. The mathematical theory assumes that the sample under test consists of a flat slab of thickness d with its parallel sides perpendicular to the axes of the conductors and completely filling the space between and around them. For use in a coaxial or shielded-pair line it consists of a disk that fits into the outer conductor or shield and has a hole or holes for the inner conductor or conductors. For use on an open-wire line the dielectric must ideally extend to infinity, although a relatively small properly shaped sample may be used if its relative dielectric constant or permeability is not too near 1 and a correction is made for the fraction of the field outside the sample.[123] In general, measurements are most convenient with a coaxial line.

In order to determine the most useful value for the thickness d of the sample, it is necessary to consider both the magnitude of the dielectric constant and permeability and the frequency at which it is to be measured. In Fig. 7.5 theoretical curves are shown of the index of refraction $n = \sqrt{\epsilon_r}$ as a function of the argument $\Delta_v = \frac{1}{2}\beta(s' - s)_{mv}$ for a range of

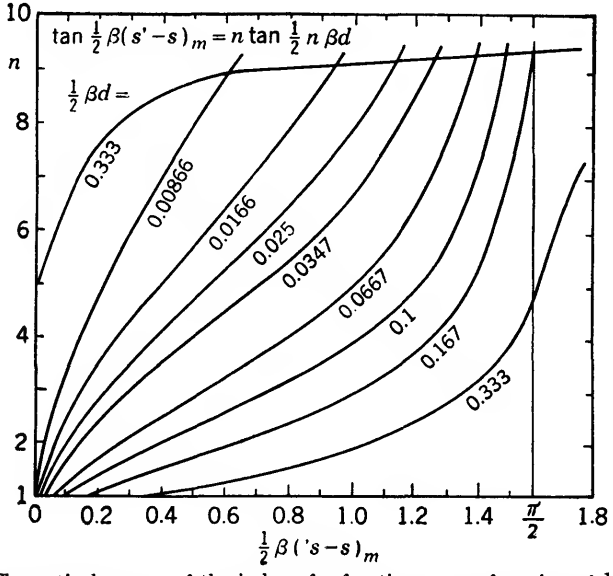


FIG. 7.5. Theoretical curves of the index of refraction n as a function of $\frac{1}{2}\beta(s' - s)_m$, with $\frac{1}{2}\beta d$ as parameter.

values of $\frac{1}{2}\beta d$ as determined from the fundamental Eq. (27b), with $\mu_r = 1$ and $B_w = 0$:

$$\tan \Delta_v = n \tan \tfrac{1}{2}n\beta d \qquad n = \sqrt{\epsilon_r},\ k \text{ odd in (12)} \tag{36}$$

With the aid of these curves it is possible to estimate the thickness d of the sample required to produce an adequate maximum value of $s' - s$, if the order of magnitude of the unknown dielectric constant is known as well as the frequency.

If the dielectric constant of a liquid is to be measured, a closed movable cell is required. Its parallel sides may be of Polyfoam or very thin solid dielectric; its inner and outer circular walls should be metal sleeves that slide over the inner and into the outer conductor of the coaxial line. By means of metal tubes of the same sizes as the sleeves, the entire section of line from the front of the dielectric sample to the reactive termination (piston) at b may be made to have constant inner and outer radii. The fact that these differ from the values between the detector and the front

of the cell is immaterial, since only the distances s', s, and d occur in the final formula.

The determination of μ_r for materials with $\epsilon_r \doteq 1$ parallels the determination of ϵ_r for materials with $\mu_r = 1$. With $B_w = 0$ and $\epsilon_r = 1$ in (27*a*), this becomes

$$\tan \Delta_i = n \tan \tfrac{1}{2}n\beta d \qquad n = \sqrt{\mu_r},\ k \text{ even in (12)} \tag{37}$$

Since this is the same as (36) except for a differently defined n and a different k in (12), the curves of Fig. 7.5 may be used.

Since $\Delta_v = \frac{1}{2}\beta(s' - s)_{mv}$ primarily depends on ϵ_r and $\Delta_i = \frac{1}{2}\beta(s' - s)_{mi}$ depends on μ_r, the curves of Fig. 7.5 are satisfactory for estimating the thickness d even in the general case when μ_r and ϵ_r both differ from unity. In general, $(s' - s)_v$ is the maximum and $(s' - s)_i$ the minimum shift when ϵ_r is greater than μ_r; $(s' - s)_i$ is the maximum and $(s' - s)_v$ the minimum shift when μ_r is greater than ϵ_r. As μ_r and ϵ_r approach each other, the maximum and minimum flatten until the shift curve is a straight line when $\mu_r = \epsilon_r$.

Measurement of Small Susceptances. The maximum-shift method is a highly sensitive procedure for measuring small lumped susceptances. The appropriate formula is obtained directly from (27*b*) by setting $d = 0$ and combining the two lumped susceptances B_w into the single lumped susceptance to be measured. Thus, with $B = 2B_w$ and $d = 0$, (27*b*) becomes

$$B = 2G_c \tan \tfrac{1}{2}\beta(s' - s)_{\max} \tag{38}$$

where $G_c = 1/R_c$ is the characteristic conductance of the line. For sufficiently small susceptances

$$B \doteq G_c\beta(s' - s)_{\max} \tag{39}$$

The extreme-shift method permits the accurate experimental determination of dielectric constants, permeabilities, and lumped susceptances from measurements of length, namely, $(s' - s)_{\max}$, $(s' - s)_{\min}$, and d. The accuracy is enhanced by the fact that in measuring the dielectric constant the sample is located at a voltage maximum, where its effect is greatest; similarly, in measuring permeability, the sample is located at a current maximum, where its effect is again greatest. Incidentally the method may also be used to determine the reactive properties of loaded sections of transmission line and of variable capacitive tuners.[125]

The adaptation of the method to measure losses is described in the next section.

8. Determination of Losses in Dielectric and Magnetic Materials Using the Maximum-shift Method. In the preceding section a method is described for determining the real effective dielectric constant $\epsilon_e = \epsilon_0\epsilon_{er}$ and the real permeability $\mu = \mu_0\mu_r$ of a sample of material. Section 7,

conditions (18), require that this sample (region 1) have small (but not necessarily zero) attenuation constant α_1 and distortion factor ϕ_{c1}. These quantities are defined as follows for a moderately low-loss line:

$$\frac{\alpha_1}{\beta_1} \doteq \frac{1}{2\omega}\left(\frac{r_1}{l_1} + \frac{g_1}{c_1}\right) \qquad \left(\frac{\alpha_1}{\beta_1}\right)^2 \ll 1 \tag{1a}$$

$$\phi_{c1} \doteq \frac{1}{2\omega}\left(\frac{r_1}{l_1} - \frac{g_1}{c_1}\right) \qquad \phi_{c1}^2 \ll 1 \tag{1b}$$

In their usual application r_1 involves only ohmic losses resulting from imperfect conductors, and g_1 involves the ohmic losses of an imperfect dielectric. As outlined in Chap. I, Sec. 4, losses in the line may result from time lags in the polarization response of a dielectric medium with a contribution to the effective conductivity and hence to g_1, or from time lags in the magnetization response of a magnetic medium with a contribution to the effective resistance r_1. Time lags in the conduction response of a medium involve contributions to the effective dielectric constant as well as to the effective conductivity. All these possible effects are included in the following general formulas for moderately low-loss lines, as obtained from Chap. I, Secs. 3 and 4:

$$\frac{r}{\omega l} = \frac{r^i}{\omega l} + \frac{\mu''}{\mu'} \equiv \frac{r^i}{\omega l} + h_m \tag{2a}$$

$$\frac{g}{\omega c} = \frac{\sigma_e}{\omega \epsilon_e} = \frac{\sigma' + \omega\epsilon''}{\omega\epsilon' - \sigma''} \equiv h_e \tag{2b}$$

Note that, if the conductors are perfect, so that the ohmic resistance $r^i = 0$, and the losses in the dielectric medium are not from conduction ($\sigma' = \sigma'' = 0$) but exclusively from time lags in polarization and magnetization, (2*a*) and (2*b*) reduce to the following symmetrical forms:

$$\frac{r}{\omega l} = \frac{\mu''}{\mu'} = h_m \qquad \frac{g}{\omega c} = \frac{\epsilon''}{\epsilon'} = h_e \tag{3}$$

It is assumed in the following that the imaginary parts of the complex permeability, complex dielectric constant, and complex conductivity are small compared with the real parts, so that these formulas are good approximations:

$$\mathfrak{y} = \mu' - j\mu'' \doteq \mu - j\mu'' \qquad \mu = \sqrt{\mu'^2 + \mu''^2} \doteq \mu' \tag{4a}$$

$$\mathfrak{e} = \epsilon' - j\epsilon'' \doteq \epsilon - j\epsilon'' \qquad \epsilon = \sqrt{\epsilon'^2 + \epsilon''^2} \doteq \epsilon' \tag{4b}$$

$$\mathfrak{d} = \sigma' - j\sigma'' \doteq \sigma - j\sigma'' \qquad \sigma = \sqrt{\sigma'^2 + \sigma''^2} \doteq \sigma' \tag{4c}$$

It follows that

$$h_m \equiv \frac{\mu''}{\mu'} \doteq \frac{\mu''}{\mu} \qquad h_e \equiv \frac{\sigma_e}{\omega\epsilon_e} \doteq \frac{\sigma + \omega\epsilon''}{\omega\epsilon - \sigma''} \tag{5}$$

By adding subscripts 1 and substituting appropriate quantities in (1*a*,*b*), the attenuation constant and distortion factor of the dielectric

and magnetic medium are

$$\frac{\alpha_1}{\beta_1} \doteq \frac{r^i}{\omega l} + h_m + h_e \qquad \left(\frac{\alpha_1}{\beta_1}\right)^2 \ll 1 \tag{6a}$$

$$\phi_{c1} \doteq \frac{r^i}{\omega l} + h_m - h_e \qquad \phi_{c1}^2 \ll 1 \tag{6b}$$

For the same line in air (vacuum) the corresponding quantities are

$$\frac{\alpha}{\beta} \doteq \phi_c \doteq \frac{r^i}{\omega l} \qquad \left(\frac{\alpha_1}{\beta_1}\right)^2 \ll 1 \tag{7}$$

With these preliminary definitions summarized, attention can be directed to the evaluation of the effective terminal function ρ of the

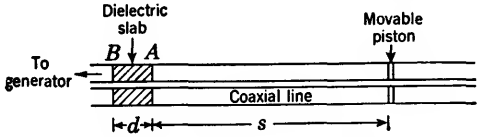


FIG. 8.1. Dielectric slab in coaxial line terminated in a movable piston.

section of line to the right of B (Fig. 8.1), including the dielectric and magnetic sample and the reactive section of length s.

The admittance looking to the right at A in Fig. 8.1 is Y_2, as defined in Sec. 7, Eq. (2). The admittance looking to the right at B is Y, as given in Sec. 7, Eq. (3). Since the effect of solid retaining walls (if the material under study is a liquid) is assumed to be *purely reactive*, there is no contribution to the dissipation, and it is adequate to treat only the simpler case without walls. This is obtained with $Y_w = 0$ in Sec. 7, Eqs. (2) and (3). The resulting expressions are

$$Y_2 = G_2 + jB_2 = Y_c \coth (\gamma s + \theta_T') \doteq Y_c(\alpha s \csc^2 \beta s - j \cot \beta s) \tag{8}$$

$$Y = G + jB = Y_{c1} \frac{Y_2 \coth \gamma_1 d + Y_{c1}}{Y_2 + Y_{c1} \coth \gamma_1 d} \tag{9}$$

The characteristic admittance of the line in the dielectric or magnetic medium is Y_{c1}, and that with the line in air is Y_c. The two quantities are given by

$$Y_c = G_c(1 + j\phi_c) \qquad G_c = \sqrt{\frac{c}{l}} \tag{10}$$

$$Y_{c1} = G_{c1}(1 + j\phi_{c1}) \qquad G_{c1} = \sqrt{\frac{c_1}{l_1}} = G_c \sqrt{\frac{\epsilon_{er}}{\mu_r}} \tag{11}$$

where ϕ_{c1} and ϕ_c are as given in (6*b*) and (7) and $\epsilon_{er} = \epsilon_e/\epsilon_0$ and $\mu_r = \mu/\mu_0$ are the relative values of the real effective dielectric constant and the real permeability.

When the dielectric or magnetic sample is in a position of *extreme shift*, the susceptance B_2 is the negative of B, as shown in Sec. 7, Eq. (28*b*).

That is,

$$B_2 = -B \tag{12}$$

so that (9) becomes

$$G - jB_2 = Y_{c1} \frac{(G_2 + jB_2) \coth \gamma_1 d + Y_{c1}}{G_2 + jB_2 + Y_{c1} \coth \gamma_1 d} \tag{13}$$

Let the admittances be normalized by dividing by Y_c, the characteristic admittance of the air-filled line. As in Sec. 7, Eq. (21), let

$$r_c \equiv \frac{Y_{c1}}{Y_c} = \frac{R_c(1 - j\phi_c)}{R_{c1}(1 - j\phi_{c1})} \doteq r_c(1 + j\phi_r) \tag{14a}$$

where $r_c = \dfrac{R_c}{R_{c1}} = \dfrac{G_{c1}}{G_c}$ $\qquad \phi_r = \phi_{c1} - \phi_c = h_m - h_e \qquad \phi_r^2 \ll 1$ (14b)

With (14a,b), (13) becomes

$$g - jb_2 = r_c \frac{(g_2 + jb_2) \coth \gamma_1 d + r_c}{g_2 + jb_2 + r_c \coth \gamma_1 d} \tag{15}$$

where $$g - jb_2 = \frac{G - jB_2}{Y_c} \qquad g_2 + jb_2 = \frac{G_2 + jB_2}{Y_c} \tag{16}$$

The real and imaginary parts may be separated using (14a) and Sec. 7, Eq. (19). For convenience let

$$C_{1r} + jC_{1i} \equiv r_c \coth \gamma_1 d \doteq r_c(\alpha_1 d \csc^2 \beta_1 d + \phi_r \cot \beta_1 d) - jr_c \cot \beta_1 d \tag{17a}$$

where use has been made of Sec. 7, Eq. (19), and a higher-order term with coefficient $\alpha_1 \phi_r d$ has been neglected. Also let

$$C_{2r} + jC_{2i} \equiv r_c^2 \doteq r_c^2(1 + j2\phi_r) \tag{17b}$$

With this shorthand notation introduced in (15), the following fundamental equations are obtained:

$$b_2^2 + 2b_2C_{1i} - C_{2r} - C_{1r}(g_2 - g) + gg_2 = 0 \tag{18a}$$

$$(g - g_2)(b_2 + C_{1i}) - 2b_2C_{1r} - C_{2i} = 0 \tag{18b}$$

Section 7, conditions (18), imply the following inequality:

$$C_{2r} \gg |C_{1r}(g - g_2) + gg_2| \tag{19}$$

since, when (19) is satisfied and with Sec. 7, Eq. (15), and

$$b_2 = -\cot(\beta s + \Phi_r') = -\cot\left(\frac{k\pi}{2} - \Delta\right) = \begin{cases} \cot \Delta & k \text{ even} \\ -\tan \Delta & k \text{ odd} \end{cases} \tag{20}$$

(18a) reduces exactly to the fundamental equations [Sec. 7, Eqs. (14a,b)] for the conditions of extreme shift. By combining Sec. 7, Eqs. (14a,b), with (20) the following alternative expressions are obtained for b_2:

$$b_2 = \begin{cases} r_c \cot \frac{1}{2}\beta_1 d & k \text{ even} \\ -r_c \tan \frac{1}{2}\beta_1 d & k \text{ odd} \end{cases} \tag{21}$$

The remaining equation, (18*b*), is to be used to determine g and, from it, ρ. Since the section of line to the right of the dielectric slab (Fig. 8.1) is essentially reactive, it may be assumed that g_2 is negligible compared with g. Hence

$$g - g_2 \doteq g \doteq \frac{2b_2C_{1r} + C_{2i}}{b_2 + C_{1i}} \tag{22}$$

With (17*a*,*b*) and (21), (22) may be expressed as follows:

$$g \doteq 2r_c[(\alpha_1 d \csc^2 \beta_1 d + \phi_r \cot \beta_1 d) \cot \tfrac{1}{2}\beta_1 d + \phi_r] \sin \beta_1 d \qquad k \text{ even} \tag{23a}$$

$$g \doteq 2r_c[(\alpha_1 d \csc^2 \beta_1 d + \phi_r \cot \beta_1 d) \tan \tfrac{1}{2}\beta_1 d - \phi_r] \sin \beta_1 d \qquad k \text{ odd} \tag{23b}$$

Use has been made of the identities

$$\tan \tfrac{1}{2}x = \csc x - \cot x \tag{24a}$$

$$\cot \tfrac{1}{2}x = \csc x + \cot x \tag{24b}$$

The terminal attenuation function ρ of a moderately low-loss line may be determined from

$$\rho = \tfrac{1}{2} \tanh^{-1} \frac{2g}{1 + b^2 + g^2} \doteq \frac{g}{1 + b^2} \tag{25}$$

The substitution of (23*a*) or (23*b*) in (25), together with the appropriate formula from (20), leads to

$$\rho_i = \frac{2r_c[(\alpha_1 d/2) \sec^2 \tfrac{1}{2}\beta_1 d + \phi_r \tan \tfrac{1}{2}\beta_1 d]}{r_c^2 + \tan^2 \tfrac{1}{2}\beta_1 d} \qquad k \text{ even} \tag{26a}$$

$$\rho_v = \frac{2r_c[(\alpha_1 d/2) \sec^2 \tfrac{1}{2}\beta_1 d - \phi_r \tan \tfrac{1}{2}\beta_1 d]}{1 + r_c^2 \tan^2 \tfrac{1}{2}\beta_1 d} \qquad k \text{ odd} \tag{26b}$$

(The subscripts i and v indicate ρ with current and voltage maximum, respectively, at the center of the slab.) In deriving (26*a*,*b*) use has been made of (24*a*) to express all arguments as $\frac{1}{2}\beta_1 d$.

Since, with k even, the dielectric sample has a current maximum at its center ($\beta_1 d < \pi$) and, with k odd, a voltage maximum, the values of ρ in (26*a*) and (26*b*) should be twice the values obtained by placing a slab of dielectric of thickness $d/2$ at an ideal short-circuited end and an ideal open end, respectively. That is, ρ in (26*a*) should be twice the value of ρ_{BS} in Sec. 6, Eq. (40*a*), and ρ in (26*b*) should be twice ρ_{BO} in Sec. 6, Eq. (35*a*). It is readily verified that this is true.

Since the circuit is always adjusted to resonance in determining the extreme shift, it is convenient to determine ρ_i and ρ_v using the resonance-curve method. Once these two quantities are known, α_1 and ϕ_r may be evaluated from (26*a*) and (26*b*), and from these h_m and h_e using (6*a*,*b*) with (14*b*). It is assumed that the constants of the line in air are known, as well as R_{c1} and β_1, which involve ϵ_r and μ_r.

9. The Double Bead and the Spacing of Beads for No Change in Impedance. Dielectric beads or slabs often must be placed at intervals along a transmission line in order to support one or more conductors and maintain the desired spacing. Since even a single dielectric bead disturbs a condition of match, a large number of beads distributed along a line might have a serious effect on the transmission properties if they happened to be so located that their effects were cumulative. In order to determine how the effect of a single bead may be magnified or reduced by the presence of other beads, let two identical slabs of dielectric, each of thickness d and separated an arbitrary distance v between adjacent parallel sides, be investigated. The configuration is shown in Fig. 9.1, where the slab nearer the load has its nearest side at a distance w from the load.

For the air-filled sections of line the propagation constant is $\gamma = \alpha + j\beta$, and the characteristic impedance is $Z_c = R_c(1 - j\phi_c)$. Although the

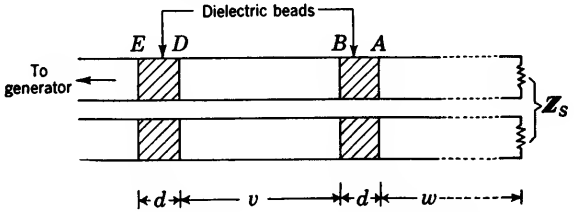


FIG. 9.1. Coaxial line with two dielectric beads.

more general case can be analyzed, let it be assumed for simplicity that losses in the dielectric are negligible, so that ϵ is real and $g_1/\omega c_1$ is negligible compared with $r_1/\omega l_1$. The propagation constant and characteristic impedance of the air-filled sections of line are

$$\gamma = \alpha + j\beta \qquad Z_c = R_c(1 - j\phi_c) \qquad \left(\frac{\alpha}{\beta}\right)^2 \doteq \phi_c^2 \ll 1 \tag{1a}$$

The parameters of the dielectric-filled sections are

$$\gamma_1 = \alpha_1 + j\beta_1 \qquad Z_{c1} = R_c(1 - j\phi_{c1}) \qquad \left(\frac{\alpha_1}{\beta_1}\right)^2 \doteq \phi_{c1}^2 \ll 1 \tag{1b}$$

Since the dielectric is lossless, it follows that

$$\alpha_1 = \alpha \qquad \beta_1 = n\beta \qquad R_{c1} = \frac{R_c}{n} \qquad n = \sqrt{\epsilon_r} \tag{2}$$

In order that the section of line between A and E (in Fig. 9.1) which includes the two beads may have no effect on the impedance of the line, the impedance looking toward the load at E must be equal to the impedance looking toward the load at A for an arbitrary load. That is,

$$Z_E = Z_A \tag{3}$$

Complex terminal functions may be defined for each impedance in terms of the characteristic impedance of either medium. Thus

$$Z_A = Z_c \coth \theta_A = Z_{c1} \coth \theta_{A1} = \frac{Z_c}{n} \coth \theta_{A1} \tag{4a}$$

$$Z_E = Z_c \coth \theta_E = Z_{c1} \coth \theta_{E1} = \frac{Z_c}{n} \coth \theta_{E1} \tag{4b}$$

Evidently (3) is equivalent to

$$\theta_E = \theta_A \qquad \text{or} \qquad \theta_{E1} = \theta_{A1} \tag{5}$$

The question, therefore, is whether (3) and (5) are possible and, if so, under what conditions.

The first step is to obtain expressions for the complex electrical length γv (v is the distance between the adjacent surfaces of the two pieces of dielectric) in terms of the function $\theta_{E1} = \theta_{A1}$ and the thickness d of each bead or slab. This is accomplished as follows: First note that, since $\theta_D = \gamma v + \theta_B$, it follows directly that

$$\gamma v = \theta_D - \theta_B \tag{6}$$

The next steps involve the evaluation of θ_D and θ_B. Since

$$\theta_{A1} = \theta_{E1} = \gamma_1 d + \theta_{D1} \tag{7}$$

and

$$Z_D = Z_c \coth \theta_D = \frac{Z_c}{n} \coth \theta_{D1} \tag{8a}$$

it follows that

$$\theta_D = \coth^{-1}\left(\frac{1}{n} \coth \theta_{D1}\right) = \tanh^{-1} (n \tanh \theta_{D1}) \tag{8b}$$

By solving (7) for θ_{D1} and substituting in (8b), the desired formula for θ_D is obtained. It is

$$\theta_D = \tanh^{-1} [n \tanh (\theta_{E1} - \gamma_1 d)] \tag{9}$$

Similarly, since

$$\theta_{B1} = \gamma_1 d + \theta_{A1} \tag{10}$$

and

$$Z_B = Z_c \coth \theta_B = \frac{Z_c}{n} \coth \theta_{B1} \tag{11a}$$

so that

$$\theta_B = \coth^{-1}\left(\frac{1}{n} \coth \theta_{B1}\right) = \tanh^{-1} (n \tanh \theta_{B1}) \tag{11b}$$

it follows that

$$\theta_B = \tanh^{-1} [n \tanh (\theta_{A1} + \gamma_1 d)] \tag{12}$$

The substitution of (9) and (12) in (6) gives the desired formula for γv:

$$\gamma v = \tanh^{-1} [n \tanh (\theta_{E1} - \gamma_1 d)] - \tanh^{-1} [n \tanh (\theta_{A1} + \gamma_1 d)] \tag{13}$$

Using the identity

$$\tanh^{-1} x \pm \tanh^{-1} y = \tanh^{-1} \frac{x + y}{1 \pm xy} \tag{14}$$

(13) may be transformed into

$$\gamma v = \tanh^{-1} \frac{n[\tanh (\theta_{E1} - \gamma_1 d) - \tanh (\theta_{A1} + \gamma_1 d)]}{1 - n^2 \tanh (\theta_{E1} - \gamma_1 d) \tanh (\theta_{A1} + \gamma_1 d)} \tag{15}$$

Each of the hyperbolic tangents in (15) may now be expanded using the identity

$$\tanh (x \pm y) = \frac{\tanh x \pm \tanh y}{1 \pm \tanh x \tanh y} \tag{16}$$

After some algebraic manipulation the result is

$$\tanh \gamma v = \frac{2n \tanh \gamma_1 d \, (\tanh^2 \theta_{A1} - 1)}{1 - \tanh^2 \theta_{A1} \tanh^2 \gamma_1 d - n^2(\tanh^2 \theta_{A1} - \tanh^2 \gamma_1 d)} \tag{17}$$

This is a complex equation for $\gamma v = (\alpha + j\beta)v$. However, since (3) cannot actually be satisfied unless the losses in the section of line between E and A (Fig. 9.1) are negligible, it is convenient to reduce (17) to a single equation in βv by setting the attenuation equal to zero. Thus

$$\gamma \doteq j\beta \qquad \gamma_1 \doteq j\beta_1 = jn\beta \tag{18}$$

With (18), (17) reduces to

$$\tan \beta v = \frac{2n \tan \beta_1 d \, (\tanh^2 \theta_{A1} - 1)}{1 + \tanh^2 \theta_{A1} \tan^2 \beta_1 d - n^2(\tanh^2 \theta_{A1} + \tan^2 \beta_1 d)} \tag{19}$$

Since the left side of (19) is real, the right side must also be real. This is possible only if $\tanh \theta_{A1}$ is either real or purely imaginary. In the latter case $\theta_{A1} = \rho_{A1} + j\Phi_{A1}$ must be imaginary, so that ρ_{A1} must vanish. Since this possibility limits the load to a pure reactance, it must be rejected. The alternative is

$$\tanh \theta_A = \frac{\tanh \rho_A + j \tan \Phi_A}{1 + j \tanh \rho_A \tan \Phi_A} \text{ is real} \tag{20}$$

For this equation there are two possible solutions. They are

$$\Phi_A = \pi \qquad \tanh \theta_A = \tanh \rho_A \tag{21a}$$

$$\Phi_A = \frac{\pi}{2} \qquad \tanh \theta_A = \coth \rho_A \tag{21b}$$

The condition $\Phi_A = \Phi_s + \beta w = \pi$ means that the edge A of the dielectric (Fig. 9.1) is at a voltage maximum; the condition $\Phi_A = \Phi_s + \beta w = \pi/2$ means that A is at a current maximum. In general, $\rho_A = \rho_s + \alpha w$. For a sufficiently small attenuation on the line it is possible to set

$$\rho_s \gg \alpha w \qquad \rho_s \doteq \rho_A \tag{22}$$

With (22) and the notation

$$S \equiv \coth \rho_s \tag{23}$$

where S is the standing-wave ratio on the line between the edge A and

the load, the conditions (21*a*,*b*) become

$$\Phi_A = \Phi_s + \beta w = \pi \qquad \tanh \theta_A = \frac{1}{S} \qquad \tanh \theta_{A1} = \frac{1}{n} \tanh \theta_A = \frac{1}{nS} \tag{24a}$$

$$\Phi_A = \Phi_s + \beta w = \frac{\pi}{2} \qquad \tanh \theta_A = S \qquad \tanh \theta_{A1} = \frac{1}{n} \tanh \theta_A = \frac{S}{n} \tag{24b}$$

If these values are substituted in (19) and the results are rearranged, the following expressions are obtained for the electrical distance βv (note that $n = \sqrt{\epsilon_r}$):

$$\text{For } \Phi_A = \pi\text{:} \quad \beta v = \tan^{-1} \frac{n(n^2S^2 - 1) \sin 2n\beta d}{(n^2S^2 - 1)(n^2 + 1) \sin^2 n\beta d - n^2(S^2 - 1)} \tag{25a}$$

$$\text{For } \Phi_A = \frac{\pi}{2}\text{:} \quad \beta v = \tan^{-1} \frac{n(n^2 - S^2) \sin 2n\beta d}{(n^2 - S^2)(n^2 + 1) \sin^2 n\beta d + n^2(S^2 - 1)} \tag{25b}$$

Matched Line with Two Beads. If the line is matched, $\rho_A = \infty$, $S = 1$, and Φ_A has no significance. The electrical distance βv between the two beads is

$$\beta v = \tan^{-1} \left(\frac{2n}{n^2 + 1} \cot n\beta d \right) \tag{26}$$

If $n\beta d$ is sufficiently small so that $\cot n\beta d \doteq 1/n\beta d$, (26) reduces to

$$\beta v \doteq \frac{\pi}{2} - \frac{1}{2} \beta d(n^2 + 1) \tag{27}$$

for a matched line. In this case the electrical distance βv_c between the centers of the beads is

$$\beta v_c = \beta(v + d) = \frac{\pi}{2} - \frac{1}{2} \beta d(n^2 - 1) \tag{28a}$$

and

$$v_c = \frac{\lambda}{4} - \frac{d}{2} (n^2 - 1) \tag{28b}$$

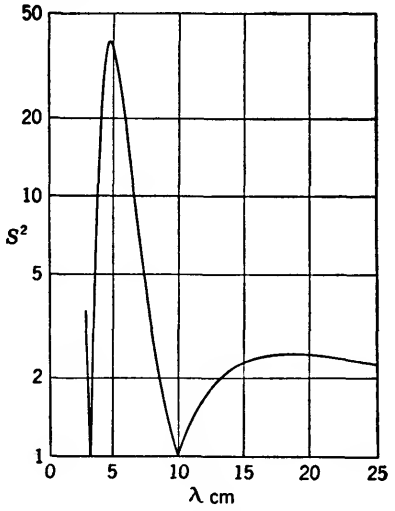


FIG. 9.2. Square of standing-wave ratio S in a matched line with two dielectric beads, each of thickness $d = 0.0635$ cm and dielectric constant $\epsilon_r = 2.6$, separated a distance $v_c = 2.03$ cm between centers.

It is seen that two sufficiently thin beads must be spaced at a distance slightly less than a quarter wavelength along a nonresonant line. The square of the standing-wave ratio introduced in an originally matched line by two beads is shown in Fig. 9.2 as a function of wavelength. It is seen that the line is matched at two wavelengths that satisfy (26).

By arranging beads or dielectric supports in pairs, with each pair spaced a distance v, as given in (26) or (27), a matched line remains nonresonant along all sections between the pairs of beads.

Resonant Line with Two Beads. If ρ_A is small and the standing-wave ratio S is very great, so that the inequalities

$$S^2 \gg 1 \qquad \epsilon S^2 \gg 1 \qquad \epsilon^2 S^2 \gg 1 \tag{29}$$

are all satisfied, the general expressions (25a) and (25b) reduce to

For $\Phi_A = \pi$: $$\beta v = \pi - \tan^{-1} \frac{2n \tan n\beta d}{1 - n^2 \tan^2 n\beta d} \tag{30a}$$

For $\Phi_A = \frac{\pi}{2}$: $$\beta v = \pi - \tan^{-1} \frac{2n \tan n\beta d}{n^2 - \tan^2 n\beta d} \tag{30b}$$

For sufficiently thin beads or slabs that satisfy the inequality

$$(n\beta d)^2 \ll 1 \tag{31}$$

the following results are obtained:

For $\Phi_A = \pi$:

$$\beta v = \pi - 2n^2 \beta d \qquad v = \frac{\lambda}{2} - 2n^2 d \qquad v_c = \frac{\lambda}{2} - d(2n^2 - 1) \tag{32a}$$

For $\Phi_A = \frac{\pi}{2}$:

$$\beta v = \pi - 2\beta d \qquad v = \frac{\lambda}{2} - 2d \qquad v_c = \frac{\lambda}{2} - d \tag{32b}$$

It is seen that for a resonant line the pair of beads must be placed almost a half wavelength apart. Note that v_c is the distance between centers.

Line with Two Lumped Shunt Capacitances. As considered in Sec. 6, a single lumped capacitance C may be represented analytically by a dielectric bead in the limit as its thickness vanishes and its dielectric constant becomes infinite. The relations are

$$C = \lim_{\substack{d \to 0 \\ n \to \infty}} cd(n^2 - 1) = \lim_{\substack{d \to 0 \\ n \to \infty}} cdn^2 \tag{33a}$$

$$\omega C R_c = \lim_{\substack{d \to 0 \\ n \to \infty}} \beta d(n^2 - 1) = \lim_{\substack{d \to 0 \\ n \to \infty}} \beta d n^2 \tag{33b}$$

$$\lim_{\substack{d \to 0 \\ n \to \infty}} n \tan n\beta d = \lim_{n \to \infty} n \tan \frac{\omega C R_c}{n} = \omega C R_c \tag{33c}$$

With these relations (25a) and (25b) may be reduced to the following:

For $\Phi_A = 0$: $$\beta v = \tan^{-1} \frac{2\omega C R_c}{\omega^2 C^2 R_c^2 - 1 + 1/S^2} \tag{34a}$$

For $\Phi_A = \frac{\pi}{2}$: $$\beta v = \tan^{-1} \frac{2\omega C R_c}{\omega^2 C^2 R_c^2 - 1 + S^2} \tag{34b}$$

For the matched line with $S = 1$ these reduce to

$$\beta v = \frac{\pi}{2} - \tan^{-1} \frac{\omega C R_c}{2} \tag{35a}$$

with $$(\omega C R_c)^2 \ll 1 \qquad v = \frac{\lambda}{4} - \frac{C}{2c} \tag{35b}$$

where c is the capacitance per unit length of the air-filled line.

For the resonant line,

For $\Phi_A = 0$: $$\beta v = \pi - 2 \tan^{-1} (\omega C R_c) \tag{36a}$$

with $$(\omega C R_c)^2 \ll 1 \qquad v = \frac{\lambda}{2} - \frac{2C}{c} \tag{36b}$$

For $\Phi_A = \frac{\pi}{2}$: $$\beta v = 0, \pi, 2\pi, \ldots \qquad v = \frac{\lambda}{2}, \lambda, \ldots \tag{37}$$

If the first capacitance is placed at a voltage maximum, the second capacitor must be somewhat less than $\lambda/2$ from it. If the first capacitance is at a current maximum, the second capacitor must be exactly a half wavelength from it.

10. The Double-slug Transformer.[16] A coaxial transmission line contains two identical slugs, each of length d, consisting either of dielectric material with relative dielectric constant ϵ_r, as shown in Fig. 10.1*a*, or of metal sleeves, as shown in Fig. 10.1*b*. The characteristic impedance of

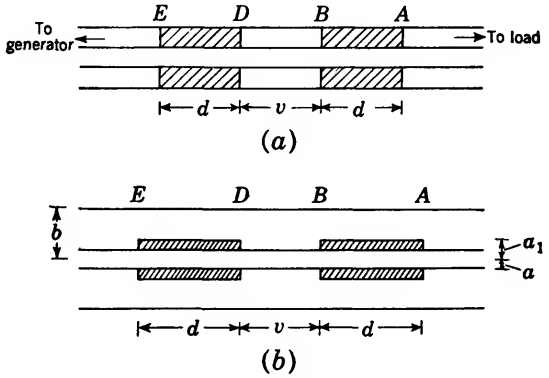


FIG. 10.1. Double-slug transformers in a coaxial line. (*a*) Dielectric-slug transformer ($\beta_1 d = \pi/2$). (*b*) Metal-sleeve transformer ($\beta d = \pi/2$).

the main line and of the section of length v between the slugs is $\boldsymbol{Z}_c$, and the propagation constant is $\gamma = \alpha + j\beta$. For the parts of the line constituting the slugs (regions 1), the parameters are $\boldsymbol{Z}_{c1}$ and $\gamma_1 = \alpha_1 + j\beta_1$. Since the transformer is to serve as a reactive device, only good dielectrics and low-loss conductors are involved. For these the reactive properties are essentially the same as for perfect dielectrics and conductors, and the losses are negligible compared with the dissipation in the load. There-

fore it is adequate to neglect attenuation in the slugs and the region between by setting

$$\gamma = j\beta \qquad Z_c = R_c \tag{1a}$$

$$\gamma_1 = j\beta_1 \qquad Z_{c1} = R_{c1} \tag{1b}$$

If the slugs are dielectric,

$$\beta_1 = \beta\sqrt{\epsilon_r} \qquad R_{c1} = \frac{R_c}{\sqrt{\epsilon_r}} \equiv \frac{R_c}{\sqrt{m}} \tag{2a}$$

If the slug consists of metal sleeves of radius a_1 greater than the radius a of the inner conductor,

$$\beta_1 = \beta \qquad R_{c1} = R_c \frac{\ln (b/a)}{\ln (b/a_1)} = \frac{R_c}{\sqrt{m}} \tag{2b}$$

The symbol m has been introduced in (2a) and (2b) to stand for either ϵ_r or $\left[\dfrac{\ln (b/a_1)}{\ln (b/a)}\right]^2$.

The properties of the transformer may be studied by deriving a formula for the complex terminal function θ_E of the arbitrarily loaded line to the right of E in Fig. 10.1. Steps in the derivation are outlined below. The impedance looking toward the load at A is

$$Z_A = Z_c \coth \theta_A = \frac{Z_c}{\sqrt{m}} \coth \theta_{A1} \tag{3a}$$

so that

$$\tanh \theta_{A1} = \frac{1}{\sqrt{m}} \tanh \theta_A \tag{3b}$$

The impedance looking to the right at B is

$$Z_B = Z_c \coth \theta_B = \frac{Z_c}{\sqrt{m}} \coth \theta_{B1} \tag{4a}$$

so that

$$\theta_B = \coth^{-1}\left(\frac{1}{\sqrt{m}} \coth \theta_{B1}\right) \tag{4b}$$

However,

$$\theta_{B1} = j\beta_1 d + \theta_{A1} \tag{5}$$

Let the length of the slugs be so chosen that

$$\beta_1 d = \frac{\pi}{2} \tag{6}$$

If (6) is used in (5), it follows with (3b) that

$$\coth \theta_{B1} = \coth\left(\frac{j\pi}{2} + \theta_{A1}\right) = \tanh \theta_{A1} = \frac{1}{\sqrt{m}} \tanh \theta_A \tag{7}$$

By substituting (7) in (4b) the following result is obtained:

$$\theta_B = \coth^{-1}\left(\frac{1}{m} \tanh \theta_A\right) \tag{8}$$

By a similar procedure it is readily shown that

$$\theta_E = \coth^{-1}\left[\frac{1}{m}\tanh\left(j\beta v + \theta_B\right)\right] \tag{9}$$

so that, with (8) in (7),

$$\theta_E = \coth^{-1}\left\{\frac{1}{m}\tanh\left[j\beta v + \coth^{-1}\left(\frac{1}{m}\tanh\theta_A\right)\right]\right\} \tag{10}$$

This is the desired expression. By expanding the hyperbolic tangent of the sum, (10) may be transformed into

$$\theta_E = \rho_E + j\Phi_E = \coth^{-1}\frac{1 + (j/m)\tanh\theta_A\tan\beta v}{\tanh\theta_A + jm\tan\beta v} \tag{11}$$

If the normalized admittance looking to the right at A is introduced by setting

$$\tanh\theta_A = \coth\theta'_A = y_A = g_A + jb_A \tag{12}$$

where

$$g_A = \frac{\sinh 2(\alpha w + \rho_s)}{\cosh 2(\alpha w + \rho_s) - \cos 2(\beta w + \Phi'_s)} \tag{13a}$$

$$b_A = \frac{-\sin 2(\beta w + \Phi'_s)}{\cosh 2(\alpha w + \rho_s) - \cos 2(\beta w + \Phi'_s)} \tag{13b}$$

and where, as usual,

$$\theta_A = \rho_A + j\Phi_A \qquad \theta'_A = \rho_A + j\Phi'_A \qquad \Phi'_A = \Phi_A - \frac{\pi}{2}$$

Φ_s and ρ_s are the terminal functions of the impedance Z_s terminating a length w of line extending from the end of the slug at A to the load.

If (12) is substituted in (11), the real and imaginary parts may be conveniently separated by introducing the following identity:

$$\coth^{-1}x = \tfrac{1}{2}\ln\frac{x+1}{x-1} \tag{14}$$

The results are

$$\rho_E = \tfrac{1}{2}\ln A \qquad \Phi_E = \tfrac{1}{2}(\psi_N + \psi_D) \tag{15}$$

where

$$A \equiv \left\{\frac{[1 + g_A - (b_A/m)\tan\beta v]^2 + [b_A + (m + g_A/m)\tan\beta v]^2}{[1 - g_A - (b_A/m)\tan\beta v]^2 + [b_A + (m - g_A/m)\tan\beta v]^2}\right\}^{\frac{1}{2}} \tag{16a}$$

$$\psi_N \equiv \tan^{-1}\frac{b_A + (m + g_A/m)\tan\beta v}{1 + g_A - (b_A/m)\tan\beta v} \tag{16b}$$

$$\psi_D = \tan^{-1}\frac{b_A + (m - g_A/m)\tan\beta v}{1 - g_A - (b_A/m)\tan\beta v} \tag{16c}$$

If the line is matched so that $Z_A = Z_s = Z_c$, $g_A = 1$, and $b_A = 0$, great

simplification is achieved. Thus

$$\rho_E = \tfrac{1}{2} \ln \sqrt{\frac{4 + (m + 1/m)^2 \tan^2 \beta v}{(m - 1/m)^2 \tan^2 \beta v}} \tag{17a}$$

$$\Phi_E = \frac{3\pi}{4} + \frac{1}{2} \tan^{-1} \left(\frac{m + 1/m}{2} \tan \beta v \right) \tag{17b}$$

The standing-wave ratio $S = \coth \rho_E$, with ρ_E as in (17a), is shown in Fig. 10.2 as a function of βv, with m as parameter. It is seen that by varying βv the double-slug transformer can introduce a value of S in the matched line ranging from 1 when $\beta v = 0$ and $\rho_E = \infty$ to a maximum $S = m^2$ when $\beta v = \pi/2$ and $\rho_E = \frac{1}{2} \ln [(m^2 + 1)/(m^2 - 1)] = \coth m^2$.

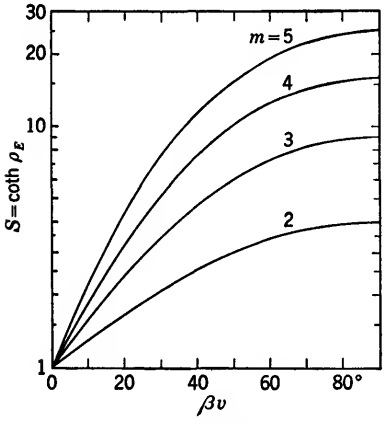


FIG. 10.2. Standing-wave ratio introduced in a matched line by a double-slug transformer when its center is fixed and the electrical distance βv between the slugs is varied.

The double-slug transformer may be adjusted in two ways: (*a*) The point midway between the slugs is fixed, and both slugs are moved simultaneously toward or away from this point, thus varying v. (*b*) Both slugs are moved in tandem with v fixed.

a. Center of Transformer Fixed; Spacing of Slugs Varied. Let the center of the transformer be fixed at a distance u from a convenient reference point between the transformer and the generator. The phase function at the reference point is

$$\Phi_u = \beta(u - d - \tfrac{1}{2}v) + \Phi_E \tag{18}$$

When the slugs are in contact, $v = 0$, and

$$(\Phi_u)_{v=0} = \beta(u - d) + (\Phi_E)_{v=0} \tag{19}$$

The phase difference between (18) and (19) is

$$\Delta\Phi_u = (\Phi_u)_{v=0} - \Phi_u = (\Phi_E)_{v=0} - \Phi_E + \tfrac{1}{2}\beta v \tag{20}$$

The value of $(\Phi_E)_{v=0}$ is obtained from the general formula (15) with (16b,c). It is

$$(\Phi_E)_{v=0} = \tfrac{1}{2} \left(\tan^{-1} \frac{b_A}{1 + g_A} + \tan^{-1} \frac{b_A}{1 - g_A} \right)$$

$$= \tfrac{1}{2} \tan^{-1} \frac{-2b_A}{g_A^2 + b_A^2 - 1} = \Phi_A \tag{21}$$

With (15) and (21) in (20), the phase difference is as follows:

$$\Delta\Phi_u = \Phi_A - \tfrac{1}{2}(\psi_N + \psi_D) + \tfrac{1}{2}\beta v \tag{22}$$

For the matched line $\Phi_A = 3\pi/4$, so that

$$\Delta\Phi_u = \tfrac{1}{2}\left[\beta v - \tan^{-1}\left(\frac{m + 1/m}{2}\tan \beta v\right)\right] \tag{23}$$

This function is represented in Fig. 10.3 as a function of βv, with m as parameter.

The electrical separation βv of the slugs for the maximum value of $\Delta\Phi_u$ for a given m is obtained by equating the derivative of $\Delta\Phi_u$ in (23) with respect to βv to zero. The result is

$$\beta v_{\max} = \tan^{-1}\sqrt{\frac{2}{m + 1/m}} \tag{24}$$

If this value of βv is substituted in (23), the maximum phase shift turns out to be

$$\begin{aligned}(\Delta\Phi_u)_{\max} &= \tfrac{1}{2}\left(\tan^{-1}\sqrt{\frac{2}{m + 1/m}} - \tan^{-1}\sqrt{\frac{m + 1/m}{2}}\right) \\ &= \tan^{-1}\sqrt{\frac{2}{m + 1/m}} - \frac{\pi}{4}\end{aligned} \tag{25}$$

The locus of maximum values of $\Delta\Phi_u$ is indicated in Fig. 10.3.

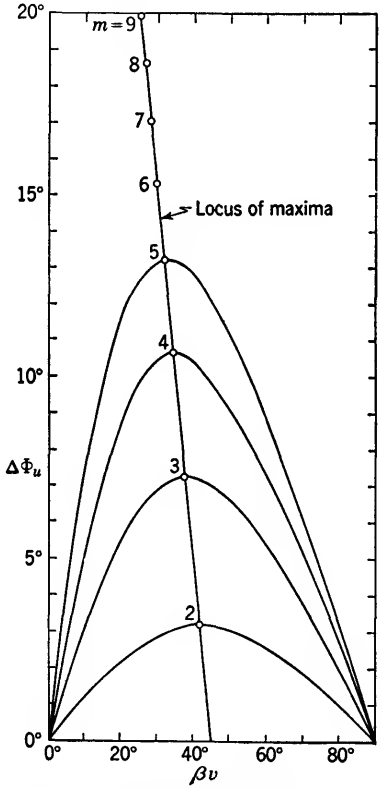


FIG. 10.3. Change in the phase function Φ_u introduced in a matched line by a double-slug transformer when its center is fixed and the electrical distance βv between the slugs is varied.

Note that the change in the phase function produced by the double-slug transformer, when its center is fixed in position in a matched line and the two slugs are moved together, is relatively small in comparison with the rather large change in attenuation function and standing-wave ratio. It is for this reason that the adjustment of the transformer by varying v, with the location of its center fixed, is significant primarily as a means for varying the attenuation function ρ_E rather than Φ_E.

b. Spacing of Slugs Fixed; Entire Transformer Moved. In order to investigate the effect of moving the entire transformer along the line,

consider an arbitrary reference point P_u at a distance u from the left side E (Fig. 10.1) of the transformer. Let the complex terminal function of the line to the right of P_u (Fig. 10.4) be $\theta_u = \rho_u + j\Phi_u$. The length of line from the right side A of the transformer to the load $\boldsymbol{Z}_s$ is w,

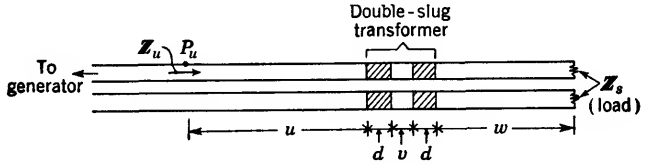


FIG. 10.4. Double-slug transformer with the distance v between slugs fixed and the entire transformer moved between a fixed load $\boldsymbol{Z}_s$ and a fixed reference point P_u.

so that the distance from the reference point P_u to the load is

$$s_t = u + 2d + v + w \tag{26}$$

This distance is kept constant as u and w are varied equally and oppositely. Evidently $u + w$ is also constant for any given value of v.

The phase function Φ_u is given by

$$\Phi_u = \beta u + \Phi_E = \beta u + \tfrac{1}{2}(\psi_N + \psi_E) \tag{27}$$

where Φ_E is given by (15) with (16b,c). In order to examine Φ_u as u and w are varied, it is necessary to express the normalized admittance $\boldsymbol{y}_A = g_A + jb_A$ in terms of the distance w. The appropriate formulas are (13a) and (13b).

Since, when the line is matched ($\boldsymbol{Z}_s = \boldsymbol{Z}_c$, $\rho_s = \infty$), the impedance terminating the transformer is always $\boldsymbol{Z}_c$ for all values of w, it follows that there is no effect whatever on θ_u as the transformer is moved, with v fixed, when the line is matched. When the line is sufficiently mismatched so that ρ_s is quite small, the following condition may be imposed:

$$(\alpha w + \rho_s)^2 \ll 1 \tag{28}$$

so that (13a,b) reduce to the following:

$$g_A \doteq (\alpha w + \rho_s) \csc^2 (\beta w + \Phi_s') = (\alpha w + \rho_s) \sec^2 (\beta w + \Phi_s) \tag{29}$$

$$b_A \doteq -\cot (\beta w + \Phi_s') = \tan (\beta w + \Phi_s) \tag{30}$$

Except over a small range near $\beta w + \Phi_s' = n\pi$, g_A is small and may be entirely neglected in determining the general nature of the variation in Φ_u. If (30) is used in (16b,c) and g_A is set equal to zero, the following expression is obtained for Φ_u, as defined in (27):

$$\Phi_u = \beta u + \tan^{-1} \frac{m \tan \beta v - \cot (\beta w + \Phi_s')}{1 + (1/m) \tan \beta v \cot (\beta w + \Phi_s')} \tag{31}$$

When $\beta v = 0$, $\Phi_u = \beta(u + w) + \Phi_s$, which is constant for all values of u and w which have a constant sum. For all other values of βv, Φ_u varies

significantly with u and w when $u + w =$ constant. For example, when $\beta v = \pi/2$,

$$\Phi_u = \beta u + \tan^{-1} [m^2 \tan (\beta w + \Phi_s')] \tag{32}$$

This formula is studied conveniently if the constant quantity

$$\beta u_0 = \beta(u + w) + \Phi_s'$$

is introduced. Note that, with

$$\beta u_0 = \Phi_u(\beta w + \Phi_s' = 0)$$

the change in phase function may be defined as follows:

$$\begin{aligned}\Delta\Phi &\equiv \Phi_u - \Phi_u(\beta w + \Phi_s' = 0) \\ &= \tan^{-1} [m^2 \tan (\beta w + \Phi_s')] \\ &\qquad - (\beta w + \Phi_s') \end{aligned} \tag{33}$$

This function is plotted in Fig. 10.5 with $\beta w + \Phi_s'$ as the variable and m as parameter. Clearly, if the load is far from matched, the phase function Φ_u may be varied over a wide range by moving a double-slug transformer for which m need not even be great.

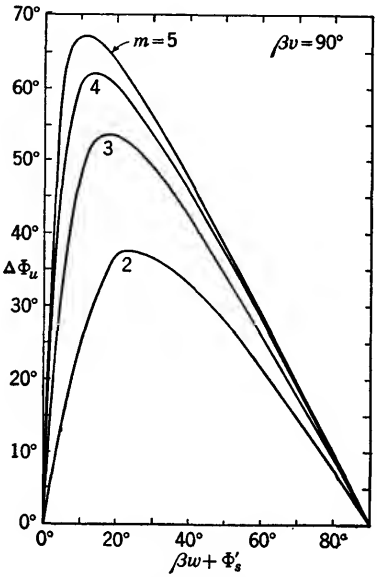


FIG. 10.5. Phase change introduced by moving a double-slug transformer with slugs separated a quarter wavelength between inner edges.

It follows directly from (15) with (16a) that ρ_E is small if g_A is small. This is conveniently shown by expressing (16a) as follows:

$$A = \sqrt{\frac{P + 2g_A}{P - 2g_A}} = \frac{P + 2g_A}{\sqrt{P^2 - 4g_A^2}} \tag{34}$$

where

$$\begin{aligned}P \equiv\ & (1 + g_A^2 + b_A^2) \cos^2 \beta v \\ & + 2b_A \left(m - \frac{1}{m}\right) \sin \beta v \cos \beta v + \left(\frac{b_A^2}{m^2} + \frac{g_A^2}{m^2} + m^2\right) \sin^2 \beta v \end{aligned} \tag{35}$$

When g_A is small, the following inequality is valid:

$$P^2 \gg g_A^2 \tag{36}$$

so that (34) reduces to $A \doteq 1 + 2g_A/P$ and

$$\rho_E = \tfrac{1}{2} \ln \left(1 + \frac{2g_A}{P}\right) \doteq \frac{g_A}{P} \tag{37}$$

It follows that ρ_E is small and that therefore $\rho_u = \alpha u + \rho_E$ also is small, since the attenuation αu of the section of line is assumed to be insignifi-

cant. By inserting (30) in (35) and neglecting g_A^2, it follows with (32) that

$$P \doteq \left(\cos^2 \beta v + \frac{1}{m^2} \sin^2 \beta v\right) \cot^2 (\beta w + \Phi_s') - \left(m - \frac{1}{m}\right) \sin 2\beta v \cot (\beta w + \Phi_s') + \cos^2 \beta v + m^2 \sin^2 \beta v \quad (38)$$

The variation of ρ_E with $\beta w + \Phi_s'$ is conveniently studied with $\beta v = \pi/2$. In this case

$$P = m^2 + \frac{\cot^2 (\beta w + \Phi_s')}{m^2} \quad (39)$$

so that, with (29),

$$\rho_E \doteq \frac{\alpha w + \rho_s}{m^2 \sin^2 (\beta w + \Phi_s') + (1/m^2) \cos^2 (\beta w + \Phi_s')} \quad (40)$$

This formula shows that $\rho_u = \rho_E + \alpha u \doteq \rho_E$ ranges between $m^2(\alpha w + \rho_s)$ and $(\alpha w + \rho_s)/m^2$ as the transformer is moved an electrical distance $\pi/2$. Note that, for moderate values of m, ρ_u is small over the entire range.

11. Lossy Terminations for Nonresonant Shielded Lines. Two types of termination which result in matched lines with standing-wave ratios $S = 1$ are useful. They are a relatively thin disk or slab of material with large leakage conductance placed at a quarter wavelength from a highly conducting piston, and a rather long section of line with a dielectric medium characterized by a moderately small leakage conductance.

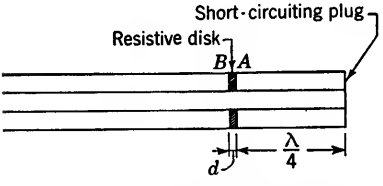


FIG. 11.1. Resistive disk with high-impedance stub terminating a coaxial line.

Resistive Disk. The properties of the resistive-disk termination may be derived directly from Sec. 6, in which the general formulas for a dielectric slab at an arbitrary location along a transmission line are given. The complex terminal function $\theta_B = \rho_B + j\Phi_B'$ of a section of line of length d, propagation constant γ_1, and characteristic impedance Z_{c1} between the planes B and A (Fig. 11.1) along an arbitrarily terminated line is given in Sec. 6, Eq. (18), in the form

$$\theta_B' = \tfrac{1}{2} \ln \frac{\coth \theta_A' + 1 + (r_c^{-1} \coth \theta_A' + r_c) \tanh \gamma_1 d}{\coth \theta_A' - 1 - (r_c^{-1} \coth \theta_A' - r_c) \tanh \gamma_1 d} \quad (1)$$

where, in the general case here considered, $r_c = Z_c/Z_{c1}$ and $\coth \theta_A'$ is the admittance looking toward the load at surface A normalized to the characteristic impedance Z_c of the main line. If the section of line to the right of the disk in Fig. 11.1 is essentially reactive and adjusted for maxi-

mum input impedance, $\theta'_A = \rho_A + j\Phi'_A \doteq j\pi/2$, so that

$$\coth \theta'_A \doteq 0 \tag{2}$$

It follows that

$$\theta'_B = \tfrac{1}{2} \ln \frac{r_c \tanh \gamma_1 d + 1}{r_c \tanh \gamma_1 d - 1} \tag{3}$$

Since the thickness d of the resistive disk may be kept very small, the conditions

$$(\alpha_1 d)^2 \ll 1 \qquad (\beta_1 d)^2 \ll 1 \tag{4}$$

are appropriate. With them the hyperbolic tangent in (3) may be replaced by its argument. Since the leakage conductance of the slab must be quite high, the condition $g^2 \gg \omega^2 c^2$ is appropriate. The parameters for this case are given in Chap. II, Sec. 13, Eqs. (47*b*). They are

$$\alpha_1 = \beta_1 = \sqrt{\frac{\omega l_1 g_1}{2}} \tag{5a}$$

$$R_{c1} = X_{c1} = \sqrt{\frac{\omega l_1}{2g_1}} = \frac{\alpha_1}{g_1} \tag{5b}$$

It follows that

$$\tanh \gamma_1 d \doteq \gamma_1 d = \alpha_1 d(1 + j) \tag{6a}$$

$$r_c = \frac{Z_c}{Z_{c1}} \doteq \frac{R_c}{R_{c1}(1 + j)} = \frac{R_c g_1}{\alpha_1(1 + j)} \tag{6b}$$

With (6*a*) and (6*b*), (3) becomes

$$\theta'_B = \rho_B + j\Phi'_B = \tfrac{1}{2} \ln \frac{R_c g_1 d + 1}{R_c g_1 d - 1} \tag{7}$$

Three cases arise as follows (note that S is the standing-wave ratio):

For $R_c g_1 d > 1$:

$$\Phi'_B = 0 \qquad \rho_B = \tfrac{1}{2} \ln \frac{R_c g_1 d + 1}{R_c g_1 d - 1} = \coth^{-1} R_c g_1 d \qquad S = R_c g_1 d \tag{8a}$$

For $R_c g_1 d < 1$:

$$\Phi'_B = \frac{\pi}{2} \qquad \rho_B = \tfrac{1}{2} \ln \frac{1 + R_c g_1 d}{1 - R_c g_1 d} = \tanh^{-1} R_c g_1 d \qquad S = \frac{1}{R_c g_1 d} \tag{8b}$$

For $R_c g_1 d = 1$:

$$\Phi'_B = \frac{\pi}{4} \qquad \rho_B = \infty \qquad S = 1 \tag{8c}$$

A comparison of these results with those for a predominantly resistive termination in Chap. II shows that the thin disk is equivalent to a lumped resistance

$$R_B = \frac{1}{g_1 d} \tag{9}$$

Lossy Line. If the losses are not primarily confined to a thin disk of relatively high leakage conductance but to a rather long section of line of length d (Fig. 11.2) with an imperfect dielectric, formula (1) is also applicable. Let it be assumed that the lossy section is terminated in a conducting plug, so that $\theta'_A = \rho_A + j\Phi'_A \doteq 0$. In this case $\coth \theta'_A \doteq \infty$, so that (1) reduces to

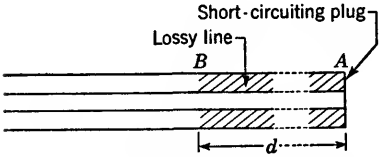


FIG. 11.2. Lossy line terminating a coaxial line.

$$\theta'_B = \tfrac{1}{2} \ln \frac{1 + r_c^{-1} \tanh \gamma_1 d}{1 - r_c^{-1} \tanh \gamma_1 d} \tag{10}$$

Since the lossy section is to be quite long, it is possible to have the attenuation per unit length moderately low, so that Chap. II, Sec. 13, formulas (1) to (9), apply. If $r/\omega l$ is negligible compared with $g/\omega c$, Chap. II, Sec. 13, formulas (46*b*), are applicable. In either case Sec. 6, Eqs. (11*c*,*d*), apply in the form

$$r_c = r_c(1 + j\phi_r) \qquad r_c = \frac{R_c}{R_{c1}} \qquad \phi_r = \phi_{c1} - \phi_c \doteq -\frac{1}{2\omega}\left(\frac{g_1}{c_1} - \frac{g}{c}\right) \tag{11}$$

It is assumed that $\phi_r^2 \ll 1$.

In order to separate real and imaginary parts in (10), note that

$$\tanh \gamma_1 d = \frac{1 - e^{-2\alpha_1 d} e^{-j2\beta_1 d}}{1 + e^{-2\alpha_1 d} e^{-j2\beta_1 d}} = \frac{1 - \delta}{1 + \delta} \tag{12}$$

where $\delta = \delta_r + j\delta_i \equiv e^{-2\alpha_1 d} e^{-j2\beta_1 d} = e^{-2\alpha_1 d}(\cos 2\beta_1 d - j \sin 2\beta_1 d)$ (13)

For sufficient attenuation it is necessary that d be long enough so that

$$\delta_r^2 \equiv e^{-4\alpha_1 d} \ll 1 \qquad \alpha_1 d \geqq 0.6 \tag{14}$$

If (11) and (12) are substituted in (10) and only the leading and first-order small terms are retained, the following results are obtained:

$$\rho_B \doteq \tfrac{1}{2} \ln \frac{r_c + 1 + \delta_r(r_c - 1)}{r_c - 1 + \delta_r(r_c + 1)} \tag{15}$$

$$\Phi'_B \doteq \tfrac{1}{2} \tan^{-1} \frac{\delta_i(r_c - 1) + \phi_r}{r_c + 1 + \delta_r(r_c - 1)} - \tfrac{1}{2} \tan^{-1} \frac{\delta_i(r_c + 1) + \phi_r}{r_c - 1 + \delta_r(r_c + 1)} \tag{16}$$

Neglected terms have the coefficients $\delta_r\phi_r$, $\delta_i\phi_r$, ϕ_r^2, and δ_i^2.

In order to have the main line exactly matched to the lossy section at B, it is necessary that ρ_B become infinite. This requires the following condition:

$$\delta_r = e^{-2\alpha_1 d} \cos 2\beta_1 d = \frac{1 - r_c}{1 + r_c} \tag{17}$$

By solving this expression for $e^{2\alpha_1 d}$ and then taking the logarithm of both sides, the following equation is obtained:

$$r_c = \tan^{-1} r_c + \ln \cos 2\beta_1 d \tag{18}$$

Alternatively, from (17),

$$r_c = \frac{R_c}{R_{c1}} = \frac{1 - \delta_r}{1 + \delta_r} = \frac{1 - e^{-2\alpha_1 d} \cos 2\beta_1 d}{1 + e^{-2\alpha_1 d} \cos 2\beta_1 d} \tag{19}$$

Evidently R_{c1} must be somewhat greater than R_c depending on the length d of the short-circuited lossy section of line and its attenuation constant α_1 and phase constant β_1.

Coaxial Resistor. Since the resistive-disk termination must be $\lambda/4$ in length and the lossy line considerably longer, both are physically cumbersome except at very short wavelengths. This is not true of the coaxial

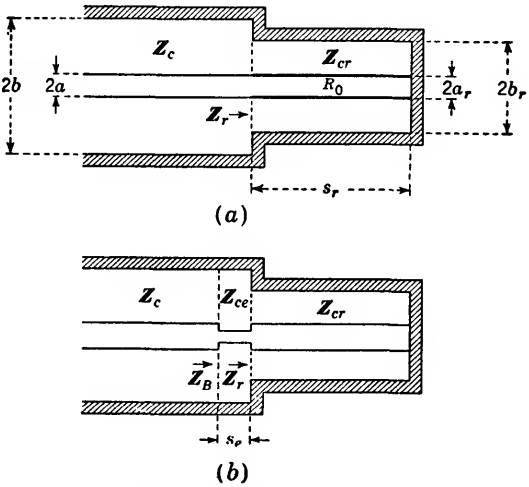


FIG. 11.3. Coaxial resistor terminating a coaxial line.

resistor,[115,128] which may be quite short (less than 0.1λ in length) and yet maintain a standing-wave ratio as low as 1.01 over a wide frequency band.

In its simplest form the coaxial resistor consists of a short section of coaxial transmission line of length s_r terminated in a short circuit, as shown in Fig. 11.3*a*. The inner conductor of this section consists of a cylinder coated with a layer of resistive material. This coating can be made so thin (e.g., of the order of 10^{-5} mm) that skin effect is negligible and its resistance per unit length is virtually independent of frequency up to 10,000 Mc/sec. It follows that the d-c resistance R_0 of this cylinder is also its high-frequency resistance in the sense that the resistance per unit length of the inner conductor is $r_r = R_0/s_r$ independent of the frequency. The outer conductor may be assumed to be lossless, since its contribution to the resistance per unit length is negligible. The characteristic impedance and the propagation constants of the coaxial line form-

ing the resistor (subscript r) and of the main line are

$$\boldsymbol{Z}_{cr} = \sqrt{\frac{l_r}{c_r}}\sqrt{1 - j\frac{r_r}{\omega l_r}} \qquad \boldsymbol{Z}_c = R_c = \sqrt{\frac{l}{c}} \tag{20}$$

$$\gamma_r = \alpha_r + j\beta_r = j\omega\sqrt{l_r c_r}\sqrt{1 - j\frac{r_r}{\omega l_r}} \qquad \gamma = j\beta = j\omega\sqrt{lc} \tag{21}$$

where the line constants are defined in the usual manner. For simplicity the main line is assumed to be lossless. Note that in the absence of magnetic and dielectric materials $lc = l_r c_r = 1/v_0^2$, so that

$$\beta = \omega\sqrt{l_r c_r} = \omega\sqrt{lc}$$

Let it be required that the resistance R_0 of the coaxial cylinder be made equal to the characteristic resistance of the main line. That is,

$$R_0 = R_c \tag{22}$$

For convenience, let the following ratio factor be introduced:

$$r_c = \sqrt{\frac{lc_r}{cl_r}} = \frac{R_c}{R_{cr}}\,(r_r = 0) = \frac{R_0}{R_{cr}}\,(r_r = 0) \tag{23}$$

With (23), (20) and (21) may be expressed as follows:

$$\frac{\boldsymbol{Z}_{cr}}{R_c} = \frac{1}{r_c}\sqrt{1 - j\frac{r_c}{\beta s_r}} = \frac{1}{\sqrt{r_c\beta s_r}}\sqrt{\frac{\beta s_r}{r_c} - j} \tag{24}$$

$$\gamma = \frac{j\sqrt{r_c\beta s_r}}{s_r}\sqrt{\frac{\beta s_r}{r_c} - j} \tag{25}$$

The input impedance of the short-circuited coaxial resistor of length s_r is $\boldsymbol{Z}_r = \boldsymbol{Z}_{cr}\tanh\gamma_r s_r$. The normalized impedance terminating the main line referred to $\boldsymbol{Z}_c$ is

$$z_{1r} = \frac{\boldsymbol{Z}_r}{\boldsymbol{Z}_c} = \frac{\boldsymbol{Z}_{cr}}{\boldsymbol{Z}_c}\tanh\gamma_r s_r = \frac{1}{\sqrt{r_c\beta s_r}}\sqrt{\frac{\beta s_r}{r_c} - j}\tanh\left(j\sqrt{r_c\beta s_r}\sqrt{\frac{\beta s_r}{r_c} - j}\right) \tag{26}$$

Since the coaxial resistor is to be kept short compared with the wavelength ($s_r \leqq 0.1\lambda$), it follows that βs_r is less than 1, so that (26) may be expanded in powers of βs_r. This leads to the formula[115]

$$z_{1r} = 1 + m + jn \tag{27}$$

where

$$m = \beta^2 s_r^2\left(\frac{2}{3} - \frac{2}{15}r_c^2\right) + \beta^4 s_r^4\left(\frac{2}{5} - \frac{68}{315}r_c^2 + \frac{62}{2{,}835}r_c^4\right) + \cdots \tag{28a}$$

$$n = \frac{\beta s_r}{r_c}\left[1 - \frac{1}{3}r_c^2 + \beta^2 s_r^2\left(\frac{1}{3} - \frac{2}{5}r_c^2 + \frac{17}{315}r_c^4\right) + \beta^4 s_r^4\left(\frac{2}{15} - \frac{34}{105}r_c^2 + \frac{62}{567}r_c^4 - \frac{1{,}382}{155{,}992}r_c^6\right) + \cdots\right] \tag{28b}$$

In practice, r_c^2 lies in the range $4 \leqq r_c^2 \leqq 4.8$, in which (27), with (28*a*) and (28*b*), is in error by less than 0.005 if $s_r/\lambda \leqq 0.1$. If m and n are small, the standing-wave ratio on the main line when terminated in z_{1r} is

$$S = \frac{1 + \Gamma}{1 - \Gamma} \doteq 1 + \sqrt{m^2 + n^2} \tag{29}$$

where $\Gamma = |(z_{1r} - 1)/(z_{1r} + 1)|$. If m, n, and S are plotted as functions of βs_r or s_r/λ with r_0^2 as a parameter, it is found that, in the range $0 \leqq s_r \leqq 0.1$, m rises most slowly when $r_c = \sqrt{5}$ and that the initial slope of n can be made to vanish when $r_c = \sqrt{3}$. The lowest standing-wave ratio occurs very nearly when $r_c = \sqrt{3}$, and this, then, is the optimum value for the simple coaxial resistor shown in Fig. 11.3*a*. However, even when $r_c = \sqrt{3}$, the standing-wave ratio increases with s_r/λ from unity at $s_r = 0$ to 1.11 when $s_r/\lambda = 0.1$.

The condition $r_c = \sqrt{3}$ is that for which the reactive part n of the normalized terminal impedance z_{1r} has a zero initial slope. Clearly, if the reactance could be compensated by other means and r_c were adjusted near the value $\sqrt{5}$, for which m in (27) is virtually zero in the range $0 \leqq s_r/\lambda \leqq 0.1$, the condition of match could be improved greatly, and the standing-wave ratio kept much nearer 1 as λ is varied in this range. One method of accomplishing this is to undercut the inner conductor of the main line for a length s_e, as shown in Fig. 11.3*b*. By applying the method outlined in Sec. 6, it can be shown that a normalized impedance $z_{1r} = 1 + m + jn$ terminating the main line on the right of the undercut section (characteristic impedance Z_{ce}) gives a normalized impedance $z_{1B} = Z_B/Z_c$ terminating the main line on the left of the undercut section. This is given by

$$z_{1B} \doteq (1 + m)\left[1 + \frac{2n}{r_e}\tan \beta s_e + \left(1 - \frac{1}{r_e^2}\right)\tan^2 \beta s_e\right] + j\left\{n + \left[r_e - \frac{(1 + m)^2 - n^2}{r_e}\right]\tan \beta s_e\right\} \tag{30}$$

where $r_e \equiv R_{ce}/R_c > 1$. The formula is a good approximation when $r_e > 1.5$, $m < 0.1$, $n < 0.5$, and $\tan \beta s_e < 0.3$.

Although both the resistive and reactive parts of the impedance terminating the main line are altered by the added undercut section, the change in the reactive part is much greater. Thus, by adjusting the undercutting to make the reactance vanish and selecting r_c to make the normalized resistance as near 1 as possible, a very low standing-wave ratio may be achieved. In general, this means a value of r_c slightly greater than $\sqrt{5}$.

The reactance vanishes when

$$\frac{s_e}{\lambda} = \frac{1}{2\pi}\tan^{-1}\frac{-n}{r_e - [(1 + m)^2 - n^2]/r_e} \tag{31}$$

and the normalized impedance of the resistor becomes

$$z_{1B} = r_B = (1 + m)\left\{1 - \frac{n^2}{r_e^2 - (1 + m)^2 + n^2} - 2\left[\frac{n^2}{r_e^2 - (1 + m)^2 + n^2}\right]^2\right\} \quad (32)$$

Although r_e may be chosen freely in theory and should preferably be large, practical limitations usually restrict it to the range $1.5 \leqq r_e \leqq 2$. In this manner a standing-wave ratio of 1.11 for a simple coaxial resistor (Fig. 11.3*a*) may be reduced to 1.01 when $s_r/\lambda = 0.1$.

The analysis of the undercut line which culminates in (32) ignores the junction effects resulting from nonuniformity in the parameters of the line over short distances on each side of the undercut section. It is shown in Sec. 14 that a change in radius of the inner conductor of a coaxial line may be expressed in terms of uniform-line theory on each side of the junction, provided a small lumped capacitance of appropriate magnitude is connected in parallel with the line at each discontinuity. Since these capacitances have been ignored in deriving (32), a further correction is required. This involves small changes in r_c and the definition of modified values of m and n. The design of a coaxial resistor that takes account of these effects is given in the literature,[115] as well as descriptions of other methods than undercutting for compensating the reactance.

12. Closed and Open Ends as Reactive Terminations in Two-wire and Coaxial Lines.[49,104] An ideal closed end for a transmission line has zero impedance, or terminal functions $\rho_s = 0$ and $\Phi_s = \pi/2$. Terminations of this kind are discussed in Chap. II, Sec. 21.

By an analysis of a closed rectangle the apparent (measurable) inductance L_{sa} of a bridge is determined in Chap. II, Sec. 20, as the sum $L_{sa} = L_s + L_T$ of an ideal inductance L_s of the bridge when terminating a fictitious line that is uniform even in the terminal zone and an inductance L_T that corrects for the difference between the actual nonuniform inductance in the terminal zone and the constant value assumed in conventional line theory. The ideal inductance L_s of the bridge is given by Chap. II, Sec. 20, Eq. (9). The lumped corrective inductance L_T of a straight bridge may also be evaluated by the general method described in Chap. II, Sec. 4, where L_T is defined by Chap. II, Sec. 4, Eq. (3), with $a_1(w) = 0$ (since there is no inductive coupling). That is,

$$L_T = \int_0^d [l_0^s(w) - l_0^s]\, dw \quad (1)$$

where

$$l_0^s(w) = \frac{k_0(w)}{2\pi\nu} \quad (2)$$

$$k_0(w) = \sinh^{-1}\frac{w}{a} - \sinh^{-1}\frac{w}{b} + \ln\frac{b}{a} \tag{3}$$

$$l_0^e = l_0^e\,(w \to \infty) = \frac{1}{\pi\nu}\ln\frac{b}{a} \tag{4}$$

The integration of (1) is easily carried out using (2), (3), and (4), with $d^2 \gg b^2$. The result is

$$L_T = -\frac{b-a}{2\pi\nu} \tag{5}$$

in agreement with Chap. II, Sec. 20, Eq. (10). The approximate general method based on Chap. II, Sec. 4, Eq. (3), is thus verified in one special case.

An experimental determination of the apparent terminal inductance $L_{sa} = L_s + L_T$ has been made for three values of the radius a_s of the terminating wire bridge, namely, $a_s = 0.0794$, 0.1588, and 0.2382 cm. The ratio $(L_s + L_T)/l_0^e$ as a function of a_s is given in Fig. 12.1. The experimental data are those of Tomiyasu; the theoretical values have been determined using Chap. II, Sec. 20, Eqs. (9) and (10). The agreement is good for the smaller radii. For the larger radii the assumption of rotational symmetry for each conductor, with the current concentrated along the axis in determining the vector potential, is not a good approximation near the corner. The mean current follows a somewhat shorter path that reduces the effective inductance L_{sa}. It is this decrease, not included in the theoretical curve in Fig. 12.1, which accounts for the smaller measured value of $(L_s + L_T)/l_0^e$.

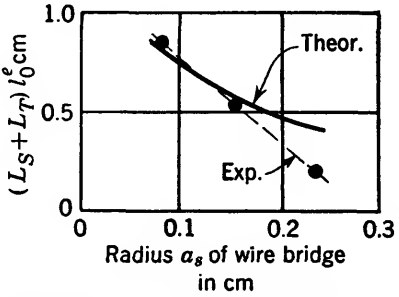


FIG. 12.1. Apparent terminal inductance of a wire bridge (Tomiyasu).

An ideal open end for a transmission line is an infinite impedance, with $\rho_s = 0$ and $\Phi_s = 0$. In practice, an open end is obtained by providing no connections between the conductors. But such an open end is not ideal in the sense that the apparent (measurable) impedance terminating the line does not have $X_{sa} = \infty$ or $\Phi_{sa} = 0$, even though the theoretical reactance of the termination is $X_s = \infty$. Owing to the rise in capacitance per unit length as the open end is approached (Chap. II, Fig. 3.2), the use of conventional transmission-line formulas with $X_s = \infty$ does not lead to the correct apparent impedance. The lumped capacitance C_T required to correct the error introduced by the use of c_0 instead of $c_0(w)$ is given by Chap. II, Sec. 4, Eq. (4) [with $\phi_1(w) = 1$, since there is no

coupling to a load], viz.,

$$C_T = \int_0^d [c_0(w) - c_0]\, dw \tag{6}$$

where, for the two-wire line,

$$c_0(w) = \frac{2\pi\epsilon}{k_0(w)} \qquad c_0 = c_0\,(w = \infty) = \frac{\pi\epsilon}{\ln\,(b/a)} \tag{7}$$

with $k_0(w)$ given by (3).

For the coaxial line

$$c_0(w) = \frac{4\pi\epsilon}{k_0(w)} \qquad c_0 = c_0\,(w = \infty) = \frac{2\pi\epsilon}{\ln\,(a_2/a_1)} \tag{8}$$

As shown in conjunction with Chap. II, Sec. 1, Eq. (32), $k_0(w)$ as given in (3) for the two-wire line is also a good approximation for the coaxial line if b is replaced by a_2, the inner radius of the shield, and a by a_1, the radius of the inner conductor. It follows that $k_0(w)$ in Chap II, Fig. 3.1, may be used for the coaxial line.

C_T in (6) has not been evaluated in closed form, but specific cases may be computed numerically. As an example, consider a two-wire line with $a = 0.1588$ cm and $b = 2$ cm or a coaxial line with $a_1 = 0.1588$ cm and $a_2 = 2$ cm. For the two-wire line $c_0 = 10.96$ $\mu\mu$f/cm, and for the coaxial line $c_0 = 21.92$ $\mu\mu$f/cm. For both lines $C_T = 0.416c_0$. It follows that, insofar as measurements on the line at some distance from the end are concerned, an open end is not equivalent to an infinite reactance but rather to the reactance of a small capacitance C_T.

An approximate simple formula for C_T may be obtained in the form of a series in inverse powers of the quantity $2 \ln (b/a)$ for the two-wire line [or $2 \ln (a_2/a_1)$ for the coaxial line]. The approximate formula is derived using $k_0(w)$, as defined in (3), in the following equivalent form:

$$k_0(w) = (1 - \delta)\left(2 \ln \frac{b}{a}\right) \tag{9}$$

where

$$\delta = \frac{\ln\,(w + \sqrt{w^2 + b^2}) - \ln\,(w + \sqrt{w^2 + a^2})}{2 \ln\,(b/a)} \tag{10}$$

With (7) and (9) it follows that

$$\frac{c_0(w) - c_0}{c_0} = \frac{\delta}{1 - \delta} \doteq \delta + \delta^2 + \cdots \tag{11}$$

Since δ is always less than 1, the denominator in the middle term in (11) may be expanded in series as indicated on the right. If the leading term is retained as a fair approximation if $2 \ln (b/a)$ is sufficiently great, it follows from (6) that

$$C_T \doteq c_0 \int_0^d \delta\, dw \tag{12}$$

With $d = 10b$ (so that b^2 and λ^2 may be neglected compared with d^2)

the integration of (12) with (10) leads to the following simple formula for the two-wire line:

$$C_T \doteq \frac{c_0(b-a)}{2\ln(b/a)} = \frac{\pi\epsilon(b-a)}{2[\ln(b/a)]^2} \tag{13}$$

(The same formula applies to the coaxial line if a_2 is substituted for b and a_1 for a.) For $a = 0.1588$ cm and $b = 2$ cm, the approximate formula (13) gives $C_T = 0.365c_0$, whereas the more accurate value obtained by numerical integration is $C_T = 0.416c_0$. In this case $b/a = 12.6$. The accuracy of (13) is improved as b/a is increased.

C_T was measured on a two-wire line ($a = 0.1588$ cm, $b = 2$ cm) with open end and by Tomiyasu using three types of ends: (1) flat closed ends, (2) hemispherical ends, and (3) open tubing. The measured capacitances in the form C_T/c_0 are listed in Table 12.1; the smallest value is for hemispherical ends. This is to be expected since both the flat end surface and the interior of the tubing are charged near the ends. The theoretical value is $C_T/c_0 = 0.42$ cm. If the length of line is measured along the surface instead of along the axis, $C_T/c_0 = 0.58$ cm, and this corrected value is in very good agreement with experiment, as shown in Table 12.1. In any event, small errors of the order of magnitude of the radius a of the conductors are to be expected in the quasi-one-dimensional analysis underlying these results.

TABLE 12.1. C_T FOR TWO-WIRE LINE

Type of end	C_T/c_0, *cm*
Flat closed	0.60
Hemispherical	0.58
Open tubing	0.65
Theoretical	0.42
Theoretical (corrected)	0.58

It is interesting to examine the distributions of scalar and vector potential difference, charge per unit length, and current near an open end. A qualitative picture is readily obtained if the conductors are assumed to be perfect. It follows from Chap. I, Sec. 4, Eqs. (9*a*,*b*), that both $V(w)$ and $W_z(w)$ satisfy the one-dimensional wave equation, so that both these functions are sinusoidally distributed *even in the terminal zone.* It follows that the known distribution of $V(w)$ outside the terminal zone, as obtained with a termination C_T, may be extended into the terminal zone. Thus in Fig. 12.2*b* the function $V(w)$ is shown as a cosine curve with its maximum at a distance C_T/c_0 beyond the actual end of the line. For a dissipationless line it follows from Chap. I, Sec. 4, Eqs. (6*a*), (7), and (8), that

$$W_z(w) = \frac{1}{j\omega}\frac{\partial V(w)}{\partial w} \tag{14}$$

so that the curve for $W_z(w)$ is a cosine curve like that for $V(w)$, but

shifted a quarter wavelength along the line (and a quarter period in time). Such a curve with an arbitrary amplitude is given in Fig. 12.2*b*.

The leading term in the distribution of charge per unit length is obtained from the relation $q(w) \doteq V(w)c_0(w)$, where $c_0(w)$ rises rapidly for the terminal zone from a constant c_0 to $2c_0$ at $w = 0$, as shown in Chap. II, Fig. 3.2. An estimated curve for $q(w)$ is sketched in Fig. 12.2, with amplitude scaled to equal that of $V(w)$ for convenient comparison.

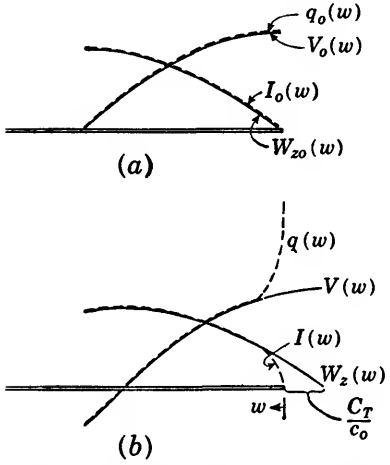


FIG. 12.2. Distributions of scalar and vector potentials, charge per unit length, and current near the end of a two-wire line. (*a*) Ideal distributions derived from uniform-line theory. (*b*) Actual distributions that take account of end effect.

The distribution of current may be derived from Chap. II, Sec. 3, Eq. (14), which, with (14), may be expressed as follows:

$$I_z(w) \doteq \frac{W_z(w)}{l_0^e(w)} + \frac{\beta_0 p_0(w)}{j\omega l_0^e(w)} V(w) \qquad (15)$$

Alternatively it is given by the equation of continuity:

$$\frac{dI_z(w)}{dw} = j\omega q(w) \qquad (16)$$

Actually it is readily sketched simply by noting that outside the terminal zone $I_z(w) = W_z(w)/l^e$ and that at $w = 0$ it must vanish. An estimated curve of $I(w)$ is shown in Fig. 12.2, with amplitude arbitrarily set equal to that of $W(w)$.

It is to be noted that the behavior of the potentials, current, and charge per unit length in Fig. 12.2*b* differs greatly from that at an *ideal* open end, as shown in Fig. 12.2*a*.

13. Junction of Two Open-wire Lines with Conductors of Different Radii. An open two-wire transmission line consists of a left-hand part extending from the generator at $z = 0$ to $z = s_l$ and a right-hand part extending from $z = s_l$ to a load at $z = s_l + s_r = s$. The distance between the centers of the wires in both parts is b; the radius of the conductors in the left-hand part is a_l, and that in the right-hand part is a_r. Without restricting the generality, let $a_l \geqq a_r$. The line is shown in Figs. 13.1 and 13.2.

Consistent with the conditions imposed on the uniform two-wire line in Chap. I, Sec. 4, let the following inequalities be assumed satisfied:

$$|\beta b|^2 \ll 1 \qquad (1)$$

$$b^2 \ll s_l^2 \qquad b^2 \ll s_r^2 \qquad (2)$$

For the present, let the restriction

$$a_r^2 \leqq a_l^2 \ll b^2 \tag{3}$$

be imposed. The more general case in which b is not so restricted is introduced later in this section.

At distances to the left and right of the junction JJ each part of the transmission line is uniform, with propagation constants γ_l and γ_r and

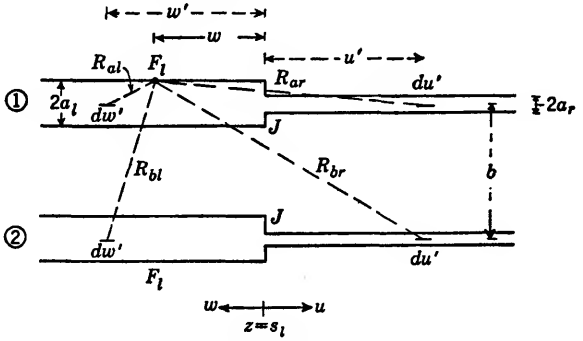


FIG. 13.1. Junction of two two-wire lines with conductors of different radii.

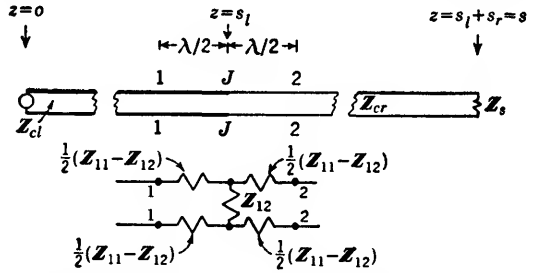


FIG. 13.2. Junction of two two-wire lines and equivalent T network of the junction.

characteristic impedances Z_{cl} and Z_{cr}. As the junction is approached. from each side, the inductance and capacitance per unit length become functions of the distances w and u from the junction owing to changes in cross-sectional dimensions and the existence of the new chargeable and current-carrying annular surfaces. In a region extending a distance $d \sim 10b$ on each side of the junction, variable parameters $\gamma(w)$ and $Z_c(w)$ must be substituted for the constant parameters γ and Z_c.

The purpose of the analysis is to replace the actual circuit, involving regions in which uniform-line theory is not applicable, with an idealized circuit that is electrically equivalent insofar as measurements on the lines *outside* a junction zone of length $2d$ are concerned. This is equivalent to replacing the section of line of length λ extending from 11 to 22 in Fig. 13.2 by an equivalent T network, as shown. If the line were uniform

between 11 and 22, the series and shunt elements would be given by Chap. III, Sec. 12, Eqs. (7*c*,*d*). Neglecting losses in this length, the elements are $\frac{1}{2}(\boldsymbol{Z}_{11} - \boldsymbol{Z}_{12}) = 0$ and $\boldsymbol{Z}_{12} = \infty$. That is, the section of lossless uniform line of length λ has no effect; it may be included or omitted as desired. Evidently, by determining the inductance and capacitance per unit length for the line sections between 11 and 22, subtracting from these the respective constant values for the uniform lines, and integrating the differences over the junction region, the series and shunt elements of the equivalent T section may be obtained in the form $\boldsymbol{Z}_{11} - \boldsymbol{Z}_{12} = j\omega L_T$ and $\boldsymbol{Z}_{12} = -j/\omega C_T$, where L_T and C_T are evaluated using the scalar and vector potential differences.

Following the general method of Chap. I, Sec. 4, and Chap. II, Sec. 1, the scalar potential difference between points F_l on the two conductors (Fig. 13.1) at a distance w to the left of the junction may be evaluated as the sum of the following three parts:

$$\boldsymbol{V}_l(w) = \boldsymbol{V}_{ll}(w) + \boldsymbol{V}_{lr}(w) + \boldsymbol{V}_{lj}(w) \tag{4}$$

where $\boldsymbol{V}_{ll}(w)$ is the contribution from the charges in the left-hand section with a charge per unit length $\boldsymbol{q}_l(w')$, $\boldsymbol{V}_{lr}(w)$ is the contribution from the charges in the right-hand section with a charge per unit length $\boldsymbol{q}_r(u')$, and $\boldsymbol{V}_{lj}(w)$ is the contribution from the charges on the two annular surfaces at the junction on which the charge density is $\mathbf{n}_j\,(r',\theta')$.

The axial component of the vector potential difference is made up of only two parts, as follows:

$$\boldsymbol{W}_{zl}\,(w) = \boldsymbol{W}_{zll}(w) + \boldsymbol{W}_{zlr}(w) \tag{5}$$

where the first term on the right is due to the current $\boldsymbol{I}_{zl}(w')$ to the left of the junction and the second term is due to $\boldsymbol{I}_{zr}(u')$ to the right of the junction. The primarily radial currents $\boldsymbol{I}_{rj}(r',\theta')$ on the annular surfaces contribute nothing to the axial component of the vector potential difference, since they are perpendicular to it.

The several components are

$$\boldsymbol{V}_{ll}(w) = \frac{1}{2\pi\xi}\int_0^{s_l} \boldsymbol{q}_l(w')\boldsymbol{P}_{ll}(w,w')\,dw' \tag{6a}$$

$$\boldsymbol{V}_{lr}(w) = \frac{1}{2\pi\xi}\int_0^{s_r} \boldsymbol{q}_r(u')\boldsymbol{P}_{lr}(w,u')\,du' \tag{6b}$$

$$\boldsymbol{W}_{zll}(w) = \frac{1}{2\pi\nu}\int_0^{s_l} \boldsymbol{I}_{zl}(w')\boldsymbol{P}_{ll}(w,w')\,dw' \tag{7a}$$

$$\boldsymbol{W}_{zlr}(w) = \frac{1}{2\pi\nu}\int_0^{s_r} \boldsymbol{I}_{zr}(u')\boldsymbol{P}_{lr}(w,u')\,du' \tag{7b}$$

where

$$\boldsymbol{P}_{ll}(w,w') = \frac{e^{-j\beta R_{al}}}{R_{al}} - \frac{e^{-j\beta R_{bl}}}{R_{bl}} \doteq \frac{1}{R_{al}} - \frac{1}{R_{bl}} \tag{8a}$$

$$\boldsymbol{P}_{lr}(w,u') = \frac{e^{-j\beta R_{ar}}}{R_{ar}} - \frac{e^{-j\beta R_{br}}}{R_{br}} \doteq \frac{1}{R_{ar}} - \frac{1}{R_{br}} \tag{8b}$$

As shown in Chap. II, Sec. 1, the approximations on the right in (8*a*,*b*) are justified if (1) is satisfied. The distances are

$$R_{al} = \sqrt{(w - w')^2 + a_l^2} \qquad R_{bl} = \sqrt{(w - w')^2 + b^2} \tag{9a}$$

$$R_{ar} = \sqrt{(w + u')^2 + a_l^2} \qquad R_{br} = \sqrt{(w + u')^2 + b^2} \tag{9b}$$

The contribution to $V_l(w)$ by the charges on the annular surfaces is

$$V_{lj}(w) = \frac{1}{2\pi\xi} \int_0^{2\pi} \int_{a_r}^{a_l} \mathfrak{n}_j'(r',\theta') P_{lj}(w,r',\theta') r'\, dr'\, d\theta' \tag{10}$$

where

$$P_{lj}(w,w') = \frac{1}{R_{alj}} - \frac{1}{R_{blj}} \tag{11}$$

R_{alj} is the distance from the point F_l to an element of charge $\mathfrak{n}_j'(r',\theta')r'\,dr'\,d\theta'$ on the annular surface belonging to the same conductor as the point F_l; R_{blj} is the distance from F_l to the corresponding element of charge $-\mathfrak{n}_j'(r',\theta')r'\,dr'\,d\theta'$ on the other annular surface.

In order to evaluate the potential differences, it is necessary to know the currents and charges on both sections of transmission line and on the annular surfaces at the junction. Since the lines are assumed to have low losses, the region near the junction may be treated as if lossless in determining L_T and C_T, so that currents as well as charges are confined to surface layers. A convenient procedure for evaluating the external inductance $l^e(w)$ and capacitance $c(w)$ per unit length is to resolve the problem into symmetrical (even currents and vector potentials, odd charges and scalar potentials) and antisymmetrical (odd currents and vector potentials, even charges and scalar potentials) parts, as in Chap. III, Sec. 12. The even and odd property is with respect to the plane through the junction perpendicular to the line. The symmetrical problem is equivalent to providing a short circuit at 22. The antisymmetrical problem is equivalent to having an ideal open circuit at 22.

Consider first the even currents and odd charges with the ideal short circuit as termination. In this case the currents must be continuous along the conductors at the junction, so that

$$I_{zl}\ (w' \to 0) = -I_{rj}\ (r' \to a_l) \tag{12a}$$

$$I_{zr}\ (u' \to 0) = -I_{rj}\ (r' \to a_r) \tag{12b}$$

where $I_{rj}(r')$ is the outward radial current on the annular surface. By integrating the θ component of the magnetic field around one of the conductors at the junction, it is readily shown by successive application of the Maxwell-Ampère theorem[9] that the total axial current entering the junction from the left must equal the current leaving on the right. It follows that (12*a*) and (12*b*) become

$$I_{zl}\ (w' \to 0) = -I_{rj}(r') = I_{zr}\ (u' \to 0) \tag{13}$$

Important conclusions follow directly from (7*b*) with (13). Since $P_{lr}(w,u')$ is the same as it would be with $a_r = a_l$, it follows that, with (13), (7*b*) is exactly what it would be if there were no change in the radius of the conductors and no annular surfaces. Therefore, insofar as the inductance per unit length is concerned, it has the constant value l_l^e from $z = 0$ to $z = s_l$ and the likewise constant value l_r^e from $z = s_l$ to $z = s_l + s_r = s$. Note that

$$l_l^e = \frac{1}{\pi\nu} \ln \frac{b}{a_l} \qquad l_r^e = \frac{1}{\pi\nu} \ln \frac{b}{a_r} \tag{14}$$

Thus there is no inductive junction effect, and no lumped inductance L_T is required on either side of the junction; $Z_{11} - Z_{12} = j\omega L_T = 0$. This means that the required lumped network can consist only of a shunt element.

The problem of odd currents and even charges when the load side of the junction is terminated in an open circuit involves continuity of charge in the form

$$q_l\ (w' \to 0) = [2\pi r' \mathfrak{n}(r',\theta')]_{r' \to a_l} \tag{15a}$$

$$q_r\ (u' \to 0) = [2\pi r' \mathfrak{n}(r',\theta')]_{r' \to a_r} \tag{15b}$$

However, since the radial components of the electric field near the junction depend on the charges on the annular surfaces as well as on the cylindrical conductors, the application of Gauss's theorem does not lead to the conclusion that $q_l\ (w' \to 0)$ is equal to $q_r\ (u' \to 0)$. On the other hand, since the transverse dimensions of the conductors on both sides of the junction are small, as required by (2) and (4), the scalar potential difference between the two conductors of the two-wire line must be the same on both sides of the junction. Therefore

$$V_l\ (w \to 0) = V_r\ (u \to 0) \tag{16}$$

where $V_l(w)$ is given by (4), with (6*a*), (6*b*), and (10), and $V_r(u)$ is given by corresponding expressions, with u and w and subscripts r and l interchanged. (Note that in the vicinity of the junction the amplitude of the periodically varying electric field is distributed essentially as if the two conductors were maintained at a constant, i.e., electrostatic, potential difference.)

Outside the junction zone where uniform-line theory is valid, the ratio of charge to voltage on each line is

$$\frac{q_l(w)}{V_l(w)} = c_{0l} = \frac{\pi\epsilon}{\ln\,(b/a_l)} \tag{17a}$$

$$\frac{q_r(w)}{V_r(u)} = c_{0r} = \frac{\pi\epsilon}{\ln\,(b/a_r)} \tag{17b}$$

Note that, with $a_l > a_r$, it follows that $c_{0l} > c_{0r}$. It is satisfactory to use these values as approximations in the junction region in order to

determine C_T as a correction for conventional line theory. In other words, the uncorrected approximate distribution of charge is used in order to determine the correction. This means that, in evaluating C_T from $V_l(w)$, (16) is applied in (17a,b) in order to determine $q_r(u')$ for use in (6b). The value is

$$q_r(u') \doteq q_l(w') \frac{c_{0r}}{c_0} = q_l(w') \frac{\ln (b/a_l)}{\ln (b/a_r)} \tag{18}$$

Also let it be assumed that the charge density on the annular surfaces is approximately rotationally symmetrical for each conductor, so that $\mathfrak{n}(r',\theta') \doteq \mathfrak{n}(r')$. This function satisfies the conditions of continuity of charge (15a,b) if it is approximated as follows:

$$\mathfrak{n}_j(r',\theta') \doteq \mathfrak{n}_j(r') \doteq \frac{q_l\ (w' = 0)}{2\pi r'} \frac{\ln (b/a_l)}{\ln (b/r')} \tag{19}$$

In calculating the potential at any point F_l (Fig. 13.1) just outside the surface of the cylindrical conductor due to the charges all along the conductor, the formulas (6a,b) based on the fundamental integral [Chap. I, Sec. 3, Eq. (30a)] are used. As indicated in the footnote discussing Chap. I, Sec. 3, Eq. (30a), this fundamental integral for the potential at the surface of a cylindrical conductor actually implies that the entire charge is concentrated in a thin line along the axis of each conductor rather than on the surface. It is a good approximation of the actual distribution along the surface if possible errors in the length of the transmission line of the order of magnitude $\pm a$ are acceptable. A similar approximation involving errors in length of the same order of magnitude may be made in evaluating the potential due to the charges on the annular surfaces. That is, the total charge on each annular surface may be treated as if concentrated at the center in determining the potential at F_l. This total charge is obtained by integrating (19) over the annulus:

$$Q_j = \int_{a_r}^{a_l} 2\pi r' \mathfrak{n}_j(r')\, dr' = q_l\ (w = 0)\ b \ln \frac{b}{a_l} \int_{a_r}^{a_l} \frac{dr'/b}{-\ln (r'/b)} \tag{20}$$

By a change of variable to $y = -\ln (r'/b)$, the integral in (20) becomes a tabulated exponential integral.† The result may be expressed as follows:

$$Q_j = \frac{\pi \epsilon K b}{c_{0l}} q_l\ (w = 0) \tag{21}$$

where c_{0l} is as defined in (17a) and where

$$K = Ei\left(\ln \frac{a_r}{b}\right) - Ei\left(\ln \frac{a_l}{b}\right) \tag{22}$$

† "Tables of Sine, Cosine, and Exponential Integrals," vol. I, W.P.A., National Bureau of Standards, 1940.

The exponential integral is

$$Ei(x) = \int_{\infty}^{-x} \frac{e^{-u}}{u}\, du \tag{23}$$

Since, in calculating $V_{ij}(w)$ from (10), the entire charge is to be treated as if concentrated on the axis at $w = u = 0$, (10) reduces to the following simple integrated form, which is a good approximation except when w is as small as a_l:

$$V_{lj}(w) = \frac{Q_j}{2\pi\epsilon}\left(\frac{1}{\sqrt{w^2 + a_l^2}} - \frac{1}{\sqrt{w^2 + b_b^2}}\right) \tag{24}$$

The potential difference between points F_l (Fig. 13.1) is given by (4) in terms of (6*a*), (6*b*) with (18), and (24). As shown in Chap. I, it is a good approximation to set $q(w) \doteq q(w')$ in the junction zone. By the same token and in the same range, q_l $(w = 0) \doteq q_l(w)$. The results are

$$V_{ll}(w) \doteq \frac{q_l(w)}{2\pi\epsilon}\int_0^{s_l} P_{ll}(w,w')\, dw' \doteq q_l(w)\left[\frac{1}{c_{0l}} - \frac{1}{c_{1l}(w)}\right] \tag{25a}$$

$$V_{lr}(w) \doteq \frac{q_l(w)}{2\pi\epsilon}\int_0^{s_r} P_{lr}(w,u')\, du' \doteq q_l(w)\left[\frac{c_{0r}}{c_{0l}c_{1l}(w)}\right] \tag{25b}$$

$$V_{lj}(w) \doteq q_l(w)\frac{Kp_l(w)}{c_{0l}} \tag{25c}$$

where the variable capacitance per unit length $c_{1l}(w)$ is defined by

$$c_{1l}(w) \equiv \frac{2\pi\epsilon}{\ln\left[(w + \sqrt{w^2 + b^2})/(w + \sqrt{w^2 + a_l^2})\right]} \tag{26a}$$

and where the dimensionless function $p_l(w)$ is

$$p_l(w) \equiv \frac{b}{2}\left(\frac{1}{\sqrt{w^2 + a_l^2}} - \frac{1}{\sqrt{w^2 + b^2}}\right) \tag{26b}$$

The addition of (25*a*), (25*b*), and (25*c*) to obtain $V_l(w)$ and the definition of $c_l(w)$ as the ratio of charge per unit length to voltage give

$$\frac{1}{c_l(w)} \equiv \frac{V_l(w)}{q_l(w)} = \frac{1}{c_{0l}}\left[1 - \frac{c_{0l} - c_{0r}}{c_{1l}(w)} + Kp_l(w)\right] \tag{27}$$

Clearly, when either of the conditions $w^2 \gg b^2$ or $a_r = a_l$ is satisfied, $c_l(w) \doteq c_{0l}$.

The corresponding expression for $c_r(u)$ on the right of the junction is obtained by interchanging subscripts l and r where they occur explicitly in (27) and substituting u for w. [Note that the subscripts occurring in K as defined in (22) should not be interchanged.] The desired formula is

$$\frac{1}{c_r(u)} \equiv \frac{V_r(u)}{q_r(u)} \equiv \frac{1}{c_{0r}}\left[1 + \frac{c_{0l} - c_{0r}}{c_{1r}(u)} + Kp_r(u)\right] \tag{28}$$

where $c_{1r}(u)$ and $p_r(u)$ are given by (26*a*) and (26*b*), with the indicated changes and substitutions. Note that $c_{1r}(u)$ and $p_r(u)$ differ very little from $c_{1l}(w)$ and $p_l(w)$ except when b is as small as a_l.

The total error in capacitance made along the left-hand section of line if c_{0l} is used in place of the true value $c_l(w)$ is given by

$$C_{Tl} = \int_0^d [c_l(w) - c_{0l}]\, dw \tag{29a}$$

The corresponding error on the right-hand section of line is

$$C_{Tr} = \int_0^d [c_r(u) - c_{0r}]\, du \tag{29b}$$

In (29*a*,*b*) d has the order of magnitude $10b$. The total shunt capacitance required to compensate for the use of uniform-line theory is the sum $C_{Tl} + C_{Tr}$. To this must be added the capacitance between the two annular rings C_{Tj}. This may be obtained approximately as follows:

By definition, $$C_{Tj} = \frac{Q_j}{V_l\,(w = 0)} \doteq \frac{\pi\epsilon K b}{c_{0l}} \frac{q_l\,(w = 0)}{V_l\,(w = 0)} \tag{30a}$$

In the evaluation of the small capacitance C_{Tj} it is adequate to assume that $q_l(w)$ and $V_l(w)$ are related according to uniform-line theory, namely, $q_l(w)/V_l(w) = c_0$, so that

$$C_{Tj} \doteq \pi\epsilon K b \tag{30b}$$

where K is as in (22).

The total lumped capacitance required in the equivalent network in Fig. 13.3 is

$$C_T = C_{Tl} + C_{Tr} + C_{Tj} \tag{31}$$

where the three terms on the right are as defined in (29*a*), (29*b*), and (30*b*). Note that, when a_l is greater than a_r, C_{Tl} and C_{Tj} are positive, whereas C_{Tr} is negative. The equivalent circuit shown in Fig. 13.3 involves only uniform sections of line and a lumped capacitance to correct for the over-all error made in assuming constant capacitances per unit length at *all* points in both lines, including the region near the junction where actually they are variable.

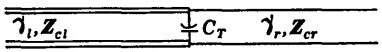


FIG. 13.3. Uniform lines with C_T to correct for the junction-zone nonuniformities.

Since a_r is less than a_l, the line to the left of the junction must behave in a manner intermediate between its behavior for $a_r = 0$ and that for $a_r = a_l$. It has been shown in Sec. 12 that near an open end, which is equivalent to $a_r = 0$, the capacitance per unit length and with it the charge per unit length increase sharply. Therefore it is to be expected that a similar but smaller increase must occur as the junction with a line

of smaller size is approached. Account of this increase in charge may be taken by including a lumped *positive* capacitance C_{Tl} at the end of a uniform section with uniform capacitance per unit length c_{0l}.

Since the uniform charge per unit length on the left-hand section of larger diameter is greater than on the right-hand section of smaller diameter, and since it is further increased near the junction, as just explained, it is evident that the contribution to the potential difference on the right by the charges on the left of the junction is relatively greater than when $a_r = a_l$. Accordingly a smaller charge per unit length is required on the right. This decrease in charge corresponds to a decrease in capacitance per unit length below the uniform value c_{0r}. If the uniform value is to be used, a correction in the form of a *negative* lumped capacitance C_{Tr} is required.

The actual evaluation of C_{Tl} and C_{Tr} has not been achieved but is unnecessary, since it is shown in Sec. 14 that C_T for the two-wire line may be determined from C_T for the coaxial line, for which graphs and tables are available.

A better approximation of the ratio of charge per unit length on the two lines near the junction is obtained by equating V_l $(w \doteq 0)$ in (27) to V_r $(u \doteq 0)$ in (28). The result is

$$\frac{q_r\,(u \doteq 0)}{q_l\,(w \doteq 0)} = \frac{c_{0r}}{c_0}\,\frac{\dfrac{c_{0r}}{c_{0l}} + \dfrac{Kb}{2}\left(\dfrac{1}{a_l} - \dfrac{1}{b}\right)}{\dfrac{c_{0l}}{c_{0r}} + \dfrac{Kb}{2}\left(\dfrac{1}{a_r} - \dfrac{1}{b}\right)} \tag{32}$$

Since $c_{0l} > c_{0r}$ and $a_l > a_r$, it is clear that the correction factor [the final factor in (32)] is less than 1. Since q_r $(u \doteq 0)$ is less than the value for a uniform line and q_l $(w \doteq 0)$ is greater than the value for a uniform line, this is as it should be.

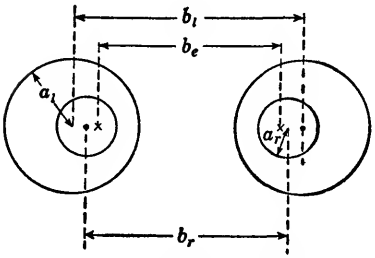


FIG. 13.4. Cross section of two two-wire lines at junction plane.

If the right-hand part of the conditions (3) is not satisfied in the sense that a_l is not necessarily very small compared with b, the results obtained above may be modified by making use of the effective radius b_e, defined in Chap. I, Sec. 7, Eq. (40*a*). Since the surfaces of all conductors must be equipotentials, their effective separation b_e in Fig. 13.4 rather than the distances between centers must be the same. That is,

$$\frac{b_l}{2} + \sqrt{\left(\frac{b_l}{2}\right)^2 - a_l^2} = \frac{b_r}{2} + \sqrt{\left(\frac{b_r}{2}\right)^2 - a_r^2} \tag{33}$$

where b_l and b_r are as shown in Fig. 13.4. If the two radii and b_l are known, b_r may be determined by solving (33) to give

$$b_r = \frac{b_l}{2} + \sqrt{\left(\frac{b_l}{2}\right)^2 - a_l^2} + a_r^2 \left[\frac{b_l}{2} + \sqrt{\left(\frac{b_l}{2}\right)^2 - a_l^2}\right]^{-1} \tag{34}$$

If b_l/a_l is substituted for b/a_l, and b_r/a_r for b/a_r in the formulas derived subject to (3), they become approximations for use when b is not sufficiently great to satisfy (3), provided (33) is satisfied.

14. Change of Radius in a Coaxial Line. If the radius of the inner conductor of a coaxial line changes from a_l to a_r at $z = s_l$, whereas the outer conductor has the uniform inner radius b, as shown in Fig. 14.1,

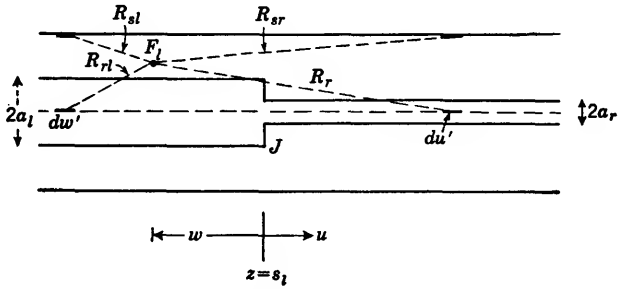


FIG. 14.1. Junction of two coaxial lines with inner conductors of different radii.

a problem arises resembling that in the preceding section. By considering the general case in its separate symmetrical and antisymmetrical parts, as in Sec. 13, it follows that there is no inductive correction near the junction and that the values of the external inductance per unit length:

$$l_l^e = \frac{1}{2\pi\nu} \ln \frac{b}{a_l} \qquad l_r^e = \frac{1}{2\pi\nu} \ln \frac{b}{a_r} \tag{1}$$

characteristic of uniform lines are valid to the left and right, respectively, of the junction. It may be concluded, as in Sec. 13, that the entire corrective network at the junction consists of a shunt capacitance C_T.

In order to determine C_T it is necessary to evaluate the potential difference $V_l(w)$ at an arbitrary distance w to the left of the junction of the two lines at $z = s_l$. This is accomplished as follows:

The potential ϕ_l at a point F_l between the inner and outer conductors (Fig. 14.1) at a radius r and at a distance w from the junction may be evaluated in three parts, viz., the potential ϕ_{ll} due to charges on the left-hand section of line of radius a_l, the potential ϕ_{lr} due to charges on the right-hand section of radius a_r, and the potential ϕ_{lj} due to charges on the annular ring at the junction. Thus

$$\phi_l(w) = \phi_{ll}(w) + \phi_{lr}(w) + \phi_{lj}(w) \tag{2}$$

The first two components are defined as follows:

$$\phi_{ll}(w) \doteq \frac{q_l(w)}{4\pi\epsilon} \int_0^{2\pi} \int_0^{\infty} P_{ll}(w,w',\theta')\, dw' \frac{d\theta'}{2\pi} \tag{3a}$$

$$\phi_{lr}(w) \doteq \frac{q_r(u)}{4\pi\epsilon} \int_0^{2\pi} \int_0^{\infty} P_{lr}(w,u',\theta')\, du' \frac{d\theta'}{2\pi} \tag{3b}$$

where

$$P_{ll}(w,w',\theta') \doteq \frac{1}{R_{rl}} - \frac{1}{R_{sl}} \tag{4a}$$

$$P_{lr}(w,u',\theta') \doteq \frac{1}{R_{rr}} - \frac{1}{R_{sr}} \tag{4b}$$

where

$$R_{rl} = \sqrt{(w' - w)^2 + r^2} \qquad R_{sl} = \sqrt{(w' - w)^2 + s^2} \tag{5a}$$

$$R_{rr} = \sqrt{(u' + w)^2 + r^2} \qquad R_{sr} = \sqrt{(u' + w)^2 + s^2} \tag{5b}$$

$$s^2 = b^2 + r^2 - 2br \cos\theta' \tag{5c}$$

The integrations with respect to w' and u' in (3a) and (3b) may be carried out as follows:

$$\int_0^{\infty} P_{ll}(w,w',\theta')\, dw' = 2 \ln \frac{s}{r} - \ln \frac{w + \sqrt{w^2 + s^2}}{w + \sqrt{w^2 + r^2}} \tag{6a}$$

$$\int_0^{\infty} P_{lr}(w,u',\theta')\, du' = \ln \frac{w + \sqrt{w^2 + s^2}}{w + \sqrt{w^2 + r^2}} \tag{6b}$$

If these expressions are substituted in (2) using (3a) and (3b), the integration with respect to θ' which involves the term $\ln (s/r)$ may be carried out just as in Chap. I, Sec. 6. The result is

$$\phi_l(w) = \frac{q_l(w)}{4\pi\epsilon} \left[2 \ln \frac{b}{r} - \int_0^{2\pi} \left(1 - \frac{c_{0r}}{c_{0l}}\right) \ln \frac{w + w^2 + s^2}{w + w^2 + r^2} \frac{d\theta'}{2\pi} \right] + \phi_{lj}(w) \tag{7}$$

In formulating (7) it has been assumed that the entire inner conductor near the junction is essentially an equipotential surface, so that

$$\phi_l(w) = \phi_r(u) \tag{8}$$

It is also assumed that the charge per unit length characteristic of the uniform line may be used to determine the corrective capacitance C_r. That is,

$$\frac{q_r(u)}{q_l(w)} \doteq \frac{c_{0r}}{c_{0l}} \tag{9}$$

where

$$c_{0r} = \frac{2\pi\epsilon}{\ln (b/a_r)} \qquad c_{0l} = \frac{2\pi\epsilon}{\ln (b/a_l)} \tag{10}$$

are the capacitances per unit length characteristic of uniform lines with radii a_r and a_l, respectively.

Since θ' occurs only in s^2, the potential difference

$$V_l(w) = [\phi_l(w)]_{r=a_l} - [\phi_l(w)]_{r=b}$$

is

$$V_l(w) \doteq \frac{q_l(w)}{4\pi\epsilon}\left[2\ln\frac{b}{a_l} - \left(1 - \frac{c_{0r}}{c_{0l}}\right)\ln\frac{w + \sqrt{w^2 + b^2}}{w + \sqrt{w^2 + a_l^2}} + \left(1 - \frac{c_{0r}}{c_{0l}}\right)\int_0^{2\pi}\ln\frac{w + \sqrt{w^2 + s_b^2}}{w + \sqrt{w^2 + s_a^2}}\frac{d\theta'}{2\pi}\right] + V_j(w) \quad (11)$$

where

$$s_a^2 = b^2 + a_l^2 - 2a_l b\cos\theta' \quad (12a)$$

$$s_b^2 = 2b^2(1 - \cos\theta') \quad (12b)$$

The logarithm in the integral in (11) has its largest value when $w = 0$ and rapidly approaches unity as w increases. However, when $w = 0$, it is readily verified by direct integration (using Pierce 523) that the integral vanishes. It may be concluded, therefore, that the last term within the brackets in (11) contributes negligibly to $V_l(w)$, so that

$$V_l(w) \doteq \frac{q_l(w)}{4\pi\epsilon}\left[2\ln\frac{b}{a_l} - \left(1 - \frac{c_{0r}}{c_{0l}}\right)\ln\frac{w + \sqrt{w^2 + b^2}}{w + \sqrt{w^2 + a_l^2}}\right] + V_j(w) \quad (13)$$

The potential difference $V_j(w) = [\phi_j(w)]_{r=a_l} - [\phi_j(w)]_{r=b}$ due to the charges on the annular ring in the junction plane may be evaluated as in Sec. 13, where there are two rings instead of one such ring. The result is like Sec. 13, Eq. (24), divided by 2, that is,

$$V_{lj}(w) = \frac{Q_j}{4\pi\epsilon}\left(\frac{1}{\sqrt{w^2 + a^2}} - \frac{1}{\sqrt{w^2 + b^2}}\right) \quad (14)$$

where

$$Q_j = \frac{2\pi\epsilon K b}{c_{0l}}\, q_l\,(w = 0) \quad (15)$$

where c_{0l} is given by (10) and K is as in Sec. 13, Eq. (22). By defining

$$c_{1l}(w) \equiv \frac{4\pi\epsilon}{\ln\left[(w + \sqrt{w^2 + b^2})/(w + \sqrt{w^2 + a_l^2})\right]} \quad (16a)$$

$$p_l(w) \equiv \frac{b}{2}\left(\frac{1}{\sqrt{w^2 + a_l^2}} - \frac{1}{\sqrt{w^2 + b^2}}\right) \quad (16b)$$

the final form of (13) is

$$\frac{V_l(w)}{q_l(w)} \equiv \frac{1}{c_l(w)} = \frac{1}{c_{0l}}\left[1 - \frac{c_{0l} - c_{0r}}{c_{1l}(w)} + Kp_l(w)\right] \quad (17)$$

The corresponding expression for $c_r(u)$ on the right of the junction is

$$\frac{V_r(u)}{q_r(u)} \equiv \frac{1}{c_r(u)} = \frac{1}{c_{0r}}\left[1 + \frac{c_{0l} - c_{0r}}{c_{1r}(u)} + Kp_r(u)\right] \quad (18)$$

where $c_{1r}(u)$ and $p_r(u)$ are as given by (16a) and (16b), with the following substitutions: u for w and subscript r for l.

Formulas (17) and (18) are the same in form as Sec. 13, Eqs. (27) and (28), for the open-wire line. However, all capacitances in (17) and (18) refer to the coaxial line with outer radius b and inner radii a_l to the left and a_r to the right of the junction. Since the formulas for the capacitances of a coaxial line differ from those for the open-wire line only by a factor 2, it follows that $c_l(w)/c_{0l}$ and $c_r(w)/c_{0r}$ are numerically the same for the coaxial and open-wire lines if the ratios b/a_l and b/a_r are the same. Accordingly C_{Tl}/c_{0l} and C_{Tr}/c_{0r}, as defined in Sec. 13, Eqs. (29a) and (29b), are also numerically the same for the coaxial and two-wire lines, with the same ratios of b/a_l and b/a_r. As in Sec. 13, the total lumped shunt capacitance required at the junction to compensate for the use of uniform-line theory on both sides of the junction is $C_{Tl} + C_{Tr}$. To this must be added the capacitance C_{Tj} between the annular ring at the junction and the coaxial shield. This is given approximately by

$$C_{Tj} = \frac{Q_j}{V_l\,(w = 0)} = \frac{2\pi\epsilon K b}{c_{0l}} \frac{q_l\,(w = 0)}{V_l\,(w = 0)} \tag{19}$$

where use has been made of (15). For the evaluation of this small capacitance it is adequate to assume that $V_l\,(w = 0)$ and $q_l\,(w = 0)$ are related, as predicted by uniform-line theory. That is,

$$\frac{q_l\,(w = 0)}{V_l\,(w = 0)} = c_{0l}$$

Accordingly

$$C_{Tj} \doteq 2\pi\epsilon K b \tag{20}$$

where K is as given by Sec. 13, Eq. (22). Note that (20) differs from the corresponding formula [Sec. 13, Eq. (30b)] by a factor 2.

The total lumped capacitance C_T required at the junction if uniform-line theory is used on each side is

$$C_T = C_{Tl} + C_{Tr} + C_{Tj} \tag{21}$$

For the same ratios b/a_l and b/a_r, the value of C_T obtained from (21) for the coaxial line is double the value obtained from Sec. 13, Eq. (31), for the open-wire line. Since the lumped susceptance $B_T = \omega C_T$ for the coaxial line has been determined by a variational analysis beyond the scope of this book, and since tables and graphs[13] of numerical values are available for a range of values of b, a_l, and a_r, the analyses of this and the preceding sections serve to justify the use of these tables and graphs for the numerical evaluation of C_T for the two-wire line.

Incidentally data for determining B_T for a coaxial line with uniform inner conductor and an outer conductor that changes from b_l to b_r at $z = s_l$ are also available (Ref. 13, p. 311).

Bifurcation of Coaxial Line. A bifurcated coaxial line is shown in Fig. 14.2*a*. If junction effects are neglected, coaxial lines 1 and 2 with characteristic impedances $\boldsymbol{Z}_{c1}$ and $\boldsymbol{Z}_{c2}$ are connected in series across coaxial line 0 with characteristic impedance $\boldsymbol{Z}_c$. Neglecting losses, the characteristic impedances are

$$\boldsymbol{Z}_c \doteq R_c = \frac{\zeta}{2\pi} \ln \frac{a_3}{a_1} \qquad \boldsymbol{Z}_{c1} \doteq R_{c1} = \frac{\zeta}{2\pi} \ln \frac{a_3}{a_2} \qquad \boldsymbol{Z}_{c2} \doteq R_{c2} = \frac{\zeta}{2\pi} \ln \frac{a_2}{a_1} \tag{22}$$

where $\zeta \doteq 120\pi$ ohms.

An approximate analysis of the junction effects in the bifurcated line could be carried out with the method used in the first part of this section.

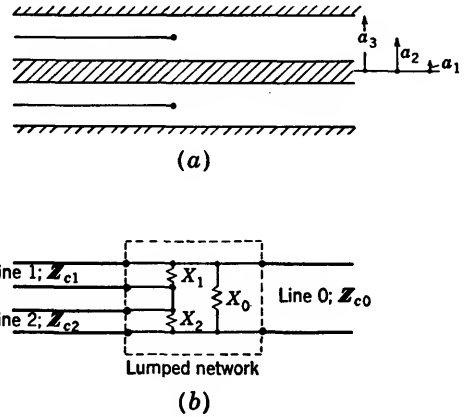


FIG. 14.2. (*a*) Bifurcated coaxial line. (*b*) The same line with an equivalent network to take account of junction effects.

However, since the results of a more rigorous analysis are available (Ref. 13, pp. 369–370), it is sufficient to repeat these. The equivalent lumped network consists of a shunt reactance across each line at the junction plane, as shown in Fig. 14.2*b*. Formulas for the three reactances are

$$X_0 = -R_c \cot \beta d \qquad X_1 = R_c \frac{a_3 - a_2}{a_3 - a_1} \cot \beta d \qquad X_2 = R_c \frac{a_2 - a_1}{a_3 - a_1} \cot \beta d \tag{23}$$

where

$$\frac{\pi d}{a_3 - a_1} = \frac{a_3 - a_2}{a_3 - a_2} \ln \frac{a_3 - a_1}{a_3 - a_2} + \frac{a_2 - a_1}{a_3 - a_1} \ln \frac{a_3 - a_1}{a_2 - a_1} \tag{24}$$

Note that X_0 is negative, also that $X_0 = -(X_1 + X_2)$, so that there is no junction correction looking from line 0 toward lines 1 and 2. Curves of $\pi d/(a_3 - a_1)$ as a function of $(a_3 - a_2)/(a_3 - a_1)$, as well as formulas for higher-order terms for d, are available in the literature. The approximation (24) is in error by less than 2 per cent, provided $2(a_3 - a_1) < 0.3\lambda$.

15. Bend in a Two-wire Line.[104,131] When a two-wire line in the yz plane is bent through an angle θ from this plane, as shown in Fig. 15.1, the two wires remain identical, so that no unbalanced currents are generated. However, the parameters of the line are not constant in the vicinity of the bend. Since resistance and leakage conductance per unit length are small, changes in them may be ignored. But this is not true of the external inductance per unit length and the capacitance per unit length. In order to evaluate these quantities near the bend, let the usual coordinate system be introduced. One part of the line extends from the generator at $z = 0$ to the bend at $z = s_l$; for convenience the variable $w = s_l - z$, measured from the bend toward the generator, is introduced. The second part of the line extends from the bend at $u = 0$ to the load at $u = s_r$ in a direction differing from the original one along the z axis by an arbitrary angle θ. As usual, the radius of the wires is a; their separation between centers is b. It is assumed that the condition $a^2 \ll b^2$ is satisfied.

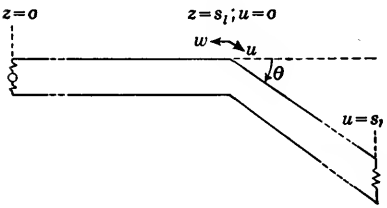


FIG. 15.1. Bend in a two-wire line.

The determination of $l^e(w)$ and $c(w)$ on one side of the junction and the equal quantities $l^e(u)$ and $c(u)$ on the other side parallels the procedure in Chap. II, Sec. 1, where the two wires of the line flared outward. Chapter II, Sec. 1, formulas (22a) and (22b), apply. The pertinent parts are

$$l^e(w) = \frac{k_0(w) + k_{0T}(w)}{2\pi\nu} \tag{1}$$

$$c(w) = \frac{2\pi\epsilon}{k_0(w) + k'_{0T}(w)} \tag{2}$$

where, as in Chap. II, Sec. 1, Eqs. (15b) and (26a),

$$k_0(w) \doteq \int_0^\infty \left(\frac{1}{R_a} - \frac{1}{R_b}\right) dw' \doteq k_0 - F_1(w) \tag{3}$$

$$k_0 = 2 \ln \frac{b}{a} \qquad F_1(w) \equiv \ln \frac{w + \sqrt{w^2 + b^2}}{w + \sqrt{w^2 + a^2}} \tag{4}$$

$$R_a = \sqrt{(w' - w)^2 + a^2} \qquad R_b = \sqrt{(w' - w)^2 + b^2} \tag{5}$$

Also

$$k_{0T}(w) \doteq \int_0^\infty \left(\frac{1}{R_{1T}} - \frac{1}{R_{2T}}\right) \cos\theta \, du' = F_2(w) \cos\theta \tag{6}$$

$$k'_{0T}(w) \doteq \int_0^\infty \left(\frac{1}{R_{1T}} - \frac{1}{R_{2T}}\right) du' = F_2(w) \tag{7}$$

where now

$$F_2(w) \equiv \ln \frac{w \cos\theta + \sqrt{w^2 + b^2}}{w \cos\theta + \sqrt{w^2 + a^2}} \tag{8}$$

and
$$R_{1T} = \sqrt{w^2 + u'^2 + 2wu' \cos\theta + a^2}$$
$$R_{2T} = \sqrt{w^2 + u'^2 + 2wu' \cos\theta + b^2} \tag{9}$$

The distances R_a and R_b from the point Q on the surface of conductor 1 at a distance w from the bend to the elements of integration dw' along the axes of the two conductors at a distance w' toward the generator from the bend are shown in Fig. 15.2, as are the distances R_{1T} and R_{2T} to the corresponding elements du' on the other side of the bend. In (3), (6), and (7) the upper limits in the integration (s_l or s_r) are replaced by infinity, since it is assumed that both sections of line are sufficiently long so that contributions from the parts that are far from the bend are negligible. The integrations are carried out using Pierce formula 160.

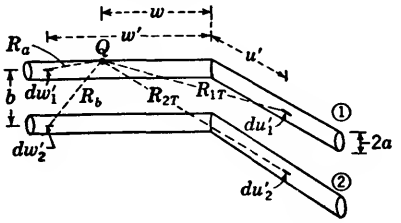


FIG. 15.2. Enlarged section of bend in a two-wire line.

It follows that
$$l^e(w) = \frac{k_0 - F_1(w) + F_2(w) \cos\theta}{2\pi\nu} \tag{10a}$$
$$c(w) = \frac{2\pi\epsilon}{k_0 - F_1(w) + F_2(w)} \tag{10b}$$

Since the inductance and capacitance per unit length of the uniform (infinitely long) line are
$$l_0^e = \frac{k_0}{2\pi\nu} \qquad c_0 = \frac{2\pi\epsilon}{k_0} \tag{11}$$

it follows that the lumped inductance L_T and capacitance C_T required to yield the same total inductance and capacitance when (11) is used in the section of line between the bend and the generator, instead of (9) and (10), are given by
$$L_T = \int_0^\infty [l^e(w) - l_0^e]\, dw = \frac{1}{2\pi\nu} \int_0^\infty [F_2(w) \cos\theta - F_1(w)]\, dw \tag{12}$$
$$C_T = \int_0^\infty [c(w) - c_0]\, dw = \frac{2\pi\epsilon}{k_0} \int_0^\infty \frac{F_1(w) - F_2(w)}{k_0 - F_1(w) + F_2(w)}\, dw \tag{13}$$

Exactly equal values are obtained for the section of line between the bend and the load by using (10a), (10b), (12), and (13), with u substituted for w, so that the total lumped series inductance at the bend is $2L_T$ and the total lumped shunt capacitance is $2C_T$, as shown in the equivalent circuit of Fig. 15.3.

The integrands in (12) and (13), as evaluated by Tomiyasu,[104] are given in Fig. 15.4 for three values of θ and $b = 2$ cm and $a = 0.1588$ cm. It is seen that the principal contributions occur in the range $w \leqq 10b$.

The second integral in (12) may be evaluated by noting that

$$\int_0^\infty \ln\,(w\cos\theta + \sqrt{w^2 + b^2})\,dw$$
$$= \int_0^\infty \ln\,(w + \sqrt{w^2 + b^2})\,dw + b\int_0^\infty \ln\,[1 - K(x)]\,dx \quad (14a)$$

so that

$$\int_0^\infty F_2(w)\,dw = \int_0^\infty F_1(w)\,dw + (b - a)\int_0^\infty \ln\,[1 - K(x)]\,dx \quad (14b)$$

Note that the shorthand

$$K(x) \equiv (1 - \cos\theta)x(\sqrt{x^2 - 1} - x) \quad (14c)$$

and the change of variable $x = w/b$ have been introduced in (14a). It is now easily verified that $K(x)$ ranges between the value 0 when $x = 0$

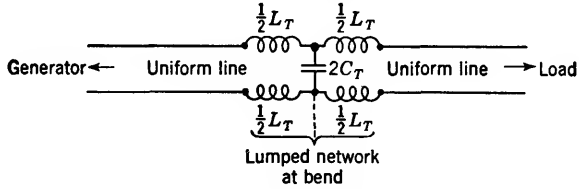


FIG. 15.3. Equivalent circuit for bent line.

to $\frac{1}{2}(1 - \cos\theta)$ when $x = \infty$. Since, for $\theta \leqq 90°$, $K(x) \leqq 0.5$, the last logarithm in (14a) may be expanded in the series

$$\ln\,[1 - K(x)] = -\left[K(x) + \frac{K^2(x)}{2} + \frac{K^3(x)}{3} + \cdots\right] \quad (15)$$

and integrated term by term. The first two terms give a satisfactory approximation, viz.,

$$\int_0^\infty \ln\,[1 - K(x)]\,dx \doteq \tfrac{1}{3}(1 - \cos\theta)$$
$$+ \tfrac{2}{15}(1 - \cos\theta)^2 + \tfrac{2}{35}(1 - \cos\theta)^3 + \cdots \quad (16)$$

The first integral on the right in (14a) is readily integrated using Dwight formula 625. Thus

$$\int_0^\infty F_1(w)\,dw = b - a \quad (17)$$

With (16) and (17) used in (12), the final formula for L_T is

$$L_T = -\frac{b - a}{2\pi\nu}\,G(\theta) \quad (18a)$$

where, with only two terms retained in the series (15) and (16),

$$G(\theta) \doteq (1 - \cos\theta)[1 - \tfrac{1}{3}\cos\theta + \tfrac{2}{15}\cos\theta\,(1 - \cos\theta)]$$
$$= (1 - \cos\theta)(1 - \tfrac{1}{5}\cos\theta - \tfrac{2}{15}\cos^2\theta) \quad (18b)$$

The function $G(\theta)$, as calculated from (18b), is shown in Fig. 15.5 as a function of θ and is listed in Table 15.1.

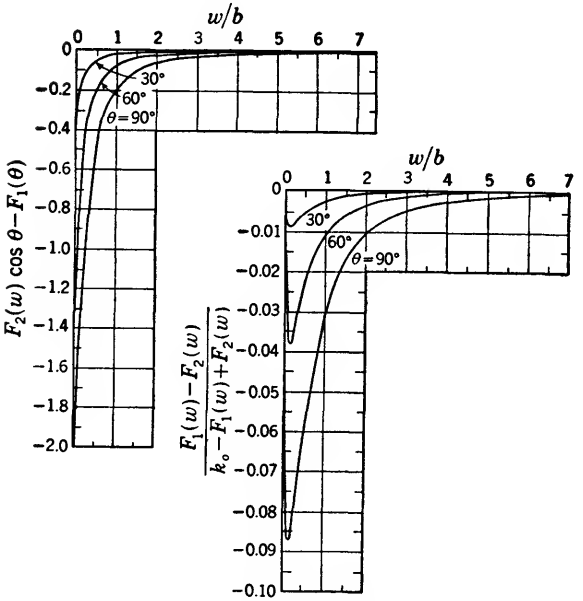


FIG. 15.4. Graphs of integrands in Eqs. (12) and (13).

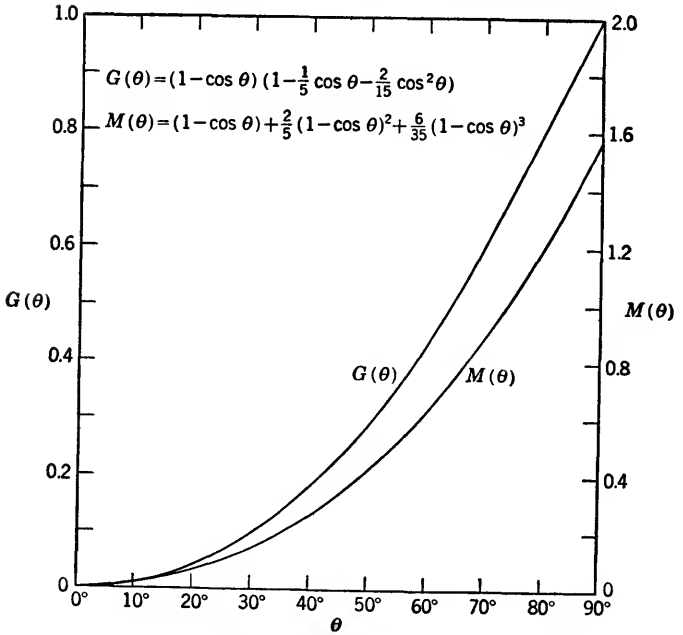


FIG. 15.5. Graphs of the functions $G(\theta)$ in $L_T \doteq -(b-a)G(\theta)/2\pi\nu$ and $M(\theta)$ in $C_T \doteq -2\pi\epsilon(b-a)M(\theta)/3k_0^2$ for a bend in a two-wire line.

TABLE 15.1. THE FUNCTION $G(\theta)$

θ, deg	$G(\theta)$
0	0.00
10	0.01
20	0.04
30	0.10
40	0.18
50	0.29
60	0.43
70	0.60
80	0.80
90	1.00

The determination of C_T using (13) may be carried out by treating the difference

$$H(w) \equiv F_2(w) - F_1(w) \tag{19}$$

[which occurs in both the numerator and the denominator of (13)] in a manner similar to that followed in the evaluation of $F_2(w) \cos \theta - F_1(w)$ in (12). Thus

$$H(w) = \ln \frac{w \cos \theta + \sqrt{w^2 + b^2}}{w + \sqrt{w^2 + b^2}} - \ln \frac{w \cos \theta + \sqrt{w^2 + a^2}}{w + \sqrt{w^2 + a^2}} \tag{20a}$$

This may be expressed in the following form:

$$H(w) = \ln \left[1 - K\left(\frac{w}{b}\right)\right] - \ln \left[1 - K\left(\frac{w}{a}\right)\right] \tag{20b}$$

where, as in (14c),

$$K(x) = (1 - \cos \theta)x(\sqrt{x^2 + 1} - x) \tag{21}$$

with $x = w/b$ or w/a.

As before, the logarithms in (20b) may be expanded in the series (15), with the result

$$H(w) = K\left(\frac{w}{a}\right) + \tfrac{1}{2}K^2\left(\frac{w}{a}\right) + \tfrac{1}{3}K^3\left(\frac{w}{a}\right) + \cdots - \left[K\left(\frac{w}{b}\right) + \tfrac{1}{2}K^2\left(\frac{w}{b}\right) + \tfrac{1}{3}K^3\left(\frac{w}{b}\right) + \cdots\right] \tag{22}$$

Since $K(x) \leqq 0.5$ for $\theta \leqq 90°$, it is readily verified that, with the assumed condition $b^2 \gg a^2$, $k_0 = 2 \ln (b/a)$ is sufficiently large so that the quantity $H(w)/k_0$ satisfies the condition

$$\frac{H(w)}{k_0} < 1 \tag{23}$$

Subject to (23), the second integrand in (13) may be expanded in powers

of $H(w)/k_0$, as follows:

$$C_T = -\frac{2\pi\epsilon}{k_0}\int_0^\infty \frac{H(w)/k_0}{1 - H(w)/k_0}\,dw \tag{24a}$$

$$= -\frac{2\pi\epsilon}{k_0}\int_0^\infty \left[\frac{H(w)}{k_0} + \frac{H^2(w)}{k_0^2} + \frac{H^3(w)}{k_0^3} + \cdots\right] dw \tag{24b}$$

The integrals in the leading term can be evaluated as in (14*b*). The result is

$$\int_0^\infty \frac{H(w)}{k_0}\,dw = \frac{(b-a)(1-\cos\theta)}{3k_0}\left[1 + \tfrac{2}{5}(1-\cos\theta) + \tfrac{6}{35}(1-\cos\theta)^2 + \cdots\right] \tag{25a}$$

The exact integration of the higher-order terms is complicated by the occurrence of cross-product terms of the form $K^n(w/a)K^m(w/b)$. Since the contribution by the terms in $K(w/a)$ is in any case small, these may be neglected in the higher-order terms, so that

$$H^2(w) \doteq \left[K\left(\frac{w}{b}\right) + \tfrac{1}{2}K^2\left(\frac{w}{b}\right) + \cdots\right]^2 = K^2\left(\frac{w}{b}\right) + K^3\left(\frac{w}{b}\right) + \cdots \tag{25b}$$

$$H^3(w) \doteq \left[K\left(\frac{w}{b}\right) + \tfrac{1}{2}K^2\left(\frac{w}{b}\right) + \cdots\right]^3 \doteq K^3\left(\frac{w}{b}\right) \tag{25c}$$

The integrations can now be carried out to give

$$\int_0^\infty \frac{H^2(w)}{k_0^2}\,dw \doteq \frac{b}{k_0^2}\left[\tfrac{4}{15}(1-\cos\theta)^2 + \tfrac{6}{35}(1-\cos\theta)^3 + \cdots\right] \tag{25d}$$

$$\int_0^\infty \frac{H^3(w)}{k_0^3}\,dw \doteq \frac{b}{k_0^3}\,\tfrac{6}{35}(1-\cos\theta)^3 + \cdots \tag{25e}$$

With (25*a*,*d*,*e*) it follows that (24*b*) becomes

$$C_T \doteq -\frac{2\pi\epsilon_0(b-a)}{3k_0^2}\left[1 - \cos\theta + \tfrac{2}{5}\left(1 + \frac{2}{k_0}\right)(1-\cos\theta)^2 + \tfrac{6}{35}\left(1 + \frac{3}{k_0} + \frac{3}{k_0^2}\right)(1-\cos\theta)^3\right] \tag{26}$$

Since the terms in a have been neglected in evaluating (25*d*) and (25*e*), the factor b occurs. Since, with $b^2 \gg a^2$, $b - a$ differs little from b, the factor $b - a$ may be substituted for b in (25*d*) and (25*e*) with little error. For most purposes the leading terms in (26) are adequate; they permit the definition of a function of θ which is independent of k_0. The leading-term formula is

$$C_T \doteq -\frac{2\pi\epsilon(b-a)}{3k_0^2}\,M(\theta) \tag{27a}$$

where $$M(\theta) = 1 - \cos\theta + \tfrac{2}{5}(1-\cos\theta)^2 + \tfrac{6}{35}(1-\cos\theta)^3 \tag{27b}$$

The function $M(\theta)$ is plotted in Fig. 15.5 and tabulated in Table 15.2.

TABLE 15.2. THE FUNCTION $M(\theta)$

θ, deg	$M(\theta)$
0	0
10	0.015
20	0.061
30	0.14
40	0.26
50	0.42
60	0.62
70	0.88
80	1.20
90	1.57

Numerical values of L_T/l_0^e and C_T/c_0 for a bend in a two-wire line, with $b = 2$ cm and $a = 0.1588$ cm, are given in Table 15.3 for $\theta = 30$, 60, and 90°. Three columns are given for C_T/c_0: one is computed using the more complete formula (26); the second column makes use of the leading-term formula (27a); the third lists values reported by Tomiyasu[104] which are determined by numerical methods. All three are in reasonably good agreement. Two columns are given for L_T/l_0^e: one is computed from (18a); the other is evaluated by numerical methods by Tomiyasu.[104] The agreement is good.

The experimental determination of the relatively small inductance $2L_T$ and capacitance $2C_T$ (Fig. 15.3) may be carried out independently by adjusting a short-circuited section of line in length to have a current maximum at the bend when $2L_T$ is measured and a charge or voltage maximum when $2C_T$ is measured. Using a two-wire line for which $b = 2$ cm and $a = 0.1588$ cm, Tomiyasu[104] determined the experimental curves shown in Fig. 15.6. The theoretical values of $2C_T/c_0$ obtained from (26) and tabulated in Table 15.3 and those of $2L_T/l_0^e$ obtained from (18a) and tabulated in Table 15.3 are also shown in Fig. 15.6. It is seen that the theoretical curve for $2C_T/c_0$ is in quite good agreement with the experimental one. On the other hand, whereas theoretical values of $2L_T/l_0^e$ are all negative in Fig. 15.6, the experimental curve shows a small

TABLE 15.3. THEORETICAL VALUES FOR C_T/c_0 AND L_T/l_0^e FOR BEND IN TWO-WIRE LINE, WITH $b = 2$ CM AND $a = 0.1588$ CM

θ, deg	C_T/c_0, cm			L_T/l_0^e, cm	
	Eq. (26)	Eq. (27a)	Numerical integration†	Eq. (18a)	Numerical integration
30	−0.017	−0.017	−0.016	−0.035	−0.033
60	−0.081	−0.077	−0.071	−0.152	−0.141
90	−0.224	−0.189	−0.189	−0.353	−0.353

† Reported by Tomiyasu.[104]

positive value when θ is less than 60°. A correction for the theoretical curve has been obtained by Tomiyasu,[104] who has shown that the discrepancy between the theoretical curve for $2L_T/l_0^e$ and the experimental results is a consequence of the fact that the elementary analysis for L_T as carried out in this section assumes rotational symmetry for the current in, and the vector potential on, the surface of the two wires throughout the bend and also an abrupt change in the direction of the current at the bend. Actually, in the case of conductors with finite radius a, neither the current nor the vector potential is rotationally symmetrical around the bend even when the condition $b^2 \gg a^2$ is satisfied. The current is more concentrated in the bend, so that the conductor behaves as if it had a radius smaller than a. However, Tomiyasu has shown that a small positive inductance L_N must be added to $2L_T$. The analysis involves elliptic integrals, and for a line with $b = 2$ cm and $a = 0.1588$ cm, Tomiyasu obtained the value

$$\frac{L_N}{l_0^e} = 0.22 \text{ cm} \qquad (28)$$

for $\theta = 30°$. By adding this value to $2L_T/l_0^e$ to obtain a total inductive correction $(2L_T + L_N)/l_0^e$, a point at $\theta = 30°$ is obtained which is in excellent agreement with experiment. Owing to increasing complications as the bend is made sharper, Tomiyasu evaluated no points for $\theta = 60$ and 90° but merely assumed that the same value of L_N given in (28) applies for $30° \leqq \theta \leqq 90°$. A curve of $(2L_T + L_N)/l_0^e$ is shown in Fig. 15.6. It is seen to agree well with experiment.

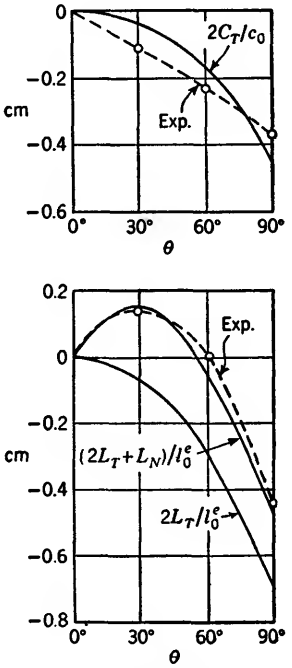


FIG. 15.6. Comparison of theoretical curves (solid lines) with experimental curves (broken lines) for $2C_T/c_0$, $2L_T/l_0^e$, and $(2L_T + L_N)/l_0^e$ (Tomiyasu).

16. T Junction in a Two-wire Line. An important type of junction consists of three sections of similar two-wire line meeting in a T. Common examples include (1) a matching or tuning stub connected at right angles to a transmission line, as shown in Fig. 16.1*a*; (2) a driven line that divides into two loaded sections in parallel, as in Fig. 16.1*b*; (3) a line that makes a right-angle bend but is supported by an insulating stub, as in Fig. 16.1*c*.

In the elementary analysis of the transmission line with a shunt stub or insulating support in Chap. III, it is assumed that conventional transmission-line formulas are valid at *all* points along all three sections

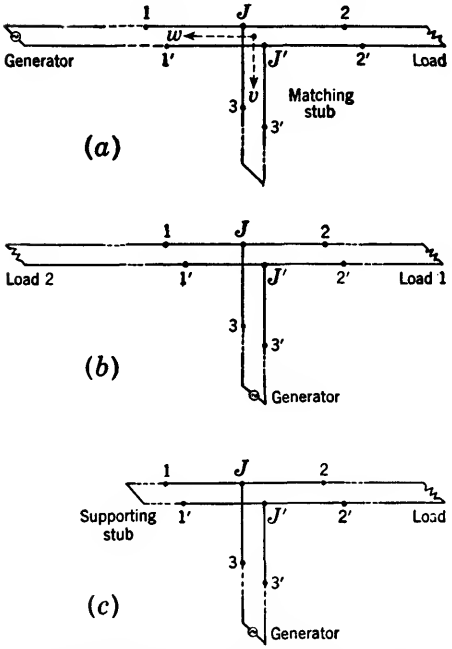


FIG. 16.1. Three types of T junctions in a two-wire line. (*a*) Line with matching stub. (*b*) Single line driving two loaded lines. (*c*) Right-angle bend with supporting stub.

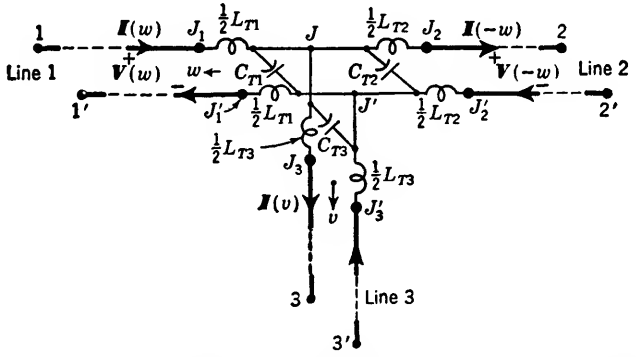


FIG. 16.2. Equivalent junction network for a shunt stub on a two-wire line.

of line, including the regions close to the junction JJ' (Fig. 16.1). Actually the external inductance and the capacitance per unit length are not constant at the values l_0^e and c_0 in the junction zone. As a consequence, it is necessary to compensate for the inaccurate use of the constant values l_0^e and c_0 by introducing a fictitious lumped network that consists of a series inductance L_T and a shunt capacitance C_T connected to each line at the common junction, as shown in Fig. 16.2. The values L_T and C_T

for each line are to be so evaluated that the impedances looking toward the junction JJ' from 11', 22', and 33' are the *measurable apparent impedances* when computed using conventional transmission-line formulas in conjunction with the lumped network.

Since the network in the vicinity of the junction is symmetrical with respect to a plane through JJ', J_3J_3', and 33' (Fig. 16.2), the problem of determining the elements of the lumped network is simplified. It is clear that

$$L_{T2} = L_{T1} \qquad C_{T2} = C_{T1} \tag{1}$$

The analysis may be carried out using even and odd currents and voltages. Let the origin of a system of coordinates be located midway between the terminals JJ', as in Fig. 16.1*a*. The coordinate w increases from JJ' toward 11' in line 1, so that currents and voltages to the left of JJ' may be designated by $I_1 = I(w)$ and $V_1 = V(w)$, and those to the right of JJ' in line 2, by $I_2 = I(-w)$ and $V_2 = V(-w)$. The coordinate v increases toward 33' in line 3, and the currents and voltages in the shunt or stub section are $I_3 = I(v)$ and $V_3 = V(v)$.

Let the currents and voltages in lines 1 and 2 be separated into even and odd parts to form symmetrical and antisymmetrical combinations, as follows:

$$I(w) = I^{(s)}(w) + I^{(a)}(w) \tag{2a}$$
$$V(w) = V^{(s)}(w) + V^{(a)}(w) \tag{2b}$$
$$I(-w) = I^{(s)}(w) - I^{(a)}(w) \tag{3a}$$
$$V(-w) = V^{(s)}(w) - V^{(a)}(w) \tag{3b}$$

By definition, let the symmetrical currents be even and the symmetrical voltages odd, so that

$$I^{(s)}(-w) = I^{(s)}(w) \qquad V^{(s)}(-w) = -V^{s}(w) \tag{4}$$
$$I^{(a)}(-w) = -I^{(a)}(w) \qquad V^{(a)}(-w) = V^{(a)}(w) \tag{5}$$

It is readily verified that definitions (4) and (5) are consistent with (2*a*,*b*) and (3*a*,*b*) and with

$$I^{(s)}(w) = \tfrac{1}{2}[I(w) + I(-w)] \qquad V^{(s)}(w) = \tfrac{1}{2}[V(w) - V(-w)] \tag{6}$$
$$I^{(a)}(w) = \tfrac{1}{2}[I(w) - I(-w)] \qquad V^{(a)}(w) = \tfrac{1}{2}[V(w) + V(-w)] \tag{7}$$

Once the currents and voltages on lines 1 and 2 have been resolved into symmetrical and antisymmetrical components using (6) and (7), each set of currents and voltages may be determined independently, and a separate set of L_T's and C_T's defined for each. Note that, in general, junction-zone networks are not the same for symmetrical currents and voltages as for antisymmetrical ones. Let the junction zone be the region in all three lines within a distance d of the junction which is short compared with the wavelength and beyond which the line parameters may be assumed constant. Usually d is of the order of magnitude of $10b$ or less.

The Symmetrical Problem. A symmetrically driven T junction is shown in Fig. 16.3. The two symmetrical branches are excited by generators that maintain currents and voltages that satisfy (4). It follows that

$$V^{(s)}\ (w = 0) = 0 \tag{8}$$

so that there may be no generator in line 3. Moreover, since the generators in lines 1 and 2 maintain zero voltage across the junction points

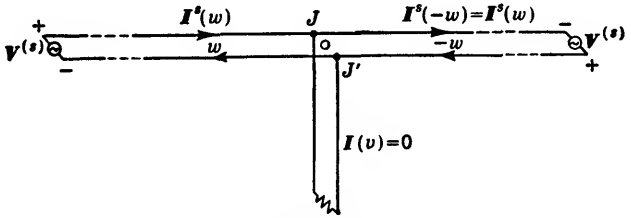


FIG. 16.3. Symmetrically driven T junction.

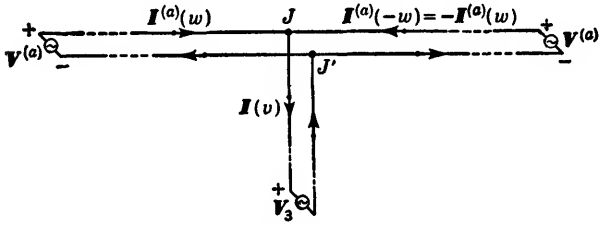


FIG. 16.4. Antisymmetrically driven T junction.

JJ', all currents, charges per unit length, and voltages in the stub line 3 are zero. Therefore lines 1 and 2 behave like a smooth line without the stub section, and

$$C^{(s)}_{T1} = C^{(s)}_{T2} = 0 \qquad L^{(s)}_{T1} = L^{(s)}_{T2} = 0 \tag{9}$$

Since there are no currents or charges in line 3, it is unnecessary to introduce $C^{(s)}_{T3}$ and $L^{(s)}_{T3}$.

The Antisymmetrical Problem. An antisymmetrically driven T junction is shown in Fig. 16.4. In general, there may be generators in all three lines, but those in lines 1 and 2 must be so adjusted that (5) is satisfied. There are no restrictions on the generator in line 3.

Kirchhoff's current law applied at JJ' in Fig. 16.4 gives

$$I^{(a)}\ (w = 0) = I^{(a)}\ (-w = 0) + I\ (v = 0) \tag{10a}$$

With (5) it follows that

$$I\ (v = 0) = 2I^{(a)}\ (w = 0) \tag{10b}$$

Since the junction zone is small compared with the wavelength, the leading terms in Maclaurin expansions of the currents are adequate. That is,

$$I^{(a)}(w) = I^{(a)}(-w) \doteq \tfrac{1}{2}I(v) \qquad |w| \leqq d,\ v \leqq d \tag{11}$$

Similarly the voltages across the three conductors in the junction zone are essentially equal:

$$V^{(a)}(w) = V^{(a)}(-w) \doteq V(v) \qquad |w| \leqq d,\ v \leqq d \tag{12}$$

Note that the equations on the left in (11) and (12) are exact and those on the right are approximate for nonzero values of b/λ.

Capacitance per Unit Length. The scalar potential differences across the three lines in the junction zone may be expressed as follows:

$$V^{(a)}(w) = V_{11}(w) + V_{12}(w) + V_{13}(w) = V^{(a)}(-w) \tag{13}$$

$$V(v) = V_{31}(v) + V_{32}(v) + V_{33}(v) \tag{14}$$

where $V_{11}(w)$ is the contribution to $V^{(a)}(w)$ by the charge per unit length $q^{(a)}(w)$ on line 1, $V_{12}(w)$ is the contribution to $V^{(a)}(w)$ by $q^{(a)}(-w)$ on line 2, and $V_{13}(w)$ is the contribution to $V^{(a)}(w)$ by $q(v)$ on line 3. Similarly $V_{31}(v)$ is the contribution to $V(v)$ by $q^{(a)}(w)$ on line 1, $V_{32}(v)$ is the contribution to $V(v)$ by $q^{(a)}(-w)$ on line 2, and $V_{33}(v)$ is the contribution to $V(v)$ by $q(v)$ on line 3. As in Chap. II, Sec. 1, the expressions for these several voltages are as follows:

$$V_{11}(w) + V_{12}(w) \doteq \frac{1}{2\pi\epsilon} \int_{-\infty}^{\infty} q^{(a)}(w') P_L(w,w')\, dw' \tag{15a}$$

$$V_{13}(w) \doteq \frac{1}{2\pi\epsilon} \int_{0}^{\infty} q(v') P_T(w,v')\, dv' \tag{15b}$$

$$V_{31}(v) + V_{32}(v) \doteq \frac{1}{2\pi\epsilon} \int_{-\infty}^{\infty} q^{(a)}(w') P_s(v,w')\, dw' \tag{16a}$$

$$V_{33}(v) \doteq \frac{1}{2\pi\epsilon} \int_{0}^{\infty} q(v') P_L(v,v')\, dv' \tag{16b}$$

where

$$P_L(w,w') \doteq \frac{1}{R_a} - \frac{1}{R_b} \qquad \begin{aligned} R_a &= \sqrt{(w'-w)^2 + a^2} \\ R_b &= \sqrt{(w'-w)^2 + b^2} \end{aligned} \tag{17a}$$

$$P_T(w,v') \doteq \frac{1}{R_{Ta}} - \frac{1}{R_{Tb}} \qquad \begin{aligned} R_{Ta} &= \sqrt{v'^2 + w^2 + a^2} \\ R_{Tb} &= \sqrt{v'^2 + w^2 + b^2} \end{aligned} \tag{17b}$$

$$P_s(v,w') \doteq \frac{1}{R_{sa}} - \frac{1}{R_{sb}} \qquad \begin{aligned} R_{sa} &= \sqrt{w'^2 + v^2 + a^2} \\ R_{sb} &= \sqrt{w'^2 + v^2 + b^2} \end{aligned} \tag{17c}$$

$$P_L(v,v') = \frac{1}{R_a} - \frac{1}{R_b} \qquad \begin{aligned} R_a &= \sqrt{(v'-v)^2 + a^2} \\ R_b &= \sqrt{(v'-v)^2 + b^2} \end{aligned} \tag{17d}$$

In carrying out the integration in (15*a*,*b*) the charge per unit length is expanded in a Taylor series about the charge per unit length at w. Similarly in (16*a*,*b*) the charge per unit length is expanded about the charge per unit length at v. As in Chap. II, Sec. 1, only the leading terms need

be retained. Using Chap. II, Sec. 1, Eqs. (15*b*) and (26*a*), the following formulas may be obtained:

$$V_{11}(w) + V_{12}(w) = \frac{q^{(a)}(w)}{2\pi\epsilon} k_0 \tag{18a}$$

$$V_{33}(v) = \frac{q(v)}{2\pi\epsilon}\left(k_0 - \ln \frac{v + \sqrt{v^2 + b^2}}{v + \sqrt{v^2 + a^2}}\right) \tag{18b}$$

where

$$k_0 = 2 \ln \frac{b}{a} \tag{19}$$

The following additional results are obtained if use is made of Sec. 15, Eq. (8), with $\theta = \pi/2$:

$$V_{13}(w) = \frac{q^a(w)}{4\pi\epsilon} \ln \frac{w^2 + b^2}{w^2 + a^2} \tag{20}$$

Similarly

$$V_{31}(v) + V_{32}(v) = \frac{q(v)}{2\pi\epsilon} \ln \frac{v^2 + b^2}{v^2 + a^2} \tag{21}$$

The variable capacitances per unit length of line may now be defined as follows. For lines 1 and 2

$$c(-w) \equiv \frac{q^{(a)}(-w)}{V^a(-w)} = c(w) \equiv \frac{q^{(a)}(w)}{V^{(a)}(w)} \tag{22a}$$

where

$$c(w) = \frac{2\pi\epsilon}{k_0 + L(w)} \tag{22b}$$

with

$$L(w) \equiv \tfrac{1}{2} \ln \frac{w^2 + b^2}{w^2 + a^2} \tag{22c}$$

Similarly, for line 3,

$$c(v) \equiv \frac{q(v)}{V(v)} = \frac{2\pi\epsilon}{k_0 + 2L(v) - M(v)} \tag{23a}$$

where

$$L(v) \equiv \tfrac{1}{2} \ln \frac{v^2 + b^2}{v^2 + a^2} \tag{23b}$$

$$M(v) \equiv \ln \frac{v + \sqrt{v^2 + b^2}}{v + \sqrt{v^2 + a^2}} \tag{23c}$$

Note that, when $|w|$ becomes sufficiently great, $c\ (w \to \infty) = c_0 = 2\pi\epsilon/k_0$. Similarly $c\ (v \to \infty) = c_0$. On the other hand, at the junction

$$c\ (w = 0) = c\ (v = 0) = \frac{2c_0}{3}$$

Inductance per Unit Length. Since the stub line 3 is perpendicular to both the other lines, there is no inductive coupling, and the junction effect in line 3 reduces to a transmission-line end correction. Thus, with Sec. 12, Eqs. (2) and (3), it follows that

$$l^e(v) = \frac{k_0(v)}{2\pi\nu} = \frac{1}{2\pi\nu}\left(\sinh^{-1} \frac{v}{a} - \sinh^{-1} \frac{v}{b} + \ln \frac{b}{a}\right) \tag{24}$$

Since for lines 1 and 2 the antisymmetrical currents are equal and oppo-

site at equal distances $|w|$ from the junction, it is readily shown that

$$l^e(w) = \frac{1}{\pi\nu}\left(\sinh^{-1}\frac{w}{a} - \sinh^{-1}\frac{w}{b}\right) \tag{25}$$

Lumped Elements. The lumped inductive elements required in each line at the common junction are defined as in Chap. II, Sec. 4. Use is also made of Sec. 12 in this chapter.

$$L_{T3} = \int_0^d [l^e(v) - l_0^e]\,dv \doteq -\frac{b-a}{2\pi\nu} \tag{26}$$

$$L_{T2} = L_{T1} = \int_0^d [l^e(w) - l_0^e]\,dw \doteq -\frac{b-a}{\pi\nu} = 2L_{T3} \tag{27}$$

Note that d is large compared with b.

The lumped capacitive elements are defined as follows:

$$C_{T3} = \int_0^d [c(v) - c_0]\,dv \tag{28a}$$

With (23*a*) this integral becomes

$$C_{T3} = -\frac{c_0}{k_0}\int_0^d \frac{2L(v) - M(v)}{1 + (1/k_0)[2L(v) - M(v)]}\,dv \tag{28b}$$

$$C_{T1} = \int_0^d [c(w) - c_0]\,dw \tag{29a}$$

With (22*b*) this last integral becomes

$$C_{T2} = C_{T1} = -\frac{c_0}{2k_0}\int_0^d \frac{2L(w)}{1 + L(w)/k_0}\,dw \tag{29b}$$

An approximate integration of (28*b*) and (29*b*) may be carried out following a procedure introduced in Sec. 15. Since k_0 is moderately large compared with unity for most lines and since $2L(v) - M(v)$ and $L(w)$ have quite small values over most of the range of integration, the denominators in (28*b*) and (29*b*) may be expanded in series, so that

$$C_{T3} \doteq -\frac{c_0}{k_0}\int_0^d \left\{2L(v) - M(v) - \frac{1}{k_0}[2L(v) - M(v)]^2 - \cdots\right\} dv \tag{30}$$

$$C_{T2} = C_{T1} = -\frac{c_0}{k_0}\int_0^d \left[L(w) - \frac{1}{k_0}L^2(w) - \cdots\right] dw \tag{31}$$

In each integral the leading or first-order terms are readily evaluated, since they have the simple forms given below:

$$(C_{T3})_1 = -\frac{c_0}{k_0}\int_0^d [\ln(v^2 + b^2) - \ln(v^2 + a^2) - \ln(v + \sqrt{v^2 + b^2}) + \ln(v + \sqrt{v^2 + a^2})]\,dv \tag{32}$$

$$(C_{T2})_1 = (C_{T1})_1 \doteq -\frac{c_0}{2k_0}\int_0^d [\ln(w^2 + b^2) - \ln(w^2 + a^2)]\,dw \tag{33}$$

These may be integrated using Dwight 623 and 625. The results are

$$(C_{T3})_1 = -\frac{c_0(\pi+1)(b-a)}{2\ln(b/a)} = -\frac{\pi(\pi+1)(b-a)\epsilon}{2[\ln(b/a)]^2} \tag{34}$$

$$(C_{T2})_1 = (C_{T1})_1 = -\frac{c_0\pi(b-a)}{4\ln(b/a)} = -\frac{\pi^2(b-a)\epsilon}{[2\ln(b/a)]^2} \tag{35}$$

These expressions are good approximations for sufficiently large values of b/a. If b/a is small, additional terms must be used in (30) and (31), or (28b) and (29b) must be evaluated numerically.

Note that all the lumped elements are negative, indicating that the actual variable inductance and capacitance per unit length are *smaller* than l_0^e and c_0 in the junction region. Therefore, if l_0^e and c_0 are to be

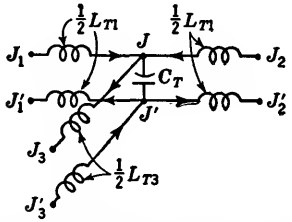


FIG. 16.5. Equivalent circuit for antisymmetrically driven T junction.

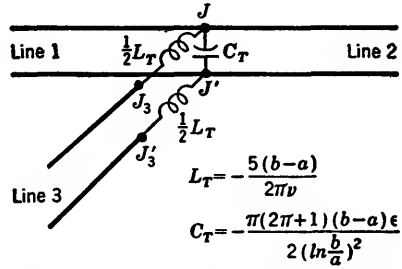


FIG. 16.6. Equivalent circuit for T junction.

used, negative lumped inductances and capacitances that decrease the total inductance and capacitance are required.

It is important to bear in mind that the values of L_T and C_T given by (26), (27), (34), and (35) apply only to that part of the current which is *odd* with respect to the junction and to that part of the voltage which is *even*. The lumped network for the antisymmetrical currents and voltages is shown in Fig. 16.5. Note that

$$C_T = C_{T1} + C_{T2} + C_{T3} \doteq -\frac{c_0(2\pi+1)(b-a)}{2\ln(b/a)} = -\frac{\pi(2\pi+1)(b-a)\epsilon}{2[\ln(b/a)]^2} \tag{36}$$

Since the *entire* antisymmetrical (odd) currents must enter line 3 from lines 1 and 2, it is obviously immaterial whether the lumped inductances L_{T1} and L_{T2} are connected in lines 1 and 2 at the junction, as in Fig. 16.5, or whether they are concentrated in line 3, as in Fig. 16.6. In the latter case the total series inductance in line 3 is

$$L_T = L_{T1} + L_{T2} + L_{T3} = 5L_{T3} = -\frac{5(b-a)}{2\pi\nu} \tag{37}$$

The advantage of Fig. 16.6 over Fig. 16.5 is that it is also the correct equivalent circuit for the symmetrical problem and therefore for the

T junction in general. Since the symmetrical voltage is zero at the junction, the presence of C_T has no effect, and since no symmetrical currents enter the stub line 3, the lumped inductances in this line also have no effect on the symmetrical currents. Therefore the equivalent circuit of Fig. 16.6 may be used for the total current and total voltage, and it is not necessary to separate the even and odd parts.

17. Junction Networks for Series Branches in Two-wire Lines; Terminal-zone Networks for Stub-supported and Center-driven Antennas and Folded Dipoles.[10,124] A balanced series junction in a two-wire line is shown in Chap. III, Fig. 14.1*b*, and in Fig. 17.1. It consists of two coplanar lines meeting at right angles. The two conductors of the

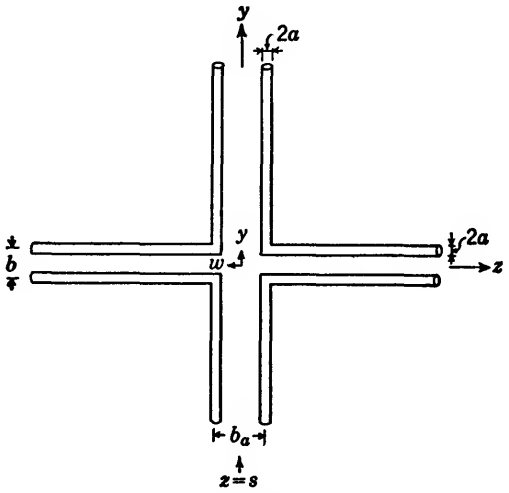


FIG. 17.1. Balanced series junction in two-wire line.

main line are parallel to the z axis; they are separated a distance b and have radii a. The conductors of the second (or auxiliary) line are parallel to the y axis; they are separated a distance b_a and also have radii a.

In order to evaluate the constants of lumped networks for each line at the junction, let the currents, voltages, and charges be resolved into symmetrical and antisymmetrical parts, as in Chap. III, Sec. 14.† It is assumed that the main line is balanced, so that $I_2(z) = -I_1(z)$.

Let the *symmetrical* case illustrated in Fig. 17.2 be defined as follows:

$$I^s(-w) = -I^s(w) \qquad I_2^s(y) = I_1^s(y) \tag{1}$$

where $w \equiv s - z$ is measured toward the left on the main line from the

† The symmetrical and antisymmetrical designations differ in this section from those in Sec. 16 in order that codirectional "antenna" currents on the auxiliary line may be designated symmetrical, as in antenna theory.[10]

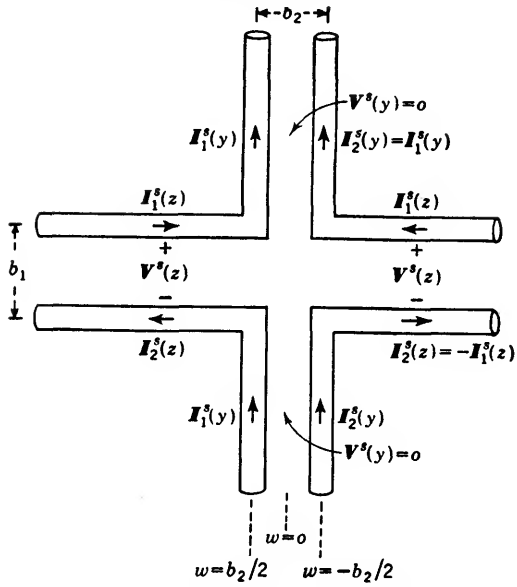


FIG. 17.2. Symmetrical currents and voltages in balanced series junction.

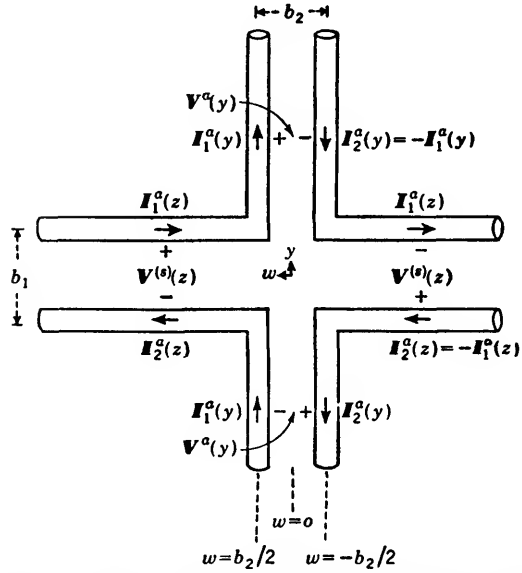


FIG. 17.3. Antisymmetrical currents and voltages in balanced series junction.

middle of the junction. With (1) the following relations also are true:

$$V^s(-w) = V^s(w) \qquad q^s(-w) = q^s(w) \tag{2a}$$
$$V^s(-y) = V^s(y) = 0 \qquad q^s(-y) = -q^s(y) \tag{2b}$$

Let the antisymmetrical case illustrated in Fig. 17.3 be defined by

$$I^a(-w) = I^a(w) \qquad I_2^a(y) = -I_1^a(y) \tag{3a}$$

Accordingly
$$V^a(-w) = -V^a(w) \qquad q^a(-w) = -q^a(w) \tag{3b}$$
$$V^a(-y) = -V^a(y) \qquad q^a(-y) = q^a(y) \tag{3c}$$

In general, the currents and voltages are superpositions of the symmetrical and antisymmetrical components. Thus

$$I(w) = I^s(w) + I^a(w) \qquad V(w) = V^s(w) + V^a(w) \tag{4a}$$
$$I(y) = I^s(y) + I^a(y) \qquad V(y) = V^s(y) + V^a(y) = V^a(y) \tag{4b}$$

The components of current on the main line are defined as follows in terms of the total quantities:

$$I^s(w) = \tfrac{1}{2}[I(w) + I(-w)] \qquad V^s(w) = \tfrac{1}{2}[V(w) - V(-w)] \tag{5a}$$
$$I^a(w) = \tfrac{1}{2}[I(w) - I(-w)] \qquad V^a(w) = \tfrac{1}{2}[V(w) + V(-w)] \tag{5b}$$

The symmetrical parts of the currents and voltages are defined so that the main line is balanced with equal and opposite currents in its two conductors, whereas the auxiliary line is *completely unbalanced* with equal and codirectional currents in its two conductors. The symmetrically driven series sections do not carry equal and opposite transmission-line currents but equal and codirectional antenna currents. These *cannot* be evaluated from transmission-line formulas. However, the appropriate junction-zone network can be determined using the methods outlined in this chapter. Such a network is useful, for example, in conjunction with lines used to center-drive balanced antennas, e.g., a tuned folded-dipole antenna.[10] By application of the theory of images, antennas over conducting planes may be analyzed when driven by a single conductor parallel to the image plane.

The antisymmetrical parts of the currents and voltages are true transmission-line currents on both the main line and the series sections.

In order to correct for the nonuniformity of the inductance and capacitance per unit length in the main line near the junction, lumped series inductances L_T and shunt capacitances C_T must be connected on each side of the junction.

Lumped Series Inductance L_T for Main-line Network. It follows by a simple modification of the formulation in Chap. II, Sec. 1, that the inductance per unit length in the main line on the left of the junction is

given by

$$l_0^e(w) = \frac{k_0(w)}{2\pi\nu} \tag{6a}$$

where

$$k_0(w) \doteq \int_{b_a/2}^{\infty} \left(\frac{1}{R_a} - \frac{1}{R_b}\right) dw' \mp \int_{-\infty}^{-b_a/2} \left(\frac{1}{R_a} - \frac{1}{R_b}\right) dw' \tag{6b}$$

Infinite limits have been substituted for the finite distances from the junction to the two ends of line 1, with the understanding that the actual distances are very great compared with the line spacing b. The

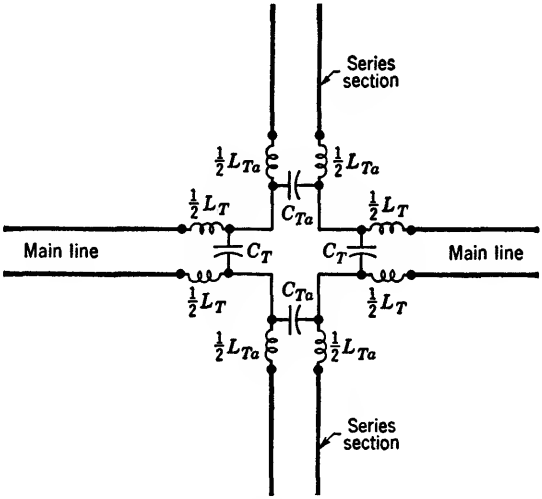


FIG. 17.4. Junction network of lumped elements for use with uniform lines.

upper sign in (6b) is for the symmetrical case, and the lower sign is for the antisymmetrical case. Note that $R_a = \sqrt{(w' - w)^2 + a^2}$ and $R_b = \sqrt{(w' - w)^2 + b^2}$. The integrations are readily carried out to give

$$k_0(w) = B \mp C + \begin{cases} 2 \ln \dfrac{b}{a} \\ 0 \end{cases} \tag{7a}$$

where

$$B \equiv \sinh^{-1} \frac{w - b_a/2}{a} - \sinh^{-1} \frac{w - b_a/2}{b} \tag{7b}$$

$$C \equiv \sinh^{-1} \frac{w + b_a/2}{a} - \sinh^{-1} \frac{w + b_a/2}{b} \tag{7c}$$

The lumped inductance required in the circuit of Fig. 17.4 to correct for the error made in using l_0^e in place of $l^e(w) = l_0^e(w)a_1(w)$ is given by Chap. II, Sec. 4, Eq. (3), viz.,

$$L_T = \int_{b_a/2}^{d+b_a/2} [l^e(w) - l_0^e]\, dw = \int_{b_a/2}^{d+b_a/2} [l_0^e(w) - l_0^e]\, dw \tag{8}$$

where $l_0^e(w)$ is given by (6a) with (7) and where $2\pi\nu l_0^e = 2 \ln b/a$. Note that $a_1(w) = 1$, since the two lines are mutually perpendicular [the ratio factor $a_1(w)$ is defined in Chap. II, Sec. 1, Eq. (24a)]. The integration in (8) may be readily performed using (7). The results are as follows:

$$\left.\begin{matrix} L_T^s \\ L_T^a \end{matrix}\right\} = \frac{-1}{2\pi\nu}\left[b - a \pm \left(\sqrt{b_a^2 + b^2} - \sqrt{b_a^2 + a^2} - b_a \ln \frac{b_a + \sqrt{b_a^2 + b^2}}{b_a + \sqrt{b_a^2 + a^2}}\right)\right] \tag{9}$$

where L_T^s applies to the symmetrical case and L_T^a to the antisymmetrical case. In the special case where $b_a = b$ and $a^2 \ll b^2$, the following simpler formula is obtained:

$$\left.\begin{matrix} L_T^s \\ L_T^a \end{matrix}\right\} = -\frac{b}{2\pi\nu}\left[1 - \frac{a}{b} \pm \left(\sqrt{2} - 1 - \ln \frac{1 + \sqrt{2}}{2}\right)\right] \tag{10}$$

Lumped Shunt Capacitance C_T for Main-line Network. The determination of the shunt capacitance in the several networks for which L_T has been evaluated is based on Chap. II, Sec. 4, formula (4), viz.,

$$C_T = \int_{b_a/2}^{d+b_a/2} [c(w) - c_0]\, dw = \int_{b_a/2}^{d+b_a/2} [c_0(w)\Phi_1(w) - c_0]\, dw \tag{11}$$

where

$$c_0(w) = \frac{2\pi\epsilon}{k_0(w)} \qquad c_0 = \frac{\pi\epsilon}{\ln (b/a)} \tag{12}$$

where $k_0(w)$ is given by (5b) and (7). The ratio factor $\Phi_1(w)$ is defined in Chap. II, Sec. 1, Eq. (24c). It is

$$\Phi_1(w) \doteq V_L(w)/V(w) \tag{13}$$

where $V_L(w)$ is the potential difference maintained exclusively by the charges on the same line where $V_L(w)$ is measured, and where

$$V(w) = V_T(w) + V_L(w)$$

is the potential difference maintained by all charges that contribute significantly, including those on the auxiliary series lines. Since $c_0(w)$ is defined by

$$c_0(w) = \frac{q_L(w)}{V_L(w)} \tag{14}$$

it follows that

$$c_0(w)\Phi_1(w) = \frac{q_L(w)}{V(w)} \tag{15}$$

so that

$$C_T = \int_{b_a/2}^{d+b_a/2} \left[\frac{q_L(w)}{V(w)} - c_0\right] dw \tag{16}$$

Since

$$c_0(w) = \frac{2\pi\epsilon}{k_0(w)} \tag{17}$$

where $k_0(w)$ is as defined in (5*b*), it follows that

$$V_L(w) = \frac{q_L(w)k_0(w)}{2\pi\epsilon} \tag{18}$$

Using (7), the symmetrical and antisymmetrical voltages maintained by charges on the main line are

$$V_L^s(w) = \frac{q_L^s(w)}{2\pi\epsilon}\left(B - C + 2\ln\frac{b}{a}\right) \tag{19}$$

$$V_L^a(w) = \frac{q_L^a(w)}{2\pi\epsilon}(B + C) \tag{20}$$

where B and C are as defined in (7*b*) and (7*c*).

The scalar potential difference maintained across the main line at a distance w from the middle of the junction is given by

$$V_T(w) \doteq \frac{1}{2\pi\epsilon}\int_{b/2}^{\infty} q_a(y')\left[\frac{1}{R_{1T}} - \frac{1}{R_{2T}} \pm \left(\frac{1}{R_{1b}} - \frac{1}{R_{2b}}\right)\right]dy' \tag{21}$$

where

$$R_{1T} = \sqrt{\left(y' - \frac{b}{2}\right)^2 + \left(w - \frac{b_a}{2}\right)^2 + a^2}$$

$$R_{2T} = \sqrt{\left(y' + \frac{b}{2}\right)^2 + \left(w - \frac{b_a}{2}\right)^2 + a^2} \tag{22a}$$

$$R_{1b} = \sqrt{\left(y' - \frac{b}{2}\right)^2 + \left(w + \frac{b_a}{2}\right)^2 + a^2}$$

$$R_{2b} = \sqrt{\left(y' + \frac{b}{2}\right)^2 + \left(w + \frac{b_a}{2}\right)^2 + a^2} \tag{22b}$$

and where $q_a(y')$ is the charge per unit length on the auxiliary line at the location y' of the element of integration dy'. As shown in general in Chap. II, Sec. 1, only the leading term need be retained in the expansion about the point w of the charge per unit length $q_a(y')$ on the auxiliary line, so that

$$q_a(y') \doteq q_L(w) \tag{23}$$

With (23) the integration in (21) is readily carried out. The result is

$$V_T(w) \doteq \frac{q_L(w)}{2\pi\epsilon}(A_1 \pm A_2) \tag{24}$$

where

$$A_1 \equiv \sinh^{-1}\frac{b}{\sqrt{(w - b_a/2)^2 + a^2}} \qquad A_2 \equiv \sinh^{-1}\frac{b}{\sqrt{(w + b_a/2)^2 + a^2}} \tag{25}$$

The upper sign in (24) defines $V_T^s(w)$, and the lower sign defines $V_T^a(w)$.

The next step in the evaluation of C_T is to express the integrand in (16) in terms of $V_L(w)$, as given in (19) and (20), and $V_T(w)$, as given in

(24). Since

$$\frac{q_L(w)}{V(w)} - c_0 = -c_0 \frac{V(w)/q_L(w) - 1/c_0}{V(w)/q_L(w)} \tag{26}$$

where

$$c_0 = \frac{\pi\epsilon}{\ln (b/a)} \tag{27}$$

it follows that the integrand in (11) may be expressed as follows in the symmetrical and antisymmetrical cases:

$$[c(w) - c_0]^s = -c_0 \frac{A_1 + A_2 + B - C}{2 \ln (b/a) + A_1 + A_2 + B - C} \equiv -c_0 H^s(w) \tag{28}$$

$$[c(w) - c_0]^a = -c_0 \frac{A_1 - A_2 + B + C - 2 \ln (b/a)}{A_1 - A_2 + B + C} \equiv -c_0 H^a(w) \tag{29}$$

where A_1 and A_2 are as in (25) and where B and C are as in (7b) and (7c).

The determination of C_T^s and C_T^a depends on the substitution of (28) and (29) in (11) and the evaluation of the integrals. Since the integration has not been carried out in closed form, graphical or numerical methods must be used if quantitative results are desired. As an alternative, the integrands (28) and (29) may be expanded in series, and approximate reasonably simple formulas for C_T obtained. Their derivation follows.

An approximate evaluation of the integrals in (11) may be carried out provided b/a is sufficiently great. As a first step, it can be shown without approximation that

$$B = \ln \frac{b}{a} - \ln D_1 \tag{30a}$$

$$C = \ln \frac{b}{a} - \ln D_2 \tag{30b}$$

where

$$D_1 \equiv \frac{w - b_a/2 + \sqrt{(w - b_a/2)^2 + b^2}}{w - b_a/2 + \sqrt{(w - b_a/2)^2 + a^2}} \tag{31}$$

$$D_2 \equiv \frac{w + b_a/2 + \sqrt{(w + b_a/2)^2 + b^2}}{w + b_a/2 + \sqrt{(w + b_a/2)^2 + a^2}} \tag{32}$$

$$B - C = \ln \frac{D_2}{D_1} \qquad B + C = 2 \ln \frac{b}{a} - \ln D_1 D_2 \tag{33}$$

If (33) is used in (28) and (29) and these are then divided by $2 \ln (b/a)$ in numerator and denominator, the following expressions are obtained:

$$H^s(w) = \frac{\delta_1}{1 + \delta_1} \qquad \delta_1 \equiv \frac{A_1 + A_2 + \ln (D_2/D_1)}{2 \ln (b/a)} \tag{34a}$$

$$H^a(w) = \frac{\delta_2}{1 + \delta_2} \qquad \delta_2 \equiv \frac{A_1 - A_2 - \ln D_1 D_2}{2 \ln (b/a)} \tag{34b}$$

If the ratio b/a is sufficiently great, both δ_1 and δ_2 are less than 1, so that

$$H(w) \doteq \delta - \delta^2 + \delta^3 - \cdots \tag{35}$$

with appropriate superscript on H and subscript on δ. It follows that,

if only the leading term is retained,

$$C_T = -c_0 \int_{b_a/2}^{d+b_a/2} H(w)\, dw \doteq -c_0 \int_{b_a/2}^{d+b_a/2} \delta\, dw$$
$$= -\frac{c_0(J_1 \pm J_2 \pm J_3 - J_4)}{2 \ln (b/a)} \tag{36}$$

where the J's are as defined below. The following approximate results apply when the condition $d^2 \gg b^2$ is valid (in general, the choice $d = 10b$ yields a satisfactory approximation):

$$J_1 \equiv \int_{b_a/2}^{d+b_a/2} A_1\, dw \doteq \int_{b_a/2}^{d+b_a/2} \sinh^{-1} \frac{b}{w - b_a/2}\, dw \doteq b\left(1 + \ln \frac{2d}{b}\right) \tag{37a}$$

$$J_2 \equiv \int_{b_a/2}^{d+b_a/2} A_2\, dw \doteq \int_{b_a/2}^{d+b_a/2} \sinh^{-1} \frac{b}{w + b_a/2}\, dw$$
$$= (d + b_a) \sinh^{-1} \frac{b}{d + b_a} - b_a \sinh^{-1} \frac{b}{b_a}$$
$$+ b \ln \frac{d + b_a + \sqrt{(d + b_a)^2 + b^2}}{b_a + \sqrt{b_a^2 + b^2}} \tag{37b}$$

$$J_3 \equiv \int_{b_a/2}^{d+b_a/2} \ln D_2\, dw \doteq b_a\left[\sqrt{1 + \frac{b^2}{b_a^2}} - 1 - \ln \tfrac{1}{2}\left(1 + \sqrt{1 + \frac{b^2}{b_a^2}}\right)\right] \tag{37c}$$

$$J_4 \equiv \int_{b_a/2}^{d+b_a/2} \ln D_1\, dw \doteq b - a \tag{37d}$$

With (37a) to (37d), C_T may be determined directly from (36) in all cases for which b/a is not too small. In general, $b/a > 10$ leads to a fair approximation, as shown later for certain special cases.

Lumped Networks in General. With L_T and C_T determined for the main line for both the symmetrical and the antisymmetrical cases, an appropriate network may be constructed for use at the junction with an auxiliary series line. Since in most practical applications the series sections involve predominantly either the symmetrical or the antisymmetrical case alone, the complication involved in a separation into symmetrical and antisymmetrical parts is avoided, and either L_T^s and C_T^s or L_T^a and C_T^a must be determined rather than both pairs.

The determination of symmetrical and antisymmetrical values of L_{Ta} and C_{Ta} for connection in the auxiliary lines, as shown in Fig. 17.4, is straightforward. In the symmetrical case the two conductors of the auxiliary line are at the same potential, and transmission-line theory has no application. The impedance of the auxiliary conductors when driven with codirectional currents must be determined by the methods of antenna theory. Note, however, that account has been taken of coupling between the auxiliary conductors and the main line in the evaluation of C_T^s and L_T^s.

When the main line is driven so that the antisymmetrical case obtains, the auxiliary lines differ in no way from the main line, so that the formulas for L_{Ta}^{a} and C_{Ta}^{a} are the same as those for L_{T}^{a} and C_{T}^{a} if b and b_a are interchanged.

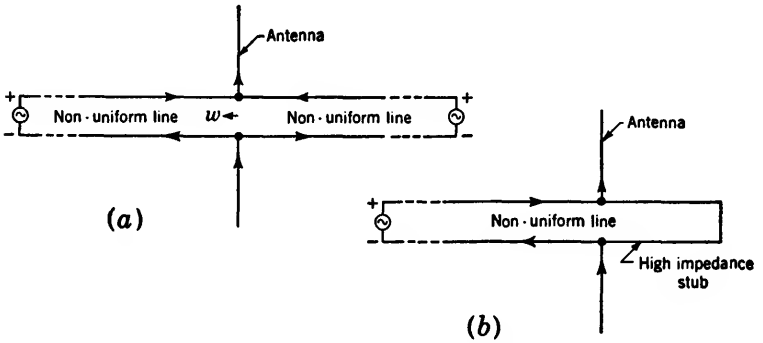


FIG. 17.5. Antenna symmetrically driven from two generators in (*a*) and with stub support in (*b*).

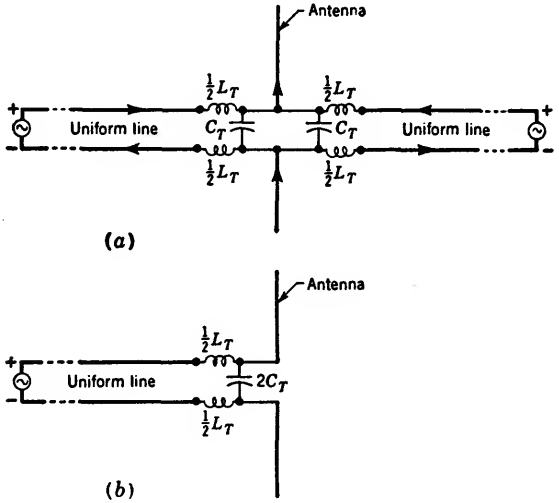


FIG. 17.6. Lumped junction networks for the circuits of Fig. 17.5.

Antenna Driven from Two Lines; Antenna with Stub Support. If the separation b_a of the two conductors of the series section is reduced to zero, these may be replaced by a single conductor, as in Fig. 17.5 or 17.6, insofar as the symmetrical case is concerned. This conductor is a center-driven antenna whose impedance cannot be determined from transmission-line theory. However, the transmission-line junction effect and the coupling between the feed line and the antenna may be obtained by specializing the general formulas derived in this section. In this

manner the constants of the junction-zone networks shown in Fig. 17.6 may be determined for use with uniform-line theory and the impedance of the isolated center-driven antenna, which is here assumed to be known.

Since the antenna in Fig. 17.5*a* is at right angles to the line and carries the sum of the equal and opposite currents of the two feeding lines, the inductive junction effect is obtained directly from L_T^s in (9) by setting b_a equal to zero. The formula is

$$L_T^s = -\frac{b-a}{\pi\nu} \tag{38}$$

and it is to be used in the circuit of Fig. 17.6*a*, in which each feeding line involves a total lumped inductance L_T^s.

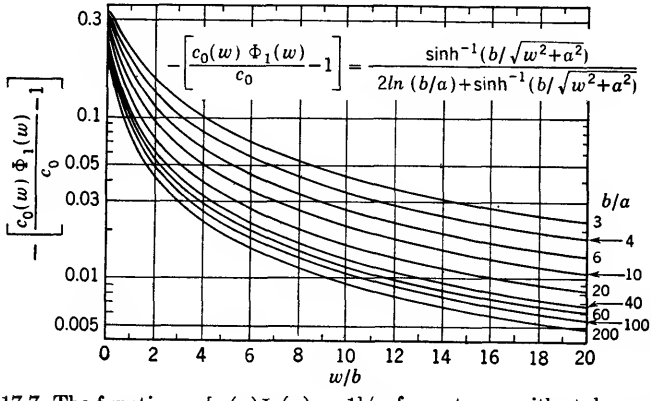


FIG. 17.7. The function $-[c_0(w)\Phi_1(w) - 1]/c_0$ for antenna with stub support.

Alternatively, if in the circuit of Fig. 17.5*b* the stub is adjusted in length to present a sufficiently high input impedance at its terminals compared with the impedance of the antenna, the current entering the stub is negligible compared with that entering the antenna or leaving the main line. It follows that the presence of the stub may be ignored except insofar as it contributes capacitively. A series inductance L_T^s need be used only in the main line, as shown in Fig. 17.6*b*.

The lumped capacitance C_T required to transform the circuits in Fig. 17.5*a* and *b* with nonuniform lines into Fig. 17.6*a* and *b* is obtained by omitting the term in A_2 in (24) and setting b_a equal to zero. The result is $A_1 = \sinh^{-1}(b/\sqrt{w^2+a^2})$ and $B = C$, so that, with A_2 absent, (28) reduces to

$$\left[\frac{c(w)-c_0}{c_0}\right]^s = -\frac{\sinh^{-1}(b/\sqrt{w^2+a^2})}{\sinh^{-1}(b/\sqrt{w^2+a^2})+2\ln(b/a)} \tag{39}$$

A plot of this quantity, proportional to the integrand in (11) for the special case under consideration, is given in Fig. 17.7 using w/b as vari-

able and b/a as parameter. The result of a numerical evaluation of (11) using (39) is shown in Fig. 17.8 in solid line. For comparison, a curve of the same quantity as evaluated from the approximate formula (36)—which is valid for sufficiently large values of b/a—is also shown. For the case at hand, J_2 in (37b) is omitted, and b_a is set equal to zero in J_1, J_3, and J_4. With $d = 10b$ the result is

$$C_T' \doteq -bc_0 \frac{1 + \ln (2d/b)}{2 \ln (b/a)} \doteq -bc_0 \frac{2}{\ln (b/a)} \tag{40}$$

The agreement of the approximate curve (shown in dashed line in Fig. 17.8) with the more accurate solid curve is increasingly good as b/a is

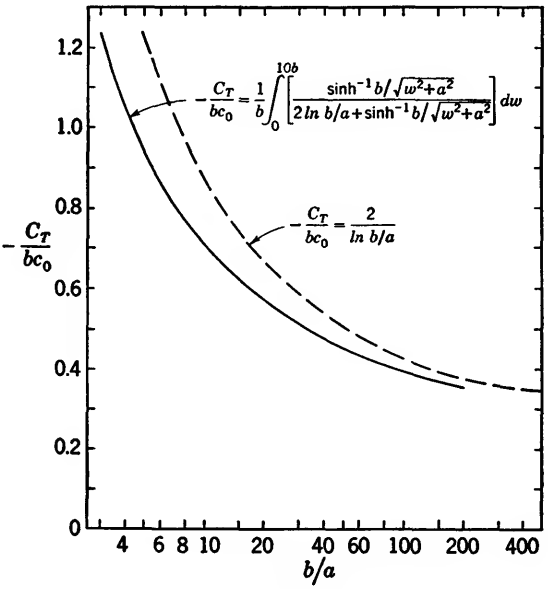


FIG. 17.8. Capacitance C_T for the junction network of Fig. 17.5; computed for $b = 0.01\lambda$.

made larger. For most practical purposes (40) may be used whenever b/a exceeds 20.

Note that in the stub-supported arrangement in Fig. 17.5b the capacitive coupling between the stub and the antenna may not be ignored, since, as a first approximation, the charge per unit length on each wire of the stub is the same as on the main line and on the antenna. The equivalent network involves C_T in parallel with the antenna for each section of line, or a total of $2C_T$, as shown in Fig. 17.6b.

Antenna as End Load on Two-wire Line. If the distance b_a between the two conductors of the auxiliary line is made infinite, the simple circuit of Fig. 17.9a remains. This consists of a two-wire line end-loaded

by a symmetrical antenna. In this case the series inductance L_T for use in the circuit of Fig. 17.9*b* is obtained from (9) by setting b_a equal to infinity. The result is

$$L_T^s = L_T^a = -\frac{b-a}{2\pi\nu} \tag{41}$$

The shunt capacitance C_T is obtained by allowing b_a to approach infinity in (28) or (29), while $w_1 \equiv w - b_a/2$ remains finite. Note that

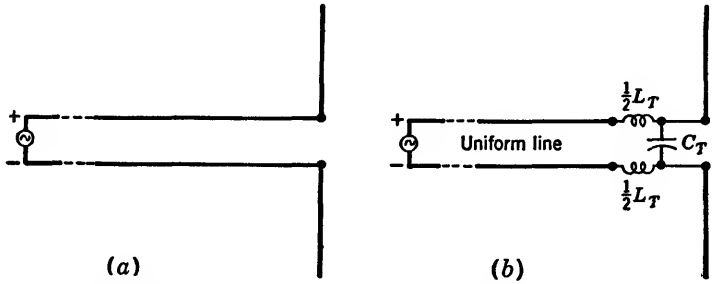


FIG. 17.9. Antenna center-driven from two-wire line. (*a*) Actual circuit with non-uniform line near junction. (*b*) Equivalent circuit for use with uniform-line theory.

w_1 is the distance $s - z$ from the end of the line and w is the distance from the point midway between the two conductors of the auxiliary line. For the special case at hand

$$A_1 = \sinh^{-1}\left(\frac{b}{\sqrt{w_1^2 + a^2}}\right)$$

$A_2 = 0$, $B = \sinh^{-1}(w_1/a) - \sinh^{-1}(w_1/b)$, and $C = \ln(b/a)$, so that

$$\frac{c(w_1) - c_0}{c_0} = -\frac{\sinh^{-1}(b/\sqrt{w_1^2 + a^2}) + \sinh^{-1}(w_1/a) - \sinh^{-1}(w_1/b) - \ln(b/a)}{\sinh^{-1}(b/\sqrt{w_1^2 + a^2}) + \sinh^{-1}(w_1/a) - \sinh^{-1}(w_1/b) + \ln(b/a)} \tag{42}$$

This quantity is plotted in Fig. 17.10 as a function of w/b, with b/a as parameter. By substituting (42) in (11) and evaluating the integral numerically, the solid curve in Fig. 17.11 is obtained. On the other hand, the approximate formula (36) using (37*a*) to (37*d*) gives the following simple results, with $b_a = \infty$ and $d = 10b$:

$$C_T \doteq -bc_0 \frac{\ln(2d/b)}{2\ln(b/a)} \doteq -bc_0 \frac{3}{2\ln(b/a)} \tag{43}$$

The approximate value of $-C_T/bc_0$ determined from (43) is shown in Fig. 17.11 in the dashed-line curve. It is seen to be in good agreement with the more accurate numerically determined solid-line curve for values

of b/a greater than 10. Since (43) is actually the first term in a series in inverse powers of 2 ln (b/a), this agreement for large values of b/a is very satisfactory.

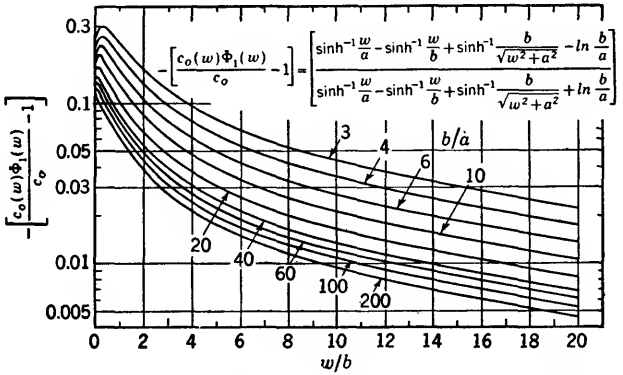


FIG. 17.10. The function $-[c_0(w)\Phi_1(w) - 1]/c_0$ for antenna as end load on a two-wire line.

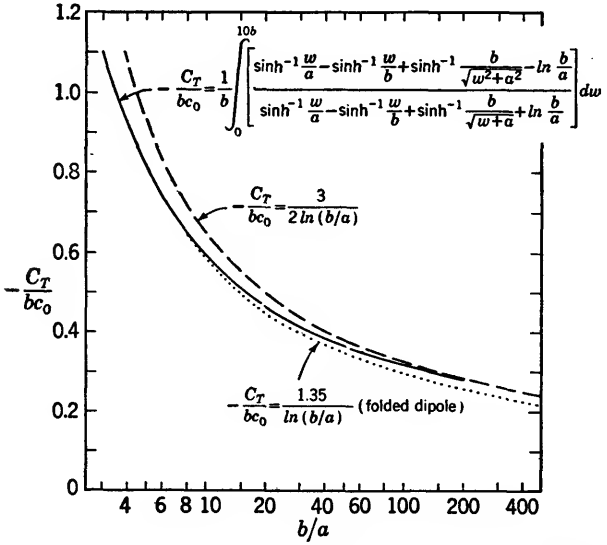


FIG. 17.11. Capacitance C_T for junction network of antenna as end load (Fig. 17.7) and folded dipole (Fig. 17.12); computed for $b = 0.01\lambda$.

The analysis of the circuit of Fig. 17.9*a* may be carried out by substituting the equivalent circuit in Fig. 17.9*b*, in which uniform-line theory may be used with L_T as in (41) and with C_T obtained from Fig. 17.11. The impedance of the antenna to be used is its isolated value, since C_T includes capacitive coupling to the line and there is no inductive coupling.

It is evident from the two special cases represented in Figs. 17.8 and

17.11 that reasonably accurate values of C_T may be evaluated from the approximate formulas (36) and (37a) to (37d), provided b/a is sufficiently great. More accurate results depend on the evaluation of the general integrals obtained from the substitution of (28) and (29) in (11).

Junction Network for Folded Dipole. The folded dipole differs from the balanced series junction in Fig. 17.1 in that there is no continuation

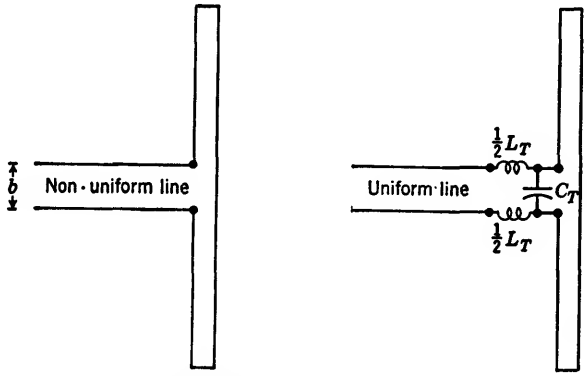


FIG. 17.12. Folded dipole and equivalent circuit.

of the main line to the right of the junction. A typical folded dipole is shown in Fig. 17.12a. In this case

$$l_0^e(w) = \frac{k_0(w)}{2\pi\nu_0} \qquad k_0(w) = \int_{b_a/2}^{\infty} \left(\frac{1}{R_a} - \frac{1}{R_b}\right) dw' \tag{44}$$

where R_a and R_b are as defined in (6). The integration gives

$$k_0(w) = B + \ln \frac{b}{a} \tag{45}$$

where B is as defined in (7b). It follows directly that the series inductance for use in Fig. 17.12b is given by

$$L_T = -\frac{b-a}{2\pi\nu_0} \tag{46}$$

The evaluation of C_T parallels the analysis following (11). Thus

$$V_L(w) = \frac{q_L(w)}{2\pi\epsilon}\left(B + \ln\frac{b}{a}\right) \tag{47}$$

$$V_T(w) = \frac{1}{2\pi\epsilon}\left[\int_{b/2}^{\infty} q_a(y')\left(\frac{1}{R_{1T}} - \frac{1}{R_{2T}}\right) dy' + \int_0^{\infty} q_a(y')\left(\frac{1}{R_{1b}} - \frac{1}{R_{2b}}\right) dy'\right] \tag{48}$$

where R_{1T}, R_{2T}, R_{1b}, and R_{2b} are as defined in (22a) and (22b). With

the same approximations as before, the integrations lead to

$$V_T(w) \doteq \frac{q_L(w)}{2\pi\epsilon} A_1' \tag{49}$$

where

$$A_1' = \sinh^{-1} \frac{b/2}{\sqrt{(w - b_a/2)^2 + a^2}} + \sinh^{-1} \frac{b/2}{\sqrt{(w - b_a/2)^2 + b^2}} \tag{50}$$

Note that A_1' differs from A_1 in (25) only in the occurrence of $b/2$ in place of b in the numerators. With $V_L(w)$ and $V_T(w)$ as defined above, it follows that

$$c(w) - c_0 = -c_0 \frac{A_1' + B - \ln (b/a)}{A_1' + B + \ln (b/a)} = -c_0 \frac{A_1' - \ln D_1}{A_1' - \ln D_1 + 2 \ln (b/a)} \tag{51}$$

where D_1 is as defined in (31). By setting

$$\delta \equiv \frac{A_1' - \ln D_1}{2 \ln (b/a)} \tag{52}$$

the first term in the series form of C_T is given by

$$C_T \doteq -c_0 \int_{b_a/2}^{d+b_a/2} \delta \, dw \tag{53}$$

Since A_1' differs from A only in the occurrence of $b/2$ in place of b, it follows with (37*a*) to (37*d*) that, with $d = 10b$,

$$C_T \doteq -bc_0 \frac{\ln (4d/b) - 1}{2 \ln (b/a)} \doteq -bc_0 \frac{1.35}{\ln (b/a)} \tag{54}$$

A curve of the approximate value of $-C_T/bc_0$ for the network in Fig. 17.12 is shown in Fig. 17.11 in dotted line. Since the corresponding approximate curve for the antenna as end load is in good agreement with the more exact value obtained numerically, it may be taken for granted that the approximate curve for the folded dipole is also a satisfactory representation, provided b/a exceeds 10.

18. Change in Spacing of a Two-wire Line. The distance between the parallel axes of the conductors of a two-wire line is b_l from $z = 0$ to a point $z = s_l$. From $z = s_l$ to $z = s_l + s_r$ the spacing is b_r. Both conductors of both sections of line, as well as the short pieces joining the two sections at $z = s_l$, have the radius a. It is assumed that the following inequalities are good approximations:

$$s_r^2 \gg b_r^2 \gg a^2 \qquad s_l^2 \gg b_l^2 \gg a^2 \tag{1}$$

A section of line near the change in spacing is shown in Fig. 18.1. In order to use uniform-line theory with the constant parameters l_{0l}^e and c_{0l} at all points to the left of the change in cross section and l_{0r}^e and c_{0r} to the right, it is necessary to determine the actual quantities $l^e(w)$ and

$c(w)$ on the left and $l^e(u)$ and $c(u)$ on the right. The variables w and u have their common origin at the junction of the two lines of different spacing, as shown in Fig. 18.1. In terms of the coordinate z, $w = s_l - z$ and $u = z - s_l$. The inductances $l^e(w)$ and $l^e(u)$ may be determined by assuming the line so driven from both ends that a current maximum is at the junction. Subject to the condition

$$(\beta b)^2 \ll 1 \tag{2}$$

the current is approximately constant in magnitude over distances $w \leqq 10b_l$ and $u \leqq 10b_r$ near the junction. The capacitances $c(w)$ and

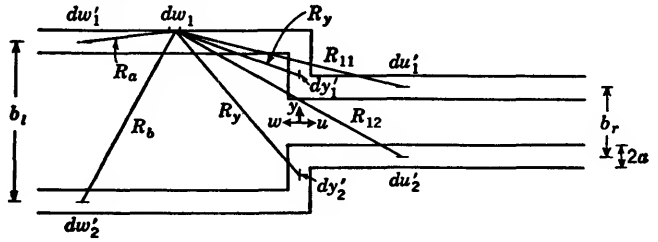


FIG. 18.1. Line with change in spacing.

$c(u)$ may be determined by reversing the generator at one end, so that a current minimum and voltage maximum are maintained at the junction. Subject to (2), the scalar potential difference in the range $w \leqq 10b_l$ and $w \leqq 10b_r$ is essentially constant.

Inductive Correction. The vector potential at dw_1 (Fig. 18.1) on the surface of conductor 1 at a distance w to the left of the junction is given by

$$A_{1z}(w) \doteq \frac{1}{4\pi\nu}\left[\int_0^\infty I(w')\left(\frac{1}{R_a} - \frac{1}{R_b}\right)dw' + \int^\infty I(u')\left(\frac{1}{R_{11}} - \frac{1}{R_{12}}\right)du'\right] \tag{3}$$

where $I(w')$ is the current in conductor 1 at a distance w' to the left of the junction and $I(u')$ is the current in conductor 1 at a distance u' to the right of the junction. It is assumed that both sections of line are balanced so that the current in conductor 2 is the negative of the current in conductor 1 for each value of w' or u'. The upper limits s_l and s_r have been replaced by infinity, since the conditions (1) on s_l and s_r lead to final results that are the same as those obtained with $s_l \doteq \infty \doteq s_r$. The exponential retardation factors $e^{-j\beta R}$ have been replaced by unity, since it is assumed that the condition $|\beta b| \ll 1$ is satisfied. The following distances occur in (3):

$$R_a = \sqrt{(w' - w)^2 + a^2} \qquad R_b = \sqrt{w' - w + b_l^2} \tag{4a}$$

$$R_{11} = \sqrt{(u' + w)^2 + m^2 + a^2} \qquad R_{12} = \sqrt{(u' + w)^2 + n^2} \tag{4b}$$

where $$m = \tfrac{1}{2}(b_l - b_r) \qquad n = \tfrac{1}{2}(b_l + b_r) \tag{4c}$$

It is assumed that $b_l \geqq b_r$.

Since the current is essentially constant in the junction zone, the leading terms in the Taylor expansions are

$$I(u') \doteq I(w) \doteq I(w') \tag{5}$$

The substitution of (5) in (3) and the subsequent integration give

$$l_l^e(w) \equiv \frac{W_z(w)}{I(w)} = \frac{2A_{1z}(w)}{I(w)} = \frac{1}{2\pi\nu}\left(2\ln\frac{b_l}{a} - \ln\frac{w+\sqrt{w^2+b_l^2}}{w+\sqrt{w^2+a^2}} + \ln\frac{w+\sqrt{w^2+n^2}}{w+\sqrt{w^2+m^2+a^2}}\right) \tag{6}$$

The lumped inductance required to permit the use of $l_{0l}^e = (1/\pi\nu)\ln(b_l/a)$ to the left of the junction is defined by

$$L_{Tl} = \int_0^d [l_l^e(w) - l_{0l}^e]\,dw \tag{7}$$

where $d \doteq 10b_l$. After the substitution of (6) in (7), the integration may be performed with the result

$$\begin{aligned} L_{Tl} &\doteq -\frac{1}{2\pi\nu}\left(m - a + \sqrt{m^2+a^2} + \frac{m^2}{d}\right) \\ &\doteq -\frac{1}{2\pi\nu}(m - a + \sqrt{m^2+a^2}) \end{aligned} \tag{8}$$

The expression for $l_r^e(u)$ is like (6), with w replaced by u and b_l by b_r. The evaluation of L_{Tr} is straightforward and results in

$$L_{Tr} \doteq \frac{1}{2\pi\nu}\frac{mb_r}{2d} \doteq 0 \tag{9}$$

Since $d \geqq 10b$, the terms with d in (8) and (9) are negligible.

The series inductance of the short conductors joining the two sections of line with different spacing is defined by

$$L_y = \frac{1}{I(0)}\left[\left(\int_{-b_l/2}^{b_l/2} - \int_{-b_r/2}^{b_r/2}\right) A_y(y)\,dy\right] \tag{10}$$

where

$$A_y(y) = \frac{1}{4\pi}\left[\left(\int_{-b_l/2}^{b_l/2} - \int_{-b_r/2}^{b_r/2}\right)\frac{dy'}{\sqrt{(y-y')^2+a^2}}\right] \tag{11}$$

These expressions may be combined to give

$$L_y = \frac{1}{4\pi\nu}\left[\int_{-b_l/2}^{b_l/2}\int_{-b_l/2}^{b_l/2}\frac{dy\,dy'}{\sqrt{(y-y')^2+a^2}} + \int_{-b_r/2}^{b_r/2}\int_{-b_r/2}^{b_r/2}\frac{dy\,dy'}{\sqrt{(y-y')^2+a^2}} - 2\int_{-b_l/2}^{b_l/2}\int_{-b_r/2}^{b_r/2}\frac{dy\,dy'}{\sqrt{(y-y')^2+a^2}}\right] \tag{12}$$

The following integrals are obtained, subject to (1):

$$L_y = \frac{1}{2\pi}\left[b_l \ln \frac{2b_l}{a} - \sqrt{b_l^2 + a^2} + a + b_r \ln \frac{2b_r}{a} - \sqrt{b_r^2 + a^2} + a \right.$$
$$\left. - 2\left(n \ln \frac{2n}{a} - \sqrt{n^2 + a^2} - m \ln \frac{2m}{a} + \sqrt{m^2 + a^2} \right) \right] \quad (13)$$

where $n = \frac{1}{2}(b_l + b_r) \qquad m = \frac{1}{2}(b_l - b_r) \qquad b_l \geqq b_r$

The total lumped inductance required at the junction in series with each conductor is $\frac{1}{2}(L_{Tl} + L_y)$, as shown in Fig. 18.2. With this lumped

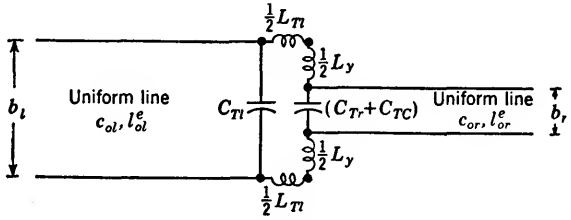


FIG. 18.2. Equivalent network for the junction in Fig. 18.1.

inductance, the inductance per unit length of each line may be assumed equal to the constant value l^e_{0l} or l^e_{0r} characteristic of uniform-line theory.

Capacitive Correction. The scalar potential at dw_1 on the surface of conductor 1 at a distance w from the change in spacing is given by the following integrals:

$$\phi_1(w) \doteq \frac{1}{4\pi\epsilon}\left[\int_0^\infty q(w') \left(\frac{1}{R_a} - \frac{1}{R_{bl}} \right) dw' + \int_0^\infty q(u') \left(\frac{1}{R_{11}} - \frac{1}{R_{12}} \right) du' \right.$$
$$\left. + \int_{\frac{1}{2}b_r}^{\frac{1}{2}b_l} \frac{q_1(y')}{R_{yl}}\, dy' + \int_{-\frac{1}{2}b_l}^{-\frac{1}{2}b_r} \frac{q_2(y')}{R_{yl}}\, dy' \right] \quad (14)$$

As in (3), exponential factors in (14) have been approximated by unity. The charges per unit length are $q_1 = q$ on conductor 1 and $q_2 = -q$ on conductor 2, with variables w', u', and y' appropriate to the three regions. In (14)

$$R_{yl} = \sqrt{(\tfrac{1}{2}b_l - y')^2 + w^2} \quad (15)$$

Since the scalar potential difference between conductors 1 and 2 is essentially constant near and at the junction when a voltage maximum is maintained across it, the charges per unit length on the two sides of the junction would be related as follows if uniform-line theory were accurate:

$$\frac{q(u')}{c_{0r}} \doteq \frac{q(w')}{c_{0l}} \quad (16)$$

where $$c_{0r} = \frac{\pi\epsilon}{\ln (b_r/a)} \qquad c_{0l} = \frac{\pi\epsilon}{\ln (b_l/a)} \quad (17)$$

In determining the departure of the scalar potential from that predicted by uniform-line theory near the junction, it is adequate to use the leading term in the unperturbed distribution of charge. That is,

$$q(w') \doteq q(w) \qquad q(u') \doteq q(w)\frac{c_{0r}}{c_{0l}} = kq(w) \tag{18}$$

where

$$k \equiv \frac{c_{0r}}{c_{0l}} = \frac{\ln (b_l/a)}{\ln (b_r/a)} \tag{19}$$

The charge per unit length on the connecting wires may be assumed to vary continuously and linearly. Thus

$$q_1(y') = q(y') \doteq q(w)\left[1 + (\tfrac{1}{2}b_l - y')\frac{k-1}{m}\right] \qquad \tfrac{1}{2}b_r \leqq y' \leqq \tfrac{1}{2}b_l \tag{20a}$$

$$q_2(y') = -q(y') \doteq -q(w)\left[1 + (\tfrac{1}{2}b_l + y')\frac{k-1}{m}\right] \qquad -\tfrac{1}{2}b_l \leqq y' \leqq -\tfrac{1}{2}b_r \tag{20b}$$

The following shorthand notation is used:

$$m \equiv \tfrac{1}{2}(b_l - b_r) \qquad n \equiv \tfrac{1}{2}(b_l + b_r) \qquad p \equiv \frac{k-1}{m} \tag{21}$$

Note that, since k does not differ much from unity in most cases and m equals or exceeds 1, p is usually quite small. With the notation introduced in (21) and with (18) and (20a,b), the following expression is obtained from (14):

$$V(w) = 2\phi_1(w) = \frac{q(w)}{2\pi\epsilon}\left\{\int_0^\infty \left(\frac{1}{R_a} - \frac{1}{R_{bl}}\right)dw' + k\int_0^\infty \left(\frac{1}{R_{11}} - \frac{1}{R_{12}}\right)du' + \int_{\frac{1}{2}b_r}^{\frac{1}{2}b_l}[1 + p(\tfrac{1}{2}b_l - y')]\frac{dy'}{R_y} - \int_{-\frac{1}{2}b_l}^{-\frac{1}{2}b_r}[1 + p(\tfrac{1}{2}b_l + y')]\frac{dy'}{R_y}\right\} \tag{22}$$

This may be integrated using standard formulas. The result is

$$V(w) = \frac{q(w)}{2\pi\epsilon}\left[2\ln\frac{b_l}{a} - F_l(w)\right] \tag{23}$$

where

$$F_l(w) = \ln\frac{w + \sqrt{w^2 + b_l^2}}{w + \sqrt{w^2 + a^2}} - k\ln\frac{w + \sqrt{w^2 + n^2}}{w + \sqrt{w^2 + m^2 + a^2}} - \operatorname{csch}^{-1}\frac{w}{m} + (1 + pb_l)\left(\operatorname{csch}^{-1}\frac{w}{b_l} - \operatorname{csch}^{-1}\frac{w}{n}\right) - p(\sqrt{w^2 + m^2} - w + \sqrt{w^2 + b_l^2} - \sqrt{w^2 + n^2}) \tag{24}$$

The capacitance per unit length on the left of the junction is

$$c_l(w) = \frac{2\pi\epsilon}{2\ln (b_l/a) - F_l(w)} \tag{25}$$

The capacitance per unit length of an infinite line is obtained by setting

$w = \infty$, for which $F(w \to \infty) = 0$. Hence

$$c_{0l} = \frac{\pi\epsilon}{\ln (b_l/a)} \tag{26}$$

In order to use uniform-line theory on the entire line to the left of the change in spacing, it is necessary to introduce a lumped capacitance C_{Tl} that compensates for the error made in using c_0 instead of $c_l(w)$. This capacitance is given by

$$C_{Tl} = \int_0^d [c_l(w) - c_0]\, dw = \frac{c_{0l}}{2 \ln (b_l/a)} \int_0^d \frac{F_l(w)}{1 - F_l(w)/[2 \ln (b_l/a)]}\, dw \tag{27}$$

where $d \doteq 10b$. This integral may be evaluated numerically. However, for sufficiently large values of b_l/a the ratio $F_l(w)/[2 \ln (b_l/a)]$ is small compared with unity, and (27) may be expanded in powers of this ratio. In particular, C_{Tl} may be approximated by the leading term in this expansion. Thus

$$C_{Tl} \doteq \frac{c_{0l}}{2 \ln (b_l/a)} \int_0^d F_l(w)\, dw \tag{28}$$

The integration in (28) can be carried out. If terms of the order of magnitude b_l^2 are neglected compared with $d^2 \doteq (10b_l)^2$, the following expression is obtained:

$$\begin{aligned} C_{Tl} \doteq \frac{c_{0l}}{2 \ln (b_l/a)} \{ & b_l - a - k(n - \sqrt{m^2 + a^2}) + \tfrac{1}{2}(1 + k)m \ln m \\ & - (1 + \tfrac{1}{2}pb_l)b_l \ln b_l + [1 + \tfrac{1}{4}(3b_l - b_r)]n \ln n \} \end{aligned} \tag{29}$$

The evaluation of C_{Tr} for the section of line to the right of the junction parallels that carried out for C_{Tl}. The potential difference at a distance u to the right of the change in spacing is given by

$$\begin{aligned} V(u) = 2\phi_1(u) = \frac{q(u)}{2\pi\epsilon} \Bigg\{ & \int_0^\infty \left(\frac{1}{R_a} - \frac{1}{R_{br}} \right) du' + \frac{1}{k} \int_0^\infty \left(\frac{1}{R_{11}} - \frac{1}{R_{12}} \right) dw' \\ & + \int_{\frac{1}{2}b_l}^{\frac{1}{2}b_l} \left[1 - \frac{p}{k} (y' - \tfrac{1}{2}b_r) \right] \frac{dy'}{R_{yr}} - \int_{-\frac{1}{2}b_l}^{-\frac{1}{2}b_r} \left[1 + \frac{p}{k} (y' + \tfrac{1}{2}b_r) \right] \frac{dy'}{R_{yr}} \Bigg\} \end{aligned} \tag{30}$$

where

$$\begin{aligned} R_a &= \sqrt{(u' - u)^2 + a^2} & R_b &= \sqrt{(u' - u)^2 + b_r^2} \\ R_{11} &= \sqrt{(u + w')^2 + m^2 + a^2} & R_{12} &= \sqrt{(u + w')^2 + n^2} \\ & & R_{yr} &= \sqrt{(\tfrac{1}{2}b_r - y)^2 + u^2} \end{aligned} \tag{31}$$

The integrations can all be carried out, and $V(u)$ expressed as follows:

$$V(u) = \frac{q(u)}{2\pi\epsilon} \left[2 \ln \frac{b_r}{a} - F_r(u) \right] \tag{32}$$

$$\text{where } F_r(u) = \ln \frac{u + \sqrt{u^2 + b_r^2}}{u + \sqrt{u^2 + a^2}} - \frac{1}{k} \ln \frac{u + \sqrt{u^2 + n^2}}{u + \sqrt{u^2 + m^2 + a^2}} - \operatorname{csch}^{-1} \frac{u}{m} + \left(1 + \frac{pb_r}{k}\right)\left(\operatorname{csch}^{-1} \frac{u}{n} - \operatorname{csch}^{-1} \frac{u}{b_r}\right) + \frac{p}{k}\left(\sqrt{u^2 + m^2} - u - \sqrt{u^2 + n^2} + \sqrt{u^2 + b_r^2}\right) \quad (33)$$

The capacitance per unit length on the right of the junction is

$$c_r(u) = \frac{2\pi\epsilon}{2 \ln (b_r/a) - F_r(u)} \quad (34)$$

The capacitance per unit length of an infinite line ($u = \infty$) is

$$c_{0r} = \frac{\pi\epsilon}{\ln (b_r/a)} \quad (35)$$

The lumped capacitance C_{Tr} required to correct for the use of c_0 in (35) in place of $c_r(u)$ in (34) is

$$C_{Tr} = \int_0^d [c_r(u) - c_{0r}]\, du = \frac{c_{0r}}{2 \ln (b_r/a)} \int_0^d \frac{F_r(u)}{1 - F_r(u)/[2 \ln (b_r/a)]}\, du \quad (36)$$

where $d \doteq 10b_r$. Corresponding to (28) for C_{Tl}, the approximate expression for C_{Tr} when b_r/a is sufficiently large is

$$C_{Tr} \doteq \frac{c_{0r}}{2 \ln (b_r/a)} \int_0^d F_r(u)\, du \quad (37)$$

If terms of magnitude b_r^2 or less are neglected compared with $d^2 \doteq (10b_r)^2$, the following result is obtained from (37):

$$C_{Tr} \doteq \frac{c_{0r}}{2 \ln (b_r/a)} \left\{2b_r - a - \frac{1}{k}(n + b_r - \sqrt{m^2 + a^2}) + \frac{k+1}{2k} m \ln m + \left(1 + \frac{pb_r}{2k}\right) b_r \ln b_r - \left[1 + \frac{p}{4k}(3b_r - b_l)\right] n \ln n\right\} \quad (38)$$

In addition to the corrections C_{Tl} and C_{Tr} required to permit the use of uniform-line theory, the capacitance between the two conductors, each of length $m = \frac{1}{2}(b_l - b_r)$, must be included. An approximate formula for the capacitance between coaxial cylinders is given by Küpfmüller (Ref. 12, p. 66). In terms of the notation of this section, the result is

$$C_{Tc} \doteq \frac{\pi\epsilon m}{\ln \left(\frac{m}{a} \sqrt{\frac{2b_r + m}{2b_r - 3m}}\right)} \quad (39)$$

The complete lumped network required to permit the use of uniform-line theory on each side of the junction of two sections of line with dif-

ferent axial separations is shown in Fig. 18.2. L_{Tr} and L_y are defined in (9) and (13), C_{Tl} in (29), C_{Tr} in (38), and C_{Tc} in (39).

19. Right-angle Bend in the Plane of a Two-wire Line. A right-angle bend in the plane of a two-wire line is shown in Fig. 19.1. Since such a bend is not symmetrical with respect to the two conductors of the transmission line, it necessarily has an unbalancing effect. An approximately equivalent lumped network for the bend is determined by separating the

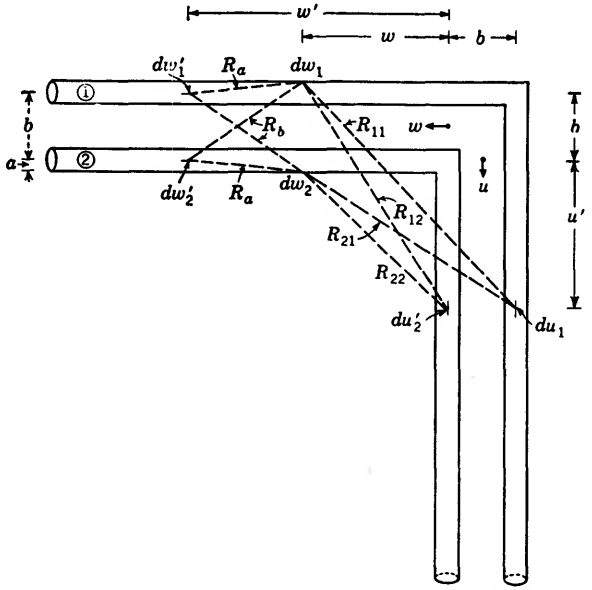


FIG. 19.1. Right-angle bend in the plane of a two-wire line.

voltage and current into symmetrical and antisymmetrical parts, as follows:

$$V(w) = V^{(s)}(w) + V^{(a)}(w) \qquad V(u) = V^{(s)}(u) + V^{(a)}(u) \tag{1}$$

$$I(w) = I^{(s)}(w) + I^{(a)}(w) \qquad I(u) = I^{(s)}(u) + I^{(a)}(u) \tag{2}$$

The symmetrical combination consists of the voltage, charge, and current maintained by the equal and codirectional generators shown in Fig. 19.2*a*; the antisymmetrical combination involves the voltage, charge, and current maintained by the equal and opposite generators shown in Fig. 19.2*b*. In terms of the coordinates illustrated in Fig. 19.1, the two cases may be summarized as follows:

Symmetrical Combination

$$I^{(s)}(w) = \tfrac{1}{2}[I(w) + I(u)] \tag{3a}$$

$$V^{(s)}(w) = \tfrac{1}{2}[V(w) - V(u)] \tag{3b}$$

$$q^{(s)}(w) = \tfrac{1}{2}[q(w) - q(u)] \tag{3c}$$

Antisymmetrical Combination

$$I^{(a)}(w) = \tfrac{1}{2}[I(w) - I(u)] \tag{4a}$$
$$V^{(a)}(w) = \tfrac{1}{2}[V(w) + V(u)] \tag{4b}$$
$$q^{(a)}(w) = \tfrac{1}{2}[q(w) + q(u)] \tag{4c}$$

Symmetrical Case. In the symmetrical case (Fig. 19.2*a*) there is a maximum of current and minimum of charge per unit length at the junction. Since the junction region extends only over a very small fraction of a wavelength, it may be assumed that the current is constant in the junction when the line is driven symmetrically and that the charge per unit length is zero.

The z component of the vector potential at an element dw on the surfaces of the horizontal conductors 1 and 2 (Fig. 19.1) is given by

$$A_{1z}(w) = \frac{1}{4\pi\nu}\int_{-b}^{\infty} I_{1z}(w')P_L(w,w')\,dw' \doteq \frac{I_{1z}(w)}{4\pi\nu}\int_{-b}^{\infty} P_L(w,w')\,dw' \tag{5a}$$

$$A_{2z}(w) = \frac{1}{4\pi\nu}\int_{0}^{\infty} I_{2z}(w')P_L(w,w')\,dw' \doteq \frac{-I_{1z}(w)}{4\pi\nu}\int_{0}^{\infty} P_L(w,w')\,dw' \tag{5b}$$

Note that z = −w and, as in Chap. II, Sec. 1, Eq. (9*a*),

$$P_L(w,w') = \frac{e^{-j\beta R_a}}{R_a} - \frac{e^{-j\beta R_b}}{R_b} \doteq \frac{1}{R_a} - \frac{1}{R_b} \tag{6a}$$

with $$R_a = \sqrt{(w' - w)^2 + a^2}$$
$$R_b = \sqrt{(w' - w)^2 + b^2} \tag{6b}$$

Since the conductor is very long to the left of the junction, the upper limit in the integrals may be made infinity. In the approximate expressions on the right in (5*a*,*b*) the leading term in the expansion of the current at w' about the point at w is substituted for the current. This is justified in Chap. II, Sec. 1. In addition, it has been assumed that $I_{2z}(w') \doteq -I_{1z}(w')$. Actually the line must be slightly unbalanced, so that the currents in the two wires are not exactly equal and opposite. However, in the approximate determination of the lumped network that is responsible for this unbalance, it is sufficiently accurate to assume the currents equal and opposite.

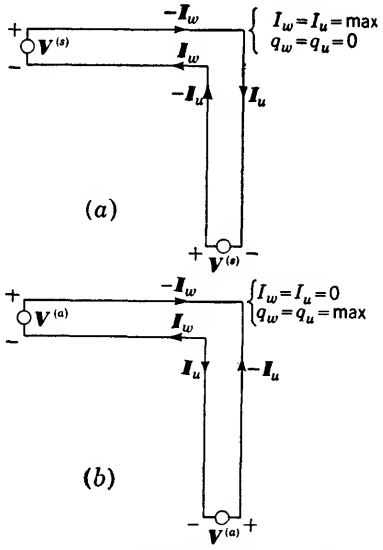


FIG. 19.2. Symmetrical and antisymmetrical driving conditions. (*a*) Symmetrical conditions. (*b*) Antisymmetrical conditions.

The integrals in (5*a*) and (5*b*) may be evaluated directly. The results are

$$A_{1z}(w) = \frac{I_{1z}(w)}{4\pi\nu}\left[2\ln\frac{b}{a} - \ln\frac{b+w+\sqrt{(b+w)^2+b^2}}{b+w+\sqrt{(b+w)^2+a^2}}\right] \tag{7a}$$

$$A_{2z}(w) = \frac{-I_{1z}(w)}{4\pi\nu}\left(2\ln\frac{b}{a} - \ln\frac{w+\sqrt{w^2+b^2}}{w+\sqrt{w^2+a^2}}\right) \tag{7b}$$

In the range $w \geqq 0$ the vector potential difference is

$$W_z(w) \equiv A_{1z}(w) - A_{2z}(w)$$
$$= \frac{I_{1z}(w)}{4\pi\nu}\left\{4\ln\frac{b}{a} - \ln\left[\frac{w+\sqrt{w^2+b^2}}{w+\sqrt{w^2+a^2}}\,\frac{b+w+\sqrt{(b+w)^2+b^2}}{b+w+\sqrt{(b+w)^2+a^2}}\right]\right\} \tag{8}$$

The inductance per unit length of line in the range $w \geqq 0$ is defined by $l_0^e(w) = W_z(w)/I_{z1}(w)$. The constant value l_0^e for uniform-line theory is given by $l_0^e(w)$ when w^2 is large compared with b^2 or when $w \to \infty$. The lumped series inductance L_T required to correct for the error made in using $l_0^e(w)$ in the range $w \geqq 0$ is given by

$$L_T = \int_0^d [l_0^e(w) - l_0^e]\,dw$$
$$= -\frac{1}{4\pi\nu}\int_0^d \ln\left[\frac{w+\sqrt{w^2+b^2}}{w+\sqrt{w^2+a^2}}\,\frac{w+b+\sqrt{(w+b)^2+b^2}}{w+b+\sqrt{(w+b)^2+a^2}}\right]dw$$

where d is of the order of magnitude of $10b$. The integration can be carried out directly to give

$$L_T = -\frac{1}{4\pi\nu}\{b[\sqrt{2} - \ln(1+\sqrt{2}) + \ln 2] - a\} = -\frac{1}{4\pi\nu}(1.21b - a) \tag{9}$$

Note that this value of L_T is considerably smaller than that given by Sec. 12, Eq. (5), for a line terminated in a conducting bridge. Since one of the conductors continues beyond the point $w = 0$ in the case of the bend but not in the case of the bridge, this is to be expected.

The section of conductor 1 extending from $w = 0$ to the corner at $w = -b$ is not a part of the two-wire line. It constitutes an additional inductance in series with conductor 1. It is defined by

$$L_1 = \int_0^b \frac{A_{1z}(w)}{I_{1z}(w)}\,dw \tag{10}$$

where $A_{1z}(w)$ is as given by (7*a*). The integration results in

$$L_1 = \frac{b}{2\pi\nu}\left(\ln\frac{b}{a} - 0.05\right) \doteq \frac{b}{2\pi\nu}\ln\frac{b}{a} \qquad \text{for } \frac{b}{a} > 5 \tag{11}$$

Since the vertical section of line is identical with the horizontal section in Fig. 19.1, the equivalent circuit for the symmetrical case is as shown in Fig. 19.3. Owing to the presence of the series inductance $2L_1$ in one conductor and not in the other, the line is unbalanced. If the voltage drop $2j\omega L_1 I_{1z}$ is replaced by an equivalent generator with emf $V_1 = -2j\omega L_1 I_{1z}$ and this is treated in two parts, as indicated in Fig. 19.4, it is clear that equal and opposite voltages $\frac{1}{2}V_1$ in the two conductors contribute to the balanced transmission-line currents, whereas equal and codirectional voltages $\frac{1}{2}V_1$ maintain currents in the two wires of the line which are equal and in the same direction. In the open-wire line these are antenna currents that radiate significantly. They cannot be determined by transmission-line theory. (In the corresponding problem with a shielded-pair line, the codirectional currents are in parallel, with the shield as the return conductor, as described in Chap. III, Sec. 14.)

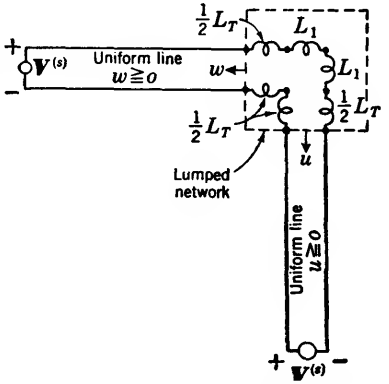


FIG. 19.3. Equivalent circuit for symmetrically driven line with bend.

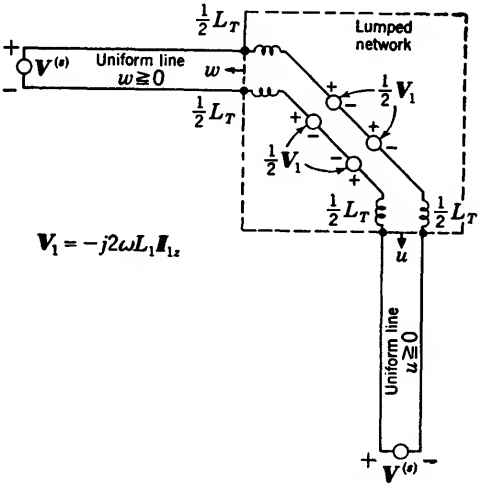


FIG. 19.4. Equivalent circuit for symmetrically driven line with bend.

Antisymmetrical Case. The antisymmetrical distribution illustrated in Fig. 19.2*b* is characterized by a vanishing current and a maximum of charge per unit length at the corners. The scalar potentials on the sur-

faces of the conductors at the elements dw_1 and dw_2 (Fig. 19.1) are

$$\phi_1(w) \doteq \frac{1}{4\pi\epsilon}\left[\int_{-b}^{\infty} q_1(w')\frac{e^{-j\beta R_a}}{R_a}\,dw' + \int_{0}^{\infty} q_2(w')\frac{e^{-j\beta R_b}}{R_b}\,dw' + \int_{-b}^{\infty} q_1(u')\frac{e^{-j\beta R_{11}}}{R_{11}}\,du' + \int_{0}^{\infty} q_2(u')\frac{e^{-j\beta R_{12}}}{R_{12}}\,du'\right] \quad (12a)$$

$$\phi_2(w) \doteq \frac{1}{4\pi\epsilon}\left[\int_{-b}^{\infty} q_1(w')\frac{e^{-j\beta R_b}}{R_b}\,dw' + \int_{0}^{\infty} q_2(w')\frac{e^{-j\beta R_a}}{R_a}\,dw' + \int_{-b}^{\infty} q_1(u')\frac{e^{-j\beta R_{21}}}{R_{21}}\,du' + \int_{0}^{\infty} q_2(u')\frac{e^{-j\beta R_{22}}}{R_{22}}\,du'\right] \quad (12b)$$

The antisymmetrical potential difference in the ranges $w \geqq 0$ and $u \geqq 0$ is

$$V^a(w) = \phi_1(w) - \phi_2(w) \doteq \frac{1}{4\pi\epsilon}\left[\int_{-b}^{\infty} q_1(w')P_L(w,w')\,dw' - \int_{0}^{\infty} q_2(w')P_L(w,w')\,dw' + \int_{-b}^{\infty} q_1(u')P_1(w,u')\,du' - \int_{0}^{\infty} q_2(u')P_2(w,u')\,du'\right] \quad (13)$$

where $P_L(w,w')$ is as defined in (6a) and where

$$P_1(w,u') = \frac{e^{-j\beta R_{11}}}{R_{11}} - \frac{e^{-j\beta R_{21}}}{R_{21}} \doteq \frac{1}{R_{11}} - \frac{1}{R_{21}} \quad (14a)$$

$$P_2(w,u') = \frac{e^{-j\beta R_{22}}}{R_{22}} - \frac{e^{-j\beta R_{12}}}{R_{12}} \doteq \frac{1}{R_{22}} - \frac{1}{R_{12}} \quad (14b)$$

R_a and R_b are defined in (6b). The other distances in (12a,b) and (14a,b) are

$$R_{11} = \sqrt{(w+b)^2 + (u'+b)^2 + a^2} \qquad R_{21} = \sqrt{(w+b)^2 + u'^2 + a^2} \quad (15a)$$

$$R_{12} = \sqrt{w^2 + (u'+b)^2 + a^2} \qquad R_{22} = \sqrt{w^2 + u'^2 + a^2} \quad (15b)$$

As a consequence of symmetry,

$$q_1(u') = q_1(w') \qquad q_2(u') = q_2(w') \quad (16)$$

Accordingly (13) may be expressed as follows:

$$V(w) \doteq \frac{1}{4\pi\epsilon}\left\{\int_{-b}^{\infty} q_1(w')[P_L(w,w') + P_1(w,w')]\,dw' - \int_{0}^{\infty} q_2(w')[P_L(w,w') + P_2(w,w')]\,dw'\right\} \quad (17)$$

Owing to the fact that conductor 1 is longer than conductor 2 by a length $2b$, the condition $q_2(w) = -q_1(w)$ (which applies when w and u are large compared with b) cannot be true at and near the corner if the total charge on conductor 1 is to be the negative of that on conductor 2,

so that the line as a whole is electrically neutral. Since conductor 1 is longer than a straight transmission line with the same mean length as the bent one by an amount b and since conductor 2 is shorter by the same amount, it follows that the charge per unit length on conductor 1 must decrease as the corner is approached, whereas the charge on conductor 2 must increase. Rough sketches of the nature of charge distributions $q_1(w)$ and $q_2(w)$ and of the electric field in the plane of the

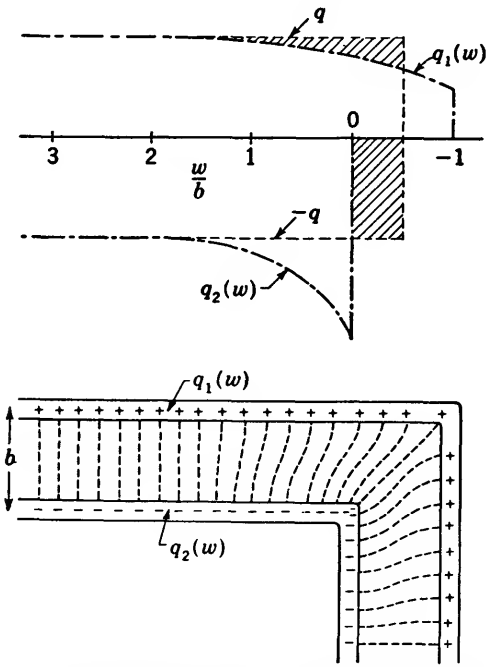


FIG. 19.5. Charge and electric-field distributions near a bend in a two-wire line (estimated).

conductors are shown in Fig. 19.5. Since the true distributions of charge are unknown and a rough approximation is adequate in order to determine the capacitance C_T for the lumped corrective network, the unperturbed distributions that would obtain if the line were straight with the same central length may be used. That is, the uniform charge per unit length q is assumed to be on conductor 1 and the uniform value $-q$ on conductor 2, both being equal in length. These uniform distributions are shown in Fig. 19.5 together with the varying ones $q_1(w)$ and $q_2(w)$. Note that the uniform charges are distributed over two conductors of equal length, so that the configuration of conductors actually assumed is that shown in Fig. 19.6. The total capacitance of this structure when uniformly charged does not differ greatly from that of the bend with the

actual *nonuniform* distributions. With each conductor in Fig. 19.6 uniformly charged in the range from $w = -b/2$ to the end of the line and from $u = -b/2$ to the other end, the scalar potential difference in the range $w \geqq 0$ is given by

$$V(w) \doteq \frac{q}{4\pi\epsilon} \int_{-b/2}^{\infty} [2P_L(w,w') + P_1(w,w') + P_2(w,w')]\, dw' \tag{18}$$

This expression may be integrated, with the following results:

$$V(w) \doteq \frac{q}{2\pi\epsilon} \left(2 \ln \frac{b}{a} - A - B + C \right) \tag{19a}$$

where

$$A \equiv \ln \frac{w + b/2 + \sqrt{(w + b/2)^2 + b^2}}{w + b/2 + \sqrt{(w + b/2)^2 + a^2}} \tag{19b}$$

$$B \equiv \ln \frac{b/2 + \sqrt{b^2/4 + (w + b)^2 + a^2}}{\sqrt{(w + b)^2 + a^2}} = \operatorname{csch}^{-1} \frac{2\sqrt{(w + b)^2 + a^2}}{b} \tag{19c}$$

$$C \equiv \ln \frac{b/2 + \sqrt{b^2/4 + w^2 + a^2}}{\sqrt{w^2 + a^2}} = \operatorname{csch}^{-1} \frac{2\sqrt{w^2 + a^2}}{b} \tag{19d}$$

The capacitance per unit length is given by

$$c(w) \equiv \frac{q}{V(w)} = \frac{2\pi\epsilon}{2 \ln (b/a) - A - B + C} \tag{20}$$

The lumped capacitance C_T required to permit the use of uniform-line theory is defined by

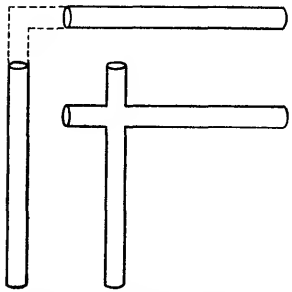


FIG. 19.6. Configuration of conductors used to determine $c(w)$ and C_T.

$$C_T \equiv \int_{-b/2}^{d-b/2} [c(w) - c_0]\, dw \tag{21}$$

where

$$c_0 \equiv \frac{\pi\epsilon}{\ln (b/a)} \tag{22}$$

With (20) and (22), it is clear that

$$c(w) - c_0 = c_0 \frac{A + B - C}{2 \ln (b/a) - A - B + C} \tag{23}$$

If (23) is substituted in (21), C_T may be evaluated. Since the integration has not been carried out in closed form, numerical methods must be used. Alternatively, if the ratio b/a is sufficiently great, the integrand in (21) may be expanded in inverse powers of the quantity $2 \ln (b/a)$, and only the leading term retained. When substituted in (21), this gives

$$C_T \doteq \frac{c_0}{2 \ln (b/a)} \int_{-b/2}^{d-b/2} (A + B - C)\, dw \tag{24}$$

If d is large compared with b, the following integrals are obtained:

$$\int_{-b/2}^{d-b/2} A\, dw \doteq b - a \tag{25a}$$

$$\int_{-b/2}^{d-b/2} (B - C)\, dw \doteq b \sinh^{-1} 1 - \frac{b^2}{2d} \doteq 0.88b \tag{25b}$$

It follows that

$$C_T \doteq \frac{(1.88b - a)c_0}{2 \ln (b/a)} \tag{26}$$

The equivalent circuit for the antisymmetrical bend is shown in Fig. 19.7, where C_T is given by (26) and uniform-line theory applies to the transmission line on each side of the bend beginning at $w = 0$ and $u = 0$ (Fig. 19.1).

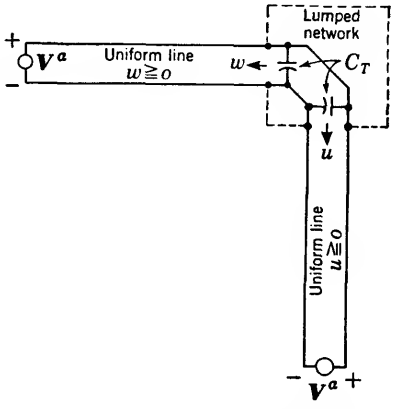


FIG. 19.7. Equivalent circuit for antisymmetrically driven line with bend.

The superposition of the symmetrical and antisymmetrical problems yields the general case of a line driven on one side of a right-angle bend by a generator $V_0 = V^s + V^a$ and loaded on the other side by an impedance Z_s that satisfies the relation $-I_s Z_s = V^s - V^a$. The appropriate lumped constant network is shown in Fig. 19.8, with L_T given by (9), L_1 by (11), and C_T by (26).

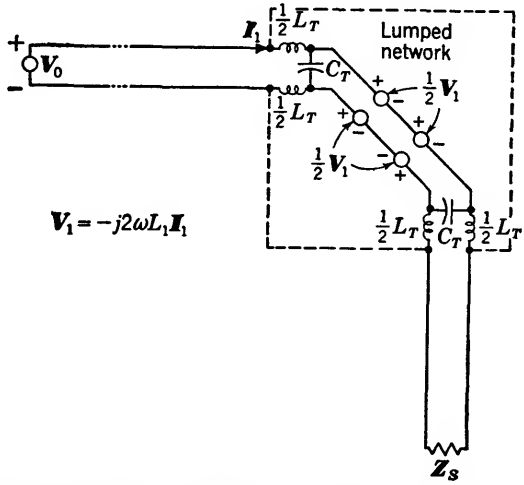


FIG. 19.8. Equivalent circuit for right-angle bend in the plane of a two-wire line.

20. Bends and T Junctions in Balanced Shielded-pair Lines. Balanced shielded-pair lines behave essentially like open two-wire lines with different line constants. If the shield is not too close to the inner conductors compared with their separation, the lumped corrective networks determined for the open two-wire line for a change in radius (Sec. 13), a bend (Sec. 15), a T junction (Sec. 16), series branches (Sec. 17), or a change in spacing (Sec. 18) may be adapted for use in corresponding situations in the balanced shielded-pair line. If the inductances and capacitances per unit length characteristic of the shielded-pair lines are substituted for the corresponding quantities for the open-wire line, reasonable approximations of the appropriate corrective networks may be obtained.

21. Bend in a Coaxial Line; T Junction. The analysis of a bend in a coaxial line cannot be carried out readily using the quasi-one-dimensional integrals for the scalar and vector potentials owing to the complicated three-dimensional nature of the problem. However, since it is possible (see Chap. I, Sec. 11) to construct a cage transmission line that has essentially the same electrical properties as a given coaxial line when both are straight, it may be expected that the behavior of the cage transmission line at a right-angle bend must approximate that of a coaxial line. Evidently the approximation improves as the number of conductors in the cage is increased. It may be assumed, therefore, that a lumped network that corrects for junction-zone errors in a cage transmission line may be applied to an equivalent coaxial line as a reasonable estimate.

Consider the bend shown in Fig. 21.1, in which the coaxial shield of inner radius a_2 is replaced by a four-conductor cage of the same radius in a region of length $d = 10a_2$ in each direction from the right-angle bend at $w = 0$, $y = 0$. The cage line is to be used only for determining the corrective network of lumped elements.

The bend in the five-wire cage line is a combination (with some added complications) of the two types of bends in a two-wire line described in Secs. 15 and 19. However, the unbalance resulting from the differences in length between conductors 1 and 3 (Fig. 21.1) and the central conductor may be ignored, since the equivalent generator in conductor 1 is equal and opposite to that in conductor 3 and the two conductors are connected in parallel at $w = 10d$, $u = 10d$. That is, the coaxial lines beyond $w = 10d$, $u = 10d$ are not unbalanced, since I_3 is smaller than $-\frac{1}{4}I$ by just the amount that I_1 exceeds $-\frac{1}{4}I$, so that $I_1 + I_3 = -\frac{1}{2}I$, where I is the current in the central conductor.

In the analysis of the coaxial line (Chap. I, Sec. 6) the potential of the shield (inner radius a_2) is zero, so that the potential difference is equal to the potential of the central conductor (radius a_1). Let it be assumed as an approximation that the same is true at the bend when the four-wire cage replaces the shield. In this case the potential differ-

ence is measured between the central conductor and wires 2 and 4 in the cage (Fig. 21.1). Let the radius of the circle around which the conductors of the cage are placed be the same as the radius a_2 of the coaxial line.

In calculating the axial vector potential on the central conductor, it may be assumed that the currents in all four conductors of the cage are equal; that is, $I_1 = I_2 = I_3 = I_4 = -\frac{1}{4}I$ in calculating the corrective inductance L_T. That is, the unperturbed current is used in calculating

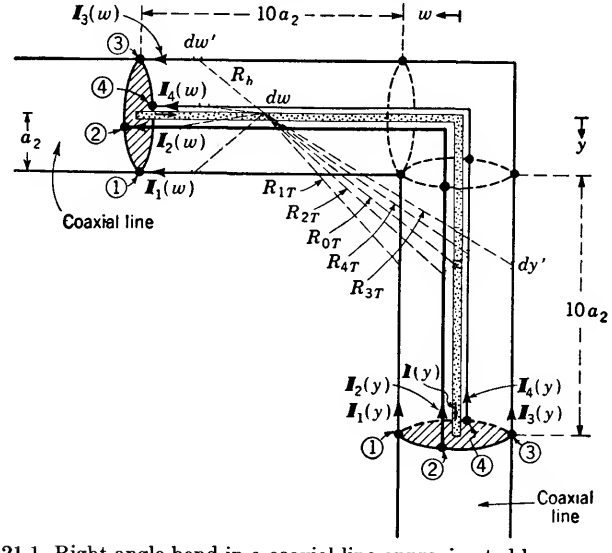


FIG. 21.1. Right-angle bend in a coaxial line approximated by a cage line.

the perturbation produced by the bend. The approximate vector potential at a point w on the central conductor of radius a_1 is given by

$$W_z(w) \doteq A_z(w) = \frac{I(w)}{4\pi\nu}\,[k_0 - F_1(w)] \tag{1a}$$

where $$k_0 - F_1(w) \equiv \int_0^d \left(\frac{1}{R_a} - \frac{1}{2R_b}\right) dw' - \int_{a_2}^d \frac{dw'}{4R_b} - \int_{-a_2}^d \frac{dw'}{4R_b} \tag{1b}$$

and $$R_a = \sqrt{(w' - w)^2 + a_1^2} \qquad R_b = \sqrt{(w' - w)^2 + a_2^2} \tag{2}$$

The corresponding expression for the scalar potential involves the complication that the charge per unit length on the shorter conductor 1 must be greater—and that in the longer conductor 3 smaller—than that in conductors 2 and 4. Account could be taken of this difference as in Sec. 19, but the simpler assumption $q_1 \doteq q_2 \doteq q_3 \doteq q_4 \doteq -\frac{1}{4}q$ will be used. The approximate scalar potential is

$$V(w) \doteq \phi_1(w) = \frac{q(w)}{4\pi\epsilon}\,[k_0 - F_1(w) + F_2(w)] \tag{3a}$$

where $k_0 - F_1(w)$ is as in (1*b*) and

$$F_2(w) \equiv \int_0^d \frac{dy'}{R_{0T}} - \int_0^d \frac{dy'}{2R_{2T}} - \int_{a_2}^d \frac{dy'}{4R_{1T}} - \int_{-a_2}^d \frac{dy'}{4R_{3T}} \tag{3b}$$

The following distances are involved:

$$R_{0T} = \sqrt{y'^2 + w^2 + a_1^2} \qquad R_{2T} = R_{4T} = \sqrt{y'^2 + w^2 + a_2'^2} \tag{4a}$$

$$R_{1T} = \sqrt{y'^2 + (w - a_2)^2} \qquad R_{3T} = \sqrt{y'^2 + (w + a_2')^2} \tag{4b}$$

The integrals $F_1(w)$ and $F_2(w)$ may be evaluated without difficulty. Subject to the condition $d^2 \gg a_2^2$, the following results are obtained:

$$k_0 = 2 \ln \frac{a_2}{a_1} \tag{5}$$

$$F_1(w) = \ln \frac{w + \sqrt{w^2 + a_2^2}}{w + \sqrt{w^2 + a_1^2}} + \tfrac{1}{4}\left(\sinh^{-1} \frac{w - a_2}{a_2} + \sinh^{-1} \frac{w + a_2}{a_2} - 2 \sinh^{-1} \frac{w}{a_2}\right) \tag{6}$$

$$F_2(w) = \tfrac{1}{4}\left[\ln (w^2 + a_2^2) + \ln |w^2 - a_2^2| - 2 \ln (w^2 + a_1^2) + \operatorname{csch}^{-1} \frac{|w - a_2|}{a_2} - \operatorname{csch}^{-1} \frac{w + a_2}{a_2}\right] \tag{7}$$

The variable inductance per unit length is

$$l^e(w) \equiv \frac{W_z(w)}{I(w)} = \frac{1}{4\pi\nu}[k_0 - F_1(w)] \qquad w \geqq 0 \tag{8}$$

The variable capacitance per unit length is

$$c(w) \equiv \frac{q(w)}{V(w)} = \frac{4\pi\epsilon}{k_0 - F_1(w) + F_2(w)} \tag{9}$$

The constant values l_0^e and c_0 are obtained by allowing w to approach infinity in (8) and (9). Since $F_1\ (w \to \infty) \to 0$ and $F_2\ (w \to \infty) \to 0$, it follows that

$$l_0^e = \frac{k_0}{4\pi\nu} = \frac{1}{2\pi\nu} \ln \frac{a_2}{a_1} \qquad c_0 = \frac{4\pi\epsilon}{k_0} = \frac{2\pi\epsilon}{\ln (a_2/a_1)} \tag{10}$$

The lumped inductance L_T and capacitance C_T that correct for the use of l_0^e and c_0 in place of $l^e(w)$ and $c(w)$ are

$$L_T = \int_0^d [l^e(w) - l_0^e]\, dw \qquad C_T = \int_0^d [c(w) - c_0]\, dw \tag{11}$$

The evaluation of L_T is simple. With (8) and (10) and the condition $d^2 \gg a_2^2$, the following is obtained:

$$L_T = -\frac{1}{4\pi\nu} \int_0^d F_1(w)\, dw \doteq -\frac{a_2 - a_1}{4\pi\nu} \tag{12}$$

The evaluation of C_T involves the integral in (11) with (9) and (10):

$$C_T = \frac{4\pi\epsilon}{k_0^2} \int_0^d \frac{F_1(w) - F_2(w)}{1 - [F_1(w) - F_2(w)]/k_0} \, dw \tag{13}$$

In general, this integral must be evaluated numerically. However, when k_0 is sufficiently great, the integrand in (13) may be expanded in powers of $1/k_0$, and the leading term used as an approximation. This is

$$C_T \doteq \frac{4\pi\epsilon}{k_0^2} \int_0^d [F_1(w) - F_2(w)] \, dw \tag{14}$$

Subject to the condition $d^2 \gg b^2$, this may be integrated into the following simple formula:

$$C_T \doteq \frac{4\pi\epsilon}{k_0^2} \left[a_2 \left(1 - \frac{\pi}{4}\right) - a_1 \right] \tag{15}$$

Since the line is identical in both directions from the bend, the same values of L_T and C_T apply. The complete equivalent network is shown in Fig. 21.2.

It is interesting to compare the approximate formulas (12) and (15) for L_T and C_T for the coaxial line with the corresponding ones for the two-wire line. These latter are obtained from Sec. 15, Eq. (18a), with $\theta = \pi/2$, and Sec. 15, Eq. (27a), with $M(\theta) = 1$. They are

$$L_T \doteq -\frac{b - a}{2\pi\nu}$$
$$C_T \doteq -\frac{2\pi\epsilon_0(b - a)}{3k_0^2} \tag{16}$$

where $k_0 = 2 \ln (b/a)$ and b is the distance between the two conductors, each of radius a. Since the inductance per unit length of the two-wire line is $l_0^e = (1/\pi\nu) \ln (b/a)$, the ratios

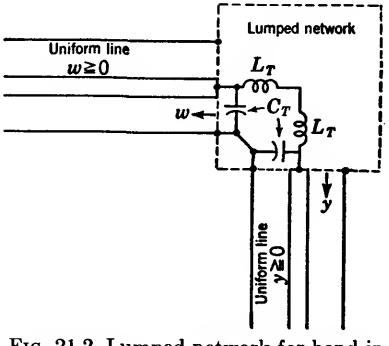


FIG. 21.2. Lumped network for bend in coaxial line.

$$\underbrace{\frac{L_T}{l_0^e} \doteq -\frac{b - a}{k_0}}_{\text{two-wire}} \qquad \underbrace{\frac{L_T}{l_0^e} \doteq -\frac{a_2 - a_1}{k_0}}_{\text{coaxial}} \tag{17}$$

are essentially the same. Note that C_T is negative for the two-wire line and positive for the coaxial line.

T Section in Coaxial Line. The analysis of a T section in a coaxial line may be carried out approximately by substituting a cage for the shield in the junction region, as shown in Fig. 21.3, and proceeding in a manner paralleling that for the right-angle bend.

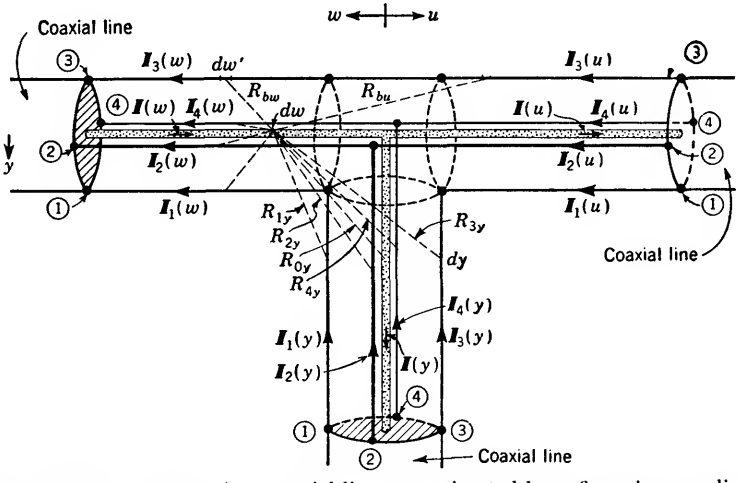


FIG. 21.3. Shunt T section in a coaxial line approximated by a five-wire cage line in the junction zone.

22. End Correction for a Coaxial Line When Driving an Antenna over a Ground Screen.[127] Consider a cylindrical antenna that is the extension of the inner conductor of a coaxial line through a hole in a conducting plane. As shown in Fig. 22.1, the radius a_1 of the antenna is also the radius of the inner conductor of the line; the radius a_2 of the hole in the ground screen is also the inner radius of the coaxial sheath. The admittance apparently loading the line at its end $w = 0$ is Y_{sa}; with perfect conductors this is the admittance looking toward the load at $w = \lambda/2$.

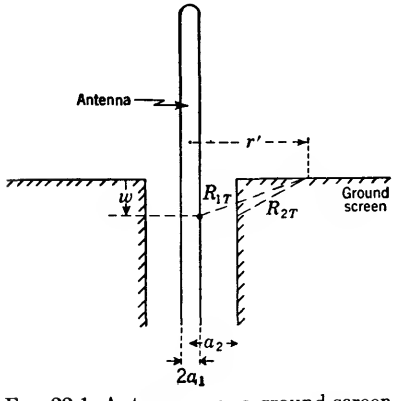


FIG. 22.1. Antenna over a ground screen.

Conventional transmission-line formulas are based on the assumptions that (1) the charges per unit length $q_1(w)$ and $q_2(w)$ on the two conductors of the line at a given cross section w are equal and opposite, so that $q_2(w) = -q_1(w)$, and that (2) the capacitance per unit length, defined as $c(w) = V(w)/q(w)$, is equal to the constant capacitance per unit length c_0, characteristic of an infinitely long line for all values of w. These are good approximations at distances d from $w = 0$ which are large compared with $a_2 - a_1$. Near $w = 0$, $q_2(w)$ is not exactly equal to $-q_1(w)$, and $c(w)$ is not a constant. Since primary interest is in the antenna and inner conductor, $c(w)$ must be defined in terms of the charge per unit

length on the inner conductor. Changes in $q(w)$ near $w = 0$ and variations in $c(w)$ from c_0 are consequences of transmission-line end effect and of the capacitive coupling between the line, on the one hand, and the antenna and ground screen, on the other.

The ideal theoretical admittance $Y_0 = 1/Z_0$ of the antenna assumes that the antenna is driven by a discontinuity in scalar potential at $w = 0$. The relations between Y_{sa} and Y_0 may be represented approximately as follows:

$$Y_{sa} \to Y_0 \text{ as } \frac{a_2}{a_1} \to 1 \tag{1}$$

$$Y_{sa} \doteq Y_0 + j\omega C_T \qquad \frac{a_2}{a_1} > 1 \tag{2}$$

where

$$C_T = \int_0^d [c(w) - c_0]\, dw \tag{3}$$

Evidently, if use is to be made of the ideal admittance Y_0 in conjunction with the measurable apparent admittance Y_{sa}, a knowledge of C_T is necessary.

Since the vector potential at w is determined from the current in the inner conductor (as shown in Chap. I, Sec. 6) and this is continuous at $w = 0$, it follows that $l^e(w) \doteq l_0^e$ for all values of $w \geqq 0$, so that

$$L_T \doteq 0 \tag{4}$$

Therefore the corrective terminal-zone network consists of the shunt capacitance C_T, defined in (3).

The evaluation of $c(w)$ and, from it, of C_T may be accomplished in the usual manner by calculating the scalar potential difference V at a distance w from the end of the line (Fig. 22.1). Since it is shown in Chap. I, Sec. 6, that the potential $\phi_2(w)$ calculated from the charges on the inner surface of the shield contributes nothing to the potential difference $V(w) = \phi_1(w) - \phi_2(w)$, it is sufficient to calculate $V(w)$ from the charges on the inner conductor, the antenna, and the ground screen. However, since the inner conductor joins the antenna with a continuous distribution of charge, the potential difference $V_{La}(w)$ for $w \geqq 0$ which is maintained by the charges on the inner conductor and the antenna is essentially the same as if the coaxial line continued. That is,

$$\frac{V_{La}(w)}{q_L(w)} = \frac{1}{c_0} = \frac{1}{2\pi\epsilon} \ln \frac{a_2}{a_1} \tag{5}$$

It follows that, with $V(w) = V_{La}(w) + V_g(w)$, where $V_g(w)$ is the potential difference at w on the line due to the charges on the ground screen,

$$\frac{V(w)}{q_L(w)} = \frac{1}{c(w)} = \left[\frac{1}{c_0} + \frac{V_g(w)}{q_L(w)}\right] \tag{6}$$

Referring to Fig. 22.1, the potential difference $V_g(w)$ is

$$V_g(w) = \frac{1}{4\pi\epsilon}\int_0^{2\pi}\int_{a_2}^{\infty}\frac{q(r')}{2\pi}\left(\frac{1}{R_{1T}} - \frac{1}{R_{2T}}\right)r'\,dr'\,d\theta' \tag{7}$$

where

$$\begin{aligned} R_{1T} &= \sqrt{r'^2 - 2a_1r'\cos\theta' + a_1^2 + w^2} \\ R_{2T} &= \sqrt{r'^2 - 2a_2r'\cos\theta' + a_2^2 + w^2} \end{aligned} \tag{8}$$

and where $q(r')$ is the total charge on a ring of unit width at radius r'. Since the charge per unit length on the line must be continuous, it may be assumed that $q(r') \doteq q_L(w)$, so that

$$V_g(w) = \frac{q_L(w)}{4\pi\epsilon}F_g(w) \tag{9}$$

where

$$F_g(w) \equiv \frac{1}{\pi}\int_0^{\pi}\int_{a_2}^{\infty}\left(\frac{1}{R_{1T}} - \frac{1}{R_{2T}}\right)r'\,dr'\,d\theta' \tag{10}$$

The substitution of (9) in (6) gives

$$\frac{c(w) - c_0}{c_0} = -\frac{F_g(w)}{F_g(w) + 2\ln(a_2/a_1)} \tag{11}$$

so that the lumped shunt capacitance required to correct for the use of c_0 in place of $c(w)$ is

$$C_T = \int_0^d [c(w) - c_0]\,dw = -c_0\int_0^d \frac{F_g(w)}{F_g(w) + 2\ln(a_2/a_1)}\,dw \tag{12}$$

where $d \doteq 10a_2$.

The exact evaluation of $F_g(w)$, as defined in (10), leads to complicated integrals of elliptic integrals. An approximate evaluation is accomplished by dividing the range of integration with respect to θ' into four regions, in each of which the integrand is assumed to be constant at a middle value. By choosing the middle values in the full range of 2π at $\theta = 0$, $\pi/2$, π, and $3\pi/2$, the integral in (10) may be approximated as follows:

$$\begin{aligned} F_g(w) \doteq\ & \tfrac{1}{4}\int_{a_2}^{\infty}\left(\frac{1}{\sqrt{(r' - a_2)^2 + w^2}} - \frac{1}{\sqrt{(r' - a_1)^2 + w^2}}\right)dr' \\ & + \tfrac{1}{2}\int_{a_2}^{\infty}\left(\frac{1}{\sqrt{r'^2 + a_2^2 + w^2}} - \frac{1}{\sqrt{r'^2 + a_1^2 + w^2}}\right)dr' \\ & + \tfrac{1}{4}\int_{a_2}^{\infty}\left(\frac{1}{\sqrt{(r' + a_2)^2 + w^2}} - \frac{1}{\sqrt{(r' + a_1)^2 + w^2}}\right)dr' \end{aligned} \tag{13}$$

This expression integrates into

$$\begin{aligned} F_g(w) = \tfrac{1}{4}\Bigg[& \sinh^{-1}\frac{a_2 - a_1}{w} + \ln\frac{w^2 + a_2^2}{w^2 + a_1^2} \\ & - 2\ln\frac{a_2 + \sqrt{2a_2^2 + w^2}}{a_2 + \sqrt{a_2^2 + a_1^2 + w^2}} - \ln\frac{2a_2 + \sqrt{4a_2^2 - w^2}}{a_2 + a_1 + \sqrt{(a_2 + a_1)^2 + w^2}}\Bigg] \end{aligned} \tag{14}$$

Since the last two terms in (14) differ only slightly from 1 even when $w = 0$, they may be neglected. The remaining terms may be arranged as follows:

$$F_g(w) \doteq \tfrac{1}{4}\left[\sinh^{-1}\frac{1 - a_1/a_2}{w/a_2} + \ln\left(1 + \frac{w^2}{a_2^2}\right) - \ln\left(\frac{a_1^2}{a_2^2} + \frac{w^2}{a_2^2}\right)\right] \quad (15)$$

The function $[c(w) - c_0]/c_0$ obtained by substituting (15) in (11) is represented graphically in Fig. 22.2, with w/a_2 as the independent variable and a_2/a_1 as parameter. Although curves are shown for a wide range

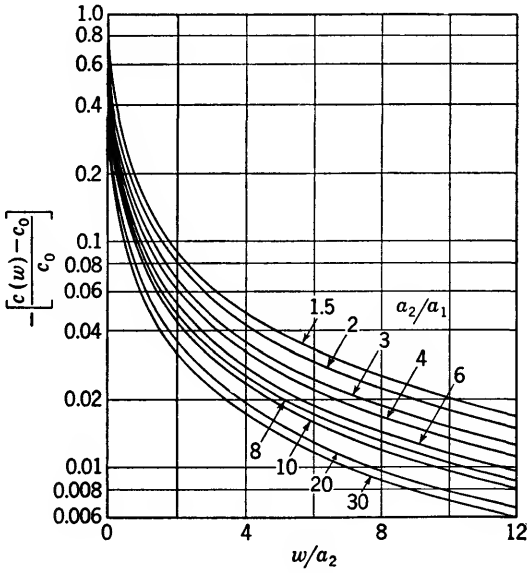


FIG. 22.2. The function $-[c(w) - c_0]/c_0$ for a coaxial line driving an antenna over a ground screen.

of values of a_2/a_1, those for which a_2/a_1 is smaller than about 7 are not accurate for determining C_T. This follows from the fact pointed out in the footnote relating to Chap. I, Sec. 3, formulas (30*a*,*b*), that the integral for the scalar potential on the surface of a cylindrical conductor, when expressed in terms of the charge per unit length, is a good approximation only when the integration is extended over distances that are at least $5a_1$ in each direction from w. Since the difference $c(w) - c_0$ is actually significant only over a range of w from zero to very small integral multiples of $a_2 - a_1$, it is clear that, in order to have $a_2 - a_1$ greater than $5a_1$, a_2/a_1 must be at least as great as 7. The validity of this argument may be questioned on the grounds that, in evaluating the part of the potential determined by the charges on the inner conductor and on the antenna, the integration is actually carried out over very

much greater distances than $5a_1$. Moreover the ratio of the uniform charge distribution on the inner conductor and the antenna to the potential difference due to this distribution yields only the constant c_0. But this argument overlooks the fact that in this approximate analysis the ratio of potential difference to charge is obtained by assuming a constant charge and determining the resultant potential difference as a function of w. Actually it is the potential difference which is constant and the charge which is a function of w; and the nonzero value of $c(w) - c_0$ within a distance of the order of magnitude of $a_2 - a_1$ of the end of the line properly corresponds to a charge distribution, and not a voltage distribution, which is nonuniform over this distance. Therefore the correct calculation of potential difference from the potential integrals using the true charge distribution would involve the determination of an effect produced by a variation in the charge per unit length which is confined to a range of the order of magnitude of $a_2 - a_1$. The contribution to the potential obtained from an integration over such a distance is not accurate unless the distance is at least $5a_1$ in each direction. Since this is approximately true only when $a_2/a_1 \geqq 7$, it follows that the curves in Fig. 22.2 are useful for determining C_T only over this range.

By determining the areas under the curves in Fig. 22.2 (when drawn to a linear scale) in the range $w/a_2 = 0$ to $w/a_2 = 10$ by numerical methods, C_T as defined in (12) may be evaluated. It is shown in solid line in Fig. 22.3 as a function of a_2/a_1 for two values of a_1/λ. As pointed out above, only the ranges $a_2/a_1 > 7$ are satisfactory approximations. The dimensionless quantity $-C_T/a_2c_0$ is shown in solid line in Fig. 22.4 for a_2/a_1 greater than 7.

In order to obtain an expression for C_T for values of a_2/a_1 near 1, it may be noted that, when $a_2 - a_1$ is small compared with a_1 and a_2, the potential at any point in the coaxial line is determined principally by the charges on the adjacent parallel surfaces, so that they may be represented approximately by parallel *planes*, i.e., cylinders of infinite radius instead of sections of circular cylinders. Moreover, since $(a_2 - a_1)/\lambda_0$ is necessarily small compared with 1, the distribution of charge near $w = 0$ must correspond closely to an electrostatic one. This suggests the determination of C_T for a coaxial line with $a_2 - a_1$ very small by representing the coaxial line by a parallel-plate region extending from $w = 0$ to $w = \infty$, with the plates separated a distance $a_2 - a_1$. One of the plates extends over the range $-\infty \leqq w \leqq \infty$; the other makes a right-angle bend at $w = 0$ and then continues to infinity.

The distribution of surface charge per unit area η on both the straight and the bent plates may be determined by conformal transformations using the Schwarz-Christoffel formula. The part of the solution of interest in the problem at hand is the distribution of charge on the straight plate in the range from $w = 0$ to $w = \infty$, where it is parallel to the

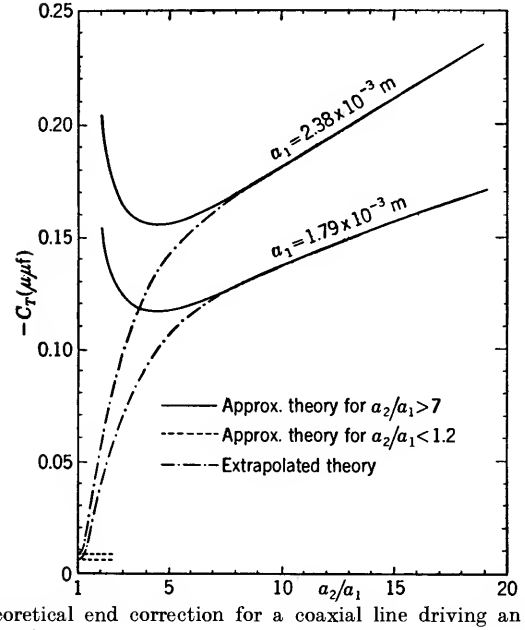


FIG. 22.3. Theoretical end correction for a coaxial line driving an antenna over a ground screen at $\lambda = 60$ cm.

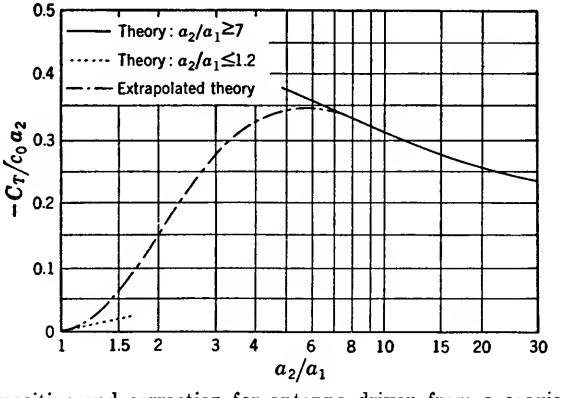


FIG. 22.4. Capacitive end correction for antenna driven from a coaxial line over a ground screen.

second plate. It is this range which corresponds to the inner conductor of the coaxial line when this has an infinite radius. The static distribution of charge may be obtained by applying a potential V across the plates. The transformations involved in the solution for the surface density of charge η are described in the literature.[1,30,32] The pertinent result is the ratio of charge density $\eta(w)$ on the straight plate at a distance w from the plane $w = 0$, where the second plate is bent to the

charge density $\eta(\infty)$ sufficiently far into the parallel-plate region so that a constant value is reached. This ratio is

$$\frac{\eta(w)}{\eta(\infty)} = \frac{1}{\sqrt{1-t}} \tag{16}$$

where the relation

$$\frac{w}{a_2 - a_1} = -\frac{1}{\pi}[2\sqrt{1-t} - \ln(\sqrt{1-t}+1) + \ln(\sqrt{1-t}-1)] \qquad t \leqq 0 \tag{17}$$

obtains. A plot of $\eta(w)/\eta(\infty)$ as a function of $w/(a_2 - a_1)$ is given in Fig. 22.5 for the part of the straight plate which forms half of the parallel-plate region near $w = 0$. The charge density on this plate *decreases* as

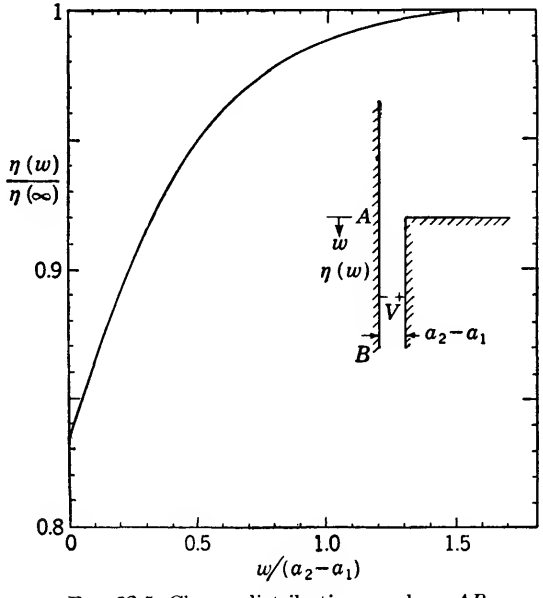


FIG. 22.5. Charge distribution on plane AB.

w decreases toward zero, whereas it is readily shown that, on the corresponding part of the bent plate, the density of charge increases as $w = 0$ is approached from within the parallel-plate region. Note particularly that the entire significant variation in $\eta(w)$ occurs in a distance of magnitude $a_2 - a_1$ from $w = 0$. A representation of the electric-field lines and the equipotentials is given in Fig. 22.6. It is significant to note that the electric lines are curved near $w = 0$, so that the electric line that ends at A (Fig. 22.6) on the straight plate originated at a point on the second plate which is not at $w = 0$.

Since V is the constant potential difference, it follows that

$$\frac{2\pi a_1 \eta(w)}{2\pi a_1 \eta(\infty)} = \frac{c(w)}{c_0} \tag{18}$$

where c_0 is the capacitance per unit length of an infinitely long line. Hence Fig. 22.4 is also a measure of the change in capacitance per unit area as w approaches zero from infinity.

In order to determine the lumped capacitance C_T required to compensate for the error made in using c_0 instead of $c(w)$ near $w = 0$, it is necessary to form (3) and to choose d sufficiently great so that $c(d) \doteq c_0$. The evaluation of C_T from (3), using (18) and Fig. 22.5, gives

$$\begin{aligned} C_T &\doteq -0.0683(2\pi a_1 \epsilon) \\ &\doteq -3.8 a_1 \quad \mu\mu\text{f} \end{aligned} \tag{19}$$

with a_1 in meters. For the two values of a_1 for which curves are shown in Fig. 22.3, $C_T = -0.0068\ \mu\mu$f for the value of $a_1 = 0.179$, and $C_T = -0.0090\ \mu\mu$f for $a_1 = 0.238$ cm. These are the limiting constant values that are good approximations for $a_2/a_1 < 1.2$. They are shown dotted in Fig. 22.3.

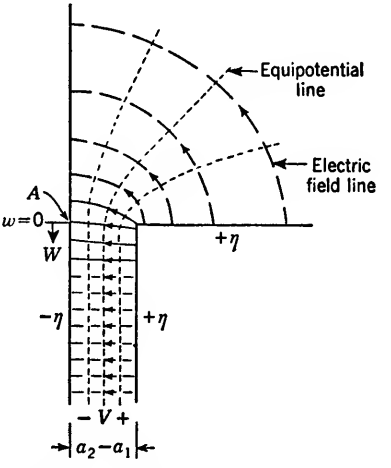


FIG. 22.6. Equipotential lines of electric field.

With approximate theoretical values available for $a_2/a_1 > 7$ and for $a_2/a_1 < 1.2$, it is possible to construct smooth, continuous curves for the range of a_2/a_1 between 1.2 and 7. Such extrapolated curves are shown in Fig. 22.3. From these the ratio $-C_T/a_2c_0$ may be computed, and the single extrapolated curve shown in Fig. 22.4 determined. Since both of the extrapolated curves in Fig. 22.3 must yield the single curve in Fig. 22.4, a check on the shapes of the curves in Fig. 22.3 is provided, and the accuracy of the single curve in Fig. 22.4 is thereby enhanced.

It may be assumed that the combined curve for the dimensionless ratio $-C_T/a_2c_0$ in Fig. 22.4 is a satisfactory approximation of the lumped corrective capacitance C_T required if uniform-line theory is used to determine the properties of an antenna as end load in the arrangement in Fig. 22.1. Satisfactory experimental verification of Fig. 22.4 has been obtained by Hartig.[120,127]

PROBLEMS

1. The input terminals 11 of a symmetrical two-terminal-pair network are connected as load to a main transmission line. The output terminals 22 of the network

are connected to an auxiliary short-circuited section of line of variable length l. The complex reflection coefficient $\Gamma = \Gamma e^{j\psi}$ of the load terminating the main line at 11 is determined from measurements on the main line to have the following values for the indicated lengths l of the auxiliary line:

l/λ	0	$\frac{1}{8}$	$\frac{1}{4}$	$\frac{3}{8}$
Γ	0.52	0.52	0.85	0.93
ψ, deg	62	127	214	235

Determine the power dissipated in the network and the power transmitted to a matched load connected across terminals 22.

2. Determine the impedance elements of a T section that is equivalent to the network between terminals 11 and 22, as described in Prob. 1.

3. The dielectric constant of a sample of material is measured using the maximum-shift method. The thickness of the sample is 2 cm; the measured maximum shift is 20 cm at a wavelength of 150 cm. What is the dielectric constant of the sample?

4. What would be the minimum shift in Prob. 3 if the sample were 4 cm thick? How is this related to the measurement of dielectric constant using a coaxial cavity and a method in which the resonant length of the cavity is determined when the cavity is empty and again when the sample is placed against the piston terminating one end of the cavity?

5. For a given sample of thickness 0.2 cm the minimum shift is 4 cm, and the maximum shift is 10 cm at a wavelength of 1 m. What are the relative dielectric constant and permeability of the sample?

6. Two polystyrene beads ($\epsilon_r = 2.6$) each of length 0.25 in. are spaced a distance v between adjacent edges in an air-filled coaxial line terminated in a matched wideband load.

(*a*) Determine v so that the standing-wave ratio $S = \coth \rho$ on the main line between the generator and the nearer bead is unity at 3,000 Mc/sec.

(*b*) With v as in (*a*) and assuming the load to be matched continuously, determine ρ and S as the frequency is varied from 1,500 to 9,000 Mc/sec. Plot S as a function of frequency on semilog paper. (It is sufficient to determine S at 1,500, 2,000, 3,000, 6,000, and 9,000 Mc/sec.)

7. Two sections of flexible coaxial line are joined by a connector. The line is filled continuously with polystyrene of dielectric constant $\epsilon_r = 2.6$. The connector has inner and outer conductors of the same size as the line, but it is filled with air for a length of 1 cm. The joined line feeds a matched load. Determine the standing-wave ratio in the section of line on each side of the connector when the operating frequency is 3,000 Mc/sec.

8. A two-wire line made of No. 9 copper wire spaced 2 cm between centers is to be matched to its load with a movable open-ended single stub. Determine the lumped elements of all necessary junction- and terminal-zone networks if the apparent impedance of the load is known.

9. A vertical antenna is driven over a horizontal ground screen by a coaxial line. The inner conductor of the line and its extension as the antenna are of copper with a radius of 0.4 cm. The coaxial line has an inner diameter of 4 cm. What is the magnitude of the lumped capacitance C_T required to correct for end effect?

10. The theoretical impedance of a center-driven antenna at antiresonance is $Z = 840 + j0$ ohms. What apparent impedance is measured on a two-wire line driving this antenna if the line spacing is 2 cm, the radius of the conductors 0.1 cm, and the frequency 150 Mc/sec?

CHAPTER VI

TRANSMISSION-LINE OSCILLATORS AND COUPLED SECTIONS OF TRANSMISSION LINE

1. Frequency Characteristics of Simple Triode Oscillators with Transmission Lines as Tank Circuits.[143,146,147,155] At ultrahigh frequencies coils and capacitors are often unsatisfactory as circuit elements, and sections of transmission line are used to replace them, especially in the tank circuits of oscillators. Various circuits are in common use, a number of which are analyzed below.

Single-tube Quarter-wave Oscillator. One of the simplest vacuum-tube oscillators makes use of a section of coaxial or two-wire line connected to the plate and grid terminals of a triode, as shown in Fig. 1.1*a*. Since

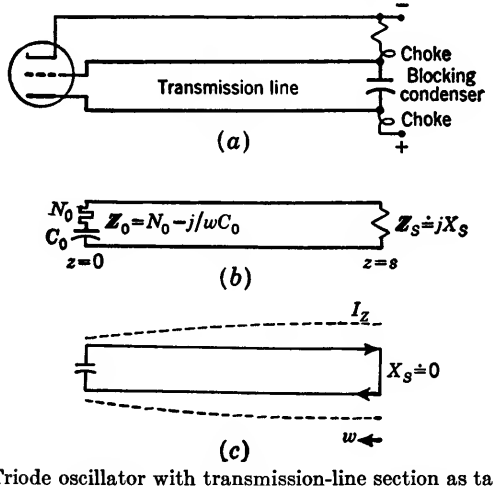


FIG. 1.1. Triode oscillator with transmission-line section as tank circuit.

the analysis of the triode as a negative-resistance device is beyond the scope of this book, it is represented simply as a series combination of a negative resistance $N_0 = -R_0$ and the output capacitance of the tube. For a triode this capacitance is

$$C_0 = \frac{C_1C_2 + C_2C_3 + C_3C_1}{C_2 + C_3} \tag{1}$$

where C_1 is the plate-grid capacitance, C_2 is the grid-filament capacitance, and C_3 is the plate-filament capacitance. Thus, insofar as the attached transmission line is concerned, the triode is replaced by the impedance

$$\boldsymbol{Z}_0 = N_0 + jX_0 = N_0 - \frac{j}{\omega C_0} \tag{2a}$$

at the end ($z = 0$) of the line, as shown in Fig. 1.1*b*. As a consequence of terminal-zone effects, the impedance that must be used in conjunction with uniform-line theory is the apparent impedance

$$\boldsymbol{Z}_{0a} = N_{0a} + jX_{0a} \tag{2b}$$

where $\boldsymbol{Z}_{0a}$ consists of an appropriate lumped network combined with $\boldsymbol{Z}_0$. In most cases it is adequate to assume $\boldsymbol{Z}_{0a} \doteq \boldsymbol{Z}_0$.

At the other end ($z = s$) the line is terminated in an impedance $\boldsymbol{Z}_s = R_s + jX_s$ which usually consists of a metal piston in the case of a coaxial line and of a conducting wire bridge of length b in the case of a two-wire line. The apparent impedances to be used in conjunction with uniform-line formulas is $\boldsymbol{Z}_{sa} = R_{sa} + jX_{sa}$.

The terminal functions at the generator end of the line may be approximated by formulas appropriate to a predominantly reactive termination. These are

$$\rho_0 = \frac{n_{10}}{x_{10}^2 + 1} \qquad \Phi_0 = \frac{\pi}{2} + \tan^{-1} x_{10} \tag{3}$$

where $n_{10} = N_0/R_c$ and $x_{10} = X_0/R_c$, if it is assumed that n_{10}^2 is small compared with $x_{10}^2 + 1$. At the other end the corresponding functions are

$$\rho_{sa} = \begin{cases} 0 & \text{for piston} \\ \frac{1}{2}\alpha b & \text{for bridge} \end{cases} \qquad \Phi_{sa} = \begin{cases} \dfrac{\pi}{2} & \text{for piston} \\ \dfrac{\pi}{2} + \beta k_{sa} & \text{for bridge} \end{cases} \tag{4}$$

where k_{sa} is as evaluated in Chap. II, Sec. 20.

The condition for resonance for the entire circuit determines the natural frequencies $f_n = \omega_n/2\pi$ at which the circuit may oscillate. It is

$$\beta_n s + \Phi_{0a} + \Phi_{sa} = n\pi \qquad n \text{ integral} \tag{5}$$

where $\beta_n = \omega_n/v = 2\pi/\lambda_n$. With (3) and (4) expressed for the wire bridge, (5) may be written as follows:

$$\beta_n(s + k_{sa}) + \tan^{-1} x_{10} = n\pi \tag{6}$$

For a piston $k_{sa} = 0$. It follows that, with $R_c = \sqrt{l/c}$ and $\beta = \omega\sqrt{lc}$,

$$x_{10} = \frac{X_0}{R_c} = -\frac{1}{\omega C_0 R_c} = -\frac{c}{\beta C_0} \tag{7}$$

so that (6) becomes

$$\beta_n \tan \beta_n s' = \frac{c}{C_0} \tag{8}$$

where the effective length is $s' = s + k_{sa}$ for a two-wire line and $s' = s$ for a coaxial line with piston. This equation determines the frequencies generated. In general, the fundamental or lowest frequency f_0 has the largest amplitude, but one or more of the higher harmonics may be maintained as well.

In practice, it is often convenient to determine the generated fundamental wavelength λ_0 as a function of the effective length s' of the section of transmission line. This length is given by

$$s' = \frac{1}{\beta_0} \tan^{-1} \frac{c}{\beta_0 C_0} = \frac{\lambda_0}{4} - \frac{1}{\beta_0} \tan^{-1} \frac{\beta_0 C_0}{c} \tag{9}$$

so that

$$\frac{\lambda_0}{4} = s' + \frac{1}{\beta_0} \tan^{-1} \frac{\beta_0 C_0}{c} \tag{10}$$

For the range that satisfies the inequality

$$\left(\frac{\beta_0 C_0}{c}\right)^2 \ll 1 \qquad \text{or} \qquad \lambda_0^2 \gg \left(\frac{2\pi C_0}{c}\right)^2 \tag{11}$$

(10) becomes

$$\frac{\lambda_0}{4} \doteq s' + \frac{C_0}{c} \tag{12}$$

This is the long-wavelength limit. It is seen that C_0/c is a length characteristic of the output capacitance of the generator. It represents the shortening effect of the tube capacitance. In the range of short lengths s' defined by

$$(\beta_0 s')^2 \ll 1 \tag{13}$$

the tangent in (8) may be approximated by its argument, so that

$$s' \doteq \frac{c}{\beta_0^2 C_0} = \lambda_0^2 \frac{c}{4\pi^2 C_0} \tag{14a}$$

It follows that the generated wavelength in the short-wavelength limit is

$$\lambda_0 \doteq A \sqrt{s'} \qquad A = 2\pi \sqrt{\frac{C_0}{c}} \tag{14b}$$

A plot of the general formula (9) is given in Fig. 1.2. The limiting ranges given by (12) and (14*b*) are indicated, as is the length C_0/c. Note that the generator has been represented by a lumped impedance. Frequently the leads from the line to the electrodes are appreciable in length. When

this is true, the origin for s' lies at a point such as 0′ to the right of the ideal value by a distance 00′ equal to the effective length of the leads. The distribution of current for the fundamental frequency is

$$\begin{aligned} I_s(w) &= I_{\max} \sin(\beta w + \Phi_{sa}) \\ &= I_{\max} \cos \beta(w + k_{sa}) \end{aligned} \quad (15)$$

where $w = s - z$ is measured from the terminating reactance X_s. A sketch of the current distribution is given in Fig. 1.1*c*.

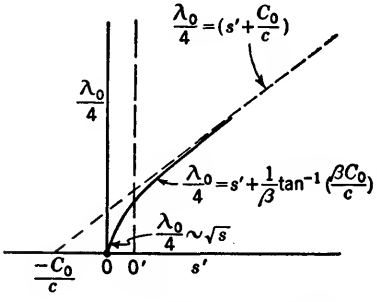


FIG. 1.2. Theoretical wavelength characteristics of transmission-line oscillator of effective length s'.

Two-tube Half-wave Oscillator. A two-tube circuit with a triode at each end of the section of transmission line is shown in Fig. 1.3. Since both ends of the line are the same as at $z = 0$ in Fig. 1.1, the condition for resonance is simply

$$\beta_n s + 2\Phi_{0a} = n\pi \qquad n \text{ integral} \quad (16)$$

With (6) and (7), the equation corresponding to (8) is

$$\beta_n \tan \tfrac{1}{2}\beta_n s = \frac{c}{C_0} \quad (17)$$

It is seen that, by setting $s' = s/2$, (17) is identically (8), so that the entire discussion following (8) and Fig. 1.2 applies to the push-pull circuit if its half length $s' = s/2$ is used as the variable.

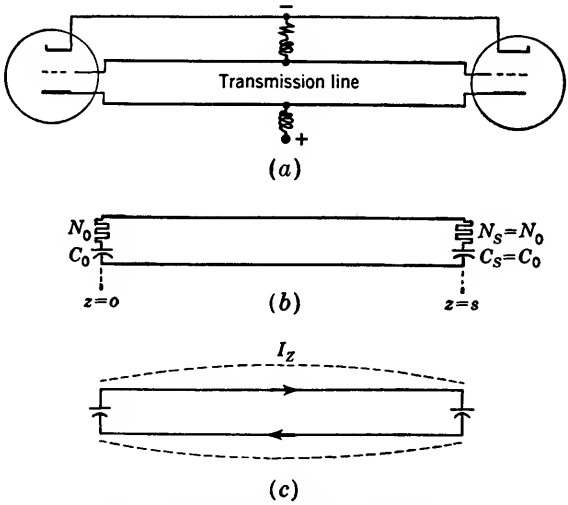


FIG. 1.3. Push-pull oscillator with transmission-line tank circuit.

The distribution of current along the transmission line is most conveniently expressed in the form

$$I_z(w) = I_{\max} \cos \beta v \tag{18}$$

where v is measured from the center of the line section.

Tuned-plate Tuned-grid Circuit for Push-Pull Operation. An adaptation of the well-known tuned-plate tuned-grid circuit for use with transmission-line sections is shown in Fig. 1.4*a*, where the plates of two

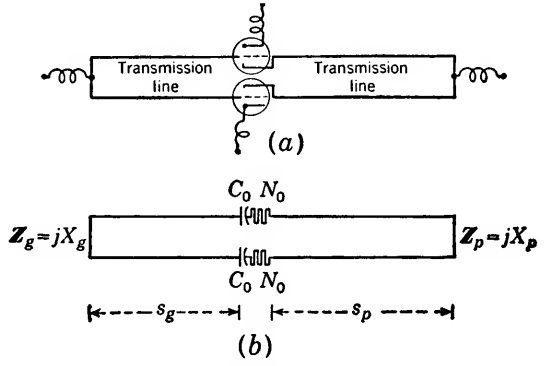


FIG. 1.4. Tuned-plate tuned-grid circuits.

tubes operated in push-pull are connected to one section of transmission line of length s_p and the two grids are connected to a second section of line of length s_g. For present purposes each tube is represented by its output capacitances C_0 in series with a negative resistance N_0. Each of the transmission lines is terminated in a short circuit or a small inductive reactance, so that

$$\Phi_p = \Phi_g = \frac{\pi}{2} + \beta k_{sa} \tag{19}$$

Let $s + k_{sa} = s'$. For a short circuit $k_{sa} = 0$ and $s = s'$.

Since all resistances are small, the natural frequency of the system may be determined by neglecting losses in the formulas for the reactances. The input reactance of a section of line of length s is

$$X_{in} = -R_c \cot (\beta s + \Phi_{sa}) \tag{20}$$

The sum of the reactances in the series circuit consisting of the two capacitances C_0 and the input impedances of the two lines must vanish at the generated frequency $f_n = \omega_n/2\pi$. That is,

$$-R_c \cot (\beta_n s_p + \Phi_p) - R_c \cot (\beta_n s_g + \Phi_g) - \frac{2}{\omega_n C_0} = 0 \tag{21}$$

With (19) this expression becomes

$$\tan \beta_n s_p' + \tan \beta_n s_g' = \frac{2c}{\beta_n C_0} \tag{22a}$$

Alternatively

$$\frac{\sin \beta_n (s_p' + s_g')}{\cos \beta_n s_p' \cos \beta s_g'} = \frac{2c}{\beta_n C_0} \tag{22b}$$

Since phase relations in a triode require that the alternating voltage across the grid be 180° out of phase with the voltage across the plate, one side of C_0 must be maximum positive when the other side is maximum negative. This occurs when the standing-wave pattern on the complete transmission line consisting of both sections has a voltage maximum across each C_0. This means

$$\beta_n s_g' = \beta_n s_p' + n\pi \qquad n \text{ integral} \tag{23}$$

With (23) in (22*a*), this reduces to

$$\beta_n \tan \beta_n s_p' = \frac{c}{C_0} \tag{24}$$

This is the same in form as (8), so that the frequency characteristics of the tuned-plate tuned-grid oscillator are essentially the same as those shown in Fig. 1.2 for the quarter-wave oscillator, except that condition (23) also must be satisfied. If $n = 0$ in (24) and s_p' determines the fundamental, as in Fig. 1.2, the grid line may exceed the plate line in length, so that the grid circuit is actually oscillating at a harmonic. This is often convenient in coupling a load to the oscillator. Alternatively s_p and s_g may both be made long enough so that each operates on a higher harmonic for the particular lengths s_p and s_g, with $n = 1, 2, \ldots$, in (24). In this case the fundamental frequency generated is determined by the requirement

$$s_g' - s_p' = \frac{\lambda}{2} \tag{25}$$

In general, the circuit oscillates at the lowest possible frequency.

Sinusoidal distributions of current on plate and grid lines are sketched in Fig. 1.5 for three possible combinations of lengths. In Fig. 1.5*a* the plate and grid lines are of equal length, and each is oscillating in its fundamental. In Fig. 1.5*b* the length of the grid line exceeds that of the plate line by a half wavelength, so that the latter oscillates in its fundamental and the former in a first harmonic. In Fig. 1.5*c* the grid and plate lines have lengths that make the proper phase relations across the plate-grid capacitance of the triode impossible if the plate line oscillates in its fundamental. The lowest frequency at which the requisite 180° phase relations are maintained occurs when the plate line oscillates in a first harmonic and the grid line in a second harmonic, with $s_g - s_p = \lambda/2$, where λ is the generated wavelength.

Double-ended Tubes with Transmission-line Tank Currents. Some triodes designed for use at ultrahigh frequencies have plate and grid connections that pass completely through the glass envelope as a short two-wire line, so that transmission-line sections may be attached on two sides, as shown in Fig. 1.6*a*. If the triode is represented by a capacitance C_0

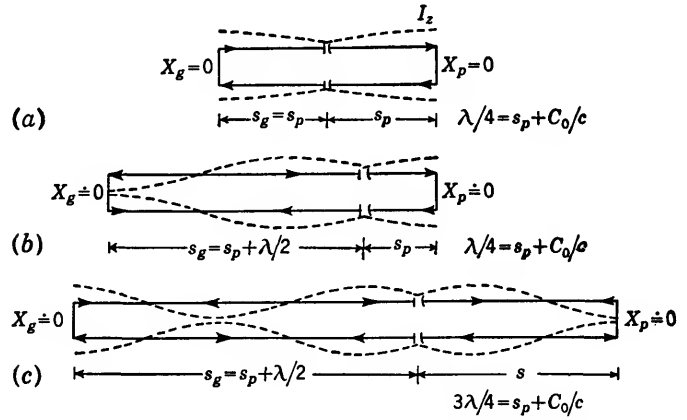


FIG. 1.5. Possible distributions of current in tuned-plate tuned-grid circuit.

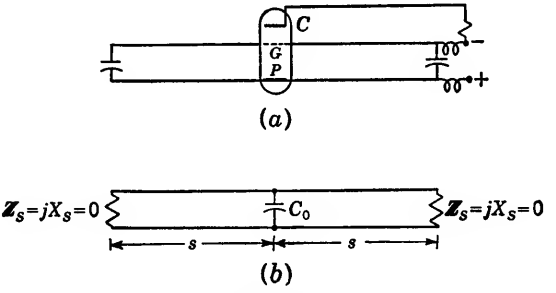


FIG. 1.6. Circuit for double-ended tube.

insofar as its reactive contribution to the current is concerned, the network of Fig. 1.6*b* is obtained (terminal-zone effects are not considered). In effect, two identical sections of transmission line are in parallel with the triode. The input reactance of each section is given by (20), so that for the two in parallel the input reactance is one-half of (20), or

$$X_{in} = -\frac{R_c}{2}\cot(\beta s + \Phi_a) = -\frac{R_c}{2}\tan \beta s' \tag{26}$$

where $s' = s + k_{sa}$. The expression on the right is for terminating reactances at the ends of the lines consisting of conducting bridges of equivalent length k_{sa}.

The generated frequency is the natural frequency of the triode in parallel with the two line sections. It is obtained by equating the reactance (26) to the reactance $-1/\omega C_0$ of the triode. Thus

$$\tan \beta_n s' = \frac{2}{\omega_n C_0 R_c} = \frac{2c}{\beta_n C_0} \tag{27}$$

This equation is like (8) except for the factor 2. It indicates that the capacitance $C_0/2$ plays the same part in determining the generated wavelength in the circuit of Fig. 1.6*b* as C_0 does in the circuit of Fig. 1.1*b*. It follows that, for triodes with the same C_0, the wavelength characteristic of the double-ended tube lies below that for the single-ended tube, as shown in Fig. 1.7.

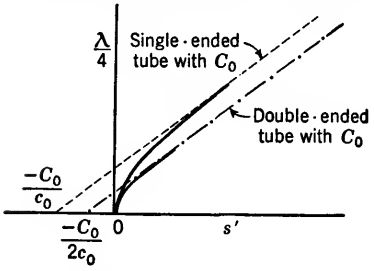


FIG. 1.7. Comparison of wavelength characteristics of single- and double-ended tubes in transmission-line oscillator.

Lighthouse-tube Reentrant Oscillator. An important type of ultrahigh-frequency oscillator makes use of the so-called lighthouse, or disk-seal, tube, in which the connections to the parallel plane electrodes consist of circular copper disks of graduated sizes. This construction permits the triode to be inserted in two concentric coaxial lines in such a manner that the inner and outer surfaces of the cylinder in contact with the grid

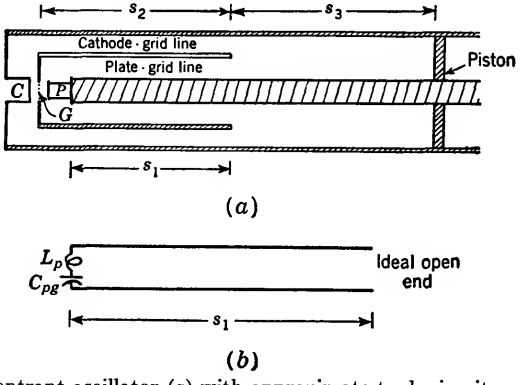


FIG. 1.8. Reentrant oscillator (*a*) with approximate tank-circuit equivalent (*b*).

disk serve, respectively, as outer conductor of the plate-grid line and inner conductor of the cathode-grid line. This construction is shown in Fig. 1.8 in a typical lighthouse-tube circuit known as the *reentrant oscillator*. Various other circuits are in use, but all are characterized by separate plate-grid and cathode-grid transmission-line circuits with a coupling link or aperture connecting them. Owing to the sections of

radial line which are bounded by the disks and contain the electrodes, none of the circuits can be represented accurately by sections of coaxial line and lumped elements. However, in the case of the reentrant circuit in which the frequency generated is primarily determined by the plate-grid section of line which is of relatively small cross-sectional size, a reasonable approximation may be achieved in terms of coaxial and lumped elements.

The circuit in Fig. 1.8*a* consists essentially of a section of bifurcated coaxial line which is equivalent to three sections of transmission line connected in series. As given in Chap. V, Sec. 14, the required junction-zone network of lumped elements in the plane of bifurcation consists of positive capacitances across the ends of the two lines 1 and 2 of smaller cross-sectional area and a negative capacitance across the large line. The plate lead extending beyond the end of the innermost coaxial conductor and the plate-grid space may be approximated by an inductance L_p in series with a capacitance C_{pg}. The proper phase relations for oscillation are obtained when the length s_3 of the large line is adjusted so that the terminating impedance for the plate-grid line in the plane of bifurcation is essentially that of an open circuit. As a consequence the frequency of oscillation is primarily determined by the plate-grid line treated as if it had an ideal open end. This cannot be shown analytically without an elaborate analysis of the entire triode circuit, which is beyond the scope of this book. For present purposes, then, the effective tank circuit is that shown in Fig. 1.8*b*. The resonant frequency is obtained from the solution of the equation

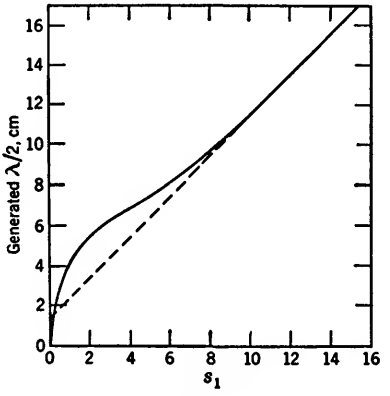


FIG. 1.9. Wavelength characteristics of reentrant oscillator.

$$\omega L_p - \frac{1}{\omega C_{pg}} = R_{c1} \cot \beta s_1 \tag{28}$$

where $R_{c1} = 60 \ln (a_2/a_1)$ ohms. The numerical solution[144] of (28) for $\lambda = 2\pi/\beta$ for a particular circuit is shown in Fig. 1.9, which is representative of the wavelength characteristic of a reentrant lighthouse-tube oscillator.

2. Frequency Characteristics of a Transmission-line Oscillator with Coupled Secondary.[152,155] Transmission-line oscillators are sometimes operated with a closely coupled secondary that modifies the frequency characteristics. Various arrangements are available, but the general

properties of most of these resemble those of the simple coupled-circuit oscillator shown in Fig. 2.1. This consists of a primary circuit which is identical with the single-circuit oscillator in Fig. 1.1*a* and which may be represented by the equivalent circuit in Fig. 1.1*b*. The secondary consists of an added section of transmission line extending beyond the bridge terminating the primary.

Let the length of the primary be s_1 and that of the secondary, s_2, so that the over-all length is $s = s_1 + s_2$. The impedance and emf of the generator at $z = 0$ are represented by the series combination of an

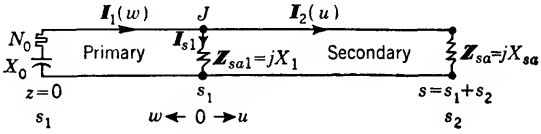


FIG. 2.1. Equivalent circuit of transmission-line oscillator with bridge-coupled secondary.

apparent negative resistance N_{0a} and reactance X_{0a}; the apparent impedance at the junction $z = s_1$ of primary and secondary is $\boldsymbol{Z}_{s1a}$, and that of the termination for the secondary at $z = s$ is $\boldsymbol{Z}_{sa}$. The corresponding apparent terminal functions are

$$\boldsymbol{\theta}_{0a} = \rho_{0a} + j\Phi_{0a} = \coth^{-1} \frac{N_{0a} + jX_{0a}}{\boldsymbol{Z}_c}, \tag{1a}$$

$$\boldsymbol{\theta}_{sa} = \rho_{sa} + j\Phi_{sa} = \coth^{-1} \frac{\boldsymbol{Z}_{sa}}{\boldsymbol{Z}_c} \tag{1b}$$

The admittances looking toward the two ends from the junction plane at $z = s_1$ are

$$\boldsymbol{Y}_1 = \boldsymbol{Y}_c \tanh (\gamma s_1 + \boldsymbol{\theta}_{0a}) \qquad \boldsymbol{Y}_2 = \boldsymbol{Y}_c \tanh (\gamma s_2 + \boldsymbol{\theta}_{sa}) \tag{2}$$

An equation representing the frequency and damping properties of the circuit in Fig. 2.1 may be derived by noting that the voltage across the coupling impedance (which is assumed to be a small inductive reactance) is

$$\boldsymbol{V}_{s1} = j\omega L_{s1}[\boldsymbol{I}_1(s_1) - \boldsymbol{I}_2(s_1)] \tag{3}$$

and that the currents in the primary and secondary where these join are

$$\boldsymbol{I}_1(s_1) = \boldsymbol{V}_{s1}\boldsymbol{Y}_1 \qquad \boldsymbol{I}_2(s_1) = -\boldsymbol{V}_{s1}\boldsymbol{Y}_2 \tag{4}$$

The negative sign for $\boldsymbol{I}_2(s)$ is a consequence of the fact that the voltage induced in the secondary is 180° out of phase with that in the primary.

By subtracting $\boldsymbol{I}_2(s_1)$ from $\boldsymbol{I}_1(s_1)$ in (4) and using (3), the following equation is obtained:

$$1 = j\omega L_{s1}(\boldsymbol{Y}_1 + \boldsymbol{Y}_2) \tag{5}$$

Since $\boldsymbol{Y}_c \doteq G_c \doteq 1/vl$, it follows that

$$\omega L_{s1}\boldsymbol{Y}_c \doteq \beta k \qquad k \equiv \frac{L_{s1}}{l} \tag{6}$$

Accordingly, with (2) and (6), (5) may be expressed as follows:

$$\frac{1}{j\beta k} = \tanh (A_1 + jF_1) + \tanh (A_2 + jF_2) \tag{7}$$

where, with $\gamma = \alpha + j\beta$,

$$A_1 \equiv \alpha s_1 + \rho_{0a} \qquad F_1 \equiv \beta s_1 + \Phi_{0a} \tag{8a}$$
$$A_2 \equiv \alpha s_2 + \rho_{sa} \qquad F_2 \equiv \beta s_2 + \Phi_{sa} \tag{8b}$$

By separating real and imaginary parts the following pair of equations is obtained:

$$-\frac{\tanh A_1}{\tanh A_2} = \frac{\cos^2 F_1}{\cos^2 F_2}\frac{1 + \tanh^2 A_1 \tan^2 F_1}{1 + \tanh^2 A_2 \tan^2 F_2} \tag{9a}$$

$$-\frac{1}{\beta k} = \frac{\tan F_1}{\cosh^2 A_1(1 + \tanh^2 A_1 \tan^2 F_1)} + \frac{\tan F_2}{\cosh^2 A_2(1 + \tanh^2 A_2 \tan^2 F_2)} \tag{9b}$$

Equations (9*a*) and (9*b*) may be solved for A_1 and β, and these values used to determine the negative resistance N_{0a} and the generated frequency. Since A_1 and A_2 may be assumed small, the following inequalities are good approximations:

$$A_1^2 \ll 1 \qquad A_2^2 \ll 1 \tag{10}$$

Eqs. (9*a*) and (9*b*) may be simplified. The results are

$$\frac{-A_1}{A_2} = \frac{\cos^2 F_1}{\cos^2 F_2}\frac{1 + A_1^2 \tan^2 F_1}{1 + A_2^2 \tan^2 F_2} \tag{11a}$$

$$-\frac{1}{\beta k} = \frac{\tan F_1}{1 + A_1^2 \tan^2 F_1} + \frac{\tan F_2}{1 + A_2^2 \tan^2 F_2} \tag{11b}$$

With (10) it follows that, except for values of F_1 or F_2 very near an odd integral multiple of $\pi/2$, these equations may be approximated by

$$\frac{-A_1}{A_2} \doteq \frac{\cos^2 F_1}{\cos^2 F_2} \tag{12a}$$

$$-\frac{1}{\beta k} \doteq \tan F_1 + \tan F_2 \tag{12b}$$

Evidently (12*b*) determines the generated frequency in terms of the lengths s_1 and s_2 and the terminal functions Φ_{0a} and Φ_{sa}. Similarly (12*a*) specifies the critical value of $-A_1$ (or N_{0a}) at which oscillations can be established. These two equations may be expressed directly in terms of the two unknowns. As shown in Sec. 1,

$$F_1 = \beta s_1' \qquad s_1' = s_1 + \frac{\Phi_{0a}}{\beta} \doteq s_1 + \frac{C_{0a}}{c} \tag{13}$$

where C_{0a} is the apparent output capacitance of the triode and c is the capacitance per unit of the line. Let

$$F_2 = \begin{cases} \beta s_2 & \text{for an ideal open end at } z = s \\ \beta(s_2 + k_{sa}) + \dfrac{\pi}{2} = \beta s_2' + \dfrac{\pi}{2} & \text{for a bridged end at } z = s \end{cases} \tag{14}$$

With (13) and (14), (12*b*) has the following form in the two cases specified in (14):

$$-\frac{1}{\beta k} = \tan \beta s_1' + \tan \beta s_2 \qquad \text{open end} \tag{15a}$$

$$-\frac{1}{\beta k} = \tan \beta s_1' - \cot \beta s_2' \qquad \text{bridged end} \tag{15b}$$

For an open end $\rho_{sa} = 0$; for a bridged end $\rho_{sa} \doteq \alpha b/2$. Since ρ_{0a} is small,

$$\rho_{0a} \doteq \frac{N_{0a}}{R_c} \tag{16}$$

With $\alpha = r/2R_c = r_a/R_c$ (where $r_a = r/2$ is the resistance of a unit length of one conductor) and (16), the damping equations derived from (12*a*) and associated with (15*a*) and (15*b*) are

$$-\frac{N_{0a} + r_a s_1'}{r_a s_2} = \frac{\cos^2 \beta s_1'}{\cos^2 \beta s_2} \qquad \text{open end} \tag{17a}$$

$$-\frac{N_{0a} + r_a s_1'}{r_a s_2'} = \frac{\cos^2 \beta s_1'}{\sin^2 \beta s_2'} \qquad \text{bridged end} \tag{17b}$$

These equations may be rearranged into the following forms convenient for numerical evaluations:

Open End at $z = s$

$$-\frac{1}{KS_1} = \tan S_1 + \tan nS_1 \tag{18a}$$

$$-\frac{N_{0a}/R_1 + 1}{n} = \frac{\cos^2 S_1}{\cos^2 nS_1} \tag{18b}$$

Bridged End at $z = s$

$$-\frac{1}{KS_1} = \tan S_1 - \cot nS_1 \tag{19a}$$

$$-\frac{N_{0a}/R_1 + 1}{n} = \frac{\cos^2 S_1}{\sin^2 nS_1} \tag{19b}$$

where $S \equiv \beta s_1' = 2\pi s_1'/\lambda$ is the electrical length of the primary, $K = k/s_1'$ is the fractional equivalent length of the coupling bridge, $R_1 = r_a s_1$ is the total resistance in the primary, and $n = s_2/s_1'$ or s_2'/s_1'. Note that N_{0a} is negative.

Equation (18*a*) has been solved graphically for S_1 as a function of the ratio n of the length of the secondary to that of the primary, with

K as parameter. Instead of plotting S_1 against n, the ratio of the quarter wavelength generated to the length s_1' of the primary, namely, $\lambda/4s_1' = \pi/2S_1$, is plotted against $n = s_2/s_1'$ in solid line in Fig. 2.2. Of the infinity of possible solutions, the first three are shown numbered in Roman. The particular branches that give possible generated wavelengths depend on the associated damping curves. These are obtained by plotting the right side of (18*b*) against n, as shown in dashed line in Fig. 2.2. Oscillations can be maintained at a wavelength specified by a particular point on a wavelength curve if N_{0a} is sufficiently great so that the left side of (18*b*) at least equals the right side. The dotted curve in Fig. 2.2 is the magnitude of the left side of (18*b*), with $N_{0a}/R_1 = -2$ plotted against n. Only wavelengths for which the corresponding point on the associated damping curve (dashed line) does *not* lie above the dotted excitation curve may be generated. In particular, as $n = s_2/s_1'$ is increased from zero, the generated quarter wavelength is given by wavelength curve I from $n = 0$ to $n = 1$, where damping curve I rises above the dotted excitation curve. From $n = 1$ to n very nearly 3 (where damping curve II rises above the excitation curve) the wavelength of curve II may be generated; beyond $n \doteq 3$, wavelengths on curve II are damped out. Beginning with n somewhat less than 3, damping curve III drops below the excitation curve, so that wavelengths of curve III may be generated. Evidently the generated wavelength behaves as follows as the secondary is increased in length from zero to $4s_1'$: At $n = 0$ the generated wavelength is that corresponding to a single-circuit oscillator with $s_1' = \lambda/4$ and a terminating inductance L_{s1}. It is this inductance which makes the generated quarter wavelength with $s_2 = 0$ greater than 1. As $n = s_2/s_1'$ is increased, the quarter wavelength increases slowly, following curve I until $n = 1$. At $n = 1$ the quarter wavelength drops abruptly to curve II, which it follows as n is increased until $n = 3$ is almost reached; then it drops to curve III, which it follows to $n = 4$. If n is now decreased, wavelength curve III is followed until a point is reached which lies directly above the intersection of damping curve III and the excitation curve. Here the generated quarter wavelength rises to curve II, which is followed to $n = 1$, where it rises to curve I. In a small range of n below 3 the generated wavelength may be given by either curve II or curve III. Such an overlapping range of instability is called a *drag loop*, since the generated wavelength tends to continue on a

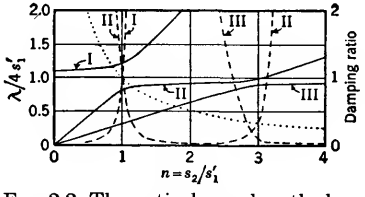


FIG. 2.2. Theoretical wavelength characteristics (solid lines), damping curves (dashed lines), and excitation curve for $N_{0a}/R_1 = -2$ (dotted curve) for coupled-circuit oscillator with open-ended secondary. The curves are for $k_1/s_1' = 0.1$.

given wavelength curve until its damping curve rises above the excitation curve. If the value of N_{0a}/R_1 is more negative than -2, the dotted excitation curve is higher, the extent of the drag loop near $n = 3$ is increased, and a drag loop (narrower than that near $n = 3$) occurs near $n = 1$. If N_{0a}/R_1 is less negative than -2, oscillations break off over a range near $n = 1$, and the drag loop near $n = 3$ is reduced. If N_{0a}/R_1 is sufficiently less negative than -2, oscillations may also break off near $n = 3$. These three possible cases are illustrated in Fig. 2.3.

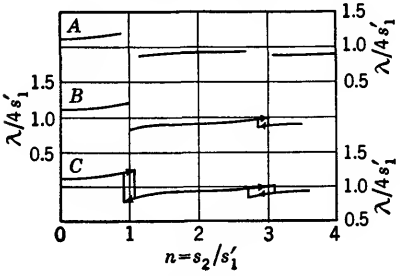


FIG. 2.3. Theoretical wavelength characteristics of a coupled-circuit oscillator with open-ended secondary. A—small excitation, $|N_{0a}/R_1| < 2$; B—critical excitation, $|N_{0a}/R_1| = 2$; C—strong excitation, $|N_{0a}/R_1| > 2$.

In order to illustrate the effect of varying the coupling inductance, the left half of the wavelength curve in Fig. 2.2 is shown in Fig. 2.4 together with two other theoretical curves for smaller values of $K = k/s_1'$. Experimental points for a typical case for which $k/s_1' < 0.03$ are also shown.

When the secondary is closed at $z = s$ instead of open, so that (19a) and (19b) apply, analogous results are obtained. Wavelength and damping curves determined from (19a,b), with $k/s_1' = 0.1$, are shown in Fig. 2.5 together with the single excitation curve $N_{0a}/R_1 = -2$.

Experimental wavelength characteristics for an oscillator in which k/s_1' is very small are shown in Fig. 2.6a when the secondary has a bridged end (curve A) and an open end (curve B). The wavelength characteristics of a different bridged-end oscillator with a somewhat greater value of k/s_1' are shown in Fig. 2.6b. The drag loops are noteworthy. A plot of the theoretical wavelength characteristic determined from Fig. 2.5, with the experimental curve of Fig. 2.6b properly scaled, is given in Fig. 2.7. The value of k_1/s_1' for the experimental curve is readily computed to be $k/s_1' = 0.044$. If this value of k/s_1' is used to calculate curves like those in Fig. 2.5, the theoretical and experimental curves practically coincide.

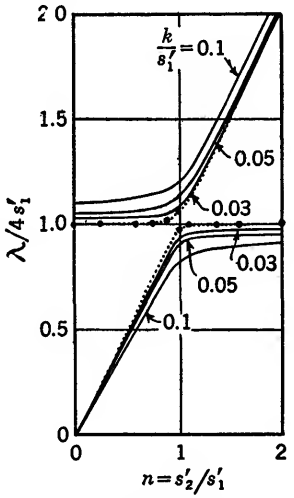


FIG. 2.4. Theoretical wavelength characteristics of the idealized coupled-circuit oscillator with open-ended secondary for three different values of the ratio k/s_1' (solid lines). A typical experimental curve following observed points is shown dotted.

It is not difficult to explain the wavelength characteristics of the

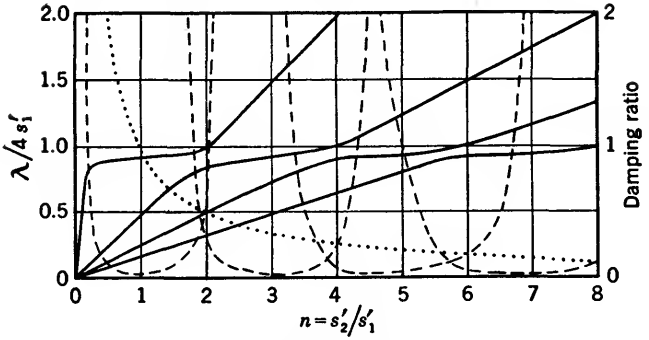
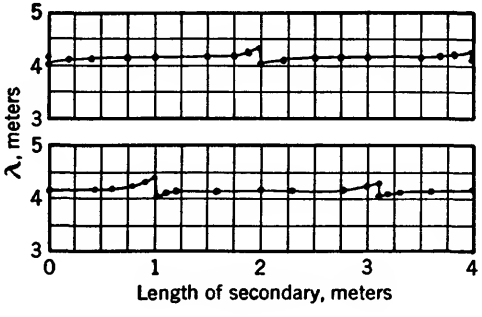
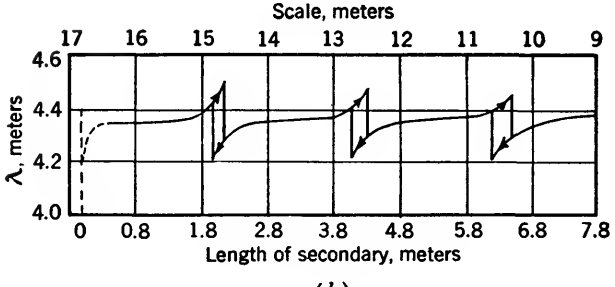


FIG. 2.5. Theoretical curves for wavelength (solid lines), damping (dashed lines), and excitation for $N_{0a}/R_1 = -2$ (dotted line) for coupled-circuit oscillator with bridged-end secondary. The curves are for $k/s_1' = 0.1$.



(*a*)



(*b*)

FIG. 2.6. Experimental wavelength characteristics of coupled-circuit oscillators. (*a*) Oscillator with bridged-end secondary in upper curve, open-end secondary in lower curve. (*b*) Different oscillator with bridged-end secondary.

coupled-circuit oscillator in a qualitative manner. The generated wavelength is determined by the complete primary-secondary circuit. In effect, the primary section of transmission line is terminated in a parallel combination of the low impedance of the inductive bridge and the variable input impedance of the secondary transmission line. When the length of the secondary line is such as to provide an input impedance that is high compared with that of the coupling bridge, the primary behaves essentially as if the secondary were a lumped high impedance in parallel. Practically the entire current enters the bridge; very little enters the secondary. As the secondary is changed in length so as to reduce its input impedance, the effective impedance of the bridge in parallel with the secondary departs more and more from that of the bridge, and an increasing current enters the secondary. Finally, when the input impedance of the line is smaller than that of the coupling bridge, the current into the secondary exceeds that into the bridge, and the wavelength increases almost linearly with increasing length of the secondary, much as if the coupling bridge were absent. But as the secondary is further increased in length, its input impedance increases and soon exceeds the impedance of the bridge. When this occurs, most of the current enters the bridge, and the wavelength is again determined by the length of the primary and its effectively lumped termination.

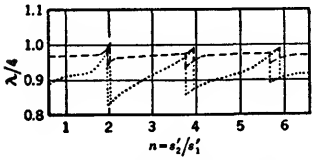


FIG. 2.7. Combined theoretical (dotted, $k/s_1' = 0.1$) and experimental (dashed, $k/s_1' = 0.044$) wavelength characteristics of coupled-circuit oscillator with bridged-end secondary.

In oscillators of the positive-grid, or Barkhausen-Kurz, type and in the magnetron, the primary circuit consists of a cloud of electrons, and the secondary includes all electrodes and attached conductors. Since the primary cannot exist without the secondary, it follows that the frequency characteristics of such an oscillator are determined both by the natural frequency of the primary cloud of electrons and by the natural frequency of the secondary circuit.[154,155]

3. Electric Field of a Conductor with Sinusoidally Distributed Current.[10] In order to determine the distributions of current and voltage along a two-wire line when this is driven by a transmission-line oscillator of a type described in Sec. 1 (or by an equivalent coupling element) coupled at an arbitrary location along the line, it is necessary to derive a formula for the electric field maintained by the currents in the oscillator. Since the relevant element of this circuit consists of a section of two-wire line carrying an essentially sinusoidally distributed current, a first step is to obtain a formula for the electromagnetic field of a single wire of arbitrary length h with a current of the general form

$$I(z') = I(0)\frac{\sin \beta_0(g - z')}{\sin \beta_0 g} = I_m \sin \beta_0(g - z') \qquad (1a)$$

where $$g \equiv h + k \qquad I_m \equiv \frac{I(0)}{\sin \beta_0 g} \tag{1b}$$

This distribution is illustrated in Fig. 3.1. By a suitable combination of conductors of this type with appropriate values of k and h, it is possible to represent most of the usual transmission-line oscillators and coupling elements.

The electric field at the point $Q(r,u)$ is most conveniently determined from the general integral [Chap. I, Sec. 3, Eq. (30b)] for the vector

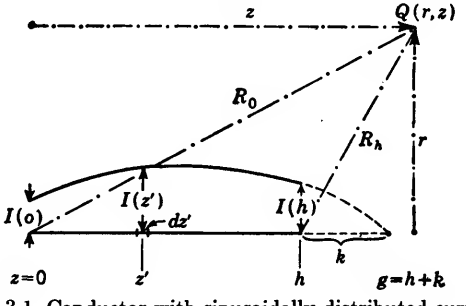


FIG. 3.1. Conductor with sinusoidally distributed current.

potential. In the notation of this section (in which the dielectric is assumed to be perfect, so that $\xi = \epsilon$ and $\beta = \beta$) it is given by

$$\mathbf{A} = \hat{z}A_z(z) \qquad A_z(z) = \frac{1}{4\pi\nu}\int_0^h I_z(z')\,\frac{e^{-j\beta R}}{R}\,dz' \tag{2a}$$

where $$R = \sqrt{(z' - z)^2 + r^2} \tag{2b}$$

The electric and magnetic fields may be calculated from (2a) using Chap. I, Sec. 3, Eqs. (7), (8a,b), forms (18), and (19). The relevant are

$$\mathbf{E} = -\frac{j\omega}{\beta^2}(\text{grad div } \mathbf{A} + \beta^2\mathbf{A}) = -\frac{j\omega}{\beta^2}\,\text{curl curl } \mathbf{A} \tag{3a}$$

$$\mathbf{B} = \text{curl } \mathbf{A} \tag{3b}$$

If (1a) is expanded in exponential form and substituted in (2a), this may be expressed as follows:

$$A_z(z) = \frac{-jI_m}{8\pi\nu}\left[e^{j\beta g}\int_0^h \frac{e^{-j\beta(R+z')}}{R}\,dz' - e^{-j\beta g}\int_0^h \frac{e^{-j\beta(R-z')}}{R}\,dz'\right] \tag{4}$$

In order to obtain a more convenient form of the integrals, let the first be multiplied by $e^{-j\beta z}$ in front of the sign and by $e^{j\beta z}$ under the sign. Similarly let the second integral be multiplied by $e^{j\beta z}$ in front of the sign and by $e^{-j\beta z}$ under it. With the abbreviations

$$u \equiv R + z' - z \qquad v \equiv R - z' + z \tag{5}$$

the following expression is obtained:

$$A_z(z) = \frac{-jI_m}{8\pi\nu}\left[e^{j\beta(g-z)}\int_0^h \frac{e^{-j\beta u}}{R}\,dz' - e^{-j\beta(g-z)}\int_0^h \frac{e^{j\beta v}}{R}\,dz'\right] \tag{6}$$

In order to express R and z' in the two integrals in terms of u and v and thus change the variables of integration, it is necessary to differentiate (5) to obtain

$$\frac{\partial u}{\partial z'} = \frac{u}{R} \qquad \frac{\partial v}{\partial z'} = -\frac{v}{R} \tag{7}$$

The limits of integration for the new variables u and v, which may be introduced at this point, are

$$\text{For } z' = 0: \quad u = u_0 = R_0 - z \qquad v = v_0 = R_0 + z \tag{8a}$$

$$\text{For } z' = h: \quad u = u_1 = R_1 + h - z \qquad v = v_1 = R_1 - h + z \tag{8b}$$

$$\text{where} \qquad R_0 = \sqrt{z^2 + r^2} \qquad R_1 = \sqrt{(z-h)^2 + r^2} \tag{8c}$$

With (7) to (8b), (6) becomes

$$A_z(z) = \frac{-jI_m}{8\pi\nu}\left[e^{j\beta(g-z)}\int_{u_0}^{u_1} \frac{e^{-j\beta u}}{u}\,du + e^{-j\beta(g-z)}\int_{v_0}^{v_1} \frac{e^{-j\beta v}}{v}\,dv\right] \tag{9}$$

Although the integrals in this formula can be expressed in terms of tabulated sine and cosine integrals, it is unnecessary to do so for the present purpose of evaluating the electric field. This is done as follows:

In cylindrical coordinates with $A_r = 0$ and $A_\theta = 0$ and rotational symmetry, so that $\partial/\partial\theta = 0$, it follows that

$$B_r = \text{curl}_r\,\mathbf{A} = \frac{1}{r}\frac{\partial A_r}{\partial\theta} = 0 \tag{10a}$$

$$B_\theta = \text{curl}_\theta\,\mathbf{A} = -\frac{\partial A_z}{\partial r} \tag{10b}$$

$$B_z = \text{curl}_z\,\mathbf{A} = 0 \tag{10c}$$

so that

$$B_\theta = \frac{jI_m}{8\pi\nu}\left[e^{j\beta(g-z)}\frac{\partial}{\partial r}\int_{u_0}^{u_1} \frac{e^{-j\beta u}}{u}\,du + e^{-j\beta(g-z)}\frac{\partial}{\partial r}\int_{v_0}^{v_1} \frac{e^{-j\beta v}}{v}\,dv\right] \tag{11}$$

Since r occurs in both limits of integration, the general formula[26] for differentiating a definite integral with respect to a parameter must be used. Note that the integrands do not involve r. Using the following derivatives of the limits of integration:

$$\frac{\partial u_0}{\partial r} = \frac{\partial v_0}{\partial r} = \frac{r}{R_0} \qquad \frac{\partial u_1}{\partial r} = \frac{\partial v_1}{\partial r} = \frac{r}{R_1} \tag{12}$$

the expression (11) may be integrated into

$$B_\theta = \frac{jI_m}{8\pi\nu}\left[e^{j\beta(g-z)}\left(\frac{r}{R_1}\frac{e^{-j\beta u_1}}{u_1} - \frac{r}{R_0}\frac{e^{-j\beta u_0}}{u_0}\right) + e^{-j\beta(g-z)}\left(\frac{r}{R_1}\frac{e^{-j\beta v_1}}{v_1} - \frac{r}{R_0}\frac{e^{-j\beta v_0}}{v_0}\right)\right] \tag{13}$$

Considerable rearrangement and simplification of (13) are possible. The final result is

$$\boldsymbol{B}_\theta = \frac{j\boldsymbol{I}_m}{4\pi\nu r}\left[e^{-j\beta R_1}\left(\cos K + j\frac{z-h}{R_1}\sin K\right) - e^{-j\beta R_0}\left(\cos G + j\frac{z}{R_0}\sin G\right)\right] \tag{14}$$

where $$K \equiv \beta k \qquad G \equiv H + K \equiv \beta(h+k) \tag{15}$$

The components of the electric field are now evaluated from (3*a*) with (3*b*) and (14). Since, with $\boldsymbol{B}_r = 0$ and $\boldsymbol{B}_z = 0$,

$$\text{curl}_r\,\mathbf{B} = -\frac{1}{r}\frac{\partial}{\partial z}(r\mathbf{B}_\theta) \tag{16a}$$

$$\text{curl}_\theta\,\mathbf{B} = 0 \tag{16b}$$

$$\text{curl}_z\,\mathbf{B} = \frac{1}{r}\frac{\partial}{\partial r}(r\mathbf{B}_\theta) \tag{16c}$$

it is clear that $\boldsymbol{E}_r$ and $\boldsymbol{E}_z$ differ from zero, whereas $\boldsymbol{E}_\theta$ vanishes. The differentiations of $r\mathbf{B}_\theta$ with respect to z and r are elementary. The results are

$$\boldsymbol{E}_r = \frac{j\zeta_0\boldsymbol{I}_m}{4\pi r}\left\{e^{-j\beta R_1}\left[\frac{z-h}{R_1}\cos K + \frac{j(z-h)^2}{R_1^2}\sin K - \frac{r^2}{\beta R_1^3}\sin K\right]\right.$$
$$\left. - e^{-j\beta R_0}\left(\frac{z}{R_0}\cos G + \frac{jz^2}{R_0^2}\sin G - \frac{r^2}{\beta R_0^3}\sin G\right)\right\} \tag{17}$$

$$\boldsymbol{E}_z = -\frac{j\zeta_0\boldsymbol{I}_m}{4\pi}\left\{e^{-j\beta R_1}\left[\frac{\cos K}{R_1} + \frac{j(z-h)}{R_1^2}\sin K + \frac{z-h}{\beta R_1^3}\sin K\right]\right.$$
$$\left. - e^{-j\beta R_0}\left(\frac{\cos G}{R_0} + \frac{jz}{R_0^2}\sin G + \frac{z}{\beta R_0^3}\sin G\right)\right\} \tag{18}$$

In calculating the electric field maintained tangent to the conductors of a transmission line by the currents in a parallel oscillator, only $\boldsymbol{E}_z$ as given by (18) is significant.

4. The Electric Field of a Driven Section of Two-wire Line.[148,151] A two-wire line of length s and spacing b is excited as a secondary by a coupled shorter section of transmission line of length h and spacing b_0, in which a current is maintained by an appropriate negative resistance. The distance between the planes containing the two parallel lines is d. For simplicity, let all conductors in the long line and the coupled section have the radius a. Thus the problem is the determination of the electric fields at points Q_1 and Q_2 in Fig. 4.1 parallel to the conductors 1 and 2 of the long line. The field is maintained by the *balanced* currents in conductors 3 and 4 of the oscillator. It is assumed that

$$\boldsymbol{I}_2 = -\boldsymbol{I}_1 \qquad \boldsymbol{I}_4 = -\boldsymbol{I}_3 \tag{1}$$

It follows that the electric fields at Q_1 and Q_2 are equal in magnitude and opposite in direction.

A distribution of current which may be adapted to represent the currents in different oscillators and variously terminated coupled sections of

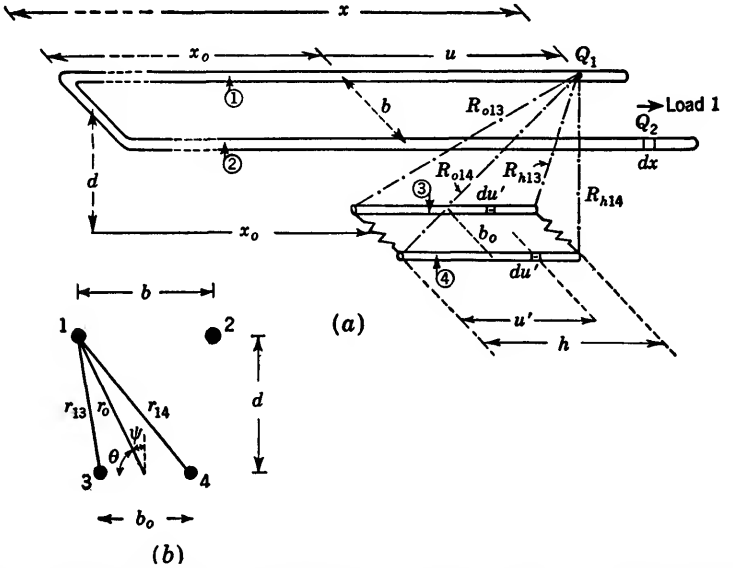


FIG. 4.1. Transmission line with coupled driven section of line. (*a*) Side view; (*b*) end view.

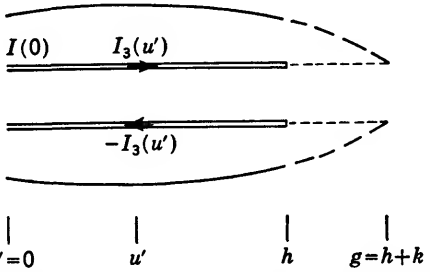


FIG. 4.2. Distribution of current along driven section of line.

line is shown in Fig. 4.2 and given analytically by

$$-I_4(u') = I_3(u') = I_3(0) \sin \beta(g - u') \qquad 0 \leqq u' \leqq h \tag{2a}$$

where

$$g \equiv h + k \tag{2b}$$

The coordinate u' locating the current is measured from the left end of the oscillator, which is at a distance x_0 from the left end of the main transmission line. This distance satisfies the inequality

$$x_0 \gg b_0 \tag{3}$$

It is desired to determine the electric field at points Q_1 and Q_2 at a distance x from the end of conductors 1 and 2.

It follows from Sec. 3, Eq. (18), with changes in notation, that the axially tangential component of the electric field maintained at a point such as Q_1 on conductor 1 by a distribution of current of the form (2a) in conductor 3 is given by

$$E_{z13} = \frac{-j\zeta_0 I_3(0)}{4\pi \sin G}\left\{e^{-j\beta R_{h13}}\left[\frac{\cos K}{R_{h13}} + \frac{j(u-h)}{R_{h13}^2}\sin K + \frac{u-h}{\beta R_{h13}^3}\sin K\right]\right.$$
$$\left. - e^{-j\beta R_{013}}\left(\frac{\cos G}{R_{013}} + \frac{ju}{R_{013}^2}\sin G + \frac{u}{\beta R_{013}^3}\sin G\right)\right\} \quad (4)$$

The field maintained at the same point Q_1 by the current in conductor 4 of the oscillator is given by (4), with all subscripts 3 replaced by 4 and the entire right side preceded by a minus sign. The following notation is involved:

$$K \equiv \beta k \qquad G \equiv H + K \equiv \beta(h + k) \quad (5)$$

$$R_{h13} = \sqrt{(u-h)^2 + r_{13}^2} = \sqrt{(u-h)^2 + r_0^2 + \frac{b_0^2}{4} - b_0 r_0 \cos\theta} \quad (6a)$$

$$R_{013} = \sqrt{u^2 + r_{13}^2} = \sqrt{u^2 + r_0^2 + \frac{b_0^2}{4} - b_0 r_0 \cos\theta} \quad (6b)$$

$$R_{h14} = \sqrt{(u-h)^2 + r_{14}^2} = \sqrt{(u-h)^2 + r_0^2 + \frac{b_0^2}{4} + b_0 r_0 \cos\theta} \quad (6c)$$

$$R_{014} = \sqrt{u^2 + r_{14}^2} = \sqrt{u^2 + r_0^2 + \frac{b_0^2}{4} + b_0 r_0 \cos\theta} \quad (6d)$$

The distances r_{13}, r_{14}, and r_0 and the angle θ are defined in Fig. 4.1b. The origin of u and u' is in the transverse plane through the left end of the oscillator or coupled section of line. That is,

$$u = x - x_0 \quad (7)$$

The resultant axially tangential electric field at Q_1 is

$$E_{z1} = E_{z13} + E_{z14} = \frac{-j\zeta_0 I_3(0)}{4\pi \sin G}\left\{\left(\frac{e^{-j\beta R_{h13}}}{R_{h13}} - \frac{e^{-j\beta R_{h14}}}{R_{h14}}\right)\cos K + j(u-h)\right.$$
$$\times\left(\frac{e^{-j\beta R_{h13}}}{R_{h13}^2} - \frac{e^{-j\beta R_{h14}}}{R_{h14}^2}\right)\sin K + (u-h)\left(\frac{e^{-j\beta R_{h13}}}{\beta R_{h13}^3} - \frac{e^{-j\beta R_{h14}}}{\beta R_{h14}^3}\right)\sin K$$
$$- \left[\left(\frac{e^{-j\beta R_{013}}}{R_{013}} - \frac{e^{-j\beta R_{014}}}{R_{014}}\right)\cos G + ju\left(\frac{e^{-j\beta R_{013}}}{R_{013}^2} - \frac{e^{-j\beta R_{014}}}{R_{014}^2}\right)\sin G\right.$$
$$\left.\left. + u\left(\frac{e^{-j\beta R_{013}}}{\beta R_{013}^3} - \frac{e^{-j\beta R_{014}}}{\beta R_{014}^3}\right)\sin G\right]\right\} \quad (8)$$

This is the general expression for the electric field at any point Q_1 along conductor 1 of the transmission line. The field at Q_2 on conductor 2 is the negative of (8).

Considerable simplification in (8) is possible under the practically most important circumstances in which the angle θ does not differ greatly from $\pi/2$, so that $\cos\theta$ is small. In particular, with $\psi \equiv \pi/2 - \theta$,

$$\cos\theta = \sin\psi \doteq \psi \qquad \psi^2 \ll 3 \tag{9}$$

With (9) and the notation

$$v_0^2 \equiv u^2 + r_0^2 + \frac{b_0^2}{4} \qquad v_1^2 \equiv (u-h)^2 + r_0^2 + \frac{b_0^2}{4} \tag{10}$$

it follows that

$$R_{h13} \doteq v_1 - f_1\psi \qquad R_{013} \doteq v_0 - f_0\psi \tag{11a}$$

$$R_{h14} \doteq v_1 + f_1\psi \qquad R_{014} \doteq v_0 + f_0\psi \tag{11b}$$

where

$$f_1 \equiv \frac{b_0 r_0}{2v_1} \qquad f_0 \equiv \frac{b_0 r_0}{2v_0} \tag{12a}$$

Evidently

$$f_1 v_1 = f_0 v_0 = \frac{b_0 r_0}{2} \tag{12b}$$

Since f_1 and f_0 are less than 1, it follows, with (9), that

$$e^{-j\beta R_{h13}} \doteq e^{-i\beta v_1}(1 + j\beta f_1\psi) \qquad e^{-j\beta R_{h14}} \doteq e^{-i\beta v_1}(1 - j\beta f_1\psi) \tag{13a}$$

$$e^{-j\beta R_{013}} \doteq e^{-i\beta v_0}(1 + j\beta f_0\psi) \qquad e^{-j\beta R_{014}} \doteq e^{-i\beta v_0}(1 - j\beta f_0\psi) \tag{13b}$$

With (9) to (13*b*), (8) reduces to the following approximate form if all terms with ψ^2 and still higher powers of ψ as a factor are neglected:

$$\begin{aligned} \boldsymbol{E}_{z1}(u) \doteq \frac{\zeta_0 \boldsymbol{I}_3(0)\psi}{2\pi \sin G} \Bigg\{ & f_1 e^{-j\beta v_1}\left[-j\,\frac{1 + j\beta v_1}{v_1^2}\cos K + (u-h)\left(\frac{2 + j\beta v_1}{v_1^3} \right.\right. \\ & \left. - \frac{j}{\beta}\,\frac{3 + j\beta v_1}{v_1^4}\right)\sin K \Bigg] - f_0 e^{-j\beta v_0}\left[-j\,\frac{1 + j\beta v_0}{v_0^2}\cos G \right. \\ & \left.\left. + u\left(\frac{2 + j\beta v_0}{v_0^3} - \frac{j}{\beta}\,\frac{3 + j\beta v_0}{v_0^4}\right)\sin G \right] \Bigg\} \end{aligned} \tag{14}$$

This is the electric field maintained at Q_1 in conductor 1 (Fig. 4.1) by the equal and opposite currents and charges in conductors 3 and 4 of the oscillator or coupled section of line.

In order to represent the electric field of transmission-line oscillators of even and odd symmetries with respect to their centers, it is advantageous to determine the field maintained at Q_1 by two sections of transmission line, of which the first is that shown in Fig. 4.1 and the second is similar but extended in the opposite direction, as shown in Fig. 4.3. The current in this second section is given by

$$-\boldsymbol{I}_4(u') = \boldsymbol{I}_3(u') = \pm \boldsymbol{I}_3(0)\sin\beta(g + u') \qquad -h \leqq u' \leqq 0 \tag{15}$$

where the upper sign applies to an oscillator in which the current is even, $I(-u') = I(u)$, and the lower sign applies to an oscillator in which the current is odd, $I(-u') = -I(u)$.

The field maintained by the current in the second section is like that given in (14) if the proper sign is prefixed and u is replaced by $-u$.

This involves the substitution of v_2 and f_2, as defined by

$$v_2^2 \equiv (u+h)^2 + r_0^2 + \frac{b_0^2}{4} \qquad f_2 = \frac{b_0 r_0}{2v_2} \tag{16}$$

for v_1 and f_1, as defined in (10) and (12a). The resulting expression is

$$E_{z1}(u) = \mp \frac{j\zeta_0 I_3(0)\psi}{2\pi \sin G} \left\{ f_2 e^{-j\beta v_2} \left[\frac{1+j\beta v_2}{v_2^2} \cos K - j(u+h)\left(\frac{2+j\beta v_2}{v_2^3} + \frac{3+j\beta v_2}{\beta v_2^4} \right) \sin K \right] - f_0 e^{-j\beta v_0} \left[\frac{1+j\beta v_0}{v_0^2} \cos G - ju \left(\frac{2+j\beta v_0}{v_0^3} + \frac{3+j\beta v_0}{\beta v_0^4} \right) \sin G \right] \right\} \tag{17}$$

The sum of (14) and (17) gives the complete electric field maintained at Q_1 by a transmission-line oscillator of length $2h$ which has an even (upper

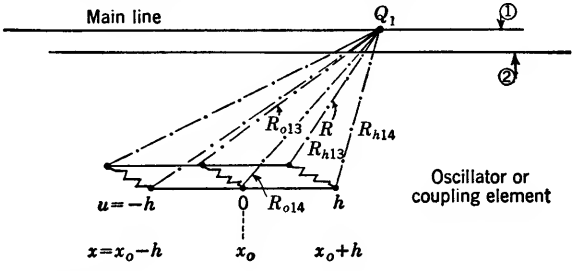


FIG. 4.3. Transmission line with coupled driven section of line or oscillator consisting of two parts each of length h.

sign) or odd (lower sign) distribution of current with respect to its center at $u = 0$ or $x = x_0$.

Even Currents and Fields. The simplest special case is the field of a half-wave section of line with vanishing currents at both ends. In this case $K = 0$, and $G = H = \pi/2$. Since the current is even, the upper sign in (17) applies. The complete field at Q_1 is

$$E_{z1}(u) = \frac{-j\zeta_0 I_3(0)\psi}{2\pi} \left(f_1 e^{-j\beta v_1} \frac{1+j\beta v_1}{v_1} + f_2 e^{-j\beta v_2} \frac{1+j\beta v_2}{v_2} \right) \tag{18}$$

Numerical computations have been made for an actual oscillator of the type shown in Fig. 1.2. The following constants apply:

$$\beta = \frac{2\pi}{\lambda} = 0.333 \text{ cm}^{-1}$$

$$2h = 20 \text{ cm} \qquad b = b_0 = 2 \text{ cm} \qquad r_0 = 10 \text{ cm} \qquad \psi = \sin^{-1} 0.1 \doteq 0.1$$

$$K = 1.237 \qquad H \equiv \beta_0 h = 0.333 \qquad G \equiv H + K = \frac{\pi}{2}$$

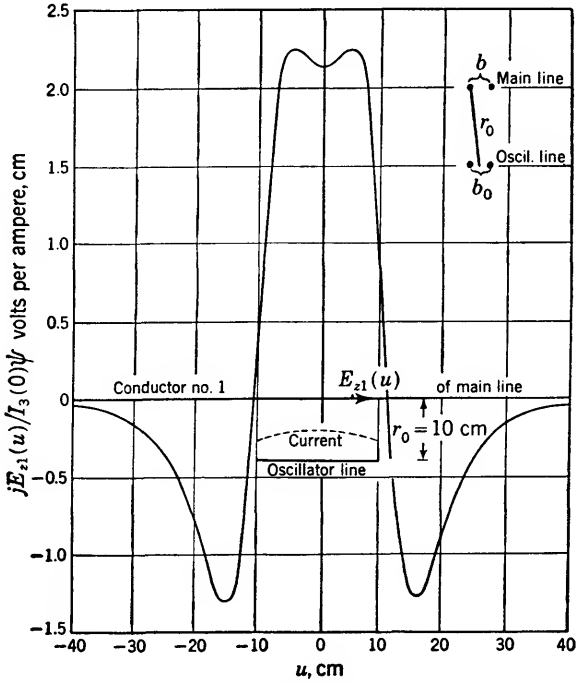


FIG. 4.4. Electric field maintained by transmission-line oscillator with even current.

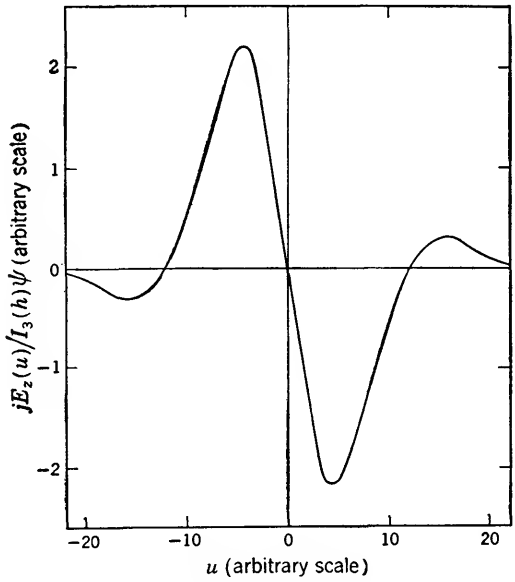


FIG. 4.5. Sketch of typical electric field maintained by transmission-line oscillator with odd current.

A graph of the quantity $jE_{z1}(u)/I_z(0)\psi$ as a function of u is given in Fig. 4.4.

Odd Currents and Fields. The simplest special case is the field of a half-wave section of line with vanishing currents at the center. In this case $K = \pi/2$, $H = \pi/2$, and $G = K + H = \pi$. Since the current at $u = 0$ vanishes, it is convenient to substitute $I_3(h) = I_3(0)/\sin G$ for the indeterminate form 0/0. The resultant field is the sum of (14) and (17), with lower sign. Thus

$$E_{z1}(u) = \frac{\zeta_0 I_3(h)}{2\pi}\left[(u-h)f_1 e^{-j\beta v_1}\left(\frac{2+j\beta v_1}{v_1^3} - \frac{j}{\beta}\frac{3+j\beta v_1}{v_1^4}\right) + (u+h)f_2 e^{-j\beta v_2}\left(\frac{2+j\beta v_2}{v_2^3} - \frac{j}{\beta}\frac{3+j\beta v_2}{v_2^4}\right)\right] \quad (19)$$

A sketch of the type of field represented by (19) is given in Fig. 4.5.

Asymmetrical Currents and Fields. If the currents are neither odd nor even with respect to the center of the oscillator or coupling element, they may be represented as the sum of even currents and odd currents. Accordingly the electric field is the sum of a field of the even type shown in Fig. 4.4 and the odd type shown in Fig. 4.5 with appropriate amplitudes and phases. If the primary section of line is terminated in its characteristic impedance at $u = h$ in Fig. 4.3, the current distribution is

$$-I_4(u') = I_3(u') = I_3(0)(\cos \beta u' - j \sin \beta u') \quad (20)$$

Since this is the sum of the even currents and $-j$ times the odd currents, it follows that the electric field of a traveling wave of current on a half wavelength of line is $E_{z1}(u)$ in (18) minus j times $E_{z1}(u)$ in (19).

5. Current and Voltage in a Line Driven by a Coupled Section of Transmission Line; Directional Coupler.[149] The current and voltage at a point z along a transmission line which extends from $z = 0$ to $z = s$ and which is driven by a pair of equal and opposite point generators with emfs $\frac{1}{2}V_x^e$ at $z = x$ are given by Chap. IV, Sec. 2, Eqs. (5) and (6). They may be expressed as follows:

$$I_z = \frac{V_x^e S_w}{Z_c S_s}\sinh(\gamma x + \theta_0) \qquad x \leqq z \leqq s \quad (1)$$

$$V_z = \frac{V_x^e C_w}{S_s}\sinh(\gamma x + \theta_0) \qquad x \leqq z \leqq s \quad (2)$$

where $S_w = \sinh(\gamma w + \theta_s)$ $\quad S_s = \sinh(\gamma s + \theta_0 + \theta_s)$

and $C_w = \cosh(\gamma w + \theta_s)$

As usual, $w \equiv s - z$.

If the line is driven by a continuous distribution of generators over a range extending from $z = x_0 - g$ to $z = x_0 + g$, it follows from the principle of superposition that the current and voltage are the super-

positions of the currents and voltages maintained by all pairs of generators localized in each element dx between $x_0 - g'$ and $x_0 + g$. Thus, if the emf maintained by the distribution of generators per unit length in conductor 1 is $E_z^e(x)$ and that in conductor 2 is $-E_z^e(x)$, the total current and voltage maintained by the entire distribution are

$$I_z = \frac{S_w}{Z_c S_s} \int_{x_0-g'}^{x_0+g} E_z^e(x) \sinh(\gamma x + \theta_0)\, dx \tag{3}$$

$$V_z = \frac{C_w}{S_s} \int_{x_0-g'}^{x_0+g} E_z^e(x) \sinh(\gamma x + \theta_0)\, dx \tag{4}$$

The electric field maintained along the conductors of the line by the current in a coupled section is equivalent to a distribution of generators. In this case the distribution of emfs per unit length $E_z^e(x)$ is replaced by $E_{z1}(u)$, as given by the sum of Sec. 4, Eqs. (14) and (17), if the currents in the oscillator have even or odd symmetry with respect to the center of the oscillator at $u = 0$ or $x = x_0$. Note that $u = x - x_0$. In the general case, in which the current in the oscillator is characterized by no particular symmetry, it may be expressed as the sum of odd and even parts, and $E_{z1}(u)$ appropriate to each part may be obtained using Sec. 4, Eqs. (14) and (17), with suitable relative amplitudes and phases.

The electric field maintained along the line by the currents in the oscillator may be expressed in a Fourier series of the following type:

$$E_{z1}(x - x_0) = \sum_{m=1}^{\infty} [a_m \cos m\beta'(x - x_0) + b_m \sin m\beta'(x - x_0)] \tag{5}$$

in the range of x between $x_0 - g$ and $x_0 + g$. The a_m's and b_m's are complex constants. For use in (3) and (4) it is more convenient to express (5) in terms of hyperbolic functions. Thus, with $\gamma' = j\beta'$,

$$E_{z1}(x - x_0) = \sum_{m=1}^{\infty} [a_m \cosh m\gamma'(x - x_0) - jb_m \sinh m\gamma'(x - x_0)] \tag{6}$$

If (6) is substituted in (3) and (4), the following integrals must be evaluated:

$$J_1 \equiv \int_{x_0-g'}^{x_0+g} \sinh(\gamma x + \theta_0) \cosh m\gamma'(x - x_0)\, dx \tag{7a}$$

$$J_2 \equiv \int_{x_0-g'}^{x_0+g} \sinh(\gamma x + \theta_0) \sinh m\gamma'(x - x_0)\, dx \tag{7b}$$

By using familiar formulas (e.g., Dwight 651.03 and 651.05) the products of two hyperbolic functions may be transformed into sums of hyperbolic functions that are readily integrated. The results are

$$J_1 = (p + q) \sinh(\gamma x_0 + \theta_0) + (p' + q') \cosh(\gamma x_0 + \theta_0) \tag{8a}$$

$$J_2 = (p' - q') \sinh(\gamma x_0 + \theta_0) + (p - q) \cosh(\gamma x_0 + \theta_0) \tag{8b}$$

where

$$p \equiv \frac{\sinh g(\gamma + m\gamma') + \sinh g'(\gamma + m\gamma')}{2(\gamma + m\gamma')} \tag{9a}$$

$$p' \equiv \frac{\cosh g(\gamma + m\gamma') - \cosh g'(\gamma + m\gamma')}{2(\gamma + m\gamma')} \tag{9b}$$

$$q \equiv \frac{\sinh g(\gamma - m\gamma') + \sinh g'(\gamma - m\gamma')}{2(\gamma - m\gamma')} \tag{9c}$$

$$q' \equiv \frac{\cosh g(\gamma - m\gamma') - \cosh g'(\gamma - m\gamma')}{2(\gamma - m\gamma')} \tag{9d}$$

By now introducing the notation

$$V_x \equiv \sum_{m=1}^{n} [a_m(p + q) - jb_m(p' - q')] \tag{10a}$$

$$W_x \equiv \sum_{m=1}^{n} [a_m(p' + q') - jb_m(p - q)] \tag{10b}$$

Eqs. (3) and (4) reduce to

$$I_z = [V_x \sinh(\gamma x_0 + \theta_0) + W_x \cosh(\gamma x_0 + \theta_0)] \frac{S_w}{Z_c S_s} \tag{11}$$

$$V_z = [V_x \sinh(\gamma x_0 + \theta_0) + W_x \cosh(\gamma x_0 + \theta_0)] \frac{C_w}{S_s} \tag{12}$$

These expressions are identical with Chap. IV, Sec. 4, Eqs. (5) and (6), for the current and voltage maintained by three pairs of equal and opposite point generators, as illustrated in Chap. IV, Fig. 4.1. Note that the

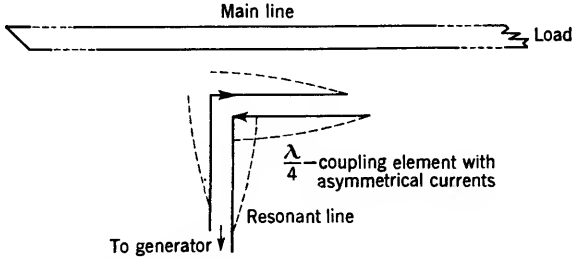


FIG. 5.1. Transmission-line coupling element with open end and asymmetrical current distribution and electric field.

coordinate x_0, which locates the point on the line opposite the center of the oscillator, replaces the coordinate x, which locates the middle pair of point generators. A coupling unit that requires this general representation is shown in Fig. 5.1. The appropriate electric fields can be constructed from combinations of Sec. 4, Eqs. (14) and (17), or from Sec. 4, Eq. (14), alone.

Even Currents. If the distribution in the driven section of line is even with respect to its center, the coefficients b_m of the sine terms in (5)

vanish, and the field maintained by these symmetrical currents is also even. If the driven section is far enough from the ends of the line so that the coordinates $z = x_0 - g'$ and $x_0 + g$ where the field is vanishingly small are points actually on the line and not beyond one or the other end, the *effective* exciting field of the even currents is also even, and $g' = g$.

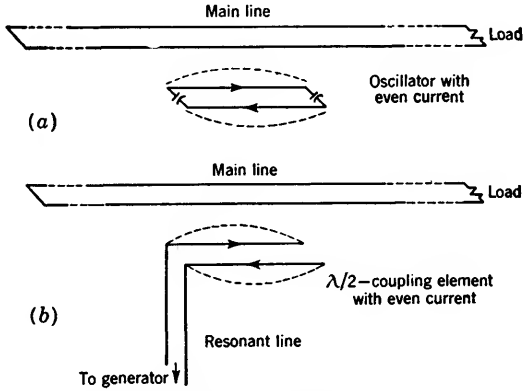


FIG. 5.2. Transmission-line oscillator and coupling element with even currents and electric fields.

It follows from (9*b*,*d*) that $\mathfrak{p}' = \mathfrak{q}' = 0$. The effective driving voltage of the even excitation is given by (10*a*,*b*), with $\mathfrak{b}_m = 0$ and $\mathfrak{p}' = \mathfrak{q}' = 0$. It is

$$\mathfrak{V}_x = \sum_{m=1}^{n} [\mathfrak{a}_m(\mathfrak{p} + \mathfrak{q})] \qquad \mathfrak{W}_x = 0 \tag{13}$$

This corresponds to a single pair of equal and opposite point generators at $z = x_0$. An oscillator and a coupling unit with this type of symmetry are shown in Fig. 5.2. The appropriate electric field is given by the sum of Sec. 4, Eqs. (14) and (17), with the upper sign. It is illustrated in Fig. 4.4 for one particular oscillator.

Odd Currents. If the distribution in the driven section is odd with respect to its center, the coefficients $\mathfrak{a}_m$ of the cosine terms in (5) vanish, and the field maintained by the odd currents is itself odd. If, in addition, the driven section is far from both ends of the line, so that the coordinates $z = x_0 - g'$ and $z = x_0 + g$ are on the line, the *effective* exciting field of the odd currents is also odd, and $g' = g$. It follows from (9*b*,*d*) that $\mathfrak{p}' = \mathfrak{q}' = 0$. The effective driving voltage of the odd excitation is given by (10*a*,*b*), with $\mathfrak{a}_m = 0$ and $\mathfrak{p}' = \mathfrak{q}' = 0$. It is

$$\mathfrak{V}_x = 0 \qquad \mathfrak{W}_x = \sum_{m=1}^{n} [-j\mathfrak{b}_m(\mathfrak{p} - \mathfrak{q})] \tag{14}$$

This corresponds to two pairs of equal and opposite point generators

located at $x_0 - g$ and $x_0 + g$, as shown in Chap. IV, Fig. 3.1. An oscillator and a coupling unit with this type of symmetry are shown in Fig. 5.3. The appropriate electric field is given by the sum of Sec. 4, Eqs. (14) and (17), with the lower sign. A typical example is sketched in Fig. 4.5.

Traveling Waves; Transmission-line Directional Coupler. As indicated at the end of Sec. 4, a traveling-wave distribution of current in the driven

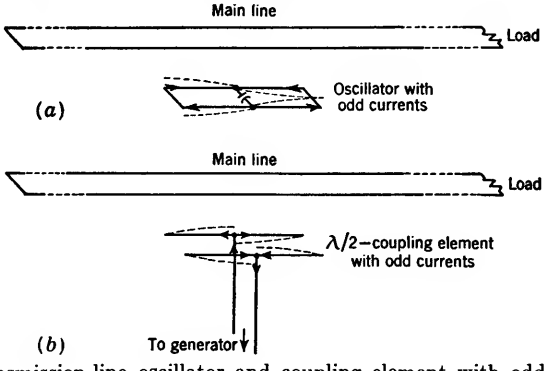


FIG. 5.3. Transmission-line oscillator and coupling element with odd currents and electric fields.

line is equivalent to a superposition of even and odd currents in time quadrature. It follows that the excitation in a coupled line must be equivalent to a superposition of one pair of equal and opposite point generators to represent the even current, and two pairs of such generators to represent the odd current. The appropriate general formulas for the current are Eq. (11) or Chap. IV, Sec. 4, Eq. (5), when $x \leqq z \leqq s$ and Chap. IV, Sec. 4, Eq. (7), when $0 \leqq z \leqq x$. If the coupled secondary line is terminated at both ends in its characteristic impedance so that $\boldsymbol{Z}_0 = \boldsymbol{Z}_c$, $\boldsymbol{Z}_s = \boldsymbol{Z}_c$, or $\rho_0 = \rho_s = \infty$, these equations reduce to

$$\boldsymbol{I}_z = \frac{\boldsymbol{V}_x + \boldsymbol{W}_x}{2\boldsymbol{Z}_c} e^{\gamma(x-z)} \qquad x \leqq z \leqq s \tag{15a}$$

$$\boldsymbol{I}_z = \frac{\boldsymbol{V}_x - \boldsymbol{W}_x}{2\boldsymbol{Z}_c} e^{-\gamma(x-z)} \qquad 0 \leqq z \leqq x \tag{15b}$$

where x is the fixed location of the point generators and z is the point along the line where the current is measured. The following are important special cases:

$$\text{For } \boldsymbol{W}_x = \boldsymbol{V}_x\text{:} \qquad \boldsymbol{I}_z = \begin{cases} \dfrac{\boldsymbol{V}_x}{\boldsymbol{Z}_c} e^{\gamma(x-z)} & x \leqq z \leqq s \\ 0 & 0 \leqq z \leqq x \end{cases} \tag{16a}$$

$$\text{For } \boldsymbol{W}_x = -\boldsymbol{V}_x\text{:} \qquad \boldsymbol{I}_z = \begin{cases} 0 & x \leqq z \leqq s \\ \dfrac{\boldsymbol{V}_x}{\boldsymbol{Z}_z} e^{-\gamma(x-z)} & 0 \leqq z \leqq x \end{cases} \tag{16b}$$

Thus, when $\boldsymbol{W}_x = \boldsymbol{V}_x$, a traveling wave of current is excited on the coupled transmission line that moves in the positive z direction toward $\boldsymbol{Z}_s = \boldsymbol{Z}_c$, whereas the line in the negative z direction is *not* excited. Alternatively, when $\boldsymbol{W}_x = -\boldsymbol{V}_x$, a traveling wave of current moves toward $\boldsymbol{Z}_0 = \boldsymbol{Z}_c$ in the negative z direction, whereas the line in the positive z direction is not excited. Since from Chap. IV, Sec. 4, Eq. (7), $\boldsymbol{W}_x \doteq j\beta g \boldsymbol{V}^e$, where $\frac{1}{2}\boldsymbol{V}^e$ is the emf of each of the four point generators, it follows with the sign convention in Chap. IV that the condition $\boldsymbol{W}_x = \boldsymbol{V}_x$ corresponds to $\boldsymbol{V}^e = -j\boldsymbol{V}_x/\beta g$ and to the current $\boldsymbol{I}_3(u') = \boldsymbol{I}_3(0)e^{-j\beta(h-u')}$, which is a traveling wave in the negative z direction. Similarly the condition $\boldsymbol{W}_x = -\boldsymbol{V}_x$ corresponds to $\boldsymbol{V}^e = j\boldsymbol{V}_x/\beta g$ and $\boldsymbol{I}_3(u') = \boldsymbol{I}_3(0)e^{j\beta(h-u')}$, which is a traveling wave in the positive z direction in the primary circuit. It follows that a traveling wave in the positive z direction in the primary section of line (terminated coupling element) induces a traveling wave in the *opposite* direction in the coupled transmission line. This behavior corresponds to that described in Chap. III, Sec. 15, for the hybrid junction when used as a directional coupler. It follows that a section of line that is terminated at both ends in its characteristic impedance and is coupled to a second line can be used as a directional coupler. Clearly, energy that reaches $\boldsymbol{Z}_0 = \boldsymbol{Z}_c$ must originate in a traveling wave in the positive z direction in the primary line, and energy that reaches $\boldsymbol{Z}_s = \boldsymbol{Z}_c$ originates in a wave traveling in the negative z direction in the primary line. Details on the construction and operation of such directional couplers are given in the literature.[142,156]

The expressions [Sec. 4, Eqs. (8), (14), and (17)] involve no restriction on the perpendicular distance d between the main line and the oscillator. That is, any degree of coupling is permissible. However, if d is small enough so that the field maintained by the currents in the line induces a significant voltage in the oscillator, the frequency generated is modified by the presence of the line, and coupled-circuit effects resembling those described in Sec. 2 are observed. These may be analyzed by introducing in each circuit appropriate generators maintained by the current in the other circuit and expressing these in the form

$$\boldsymbol{V} = -\boldsymbol{I}\boldsymbol{Z}_m$$

In this manner two simultaneous equations, each involving the currents in both circuits, are obtained, just as in Sec. 2, where the mutual impedance consists simply of an inductance in common.

If the coupling between the oscillator and the main transmission line is loose, so that there is no significant modification of the current in the oscillator or of the frequency generated by it, the equivalent induced emfs $\boldsymbol{V}_x$ and $\boldsymbol{W}_x$ may be treated as constant pairs of point generators.

6. Coupled Transmission Lines. When two transmission lines are sufficiently close and so oriented that the currents and charges in the one

induce significant currents and charges in the other, a mutual interference of the signals transmitted along the lines occurs. At low frequencies this is known as cross talk. At audio frequencies the induced voltages may be derived from relatively simple electrostatic and magnetostatic analyses involving the determination of mutual capacitances and inductances. The general or high-frequency problem of determining the interaction between two transmission lines is much more complicated. A special case of the general problem is analyzed in Secs. 4 and 5, where it is assumed that the two lines lie in parallel planes at the corners of a regular trapezoid, so that both lines remain balanced.

In a more general case the two lines may be assumed parallel but with arbitrary relative positions. The currents are those of transmission lines with arbitrary loads. In general, they are not sinusoidal but are derived

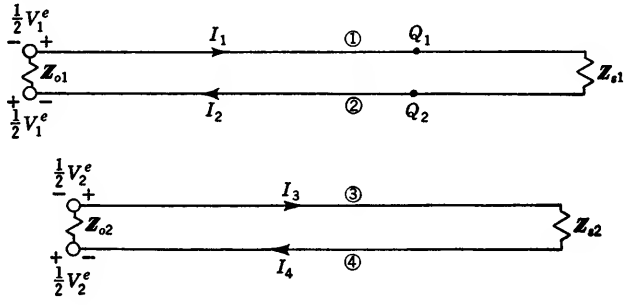


FIG. 6.1. Coupled two-wire lines.

from a hyperbolic sine or cosine of complex argument, as given by Chap. IV, Sec. 2, Eq. (7). The electric field of such a distribution in a single conductor may be determined by using this current instead of Sec. 3, Eq. (1*a*), in the integral [Sec. 3, Eq. (2*a*)]. The field of the currents and charges in the two conductors (e.g., 3 and 4 in Fig. 6.1) of one line at a point Q_1 on conductor 1 of the second line is obtained by superimposing the field of the currents and charges in each of the conductors 3 and 4 at Q_1. Since the positions of the two parallel transmission lines are arbitrary, the field at Q_2 on conductor 2 is not the negative of that at Q_1. However, it may be determined by superimposing the fields of conductors 3 and 4 at Q_2. The fields along each of the conductors 1 and 2 may then be treated as a distribution of point generators. However, they are not equal and opposite in the two conductors, so that the line is unbalanced. The balanced part of the current, which contributes to the balanced current maintained in the line by its driving generators, may be determined in a manner analogous to that used in Sec. 5. The unbalanced current must be analyzed by the methods of antenna theory.[10]

If each of the coupled lines consists of a single conductor parallel and close to a large metal plane, each conductor with its image is equivalent

to a two-wire line and may be analyzed as such following the general method used in Secs. 4 and 5.

7. Admittance of Bridge-coupled Sections of Low-loss Transmission Line; Coupled-circuit Effects Involving Minima and Double Peaks.[150,158] Consider the problem of determining the input admittance Y_1 of the transmission line shown in Fig. 7.1. It consists of a section of line of length w (to be called the primary), which is terminated in an inductive reactance ωL in parallel with the input impedance Z_2 of a second section of line of length u (to be called the secondary), which is terminated in an

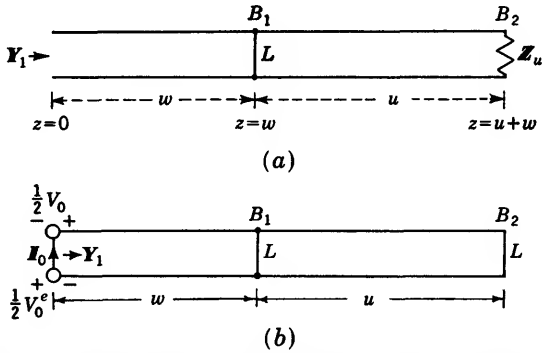


FIG. 7.1. Bridge-coupled sections of transmission line (*a*) with arbitrary termination Z_u and (*b*) with inductive bridge L as termination and a pair of point generators at the input terminals.

arbitrary impedance Z_u. Note that the coupled-circuit oscillator, for which the natural frequencies are determined in Sec. 2, consists essentially of this same circuit, but with a negative resistance connected across the input terminals and with Z_u specialized to be a short circuit or an open circuit. It is shown in Chap. III, Sec. 1, that the normalized input admittance $y_1 = Y_1/Y_c$ of a section of line of length w, when terminated in an arbitrary normalized admittance $y_{1w} = Y_w/Y_c$, is

$$y_1 = \frac{y_{1w} + \tanh \gamma w}{y_{1w} \tanh \gamma w + 1} = \frac{y_{1w} \cosh \gamma w + \sinh \gamma w}{y_{1w} \sinh \gamma w + \cosh \gamma w} \tag{1}$$

$Y_c = G_c(1 + j\phi_c)$ is the characteristic admittance of the line and $\gamma = \alpha + j\beta$ is its propagation constant.

The Normalized Terminal Admittance of the Primary. In the circuit shown in Fig. 7.1 the normalized terminal admittance of the primary is

$$y_{1w} = \frac{1}{j\beta k} + y_2 \tag{2}$$

where y_2 is the normalized input admittance of the second section of line

and where, with v the phase velocity and l the inductance per loop unit length,

$$\beta k = \frac{\omega L}{vl} = \omega L G_c \tag{3}$$

The normalized input admittance of the second section of line may be expressed in the completely hyperbolic form, as follows:

$$\boldsymbol{y}_2 = \coth (A + jF') \tag{4a}$$

where $$A \equiv \alpha u + \rho_u \qquad F' \equiv \beta u + \Phi'_u \tag{4b}$$

The terminal functions ρ and Φ' are discussed in Chap. II, Sec. 15. Using Chap. III, Sec. 1, Eqs. (16b) and (17b), the input conductance and susceptance defined by $\boldsymbol{y}_2 = g_2 + jb_2$ are

$$g_2 = \frac{\sinh A \cosh A}{\sinh^2 A + \sin^2 F'} \doteq \frac{A}{A^2 + \sin^2 F'} \tag{5a}$$

$$b_2 = \frac{-\sin F' \cos F'}{\sinh^2 A + \sin^2 F'} \doteq \frac{-\sin F' \cos F'}{A^2 + \sin^2 F'} \tag{5b}$$

The expressions on the right in (5a) and (5b) apply to a line with low over-all attenuation which satisfies the following inequalities:

$$A^2 = (\alpha u + \rho_u)^2 \ll 1 \qquad \left(\frac{\alpha}{\beta}\right)^2 \ll 1 \tag{6}$$

With (5a) and (5b) substituted in (2), $\boldsymbol{y}_{1w} = g_{1w} + jb_{1w}$ is obtained. Thus

$$g_{1w} \doteq g_2 \doteq \frac{A}{A^2 + \sin^2 F'} \tag{7a}$$

$$b_{1w} \doteq -\left(\frac{1}{\beta k} + \frac{\sin F' \cos F'}{A^2 + \sin^2 F'}\right) \tag{7b}$$

These are the final expressions for the normalized conductance and susceptance of the termination of line 1.

For later reference it is convenient to examine certain ranges of F' for which (7a) and (7b) assume simple forms. Consider first the *principal ranges*, which include all values of $F' = \beta u + \Phi'_u$ which satisfy the following inequality:

$$\sin^2 F' \gg A^2 \tag{8}$$

In these ranges (7a,b) become

$$g_{1w} \doteq A \csc^2 F' \qquad b_{1w} \doteq -\left(\frac{1}{\beta k} + \cot F'\right) \tag{9}$$

For sufficiently small values of the attenuation function A, as required by (6), the ranges of F' excluded by (8) depart only slightly from the points

$$F' \equiv \beta u + \Phi'_u = n\pi \qquad n \text{ integral} \tag{10}$$

so that $$g_{1w} = \frac{1}{A} \qquad b_{1w} = -\frac{1}{\beta k} \tag{11}$$

In order to examine small ranges near the points defined in (10), let

$$F' \equiv \beta u + \Phi'_u = n\pi + \beta d \qquad n = 1, 2, \ldots \tag{12}$$

where d is a small positive or negative quantity that is assumed to satisfy the inequality $(\beta d)^2 \ll 1$. With (12) it follows that

$$\sin F' \cos F' = \tfrac{1}{2} \sin 2F' = \tfrac{1}{2} \sin 2\beta d \doteq \beta d \tag{13a}$$

$$\sin^2 F' = \sin^2 \beta d = (\beta d)^2 \tag{13b}$$

Hence

$$g_{1w} = \frac{A}{A^2 + (\beta d)^2} \tag{14a}$$

$$b_{1w} = -\left[\frac{1}{\beta k} + \frac{\beta d}{A^2 + (\beta d)^2}\right] \tag{14b}$$

The magnitude of the normalized admittance at $F' = n\pi + \beta d$ is

$$y_{1w} = \sqrt{g_{1w}^2 + b_{1w}^2} = \frac{[\beta^4 d^4 + 2\beta^3 d^3 \beta k + \beta^2 d^2(\beta^2 k^2 + 2A^2) + \beta^2 k^2 A^2 + A^4]^{\frac{1}{2}}}{\beta k(A^2 + \beta^2 d^2)} \tag{15a}$$

where

$$A = \frac{\alpha}{\beta}\beta u + \rho_u = \frac{\alpha}{\beta}(n\pi - \Phi'_u + \beta d) + \rho_u \equiv A_n + \alpha d \doteq A_n \tag{15b}$$

where

$$A_n = \frac{\alpha n \pi}{\beta} \tag{15c}$$

Since βd may be positive or negative, it is evident that b_{1w} may vanish. The required values of βd are

$$\text{For } b_{1w} = 0: \qquad \beta d \doteq -\frac{\beta k}{2}\left[1 \pm \sqrt{1 - \left(\frac{2A_n}{\beta k}\right)^2}\right] \doteq \begin{cases} -\beta k \\ -\dfrac{A_n^2}{\beta k} \end{cases} \tag{16a}$$

The corresponding values of g_{1w} are

$$g_{1w} \doteq -\frac{A_n}{\beta d \beta h} = \frac{2A_n}{(\beta k)^2[1 \pm \sqrt{1 - (2A_n/\beta k)^2}]} \doteq \begin{cases} \dfrac{A_n}{\beta^2 k^2} \\ \dfrac{1}{A_n} \end{cases} \tag{16b}$$

By differentiating b_{1w} in (14b) with respect to βd and equating the derivative to zero, the maxima and minima of b_{1w} are located. They occur at

$$\beta d = \pm A_n\left(1 \mp \frac{\alpha}{\beta}\right) \tag{17a}$$

and have the values

$$b_{1w} = -\frac{1}{\beta k}\left(1 \pm \frac{\beta k}{2A_n^2}\right) \tag{17b}$$

The corresponding values of g_{1w} are

$$g_{1w} = \frac{1 \pm \alpha/\beta}{2A_n} \tag{17c}$$

The maximum value of g_{1w} may be located in the same manner. Its location and magnitude are given by

$$\beta d \doteq 0 \qquad (g_{1w})_{\max} \doteq \frac{1}{A_n} \tag{18}$$

The minima of g_{1w} occur in the range specified in (8) where (9) applies. They occur at values of u somewhat smaller than those defined by

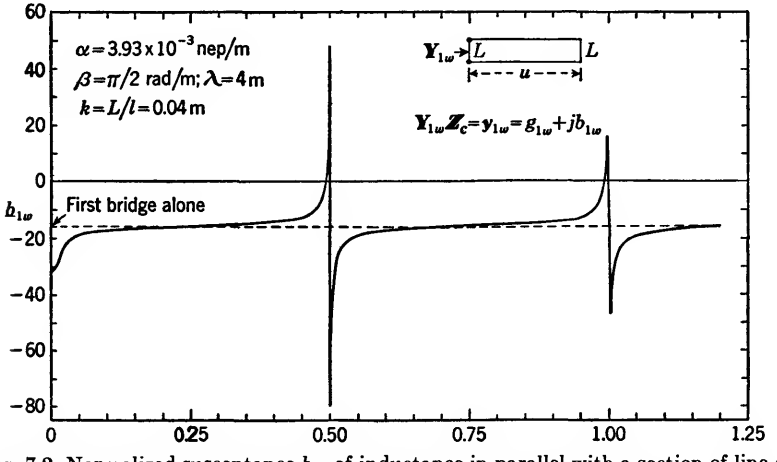


FIG. 7.2. Normalized susceptance b_{1w} of inductance in parallel with a section of line of length u terminated in an equal inductance.

$F' \equiv \beta u + \Phi'_u = [(2n + 1)/2]\pi$ and have magnitudes close to $A = \alpha u$. Extreme values of the magnitude y_{1w} may be obtained by differentiating (15a) with respect to βd. With n integral, they are located at

$$\beta d = 0 \quad \text{or} \quad \beta u = n\pi - \Phi'_u \quad \text{for the maxima} \tag{19}$$

$$\beta d \doteq -\beta h \quad \text{or} \quad \beta u = n\pi - \beta k - \Phi'_u \quad \text{for the minima} \tag{20}$$

It is seen that the minima of y_{1w} virtually coincide with one of the sets of values for which $b_{1w} = 0$. The extreme magnitudes of y_{1w} are

$$(y_{1w})_{\max} \doteq \frac{1}{A_n} \qquad (y_{1w})_{\min} \doteq \frac{A_n^2}{\beta k} \tag{21}$$

Graphs of the normalized input susceptance b_{1w}, the conductance g_{1w}, and the magnitude of the admittance $y_{1w} = \sqrt{g_{1w}^2 + b_{1w}^2}$ are shown in Figs. 7.2 to 7.4 for a special case in which the termination of the second section of the line is also an inductive reactance ωL. That is, $Z_u \doteq j\omega L$, so that $\Phi'_u = \beta k$ and $\rho_u \doteq 0$. It follows that $F' = \beta(u + k)$. The numerical values of the several constants given in the figures are those of a particular apparatus. Numerical data are given in Table 7.1.

A study of Figs. 7.2 and 7.3 reveals that wide ranges of normalized terminal conductance and susceptance are available. The susceptance remains near the value characteristic of the first bridge alone, except near $F' = \beta(u + k) = n\pi$, where it varies rapidly between high positive and negative values. The conductance is quite small except near the points $F' = n\pi$, where it rises to high maxima. The magnitude of the normalized admittance shown in Fig. 7.4 is characterized by adjacent minima and maxima near $F' = n\pi$. As indicated in (19) and (20), the maxima occur at $\beta u = n\pi - \beta k$ and the minima at $\beta u = n\pi - 2\beta k$ for the special case represented in Fig. 7.4, in which $\Phi_u' = \beta k$. The latter formula is convenient to use in the experimental determination of k for a conducting bridge, as discussed later in this section.

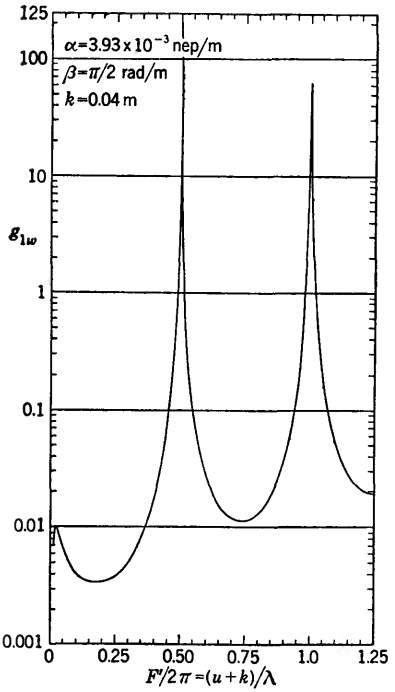


FIG. 7.3. Normalized conductance associated with the susceptance in Fig. 7.2.

The Input Admittance of the Primary in the Bridge-coupled Section. The real and imaginary parts of (1) may be separated by introducing $\boldsymbol{y}_{1w} = g_{1w} + jb_{1w}$. The following results

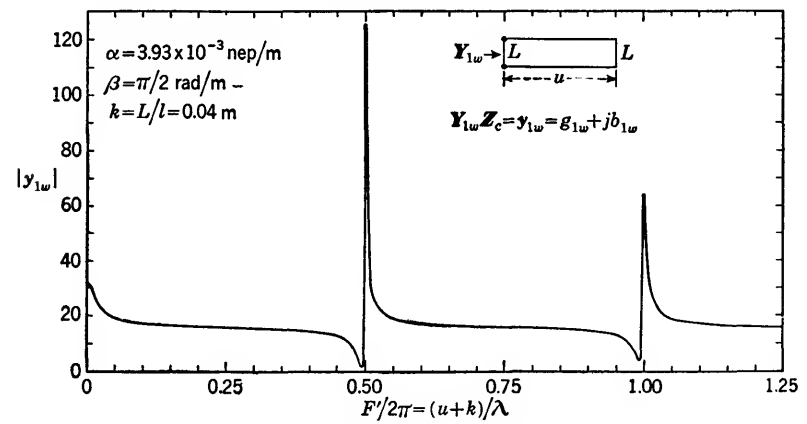


FIG. 7.4. Magnitude of normalized input admittance associated with the susceptance and conductance of Figs. 7.2 and 7.3.

TABLE 7.1. NUMERICAL VALUES OF b_{1w} AND g_{1w} FOR THE FOLLOWING PARAMETERS:

$\beta = \frac{\pi}{2}$ radians/m; $k = 0.04$ m; $\alpha = 3.93 \times 10^{-3}$ neper/m

$F'/\beta = u + k$, m	b_{1w}	g_{1w}	y_{1w}	$F'/\beta = u + k$, m	b_{1w}	g_{1w}	y_{1w}
0.05	−28.6	0.0068	28.6	2.50	−16.9	0.0193	16.9
0.08	.....	0.0099		3.00	−15.9	0.0116	15.9
0.10	−22.2	0.0096	22.2	3.50	−14.9	0.0272	14.9
0.20	−19.0	0.0066	19.0	3.80	−12.8	0.155	12.8
0.50	−16.9	0.0036	16.9	3.90	−9.6	0.616	9.6
1.00	−15.9	0.0038	15.9	3.95	−3.2	2.397	4.0
1.50	−14.9	0.0115	14.9	3.96	−0.99	3.666	3.8 min
1.80	−12.8	0.0726	12.8	3.963	0.0	4.178	4.2
1.90	−9.6	0.297	9.6	3.97	+3.18	6.255	7.0
1.95	−3.2	1.200	3.41	3.98	+9.54	12.54	15.7
1.96	−0.2	1.885	1.9 min	3.99	+15.9 max	31.43	35.2
1.9606	0.0	1.940	1.94	3.9973	0.0	36.39	36.4
1.97	+4.7	3.231	5.7	4.00	−15.9	63.03	65.0
1.98	+14.1	7.273	15.9	4.01	−47.7 min	31.59	57.2
1.995	+47.7 max	62.23	78.5	4.02	−41.4	12.67	43.3
1.9994	0.0	123.3	123.3	4.03	−35.0	6.350	35.6
2.00	−15.9	124.8 max	125.8 max	4.04	−30.9	3.740	31.1
2.005	−79.5 min	62.55	101.2	4.05	−28.6	2.458	28.7
2.01	−66.7	25.08	71.3	4.10	−22.2	0.648	22.2
2.03	−36.6	3.331	36.8	4.20	−19.0	0.172	19.0
2.05	−28.6	1.264	28.6	4.50	−16.9	0.0351	16.9
2.10	−22.2	0.329	22.2	5.00	−15.9	0.0195	15.9
2.20	−19.0	0.0891	19.0				

are obtained:

$$\boldsymbol{y}_1 = \frac{D \cos(\beta w + \delta) + jE \sin(\beta w + \epsilon)}{E \cos(\beta w + \epsilon) + jD \sin(\beta w + \delta)} \tag{22a}$$

where

$$D \equiv [(g_{1w} + \alpha w)^2 + b_{1w}^2 \alpha^2 w^2]^{\frac{1}{2}} \qquad E \equiv [(1 + g_{1w}\alpha w)^2 + b_{1w}^2]^{\frac{1}{2}} \tag{22b}$$

$$\delta \equiv \tan^{-1} \frac{b_{1w}\alpha w}{g_{1w} + \alpha w} \qquad \epsilon \equiv \tan^{-1} \frac{b_{1w}}{1 + g_{1w}\alpha w} \tag{22c}$$

It follows that, with $\boldsymbol{y}_1 = g_1 + jb_1 = y_1 e^{j\theta_1}$,

$$g_1 = \frac{DE \cos(\delta - \epsilon)}{D^2 \sin^2(\beta w + \delta) + E^2 \cos^2(\beta w + \epsilon)} \tag{23a}$$

$$b_1 = \frac{\frac{1}{2}[E^2 \sin 2(\beta w + \epsilon) - D^2 \sin 2(\beta w + \delta)]}{D^2 \sin^2(\beta w + \delta) + E^2 \cos^2(\beta w + \epsilon)} \tag{23b}$$

$$y_1 = \left[\frac{D^2 \cos^2(\beta w + \delta) + E^2 \sin^2(\beta w + \epsilon)}{D^2 \sin^2(\beta w + \delta) + E^2 \cos^2(\beta w + \epsilon)}\right]^{\frac{1}{2}} \tag{23c}$$

$$\theta_1 = \tan^{-1} \frac{E^2 \sin 2(\beta w + \epsilon) - D^2 \sin 2(\beta w + \delta)}{2DE \cos(\delta - \epsilon)} \tag{23d}$$

Special Case with Self-resonant Primary. An interesting special case is obtained when the primary circuit is adjusted to be self-resonant before the secondary is connected. Input resonance for a section of line of length w, when terminated in an inductive bridge of equivalent length k, is defined by $\beta(w + k) = m\pi$, where m is an integer. With this set of values of βw, the magnitude y_1 in (23c) may be transformed into

$$y_1 = \left[\frac{F^2 \cos^2 \beta k - 2b_{1w}(1 - \alpha^2 w^2) \sin \beta k \cos \beta k + G^2 \sin^2 \beta k}{G^2 \cos^2 \beta k + 2b_{1w}(1 - \alpha^2 w^2) \sin \beta k \cos \beta k + F^2 \sin^2 \beta k}\right]^{\frac{1}{2}} \quad (24)$$

where $F^2 \equiv b_{1w}^2 + (g_{1w} + \alpha w)^2 \qquad G^2 \equiv b_{1w}^2 \alpha^2 w^2 + (1 + g_{1w}\alpha w)^2 \quad (25)$

In most practically interesting cases the following inequalities are satisfied:

$$(\alpha w)^2 \ll 1 \qquad (\beta k)^2 \ll 1 \quad (26)$$

With (26) the magnitude (24) reduces to

$$y_1 \doteq \left[\frac{(b_{1w} - \beta k)^2 + (g_{1w} + \alpha w)^2}{(b_{1w}^2 + g_{1w}^2)(\alpha^2 w^2 + \beta^2 k^2) + 2(g_{1w}\alpha w + b_{1w}\beta k) + 1}\right]^{\frac{1}{2}} \quad (27)$$

The general behavior of y_1 in (27) as a function of the electrical length βu of the secondary may be determined by considering the orders of magnitude of b_{1w} and g_{1w}. Thus, in the principal ranges specified in (8), g_{1w} is small compared with b_{1w}, which remains almost constant near $-1/\beta k$, as is clear from Figs. 7.2 and 7.3. With this value of b_{1w} substituted in (27), the leading term in the numerator is $b_{1w}^2 = 1/\beta^2 k^2$. The terms $b_{1w}^2\beta^2 k^2 + 2b_{1w}\beta k + 1$ in the denominator cancel, and the leading term is $b_{1w}^2 \alpha^2 w^2 = \alpha^2 w^2/\beta^2 k^2$. It follows that y_1 remains approximately constant at the value

$$y_1 \doteq \frac{1}{\alpha w} \quad (28)$$

in the range defined in (8). However, this is the value characteristic of the self-resonant primary alone, with the secondary removed. Thus it is to be expected that y_1 is sensibly constant at the large value $1/\alpha w$, except when the secondary length is such that $F' = \beta u + \Phi_u'$ is near $n\pi$, where both b_{1w} and g_{1w} become large.

In the ranges of u for which $F' = \beta u + \Phi_u'$ is near $n\pi$, g_{1w} is very large compared with αw and βk, and b_{1w} varies between large positive and negative values. It follows that in these ranges the numerator in (27) reduces to $b_{1w}^2 + g_{1w}^2 = y_{1w}^2$. Thus

$$y_1 = \frac{y_{1w}}{[y_{1w}^2(\alpha^2 w^2 + \beta^2 k^2) + 2(g_{1w}\alpha w + b_{1w}\beta k) + 1]^{\frac{1}{2}}} \quad (29)$$

Although, with (26), αw and βk are both small, y_{1w} may be sufficiently great so that all terms in the denominator contribute significantly. Nevertheless, since y_{1w} is the entire numerator, it may be expected that

the variation of y_1 with u will resemble that of y_{1w}. That is, there should be maxima near $\beta u = n\pi - \Phi'_u$ and minima near $\beta u = n\pi - \beta k - \Phi'_u$. Since these minima of y_{1w} coincide with zero values of b_{1w}, and g_{1w} is sufficiently small so that the leading term in the denominator of (29) is 1, it follows that the minima in y_1 must occur essentially at the same values of βu as the minima in y_{1w}. Graphs of the magnitude y_1 as functions of the length u of the secondary are given in Figs. 7.5 and 7.6 for various conditions. Figure 7.5 has been evaluated for a rather long primary circuit for a reason that is discussed below. As a consequence, the high maxima in y_{1w} shown in Fig. 7.4 have corresponding maxima in y_1 which

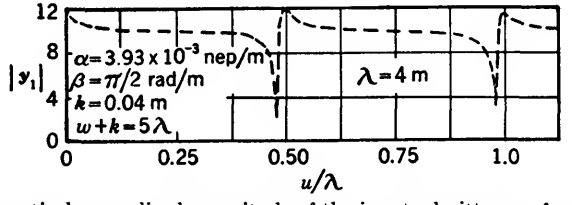


FIG. 7.5. Theoretical normalized magnitude of the input admittance of a self-resonant section of line of electrical length $\beta(w + k) = 10$, when terminated in an inductance $L = kl$ in parallel with a second section of line of electrical length u also terminated in $L = kl$.

are very much reduced. On the other hand, the minima of y_1 are comparable with those of y_{1w}. In Fig. 7.6, y_1 is shown for several values of w, α, and k. It is seen that, whereas the maxima may be greatly altered, the minima are all sharp and actually occur at

$$\beta u = n\pi - 2\beta k \tag{30}$$

in all cases when $\Phi'_u = \beta k$.

The Determination of the Equivalent Length k of a Conducting Bridge. Use may be made of the simple formula (30) to determine the equivalent length k of each of two identical conducting bridges by direct experimental measurement. Clearly, if the sharp minima (in Fig. 7.5 or 7.6) in the magnitude of the normalized input admittance can be located, the distance between the fixed bridge terminating the primary and the identical bridge terminating the extensible secondary, when this has a length to give the first minimum in y_1, is

$$u = \frac{\lambda}{2} - 2k \tag{31}$$

and the distances between adjacent successive minima are $\lambda/2$. Thus, by locating the first and second minimum relative to the fixed bridge (these are shown, for example, in Fig. 7.5), both $\lambda/2 - 2k$ and $\lambda/2$ may be measured. From these measurements $2k$ is determined.

It is not necessary actually to measure the input admittance $\boldsymbol{Y}_1$ of the bridge-coupled circuit, shown in Fig. 7.1 (with $\boldsymbol{Z}_u = j\omega L$) as a function

of u, in order to locate the minima in $y_1 = Y_1/Y_c \doteq Y_1/G_c$. Since the normalized input admittance is defined by

$$y_1 = \frac{I_0}{V_0 Y_c} \tag{32}$$

where I_0 is the current and V_0 is the voltage at the input terminals $z = 0$

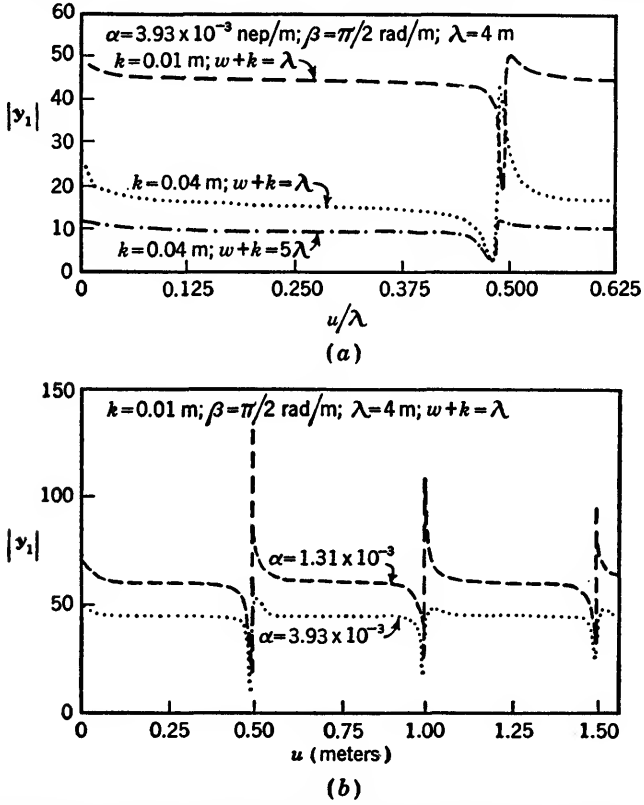


FIG. 7.6. Magnitude of normalized admittance (a) for different values of $L = kl$ and w and (b) for different values of the attenuation constant α.

of the primary, it is clear that $|y_1|$ is proportional to $|I_0|$. Hence, if an impedanceless ammeter is connected in series with an impedanceless generator across the input terminals of the primary in Fig. 7.1, and the magnitude of the current I_0 is observed as u is changed (with $Z_u = j\omega L$), the minima of I_0 coincide with those of y_1.

In practice, the combination of an impedanceless ammeter in series with an impedanceless generator is unavailable, and a finite value of Z_0 is unavoidable. However, an actual circuit consisting of a primary of length w', driven by a generator in series with an ammeter, and their

combined impedance Z_0 at $z = 0$ may be approximated by an ideal circuit consisting of a primary of length $w > w'$, driven by an impedanceless generator in series with an impedanceless ammeter. The requirement that the input currents in the two cases be the same is simply

$$Z_{1in}(w') + Z_0 = Z_{1in}(w) \tag{33a}$$

or, in terms of normalized values,

$$\coth(\gamma' w' + \theta_w) + z_{10} = \coth(\gamma w + \theta_0) \tag{33b}$$

In (33*b*) it has been assumed that the characteristic impedances of the

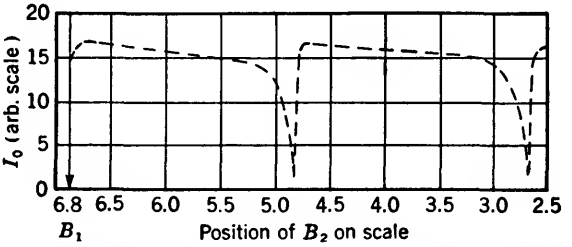


FIG. 7.7. Experimentally determined magnitude of current entering primary as length of bridge-coupled secondary is increased. B_1 is the location of the bridge terminating the primary; B_2 is the location of the bridge terminating the secondary. Line and bridges are of No. 12 copper wire; $\lambda = 4.3$ m.

actual and the equivalent sections of line are the same, but the propagation constants γ' and γ may differ in their real parts. That is, $\gamma' = \alpha' + j\beta$, and $\gamma = \alpha + j\beta$.

In the principal ranges of the input impedances, Chap. III, Sec. 2, Eqs. (32*a*,*b*), may be used in (33*b*) to separate the real and imaginary parts. This leads to the following pair of equations for determining w and α of the equivalent section of line:

$$x_{10} - \cot(\beta w' + \Phi_w) = -\cot(\beta w + \Phi_w) \tag{34a}$$

$$2r_{10} + \sinh 2(\alpha' w' + \rho_w) \csc^2(\beta w' + \Phi_w) = \sinh 2(\alpha w + \omega_w) \csc^2(\beta w + \Phi_w) \tag{34b}$$

From (34*a*)

$$\beta w = \cot^{-1}[\cot(\beta w' + \Phi_w) - x_{10}] - \Phi_w - n\pi \qquad n \text{ integral} \tag{35}$$

If w, as given by (35), is substituted in (34*b*), a value of α may be determined for each choice of the integer n. In general, it is convenient to select that value of n which will make α and α' as nearly equal as possible. Actually, since the location of the minima in y_1 is not sensitive to the precise value of α, it is often adequate (especially if w is large) to select the value of n which makes α as near α' as possible and then to approximate α by α'.

In Fig. 7.7 is shown an experimentally determined curve of an amplitude proportional to I_0 in a current indicator across the input terminals

of a bridge-coupled line. The secondary circuit and the coupling and terminating bridges are those described in connection with the numerical values in Table 7.1 and the curves of Figs. 7.2 to 7.4. By observing the successive amplitudes of six resonance maxima in the primary circuit when w was varied with the secondary absent, the approximate length of an equivalent circuit with impedanceless detector and generator was determined. The total equivalent length w of the primary turned out to be 5λ (to the nearest half wavelength in determining α, which was then made equal to α'). Thus the curve of y_1 in Fig. 7.5 is the approximate theoretical equivalent of Fig. 7.7. The agreement is seen to be excellent.

By determining the values of u for the two minima in Fig. 7.7, the wavelength of the generated signal and the equivalent length k of the identical bridges may be determined. In this particular case the distance between the two minima is 2.15 m, so that $\lambda = 4.30$ m; the distance between the coupling bridge B_1 and B_2 when at the first minimum is 2.07 m, so that $k = (2.15 - 2.07)/2 = 0.04$ m.

Double-hump Phenomena. Interesting coupled-circuit effects sometimes known as "double-hump phenomena" are easily obtained with the circuit of Fig. 7.1. In principle, double humps depend on a superposition of the conventional resonance peaks described in Chap. IV, Sec. 9, and coupled-circuit minima of the types shown in Figs. 7.5 to 7.7. Depending on the particular tuning adjustments, the minima may be made to occur exactly at the center of a simple resonance maximum or displaced toward one or the other side. The appropriate conditions may be described in conjunction with the circuit of Fig. 7.1*b*.

In order to obtain conventional resonance maxima of I_0 in Fig. 7.1*b* or of normalized input admittance in Fig. 7.1*a* by moving the conducting bridge B_1 (Fig. 7.1*b*), it is necessary that the secondary circuit have a negligible reaction on the primary when βw is near and at its resonant values, defined by $\beta w + \Phi_0 + \Phi_w = m\pi$, where m is an integer with βw positive. In the circuit of Fig. 7.1*b*, $\Phi_0 = \pi/2$, and $\Phi_w = \pi/2 + \beta k$, so that the condition for resonance in this case is simply $\beta(w + k) = m\pi$, with $m = 1, 2, \ldots$. The reaction of the secondary is negligible if its electrical effective length $\beta u + \Phi_u = \beta(u + k) = n\pi + \pi/2$, where n is an integer. Thus, if the electrical length $\beta s = \beta(u + w)$ is near $N\pi + \pi/2$, where N is an integer, the resonant values of βw coincide with values of βu for which the effect of the secondary is negligible. Hence, if B_1 in Fig. 7.1*a* or *b* is moved with B_2 fixed, so that $\beta s \doteq N\pi + \pi/2$, the normalized input admittance y_1 in Fig. 7.1*a* or the magnitude of the current in Fig. 7.1*b* will have maxima when $\beta(w + k) = m\pi$. A theoretical curve of y_1, which is proportional to I_0, is curve f in Fig. 7.8. This curve was computed for the long primary circuit previously described. Similar but sharper curves are obtained for smaller values of w, as described in Chap. IV, Sec. 8.

The maxima shown in Fig. 7.8 may be split by a minimum of the type illustrated in Fig. 7.5 if the over-all electrical length βs is adjusted to a value such that $\beta u = m\pi - 2\beta k$ when $\beta w = n\pi - \beta k$. That is, when $\beta s = N\pi - 3\beta k$, the reaction of the secondary should split the primary maximum symmetrically as B_1 in Fig. 7.1 is moved through an appropriate range.

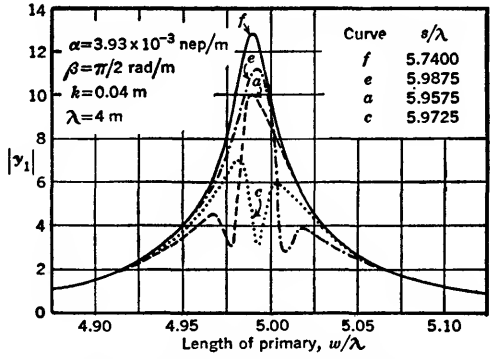


FIG. 7.8. Theoretical normalized input admittance of primary as a function of the length w of the primary with bridge-coupled secondary of length u; $s = w + u$.

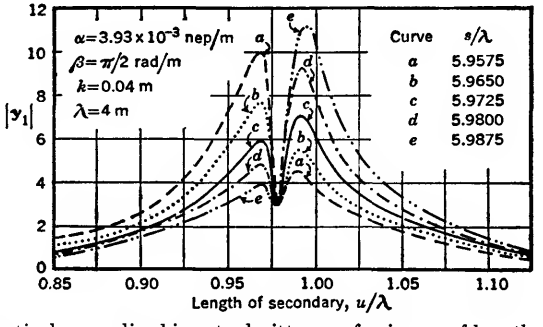


FIG. 7.9. Theoretical normalized input admittance of primary of length w as a function of the length u of a bridge-coupled secondary; $s = w + u$.

Theoretical curves of y_1 as a function of the length w of the primary, with βs set at three values near $\beta u = 2\pi - 2\beta k$, are marked a, c, and e in Fig. 7.8. The same curves and two additional ones plotted as a function of the length u of the secondary are shown in Fig. 7.9. It is clear from Figs. 7.8 and 7.9 that the minimum resulting from the interaction with the secondary occurs at $\beta u = 2\pi - \beta k$ and that its location with respect to the primary maximum is determined by βs. The experimental verification of the double humps is shown in Figs. 7.10 and 7.11, where I_0 is plotted as a function of βw and βu. These curves were obtained with the same line as used for the curves in Fig. 7.7. A single resonance peak

with the secondary detuned is shown in curve *f* of Fig. 7.10. The remaining curves in Fig. 7.10 and all the curves in Fig. 7.11 have the electrical length βu of the secondary near $2\pi - 2\beta k$, as indicated. The correspondence between Figs. 7.8 and 7.10 is evident, as is that between Figs. 7.9 and 7 11.

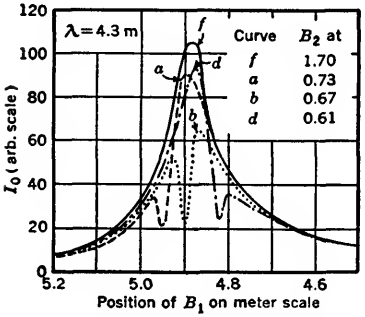


FIG. 7.10. Experimentally determined I_0 as a function of the position of the bridge B_1 in Fig. 7.1, with B_2 fixed at the indicated scale points.

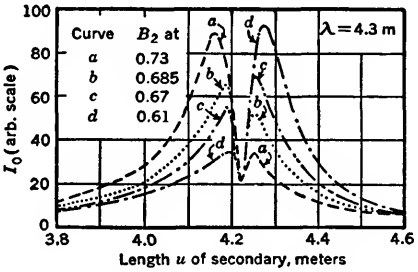


FIG. 7.11. Experimentally determined I_0 as a function of the length of the secondary when varied by moving B_1, with B_2 fixed at the indicated scale points.

8. Transmission-line Measurements with a Multiple-frequency Source; Filter Sections.[79,149,152] Throughout the preceding sections and chapters it has been assumed that the oscillators driving a transmission line generate only a single frequency. If one or more harmonic frequencies are generated together with the fundamental, the current and voltage distributions along the line are the superpositions of the individual currents and voltages of the several frequencies.

An oscillator or a coupling element that maintains an electric field that is even with respect to its center may involve a fundamental with a third harmonic. In this case the equivalent pair of equal and opposite point generators at $z = x$ has a combined emf V_{x1}^e for the fundamental frequency f_1 and an emf V_{x3}^e for the harmonic frequency f_3. For a line extending from $z = 0$ to $z = s$, the resultant voltage across the line in the range $x \leqq z \leqq s$ is obtained using Chap. IV, Sec. 2, Eq. (6). It is

$$V_z = V_{x1}^e \frac{\sinh(\gamma_1 x + \theta_{01}) \cosh(\gamma_1 w + \theta_{s1})}{\sinh(\gamma_1 s + \theta_{01} + \theta_{0s})} + V_{x3}^e \frac{\sinh(\gamma_3 x + \theta_{03}) \cosh(\gamma_3 w + \theta_{s3})}{\sinh(\gamma_3 s + \theta_{03} + \theta_{s3})} \quad (1)$$

where $w = s - z$, the subscript 1 refers to the fundamental, and the subscript 3 refers to the harmonic.

An oscillator or coupling element that maintains an electric field that is odd with respect to its center may involve a fundamental and a second

harmonic. In this case two pairs of equal and opposite point generators symmetrically placed with respect to their center at $z = x$ are required, and the voltage at a point z in the range $0 \leqq z \leqq x$ along the line is obtained from Chap. IV, Sec. 3, Eq. (6). It is

$$V_z = W_{x1}^e \frac{\cosh(\gamma_1 z + \theta_{01}) \cosh(\gamma_1 y + \theta_{s1})}{\sinh(\gamma_1 s + \theta_{01} + \theta_{s1})} + W_{x2}^e \frac{\cosh(\gamma_2 z + \theta_{02}) \cosh(\gamma_2 y + \theta_{s2})}{\sinh(\gamma_2 s + \theta_{02} + \theta_{s2})} \quad (2)$$

where $y = s - x$ and the subscripts 1 and 2 refer, respectively, to the fundamental and the second harmonic.

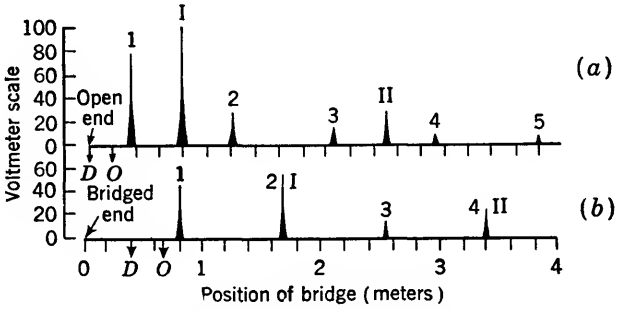


FIG. 8.1. Experimental resonance curves of oscillator with second harmonic. Peaks of the fundamental are numbered in Roman; those of the harmonic, in Arabic. D locates the voltage detector, O locates the center of the oscillator with odd field distribution. (a) Open end at left; (b) bridged end at left.

As an explicit application of (2), consider a transmission line excited by a loosely coupled oscillator of the type shown in Fig. 1.6a which maintains an electric field that is odd with respect to the point x opposite its center and includes a fundamental and a second harmonic. Such an oscillator induces a maximum voltage in a resonant line when coupled at a point of maximum voltage. A voltage detector is loosely coupled to the open end of the line at $z = 0$ (D in Fig. 8.1a), and the oscillator is near it (at 0 in Fig. 8.1a). When a large conducting disk is moved along the line as a short-circuiting termination, the voltage at $z = 0$ varies, as shown in Fig. 8.1a. The observed curve consists of two families of resonance curves of the type described in Chap. IV, Sec. 7. One family is characteristic of the fundamental (numbered in Roman), and the other family is characteristic of the second harmonic (numbered in Arabic). In each family the distances between successive maxima are half wavelengths.

The formula (2) may be specialized to apply to the specific case represented in Fig. 8.1a by setting $\theta_{01} = \theta_{02} \doteq 0$, $\theta_{s1} = \theta_{s2} = j\pi/2$, and

$\beta_2 = 2\beta_1$. The conditions for resonance for the fundamental and second harmonic are, respectively,

$$\beta_1 s + \Phi_{01} + \Phi_{s1} = \beta_1 s + \frac{\pi}{2} = n_1\pi \qquad n_1 = 1, 2, \ldots \tag{3a}$$

$$\beta_2 s + \Phi_{02} + \Phi_{s2} = \beta_2 s + \frac{\pi}{2} = n_2\pi \qquad n_2 = 1, 2, \ldots \tag{3b}$$

These are equivalent to

$$s = \frac{n_1\lambda_1}{2} - \frac{\lambda_1}{4} \tag{4a}$$

$$s = \frac{n_2\lambda_2}{2} - \frac{\lambda_2}{4} = \frac{n_2\lambda_1}{4} - \frac{\lambda_1}{8} \tag{4b}$$

Thus resonances for the fundamental occur when $s = \lambda_1/4, 3\lambda_1/4, 5\lambda_1/4, \ldots$, and those for the second harmonic when $s = \lambda_1/8, 3\lambda_1/8, 5\lambda_1/8, \ldots$. These conclusions are in agreement with Fig. 8.1*a*. If the attenuation is neglected in the numerator, (2) reduces to the following simple form, as applied to the conditions characteristic of Fig. 8.1*a*:

$$V_0 = jW_{z1}^{e} \frac{\sin \beta_1(s - x)}{\cosh \gamma_1 s} + jW_{z2}^{e} \frac{\sin \beta_2(s - x)}{\cosh \gamma_2 s} \tag{5}$$

If the end of the line at $z = 0$ is terminated in a conducting bridge with an equivalent length k_0, the terminal phase function is $\Phi_0 = \pi/2 + \beta k_0$. In this case the maxima in the voltage distributions of the fundamental and the harmonic have no locations in common, so that it is not possible to place a voltage detector or an oscillator with a field of odd symmetry in a position where it detects or induces a maximum. (On the other hand, a current detector and an oscillator with a field of even symmetry could be coupled to the bridge at $z = 0$ or at half wavelengths of the fundamental from it.) Actually, adequate voltages of both frequencies were received when the detector was placed near $\beta_1(z + k) = \pi/8$ (D in Fig. 8.1*b*), and the oscillator as close to it as physical conditions permitted. This turned out to be at 0 (Fig. 8.1*b*), which is rather close to a voltage node of the harmonic. With $\theta_{01} = \theta_{02} = j(\pi/2 + \beta_1 k_0)$, $\theta_{s1} = \theta_{s2} = j\pi/2$, and $\beta_2 = 2\beta_1$, the conditions for resonance for the fundamental and second harmonic are, respectively,

$$s + k_0 = \frac{n_1\lambda_1}{2} \qquad s + k_0 = \frac{n_2\lambda_2}{2} = \frac{n_2\lambda_1}{4} \tag{6}$$

Thus the resonances for the fundamental occur when $s + k = \lambda_1/2, \lambda_1, 3\lambda_1/2$, etc., and those for the harmonic at $s + k = \lambda_1/4, \lambda_1/2, 3\lambda_1/4, \lambda_1$, etc. Clearly every other resonance maximum of the harmonic coincides with a resonance maximum of the fundamental. An experimental curve

illustrating this is shown in Fig. 8.1*b*. The equation for these curves is

$$V_z \doteq -W^e_{x1} \frac{\cos [\beta_1(z + k)] \sin \beta_2(s - x)}{\sinh [\gamma_1(s + k)]} - W^e_{x2} \frac{\cos [\beta_2(z + k)] \sin \beta_2(s - x)}{\sinh [\gamma_2(s + k)]} \quad (7)$$

It is clear from (4) that by a proper choice of either z or x the contribution to V_z at resonance by either the fundamental or the harmonic may be made very small. This means that the oscillator may be so located (by a choice of x) that it induces either no fundamental or no harmonic voltage in the line, or that the detector is so situated that either the fundamental or the harmonic voltage is small at the point of coupling. Note that the locations for negligible response of a symmetrical current indicator are a quarter wavelength from the corresponding locations for a voltage indicator. Similarly the locations for negligible induced voltage by an oscillator with an even electric field (one pair of point generators) are shifted a quarter wavelength from the locations for negligible induced current by an oscillator with an odd electric field (two pairs of point generators).

It is seen that, by an appropriate location of the oscillator (or coupling element) and of the detector probe and by a proper choice of the terminations, a resonance maximum of the fundamental or of the second harmonic may be located at the minimum of the other. In this manner resonance-curve measurements may be made using either the fundamental or the harmonic if the losses in the circuit are sufficiently low and the relative amplitudes are not so different that the minima of the one frequency are not negligible compared with the maxima of the other.

Coupled-circuit measurements involving the sharp minima in resonance curves described in Sec. 7 may be made with the fundamental or the second harmonic. This is illustrated in Fig. 8.2*a* and *b* by a set of experimental curves. The curves in Fig. 8.2*a* correspond closely to those in Fig. 8.1*a*. Below them in Fig. 8.2*b* is a related set of coupled-circuit curves like those in Fig. 7.7. The upper curve is obtained by observing the voltage at D in a self-resonant primary circuit formed by locating an inductive bridge at B_1 and then moving a conducting disk beyond it to increase the length of the secondary. In this case the primary is tuned to the fundamental. The lower curve in Fig. 8.2*b* is obtained in the same manner as the upper one, but with the primary circuit tuned to the harmonic by locating the conducting bridge at B_2.

The separation of a fundamental frequency from a harmonic by proper location along the transmission line of the points of coupling and detection is useful only when the over-all loss on the line is low and sharp resonance curves can be obtained. A more generally useful method of suppressing a harmonic without interfering with the fundamental, or vice versa, is to

arrange a pair of shunt stubs so that they present a low impedance to the frequency to be suppressed and a high impedance to the frequency to be transmitted. For maximum effectiveness the stubs are separated a distance equal to a quarter wavelength of the frequency to be suppressed.

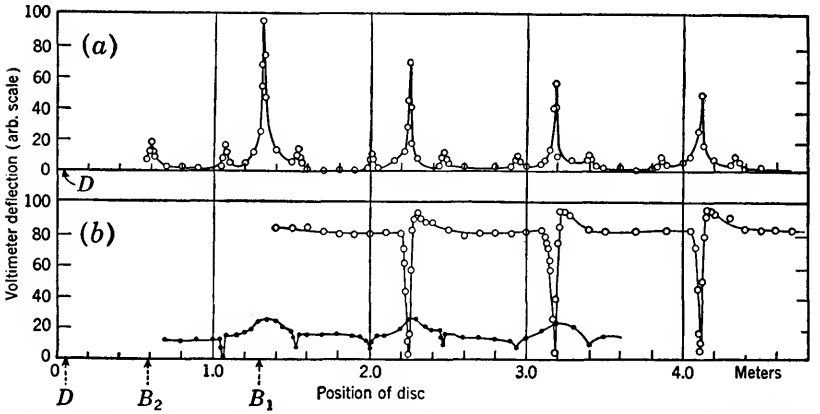


FIG. 8.2. (*a*) Resonance curves of a source with a second harmonic. (*b*) Coupled-circuit curves with conducting bridge at B_1 (for upper curve) or B_2 (for lower curve).

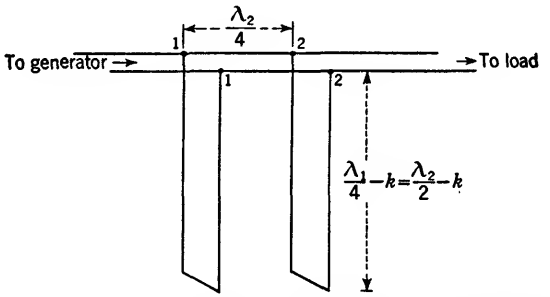


FIG. 8.3. Combination of stubs to suppress the second harmonic from the line to the right of the stubs without interfering with the fundamental.

A circuit for suppressing all even harmonics and passing the fundamental is shown in Fig. 8.3. On the other hand, the fundamental is suppressed and the second harmonic passed to the right of the junction 22 in Fig. 8.4.

It is slightly more difficult to suppress the third harmonic while the fundamental is passed. One method using two stubs in parallel is illustrated in Fig. 8.5. The $\lambda_3/4$ open stub and the $\lambda_3/2$ closed stub both present a low impedance at 11 for the third harmonic, so that this is suppressed from the line to the right of 22. Neglecting losses, the admittance of the parallel combination of stubs for the fundamental frequency

is approximately

$$Y_{in} \doteq -jY_c(\cot \beta s_0 - \tan \beta s_c) = -jY_c\left(\cot \frac{\pi}{6} - \tan \frac{\pi}{3}\right) = 0$$

so that the fundamental is passed without attenuation.

In effect, the stub combinations in Figs. 8.3 to 8.5 are special types of filter circuits using sections of transmission line as their elements. They are effective in suppressing only particular frequencies, such as may be

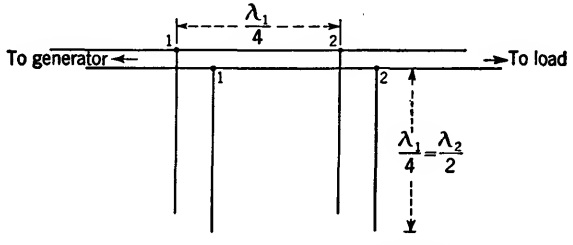


FIG. 8.4. Combination of stubs to suppress the fundamental from the line to the right of the stubs without interfering with the second harmonic.

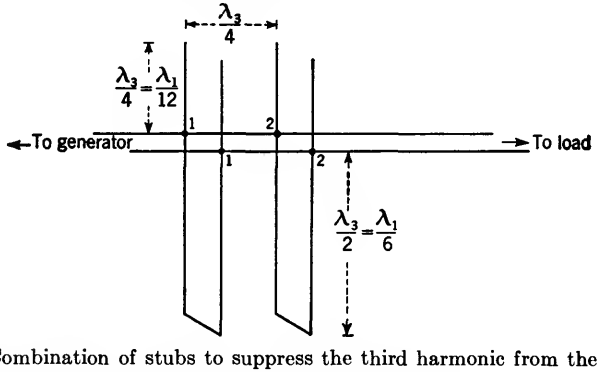


FIG. 8.5. Combination of stubs to suppress the third harmonic from the line to the right of the stubs without interfering with the fundamental.

encountered when simple generators of the types described in Sec. 1 are used unmodulated. When high-frequency generators are modulated, various frequencies are introduced, and more complicated filters are required. At high frequencies these are advantageously constructed of sections of transmission line (usually coaxial). Since their transmission and suppression properties are described in terms of the general theory of wave filters, their analysis is beyond the scope of this book.

9. Radiation from Open-wire Lines.[141,157] The derivation of the differential equations for the current and voltage along a two-wire line in Chap. I involves neglecting terms of the order of magnitude $|\beta b|^2$. It is these terms which specify radiation from the line. Accordingly neither the distribution of current along a section of line nor its input imped-

ance as determined from solutions of the conventional equations includes or takes account of radiation. Since the power radiated from a circuit depends on the entire configuration of conductors and cannot be assigned piecewise to the several parts, it is necessary to consider the complete circuit consisting of the line *and* the terminations at both ends if the radiated power is to be evaluated.

Consider a two-wire line extending from $z = 0$ to $z = s$ in air. The generator is at $z = 0$; it has an impedance $\boldsymbol{Z}_0$. The load at $z = s$ is $\boldsymbol{Z}_s$. The impedance seen by the generator is

$$\boldsymbol{Z} = \boldsymbol{Z}_0 + \boldsymbol{Z}_c \tanh (\gamma s + \boldsymbol{\theta}_s') + R_0^e \tag{1}$$

where, as usual, $\gamma = \alpha + j\beta$ and $\boldsymbol{\theta}_s' = \rho_s + j\Phi_s' = \tanh^{-1} (\boldsymbol{Z}_s/\boldsymbol{Z}_c)$ and where R_0^e is the external or radiation resistance referred to the current $\boldsymbol{I}_0$. It is defined by

$$R_0^e = \frac{2P}{I_0^2} \tag{2}$$

where P is the average radiated power. The distribution of current as determined by line theory is obtained from Chap. IV, Sec. 2, Eq. (5). It is

$$\boldsymbol{I}_z = \boldsymbol{I}_0 \frac{\cosh [\gamma(s - z) + \boldsymbol{\theta}_s']}{\cosh (\gamma s + \boldsymbol{\theta}_s')} \tag{3}$$

There are several methods of evaluating R_0^e, but since all depend on antenna theory, they are not described here. The result is as follows:

$$R_0^e = \frac{\zeta_0}{4\pi} \beta_0^2 b^2 \frac{\cosh (\alpha s + 2\rho_s)}{|\cosh (\gamma s + \boldsymbol{\theta}_s')|^2} \left(\cosh \alpha s - \frac{\sin 2\beta s}{2\beta s} \right) \tag{4}$$

In the derivation of (4) it is assumed that the terminal impedances $\boldsymbol{Z}_0$ and $\boldsymbol{Z}_s$ are effectively lumped, so that it may be assumed that the currents $\boldsymbol{I}_0$ and $\boldsymbol{I}_s$ are constant in amplitude from one of the line wires to the other. Except for higher-order terms these terminations are equivalent to filaments of current $\boldsymbol{I}_0$ and $\boldsymbol{I}_s$ of length b in their contribution to R_0^e.

The general formula (4) is simplified when applied to important special cases.

Nonresonant Line. A nonresonant line is characterized by $\rho_s = \infty$ However, the same results obtain to an excellent approximation when ρ_s exceeds 3. The appropriate form of (4) is

$$R_0^e \doteq \frac{\zeta_0}{2\pi} \beta^2 b^2 \left(\cosh \alpha s - \frac{\sin 2\beta s}{2\beta s} \right) e^{-\alpha s} \tag{5}$$

Usually αs is sufficiently small so that the following formula is a good approximation of the radiation resistance, referred to the input current

of a low-loss line terminated in its characteristic impedance:

$$R_0^e \doteq \frac{\zeta_0}{2\pi} \beta^2 b^2 \left(1 - \frac{\sin 2\beta s}{2\beta s}\right) \tag{6}$$

This formula is further simplified if $2\beta s = n\pi$ or if βs is sufficiently great. In these cases

$$R_0^e \doteq \frac{\zeta_0}{2\pi} \beta^2 b^2 = 60\beta^2 b^2 \qquad \text{ohms} \tag{7}$$

A graph of (6) is given in Fig. 9.1.

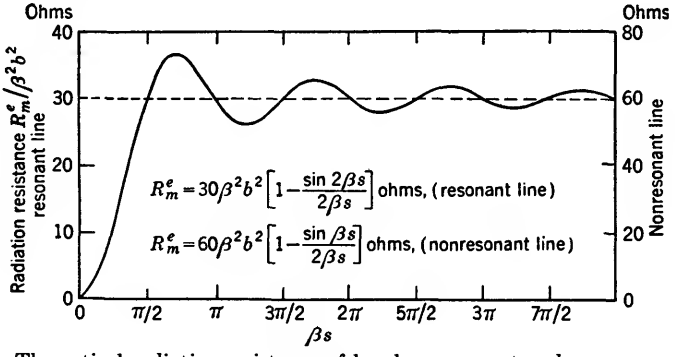


FIG. 9.1. Theoretical radiation resistance of low-loss resonant and nonresonant lines.

Low-loss Line with Low-loss Terminations. If the losses in the line and its terminations are sufficiently small so that the inequality $(\alpha s + 2\rho_s) < 0.1$ is satisfied, the following simplification of (4) applies:

$$R_0^e \doteq \frac{\zeta_0}{4\pi} \beta^2 b^2 \sec^2 (\beta s + \Phi_s') \left(1 - \frac{\sin 2\beta s}{2\beta s}\right) \tag{8}$$

Since the approximations implicit in this formula are equivalent to neglecting all losses in determining the distribution of current, this is purely sinusoidal. Accordingly the input current I_0 vanishes when $\beta s + \Phi_s' = (2n + 1)\pi/2$ and R_0^e becomes infinite. If a different reference current is chosen, in particular, the maximum I_m of the sinusoidal distribution, a radiation resistance R_m^e referred to I_m may be defined. With (8), it is

$$R_m^e \equiv \frac{2P}{I_m^2} \doteq \frac{\zeta_0}{4\pi} \beta^2 b^2 \left(1 - \frac{\sin 2\beta s}{2\beta s}\right) \tag{9}$$

When $2\beta s = n\pi$ or when βs is sufficiently long, (9) reduces to

$$R_m^e \doteq \frac{\zeta_0}{4\pi} \beta^2 b^2 \doteq 30\beta^2 b^2 \qquad \text{ohms} \tag{10}$$

A graph of (9) is given in Fig. 9.1. It is seen to differ from (6) for the

nonresonant low-loss line only by a factor 2. Note that (9) and (10) apply to lines with open or short-circuited ends or to lines with lumped reactive terminations of any type.

Although the radiation resistance of a two-wire line with closely spaced conductors is very small, it is not necessarily negligible in comparison with the corresponding ohmic resistance. If the two conductors of the line are of copper and of sufficiently large diameter and the line is terminated in essentially reactive impedances, such as metal disks, conducting bridges, or open ends, the power dissipated in heat may be as small as or smaller than the power radiated. Owing to the small over-all attenuation, standing-wave ratios may be enormous. This is true, in particular, of heavy single conductors placed close to and parallel to a large highly conducting plane. In this case ohmic losses in the conducting plane are usually negligible, and the radiation resistance is one-half that given in (9) or (10) if b is the distance between the axis of the conductor and the axis of its image or twice the distance between the axis of the conductor and the conducting plane. If the single conductor is sufficiently large in diameter and the distance b is not too small, the power radiated may be made to exceed greatly the power dissipated in heat. In this case the section of resonant line is a reasonably efficient antenna.

If the distance b between the axes of the two conductors of a two-wire line (or a single conductor and its image in a conducting plane) is not large compared with the radius a of the conductors, the effective centers of the currents in the two conductors are moved closer together than b. In this case the effective separation

$$b_e = \frac{b}{2}\left[1 + \sqrt{1 - \left(\frac{2a}{b}\right)^2}\right] \tag{11}$$

may be used in place of the distance b between axes.

An experimental determination of the radiation resistance of resonant sections of two-wire line has been carried out by Chipman[141] and his collaborators. The procedure was to determine the widths of the resonance curves at the half-power points of a section of two-wire line projecting vertically above a highly conducting metal plane when enclosed in a metal shield and with the shield removed. The line consisted of silver conductors of diameter $2a = 0.100$ in. separated a distance $b = 1.00$ in. between centers. It was adjusted to resonance with open and short-circuited ends for a range of lengths extending from $\lambda/4$ to 4λ at frequencies of 342 to 1,420 Mc/sec. For the short-circuited line a brass shield 4 in. in inside diameter was used; for the open line the shield was of aluminum 4.5 in. in diameter.

The width W of the resonance curve between half-power points is

related to the over-all attenuation by the formula

$$\frac{\beta W}{2} = \alpha s + \rho_0 + \rho_s \tag{12}$$

where s is the length of the line and ρ_0 and ρ_s are the attenuation functions of the terminations at the two ends $z = 0$ and $z = s$. This formula does not include attenuation due to radiation, but it may be generalized to include radiation by adding a function ρ_r. Thus

$$\frac{\beta W}{2} = \alpha s + \rho_0 + \rho_s + \rho_r \tag{13}$$

Since the characteristic impedance and, with it, the attenuation constant of the line change when the shield is removed quite irrespective of radiation, it is advantageous to multiply (12) and (13) through by the characteristic impedance appropriate, respectively, for the shielded and unshielded line. Let the subscript 1 be used for the former and the subscript 2 for the latter. The two equations are

$$\frac{\beta R_{c1} W_1}{2} = r_1 s + R_{c1}(\rho_0 + \rho_s) \tag{14}$$

$$\frac{\beta R_{c2} W_2}{2} = r_2 s + R_{c2}(\rho_0 + \rho_s + \rho_r) \tag{15}$$

where r_1 and r_2 are the resistances per loop unit length of the shielded-pair and the open two-wire lines and R_{c1} and R_{c2} are the characteristic impedances. Since $\boldsymbol{Z}_0$ is a low-impedance essentially reactive termination, $\rho_0 \doteq r_{10} = R_0/R_c$. It follows that $R_{c1}\rho_0 \doteq R_{c2}\rho_0 \doteq R_0$. Similarly $\boldsymbol{Z}_s$ is either a short circuit or an open circuit for which $\rho_s \doteq 0$. It follows that, if (15) is subtracted from (14), the following result is obtained (since ρ_r represents a small pure resistance, it is logical to set $\rho_r \doteq R^e/R_{c2}$, so that $R_{c1}\rho_r \doteq R_0^e \doteq R_m^e$):

$$R_m^e \doteq \frac{\beta}{2}(R_{c2}W_2 - R_{c1}W_1) - s(r_2 - r_1) \tag{16}$$

The difference in ohmic resistance per unit length of the shielded and unshielded lines arises from the small eddy currents in the shield, when this is present, and a small change in transverse distribution. Actually, with as large a shield as used in the experimental measurements, these changes are insignificant, and it is a good approximation to set $r_1 \doteq r_2$. It follows that

$$R_m^e \doteq \tfrac{1}{2}\beta(R_{c2}W_2 - R_{c1}W_1) \tag{17}$$

By measuring the half-power widths W_1 and W_2, Chipman et al. determined R_m^e. For each of 13 different frequencies, measurements were made using either open-end or closed-end lines. At each frequency a

number of different resonant lengths were used. The mean value of the measured R_m^e and the ranges for the several lengths of line are shown in Fig. 9.2. The theoretical curve $R_m^e = 15\beta^2 b^2$ is also shown. (Note that the factor 15 occurs in place of 30 when the line is over an infinite image plane and radiates into a half space.) Although a few of the experimental points lie on the theoretical curve, most of them are considerably below it. In general, they lie more closely along a line defined by $R_m^e = 13.75\beta^2 b^2$. It is difficult to achieve high experimental accuracy in radiation problems, and the theoretical formula is also approximate in the sense that it depends on a distribution of current which is valid strictly only when there is no radiation. Therefore an 8 per cent difference in the constant factor multiplying $\beta^2 b^2$ and the excellent agreement with which R^e obeys a square law in βb are quite acceptable.

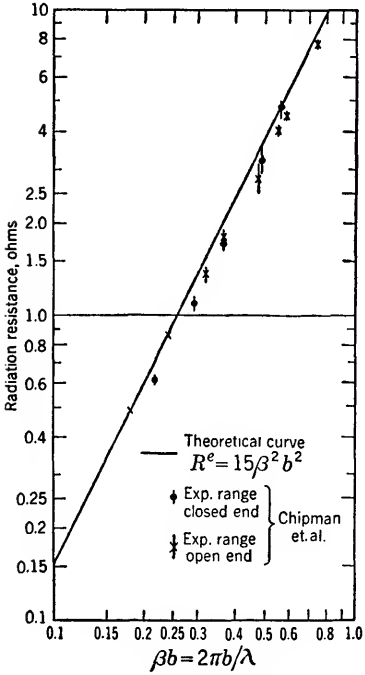


FIG. 9.2. Radiation resistance of resonant two-wire line over an image plane. Theoretical curve in solid line; experimental points by Chipman et al.

Radiation from a two-wire line is greatly increased if the line is even slightly unbalanced. In this case the part of the current in the two conductors which is given by $I_1 + I_2$ is in the same direction in the two wires, so that these act like an antenna carrying this current.

Radiation from a coaxial line with small cross section may be ignored so long as no currents exist on the outside of the shield. However, if a coaxial line is used with a balanced load, e.g., a center-driven symmetrical antenna, currents may be excited on the outside of the shield, and this then behaves like an antenna.

PROBLEMS

1. A triode of the double-ended type has the following interelectrode capacitances: grid plate, 2 $\mu\mu$f; grid filament, 2 $\mu\mu$f; plate filament, 0.4 $\mu\mu$f. Determine and plot the generated frequency as a function of the length of two identical effectively short-circuited sections of two-wire line attached to the grid-plate leads, one on each side of the tube.

2. What are the wavelength characteristics of the triode oscillator in the preceding problem if only one section of the two-wire line is used?

3. A ring oscillator consists of a closed square of two-wire line. A double-ended tube is connected at the center of each side of the square. If the equivalent capacitance of each tube is C_0, what are the wavelength characteristics of the oscillator as a function of the length of one side of the square? (Neglect the effect of the corners.)

4. Determine the effect of the corners in the ring oscillator in Prob. 4 in modifying the natural frequency generated.

5. The coupled-circuit oscillator described in Sec. 2 is modified by cutting the coupling bridge in the middle and inserting a small effectively lumped capacitance in series with it. Determine the effect of such a capacitance on the frequency or wavelength generated as a function of the magnitude of the capacitance.

6. A transmission line consists of a single silvered brass tube $\frac{1}{4}$ in. in diameter placed parallel to, and with its center at a distance of $\frac{1}{2}$ in. from, a very large highly conducting plane (assumed perfectly conducting and infinite in extent). The line is driven at one end by a generator at a frequency of 750 Mc/sec; the other end is terminated in a large metal disk (which may be assumed equivalent to a perfect short circuit).

(*a*) Compare the power dissipated as heat in the line with the power radiated as the length of the line is increased from one-quarter to two wavelengths.

(*b*) What are the successive maximum and minimum values of the input resistance of the line in this range of length?

BIBLIOGRAPHY

BOOKS

1. Bewley, L. V.: "Two-dimensional Fields in Electrical Engineering," The Macmillan Company, New York, 1948.
2. Everitt, W. L.: "Communication Engineering," 2d ed., McGraw-Hill Book Company, Inc., New York, 1937.
3. Guillemin, E. A.: "Communication Networks," vol. II, chaps. I–III, John Wiley & Sons, Inc., New York, 1935.
4. Jackson, Willis: "High Frequency Transmission Lines," 3d ed., Methuen & Co., Ltd., London, and John Wiley & Sons, Inc., New York, 1951.
5. Johnson, W. C.: "Transmission Lines and Networks," McGraw-Hill Book Company, Inc., New York, 1950.
6. Karakash, John J.: "Transmission Lines and Filter Networks," The Macmillan Company, New York, 1950.
7. Kennelly, A. E.: "Chart Atlas of Complex Hyperbolic and Circular Functions," 3d ed., Harvard University Press, Cambridge, Mass., 1924; "Tables of Complex Hyperbolic and Circular Functions," 2d ed., Harvard University Press, Cambridge, Mass., 1921.
8. King, D. D.: "Measurements at Centimeter Wavelength," D. Van Nostrand Company, Inc., New York, 1952.
9. King, R. W. P.: "Electromagnetic Engineering," vol. I, McGraw-Hill Book Company, Inc., New York, 1945.
10. King, R. W. P.: "Theory of Linear Antennas," Harvard University Press, Cambridge, Mass. (in press).
11. King, R. W. P., H. R. Mimno, and A. H. Wing: "Transmission Lines, Antennas, and Wave Guides," McGraw-Hill Book Company, Inc., New York, 1945.
12. Küpfmüller, K.: "Theoretische Elektrotechnik," Springer-Verlag OHG, Berlin, 1932.
13. Marcuvitz, N.: "Waveguide Handbook," McGraw-Hill Book Company, Inc., New York, 1951.
14. Montgomery, C. G.: "Technique of Microwave Measurements," McGraw-Hill Book Company, Inc., New York, 1947.
15. Montgomery, C. G., R. H. Dicke, and E. M. Purcell: "Principles of Microwave Circuits," McGraw-Hill Book Company, Inc., New York, 1948.
16. Moreno, T.: "Microwave Transmission Design Data," McGraw-Hill Book Company, Inc., New York, 1948.
17. Pierce, G. W., "Electric Oscillations and Electric Waves," McGraw-Hill Book Company, Inc., New York, 1920.
18. Pipes, L. A.: "Applied Mathematics for Engineers and Physicists," McGraw-Hill Book Company, Inc., New York, 1946.
19. Radio Research Laboratory: "Very High-frequency Techniques," vols. I–II, McGraw-Hill Book Company, Inc., New York, 1947.
20. Ragan, G. L.: "Microwave Transmission Circuits," McGraw-Hill Book Company, Inc., New York, 1948.

21. Ramo, S., and J. R. Whinnery: "Fields and Waves in Modern Radio," John Wiley & Sons, Inc., New York, 1944.
22. "Reference Data for Radio Engineers," 3d ed., Federal Telephone and Radio Corporation, New York, 1949.
23. Ryder, John D.: "Networks, Lines and Filters," Prentice-Hall Inc., New York, 1949.
24. Skilling, H. H.: "Electric Transmission Lines," McGraw-Hill Book Company, Inc., New York, 1951.
25. Slater, J. C.: "Microwave Transmission," McGraw-Hill Book Company, Inc., New York, 1942.
26. Sokolnikoff, I. S. and E. S.: "Higher Mathematics for Engineers and Physicists," McGraw-Hill Book Company, Inc., New York, 1934.
27. Sommerfeld, A.: "Lectures on Theoretical Physics," vol. III, "Electrodynamics," Academic Press, Inc., New York, 1952. ("Vorlesungen über Theoretische Physik. III. Elektrodynamik," especially pp. 198–211, Dieterich'sche Verlagsbuchhandlung, Wiesbaden, 1948.)
28. Stratton, J.: "Electromagnetic Theory," McGraw-Hill Book Company, Inc., New York, 1941.
29. Terman, F. E.: "Radio Engineers' Handbook," McGraw-Hill Book Company, Inc., New York, 1943.
30. Thomson, J. J.: "Recent Researches in Electricity and Magnetism," Clarendon Press, Oxford, 1893.
31. Ware, L. A., and H. R. Reed: "Communication Circuits," 3d ed., John Wiley & Sons, Inc., New York, 1949.
32. Weber, E.: "Electromagnetic Fields," vol. I, John Wiley & Sons, Inc., New York, 1950.
33. Weissfloch, A.: "Schaltungstheorie und Messtechnik des Dezimeter- und Zentimeter-Wellengebietes," Verlag Birkhäuser, Basel, 1954.

PAPERS

References Primarily for Chaps. I and II

34. Angelakos, D. J.: A Coaxial Line Filled with Two Non-concentric Dielectrics, Technical Report No. 102, Series No. 60, University of California, Division of Electrical Engineering, Berkeley, Calif., November, 1953.
35. Arnold, A. H. M.: Proximity Effect in Solid and Hollow Round Conductors, *J. Inst. Elec. Engrs. London*, pt. II, **88**: 349 (1941).
36. Assadourian, F., and F. Rimai: Simplified Theory of Microstrip Transmission Systems, *Proc. IRE*, **40**: 1651 (1952).
37. Brick, D.: Radiation of a Hertzian Dipole over a Coated Conductor, *Proc. Inst. Elec. Engrs. London*, pt. C (1955); Monograph 113, Radio Section (1954).
38. Brown, G. H.: Characteristics of Unbalanced Overhead Transmission Lines, *Broadcast Rev.*, May, 1941.
39. Carson, J. R.: The Present Status of Wire-transmission Theory and Some of Its Outstanding Problems, *Bell System Tech. J.*, **7**: 268 (1928).
40. Carson, J. R.: Wave Propagation over Parallel Wires. The Proximity Effect, *Phil. Mag.*, ser. 6, **41**: 607 (1921).
41. Carson, J. R., and R. S. Hoyt: Propagation of Periodic Currents over a System of Parallel Wires, *Bell System Tech. J.*, **6**: 495 (1927).
42. Colebrook, F. M.: Transmission-line Theory, *Wireless Eng.*, **21**: 167 (1944).
43. Frankel, S.: Characteristic Impedance of Parallel Wires in Rectangular Troughs, *Proc. IRE*, **30**: (1942).

44. Fubini, E., W. Fromm, and H. Keen: New Techniques for High-Q Strip Microwave Components, *Convention Record of the IRE, 1954 National Convention*, pt. 8: 91 (1954).
45. Goubau, G.: Surface Waves and Their Application to Transmission Lines, *J. Appl. Phys.*, **21**: 1119 (1950).
46. Hikosaburo, A.: Ellipse Diagram of a Lecher-wire System, *Proc. IRE*, **21**: 303 (1933).
47. Jackson, W., and L. G. H. Huxley: The Solution of Transmission-line Problems by the Use of the Circle Diagram of Impedance, *J. Inst. Elec. Engrs. London*, pt. III, **91**: 105 (1944).
48. King, R.: The Telegraphist's Equations at Ultra-high Frequencies, *Physics*, **6**: 121 (1935).
49. King, R., and K. Tomiyasu: Terminal Impedance and Generalized Two-wire Line Theory, *Proc. IRE*, **37**: 1134 (1949). Part I in Technical Report No. 74, Cruft Laboratory, Harvard University, 1949.
50. Laport, E. A.: Open-wire Radio-frequency Transmission Lines, *Proc. IRE*, **31**: 271 (1943).
51. Levin, S. A.: Electromagnetic Waves Guided by Parallel Wires, *Trans. AIEE*, **46**: 983 (1927).
52. Mie, G.: Elektrische Wellen an zwei parallelen Drähten, *Ann. Physik*, **2**: 201 (1900).
53. Namiki, M., and H. Takahashi: Some Variational Principles for Problems in Transmission Lines, *J. Appl. Phys.*, **23**: 1056 (1952).
54. Pipes, L. A.: Matrix Theory of Multiconductor Transmission Lines, *Phil. Mag.*, ser. 7, **24**: 97 (1937).
55. Pipes, L. A.: Steady-state Analysis of Multiconductor Transmission Lines, *J. Appl. Phys.*, **12**: 782 (1941).
56. Rice, S. O.: Steady-state Solutions of Transmission-line Equations, *Bell System Tech. J.*, **20**: 131 (1941).
57. Sim, A. C.: New High-frequency Proximity Effect Formula, *Wireless Engr.*, **30**: 203 (1953).
58. Smith, H. P.: An Improved Transmission-line Calculator, *Electronics*, **17**: 130 (1944).
59. Tai, C. T.: High-frequency Polyphase Transmission Lines, *Proc. IRE*, **36**: 1370 (1948).
60. Walker, L. R., and N. Wax: Non-uniform Transmission Lines and Reflection Coefficients, *J. Appl. Phys.*, **17**: 1043 (1946).
61. Zinke, O.: Grundlagen der Strom- u. Spannungsverteilung auf Antennen, *Archiv Elektrotech.*, **35**: 67 (1941).

References Primarily for Chaps. III and IV

62. Andrews, H. W.: Image-plane and Coaxial-line Measuring Equipment at 600 Mc/s, Technical Report No. 177, Cruft Laboratory, Harvard University, 1953.
63. Bloch, A., F. J. Fisher, and G. J. Hunt: New Equipment for Impedance Matching and Measurement at Very High Frequencies, *Proc. Inst. Elec. Engs., London*, pt. III, **100**: 93 (1953).
64. Bruckmann, H.: Widerstandsmessungen mit der Paralleldrahtleitung, *Hochfrequenztech.*, **51**: 128 (1938).
65. Cafferata, H.: The Calculation of Input or Sending-end Impedances of Feeders and Cables Terminated in Complex Loads, *Marconi Rev.*, **6**: 12 (1937).

66. Carter, P. S.: Charts for Transmission-line Measurements and Computations, *RCA Rev.*, **3**: 355 (1938–1939).
67. Chipman, R. A.: A Resonance-curve Method for the Absolute Measurement of Impedance at Frequencies of the Order 300 Mc/s, *J. Appl. Phys.*, **10**: 27 (1939).
68. Clayton, R. J., J. E. Houldin, H. R. L. Lamont, and W. E. Willshaw: Radio Measurements in the Decimetre and Centimetre Wavebands, *J. Inst. Elec. Engrs. London*, pt. III, **93**: 97 (1946).
69. Cox, C. R.: Design Data for Beaded Coaxial Lines, *Electronics*, **19**: 130 (1946).
70. Diamond, J. M.: Shorted Stubs of High Resonant Impedance, *Proc. IRE*, **40**: 188 (1952).
71. Duffin, W. J.: Three-probe Method of Impedance Measurement, *Wireless Engr.*, **29**: 317 (1952).
72. Essen, L.: The Measurement of Balanced and Unbalanced Impedances at Frequencies near 500 Mc/s and Its Application to the Determination of the Propagation Constant of Cables, *J. Inst. Elec. Engrs. London*, pt. III, **91**: 84 (1944).
73. Essen, L., and A. C. Gordon-Smith: The Measurement of Frequencies in the Range 100 Mc/s to 10,000 Mc/s, *J. Inst. Elec. Engrs. London*, pt. III, **92**: 291 (1945).
74. Frankel, S.: Characteristic Functions of Transmission Lines, *Communications*, March, 1942.
75. Fubini, E. G., and P. S. Sutro: A Wide-band Transformer from an Unbalanced to a Balanced Line, *Proc. IRE*, **35**: 1153 (1947).
76. Hoag, J. B.: Measurement of the Frequency of Ultra-radio Waves, *Proc. IRE*, **21**: 29 (1933).
77. Kaufman, H.: Scheinwiderstandsmessungen im Dezimeterwellengebiet, *Hochfrequenztech.*, **53**: 61 (1939).
78. King, D. D.: Impedance Measurement on Transmission Lines, *Proc. IRE*, **35**: 509 (1947).
79. King, R.: Electrical Measurements at Ultra-high Frequencies, *Proc. IRE*, **23**: 885 (1935).
80. King, R.: General Amplitude Relations for Transmission Lines with Unrestricted Line Parameters, Terminal Impedances, and Driving Point, *Proc. IRE*, **29**: 640 (1941).
81. King, R.: Transmission-line Theory and Its Application, *J. Appl. Phys.*, **14**: 577–600 (1943).
82. Klopfenstein, R. W.: Design of Transmission-line Tuning Elements for Minimum Dissipation, *Proc. IRE*, **39**: 1089 (1951).
83. Kostrize, J. A.: Microstrip Components, *Proc. IRE*, **40**: 1658 (1952).
84. Labus, J. W.: Measurement of Resistances and Impedances at High Frequencies, *Proc. IRE*, **19**: 452 (1931).
85. Macalpine, W. W.: Computation of Impedance and Efficiency of Line with High Standing-wave Ratio, *Elec. Commun.*, **30**: 238 (1953).
86. Matthews, E. W.: A Shielded Two-wire Hybrid Junction and Its Use as an Ultra-high Frequency Impedance Bridge, Ph.D. Thesis, Harvard University, Division of Applied Science, 1954.
87. Medhurst, R. G., and S. D. Pool: Correction Factors for Slotted Measuring Lines at Very High Frequencies, *Proc. Inst. Elec. Engrs. London*, pt. III, **97**: 223 (1950).
88. Meinke, H. H.: Fortschritte der Dezimeterwellen-Messtechnik, *Frequenz*, **2**: 41 (1948).

89. Morita, T.: Measurement of Current and Charge Distributions on Cylindrical Antenna, *Proc. IRE*, **38**: 898 (1950). Technical Report No. 66, Cruft Laboratory, Harvard University, 1949.
90. Morita, T., and L. Sheingold: A Coaxial Magic-T, Technical Report No. 162, Cruft Laboratory, Harvard University, 1952.
91. Nergaard, L. S.: A Survey of Ultra-high Frequency Measurements, *RCA Rev.*, **3**: 156 (1938–1939).
92. Nergaard, L. S., and B. Salzberg: Resonant Impedance of Transmission Lines, *Proc. IRE*, **27**: 579 (1939).
93. Paine, R. C.: Graphical Solution of Voltage and Current Distribution and Impedance of Transmission Lines, *Proc. IRE*, **32**: 686 (1944).
94. Roder, Hans: Graphical Methods for Problem Involving Radio-frequency Transmission Lines, *Proc. IRE*, **21**: 290 (1933).
95. Roosenstein, H. O.: The Conduction of High-frequency Oscillatory Energy, *Proc. IRE*, **19**: 1849 (1931); *Hochfrequenztech.*, **36**: 81, 120 (1930).
96. Russell, A.: Effective Resistance and Inductance of Concentric Mains, *Phil. Mag.*, ser. 6, **17**: 524 (1909).
97. Salinger, H.: The Quarter-wave Step-up Transformer, *Proc. IRE*, **32**: 553 (1944).
98. Schmidt, O.: Das Paralleldrahtsystem als Messinstrument, *Hochfrequenz. u. Elektroakustik*, **41**: 1 (1933).
99. Smith, P. H.: Optimum Coax Diameters, *Electronics*, **23**: 111 (1950).
100. Sterba, E. J., and C. B. Feldman: Transmission Lines for Short-wave Radio, *Proc. IRE*, **20**: 1163 (1932).
101. Tai, C. T.: Shunt and Series Sections of Transmission Line for Impedance Matching, *J. Appl. Phys.*, **17**: 44 (1946).
102. Terman, F. E.: Resonant Lines in Radio Circuits, *Elec. Eng.*, **53**: 1046 (1934).
103. Tomiyasu, K.: Antennas and Open-wire Lines. Part II. Measurements on Two-wire Lines, *J. Appl. Phys.*, **20**: 892 (1949).
104. Tomiyasu, K.: Terminal Impedance and Generalized Two-wire Line Theory. Part II. Effect of a Bend, Technical Report No. 74, Cruft Laboratory, Harvard University, 1945.
105. Tomiyasu, K.: Unbalanced Terminations on a Shielded-pair Line, Technical Report No. 86, Cruft Laboratory, Harvard University, 1949.
106. Tomiyasu, K.: The Unbalance Squelcher, *Rev. Sci. Instr.*, **19**: 675 (1948).
107. Wheeler, H. A.: Transmission-line Impedance Curves, *Proc. IRE*, **38**: 1400 (1950).
108. Wholey, W. B., and W. H. Eldred: A New Type of Slotted-line Section, *Proc. IRE*, **38**: 244 (1950).
109. Wing, A. H., and J. Eisenstein: Single and Double-stub Impedance Matching, *J. Appl. Phys.*, **15**: 615 (1944).
110. Witt, B. J.: Concentric Tube Lines, *Marconi Rev.*, **5**: 20 (1936).

References Primarily for Chap. V

111. Angelakos, D. J.: Current and Charge Distributions on Antennas and Open-wire Lines, *J. Appl. Phys.*, **22**: 910 (1951).
112. Arditi, Maurice: Experimental Determination of the Properties of Microstrip Components, *Elec. Commun.*, **30**: 283 (1953).
113. Brennecke, C. G.: Equivalent T and Pi Sections for the Quarter-wavelength Line, *Proc. IRE*, **32**: 15 (1944).
114. Cornes, R. W.: A Coaxial Line Support for 0 to 4000 Mc, *Proc. IRE*, **37**: 94 (1949).

115. Crosby, D. R., and C. H. Pennypacker: Radio-frequency Resistors as Uniform Transmission Lines, *Proc. IRE*, **34**: 62 (1946).
116. Deschamps, G. A.: Application of Non-Euclidean Geometry to the Analysis of Waveguide Junctions, Report URSI-IRE Spring Meeting, 1952.
117. Deschamps, G. A.: New Chart for the Solution of Transmission-line and Polarization Problems, *Trans. IRE*, Professional Group on Microwave Theory and Techniques, **1**: 5 (1953).
118. Felsen, L. B., and A. A. Oliner: Determination of Equivalent Circuit Parameters for Dissipative Microwave Structures, *Proc. IRE*, **42**: 477 (1954).
119. Hartig, E. O.: A Study of Coaxial Line Discontinuities Using a Variational Method, Technical Report No. 108, Cruft Laboratory, Harvard University, 1950.
120. Hartig, E. O.: Circular Apertures and Their Effects on Half-dipole Impedances, Technical Report No. 107, Cruft Laboratory, Harvard University, 1950.
121. Hollway, D. L.: An Instrument for Dielectric Measurements in the Frequency Range 100–300 Mc/s, *Proc. Inst. Elec. Engrs. London*, pt. III, **99**: 364 (1952).
122. Kaden, H., and G. Ellenberger: Reflexionsfreie Stützscheiben in Koaxialen Leitungen, *Arch. elektr. Übertrag.*, **3**: 313 (1949).
123. King, R.: An Absolute Method for Measuring Dielectric Constants of Fluids and Solids at Ultra-high Frequencies, *Rev. Sci. Instr.*, **8**: 201 (1937).
124. King, R.: Antennas and Open-wire Lines. Part I. Theory and Summary of Measurements, *J. Appl. Phys.*, **20**: 832 (1949).
125. King, R.: Capacitance at Ultra-high Frequencies, *Phil. Mag.*, ser. 7, **25**: 339 (1938).
126. King, R.: Eine Zuzammenfassende Untersuchung über stehende elektrische Drahtwellen, *Ann. Physik*, ser. 5, **7**: 805 (1930).
127. King, R.: End-correction for Coaxial Line Driving an Antenna over a Ground Screen, Technical Report No. 174, Cruft Laboratory, Harvard University, 1953 (*Trans. IRE*, AP-3, April, 1955).
128. Kohn, C. T.: The Design of a Radio Frequency Coaxial Resistor, *Proc. Inst. Elec. Engrs. London*, pt. IV, Monograph 83 (1953).
129. Lamont, H. R. L.: Theory of Resonance in Microwave Transmission Lines with Discontinuous Dielectric, *Phil. Mag.*, ser. 7, **29**: 521 (1940).
130. Lamont, H. R. L.: The Use of the Wave Guide for Measurement of Microwave Dielectric Constants, *Phil. Mag.*, ser. 7, **30**: 1 (1940).
131. Matsumoto, K.: On the Turning Point and Branching Point of Lecher Wires, *J. Inst. Elec. Commun. Engrs. Japan*, **26**: 203 (1951).
132. Miles, J. W.: Plane Discontinuities in Coaxial Lines, *Proc. IRE*, **35**: 1498 (1947).
133. Oliver, M. H.: Discontinuities in Concentric-line Impedance-measuring Apparatus, *Proc. Inst. Elec. Engrs. London*, pt. III, **97**: 29 (1950).
134. Powles, J. G., and W. Jackson: Measurement of the Dielectric Properties of High-permittivity Materials at Centimetre Wavelengths, *Proc. Inst. Elec. Engrs. London*, pt. III, **96**: 383 (1949).
135. Storer, J. E., L. S. Sheingold, and S. Stein: A Simple Graphical Analysis of Waveguide Junctions, *Proc. IRE*, **41**: 1004 (1953).
136. Weissfloch, A.: Ein Transformationsglied für Dezimeter- und Zentimeterwellen mit geringer Frequenz Abhängigkeit, *Elek. Nachr. Tech.*, **20**: 189 (1943).
137. Weissfloch, A.: Ein Transformationssatz über Verlustlose Vierpole und seine Anwendung auf die experimentelle Untersuchung von Dezimeter- und Zentimeterwellen-Schaltungen, *Hochfrequenztech.*, **60**: 67 (1942).

138. Weissfloch, A.: Kreisgeometrische Vierpoltheorie und Ihre Bedeutung für Messtechnik und Schaltungstheorie des Dezimeter- und Zentimeterwellengebietes, *Hochfrequenztech.*, **61**: 100 (1943).
139. Whinnery, J. R., and H. W. Jamieson: Equivalent Circuits for Discontinuities in Transmission Lines, *Proc. IRE*, **32**: 98 (1944).
140. Whinnery, J. R., H. W. Jamieson, and T. E. Robbins: Coaxial-line Discontinuities, *Proc. IRE*, **32**: 695 (1944).

References Primarily for Chap. VI

141. Chipman, R. A., E. F. Clark, N. A. Hoy, and M. Yurko: Radiation Resistance of Resonant Transmission Lines, *J. Appl. Phys.*, **23**: 613 (1952). (This paper contains an extensive list and a discussion of earlier work on radiation from lines.)
142. Firestone, W. L.: Analysis of Transmission-line Directional Couplers, *Proc. IRE*, **42**: 1529 (1954).
143. Gavin, M. R.: Triode Oscillators for Ultra-short Wavelengths, *Wireless Engr.*, **16**: 287 (1939).
144. Gureivitsch, A. M., and J. R. Whinnery: Microwave Oscillators Using Disk-seal Tubes, *Proc. IRE*, **35**: 462 (1947).
145. Hansen, W. W.: On the Resonant Frequency of Closed Concentric Lines, *J. Appl. Phys.*, **10**: 38 (1939).
146. King, R.: A Continuously Variable Oscillator for Parallel Line Measurements at 100 to 2000 Megacycles per Second, *Rev. Sci. Instr.*, **11**: 270 (1940).
147. King, R.: A General Reciprocity Theorem for Transmission Lines at Ultra-high Frequencies, *Proc. IRE*, **28**: 223 (1940).
148. King, R.: A Generalized Coupling Theorem for Ultra-high Frequency Circuits, *Proc. IRE*, **28**: 84 (1940).
149. King, R.: A Variable Oscillator for Ultra-high Frequency Measurements, *Rev. Sci. Instr.*, **10**: 325 (1939).
150. King, R.: Amplitude Characteristics of Coupled Circuits Having Distributed Constants, *Proc. IRE*, **21**: 1142 (1933).
151. King, R.: Application of Low-frequency Circuit Analysis to the Problem of Distributed Coupling in Ultra-high Frequency Circuits, *Proc. IRE*, **27**: 715 (1939).
152. King, R.: Beam Tubes as Ultra-high Frequency Generators, *J. Appl. Phys.*, **10**: 638 (1939).
153. King, R.: Coupled Antennas and Transmission Lines, *Proc. IRE*, **31**: 626 (1943).
154. King, R.: Parasitic Electronic Oscillations and Coupling Frequencies in a Power Tube, *J. Appl. Phys.*, **11**: 615 (1940).
155. King, R.: Wavelength Characteristics of Coupled Circuits Having Distributed Constants, *Proc. IRE*, **20**: 1368 (1932).
156. Oliver, B. M.: Directional Electromagnetic Couplers, *Proc. IRE*, **42**: 1686 (1954).
157. Storer, J. E., and R. King: Radiation Resistance of Two-wire Line, *Proc. IRE*, **39**: 1408 (1951).
158. Takagishi, E.: On a Double-hump Phenomenon of Current through a Bridge across Parallel Lines, *Proc. IRE*. **18**: 513 (1930).
159. Tomiyasu, K.: Loading and Coupling Effects of Standing-wave Detectors, *Proc. IRE*, **37**: 1405 (1949).
160. King, R. W. P., C. W. Harrison, Jr., and D. H. Denton, Jr.: Transmission-Line Missile Antennas, *Trans. IRE*, AP–8 : 88 (1960).

INDEX OF SYMBOLS

Symbol	*Definition*	*Page*
$\mathbf{A}$	vector potential	8
A_s, A_w	over-all attenuation function	87
a	radius of conductors of two-wire line	13
$a_1(w)$	ratio function	63
$\mathbf{B}$	magnetic vector	8
b	distance between conductors of two-wire line	13
$\mathbf{C}$	amplitude function	86
$\mathbf{C}_w$	amplitude function	87
C_x, C_z	amplitude functions	250
C_T	lumped shunt capacitance	401
c	capacitance per unit length	7
$c(w)$	capacitance per unit length	63
$\mathbf{E}$	electric vector	8
F_s, F_w	over-all phase functions	87
$f(h)$	real part of complex radical	92
g	conductance per unit length	7
$g(h)$	imaginary part of complex radical	92
$g(w)$	conductance per unit length	63
h_e	loss tangent of dielectric material	8
h_m	loss tangent of magnetic material	9
I_z	current in transmission line	5
$I_{zL}(w)$	current in line	60
I_{zT}	current in load	60
$I_y^a(y)$	antisymmetrical or equal and opposite currents	213
$I_y^s(y)$	symmetrical or codirectional currents	213
$\mathbf{i}$, $\boldsymbol{i}$	volume density of current—real, complex	11
k_0	constant	17
$k_0(w)$, $k_1(w)$	parameters	16
L	power loss	244
L_s	inductance of termination	121
L_{sa}	apparent terminal inductance	122
L_T	inductance due to end effect	121
L^e	external inductance	121
l	inductance per unit length	6
$l_{1,\,2}$	inductance per unit length of conductor 1, 2	5
l^e	external inductance per unit length	17
$l^e(w)$	external inductance per unit length	63
l^i	internal inductance per unit length	18
n	index of refraction	334

Symbol	*Definition*	*Page*
P_L	power in line	252
P_s	power to load	243
P_z	power to line beyond point z	251
P_0	power to line	243
$\boldsymbol{p}$	parameter in method of symmetrical components	41
p	ratio factor	266
$\boldsymbol{p}(w)$, $\boldsymbol{p}'(w)$, $\boldsymbol{p}_0(w)$		63
Q	quality factor	270
$\boldsymbol{q}$	charge per unit length	7
$\boldsymbol{q}_L(w)$	charge per unit length on line	60
$\boldsymbol{q}_T(u)$	charge per unit length on load	60
R	distance between two points	11
R_a	distance to conductor	15
R_b	distance to conductor	15
R_{s1}	distance between points in coaxial line	21
R_{1T}, R_{2T}	distances from point on line to points on termination	61
R_0^e	radiation (external) resistance of two-wire line	488
R_m^e	radiation resistance	489
r	resistance per unit length of line	6
$r_{1,\,2}$	resistance per unit length of conductor 1, 2	5
r^i	internal resistance per unit length of line	18
$r_{1,\,2}^i$	internal resistance per unit length of conductor 1, 2	18
$\boldsymbol{S}$	amplitude function	86
$\mathbf{S}$	scattering matrix	305
S, SWR	standing-wave ratio	260
S_I	current standing-wave ratio	261
S_V	voltage standing-wave ratio	261
$\boldsymbol{S}_0$, $\boldsymbol{S}_s$, $\boldsymbol{S}_w$	amplitude functions	87
S_x, S_y	amplitude functions	250
$\boldsymbol{S}_{11}$, $\boldsymbol{S}_{12}$, $\boldsymbol{S}_{21}$, $\boldsymbol{S}_{22}$	elements of scattering matrix	305
$s_{1,\,2}$	distance between points in coaxial line	21
$\mathbf{U}$	unit matrix	305
$V(w)$	scalar potential difference	15
$V_L(w)$	scalar potential difference due to charges on line	60
$\bar{V}_s$	modified amplitude	86
$V_T(w)$	scalar potential difference due to charges on load	60
V_x^e	generator voltage at x along line	245
V_z	potential difference across transmission line	5
$\boldsymbol{V}^a$	antisymmetrical or equal and opposite voltages	213
$\boldsymbol{V}^s$	symmetrical or codirectional voltages	213
v_g	group velocity	54
v_p	phase velocity	52
v_z	instantaneous real voltage at distance z	87
v_0, v, $\boldsymbol{v}$	velocity of electromagnetic waves in free space, dielectric medium, lossy medium	10
v_0	instantaneous potential difference	50

Symbol	*Definition*	*Page*
W	power ratio	252
W	width of resonance curve	491
$W_z(w)$	vector potential difference	15
$W_{zL}(w)$	vector potential difference due to currents in line	60
$W_{zT}(w)$	vector potential due to currents in load	60
W_x^e	voltage of equal and opposite doublet	247
w	distance measured from load end of line	13
w	distance measured from load end of line	80
x^i	internal reactance per unit length of line	18
$x^i_{1,2}$	internal reactance per unit length of conductor 1, 2	18
Y_c	characteristic admittance	49
Y^a	antisymmetrical input admittance	214
Y^s	symmetrical input admittance	215
y	admittance per unit length of line	7
$y(w)$, $y_0(w)$	admittance per unit length	63
$y_T(w)$	admittance per unit length	63
y_1	normalized admittance	103
Z_c	characteristic impedance	49
Z_t	transfer impedance	216
Z_0, Z_s	terminating impedances	74
Z_{0a}, Z_{sa}	apparent terminating impedances	74
Z_{11}, Z_{22}	self-impedances	216
Z_{12}, Z_{21}	mutual impedances	216
Z^a	antisymmetrical input impedance	214
Z^s	symmetrical input impedance	215
z	impedance per unit length of line	7
$z(w)$	impedance per unit length	66
z^i	internal impedance per unit length of line	18
$z^i_{1,2}$	internal impedance per unit length of conductor 1, 2	18
z_1	normalized impedance	103
α	attenuation constant	52
β	complex wave number	9
β_0, β, β	wave number in free space, dielectric medium, lossy medium	10
Γ_0, Γ_s	voltage reflection coefficients of terminations	76
Γ_{sa}	apparent terminal reflection coefficient of Z_{sa}	280
γ	complex propagation constant of line	7
$\gamma(w)$	complex propagation constant	68
ϵ	angle of amplitude function	86
ϵ	absolute permittivity	8
ϵ', ϵ''	real and imaginary parts of complex permittivity	8
ϵ_r	relative permittivity	9
ϵ_0	permittivity of free space	9
ϵ_w	angle of amplitude function	87
ϵ_x	angle of amplitude function	250
ϵ_z	angle of amplitude function	250

Symbol	*Definition*	*Page*
$\zeta_0, \zeta, \boldsymbol{\zeta}$	characteristic resistance of free space, dielectric medium	10
$\boldsymbol{\eta}$	surface density of charge—real, complex	11
$\boldsymbol{\theta}$	complex constant (terminal function)	49
$\boldsymbol{\theta}, \boldsymbol{\theta}'$	complex terminal functions	84
$\boldsymbol{\theta}_0, \boldsymbol{\theta}_s$	complex terminal functions of $\boldsymbol{Z}_0, \boldsymbol{Z}_s$	84
μ', μ''	real and imaginary parts of complex permeability	9
μ_0	permeability of free space	9
$\boldsymbol{\nu}$	reluctivity (reciprocal permeability)	9
$\boldsymbol{\nu}_r$	relative reluctivity	9
ν_0	reluctivity of free space	9
$\boldsymbol{\xi}$	complex dielectric factor	8
ρ	terminal attenuation function	84
ρ_0, ρ_s	terminal attenuation functions of $\boldsymbol{Z}_0, \boldsymbol{Z}_s$	86
ρ_{0a}, ρ_{sa}	apparent terminal attenuation functions for $\boldsymbol{Z}_{0a}, \boldsymbol{Z}_{sa}$	276
$\rho_{1,\,2}$	constant parameter in definition of circle diagram	26
σ	angle of amplitude function	86
$\sigma_0, \sigma_s, \sigma_w$	angles of amplitude functions	37
σ_x	angle of amplitude function	250
σ', σ''	real and imaginary parts of complex conductivity	9
Φ, Φ'	terminal phase functions	84
Φ_0, Φ_s	terminal phase functions of $\boldsymbol{Z}_0, \boldsymbol{Z}_s$	86
Φ_{0a}, Φ_{sa}	apparent terminal phase functions for $\boldsymbol{Z}_{0a}, \boldsymbol{Z}_{sa}$	273
$\boldsymbol{\Phi}_1(w)$	ratio function	63
ϕ	scalar potential	8
ϕ_c	distortion factor	93
ψ_{sa}	angle of complex apparent reflection coefficient of $\boldsymbol{Z}_{sa}$	280
ψ_0, ψ_s	angles of complex reflection coefficients	76

INDEX

ABCD constants, 84, 194, 289, 290
Active networks (*see* Oscillators)
Admittance, of bridge-coupled sections of line, 470–482
  characteristic, definition, 49
  input, of line section, 147–152, 161–169
    graphs, 162–169
    schematic diagrams, 162
    symmetrical, 196
  of loaded line section, 168, 169
  of low-loss line, critical values, 160, 161
  normalized input, of line section, 133–135
    determination using circle diagram, 108
  per unit length, 7
    of coaxial cage line, 45
    of coaxial line, 22
    of four-wire line, 20
    generalized, in terminal zone, 63, 69
    of shielded eccentric line, 33
    of shielded-pair line, circular, 36, 38
      rectangular, 36, 39
    of single line over image plane, 29, 46
    of strip line, 46
    of three-phase cable, 43
    of three-wire line, 41
    of two-wire line, closely spaced, 28, 29
      with unequal conductors, 28
      widely spaced, 17
  terminal-zone, definition, 73
    discussion, 72, 73
Admittance matrix, 198, 199
Antenna, end-loading two-wire line, junction network for, 407–410
  folded dipole, 210
    junction network for, 410–411
  over ground screen, junction network for, 430–437
  shielded loop, 223, 224
  stub-supported, junction network for, 405–407
Antiresonance, input of line section, 149, 150
    low-loss, 150
  normalized input, 150–152
Attenuation, circles of constant, for line section, 137
Attenuation constant of transmission line, definition, 52
  general formulas, 91–93
  with high attenuation, 99
  with large leakage, 100
  with low attenuation, 95–98
  with low distortion, 98, 99
  measurement of, 275, 276
  and width of resonance and distribution curves, 268, 269
Attenuation function, of conducting bridge, 125, 126
  definition, 84
  description, 102–104
  of line section, 135
  measurement, 279, 280
  negative, 128–130
  for reactive termination, 118
  for resistive termination, 114
  significance, 86
  and width of resonance and distribution curves, 268, 269
Attenuator, lossy, 98, 99

Balun, 220–224
Beads in line, 346–351
  impedance transformation through use of, 351–358
  standing-wave ratio, due to single bead, 324
    due to two beads, 349
Bend, in coaxial line, 426–430
  in shielded-pair line, 426
  in two-wire line, 382–389
Bilinear transformation, 109
Boundary conditions, at discontinuity in dielectric, 320
  at terminations of line, 73–76
Bridge, conducting, attenuation function, 123
    equivalent length, 124, 125
    phase function, 123
    reactance, 122
    resistance, 122
    resistive wire, 127
    tandem, 127

Bridge, conducting, transmission-line, using hybrid junction, 230
wire, 120

Cable, ocean, 100, 101
three-phase, 41
Cage line, 43
constants of, 45
Capacitance, lumped, to correct open end, 365–367
per unit length, for coaxial cage line, 45
of coaxial line, 22
in equivalent circuit of line, 3, 4
of four-wire line, 20
generalized, in terminal zone, 63
of shielded eccentric line, 33
of shielded-pair line, circular, 36, 38
rectangular, 38, 39
of single line over image plane, 29, 46
of strip line, 46
of three-phase cable, 43
of three-wire line, 41
of two-wire line, closely spaced, 28, 29
with unequal conductors, 28
widely spaced, 17
Characteristic admittance, definition, 49
Characteristic impedance, definition, 49
discussion of significance, 76
general forms, 93
of line, of dielectric medium, 10
of free space, 10
of imperfect dielectric medium, 10
matrix for, 305
measurement, 282–284
Characteristic resistance, definition, 49
Charge per unit length, definition, 7
discontinuity in, across boundary, 321
near open end of line, 367, 368
Circle diagram, applications, 107, 108, 147
construction, 104–110
equations for, derivation, 104–106
for equipotentials of two-wire line, 27
polar form, 111
rectangular form, 106, 107
Smith chart, 111
Circuit, equivalent, of infinite line, 4, 5
Closed end of line, 364–368
Coaxial line, analysis, 20–23
bend in, 426–430
bifurcation, 381, 382
change of radius in, 377–381
constants, 22
discontinuous dielectric in, 23
electric field in, 23
end-correction for, when driving antenna, 430–437
Coaxial line, magnetic field in, 22
Coaxial mode suppressor, 207
Coefficient of reflection (*see* Reflection coefficient)
Conditions for infinite line equations to apply to finite line, 49
Conductance, input, of line section, 147–153, 162, 166–169
extreme, 153–157
graphs of, 162, 166–169
of loaded line section, graphs of, 168, 169
leakage (*see* Leakage conductance per unit length)
normalized input, of line section, 135
Conductivity, complex, 8
measurement, 285, 286
real effective, 9
Constants of line in equivalent circuit, 3, 4 (*See also* specific constants)
Continuity equation, 7
Coupled-circuit phenomena, 480–482
Coupler, directional (*see* Directional coupler)
Coupling effects at termination, general description, 68–71
Cross talk, 469
Curl, 8
Current and scattering matrix, 305
Current density, 11
Currents on line, balanced, 6
codirectional, 6
continuity across boundary, 321
driven by coupled section of line, 463–468
even and odd, 195–197
nonresonant, 243–244
with one pair of generators, 244–246
near open end, 367, 368
on outside of shield, 6
polar form, 249–251
resonant distribution, 262–265
symmetrical and antisymmetrical, 196
with three pairs of generators, 248–249
with two pairs of generators, 246–248
unbalanced, 6

Deschamps' method for determining scattering matrix, 304–314
Dielectric, discontinuous, in coaxial line, 23
loss tangent for, 8
Dielectric constant, complex, 8
measurement of, by Drude's method, 285–286
by shift method, 329–34'
relative, 9
real effective, 9

Dielectric factor, complex, 8
Dielectric and magnetic slab in matched line, 323
Dielectric slab in line, general analysis, 317–328
  at open circuit, 326
  at short circuit, 327, 328
Dielectric slabs or beads in line, 346–351
Differential equation, generalized first-order, for current, 66
  second-order, for voltage, 48
Differential equations, first-order, for current and voltage, 7, 48
  generalized, for transmission lines, 64–68
  of line, derivation of, conventional, 3–7
    electromagnetic, 13–19
    restrictions on, 4–5
  for potential functions, 14–15, 24–25
  solution of (*see* Solution of differential equations)
Directional coupler, hybrid junction as, 235–237
  transmission line, 467
Discontinuities (*see* specific discontinuities)
Disk, conducting, as termination, 127, 128
  resistive, 358, 359
Dispersion, anomalous, 54
  definition for transmission line, 53
  normal, 54
Distortion factor, definition, 93
Distortionless line, 98, 99
Distribution of voltage along infinite line, 50–56
Distribution curve, current or voltage, 257–259
  definition, 257–259
  for moving generators, 258, 259
  width at half-power points, 266–269
Distribution-curve method for measuring, 275, 279, 280
Distribution-curve ratio, 259–262
Div, 8
Double-hump phenomena, 480–482
Double-slug tuner, 351–353
Double-stub tuner, 184–190

Eccentric line, 31
  constants, 33
Eccentricity in coaxial line, 33
Effective spacing for closely spaced two-wire line, 29
Efficiency of transmission, maximum, 253
  general formula, 253
  with nonresonant line, 244
Electric field, 8
  of asymmetrical currents, 463
  boundary conditions at discontinuous dielectric, 320
  in closely spaced two-wire line, 31
  in coaxial line, 23
  of conductor with sine current, 454–457
  of even currents, 461, 462
  of odd currents, 463
  of section of two-wire line, 457–463
  at surface of conductors of line, 17
  of two-wire line, 31, 457–463
End correction for coaxial line driving antenna, 430–437
End effects, general description, 68–71
Equations, current, for π-network, 291
  differential (*see* Differential equations)
  Helmholtz, for potentials, 14
  transmission-line, 18
    conditions for, 19
  voltage, for T network, 290
Equipotentials, of line with unequal conductors, 25, 26
  of shielded-pair line, 37
  of two-wire line, 25, 26
  of unbalanced shielded-pair line, 37
Equivalent circuits (*see* Junction networks)
Equivalent length of line, 136
Equivalent Π network of line section, 198, 199
Equivalent point generators, for even currents in coupled section, 465, 466
  for odd currents in coupled section, 466, 467
  for traveling waves in coupled section, 468, 469
Equivalent T of junction, series elements, 202
  shunt element, 202
Equivalent T network of line section, 195–198
Exponential solutions, 73–83

$f(h)$, definition, 92
Field (*see* Electric field; Magnetic field)
Filter, transmission-line, 482–487
Flat line (*see* Matched line)
Folded dipole antenna, 210
Four-terminal network, 194–203
Four-wire line, with conductors at corners of square, 19
  constants of, 20
  with conductors in one plane, 34
Free space, constants of, 9, 10
Frequency measurement, 275

$g(h)$, definition, 92
Generators, point, 244–249
  distributed equivalents, 463–467
Grad, 8
Group velocity, definition, 54
  significance, 54, 56
Guided mode in strip line, 47
Gyrator, ideal, scattering matrix for, 201

Half-power points in resonance and distribution curves, 268, 269
Half-wave transformer, 326
Harmonics, in driving generator, 482–487
  measurements on line with, 482–486
  suppression, 485–487
Hybrid junction, 225–241
  admittance matrix, 228, 229
  analysis of equivalent circuit, 227–230
  as bridge, 230
  circuit for coaxial line, 226, 237, 238
  circuit for two-wire or shielded-pair line, 225
  as directional coupler, 235–237
  equivalent circuit, 227
  with high-impedance stubs for two-wire line, 238
  as line stretcher, 230–232
  for measuring phase, balanced-detector method, 233–235
    ratio method, 232, 233
  ring-circuit form, 239–241
  with shielded loop, 237
  special cases, 229, 230
  without transformer, 236–239
Hyperbolic functions, definition, 83
  in polar form, 86, 87
Hyperbolic solutions, 83–91

Image in cylinder, 34
Image-plane line, 29, 34, 41, 45
  constants, 29, 36, 38, 39, 46
Impedance, apparent terminal, definition, 71
    determined from measurements, 75, 280–282
    of wire bridge, 122
  and circle diagrams, 106–112, 146, 147
  characteristic (*see* Characteristic impedance)
  input, of line section, 147–152
      antisymmetrical, 196
      maximum, 164–172
      schematic diagrams of, 161, 163
    of loaded line section, graphs, 163, 168
    of low-loss line, critical values, 160, 161
Impedance, measurement, 280–282
      through junction, 314–317
  normalized input, of line section, 133–135
  per unit length, 6
    in equivalent circuit of line, 3, 4
    external, 17, 18
    generalized, for terminal zone, 66
    internal, of coaxial cage line, 45
      of coaxial line, 22
      of four-wire line, 20
      of shielded-pair line, circular, 36, 38
        rectangular, 38, 39
      of single line over image plane, 20
      of strip line, 46
      of three-phase cable, 43
      of three-wire line, 41
      of tubular conductors, 30
      of two-wire line, closely spaced, 30
        unequal conductors, 30
        widely spaced, 18
    terminal, apparent, 71
    terminal-zone, definition, 73
      discussion, 72, 73
  transfer, for series sections of line, 216–219
Impedance matching (*see* Matching)
Impedance matrix, 197, 198, 304
Impedance transformation (*see* Matching)
Incident wave on line, 80
Inductance, apparent, of rectangle, 122
  correction, for rectangle, 121
    for wire bridge, 364, 365
  per unit length, of coaxial cage line, 45
    of coaxial line, 22
    complex, for two-wire line, 17, 18
    in equivalent circuit of line, 3, 4
    of four-wire line, 20
    generalized in terminal zone, 63, 69
    of shielded eccentric line, 33
    of shielded-pair line, circular, 36, 38
      rectangular, 38, 39
    of single line over image plane, 29, 46
    of strip line, 46
    of three-phase cable, 43
    of three-wire line, 41
    total, 48
    of two-wire line, closely spaced, 28, 29, 121
      with unequal conductors, 28
      widely spaced, 17, 121
  of rectangle, 121
Infinite line, general solution for, 49
    exponential form, 49
    hyperbolic forms, 49
    interpretation of, 50–56
    with power coefficients, 49

Input-output equations, 289
Insertion loss, 253
Insulator, line section as, 164–172

Junction, of two coaxial lines with different inner conductors, 377–381
of two-wire lines of different dimensions, 368–377, 411–417
Junction networks, for antenna, as end load, 407–411
over ground screen, 430–437
with stub support, 405–407
for bend, in coaxial line, 426–430
in plane of two-wire line, 418–425
for bends and T junctions in shielded-pair lines, 426
for bifurcation of coaxial line, 381, 382
for change, in radius of coaxial line, 377–380
in spacing of two-wire line, 411–417
for folded dipole, 410, 411
for open end, 366, 367
for series branches in two-wire line, 397–411
for T junction in two-wire line, 389–397
for two-wire lines of different radii, 368–377
for wire bridge, 120–127, 364, 365

$k_0(w)$, definition, 16
for infinite line, 17
$k_1(w)$, definition, 16
for infinite line, 17
Kirchhoff's laws applied to equivalent circuit of line, 5

Laplace's equation for transverse problem in lines, 25
Laplacian operator, 10
Leakage conductance per unit length, of coaxial cage line, 45
of coaxial line, 22
in equivalent circuit of line, 3, 4
of four-wire line, 20
generalized, in terminal zone, 63
of shielded eccentric line, 33
of shielded-pair line, circular, 36, 38
rectangular, 38, 39
of single line over image plane, 29
of three-phase cable, 43
of three-wire line, 41
of two-wire line, closely spaced, 28, 29
with unequal conductors, 28
widely spaced, 17
Lecher wires (*see* Two-wire line)
Length, equivalent, of line, for attenuation, 136
for phase shift, 136
Line stretcher, hybrid junction as, 230–232
Load, reactive, 117–120
Loop antenna, 223, 224
Lorentz condition, 8, 12, 13
Loss, insertion, 253
measurement of, for dielectric and magnetic materials, 341–346
transmission, on nonresonant line, 244
Loss tangent, 8
Lossy attenuator, 98, 99
Lossy line, 360
Lossy terminations, 358–364
Lumped equivalent of line section, 194–203

Magnetic field, 8
in closely spaced two-wire line, 30
in coaxial line, 22
on terminating disk, 128
Magnetization, time lags in, 9
Matched line, 149
with dielectric and magnetic slab, 323–327
half-wave slab, 326
quarter-wave slab, 325
thin slab, 325
loaded with lumped capacitances or inductances, 328, 329
unaffected by dielectric slab, conditions of, 323
Matching, 172–194
double-stub, 184–190
examples, 187–190
general formulation, 172–174
quarter-wave transformer, 176
series transformer, 174–177
limitations, 176, 177
single movable stub, 178–184
examples, 180–184
shunt sections, 190–193
examples, 192–193
stub with resistive load, curves, 180
Matrices, impedance, admittance, and scattering, relations between, 201–203
Matrix, admittance, 198, 199
of hybrid junction, 229
impedance, 197, 198, 304
scattering (*see* Scattering matrix)
Matrix elements, scattering, determination of, 304–314
interpretation of, 201, 305
of symmetrical T section, 293

Measurements, with hybrid junction, 230–236
methods, Chipman's (resonance-curve method), 273, 279, 280
Deschamps', 304–317
distribution-curve, 274, 275, 278–280
maximum-minimum-shift, 329–345
resonance-curve, 273, 276, 278–280
three-probe, 281, 282
Weissfloch tangent, 294–304
with multiple-frequency source, 482–487
transmission-line, theory of, 272–286
Methods of analysis, 1
based on electric-circuit theory, 1, 3
electromagnetic, 2
Microstrip, 46, 47
Modulated voltage applied to infinite line, 53
Multiple-frequency source, measurements with, 482–487

Nabla operator, 10
Natural frequencies of oscillation (*see* Oscillators)
Network, four-terminal, for line, 84
two-terminal pair, 288–294
Nonreciprocal elements in scattering matrix, 201
Nonresonant section of line, 148

Open end of line, current and voltage near, 367, 368
equivalent circuit for, 364–366
Open-wire line (*see* Two-wire line)
Optimum termination for line, 253
Oscillators, with coupled secondary, 447–454
with double-end triode, 445, 446
with lighthouse tube, 446, 447
push-pull, with triode, 442, 443
reentrant, 446, 447
with single triode, 439, 442
tuned-plate tuned-grid, 443–445

Parallel-strip line 45, 46
Parallel-wire line (*see* Two-wire line)
Permeability, 9
complex, 9, 18
measurement of, 285, 286
by shift method, 329–341
Permittivity (*see* Dielectric constant)
Phase, circles of constant, 137
comparison of, 284, 285
measurement of, balanced-detector method, 233–235
Phase, measurement of, with hybrid junction, 233–235
ratio method, 232, 233
of voltage on infinite line, 51
Phase constant, of dielectric medium, 10
of free space, 10
general forms of, 92
generalized, in terminal zone, 63
of imperfect dielectric, 10
measurement of, 273–275
of transmission line, definition, 53
general formulas, 91–93
with high attenuation, 99
with large leakage, 100
with low attenuation, 95–98
with low distortion, 98, 99
with no attenuation, 98
Phase function, of conducting bridge, 123
definition, 84
description, 102–104
of disk, 127
of line section, 135
measurement, 276–278
of piston, 127
of reactive termination, 118, 119
of resistive termination, $x_1 = 0$, 114
$X = 0$, 117
significance, 86
tabulation for different terminations, 104
Phase measurement (*see* Phase)
Phase velocity (*see* Velocity)
Π network as load for two lines, 288–294
Piston as termination, 127
Potential, scalar, 8
separation into parts due to line and termination, 13, 65
vector, 8
separation into components due to line and termination, 12, 65
Potential difference, due to charges and currents, on line, 59, 60
on termination, 59, 60
generalized for terminated two-wire line, 61
scalar, 15
vector, 15
Potentials and potential differences, for coaxial cage line, 44
for coaxial line, 21, 22
for cylindrical conductors, 11, 13
for four-wire line, 20
Helmholtz integrals, 11
ratio functions, definitions, 63
for shielded eccentric line, 32, 33
for shielded-pair line, 35, 37
for terminated line, 58, 59
for three-phase cable, 42
for three-wire line, 40

Potentials and potential differences, for
two-wire line, closely spaced, 25–29
with unequal conductors, 25, 26
widely spaced, 11, 15, 16
Power factor, 129*n*.
(*See also* Loss tangent)
Power transfer along line, 251–254
Propagation constant, complex, 7, 25, 49
general forms, 91–93
generalized, for terminal zone, 68
in terms of separation constant, 25
Proximity effect, internal impedance with, 30
Pulse applied to transmission line, 55

Q of line, 269–272
external, 271
loaded, 271
unloaded, 271
Quarter-wave transformer, 176

Radiation from two-wire line, 487–492
condition to make negligible, 16, 17
nonresonant line, 488, 489
resonant low-loss line, 489, 490
Rat race, 239–241
Ratio, distribution-curve, 259–262
resonance-curve, 259–262
standing-wave, 260–263
Ratio method for measuring phase, 232, 233
Reactance, input, of line section, 147–152
extreme, 157–160
graphs, 161, 163–165, 168
loaded, graphs, 163, 168
nonresonant, 148
schematic diagrams of, 161
normalized, 102
contours of constant, 137
of line section, 135
tables, 142–146
Reactive load, 117–120
Reciprocal elements in scattering matrix, 201
Reflected wave, amplitude, 201
on line, 80
Reflection coefficient, definition, 76
discussion, 78
elements of scattering matrix, 201
formulas for, 134
greater than unity, 128–130, 252*n*.
measurement, 280
through junction, 314–317
as ratios of currents and voltages, 83
relation to terminal functions, 101, 280
Reflections on terminated line, 77–80
Reluctivity, 9
Resistance, characteristic, 49
input, of line section, 147–152
extreme, 153–157, 164–172
graphs, 161, 163–165, 168
loaded, graphs, 163, 168
maximum, 164–172
nonresonant, 148
schematic diagrams, 161
normalized, 102
contours of constant, 136
of line section, 135
tables, 138–141
per unit length, in equivalent circuit of line, 3, 4
generalized to include magnetic losses, 19
(*See also* Impedance per unit length, internal)
of wire bridge, 120–127
Resistive disk termination, 358, 359
Resistor, coaxial, 361–364
Resonance, conditions for, 255, 256
input, of line section, 149
low-loss, 149, 150
normalized input, 150–153
Resonance-curve method for measuring, 273, 279, 280
Resonance-curve ratio, 259–262
Resonance curves, definition, 254–257
with multiple-frequency source, 483
width at half-power points, 266–269
Resonant section of line, 148, 149
Ring circuit, 239–241

Sandwich line, 46
Scalar potential, 8, 13, 15, 65
(*See also* Voltage)
Scattering matrix, 199–203, 305
determination of elements, 304–314
interpretation, 307
Separation constant, 24
Series branch in two-wire line, 397–401
Series expansions of charge and current in line, 15
Series section of twin line, 209–223
antisymmetrical problem for, 213, 214
coaxial mode in, 218
equal twin and coaxial modes in, 219
symmetrical problem for, 214, 215
twin mode in, 217
Series stubs, 209–223
on balanced line, 211, 212
Shielded line with eccentric inner conductor, 31
constants, 33
Shielded loop antenna, 223–224
Shielded-pair line, 34–39

Shielded-pair line, balanced, 35, 36
with circular shield, 34–37
constants, 36–39
with rectangular shield, 38, 39
series section (*see* Series section of twin line)
unbalanced, 37, 38, 203–224
Short-circuiting bar or wire, 120
Shunt sections, matching with, 190–193
Signal velocity, 56
Single-stub tuner, 177–184
Single-wire line over image plane, constants, 29, 46
Smith chart, derivation of equations for, 108–112
with scales of ρ, Γ, Φ, 112
Solution of differential equations, for infinite line, 48
for terminated line, exponential, 73–76
hyperbolic forms, 83–86
instantaneous, 86–91
incident- and reflected-wave form, 79–83
infinite-series form, 77–79
Squelcher, unbalance, 207–209
Standing-wave ratio, 260–263
Standing waves (*see* Distribution curve)
Strip line, 45, 46
Stub, single movable, for matching, 177–184
Stub matching, 177–193
Stub support, 164–172
for antenna, 405–407
Suppressor, of coaxial mode in shielded-pair line, 207–209
of fundamental while passing even harmonics, 487
of second harmonic while passing fundamental, 486
of third harmonic while passing fundamental, 487
Susceptance, input, of line section, 147–153
extreme, 157–160
graphs, 162, 166–169
loaded, graphs, 168, 169
schematic diagram, 162
normalized, 135
Symmetrical networks, 293

T junction in two-wire line, 389–397
T network as load for two lines, 288–294
Tangent relation, Weissfloch, 296, 297
TEM mode in strip lines, 47
Terminal function, complex, compared with reflection coefficient, 84
definition, 84, 85
graphical representations, 104–107
relation to reflection coefficient, 101
Terminal impedance, apparent, 71
idealized, 72
Terminal zone, definition, 68–71
length, 68
Terminal-zone network, description, 71–73
Terminated line, 58–130
Termination, lossy, 358–364
open-end, 365, 366
reactive, 117–120
resistive, 112–117
wire-bridge, 364, 365
Three-phase line, 39–43
Three-probe method, 281, 282
Three-wire line, 39–43
Transfer impedance for series sections of line, 216–219
Transformer, double-slug, 351–358
equivalent, experimental determination of, 298–304
for two-terminal pair network, 294–304
with hybrid junction, 227
elimination of, 236, 237
impedance, 172–174
quarter-wave, 176
series, 174–177
Transmission coefficient, 305
element of scattering matrix, 201
Transmission lines, change in cross section, 317–328
coaxial (*see* Coaxial line)
coaxial cage, 43
constants, 45
coupled, 457–470
distortionless, 98, 99
eccentric, 31
constants, 33
equivalent uniform, in terminal zone, 71
flat (*see* Matched line; Matching)
four-wire, 19
constants, 20
with high attenuation, conditions and constants, 99
image, 29, 34, 41, 45
constants, 29, 36, 38, 39, 46
with large leakage and negligible resistance, 100
lossless, 98
formulas for current and voltage, 86
lossy, 360
with low attenuation, negligible leakage conductance, 98
per unit length, 95–96
factors of higher order for, 96, 97
with low distortion, 98
matched (*see* Matched line; Matching)
n-phase, 39, 43

Transmission lines, *n*-wire, 39, 43
nonresonant, 243, 244
resonant, current and voltage, 262–265
sandwich, 46
shielded, 31, 34, 43
shielded-pair (*see* Shielded-pair line)
single conductor over image plane, 29, 45
strip, 45
constants, 46
terminated, 58
three-phase, 41
constants, 43
three-wire, 39
constants, 41
twin (*see* Shielded-pair line)
two-wire (*see* Two-wire line)
Transmitted wave, amplitude of, 201
Transverse problem, equation for, 25
Traveling wave on line, 52
Tuner, double-slug, 351–353
double-stub, 184–190
single-stub, 177–184
triple-stub, 241
Twin line (*see* Shielded-pair line)
Two-terminal pair, equivalent transformer, 294–304
Two-wire line, analysis, 13–20, 23–31
bend in, 382–389
change in spacing, 411–417
closely spaced, 23–31
effective spacing for, 29
constants, 17, 28, 29
electric field, 31
magnetic field, 30
plane of, bend in, 418–425
radiation from (*see* Radiation from two-wire line)
series branches in, 397–411
shielded, 34–39
T junction in, 389–397
unbalanced, 224, 397–399

Unbalance squelcher, terminated, 209
Tomiyasu's, 207
Unbalanced generator, 208
Unbalanced line, open-wire, 209, 210
shielded-pair, 203–209
Unbalanced load, difference impedance for, 203
equivalent generators for, 204
terminating shielded-pair line, 203–209

Variables, separation of, 24
Vector potential, definition, 8
discontinuity across boundary in line, 321
near open end, 367, 368
Vector potential, for terminated line, 66
for two-wire line, 30
(*See also* Potentials and potential differences)
Velocity, characteristic, of dielectric medium, 10
of free space, 10
of imperfect dielectric medium, 10
group, definition, 54
significance, 54, 56
phase, definition, 52, 53
general forms, 94
in hyperbolic form of solution, 88–91
in incident- and reflected-wave form of solution, 80
in infinite-series form of solution, 77
lower frequency limit, 94
measurement, 275
in ocean cable, 100
significance, 52–54
upper frequency limit, 94
varying, for finite line, 89
signal, 56
Voltage, continuity across boundary, 320–321
distribution, on nonresonant line, 243, 244
on resonant line, 262–265
instantaneous, along finite line, 77, 87
along infinite line, 50
as infinite series, 77
on line, driven by coupled section of line, 463–468
with one pair of point generators, 244–246
with three pairs of point generators, 248, 249
with two pairs of point generators, 246–248
near open end, 367, 368
polar form for line, 249–251
and scattering matrix, 305
Voltages on line, even and odd, 195–197
symmetrical and antisymmetrical, 196, 293, 391, 398, 399, 418, 419

Wave, incident, 80
reflected, 80
Wavelength, definition for infinite line, 51, 52
measurement, 273–275
Waves, of current on infinite line, running, 52
traveling, 52
of voltage, 52
Weissfloch tangent relation, 296, 297

Zone, terminal, 68–71

CATALOGUE OF DOVER BOOKS

PHYSICS

General physics

FOUNDATIONS OF PHYSICS, R. B. Lindsay & H. Margenau. Excellent bridge between semi-popular works & technical treatises. A discussion of methods of physical description, construction of theory; valuable for physicist with elementary calculus who is interested in ideas that give meaning to data, tools of modern physics. Contents include symbolism, mathematical equations; space & time foundations of mechanics; probability; physics & continua; electron theory; special & general relativity; quantum mechanics; causality. "Thorough and yet not overdetailed. Unreservedly recommended," NATURE (London). Unabridged, corrected edition. List of recommended readings. 35 illustrations. xi + 537pp. 5⅜ x 8.
S377 Paperbound **$2.75**

FUNDAMENTAL FORMULAS OF PHYSICS, ed. by D. H. Menzel. Highly useful, fully inexpensive reference and study text, ranging from simple to highly sophisticated operations. Mathematics integrated into text—each chapter stands as short textbook of field represented. Vol. 1: Statistics, Physical Constants, Special Theory of Relativity, Hydrodynamics, Aerodynamics, Boundary Value Problems in Math. Physics; Viscosity, Electromagnetic Theory, etc. Vol. 2: Sound, Acoustics, Geometrical Optics, Electron Optics, High-Energy Phenomena, Magnetism, Biophysics, much more. Index. Total of 800pp. 5⅜ x 8.
Vol. 1 S595 Paperbound **$2.00**
Vol. 2 S596 Paperbound **$2.00**

MATHEMATICAL PHYSICS, D. H. Menzel. Thorough one-volume treatment of the mathematical techniques vital for classic mechanics, electromagnetic theory, quantum theory, and relativity. Written by the Harvard Professor of Astrophysics for junior, senior, and graduate courses, it gives clear explanations of all those aspects of function theory, vectors, matrices, dyadics, tensors, partial differential equations, etc., necessary for the understanding of the various physical theories. Electron theory, relativity, and other topics seldom presented appear here in considerable detail. Scores of definitions, conversion factors, dimensional constants, etc. "More detailed than normal for an advanced text . . . excellent set of sections on Dyadics, Matrices, and Tensors," JOURNAL OF THE FRANKLIN INSTITUTE. Index. 193 problems, with answers. x + 412pp. 5⅜ x 8.
S56 Paperbound **$2.00**

THE SCIENTIFIC PAPERS OF J. WILLARD GIBBS. All the published papers of America's outstanding theoretical scientist (except for "Statistical Mechanics" and "Vector Analysis"). Vol I (thermodynamics) contains one of the most brilliant of all 19th-century scientific papers—the 300-page "On the Equilibrium of Heterogeneous Substances," which founded the science of physical chemistry, and clearly stated a number of highly important natural laws for the first time; 8 other papers complete the first volume. Vol II includes 2 papers on dynamics, 8 on vector analysis and multiple algebra, 5 on the electromagnetic theory of light, and 6 miscellaneous papers. Biographical sketch by H. A. Bumstead. Total of xxxvi + 718pp. 5⅝ x 8⅜.
S721 Vol I Paperbound **$2.00**
S722 Vol II Paperbound **$2.00**
The set **$4.00**

BASIC THEORIES OF PHYSICS, Peter Gabriel Bergmann. Two-volume set which presents a critical examination of important topics in the major subdivisions of classical and modern physics. The first volume is concerned with classical mechanics and electrodynamics: mechanics of mass points, analytical mechanics, matter in bulk, electrostatics and magnetostatics, electromagnetic interaction, the field waves, special relativity, and waves. The second volume (Heat and Quanta) contains discussions of the kinetic hypothesis, physics and statistics, stationary ensembles, laws of thermodynamics, early quantum theories, atomic spectra, probability waves, quantization in wave mechanics, approximation methods, and abstract quantum theory. A valuable supplement to any thorough course or text.
Heat and Quanta: Index. 8 figures. x + 300pp. 5⅜ x 8½. S968 Paperbound **$1.75**
Mechanics and Electrodynamics: Index. 14 figures. vii + 280pp. 5⅜ x 8½.
S969 Paperbound **$1.75**

THEORETICAL PHYSICS, A. S. Kompaneyets. One of the very few thorough studies of the subject in this price range. Provides advanced students with a comprehensive theoretical background. Especially strong on recent experimentation and developments in quantum theory. Contents: Mechanics (Generalized Coordinates, Lagrange's Equation, Collision of Particles, etc.), Electrodynamics (Vector Analysis, Maxwell's equations, Transmission of Signals, Theory of Relativity, etc.), Quantum Mechanics (the Inadequacy of Classical Mechanics, the Wave Equation, Motion in a Central Field, Quantum Theory of Radiation, Quantum Theories of Dispersion and Scattering, etc.), and Statistical Physics (Equilibrium Distribution of Molecules in an Ideal Gas, Boltzmann statistics, Bose and Fermi Distribution, Thermodynamic Quantities, etc.). Revised to 1961. Translated by George Yankovsky, authorized by Kompaneyets. 137 exercises. 56 figures. 529pp. 5⅜ x 8½. S972 Paperbound **$2.50**

ANALYTICAL AND CANONICAL FORMALISM IN PHYSICS, André Mercier. A survey, in one volume, of the variational principles (the key principles—in mathematical form—from which the basic laws of any one branch of physics can be derived) of the several branches of physical theory, together with an examination of the relationships among them. Contents: the Lagrangian Formalism, Lagrangian Densities, Canonical Formalism, Canonical Form of Electrodynamics, Hamiltonian Densities, Transformations, and Canonical Form with Vanishing Jacobian Determinant. Numerous examples and exercises. For advanced students, teachers, etc. 6 figures. Index. viii + 222pp. 5⅜ x 8½. S1077 Paperbound **$1.75**

Acoustics, optics, electricity and magnetism, electromagnetics, magneto-hydrodynamics

THE THEORY OF SOUND, Lord Rayleigh. Most vibrating systems likely to be encountered in practice can be tackled successfully by the methods set forth by the great Nobel laureate, Lord Rayleigh. Complete coverage of experimental, mathematical aspects of sound theory. Partial contents: Harmonic motions, vibrating systems in general, lateral vibrations of bars, curved plates or shells, applications of Laplace's functions to acoustical problems, fluid friction, plane vortex-sheet, vibrations of solid bodies, etc. This is the first inexpensive edition of this great reference and study work. Bibliography. Historical introduction by R. B. Lindsay. Total of 1040pp. 97 figures. 5⅜ x 8.
S292, S293, Two volume set, paperbound, **$4.70**

THE DYNAMICAL THEORY OF SOUND, H. Lamb. Comprehensive mathematical treatment of the physical aspects of sound, covering the theory of vibrations, the general theory of sound, and the equations of motion of strings, bars, membranes, pipes, and resonators. Includes chapters on plane, spherical, and simple harmonic waves, and the Helmholtz Theory of Audition. Complete and self-contained development for student and specialist; all fundamental differential equations solved completely. Specific mathematical details for such important phenomena as harmonics, normal modes, forced vibrations of strings, theory of reed pipes, etc. Index. Bibliography. 86 diagrams. viii + 307pp. 5⅜ x 8. S655 Paperbound **$1.50**

WAVE PROPAGATION IN PERIODIC STRUCTURES, L. Brillouin. A general method and application to different problems: pure physics, such as scattering of X-rays of crystals, thermal vibration in crystal lattices, electronic motion in metals; and also problems of electrical engineering. Partial contents: elastic waves in 1-dimensional lattices of point masses. Propagation of waves along 1-dimensional lattices. Energy flow. 2 dimensional, 3 dimensional lattices. Mathieu's equation. Matrices and propagation of waves along an electric line. Continuous electric lines. 131 illustrations. Bibliography. Index. xii + 253pp. 5⅜ x 8.
S34 Paperbound **$1.85**

THEORY OF VIBRATIONS, N. W. McLachlan. Based on an exceptionally successful graduate course given at Brown University, this discusses linear systems having 1 degree of freedom, forced vibrations of simple linear systems, vibration of flexible strings, transverse vibrations of bars and tubes, transverse vibration of circular plate, sound waves of finite amplitude, etc. Index. 99 diagrams. 160pp. 5⅜ x 8. S190 Paperbound **$1.35**

LIGHT: PRINCIPLES AND EXPERIMENTS, George S. Monk. Covers theory, experimentation, and research. Intended for students with some background in general physics and elementary calculus. Three main divisions: 1) Eight chapters on geometrical optics—fundamental concepts (the ray and its optical length, Fermat's principle, etc.), laws of image formation, apertures in optical systems, photometry, optical instruments etc.; 2) 9 chapters on physical optics—interference, diffraction, polarization, spectra, the Rayleigh refractometer, the wave theory of light, etc.; 3) 23 instructive experiments based directly on the theoretical text. "Probably the best intermediate textbook on light in the English language. Certainly, it is the best book which includes both geometrical and physical optics," J. Rud Nielson, PHYSICS FORUM. Revised edition. 102 problems and answers. 12 appendices. 6 tables. Index. 270 illustrations. xi +489pp. 5⅜ x 8½. S341 Paperbound **$2.45**

PHOTOMETRY, John W. T. Walsh. The best treatment of both "bench" and "illumination" photometry in English by one of Britain's foremost experts in the field (President of the International Commission on Illumination). Limited to those matters, theoretical and practical, which affect the measurement of light flux, candlepower, illumination, etc., and excludes treatment of the use to which such measurements may be put after they have been made. Chapters on Radiation, The Eye and Vision, Photo-Electric Cells, The Principles of Photometry, The Measurement of Luminous Intensity, Colorimetry, Spectrophotometry, Stellar Photometry, The Photometric Laboratory, etc. Third revised (1958) edition. 281 illustrations. 10 appendices. xxiv + 544pp. 5½ x 9¼. S319 Clothbound **$10.00**

EXPERIMENTAL SPECTROSCOPY, R. A. Sawyer. Clear discussion of prism and grating spectrographs and the techniques of their use in research, with emphasis on those principles and techniques that are fundamental to practically all uses of spectroscopic equipment. Beginning with a brief history of spectroscopy, the author covers such topics as light sources, spectroscopic apparatus, prism spectroscopes and graphs, diffraction grating, the photographic process, determination of wave length, spectral intensity, infrared spectroscopy, spectrochemical analysis, etc. This revised edition contains new material on the production of replica gratings, solar spectroscopy from rockets, new standard of wave length, etc. Index. Bibliography. 111 illustrations. x + 358pp. 5⅜ x 8½. S1045 Paperbound **$2.00**

FUNDAMENTALS OF ELECTRICITY AND MAGNETISM, L. B. Loeb. For students of physics, chemistry, or engineering who want an introduction to electricity and magnetism on a higher level and in more detail than general elementary physics texts provide. Only elementary differential and integral calculus is assumed. Physical laws developed logically, from magnetism to electric currents, Ohm's law, electrolysis, and on to static electricity, induction, etc. Covers an unusual amount of material; one third of book on modern material: solution of wave equation, photoelectric and thermionic effects, etc. Complete statement of the various electrical systems of units and interrelations. 2 Indexes. 75 pages of problems with answers stated. Over 300 figures and diagrams. xix +669pp. 5⅜ x 8. S745 Paperbound **$2.75**

MATHEMATICAL ANALYSIS OF ELECTRICAL AND OPTICAL WAVE-MOTION, Harry Bateman. Written by one of this century's most distinguished mathematical physicists, this is a practical introduction to those developments of Maxwell's electromagnetic theory which are directly connected with the solution of the partial differential equation of wave motion. Methods of solving wave-equation, polar-cylindrical coordinates, diffraction, transformation of coordinates, homogeneous solutions, electromagnetic fields with moving singularities, etc. Index. 168pp. 5⅜ x 8. S14 Paperbound **$1.75**

PRINCIPLES OF PHYSICAL OPTICS, Ernst Mach. This classical examination of the propagation of light, color, polarization, etc. offers an historical and philosophical treatment that has never been surpassed for breadth and easy readability. Contents: Rectilinear propagation of light. Reflection, refraction. Early knowledge of vision. Dioptrics. Composition of light. Theory of color and dispersion. Periodicity. Theory of interference. Polarization. Mathematical representation of properties of light. Propagation of waves, etc. 279 illustrations, 10 portraits. Appendix. Indexes. 324pp. 5⅜ x 8. S178 Paperbound **$1.75**

THE THEORY OF OPTICS, Paul Drude. One of finest fundamental texts in physical optics, classic offers thorough coverage, complete mathematical treatment of basic ideas. Includes fullest treatment of application of thermodynamics to optics; sine law in formation of images, transparent crystals, magnetically active substances, velocity of light, apertures, effects depending upon them, polarization, optical instruments, etc. Introduction by **A. A.** Michelson. Index. 110 illus. 567pp. 5⅜ x 8. S532 Paperbound **$2.45**

ELECTRICAL THEORY ON THE GIORGI SYSTEM, P. Cornelius. A new clarification of the fundamental concepts of electricity and magnetism, advocating the convenient m.k.s. system of units that is steadily gaining followers in the sciences. Illustrating the use and effectiveness of his terminology with numerous applications to concrete technical problems, the author here expounds the famous Giorgi system of electrical physics. His lucid presentation and well-reasoned, cogent argument for the universal adoption of this system form one of the finest pieces of scientific exposition in recent years. 28 figures. Index. Conversion tables for translating earlier data into modern units. Translated from 3rd Dutch edition by L. J. Jolley. x + 187pp. 5½ x 8¾. S909 Clothbound **$6.00**

ELECTRIC WAVES: BEING RESEARCHES ON THE PROPAGATION OF ELECTRIC ACTION WITH FINITE VELOCITY THROUGH SPACE, Heinrich Hertz. This classic work brings together the original papers in which Hertz—Helmholtz's protegé and one of the most brilliant figures in 19th-century research—probed the existence of electromagnetic waves and showed experimentally that their velocity equalled that of light, research that helped lay the groundwork for the development of radio, television, telephone, telegraph, and other modern technological marvels. Unabridged republication of original edition. Authorized translation by D. E. Jones. Preface by Lord Kelvin. Index of names. 40 illustrations. xvii + 278pp. 5⅜ x 8½. S57 Paperbound **$1.75**

PIEZOELECTRICITY: AN INTRODUCTION TO THE THEORY AND APPLICATIONS OF ELECTROMECHANICAL PHENOMENA IN CRYSTALS, Walter G. Cady. This is the most complete and systematic coverage of this important field in print—now regarded as something of scientific classic. This republication, revised and corrected by Prof. Cady—one of the foremost contributors in this area—contains a sketch of recent progress and new material on Ferroelectrics. Time Standards, etc. The first 7 chapters deal with fundamental theory of crystal electricity. 5 important chapters cover basic concepts of piezoelectricity, including comparisons of various competing theories in the field. Also discussed: piezoelectric resonators (theory, methods of manufacture, influences of air-gaps, etc.); the piezo oscillator; the properties, history, and observations relating to Rochelle salt; ferroelectric crystals; miscellaneous applications of piezoelectricity; pyroelectricity; etc. "A great work," W. A. Wooster, NATURE. Revised (1963) and corrected edition. New preface by Prof. Cady. 2 Appendices. Indices. Illustrations. 62 tables. Bibliography. Problems. Total of 1 + 822pp. 5⅜ x 8½.
S1094 Vol. I Paperbound **$2.50**
S1095 Vol. II Paperbound **$2.50**
Two volume set Paperbound **$5.00**

MAGNETISM AND VERY LOW TEMPERATURES, H. B. G. Casimir. A basic work in the literature of low temperature physics. Presents a concise survey of fundamental theoretical principles, and also points out promising lines of investigation. Contents: Classical Theory and Experimental Methods, Quantum Theory of Paramagnetism, Experiments on Adiabatic Demagnetization. Theoretical Discussion of Paramagnetism at Very Low Temperatures, Some Experimental Results, Relaxation Phenomena. Index. 89-item bibliography. ix + 95pp. 5⅜ x 8.
S943 Paperbound **$1.25**

SELECTED PAPERS ON NEW TECHNIQUES FOR ENERGY CONVERSION: THERMOELECTRIC METHODS; THERMIONIC; PHOTOVOLTAIC AND ELECTRICAL EFFECTS; FUSION, Edited by Sumner N. Levine. Brings together in one volume the most important papers (1954-1961) in modern energy technology. Included among the 37 papers are general and qualitative descriptions of the field as a whole, indicating promising lines of research. Also: 15 papers on thermoelectric methods, 7 on thermionic, 5 on photovoltaic, 4 on electrochemical effect, and 2 on controlled fusion research. Among the contributors are: Joffe, Maria Telkes, Herold, Herring, Douglas, Jaumot, Post, Austin, Wilson, Pfann, Rappaport, Morehouse, Domenicali, Moss, Bowers, Harman, Von Doenhoef. Preface and introduction by the editor. Bibliographies. xxviii + 451pp. 6⅛ x 9¼. S37 Paperbound **$3.00**

SUPERFLUIDS: MACROSCOPIC THEORY OF SUPERCONDUCTIVITY, Vol. I, Fritz London. The major work by one of the founders and great theoreticians of modern quantum physics. Consolidates the researches that led to the present understanding of the nature of superconductivity. Prof. London here reveals that quantum mechanics is operative on the macroscopic plane as well as the submolecular level. Contents: Properties of Superconductors and Their Thermodynamical Correlation; Electrodynamics of the Pure Superconducting State; Relation between Current and Field; Measurements of the Penetration Depth; Non-Viscous Flow vs. Superconductivity; Micro-waves in Superconductors; Reality of the Domain Structure; and many other related topics. A new epilogue by M. J. Buckingham discusses developments in the field up to 1960. Corrected and expanded edition. An appreciation of the author's life and work by L. W. Nordheim. Biography by Edith London. Bibliography of his publications. 45 figures. 2 Indices. xviii + 173pp. 5⅜ x 8⅜. S44 Paperbound **$1.45**

SELECTED PAPERS ON PHYSICAL PROCESSES IN IONIZED PLASMAS, Edited by Donald H. Menzel, Director, Harvard College Observatory. 30 important papers relating to the study of highly ionized gases or plasmas selected by a foremost contributor in the field, with the assistance of Dr. L. H. Aller. The essays include 18 on the physical processes in gaseous nebulae, covering problems of radiation and radiative transfer, the Balmer decrement, electron temperatives, spectrophotometry, etc. 10 papers deal with the interpretation of nebular spectra, by Bohm, Van Vleck, Aller, Minkowski, etc. There is also a discussion of the intensities of "forbidden" spectral lines by George Shortley and a paper concerning the theory of hydrogenic spectra by Menzel and Pekeris. Other contributors: Goldberg, Hebb, Baker, Bowen, Ufford, Liller, etc. viii + 374pp. 6⅛ x 9¼. S60 Paperbound **$2.95**

THE ELECTROMAGNETIC FIELD, Max Mason & Warren Weaver. Used constantly by graduate engineers. Vector methods exclusively: detailed treatment of electrostatics, expansion methods, with tables converting any quantity into absolute electromagnetic, absolute electrostatic, practical units. Discrete charges, ponderable bodies, Maxwell field equations, etc. Introduction. Indexes. 416pp. 5⅜ x 8. S185 Paperbound **$2.00**

THEORY OF ELECTRONS AND ITS APPLICATION TO THE PHENOMENA OF LIGHT AND RADIANT HEAT, H. Lorentz. Lectures delivered at Columbia University by Nobel laureate Lorentz. Unabridged, they form a historical coverage of the theory of free electrons, motion, absorption of heat, Zeeman effect, propagation of light in molecular bodies, inverse Zeeman effect, optical phenomena in moving bodies, etc. 109 pages of notes explain the more advanced sections. Index. 9 figures. 352pp. 5⅜ x 8. S173 Paperbound **$1.85**

FUNDAMENTAL ELECTROMAGNETIC THEORY, Ronold P. King, Professor Applied Physics, Harvard University. Original and valuable introduction to electromagnetic theory and to circuit theory from the standpoint of electromagnetic theory. Contents: Mathematical Description of Matter—stationary and nonstationary states; Mathematical Description of Space and of Simple Media—Field Equations, Integral Forms of Field Equations, Electromagnetic Force, etc.; Transformation of Field and Force Equations; Electromagnetic Waves in Unbounded Regions; Skin Effect and Internal Impedance—in a solid cylindrical conductor, etc.; and Electrical Circuits—Analytical Foundations, Near-zone and quasi-near zone circuits, Balanced two-wire and four-wire transmission lines. Revised and enlarged version. New preface by the author. 5 appendices (Differential operators: Vector Formulas and Identities, etc.). Problems. Indexes. Bibliography. xvi + 580pp. 5⅜ x 8½. S1023 Paperbound **$2.75**

Hydrodynamics

A TREATISE ON HYDRODYNAMICS, A. B. Basset. Favorite text on hydrodynamics for 2 generations of physicists, hydrodynamical engineers, oceanographers, ship designers, etc. Clear enough for the beginning student, and thorough source for graduate students and engineers on the work of d'Alembert, Euler, Laplace, Lagrange, Poisson, Green, Clebsch, Stokes, Cauchy, Helmholtz, J. J. Thomson, Love, Hicks, Greenhill, Besant, Lamb, etc. Great amount of documentation on entire theory of classical hydrodynamics. Vol I: theory of motion of frictionless liquids, vortex, and cyclic irrotational motion, etc. 132 exercises. Bibliography. 3 Appendixes. xii + 264pp. Vol II: motion in viscous liquids, harmonic analysis, theory of tides, etc. 112 exercises, Bibliography. 4 Appendixes. xv + 328pp. Two volume set. 5⅜ x 8.
S724 Vol I Paperbound **$1.75**
S725 Vol II Paperbound **$1.75**
The set **$3.50**

HYDRODYNAMICS, Horace Lamb. Internationally famous complete coverage of standard reference work on dynamics of liquids & gases. Fundamental theorems, equations, methods, solutions, background, for classical hydrodynamics. Chapters include Equations of Motion, Integration of Equations in Special Gases, Irrotational Motion, Motion of Liquid in 2 Dimensions, Motion of Solids through Liquid-Dynamical Theory, Vortex Motion, Tidal Waves, Surface Waves, Waves of Expansion, Viscosity, Rotating Masses of liquids. Excellently planned, arranged; clear, lucid presentation. 6th enlarged, revised edition. Index. Over 900 footnotes, mostly bibliographical. 119 figures. xv + 738pp. 6⅛ x 9¼. S256 Paperbound **$3.25**

ENGINEERING AND TECHNOLOGY

General and mathematical

ENGINEERING MATHEMATICS, Kenneth S. Miller. A text for graduate students of engineering to strengthen their mathematical background in differential equations, etc. Mathematical steps very explicitly indicated. Contents: Determinants and Matrices, Integrals, Linear Differential Equations, Fourier Series and Integrals, Laplace Transform, Network Theory, Random Function . . . all vital requisites for advanced modern engineering studies. Unabridged republication. Appendices: Borel Sets; Riemann-Stieltjes Integral; Fourier Series and Integrals. Index. References at Chapter Ends. xii + 417pp. 6 x 8½. S1121 Paperbound **$2.00**

MATHEMATICAL ENGINEERING ANALYSIS, Rufus Oldenburger. A book designed to assist the research engineer and scientist in making the transition from physical engineering situations to the corresponding mathematics. Scores of common practical situations found in all major fields of physics are supplied with their correct mathematical formulations—applications to automobile springs and shock absorbers, clocks, throttle torque of diesel engines, resistance networks, capacitors, transmission lines, microphones, neon tubes, gasoline engines, refrigeration cycles, etc. Each section reviews basic principles of underlying various fields: mechanics of rigid bodies, electricity and magnetism, heat, elasticity, fluid mechanics, and aerodynamics. Comprehensive and eminently useful. Index. 169 problems, answers. 200 photos and diagrams. xiv + 426pp. 5⅜ x 8½. S919 Paperbound **$2.00**

MATHEMATICS OF MODERN ENGINEERING, E. G. Keller and R. E. Doherty. Written for the Advanced Course in Engineering of the General Electric Corporation, deals with the engineering use of determinants, tensors, the Heaviside operational calculus, dyadics, the calculus of variations, etc. Presents underlying principles fully, but purpose is to teach engineers to deal with modern engineering problems, and emphasis is on the perennial engineering attack of set-up and solve. Indexes. Over 185 figures and tables. Hundreds of exercises, problems, and worked-out examples. References. Two volume set. Total of xxxiii + 623pp. 5⅜ x 8.
S734 Vol I Paperbound **$1.85**
S735 Vol II Paperbound **$1.85**
The set **$3.70**

MATHEMATICAL METHODS FOR SCIENTISTS AND ENGINEERS, L. P. Smith. For scientists and engineers, as well as advanced math students. Full investigation of methods and practical description of conditions under which each should be used. Elements of real functions, differential and integral calculus, space geometry, theory of residues, vector and tensor analysis, series of Bessel functions, etc. Each method illustrated by completely-worked-out examples, mostly from scientific literature. 368 graded unsolved problems. 100 diagrams. x + 453pp. 5⅝ x 8⅜. S220 Paperbound **$2.00**

THEORY OF FUNCTIONS AS APPLIED TO ENGINEERING PROBLEMS, edited by R. Rothe, F. Ollendorff, and K. Pohlhausen. A series of lectures given at the Berlin Institute of Technology that shows the specific applications of function theory in electrical and allied fields of engineering. Six lectures provide the elements of function theory in a simple and practical form, covering complex quantities and variables, integration in the complex plane, residue theorems, etc. Then 5 lectures show the exact uses of this powerful mathematical tool, with full discussions of problem methods. Index. Bibliography. 108 figures. x + 189pp. 5⅜ x 8.
S733 Paperbound **$1.35**

Aerodynamics and hydrodynamics

AIRPLANE STRUCTURAL ANALYSIS AND DESIGN, E. E. Sechler and L. G. Dunn. Systematic authoritative book which summarizes a large amount of theoretical and experimental work on structural analysis and design. Strong on classical subsonic material still basic to much aeronautic design . . . remains a highly useful source of information. Covers such areas as layout of the airplane, applied and design loads, stress-strain relationships for stable structures, truss and frame analysis, the problem of instability, the ultimate strength of stiffened flat sheet, analysis of cylindrical structures, wings and control surfaces, fuselage analysis, engine mounts, landing gears, etc. Originally published as part of the CALCIT Aeronautical Series. 256 illustrations. 47 study problems. Indexes. xi + 420pp. 5⅜ x 8½.
S1043 Paperbound **$2.25**

FUNDAMENTALS OF HYDRO- AND AEROMECHANICS, L. Prandtl and O. G. Tietjens. The well-known standard work based upon Prandtl's lectures at Goettingen. Wherever possible hydrodynamics theory is referred to practical considerations in hydraulics, with the view of unifying theory and experience. Presentation is extremely clear and though primarily physical, mathematical proofs are rigorous and use vector analysis to a considerable extent. An Enginering Society Monograph, 1934. 186 figures. Index. xvi + 270pp. 5⅜ x 8.
S374 Paperbound **$1.85**

FLUID MECHANICS FOR HYDRAULIC ENGINEERS, H. Rouse. Standard work that gives a coherent picture of fluid mechanics from the point of view of the hydraulic engineer. Based on courses given to civil and mechanical engineering students at Columbia and the California Institute of Technology, this work covers every basic principle, method, equation, or theory of interest to the hydraulic engineer. Much of the material, diagrams, charts, etc., in this self-contained text are not duplicated elsewhere. Covers irrotational motion, conformal mapping, problems in laminar motion, fluid turbulence, flow around immersed bodies, transportation of sediment, general charcteristics of wave phenomena, gravity waves in open channels, etc. Index. Appendix of physical properties of common fluids. Frontispiece + 245 figures and photographs. xvi + 422pp. 5⅜ x 8. S729 Paperbound **$2.25**

WATERHAMMER ANALYSIS, John Parmakian. Valuable exposition of the graphical method of solving waterhammer problems by Assistant Chief Designing Engineer, U.S. Bureau of Reclamation. Discussions of rigid and elastic water column theory, velocity of waterhammer waves, theory of graphical waterhammer analysis for gate operation, closings, openings, rapid and slow movements, etc., waterhammer in pump discharge caused by power failure, waterhammer analysis for compound pipes, and numerous related problems. "With a concise and lucid style, clear printing, adequate bibliography and graphs for approximate solutions at the project stage, it fills a vacant place in waterhammer literature," WATER POWER. 43 problems. Bibliography. Index. 113 illustrations. xiv + 161pp. 5⅜ x 8½. S1061 Paperbound **$1.65**

AERODYNAMIC THEORY: A GENERAL REVIEW OF PROGRESS, William F. Durand, editor-in-chief. A monumental joint effort by the world's leading authorities prepared under a grant of the Guggenheim Fund for the Promotion of Aeronautics. Intended to provide the student and aeronautic designer with the theoretical and experimental background of aeronautics. Never equalled for breadth, depth, reliability. Contains discussions of special mathematical topics not usually taught in the engineering or technical courses. Also: an extended two-part treatise on Fluid Mechanics, discussions of aerodynamics of perfect fluids, analyses of experiments with wind tunnels, applied airfoil theory, the non-lifting system of the airplane, the air propeller, hydrodynamics of boats and floats, the aerodynamics of cooling, etc. Contributing experts include Munk, Giacomelli, Prandtl, Toussaint, Von Karman, Klemperer, among others. Unabridged republication. 6 volumes bound as 3. Total of 1,012 figures, 12 plates. Total of 2,186pp. Bibliographies. Notes. Indices. 5⅜ x 8. S328-S330 Clothbound, The Set **$17.50**

APPLIED HYDRO- AND AEROMECHANICS, L. Prandtl and O. G. Tietjens. Presents, for the most part, methods which will be valuable to engineers. Covers flow in pipes, boundary layers, airfoil theory, entry conditions, turbulent flow in pipes, and the boundary layer, determining drag from measurements of pressure and velocity, etc. "Will be welcomed by all students of aerodynamics," NATURE. Unabridged, unaltered. An Engineering Society Monograph, 1934. Index. 226 figures, 28 photographic plates illustrating flow patterns. xvi + 311pp. 5⅜ x 8. S375 Paperbound **$1.85**

SUPERSONIC AERODYNAMICS, E. R. C. Miles. Valuable theoretical introduction to the supersonic domain, with emphasis on mathematical tools and principles, for practicing aerodynamicists and advanced students in aeronautical engineering. Covers fundamental theory, divergence theorem and principles of circulation, compressible flow and Helmholtz laws, the Prandtl-Busemann graphic method for 2-dimensional flow, oblique shock waves, the Taylor-Maccoll method for cones in supersonic flow, the Chaplygin method for 2-dimensional flow, etc. Problems range from practical engineering problems to development of theoretical results. "Rendered outstanding by the unprecedented scope of its contents . . . has undoubtedly filled a vital gap," AERONAUTICAL ENGINEERING REVIEW. Index. 173 problems, answers. 106 diagrams. 7 tables. xii + 255pp. 5⅜ x 8. S214 Paperbound **$1.45**

HYDRAULIC TRANSIENTS, G. R. Rich. The best text in hydraulics ever printed in English . . . by one of America's foremost engineers (former Chief Design Engineer for T.V.A.). Provides a transition from the basic differential equations of hydraulic transient theory to the arithmetic intergration computation required by practicing engineers. Sections cover Water Hammer, Turbine Speed Regulation, Stability of Governing, Water-Hammer Pressures in Pump Discharge Lines, The Differential and Restricted Orifice Surge Tanks, The Normalized Surge Tank Charts of Calame and Gaden, Navigation Locks, Surges in Power Canals—Tidal Harmonics, etc. Revised and enlarged. Author's prefaces. Index. xiv + 409pp. 5⅜ x 8½. S116 Paperbound **$2.50**

HYDRAULICS AND ITS APPLICATIONS, A. H. Gibson. Excellent comprehensive textbook for the student and thorough practical manual for the professional worker, a work of great stature in its area. Half the book is devoted to theory and half to applications and practical problems met in the field. Covers modes of motion of a fluid, critical velocity, viscous flow, eddy formation, Bernoulli's theorem, flow in converging passages, vortex motion, form of effluent streams, notches and weirs, skin friction, losses at valves and elbows, siphons, erosion of channels, jet propulsion, waves of oscillation, and over 100 similar topics. Final chapters (nearly 400 pages) cover more than 100 kinds of hydraulic machinery: Pelton wheel, speed regulators, the hydraulic ram, surge tanks, the scoop wheel, the Venturi meter, etc. A special chapter treats methods of testing theoretical hypotheses: scale models of rivers, tidal estuaries, siphon spillways, etc. 5th revised and enlarged (1952) edition. Index. Appendix. 427 photographs and diagrams. 95 examples, answers. xv + 813pp. 6 x 9. S791 Clothbound **$8.00**

FLUID MECHANICS THROUGH WORKED EXAMPLES, D. R. L. Smith and J. Houghton. Advanced text covering principles and applications to practical situations. Each chapter begins with concise summaries of fundamental ideas. 163 fully worked out examples applying principles outlined in the text. 275 other problems, with answers. Contents: The Pressure of Liquids on Surfaces; Floating Bodies; Flow Under Constant Head in Pipes; Circulation; Vorticity; The Potential Function; Laminar Flow and Lubrication; Impact of Jets; Hydraulic Turbines; Centrifugal and Reciprocating Pumps; Compressible Fluids; and many other items. Total of 438 examples. 250 line illustrations. 340pp. Index. 6 x 8⅞. S981 Clothbound **$6.00**

THEORY OF SHIP MOTIONS, S. N. Blagoveshchensky. The only detailed text in English in a rapidly developing branch of engineering and physics, it is the work of one of the world's foremost authorities—Blagoveshchensky of Leningrad Shipbuilding Institute. A senior-level treatment written primarily for engineering students, but also of great importance to naval architects, designers, contractors, researchers in hydrodynamics, and other students. No mathematics beyond ordinary differential equations is required for understanding the text. Translated by T. & L. Strelkoff, under editorship of Louis Landweber, Iowa Institute of Hydraulic Research, under auspices of Office of Naval Research. Bibliography. Index. 231 diagrams and illustrations. Total of 649pp. 5⅜ x 8½. Vol. I: S234 Paperbound **$2.00**
Vol. II: S235 Paperbound **$2.00**

THEORY OF FLIGHT, Richard von Mises. Remains almost unsurpassed as balanced, well-written account of fundamental fluid dynamics, and situations in which air compressibility effects are unimportant. Stressing equally theory and practice, avoiding formidable mathematical structure, it conveys a full understanding of physical phenomena and mathematical concepts. Contains perhaps the best introduction to general theory of stability. "Outstanding," Scientific, Medical, and Technical Books. New introduction by K. H. Hohenemser. Bibliographical, historical notes. Index. 408 illustrations. xvi + 620pp. 5⅜ x 8⅜. S541 Paperbound **$2.95**

THEORY OF WING SECTIONS, I. H. Abbott, A. E. von Doenhoff. Concise compilation of subsonic aerodynamic characteristics of modern NASA wing sections, with description of their geometry, associated theory. Primarily reference work for engineers, students, it gives methods, data for using wing-section data to predict characteristics. Particularly valuable: chapters on thin wings, airfoils; complete summary of NACA's experimental observations, system of construction families of airfoils. 350pp. of tables on Basic Thickness Forms, Mean Lines, Airfoil Ordinates, Aerodynamic Characteristics of Wing Sections. Index. Bibliography. 191 illustrations. Appendix. 705pp. 5⅜ x 8. S558 Paperbound **$3.25**

WEIGHT-STRENGTH ANALYSIS OF AIRCRAFT STRUCTURES, F. R. Shanley. Scientifically sound methods of analyzing and predicting the structural weight of aircraft and missiles. Deals directly with forces and the distances over which they must be transmitted, making it possible to develop methods by which the minimum structural weight can be determined for any material and conditions of loading. Weight equations for wing and fuselage structures. Includes author's original papers on inelastic buckling and creep buckling. "Particularly successful in presenting his analytical methods for investigating various optimum design principles," AERONAUTICAL ENGINEERING REVIEW. Enlarged bibliography. Index. 199 figures. xiv + 404pp. 5⅝ x 8⅜. S660 Paperbound **$2.45**

Electricity

TWO-DIMENSIONAL FIELDS IN ELECTRICAL ENGINEERING, L. V. Bewley. A useful selection of typical engineering problems of interest to practicing electrical engineers. Introduces senior students to the methods and procedures of mathematical physics. Discusses theory of functions of a complex variable, two-dimensional fields of flow, general theorems of mathematical physics and their applications, conformal mapping or transformation, method of images, freehand flux plotting, etc. New preface by the author. Appendix by W. F. Kiltner. Index. Bibliography at chapter ends. xiv + 204pp. 5⅜ x 8½. S1118 Paperbound **$1.50**

FLUX LINKAGES AND ELECTROMAGNETIC INDUCTION, L. V. Bewley. A brief, clear book which shows proper uses and corrects misconceptions of Faraday's law of electromagnetic induction in specific problems. Contents: Circuits, Turns, and Flux Linkages; Substitution of Circuits; Electromagnetic Induction; General Criteria for Electromagnetic Induction; Applications and Paradoxes; Theorem of Constant Flux Linkages. New Section: Rectangular Coil in a Varying Uniform Medium. Valuable supplement to class texts for engineering students. Corrected, enlarged edition. New preface. Bibliography in notes. 49 figures. xi + 106pp. 5⅜ x 8. S1103 Paperbound **$1.25**

INDUCTANCE CALCULATIONS: WORKING FORMULAS AND TABLES, Frederick W. Grover. An invaluable book to everyone in electrical engineering. Provides simple single formulas to cover all the more important cases of inductance. The approach involves only those parameters that naturally enter into each situation, while extensive tables are given to permit easy interpolations. Will save the engineer and student countless hours and enable them to obtain accurate answers with minimal effort. Corrected republication of 1946 edition. 58 tables. 97 completely worked out examples. 66 figures. xiv + 286pp. 5⅜ x 8½.
S974 Paperbound **$1.85**

GASEOUS CONDUCTORS: THEORY AND ENGINEERING APPLICATIONS, J. D. Cobine. An indispensable text and reference to gaseous conduction phenomena, with the engineering viewpoint prevailing throughout. Studies the kinetic theory of gases, ionization, emission phenomena; gas breakdown, spark characteristics, glow, and discharges; engineering applications in circuit interrupters, rectifiers, light sources, etc. Separate detailed treatment of high pressure arcs (Suits); low pressure arcs (Langmuir and Tonks). Much more. "Well organized, clear, straightforward," Tonks, Review of Scientific Instruments. Index. Bibliography. 83 practice problems. 7 appendices. Over 600 figures. 58 tables. xx + 606pp. 5⅜ x 8. S442 Paperbound **$2.95**

INTRODUCTION TO THE STATISTICAL DYNAMICS OF AUTOMATIC CONTROL SYSTEMS, V. V. Solodovnikov. First English publication of text-reference covering important branch of automatic control systems—random signals; in its original edition, this was the first comprehensive treatment. Examines frequency characteristics, transfer functions, stationary random processes, determination of minimum mean-squared error, of transfer function for a finite period of observation, much more. Translation edited by J. B. Thomas, L. A. Zadeh. Index. Bibliography. Appendix. xxii + 308pp. 5⅜ x 8. S420 Paperbound **$2.25**

TENSORS FOR CIRCUITS, Gabriel Kron. A boldly original method of analyzing engineering problems, at center of sharp discussion since first introduced, now definitely proved useful in such areas as electrical and structural networks on automatic computers. Encompasses a great variety of specific problems by means of a relatively few symbolic equations. "Power and flexibility . . . becoming more widely recognized," Nature. Formerly "A Short Course in Tensor Analysis." New introduction by B. Hoffmann. Index. Over 800 diagrams. xix + 250pp. 5⅜ x 8. S534 Paperbound **$2.00**

SELECTED PAPERS ON SEMICONDUCTOR MICROWAVE ELECTRONICS, edited by Sumner N. Levine and Richard R. Kurzrok. An invaluable collection of important papers dealing with one of the most remarkable devolopments in solid-state electronics—the use of the p-n junction to achieve amplification and frequency conversion of microwave frequencies. Contents: General Survey (3 introductory papers by W. E. Danielson, R. N. Hall, and M. Tenzer); General Theory of Nonlinear Elements (3 articles by A. van der Ziel, H. E. Rowe, and Manley and Rowe); Device Fabrication and Characterization (3 pieces by Bakanowski, Cranna, and Uhlir, by McCotter, Walker and Fortini, and by S. T. Eng); Parametric Amplifiers and Frequency Multipliers (13 articles by Uhlir, Heffner and Wade, Matthaei, P. K. Tien, van der Ziel, Engelbrecht, Currie and Gould, Uenohara, Leeson and Weinreb, and others); and Tunnel Diodes (4 papers by L. Esaki, H. S. Sommers, Jr., M. E. Hines, and Yariv and Cook). Introduction. 295 Figures. xiii + 286pp. 6½ x 9¼. S1126 Paperbound **$2.25**

THE PRINCIPLES OF ELECTROMAGNETISM APPLIED TO ELECTRICAL MACHINES, B. Hague. A concise, but complete, summary of the basic principles of the magnetic field and its applications, with particular reference to the kind of phenomena which occur in electrical machines. Part I: General Theory—magnetic field of a current, electromagnetic field passing from air to iron, mechanical forces on linear conductors, etc. Part II: Application of theory to the solution of electromechanical problems—the magnetic field and mechanical forces in non-salient pole machinery, the field within slots and between salient poles, and the work of Rogowski, Roth, and Strutt. Formery titled "Electromagnetic Problems in Electrical Engineering." 2 appendices. Index. Bibliography in notes. 115 figures. xiv + 359pp. 5⅜ x 8½. S246 Paperbound **$2.25**

Mechanical engineering

DESIGN AND USE OF INSTRUMENTS AND ACCURATE MECHANISM, T. N. Whitehead. For the instrument designer, engineer; how to combine necessary mathematical abstractions with independent observation of actual facts. Partial contents: instruments & their parts, theory of errors, systematic errors, probability, short period errors, erratic errors, design precision, kinematic, semikinematic design, stiffness, planning of an instrument, human factor, etc. Index. 85 photos, diagrams. xii + 288pp. 5⅜ x 8. S270 Paperbound **$2.00**

A TREATISE ON GYROSTATICS AND ROTATIONAL MOTION: THEORY AND APPLICATIONS, Andrew Gray. Most detailed, thorough book in English, generally considered definitive study. Many problems of all sorts in full detail, or step-by-step summary. Classical problems of Bour, Lottner, etc.; later ones of great physical interest. Vibrating systems of gyrostats, earth as a top, calculation of path of axis of a top by elliptic integrals, motion of unsymmetrical top, much more. Index. 160 illus. 550pp. 5⅜ x 8. S589 Paperbound **$2.75**

MECHANICS OF THE GYROSCOPE, THE DYNAMICS OF ROTATION, R. F. Deimel, Professor of Mechanical Engineering at Stevens Institute of Technology. Elementary general treatment of dynamics of rotation, with special application of gyroscopic phenomena. No knowledge of vectors needed. Velocity of a moving curve, acceleration to a point, general equations of motion, gyroscopic horizon, free gyro, motion of discs, the damped gyro, 103 similar topics. Exercises. 75 figures. 208pp. 5⅜ x 8. S66 Paperbound **$1.65**

STRENGTH OF MATERIALS, J. P. Den Hartog. Distinguished text prepared for M.I.T. course, ideal as introduction, refresher, reference, or self-study text. Full clear treatment of elementary material (tension, torsion, bending, compound stresses, deflection of beams, etc.), plus much advanced material on engineering methods of great practical value: full treatment of the Mohr circle, lucid elementary discussions of the theory of the center of shear and the "Myosotis" method of calculating beam deflections, reinforced concrete, plastic deformations, photoelasticity, etc. In all sections, both general principles and concrete applications are given. Index. 186 figures (160 others in problem section). 350 problems, all with answers. List of formulas. viii + 323pp. 5⅜ x 8. S755 Paperbound **$2.00**

PHOTOELASTICITY: PRINCIPLES AND METHODS, H. T. Jessop, F. C. Harris. For the engineer, for specific problems of stress analysis. Latest time-saving methods of checking calculations in 2-dimensional design problems, new techniques for stresses in 3 dimensions, and lucid description of optical systems used in practical photoelasticity. Useful suggestions and hints based on on-the-job experience included. Partial contents: strained and stress-strain relations, circular disc under thrust along diameter, rectangular block with square hole under vertical thrust, simply supported rectangular beam under central concentrated load, etc. Theory held to minimum, no advanced mathematical training needed. Index. 164 illustrations. viii + 184pp. 6⅛ x 9¼. S720 Paperbound **$2.00**

APPLIED ELASTICITY, J. Prescott. Provides the engineer with the theory of elasticity usually lacking in books on strength of materials, yet concentrates on those portions useful for immediate application. Develops every important type of elasticity problem from theoretical principles. Covers analysis of stress, relations between stress and strain, the empirical basis of elasticity, thin rods under tension or thrust, Saint Venant's theory, transverse oscillations of thin rods, stability of thin plates, cylinders with thin walls, vibrations of rotating disks, elastic bodies in contact, etc. "Excellent and important contribution to the subject, not merely in the old matter which he has presented in new and refreshing form, but also in the many original investigations here published for the first time," NATURE. Index. 3 Appendixes. vi + 672pp. 5⅜ x 8. S726 Paperbound **$2.95**

APPLIED MECHANICS FOR ENGINEERS, Sir Charles Inglis, F.R.S. A representative survey of the many and varied engineering questions which can be answered by statics and dynamics. The author, one of first and foremost adherents of "structural dynamics," presents distinctive illustrative examples and clear, concise statement of principles—directing the discussion at methodology and specific problems. Covers fundamental principles of rigid-body statics, graphic solutions of static problems, theory of taut wires, stresses in frameworks, particle dynamics, kinematics, simple harmonic motion and harmonic analysis, two-dimensional rigid dynamics, etc. 437 illustrations. xii + 404pp. 5⅜ x 8½. S1119 Paperbound **$2.00**

THEORY OF MACHINES THROUGH WORKED EXAMPLES, G. H. Ryder. Practical mechanical engineering textbook for graduates and advanced undergraduates, as well as a good reference work for practicing engineers. Partial contents: Mechanisms, Velocity and Acceleration (including discussion of Klein's Construction for Piston Acceleration), Cams, Geometry of Gears, Clutches and Bearings, Belt and Rope Drives, Brakes, Inertia Forces and Couples, General Dynamical Problems, Gyroscopes, Linear and Angular Vibrations, Torsional Vibrations, Transverse Vibrations and Whirling Speeds (Chapters on vibrations considerably enlarged from previous editions). Over 300 problems, many fully worked out. Index. 195 line illustrations. Revised and enlarged edition. viii + 280pp. 5⅝ x 8¾. S980 Clothbound **$5.00**

THE KINEMATICS OF MACHINERY: OUTLINES OF A THEORY OF MACHINES, Franz Reuleaux. The classic work in the kinematics of machinery. The present thinking about the subject has all been shaped in great measure by the fundamental principles stated here by Reuleaux almost 90 years ago. While some details have naturally been superseded, his basic viewpoint has endured; hence, the book is still an excellent text for basic courses in kinematics and a standard reference work for active workers in the field. Covers such topics as: the nature of the machine problem, phoronomic propositions, pairs of elements, incomplete kinematic chains, kinematic notation and analysis, analyses of chamber-crank trains, chamber-wheel trains, constructive elements of machinery, complete machines, etc., with main focus on controlled movement in mechanisms. Unabridged republication of original edition, translated by Alexander B. Kennedy. New introduction for this edition by E. S. Ferguson. Index. 451 illustrations. xxiv + 622pp. 5⅜ x 8½. S1124 Paperbound **$3.00**

ANALYTICAL MECHANICS OF GEARS, Earle Buckingham. Provides a solid foundation upon which logical design practices and design data can be constructed. Originally arising out of investigations of the ASME Special Research Committee on Worm Gears and the Strength of Gears, the book covers conjugate gear-tooth action, the nature of the contact, and resulting gear-tooth profiles of: spur, internal, helical, spiral, worm, bevel, and hypoid or skew bevel gears. Also: frictional heat of operation and its dissipation, friction losses, etc., dynamic loads in operation, and related matters. Familiarity with this book is still regarded as a necessary prerequisite to work in modern gear manufacturing. 263 figures. 103 tables. Index. x + 546pp. 5⅜ x 8½. S1073 Paperbound **$2.75**

Optical design, lighting

THE SCIENTIFIC BASIS OF ILLUMINATING ENGINEERING, Parry Moon, Professor of Electrical Engineering, M.I.T. Basic, comprehensive study. Complete coverage of the fundamental theoretical principles together with the elements of design, vision, and color with which the lighting engineer must be familiar. Valuable as a text as well as a reference source to the practicing engineer. Partial contents: Spectroradiometric Curve, Luminous Flux, Radiation from Gaseous-Conduction Sources, Radiation from Incandescent Sources, Incandescent Lamps, Measurement of Light, Illumination from Point Sources and Surface Sources, Elements of Lighting Design. 7 Appendices. Unabridged and corrected republication, with additions. New preface containing conversion tables of radiometric and photometric concepts. Index. 707-item bibliography. 92-item bibliography of author's articles. 183 problems. xxiii + 608pp. 5⅜ x 8½. S242 Paperbound **$2.85**

OPTICS AND OPTICAL INSTRUMENTS: AN INTRODUCTION WITH SPECIAL REFERENCE TO PRACTICAL APPLICATIONS, B. K. Johnson. An invaluable guide to basic practical applications of optical principles, which shows how to set up inexpensive working models of each of the four main types of optical instruments—telescopes, microscopes, photographic lenses, optical projecting systems. Explains in detail the most important experiments for determining their accuracy, resolving power, angular field of view, amounts of aberration, all other necessary facts about the instruments. Formerly "Practical Optics." Index. 234 diagrams. Appendix. 224pp. 5⅜ x 8. S642 Paperbound **$1.65**

APPLIED OPTICS AND OPTICAL DESIGN, A. E. Conrady. With publication of vol. 2, standard work for designers in optics is now complete for first time. Only work of its kind in English; only detailed work for practical designer and self-taught. Requires, for bulk of work, no math above trig. Step-by-step exposition, from fundamental concepts of geometrical, physical optics, to systematic study, design, of almost all types of optical systems. Vol. 1: all ordinary ray-tracing methods; primary aberrations; necessary higher aberration for design of telescopes, low-power microscopes, photographic equipment. Vol. 2: (Completed from author's notes by R. Kingslake, Dir. Optical Design, Eastman Kodak.) Special attention to high-power microscope, anastigmatic photographic objectives. "An indispensable work," J., Optical Soc. of Amer. "As a practical guide this book has no rival," Transactions, Optical Soc. Index. Bibliography. 193 diagrams. 852pp. 6⅛ x 9¼.
Vol. 1 S366 Paperbound **$2.95**
Vol. 2 S612 Paperbound **$2.95**

Miscellaneous

THE MEASUREMENT OF POWER SPECTRA FROM THE POINT OF VIEW OF COMMUNICATIONS ENGINEERING, R. B. Blackman, J. W. Tukey. This pathfinding work, reprinted from the "Bell System Technical Journal," explains various ways of getting practically useful answers in the measurement of power spectra, using results from both transmission theory and the theory of statistical estimation. Treats: Autocovariance Functions and Power Spectra; Direct Analog Computation; Distortion, Noise, Heterodyne Filtering and Pre-whitening; Aliasing; Rejection Filtering and Separation; Smoothing and Decimation Procedures; Very Low Frequencies; Transversal Filtering; much more. An appendix reviews fundamental Fourier techniques. Index of notation. Glossary of terms. 24 figures. XII tables. Bibliography. General index. 192pp. 5⅜ x 8. S507 Paperbound **$1.85**

CALCULUS REFRESHER FOR TECHNICAL MEN, A. Albert Klaf. This book is unique in English as a refresher for engineers, technicians, students who either wish to brush up their calculus or to clear up uncertainties. It is not an ordinary text, but an examination of most important aspects of integral and differential calculus in terms of the 756 questions most likely to occur to the technical reader. The first part of this book covers simple differential calculus, with constants, variables, functions, increments, derivatives, differentiation, logarithms, curvature of curves, and similar topics. The second part covers fundamental ideas of integration, inspection, substitution, transformation, reduction, areas and volumes, mean value, successive and partial integration, double and triple integration. Practical aspects are stressed rather than theoretical. A 50-page section illustrates the application of calculus to specific problems of civil and nautical engineering, electricity, stress and strain, elasticity, industrial engineering, and similar fields.—756 questions answered. 566 problems, mostly answered. 36 pages of useful constants, formulae for ready reference. Index. v + 431pp. 5⅜ x 8. T370 Paperbound **$2.00**

METHODS IN EXTERIOR BALLISTICS, Forest Ray Moulton. Probably the best introduction to the mathematics of projectile motion. The ballistics theories propounded were coordinated with extensive proving ground and wind tunnel experiments conducted by the author and others for the U.S. Army. Broad in scope and clear in exposition, it gives the beginnings of the theory used for modern-day projectile, long-range missile, and satellite motion. Six main divisions: Differential Equations of Translatory Motion of a projectile; Gravity and the Resistance Function; Numerical Solution of Differential Equations; Theory of Differential Variations; Validity of Method of Numerical Integration; and Motion of a Rotating Projectile. Formerly titled: "New Methods in Exterior Ballistics." Index. 38 diagrams. viii + 259pp. 5⅜ x 8½. S232 Paperbound **$1.75**

LOUD SPEAKERS: THEORY, PERFORMANCE, TESTING AND DESIGN, N. W. McLachlan. Most comprehensive coverage of theory, practice of loud speaker design, testing; classic reference, study manual in field. First 12 chapters deal with theory, for readers mainly concerned with math. aspects; last 7 chapters will interest reader concerned with testing, design. Partial contents: principles of sound propagation, fluid pressure on vibrators, theory of moving-coil principle, transients, driving mechanisms, response curves, design of horn type moving coil speakers, electrostatic speakers, much more. Appendix. Bibliography. Index. 165 illustrations, charts. 411pp. 5⅜ x 8.
S588 Paperbound **$2.25**

MICROWAVE TRANSMISSION, J. C. Slater. First text dealing exclusively with microwaves, brings together points of view of field, circuit theory, for graduate student in physics, electrical engineering, microwave technician. Offers valuable point of view not in most later studies. Uses Maxwell's equations to study electromagnetic field, important in this area. Partial contents: infinite line with distributed parameters, impedance of terminated line, plane waves, reflections, wave guides, coaxial line, composite transmission lines, impedance matching, etc. Introduction. Index. 76 illus. 319pp. 5⅜ x 8.
S564 Paperbound **$1.50**

MICROWAVE TRANSMISSION DESIGN DATA, T. Moreno. Originally classified, now rewritten and enlarged (14 new chapters) for public release under auspices of Sperry Corp. Material of immediate value or reference use to radio engineers, systems designers, applied physicists, etc. Ordinary transmission line theory; attenuation; capacity; parameters of coaxial lines; higher modes; flexible cables; obstacles, discontinuities, and injunctions; tunable wave guide impedance transformers; effects of temperature and humidity; much more. "Enough theoretical discussion is included to allow use of data without previous background," Electronics. 324 circuit diagrams, figures, etc. Tables of dielectrics, flexible cable, etc., data. Index. ix + 248pp. 5⅜ x 8.
S459 Paperbound **$1.65**

RAYLEIGH'S PRINCIPLE AND ITS APPLICATIONS TO ENGINEERING, G. Temple & W. Bickley. Rayleigh's principle developed to provide upper and lower estimates of true value of fundamental period of a vibrating system, or condition of stability of elastic systems. Illustrative examples; rigorous proofs in special chapters. Partial contents: Energy method of discussing vibrations, stability. Perturbation theory, whirling of uniform shafts. Criteria of elastic stability. Application of energy method. Vibrating systems. Proof, accuracy, successive approximations, application of Rayleigh's principle. Synthetic theorems. Numerical, graphical methods. Equilibrium configurations, Ritz's method. Bibliography. Index. 22 figures. ix + 156pp. 5⅜ x 8.
S307 Paperbound **$1.50**

ELASTICITY, PLASTICITY AND STRUCTURE OF MATTER, R. Houwink. Standard treatise on rheological aspects of different technically important solids such as crystals, resins, textiles, rubber, clay, many others. Investigates general laws for deformations; determines divergences from these laws for certain substances. Covers general physical and mathematical aspects of plasticity, elasticity, viscosity. Detailed examination of deformations, internal structure of matter in relation to elastic and plastic behavior, formation of solid matter from a fluid, conditions for elastic and plastic behavior of matter. Treats glass, asphalt, gutta percha, balata, proteins, baker's dough, lacquers, sulphur, others. 2nd revised, enlarged edition. Extensive revised bibliography in over 500 footnotes. Index. Table of symbols. 214 figures. xviii + 368pp. 6 x 9¼.
S385 Paperbound **$2.45**

THE SCHWARZ-CHRISTOFFEL TRANSFORMATION AND ITS APPLICATIONS: A SIMPLE EXPOSITION, Miles Walker. An important book for engineers showing how this valuable tool can be employed in practical situations. Very careful, clear presentation covering numerous concrete engineering problems. Includes a thorough account of conjugate functions for engineers—useful for the beginner and for review. Applications to such problems as: Stream-lines round a corner, electric conductor in air-gap, dynamo slots, magnetized poles, much more. Formerly "Conjugate Functions for Engineers." Preface. 92 figures, several tables. Index. ix + 116pp. 5⅜ x 8½.
S1149 Paperbound **$1.25**

THE LAWS OF THOUGHT, George Boole. This book founded symbolic logic some hundred years ago. It is the 1st significant attempt to apply logic to all aspects of human endeavour. Partial contents: derivation of laws, signs & laws, interpretations, eliminations, conditions of a perfect method, analysis, Aristotelian logic, probability, and similar topics. xviii + 424pp. 5⅜ x 8.
S28 Paperbound **$2.00**

SCIENCE AND METHOD, Henri Poincaré. Procedure of scientific discovery, methodology, experiment, idea-germination—the intellectual processes by which discoveries come into being. Most significant and most interesting aspects of development, application of ideas. Chapters cover selection of facts, chance, mathematical reasoning, mathematics, and logic; Whitehead, Russell, Cantor; the new mechanics, etc. 288pp. 5⅜ x 8.
S222 Paperbound **$1.35**

FAMOUS BRIDGES OF THE WORLD, D. B. Steinman. An up-to-the-minute revised edition of a book that explains the fascinating drama of how the world's great bridges came to be built. The author, designer of the famed Mackinac bridge, discusses bridges from all periods and all parts of the world, explaining their various types of construction, and describing the problems their builders faced. Although primarily for youngsters, this cannot fail to interest readers of all ages. 48 illustrations in the text. 23 photographs. 99pp. 6⅛ x 9¼.
T161 Paperbound **$1.00**

Technological, historical

A DIDEROT PICTORIAL ENCYCLOPEDIA OF TRADES AND INDUSTRY, Manufacturing and the Technical Arts in Plates Selected from "L'Encyclopédie ou Dictionnaire Raisonné des Sciences, des Arts, et des Métiers" of Denis Diderot. Edited with text by C. Gillispie. This first modern selection of plates from the high point of 18th century French engraving is a storehouse of valuable technological information to the historian of arts and science. Over 2000 illustrations on 485 full-page plates, most of them original size, show the trades and industries of a fascinating era in such great detail that the processes and shops might very well be reconstructed from them. The plates teem with life, with men, women, and children performing all of the thousands of operations necessary to the trades before and during the early stages of the industrial revolution. Plates are in sequence, and show general operations, closeups of difficult operations, and details of complex machinery. Such important and interesting trades and industries are illustrated as sowing, harvesting, beekeeping, cheesemaking, operating windmills, milling flour, charcoal burning, tobacco processing, indigo, fishing, arts of war, salt extraction, mining, smelting, casting iron, steel, extracting mercury, zinc, sulphur, copper, etc., slating, tinning, silverplating, gilding, making gunpowder, cannons, bells, shoeing horses, tanning, papermaking, printing, dyeing, and more than 40 other categories. Professor Gillispie, of Princeton, supplies a full commentary on all the plates, identifying operations, tools, processes, etc. This material, presented in a lively and lucid fashion, is of great interest to the reader interested in history of science and technology. Heavy library cloth. 920pp. 9 x 12. T421 Two volume set **$18.50**

CHARLES BABBAGE AND HIS CALCULATING ENGINES, edited by P. Morrison and E. Morrison. Babbage, leading 19th century pioneer in mathematical machines and herald of modern operational research, was the true father of Harvard's relay computer Mark I. His Difference Engine and Analytical Engine were the first machines in the field. This volume contains a valuable introduction on his life and work; major excerpts from his autobiography, revealing his eccentric and unusual personality; and extensive selections from "Babbage's Calculating Engines," a compilation of hard-to-find journal articles by Babbage, the Countess of Lovelace, L. F. Menabrea, and Dionysius Lardner. 8 illustrations, Appendix of miscellaneous papers. Index. Bibliography. xxxviii + 400pp. 5⅜ x 8. T12 Paperbound **$2.00**

HISTORY OF HYDRAULICS, Hunter Rouse and Simon Incé. First history of hydraulics and hydrodynamics available in English. Presented in readable, non-mathematical form, the text is made especially easy to follow by the many supplementary photographs, diagrams, drawings, etc. Covers the great discoveries and developments from Archimedes and Galileo to modern giants—von Mises, Prandtl, von Karman, etc. Interesting browsing for the specialist; excellent introduction for teachers and students. Discusses such milestones as the two-piston pump of Ctesibius, the aqueducts of Frontius, the anticipations of da Vinci, Stevin and the first book on hydrodynamics, experimental hydraulics of the 18th century, the 19th-century expansion of practical hydraulics and classical and applied hydrodynamics, the rise of fluid mechanics in our time, etc. 200 illustrations. Bibliographies. Index. xii + 270pp. 5¾ x 8.
S1131 Paperbound **$2.00**

BRIDGES AND THEIR BUILDERS, David Steinman and Sara Ruth Watson. Engineers, historians, everyone who has ever been fascinated by great spans will find this book an endless source of information and interest. Dr. Steinman, recipient of the Louis Levy medal, was one of the great bridge architects and engineers of all time, and his analysis of the great bridges of history is both authoritative and easily followed. Greek and Roman bridges, medieval bridges, Oriental bridges, modern works such as the Brooklyn Bridge and the Golden Gate Bridge, and many others are described in terms of history, constructional principles, artistry, and function. All in all this book is the most comprehensive and accurate semipopular history of bridges in print in English. New, greatly revised, enlarged edition. 23 photographs, 26 line drawings. Index. xvii + 401pp. 5⅜ x 8. T431 Paperbound **$2.00**

Prices subject to change without notice.

Dover publishes books on art, music, philosophy, literature, languages, history, social sciences, psychology, handcrafts, orientalia, puzzles and entertainments, chess, pets and gardens, books explaining science, intermediate and higher mathematics, mathematical physics, engineering, biological sciences, earth sciences, classics of science, etc. Write to:

Dept. catrr.
Dover Publications, Inc.
180 Varick Street, N.Y. 14, N.Y.

(continued from front flap)

Mathematical Tables of Elementary and Some Higher Mathematical Functions, Herbert B. Dwight. $1.75

The Theory and Operation of the Slide Rule, John P. Ellis. $1.50

Differential Equations for Engineers, Philip Franklin. $1.65

Hydraulics and Its Applications, A. H. Gibson. Clothbound $8.00

A Treatise on Gyrostatics and Rotational Motion, Andrew Gray. $2.75

Inductance Calculations: Working Formulas and Tables, Frederick W. Grover. $1.85

The Principles of Electromagnetism Applied to Electrical Machines, Bernard Hague. $2.25

Elasticity, Plasticity and Structure of Matter, Roelof Houwink. $2.45

Applied Mechanics for Engineers, Sir Charles Inglis. $2.00

Tables of Functions with Formulae and Curves, Eugene Jahnke and Fritz Emde. $2.00

Photoelasticity: Principles and Methods, H. T. Jessop and F. C. Harris. $2.00

Optics and Optical Instruments, B. K. Johnson. $1.65

Mathematics of Modern Engineering, Ernest G. Keller and Robert E. Doherty. Two volume set $3.70

Fundamental Electromagnetic Theory, Ronold P. King. $2.75

Calculus Refresher for Technical Men, A. Albert Klaf. $2.00

Trigonometry Refresher for Technical Men, A. Albert Klaf. $2.00

Stress Waves in Solids, H. Kolsky. $1.55

Tensors for Circuits, Gabriel Kron. $2.00

The Dynamical Theory of Sound, Horace Lamb. $1.50

Hydrodynamics, Horace Lamb. $3.75

Selected Papers on New Techniques for Energy Conversion, edited by Sumner N. Levine. $3.00

Selected Papers on Semiconductor Microwave Electronics, edited by Sumner N. Levine and Richard M. Kurzrok. $2.25

Fundamentals of Electricity and Magnetism, Leonard B. Loeb. $2.75

The Principles of Electrochemistry, Duncan A. MacInnes. $2.45

Loud Speakers: Theory, Performance, Testing, and Design, Norman W. McLachlan. $2.25

Paperbound unless otherwise indicated. Prices subject to change without notice. Available at your book dealer or write for free catalogues to Dept. Eng., Dover Publications, Inc., 180 Varick St., N. Y., N. Y. 10014. Please indicate field of interest. Dover publishes over 125 new books and records each year on such fields as mathematics, physics, explaining science, art, languages, philosophy, classical records, and others.

Transmission-line Theory

BY RONOLD W. P. KING

Professor of Applied Physics, Harvard University

Within the last decade, electrical science has become the province not so much of the physicist, but of the engineer. For these people, a knowledge of electromagnetic theory is, of course, essential. It is the contention of Professor King, a well-known authority who has taught at Harvard for many years and has made significant contributions to applied physics, that one of the best approaches to electromagnetic theory for the engineer is through the conventional transmission line, for, in this way, it is possible to introduce fundamental concepts without becoming involved in all the complications of vector line theory.

His book, now reprinted in a corrected edition with a new index of symbols, is the standard English-language reference work on transmission-line theory. In its first chapter, the transmission-line equations for an infinite line are deduced both in the conventional manner and from electromagnetic fundamentals for various cross-sections. In chapter two, the derivation of these equations is specialized to lines of finite length, and the basic method of treating terminated lines is formulated. Chapter three is concerned with the impedance of sections of transmission line and their use as shunt and series elements. The next two chapters discuss distributions of current and voltage, the transfer of power, distribution and resonance curves, discontinuities and nonuniformities along smooth lines, the Weissfloch tangent relation, Deschamps's method for determining the properties of junctions, T junctions, end corrections, etc. The final chapter is devoted to transmission-line oscillators, coupled-circuit phenomena on lines, and radiation.

Designed as a fundamental introduction to more serious work in wave guides and antennas, this book is primarily analytic in treatment. Little more than a sound knowledge of differential and integral calculus and elementary differential equations is supposed, however. Each chapter concludes with a selection of problems, making the book useful as a classroom text and for testing comprehension. Electrical engineers and students, and physicists interested in an important modern approach to these topics will find the book invaluable as a text or a reference.

"Invaluable to anyone who wishes to use transmission-line theory effectively . . . should put the reader in a position to tackle new problems with confidence," T. Teichmann, PHYSICS TODAY. "Used as a text or reference, this book undoubtedly is one of the most complete treatments of the subject to date," J. OF FRANKLIN INSTITUTE.

Corrected (1964), unabridged republication. Author's preface. Bibliography. Subject index. New index of symbols. 255 figures. 9 tables. 62 problems, chapter ends. xiv + 513 pp. 5⅜ x 8½. S1285 Paperbound $3.50

PUBLISHERS LIST PRICE

A DOVER EDITION DESIGNED FOR YEARS OF USE!

We have spared no pains to make this the best book possible. Our paper is opaque, with minimal show-through; it will not discolor or become brittle with age. Pages are sewn in signatures, in the method traditionally used for the best books. Books open flat for easy reference. Pages will not drop out, as often happens with paperbacks held together with glue. The binding will not crack and split. This is a permanent book.

KING

Transmission-line Theory

Dover

S1285